ol. 93 October 1, 1977
omplete in one issue

ISSN 0003-2670

ANALYTICA CHIMICA ACTA

International journal devoted to all branches of analytical chemistry

EDITORS

A. M. G. MACDONALD (Birmingham, Great Britain)

D. M. W. ANDERSON (Edinburgh, Great Britain)

Editorial Advisers

R. Belcher, Birmingham
E. A. M. F. Dahmen, Enschede
G. den Boef, Amsterdam
G. Duyckaerts, Liège
D. Dyrssen, Göteborg
T. Fujinaga, Kyoto
G. G. Guilbault, New Orleans, La.
G. M. Hieftje, Bloomington, Ind.
J. Hoste, Ghent
A. Hulanicki, Warsaw
E. Jackwerth, Dortmund
G. Johansson, Lund
D. C. Johnson, Ames, Iowa
J. H. Knox, Edinburgh
D. E. Leyden, Denver, Colo.
H. Malissa, Vienna
G. H. Morrison, Ithaca, N.Y.
E. Pungor, Budapest
J. P. Riley, Liverpool
J. W. Robinson, Baton Rouge, La.
J. Růžička, Copenhagen
D. E. Ryan, Halifax, N.S.
W. Simon, Zürich
R. K. Skogerboe, Fort Collins, Colo.
W. I. Stephen, Birmingham
G. Tölg, Schwäbisch Gmünd, B.R.D.
A. Townshend, Birmingham
B. Tremillon, Paris
A. Walsh, Melbourne
H. Weisz, Freiburg i Br.
P. W. West, Baton Rouge, La.
T. S. West, Aberdeen
Yu. A. Zolotov, Moscow
P. Zuman, Potsdam, N.Y.

ELSEVIER SCIENTIFIC PUBLISHING COMPANY

ANALYTICA CHIMICA ACTA

International journal devoted to all branches of analytical chemistry
Revue internationale consacrée à tous les domaines de la chimie analytique
Internationale Zeitschrift für alle Gebiete der analytischen Chemie

PUBLICATION SCHEDULE FOR 1977 (incorporating the section on Computer Techniques and Optimization).

	J	F	M	A	M	J	J	A	S	O	N	D
Analytica Chimica Acta	88/1	88/2	89/1	89/2	90	91/1	91/2	92/1	92/2	93	94/1	94/2
Section on Computer Techniques and Optimization									95/ 1+2			95/3+4

Scope. *Analytica Chimica Acta* publishes original papers, short communications, and reviews dealing with every aspect of modern chemical analysis, both fundamental and applied. The section on *Computer Techniques and Optimization* is devoted to new developments in chemical analysis by the application of computer techniques and by interdisciplinary approaches, including statistics, systems theory and operation research.

Submission of Papers. Manuscripts (three copies) should be submitted to:
for *Analytica Chimica Acta*: Dr. A.M.G. Macdonald, Department of Chemistry, The University, P.O. Box 363, Birmingham B15 2TT, England.
for the section on *Computer Techniques and Optimization*: Dr. J.T. Clerc, Laboratorium für Organische Chemie, Swiss Federal Institute of Technology, Universitätstrasse 16, CH-8092 Zürich, Switzerland.

Information for Authors. Papers in English, French and German are published. There are no page charges. Manuscripts should conform in layout and style to the papers published in this Volume. Authors should consult Vol. 93, p. 379 for detailed information. Reprints of this information are available from the Editors or from: Elsevier Editorial Services Ltd., Mayfield House, 256 Banbury Road, Oxford OX2 7DE (Great Britain).

Reprints. Fifty reprints will be supplied free of charge. Additional reprints (minimum 100) can be ordered. An order form containing price quotations will be sent to the authors together with the proofs of their article.

Advertisements. Advertisement rates are available from the publisher.

Subscriptions. Subscriptions should be sent to: Elsevier Scientific Publishing Company, P.O. Box 211, Amsterdam, The Netherlands. The section on *Computer Techniques and Optimization* can be subscribed to separately.

Publication. *Analytica Chimica Acta* (including the section on *Computer Techniques and Optimization*) appears in 8 volumes in 1977. The subscription for 1977 (Vols. 88–95) is Dfl. 920.00 plus Dfl. 112.00 (postage) (Total approx. US $ 420.95). The subscription for the *Computer Techniques and Optimization* section only (Vol. 95) is Dfl. 115.00 plus Dfl. 14.00 (postage) (Total approx. US $ 52.75). Journals are sent automatically by air mail to the U.S.A. and Canada at no extra cost and to Japan, Australia and New Zealand for a small additional postal charge. All earlier volumes (Vols. 1–87) are available at Dfl. 115.- (plus postage).

Claims for issues not received should be made within three months of publication of the issue, otherwise they cannot be honoured free of charge.

© ELSEVIER SCIENTIFIC PUBLISHING COMPANY – 1977

All rights reserved. No part of this publication may be reproduced, stored in a retrieval system or transmitted in any form or by any means, electronic, mechanical photocopying, recording or otherwise, without the prior written permission of the publisher, Elsevier Scientific Publishing Company, P.O. Box 330, Amsterdam, The Netherlands.

Submission of an article for publication implies transfer of the copyright from the author to the publisher, and is also understood to imply that the article is not under consideration for publication elsewhere.

Printed in The Netherlands

salon du laboratoire 1977

Paris, porte de Versailles

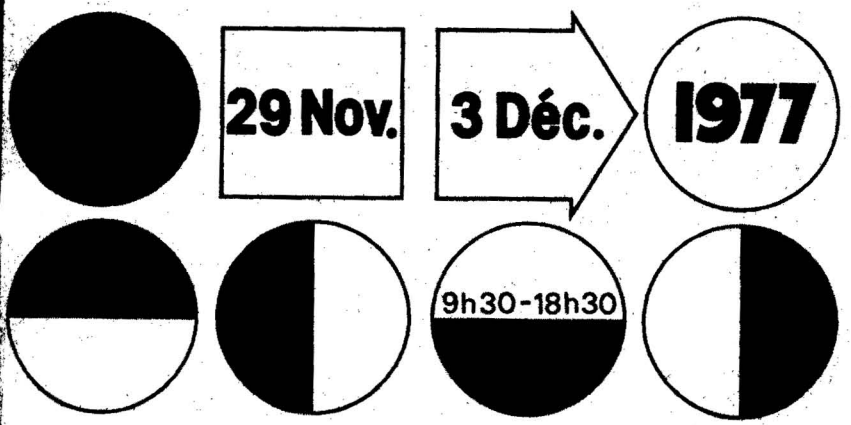

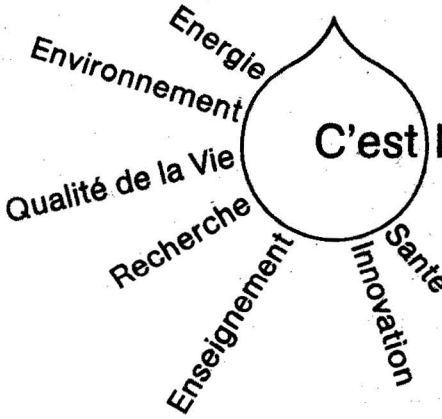

C'est la raison d'être du Laboratoire.

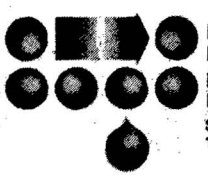

La 67e Exposition de Physique a lieu conjointement avec le Salon du Laboratoire. L'entrée des deux expositions est commune.

Le Congrès de Chimie Analytique - 33e Congrès du G.A.M.S. - se tiendra aux mêmes lieux et dates que ce salon.

Salon organisé par l'Association pour le Salon du Laboratoire régie par la loi de 1901
12, rue Chabanais - 75002 PARIS - France - Tél. 742.79.00

399

Verdere inlichtingen, folder en voordelig reisarrangement worden gaarne verstrekt door de
STICHTING TER BEVORDERING VAN DE FRANSE VAKBEURZEN
Prins Hendrikkade 20-21 - Amsterdam-C. - Telefoon (020) 248670 en 239204

Six new volumes in 1976/1977:

Rodd's Chemistry of Carbon Compounds (Second Edition)

S. COFFEY *(Editor)*

This series, now in the process of being entirely rewritten in the second edition, has established itself as the standard reference work on organic chemistry throughout the world. Since the publication of the first volume of the first edition, the tendency for the organic chemist to make use of the work and techniques of the physicist and the physical chemist, and for the theoretical organic chemist to take advantage of ideas developed in the fields of mathematics and physics, especially atomic physics, has increased markedly. This is clearly reflected in this new edition.

"...Once again a team of authors and a redoubtable, indefatigable editor have put the world of organic chemists in their debt."
-NATURE

"The wealth of factual material, references to the original writings and surveys of modern ideas presented in this series should win the gratitude of chemists the world over."
-CHEMICAL PROCESSING

VOLUME I: ALIPHATIC COMPOUNDS

Part E: Trihydric Alcohols, their Oxidation Products and Derivatives
March 1976 xviii + 488 pages US $75.50/Dfl. 185.00 Subscription price: US $65.50/Dfl. 160.00 ISBN 0-444-40680-8

Part G: Tetrahydric Alcohols, their Analogues, Derivatives and Oxidation Products; Cumulative Index to Volume 1, Parts A-G
Sept. 1976 xiv + 344 pages US $54.95/Dfl. 135.00 Subscription price: US $46.95/Dfl. 115.00 ISBN 0-444-41447-9

VOLUME III: AROMATIC COMPOUNDS

Part D: Monobenzenoid and Phenolic Aralkyl Compounds, their Derivatives and Oxidation Products: Depsides, Tannins, Lignans, Lignin and Humic Acid
Aug. 1976 xx + 322 pages US $57.25/Dfl. 140.00 Subscription price: US $48.95/Dfl. 120.00 ISBN 0-444-41209-3

VOLUME IV: HETEROCYCLIC COMPOUNDS

Part F: Six-membered Heterocyclic Compounds with a Single Atom in the Ring; Pyridine, Polymethylenepyridines, Quinoline, Isoquinoline and their Derivatives
Dec. 1976 xviii + 486 pages US $75.50/Dfl. 185.00 Subscription price: US $64.95/Dfl. 159.00 ISBN 0-444-41503-3

Part B: Five-Membered Heterocyclic Compounds with a Single Hetero-Atom in the Ring: Alkaloids, Dyes and Pigments
Feb. 1977 xx + 462 pages US $75.50/Dfl. 185.00 Subscription price: US $64.95/Dfl. 159.00 ISBN 0-444-41504-1

Part E: Six-membered Monoheterocyclic Compounds containing Oxygen, Sulphur, Selenium, Tellurium, Silicon, Germanium, Tin, Lead or Iodine as the Hetero Atom
Aug. 1977 xviii + 494 pages US $79.75/Dfl. 195.00 Subscription price: US $68.95/Dfl. 169.00 ISBN 0-444-41363-4

Detailed information on these volumes may be obtained from:
Elsevier Promotion Department, P.O. Box 330, Amsterdam, The Netherlands.

The Dutch guilder price is definitive. US $ prices are subject to exchange rate fluctuations.

ELSEVIER

P.O. Box 211, Amsterdam
The Netherlands
52 Vanderbilt Ave
New York, N.Y. 10017

7019E

Sulfur, Energy, and Environment

BEAT MEYER, *Chemistry Department, University of Washington, Seattle, U.S.A.*

This interdisciplinary book describes the properties of sulfur and deals with those aspects of production, use and recovery of sulfur which are important in relation to energy production and environmental protection. Supported by 94 figures, 72 tables and 1500 references, the 15 chapters present a short introduction, a critical review and a reference guide in 14 major areas of the field. A large number of topics are highlighted, such as sulfur based materials and their potential for future utilization, problems of waste and legislation at the interface of scientific and societal concern, and the extensive use of sulfur in agriculture and food preparation. In addition to presenting trends in energy uses, sources, and technology, and trends in the supply and demand of sulfur compounds, the concluding chapter discusses the relationship between scientific initiative and industrial and public demands.
Designed for specialists and non-specialists, this book will serve as a valuable reference guide for scientists, engineers, civil servants, managers, political and social scientists, and lawyers connected with practical or theoretical work involving sulfur.

CONTENTS: **Chapters 1. Introduction. 2. History. 3. Properties.** Elemental Sulfur. Hydrogen Sulfide, Polysulfides, and Sulfanes. Sulfur Oxides and Oxyacids. Corrosion. **4. Analytical Chemistry.** Quantitative Analysis of Total Sulfur. Qualitative Analysis. Sulfur Isotopes. Impurities in Elemental Sulfur. **5. Occurrence and Sources of Sulfur.** Natural Deposits. Secondary Sources. **6. The Sulfur Cycles.** The Global Sulfur Cycle. Hydrosphere. Atmospheric Sulfur Budget. The Anthropogenic Sulfur Cycle. **7. Sulfur Production.** Production of Elemental Sulfur. By-Product Sulfur. **8. Recovery from Combustion Gases.** Coal Combustion Chemistry. Abatement Methods. Abatement Chemistry. **9. Environmental Control and Legislation.** Waste, Disposal, and Education. Air Pollution Legislation. **10. Medical Use and Health Effects.** Elemental Sulfur. Hydrogen Sulfide. Sulfides. Thiosulfate. Polythionates. Sulfite. Sulfur Dioxide. **11. Sulfur in Agriculture and Food.** Sulfur in Agriculture. Sulfur as Fungicide and Insecticide. Sulfur in the Food Industry. **12. Industrial Uses of Sulfur and its Compounds. 13. Sulfur Polymers.** Polymeric Elemental Sulfur. Inorganic Polymers. Organic Polymers. Polymer Mixtures and Blends. **14. Sulfur Containing Materials.** Sulfur-Asphalt. Sulfur-Concrete. Sulfur Foam. Cardboard. Wood-Sulfur Products. Batteries. Sulfur Impregnated Ceramics. Application of Sulfur Compositions. **15. Future Trends.** Sulfur, Energy, and Environment. Chemistry, Government, and Education. Conclusions. **Appendix. Bibliography. Author Index. Subject Index.**

June 1977 xii + 448 pages US $39.60/Dfl. 97.00 ISBN 0-444-41595-5

The Dutch guilder price is definitive. US $ prices are subject to exchange rate fluctuations.

ELSEVIER

P.O. Box 211, Amsterdam
The Netherlands
52 Vanderbilt Ave
New York, N.Y. 10017

7038

Nucleation Phenomena

edited by A.C. ZETTLEMOYER, *Lehigh University, Bethlehem, Penn., U.S.A.*

Reprinted from Advances in Colloid and Interface Science, Vol. 7

The broad interest in nucleation is evident from the fact that industrial laboratories as well as academic groups are working in the field. Although there is much work in progress in the field of nucleation, no journal deals specifically with this subject.

This compilation should serve as a reference treatise for those interested in nucleation. It will be useful in courses on statistical mechanics, thermodynamics, and colloid science, and will also be suitable as a basic text in some subjects.

Most of the material in the seven chapters of this book is directed at homogeneous nucleation. Theoretical contributions include: the replacement free energy approach of Reiss (*University of California at Los Angeles, work done at Bell Laboratories*), the statistical mechanics of liquid droplets by Kikuchi (*Hughes Research Laboratories*), the Fisher's droplet model approach by Stauffer and Kiang (*University of Saarlande and National Center for Atmospheric Research*), atomistic models of microclusters by Burton and Briant (*Exxon Research Corporation and General Electric Research and Development Center*), a further contribution on statistical mechanics of homogeneous nucleation from Pound and Nishioka (*Stanford University and Tokushima University*), and computer simulations of nucleation processes using the lattice gas model by Binder (*University of Saarlande*). The major experimental contribution is the elegant gasdynamics technique for homogeneous nucleation by Wegener and Wu (*Yale University*).

June 1977 viii + 418 pages US$ 49.00/Dfl. 120.00 ISBN 0-444-41586-6

The Dutch guilder price is definitive. US$ prices are subject to exchange rate fluctuations.

ELSEVIER

P.O. Box 211, Amsterdam
The Netherlands
52 Vanderbilt Ave
New York, N.Y. 10017

7033

ANALYTICA CHIMICA ACTA
VOL. 93 (1977)

ANALYTICA CHIMICA ACTA

International journal devoted to all branches of analytical chemistry

EDITORS

A. M. G. MACDONALD (Birmingham, Great Britain)

D. M. W. ANDERSON (Edinburgh, Great Britain)

Editorial Advisers

R. Belcher, Birmingham
E. A. M. F. Dahmen, Enschede
G. den Boef, Amsterdam
G. Duyckaerts, Liège
D. Dyrssen, Göteborg
T. Fujinaga, Kyoto
G. G. Guilbault, New Orleans, La.
G. M. Hieftje, Bloomington, Ind.
J. Hoste, Ghent
A. Hulanicki, Warsaw
E. Jackwerth, Dortmund
G. Johansson, Lund
D. C. Johnson, Ames, Iowa
J. H. Knox, Edinburgh
D. E. Leyden, Denver, Colo.
H. Malissa, Vienna
G. H. Morrison, Ithaca, N.Y.
E. Pungor, Budapest
J. P. Riley, Liverpool
J. W. Robinson, Baton Rouge, La.
J. Růžička, Copenhagen
D. E. Ryan, Halifax, N.S.
W. Simon, Zürich
R. K. Skogerboe, Fort Collins, Colo.
W. I. Stephen, Birmingham
G. Tölg, Schwäbisch Gmünd, B.R.D.
A. Townshend, Birmingham
B. Tremillon, Paris
A. Walsh, Melbourne
H. Weisz, Freiburg i Br.
P. W. West, Baton Rouge, La.
T. S. West, Aberdeen
Yu. A. Zolotov, Moscow
P. Zuman, Potsdam, N.Y.

ELSEVIER SCIENTIFIC PUBLISHING COMPANY

Anal. Chim. Acta, Vol. 93 (1977)

© ELSEVIER SCIENTIFIC PUBLISHING COMPANY, 1977

All rights reserved. No part of this publication may be reproduced, stored in a retrieval system or transmitted in any form or by any means, electronic, mechanical photocopying, recording or otherwise, without the prior written permission of the publisher, Elsevier Scientific Publishing Company, P.O. Box 330, Amsterdam, The Netherlands.
Submission of an article for publication implies the transfer of the copyright from the author to the publisher and is also understood to imply that the article is not being considered for publication elsewhere.
PRINTED IN THE NETHERLANDS

Analytica Chimica Acta, 93 (1977) 1
© Elsevier Scientific Publishing Company, Amsterdam — Printed in The Netherlands

EDITORIAL ANNOUNCEMENT

Important advances have been made in chemical analysis by the application of computer techniques, and with the wider availability of computers, many interesting developments can be expected. With the intention of encouraging such applications, it has been decided to devote a special section of *Analytica Chimica Acta* to non-trivial applications of computer techniques. Expert help in the organization of this new section has been sought, and we are pleased to announce that Dr. J. T. Clerc and Dr. E. Ziegler have agreed to take responsibility for the issues devoted to *Computer Techniques and Optimization*. Guidance on the submission of manuscripts and on subscriptions can be found on the cover of this issue.

The distinction between papers that are of wide analytical interest and papers of more specialized interest can be very fine; authors will therefore be free to choose whether their papers are published in the general issues of *Analytica Chimica Acta* or in the section devoted to *Computer Techniques and Optimization*.

Subscribers to *Analytica Chimica Acta* will receive these issues as a part of their subscriptions. Those particularly interested in the topic of the new section may subscribe separately to these issues.

We wish our new editorial colleagues every success in this venture.

A. M. G. Macdonald
D. M. W. Anderson

Analytica Chimica Acta, 93 (1977) 3—18
©Elsevier Scientific Publishing Company, Amsterdam — Printed in The Netherlands

PRECISE TWIN EBULLIOMETRY

WALACE A. de OLIVEIRA[§] and LOUIS MEITES*

Department of Chemistry, Clarkson College of Technology, Potsdam, New York 13676 (U.S.A.)

(Received 4th April 1977)

SUMMARY

A simple twin ebulliometer is described that makes it possible to achieve a standard error of about 45 μdeg in measuring the difference between the boiling temperatures of two aqueous solutions in the vicinity of 760 torr. Sodium chloride is recommended as a reference electrolyte in aqueous twin ebulliometry, and precise information is given on the concentration dependence of the osmotic and mean ionic activity coefficients of aqueous solutions of sodium chloride over the range 0—1 m. A quick and simple procedure is described for using this information to evaluate the osmotic coefficients of other solutions by twin ebulliometry, and is applied to an investigation of the osmotic and mean ionic activity coefficients of aqueous solutions of lithium chloride at 100°C. The potentialities of twin ebulliometry are judged to be superior to those of cryoscopy and comparable with those of thermoelectric vapor-pressure osmometry.

The boiling point of a solution is an important colligative property, and apparatus and procedures for its measurement have been much studied and greatly refined since the pioneering work of Beckmann [1]. In general, the boiling-point elevation, rather than the boiling temperature itself, is of interest. It is often convenient to define the boiling-point elevation as the difference between the boiling temperature of a solution and that of the pure solvent. The boiling-point elevation thus defined can be evaluated by differential ebulliometry [2], in which a single ebulliometer is employed. The difference between the boiling and condensation temperatures may be measured directly [3], or these two temperatures may be measured separately [4].

Differential ebulliometry has been widely used for the evaluation of number-average molecular weights, and there are several excellent recent reviews in this field [5—8]. Other applications of ebulliometry include evaluations of osmotic and activity coefficients and partial molal heat capacities [9—13], evaluations of association constants and other equilibrium constants [14—17], and studies of the rates of reactions [18—20].

---

§This paper is based in part on a Thesis submitted by Walace A. de Oliveira to the Faculty of Clarkson College of Technology in partial fulfillment of the requirements for the Ph.D. degree in July, 1975.

Twin ebulliometry was first described by Washburn and Read [21]. It has found occasional use [22—25], but is much less well known than differential ebulliometry. It entails the use of two identical ebulliometers. One of these contains the solution being studied; the other contains a reference solution. In this arrangement the difference between the two boiling temperatures can be measured directly, and virtually without interference from fluctuations of atmospheric pressure.

Although the reference ebulliometer has always contained the pure solvent in prior work with twin ebulliometry, this is often not the best choice. Unless the boiling temperature of the solution being studied is very close to that of the solvent, small variations will be masked by the relative error of the measured difference. Better precision can be obtained by using a stable solution whose boiling temperature is known accurately and only very slightly different from that of the solution being studied. Moreover, twin ebulliometry makes it possible to observe the effect of a small concentration of one solute in the presence of a large excess of another, and this is most easily done by using the supporting electrolyte, rather than the pure solvent, in the reference ebulliometer.

The present investigation was aimed at developing and testing a simple twin ebulliometric apparatus that would yield data comparable with those that can be achieved in the present state of the art for measurements of small differences of temperature [26], and at obtaining data of primary-standard grade on the concentration dependence of the boiling temperatures of solutions of some substance that would then serve as a reference in subsequent twin ebulliometric measurements.

EXPERIMENTAL

Apparatus

The final form of the ebulliometer adopted is shown in Fig. 1. Equilibrium between vapor and liquid is established by means of a Cottrell pump of conventional design [6]; a single arm of relatively large diameter (4 mm) was used to minimize superheating. The pump delivers liquid to a point about 6 cm above the tip of the thermistor well B. From that point it streams down the glass spiral C, while maintaining intimate contact with the outside of the well, before returning to the body of the solution at D. The activated surface F was prepared by sintering a thin layer of 20—60-mesh particles of ground glass to the bottom of the flask, using the lowest possible temperature to minimize fusing the sharp edges of the particles. The ebulliometer is connected at the ground joint A to a small water-cooled condenser that is operated at total reflux. Provision is made for withdrawing samples of the boiling solution for analysis through the Teflon stopcock E. The volume of solution is purposely made large to minimize the importance of the hold-up volume.

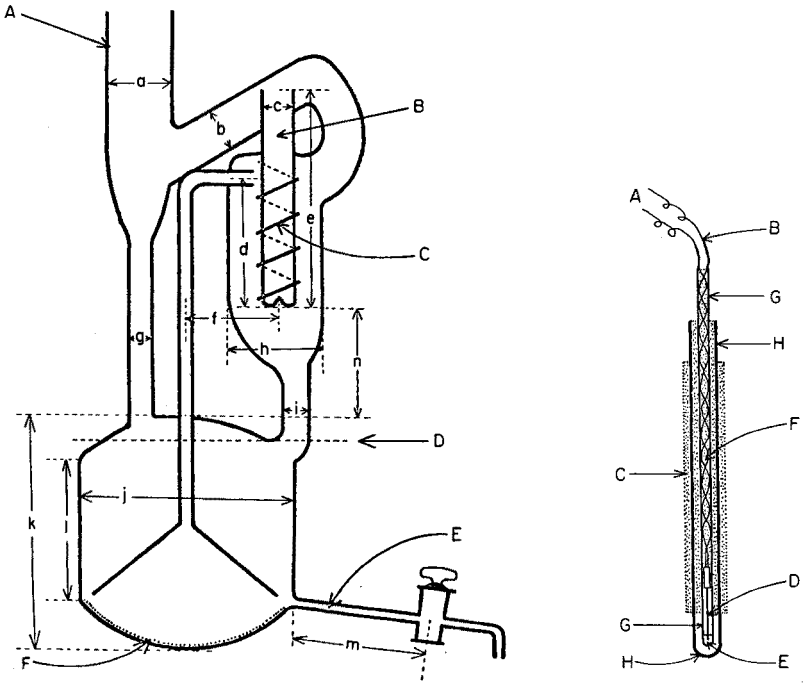

Fig. 1. The ebulliometer. Dimensions (in mm) are a = 22, b = 10, c = i = 11, d = 63, e = 98, f = h = 38, j = 80, k = 95, l = 60, m = 55, and n = 45.

Fig. 2. The thermistor assembly. A, leads to the Wheatstone bridge; B, electrical shielding; C, glass wool tightly wrapped around the inner tube G (i.d. = 3 mm, o.d. = 5 mm); D, thermistor; E, mercury; F, glass wool tightly wrapped around the thermistor leads; H, outer tube (i.d. = 7.8 mm, o.d. = 10 mm).

The boiling temperature was sensed with a Type T63A21 bead-in-glass thermistor (Victory Engineering Corp., Springfield, N.J.) having a nominal resistance of 2.5 MΩ at 25°C. At 100°C the resistance of such a thermistor is about 95 kΩ and its temperature coefficient of resistance is about −3.5% deg^{-1}. To damp momentary fluctuations arising from superheating, thermistor assemblies were prepared in the following way. About 1 g of mercury was placed in the bottom of a glass tube (12 cm long, i.d. 3 mm), a thermistor was inserted into the tube so that its bead was immersed in the mercury, and glass wool was packed as tightly as possible round the thermistor and its leads while the thermistor was kept accurately aligned along the axis of the tube. This inner tube was then similarly placed inside a larger tube (10 cm long, i.d. 8 mm) which was tightly packed with glass wool, and a final layer of glass wool was wrapped around the outer tube so that the entire assembly (Fig. 2) would fit snugly into the thermistor well of the ebulliometer. The mercury in the inner tube served to minimize fluctuations of temperature caused by convection around the thermistor bead [27, 28]. Other materials, such as powdered chalk and tightly packed glass wool, also

served to damp out momentary fluctuations of temperature, but gave much slower overall response because of their lower thermal conductivities.

Two identical ebulliometers were constructed and heavily lagged with polyurethane foam to insulate them from drafts. Each ebulliometer was provided with an electric heating mantle powered by its own autotransformer. The mantles were covered with a heavy layer of glass wool, to avoid overheating the polyurethane foam, before the latter was applied; in addition aluminum foil was wrapped around the upper portion of the ebulliometer to provide an additional barrier against convection and radiation.

Each of a number of new thermistors was mounted in a glass tube like G in Fig. 2, and the resulting partial assemblies were allowed to stand in boiling water with a current of approximately 15 μA flowing through the thermistors in series. The resistances of the individual thermistors were measured occasionally with a Hewlett-Packard Model 3450A digital multimeter. When no further variations of the ratios of resistances could be detected, the partial assemblies were transferred to an oil thermostat, and the individual resistances were measured at a number of different temperatures between 25°C and 99.5°C. Calibrated thermometers were used in measuring these temperatures, and great care was taken to ensure that equilibrium was attained at each temperature. The resistance—temperature data were fitted [29] to the familiar equation

$$R = R_0 \exp\left[B\left(\frac{1}{T} - \frac{1}{T_0}\right)\right] \tag{1}$$

to evaluate R_0, the resistance at 373.15°C (= T_0), and the temperature coefficient of resistance α (= $-B/T_0^2$) at that temperature. Robertson et al. [30] reported that other equations gave better fits to such data, but this was not confirmed in our work. The resulting values made it possible to select a pair of thermistors whose resistances at 100°C differed by only a few tenths of a per cent and whose temperature coefficients of resistance were virtually identical. Complete thermistor assemblies, as shown in Fig. 2, were made for these two thermistors and used throughout the remainder of the work. Whenever they were not in use, they were stored in boiling water, and the current flowing through the thermistors was never interrupted for more than a few seconds.

The two thermistors, one in each ebulliometer, were connected as two of the four arms of a d.c. Wheatstone bridge. Each of the other two arms consisted of three Type 216-RBPJ wire-wound precision resistors (Consolidated Resistance Co. of America, Inc., Yonkers, N.Y.) so chosen as to balance the bridge as closely as possible when the thermistors were at the same temperature. The bridge was powered by a Model DAS-46A "Dial-a-Source" (General Resistance Co., Mount Vernon, N.Y.) which provided a stable and accurate d.c. voltage having any desired value up to 10 V. The imbalance e.m.f. of the bridge was usually presented directly to the input terminals of a Model SRLG Y-T strip-chart recorder (E. H. Sargent and Co.,

Inc., Chicago, Ill.) operated at its maximum sensitivity (0.37 mV full-scale, or 14.6 μV cm^{-1}).

Experimental variables and performance characteristics

The sensitivity of the apparatus is described by the Wheatstone bridge equation [28]

$$\frac{de}{dT_A} = \frac{R_A R_B}{(R_A + R_B)^2} \alpha_A E \qquad (2)$$

where de is the change of imbalance e.m.f. resulting from a small change dT_A in the temperature of the thermistor (denoted by the subscript A) in the sample ebulliometer; R_A and R_B are the resistances of the thermistors in the sample and reference ebulliometers; α_A is the temperature coefficient of the thermistor in the sample ebulliometers; and E is the e.m.f. applied to the bridge. If the temperature in the reference ebulliometer is constant, and if dT_A is so small that the variations of R_A and α_A can be neglected, this indicates that de should be proportional to dT_A.

Increasing the power that is dissipated in a thermistor increases the noise level by increasing the extent of thermal convection in the liquid surrounding the thermistor [27, 28]. The effect of power dissipation on the noise level was investigated by using a Hewlett-Packard Model 3480A digital voltmeter to measure the imbalance e.m.f. at 30-s intervals during 15-min periods in which distilled water was boiling in each of the ebulliometers, with the results shown in Fig. 3. The minimum value of s/E ($9 \cdot 10^{-8}$), where s is the standard deviation of the mean of the 30 individual values of e, is attained with E = 4 V. If E is increased above this value, s/E increases because of the increase of thermal convection; decreasing E below this value also increases s/E because other sources of noise and the finite resolution of the meter combine to keep s nearly constant. The standard deviation of a difference of temperature measured in this fashion is proportional to s/E, and may be estimated from eqn. (2) to be approximately 10^{-5} degree. The value of E at the minimum corresponds to a power dissipation of 40 μW, which is appreciably higher than the optimum value for thermistors immersed in water [27] because the thermal conductivity, viscosity, and coefficient of thermal expansion are all more favorable for mercury than for water.

The efficiency of a Cottrell pump depends on the geometry of the system, and Fig. 4 shows how the measured difference of boiling temperatures changes when the volume of liquid in one ebulliometer is varied while the volume in the other is kept constant. The measured difference is constant over the range of volumes from about 290 to 310 cm^3, which corresponds to the level of "D" in Fig. 1. If the volume of liquid exceeds 310 cm^3, superheating is not entirely relieved in the pump; if it is below 290 cm^3, the action of the pump does not suffice to bring the thermistor assembly to equilibrium with the boiling liquid; if it is below about 230 cm^3, the pump does not operate at all and the thermistor senses the condensation

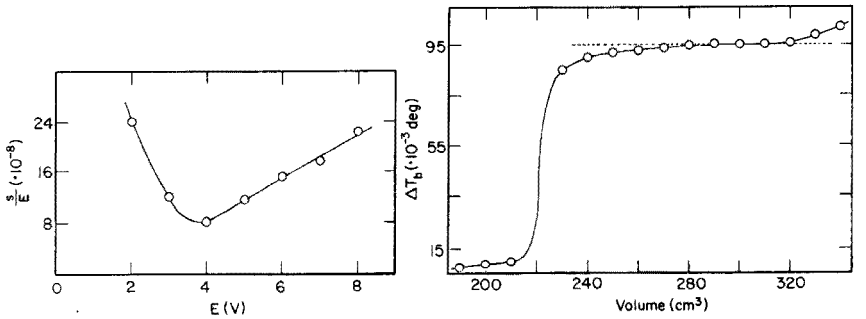

Fig. 3. Effect of the e.m.f., E, applied to the Wheatstone bridge on the standard deviation of the mean of 30 measured values of the imbalance e.m.f., e.

Fig. 4. Effect of the volume of an approximately 0.1 m solution of sodium chloride on the measured difference ΔT_b between the boiling temperature of this solution in one ebulliometer and that of distilled water in another. The horizontal dashed line is drawn to emphasize the variation of ΔT_b outside the range $290 \leqslant V \leqslant 310$ cm³.

temperature rather than the boiling temperature. In addition, the precision of measurement reaches a maximum when the volume is between 305 and 310 cm³ (with 0.5 F sodium chloride): this optimum volume increases very slightly as the density of the solution increases, reaching 315 cm³ with 1 F sodium or lithium chloride. Volumes within 1% of the optimum were used in making all the measurements reported here.

Varying the power supplied to either heating mantle has a generally similar effect, which is shown in Fig. 5 for a typical set of conditions. There is an optimum range over which the measured difference of boiling temperatures is constant. Above this range, boiling becomes so rapid that some superheating is transmitted to the thermistor assembly; below it, the rate of boiling becomes too low to maintain the thermistor assembly at the boiling temperature. No variation of the precision of measurement could be detected on varying the e.m.f. applied to the heater as long as this remained within the optimum range.

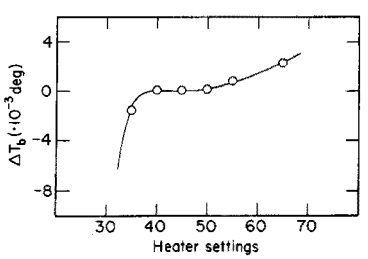

Fig. 5. Effect of the "heater setting" (the fraction of the line voltage applied to one heating mantle) on the measured value of ΔT_b. The measurements were made with an approximately 0.1 m solution of sodium chloride in each ebulliometer and with a constant voltage applied to the heating mantle of the reference ebulliometer.

As equilibrium is approached, the concentration of solute in the boiling liquid increases because of solvent hold-up. A known volume of an approximately 0.1 *F* solution of sodium chloride was brought to equilibrium and a sample of the boiling liquid was removed through the stopcock. This sample and the original solution were analyzed by potentiometric titration with standard silver nitrate. For a typical ebulliometer the data showed that the hold-up volume was 3.6 cm^3; most of this corresponds to condensate on the walls of the reflux condenser. There was no detectable loss of water by evaporation through the condenser even when boiling was prolonged for as much as 90 h, and varying the rate of flow or the temperature of the water in the jacket of the condenser within the limits 3—6 $dm^3\ min^{-1}$ or 4—17°C had no effect.

The optimum values of these experimental variables will depend on the geometry of the ebulliometers and such properties as the densities, viscosities, and thermal conductivities of the boiling solutions, and should be evaluated for each individual ebulliometer with a solution whose composition is representative of the solutions to be investigated. The optimum ranges are wide enough to accommodate moderate variations of composition, but the conditions that are best suited to work with dilute aqueous solutions may have to be modified in work with concentrated ones or with solutions in another solvent.

The rate of response to changes of boiling temperature was evaluated by bringing the apparatus to equilibrium with distilled water in each ebulliometer, and then adding approximately 0.25 g of solid sodium chloride to one ebulliometer by means of a long-stem funnel inserted through the reflux condenser. The difference of temperature was recorded against time until a new equilibrium had been attained, and the half-time was found to be 95 s. This is an overall figure that reflects the rates of several processes (recovery from the addition of material that was probably at a temperature somewhat below 100°C, dissolution of the salt, and the attainment of uniform composition) but is probably chiefly dependent on the time constant of the thermistor assembly. Although the overall response is amply fast for equilibrium measurements, a faster one would of course be desirable in rate studies.

Procedure

The upper portions of the ebulliometers were cleaned with an alkaline solution of permanganate before beginning each experiment. Care was taken to ensure that their activated portions did not come into contact with this solution. The ebulliometers were rinsed with water, then with 0.1 F solution of hydroxylammonium chloride to destroy permanganate ion and oxides of manganese, and finally again with water, and were then thoroughly dried by aspiration of clean air. They were then mounted in position, charged with the appropriate volumes of the desired solutions, and attached to the reflux condensers. The heaters were then actuated and the thermal insulation was assembled.

When boiling had begun in each ebulliometer, the thermistor assemblies were removed from the flask of boiling water in which they were stored between experiments, and inserted into the thermistor wells. The thermistors were then connected to the Wheatstone bridge, the output of which was recorded until it had become constant, thus establishing the value of e that corresponded to equality of the two boiling temperatures T_b (or boiling-point elevations θ). A weighed amount of solid was then added to one ebulliometer through the condenser, and the resulting change of boiling temperature was calculated, by means of eqn. (2), from the change of e that occurred while the new equilibrium was being reached.

Distilled water, reagent-grade salts, and calibrated volumetric glassware were used throughout. Sodium chloride and lithium chloride were oven-dried to constant weight and stored in vacuum desiccators.

RESULTS AND DISCUSSION

The first desideratum was the establishment of an ebulliometric standard, for which the boiling-point elevation of an aqueous solution could be accurately calculated at any desired concentration. Most of the compounds used for ebulliometric determinations of molecular weights [7, 8] are insoluble in water, or nearly so; one with a solubility suitable for our purposes was therefore sought. Succinonitrile and glycerol were investigated briefly, but both departed so widely from ideal behavior that sodium chloride was finally selected.

Average values of $\Delta\theta/\Delta m$ (θ = boiling-point elevation, m = molality) were obtained for solutions containing sixteen different concentrations of sodium chloride ranging from 0 to 1.0 m. After the ebulliometers had been charged with a solution of approximately the desired concentration and boiling equilibrium had been established, a small amount (typically 0.3 g) of sodium chloride was added to one, and the resulting value of $\Delta\theta$ was calculated as described above. The corresponding value of Δm was easily obtained from the known volume and composition of the initial solution, the weight of sodium chloride added to it, and the hold-up volume for the ebulliometer, and thus one value of $\Delta\theta/\Delta m$ was secured. An approximately equal weight of sodium chloride was then added to the other ebulliometer, and another value of $\Delta\theta/\Delta m$ was obtained in the same way. One or two repetitions of this procedure yielded a total of four to six individual values of $\Delta\theta/\Delta m$. The additions of sodium chloride were so small that the average value of m did not change substantially, and as a result the individual values of $\Delta\theta/\Delta m$ always agreed within the estimated uncertainty of measurement. The average of the individual values of $\Delta\theta/\Delta m$ was assigned to the average value of m for the solutions employed in obtaining them. The ebulliometers were emptied, cleaned thoroughly, and charged with a new solution containing a different concentration of sodium chloride to obtain the next average value in the same fashion.

By assuming the difference between the molal heat capacities of a vapor and the boiling liquid to be independent of temperature over the range of interest, it is easily shown [6, 10] that

$$\ln a_1 = -\frac{\Delta H_0 \theta}{R\,T_0^2}\left(1 - \frac{b}{\Delta H_0}\theta + \frac{c}{\Delta H_0}\theta^2 - \ldots\right) \tag{3}$$

where a_1 is the activity of the solvent, ΔH_0 is the molal enthalpy of vaporization of the pure solvent at its normal boiling temperature T_0, and b and c are constants. Differentiating eqn. (3) with respect to θ, combining the result with the Gibbs—Duhem equation, rearranging, and introducing the ebulliometric constant K_b ($= M_1 R T_0^2/1000\,\Delta H_0$), gives

$$\mathrm{d}\ln a_2\ (= \mathrm{d}\ln a_\pm^2) = \frac{\mathrm{d}\theta}{K_b m}\left(1 - \frac{2b}{\Delta H_0}\theta + \frac{3c}{\Delta H_0}\theta^2 - \ldots\right) \tag{4}$$

where a_2 is the activity of the solute and $a_\pm$ is its mean ionic activity. Replacing $a_\pm$ by $\gamma_\pm m$ and dividing by $\mathrm{d}m$ yields

$$\frac{\mathrm{d}\ln\gamma_\pm}{\mathrm{d}m} + \frac{1}{m} = \frac{1}{2K_b m}\frac{\mathrm{d}\theta}{\mathrm{d}m}\left(1 - \frac{2b}{\Delta H_0}\theta + \frac{3c}{\Delta H_0}\theta^2 - \ldots\right) \tag{5}$$

Following Lewis and Randall [31] the Hückel equation [32, 33] for $\gamma_\pm$ may be written in the form

$$\ln\gamma_\pm = -\frac{2.3026\,A\,m^{\frac{1}{2}}}{1 + V_1 m^{\frac{1}{2}}} + V_2 m \tag{6}$$

where V_1 and V_2 are adjustable parameters whose significance will be discussed below. Differentiating this with respect to m, combining the result with eqn. (5), and introducing the appropriate numerical values of the quantities A, b, c, ΔH_0, and K_b yields

$$1.026 - \frac{0.70743\,m^{\frac{1}{2}}}{(1 + V_1 m^{\frac{1}{2}})^2} + V_2' m = (1 - 6.320\cdot10^{-3}\theta + 2.35\cdot10^{-5}\theta^2)\frac{\mathrm{d}\theta}{\mathrm{d}m} \tag{7}$$

where the substitution $V_2' = 2K_b V_2$ has been made for convenience. Because θ never exceeded about 1 degree in this work, the last term within the parentheses on the right-hand side of eqn. (7) was negligible, and even the second term is so small that the empirical approximation $\theta = 0.95\,m$ provides a sufficiently accurate description of it. Equation (7) was consequently rewritten in the form

$$\frac{\mathrm{d}\theta}{\mathrm{d}m} = \left[1.026 - \frac{0.70743\,m^{\frac{1}{2}}}{(1 + V_1 m^{\frac{1}{2}})^2} + V_2' m\right] \Big/ (1 - 6.00\cdot10^{-3}m) \tag{8}$$

A general multiparametric curve-fitting program [29] was employed to find the best values $V_1 = 1.45248$ and $V_2' = 0.096541$, which yielded a fit for which the standard deviation was $2.0\cdot10^{-3}$ deg mol^{-1} kg. Since the average value of $\mathrm{d}\theta/\mathrm{d}m$ over the range investigated was 0.95 deg mol^{-1} kg, this absolute standard deviation corresponds to a relative standard deviation of

0.21%; since the average measured value of $\Delta\theta$ was approximately $21 \cdot 10^{-3}$ deg, this relative standard deviation corresponds in turn to a standard error of $45 \cdot 10^{-6}$ deg in the individual measurements. It was estimated above that the noise level led to a standard error of about $10 \cdot 10^{-6}$ deg for measurements made in a single experiment. The figure of $45 \cdot 10^{-6}$ deg exceeds this because it includes the effects of uncertainties in Δm, the total and hold-up volumes, the heater outputs, and any day-to-day fluctuations in the temperature coefficients of resistance of the thermistors. Several other experimenters have achieved "sensitivities" that lie between [34—37] or approach [38] these values, and Zichy [39] claims to have obtained one of $2.4 \cdot 10^{-6}$ deg with a differential ebulliometer much more complicated than the apparatus described here.

Integrating eqn. (7) and introducing the best values of V_1 and V_2' gives

$$\begin{aligned} f(\theta) &= \theta - 3.160 \cdot 10^{-3}\theta^2 + 7.83 \cdot 10^{-6}\theta^3 - \ldots \\ &= 1.026m - 0.46172 \left[1 + 1.45248m^{\frac{1}{2}} - 2\ln(1 + 1.45248m^{\frac{1}{2}}) \right. \\ &\quad \left. - \frac{1}{1 + 1.45248m^{\frac{1}{2}}}\right] + 0.04827m^2 \end{aligned} \tag{9}$$

while the osmotic coefficient ϕ is given by

$$\phi = \frac{0.9746}{m} f(\theta) \tag{10}$$

Values of θ, ϕ, and $-\ln \gamma_{\pm}$ calculated from these equations are given in Table 1 for various round values of m up to 1 m. The best previous values appear to be those of Smith [10], who also used an ebulliometric technique. Eleven of the twelve values of ϕ given by Smith differ from ours by amounts equal to or smaller than those corresponding to his claimed uncertainty of $\pm 0.2 \cdot 10^{-3}$ deg in θ, but the differences vary systematically with m as shown in Fig. 6.

These primary-standard data for sodium chloride form the basis of a very simple and convenient null method for evaluating the boiling-point elevations and osmotic and activity coefficients of other boiling aqueous solutions. To illustrate this method it was applied to solutions of lithium chloride over the 0—1 m range of concentrations.

Each experiment was begun by charging both ebulliometers with water, bringing them to boiling equilibrium, and measuring the imbalance e.m.f., e_0, of the bridge. Enough solid lithium chloride was then added to one ebulliometer to give a solution of approximately the desired concentration, and enough solid sodium chloride was added to the other to give a solution for which the boiling-point elevation was slightly smaller than that for the lithium chloride solution. The concentration (mol kg^{-1} of water) of sodium chloride in this solution was denoted as c_1 and the corresponding imbalance e.m.f. as e_1.

TABLE 1

Values of θ, ϕ, and ln $\gamma_{\pm}$ for boiling aqueous solutions of sodium chloride at round concentrations

Concentration of sodium chloride, mol kg^{-1} of water	θ (deg)	ϕ	$-\ln \gamma_{\pm}$
0.010	0.00988	0.9630	0.1195
0.020	0.01953	0.9520	0.1599
0.030	0.02908	0.9448	0.1880
0.040	0.03856	0.9395	0.2100
0.050	0.04799	0.9353	0.2281
0.060	0.05738	0.9320	0.2435
0.070	0.06675	0.9292	0.2570
0.080	0.07609	0.9269	0.2689
0.090	0.08542	0.9249	0.2797
0.100	0.09474	0.9231	0.2894
0.120	0.11335	0.9203	0.3065
0.140	0.13194	0.9181	0.3211
0.160	0.15052	0.9165	0.3338
0.180	0.16910	0.9152	0.3451
0.200	0.18770	0.9142	0.3550
0.250	0.23427	0.9127	0.3759
0.300	0.28100	0.9121	0.3924
0.350	0.32792	0.9122	0.4058
0.400	0.37507	0.9128	0.4169
0.450	0.42246	0.9138	0.4262
0.500	0.47010	0.9150	0.4340
0.550	0.51800	0.9165	0.4406
0.600	0.56617	0.9181	0.4462
0.650	0.61460	0.9198	0.4509
0.700	0.66332	0.9217	0.4550
0.750	0.71231	0.9236	0.4584
0.800	0.76159	0.9256	0.4612
0.850	0.81114	0.9277	0.4635
0.900	0.86098	0.9299	0.4655
0.950	0.91111	0.9321	0.4670
1.000	0.96152	0.9343	0.4682

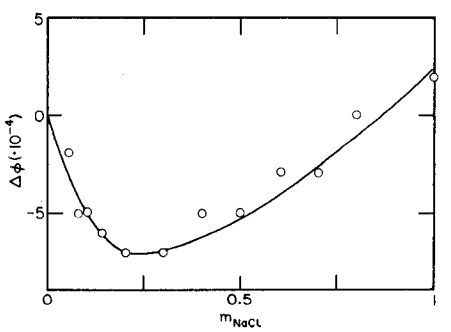

Fig. 6. The effect of the concentration of sodium chloride on the difference between the osmotic coefficient obtained by Smith [10] and the one obtained in this work.

In the present work the temperature coefficients of resistance of the thermistors were known, and it was therefore possible to estimate the concentration of sodium chloride to be added by measuring e with the lithium chloride solution in one ebulliometer and water in the other, computing the boiling-point elevation for the lithium chloride by means of eqn. (2), and interpolating in Table 1 to find a concentration of sodium chloride for which the boiling-point elevation would be a little smaller. With uncalibrated thermistors the same result could have been secured by observing the value of e with lithium chloride in the sample ebulliometer and water in the reference ebulliometer, adding a little sodium chloride to the latter and observing the new value of e, and using linear extrapolation to calculate how much more sodium chloride would be needed to bring e to nearly the same value, e_0, that it had had with water in each ebulliometer.

Next a small increment of sodium chloride was added to the sodium chloride solution, so that its boiling-point elevation was slightly larger than that for the lithium chloride solution. If the concentration of the sodium chloride is then c_2 (mol kg^{-1} of water) and the measured imbalance in e.m.f. is e_2, and if the difference $c_2 - c_1$ is small enough to justify the assumption that the osmotic coefficient for sodium chloride is constant over the range from c_1 to c_2, then the activity of water in the lithium chloride is equal to that in a c m solution of sodium chloride, where

$$c = \frac{(e_1 - e_0)c_2 + (e_0 - e_2)c_1}{2e_0 + e_1 - e_2} \tag{11}$$

The values in Table 1 show how small $c_2 - c_1$ must be to justify the stated assumption in any particular range of concentrations: in general, the error entailed by this assumption will be consistent with the standard deviation of $45 \cdot 10^{-6}$ deg in the measurement of a difference of boiling temperatures, which was attained in this work, if $c_2 - c_1$ is of the order of $0.02m$. If substantially more precise measurements could be made, a more exact interpolation could be effected with the aid of eqns. (9) and (10). The measurements can be completed within a few minutes after the initial boiling equilibrium has been attained.

The values of c thus obtained for solutions containing different concentrations of lithium chloride were used to compute the osmotic coefficients from the relation

$$\phi_{LiCl} = \frac{c}{m_{LiCl}} \phi_{NaCl} \tag{12}$$

and these were fitted to the equation

$$\phi = 1 - \frac{1.3790}{V_1^3 m}\left[1 + V_1 m^{\frac{1}{2}} - 2\ln(1 + V_1 m^{\frac{1}{2}}) - \frac{1}{1 + V_1 m^{\frac{1}{2}}}\right] + \frac{V_2 m}{2} \tag{13}$$

which has the same form as a combination of eqns. (9) and (10). The best fit was obtained with $V_1 = 1.42929$ and $V_2 = 0.18775$. It corresponded to

a relative standard deviation of 0.25% in the measurements, which was nearly the same as that for the data on sodium chloride. These values yield

$$\ln \gamma_{\pm} = -\frac{1.3790 m^{\frac{1}{2}}}{1 + 1.42929 m^{\frac{1}{2}}} + 0.18775 m \qquad (14)$$

for the mean ionic molality activity coefficients of lithium chloride in boiling aqueous solutions. Graphical integration [40] based on the equation

$$\ln \gamma_{\pm} = (\phi - 1) - 2 \int_0^m \frac{1 - \phi}{m^{\frac{1}{2}}} \, dm^{\frac{1}{2}} \qquad (15)$$

gave values of $\gamma_{\pm}$ indistinguishable from, but somewhat less regular than, those computed from eqn. (14).

As the literature appears to contain no prior data on the osmotic or activity coefficients for aqueous solutions of lithium chloride at 100°C, values of $\gamma_{\pm}$ were calculated from the equation

$$\log \gamma_{\pm}\,(100°C) = \log \gamma_{\pm}\,(25°C) - 7.366 \cdot 10^{-5} \bar{L}_2\,(25°C) - 2.555 \cdot 10^{-3} \bar{J}_2\,(25°C) \qquad (16)$$

which was derived by Harned and Owen [33], together with their values for $\bar{L}_2$, the relative partial molal heat content of lithium chloride, and those of Gucker and Schminke [41] for $\bar{J}_2$, the relative partial molal heat capacity of lithium chloride. With Robinson's values [42, 43] for $\gamma_{\pm}$ at 25°C, the agreement with our experimental results at 100°C was within 0.001 unit in $\gamma_{\pm}$ up to 0.4 *m* lithium chloride, but deteriorated at higher concentrations. Oddly enough, the older values obtained by Robinson and Sinclair [44] gave nearly perfect agreement over the entire range of concentrations. Equation (14) is therefore as reliable at 100°C as the data available for lithium chloride at 25°C.

Converting the values of V_1 and V_2 for sodium chloride and lithium chloride to the molarity scale and combining the results with the value of the numerical coefficient B in the familiar form of the Hückel equation

$$\log \gamma_{\pm} = -\frac{A \mu^{\frac{1}{2}}}{1 + B \mathring{a} \mu^{\frac{1}{2}}} + B' \mu \qquad (17)$$

gave the following values (accompanied by their standard deviations) for the distances of closest approach $\mathring{a}$ and the salting coefficient B′:

	NaCl	LiCl
$\mathring{a}$, Å	4.28 (±0.05)	4.21 (±0.06)
B′, dm³ mol⁻¹	0.0428 (±0.0011)	0.084 (±0.002)

Harned and Owen [33] gave 4.0 and 4.25 Å for the distances of closest approach at 25°C. There is little prior information on the variation of $\mathring{a}$ with temperature: Harned and Cook [45] found $\mathring{a}$ for sodium chloride to be independent of temperature from 0 to 40°C, and Robinson and Harned [46]

กรมวิทยาศาสตร์

reported that $\mathring{a}$ for lithium chloride appeared to be independent of temperature over a similar range. It is consistent with these observations that the present values of $\mathring{a}$ at 100°C are nearly the same as the corresponding ones at 25°C. For each of these electrolytes, the salting coefficient is smaller at 100°C than at 25°C (where they are 0.0521 for sodium chloride and 0.121 for lithium chloride [33]); these changes of B′ unaccompanied by significant changes of $\mathring{a}$ are difficult to reconcile with the generally accepted idea that B′ is a measure of the partial molal volume of the solute.

Rossotti and Rossotti [47] stigmatized the use of ebulliometry in fundamental physicochemical investigations in the following words: "the technique has been little used for quantitative work, since elevations of boiling point can be measured less precisely than depressions of freezing point. Moreover, a bulk electrolyte cannot be used to control the osmotic coefficients". In view of the simplicity of the apparatus used here and the precision and reliability of the results obtained, and also of the difficulties caused by supercooling in cryoscopic work, the first of these objections seems to have been largely overcome, whereas the second is untrue of twin ebulliometry. A major advantage of twin ebulliometry is that measurements can be made over a wide range of temperatures by adjusting the ambient pressure to which the ebulliometers are exposed [48], whereas this is scarcely possible in cryoscopy.

It is of interest to compare the potentialities of twin ebulliometry with those of thermoelectric vapor-pressure osmometry, which is widely used for similar purposes. Adicoff and Murbach [49] found, for example, that the change of resistance ΔR of a thermistor covered with a film of a c M solution of any of a number of solutes in toluene was given by $\Delta R = 301c$ when the solution was in equilibrium with toluene vapor at 25°C, and also found the standard error of a single measurement of ΔR to be 0.025 Ω. The limit of detection, defined as the concentration at which the measured response is twice the standard error of a single measurement, was accordingly $2 \cdot 0.025/301 = 1.6 \cdot 10^{-4}$ M. If the standard error, $45 \cdot 10^{-6}$ deg, achieved in this work could be duplicated in boiling toluene, for which the ebullioscopic constant is equal to 3.55 deg mol^{-1} kg, the comparable limit of detection for twin ebulliometry would be $2 \cdot 45 \cdot 10^{-6}/3.55 = 2.5 \cdot 10^{-5}$ M, nearly an order of magnitude better. Adicoff and Murbach judged thermoelectric vapor-pressure osmometry to be the superior technique, but did so on the basis of a substantial underestimate of the precision that could be attained ebulliometrically. Even the simple and inexpensive ebulliometric apparatus described here yields a precision comparable with that of the extremely sophisticated thermoelectric vapor-pressure osmometer built by Wachter, Simon and co-workers [50, 51].

This work was supported by grant number GP-10325 and grant number MPS 74-17519 from the National Science Foundation, and by a fellowship awarded to W. A. de O. by CAPES — Brazil.

REFERENCES

1 E. Beckmann, Z. Phys. Chem. (Frankfurt am Main), 4 (1889) 532.
2 W. Swietoslawski and J. R. Anderson, Ebulliometry, in A. Weissberger (Ed.), Techniques of Organic Chemistry, Vol. 1, Part 1, Interscience, New York, 1959.
3 W. Swietoslawski, Ebulliometric Measurements, Reinhold, New York, 1945.
4 A. W. C. Menzies and S. L. Wright, Jr., J. Am. Chem. Soc., 43 (1921) 2314.
5 F. H. Stross, Molecular Weight Determination of Oils, in Symposium on Composition of Petroleum Oils, New Orleans, 1957; A.S.T.M. Spec. Tech. Pub., No. 224, (1958) 265.
6 R. S. Lehrle, Ebulliometry Applied to Polymer Solutions, in J. C. Roble and F. W. Peaker (Eds.), Progress in High Polymers, Vol. 1, Academic Press, New York, 1961.
7 C. A. Glover, Determination of Molecular Weights by Ebulliometry, in C. N. Reilley and F. W. McLafferty (Eds.), Advances in Analytical Chemistry and Instrumentation, Vol. 5, Interscience, New York, 1966; Determination of Number-Average Molecular Weights by Ebulliometry, in M. Ezrin (Ed.), Polymer Molecular Weight Methods, Am. Chem. Soc., Washington, D.C., (1973).
8 R. V. Bonnar, M. Dimbat and F. H. Stross, Number-Average Molecular Weights, Interscience, New York, 1958, p. 77.
9 B. Saxton and R. P. Smith, J. Am. Chem. Soc., 54 (1932) 2626.
10 R. P. Smith, J. Am. Chem. Soc., 61 (1939) 497, 500.
11 R. P. Smith and D. S. Hirtle, J. Am. Chem. Soc., 61 (1939) 1123.
12 G. C. Johnson and R. P. Smith, J. Am. Chem. Soc., 63 (1941) 1352.
13 G. Cocco, C. Dejok, and O. Devoto, Chem. Phys. Lett., 11 (1971) 198.
14 W. Swietoslawski, Ebulliometric Measurements, Chapter 17, Reinhold, New York, 1945.
15 G. Allen and E. F. Caldin, Trans. Faraday Soc., 49 (1953) 895.
16 R. S. Rodgers and L. M. Mukherjee, J. Chem. Phys., 52 (1970) 4550.
17 A. D. Adler, J. A. O'Malley, and A. J. Herr, Jr., J. Phys. Chem., 71 (1967) 2896.
18 C. Heitler, Chem. Ind. (London), (1952) 875.
19 C. Heitler, J. Chem. Soc., (1963) 4885.
20 S. Garbutt and D. L. Gerrard, J. Chem. Soc. Perkin Trans., 2, 6 (1972) 782.
21 E. W. Washburn and J. W. Read, J. Am. Chem. Soc., 41 (1919) 729.
22 B. J. Mair, J. Res. Natl. Bur. Standards, 14 (1935) 345.
23 A. J. Davies, A. E. Phillpotts, and B. W. Swanson, Proc. 4th World Petrol. Congr., Section V/C, Colombo, Rome, 1955, p. 351.
24 M. Dimbat and F. H. Stross, Anal. Chem., 29 (1957) 1517.
25 M. Ezrin and G. C. Claver, Am. Chem. Soc., Div. Polymer Chem., Prepr., 3(1) (1962) 308.
26 L. Lampugnani and L. Meites, Thermochim. Acta, 5 (1973) 351.
27 T. Meites, L. Meites, and J. N. Jaitly, J. Phys. Chem., 73 (1969) 3801.
28 P. W. Carr, Crit. Rev. Anal. Chem., 2 (1972) 505.
29 L. Meites, The General Multiparametric Curve-Fitting Program CFT3, Computing Laboratory, Department of Chemistry, Clarkson College of Technology, Potsdam, New York, 1974.
30 E. C. Robertson, R. Raspet, J. H. Swartz, and M. E. Lillard, Geol. Surv. Bull. 1203-B, U.S. Government Printing Office, Washington, D.C., 1966.
31 G. N. Lewis and M. Randall, Thermodynamics, McGraw-Hill, New York, 2nd edn., 1961, p. 344.
32 R. A. Robinson and R. H. Stokes, Electrolyte Solutions, Butterworths, London, 1955, pp. 222—60.
33 H. S. Harned and B. B. Owen, The Physical Chemistry of Electrolyte Solutions, 3rd edn., Reinhold, New York, 1958, pp. 504—12.
34 R. S. Lehrle and T. G. Majury, J. Polymer Sci., 29 (1958) 219.

35 C. A. Glover and R. R. Stanley, Anal. Chem., 33 (1961) 447.
36 J. E. Barney and W. A. Pavelich, Anal. Chem., 34 (1962) 1625.
37 T. Daniels and R. S. Lehrle, J. Polymer. Sci., C16 (1969) 4533.
38 P. Parrini and M. S. Vacanti, Makromol. Chem., 175 (1974) 935.
39 E. L. Zichy, Soc. Chem. Ind. (London), Monograph no. 17 (1963) 122.
40 M. Randall, J. Am. Chem. Soc., 48 (1926) 2512.
41 F. T. Gucker, Jr. and K. H. Schminke, J. Am. Chem. Soc., 54 (1932) 1358.
42 R. A. Robinson, Trans. Faraday Soc., 41 (1945) 756.
43 R. A. Robinson and R. H. Stokes, Trans. Faraday Soc., 45 (1949) 612.
44 R. A. Robinson and D. A. Sinclair, J. Am. Chem. Soc., 56 (1934) 1830.
45 H. S. Harned and M. A. Cook, J. Am. Chem. Soc., 61 (1939) 495.
46 R. A. Robinson and H. S. Harned, Chem. Rev., 28 (1941) 419.
47 F. J. C. Rossotti and H. Rossotti, The Determination of Stability Constants, McGraw-Hill, New York, 1961, p. 264.
48 G. Allen and E. F. Caldin, Trans. Faraday Soc., 49 (1953) 895.
49 A. Adicoff and W. J. Murbach, Anal. Chem., 39 (1967) 302.
50 R. E. Dohner, A. H. Wachter, and W. Simon, Helv. Chim. Acta, 50 (1967) 2193.
51 A. H. Wachter and W. Simon, Anal. Chem., 41 (1969) 90.

Analytica Chimica Acta, 93 (1977) 19—31
©Elsevier Scientific Publishing Company, Amsterdam — Printed in The Netherlands

HIGH-RESOLUTION FIELD DESORPTION MASS SPECTROMETRY
Part VII. Explosives and Explosive Mixtures§

H.-R. SCHULTEN* and W. D. LEHMANN

Institute of Physical Chemistry, University of Bonn, Wegelerstr, 12, 5300 Bonn (W. Germany)

(Received 26th April 1977)

SUMMARY

Standard explosives and technical mixtures of explosives have been investigated by field desorption mass spectrometry. The compounds investigated gave intense molecular ions or protonated molecules and structurally significant fragmentation. For comparison, the corresponding electron impact and chemical ionization mass spectrometry data are reported. Emission-controlled field desorption, photographic detection, and accurate mass measurements enabled the components of the technical mixtures to be identified. An example of the determination of an additive in a technical product by field desorption mass spectrometry and stable isotope dilution is given. The use of these techniques for quality control of explosives and for forensic investigations appears to be promising.

Electron-impact mass spectrometry (e.i.m.s.) is an established tool for the analysis of explosives [1—7]. However, identification of these compounds is frequently difficult because the e.i. spectra are characterized by a large number of fragment ions. Often the molecular ions are of very low intensity or are not observed. Therefore chemical ionization (c.i.) m.s. has been introduced for the identification of explosives [8, 9]. The results obtained with methane, isobutane, and water [10] as reagent gases show the advantages of this ionization method because of its enhanced molecular or quasi-molecular ion intensities.

Field desorption (f.d.) m.s. is the method of choice for molecular weight determination of highly polar and thermally labile compounds [11, 12]. Further the high molecular ion intensities and low fragmentation make f.d.m.s. particularly well suited for the analysis of mixtures. The method has provided a good indication of the composition of complexes of antibiotics [13] and steroid conjugates [14]. Mixtures of dyestuffs [15], pesticides [11, 16], drugs [17], parent pesticides [16] or drugs [18] together with some of their metabolites, and of mycotoxins in extracts of foodstuffs [19] have been investigated successfully. The usefulness of f.d.m.s. for the examination of mixtures of PTH-amino acids [20] and small oligopeptides

§ Part VI: H.-R. Schulten and W. D. Lehmann, Anal. Chim. Acta, 87 (1976) 103.

[12, 21] has been demonstrated; the f.d. spectra consisted almost exclusively of molecular ions.

In an effort to explore the behaviour of thermally labile substances under the conditions of field desorption, and to elucidate the analytical potential of the f.d. technique, a number of standard explosives and technical explosive mixtures have been studied with the objective of establishing the optimal experimental conditions for obtaining informative f.d. spectra with respect to molecular weight determination and structurally significant fragmentation, the characteristic features of these classes of compound in f.d.m.s., and the potential of the f.d. technique for the qualitative and quantitative determination of the components of technical explosive mixtures.

EXPERIMENTAL

The f.d. spectra were obtained with a modified CEC 21-110B instrument [22] by the photographic detection system with vacuum evaporated AgBr plates (Ionomet, Waban, Mass.). The resolution obtained was better than 15 000 (at half peak width), and the average accuracy in the mass determination was ±2 millimass units. For accurate mass measurements (the text and the figures give the theoretical masses) reference masses were taken from the field ionization mass spectrum of perfluorotributylamine. Field desorption emitters, used in all experiments, were prepared by high-temperature activation of 10-μm diameter tungsten wires [23]. The distribution and morphology of the microneedles produced were as shown previously [24]. F.d. emitters with an average length of 30 μm for the carbon microneedles were used as standards. The ionization efficiency and the adjustment of the f.d. emitter were determined by means of *m/e* 58 of acetone in the field ionization mode. In general, 1×10^{-6} g was applied as sample to the standard emitter via the syringe technique [25]. The solvent for all compounds was acetone. All f.d. spectra (with the exceptions of (I), (II), and (III)) were produced by emission-controlled f.d. at a threshold of 2×10^{-8} A measured between the field anode and the slotted cathode plate at 2-mm distance and at +10 to −2 kV accelerating voltage.

The recorded mass range on the photoplate extended from *m/e* 17 to *m/e* 560. Because of the small dynamic range of the photographic detection system, the observed ion intensities cannot be correlated directly with the true isotopic pattern of the recorded ions. To illustrate that this effect results from the ion response of the photographic emulsion, the molecular ion group of pentaerythritol tetranitrate (IV) was recorded electrically on a Varian MAT 731 mass spectrometer (Fig. 1).

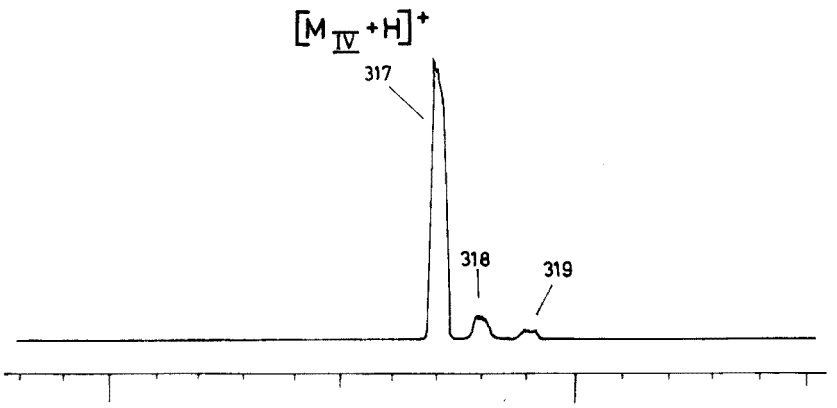

Fig. 1. F.d. mass spectrum of pentaerythritol tetranitrate (IV) obtained with electric detection, resolution 2000 (10% valley), scan speed 2.6 mm s^{-1}, emitter heating current 11 mA. The $[M + H]^+$ ion at *m/e* 317 and two isotopic satellite peaks at *m/e* 318 and *m/e* 319 are found. The experimental values for the isotopic distribution are (M + 1):(M + 2):(M + 3) = 100:7.98:2.66. The theoretical values according to the elemental composition $C_5H_9N_4O_{12}$ are 100:7.66:2.45.

RESULTS AND DISCUSSION

Aromatic nitro compounds

Apart from the absolute temperature of the sample and the amount adsorbed on the f.d. emitter, the rate of desorption from the emitter surface has a strong influence on the appearance of the f.d. spectra. For direct heating of the emitter, the temperature is controlled by the emitter heating current (e.h.c.). To obtain minimal fragmentation, the emitter heating current is set at the lowest level which produces a detectable ion current. The term 'best anode temperature' (b.a.t.) is used to characterize these experimental conditions [26].

The f.d. spectrum of 2,4,6-trinitrotoluene (TNT, I) in Fig. 2 was recorded at the b.a.t. (7 mA e.h.c.) and clearly demonstrated the characteristic feature of f.d. to produce mass spectra of a wide variety of compounds that contain only the molecular ion group.

For comparison with conventional mass spectrometric techniques such as electron impact and chemical ionization, the data for the relative intensities (rel. int.) of the molecular ions and the *m/e* values of the base peaks of the standard explosives are given. The base peak of compound (I) in e.i.m.s. is generated by the $[M—OH]^+$ ion at *m/e* 210 and the molecular ion is observed with 2.5% relative intensity [1]. With c.i.m.s., however, methane as well as isobutane as reagent gas form the $[M + 1]^+$ ion with 100% relative intensity [8].

The f.d. spectrum of 1,3,5-trinitrobenzene (TNB, II) was recorded at 9 mA e.h.c., corresponding to an emitter temperature slightly above the b.a.t. in order to produce structurally significant fragment ions. As shown in Fig. 3 the $[M]^+$ ion is the base peak in the f.d. spectrum and fragment ions, resulting

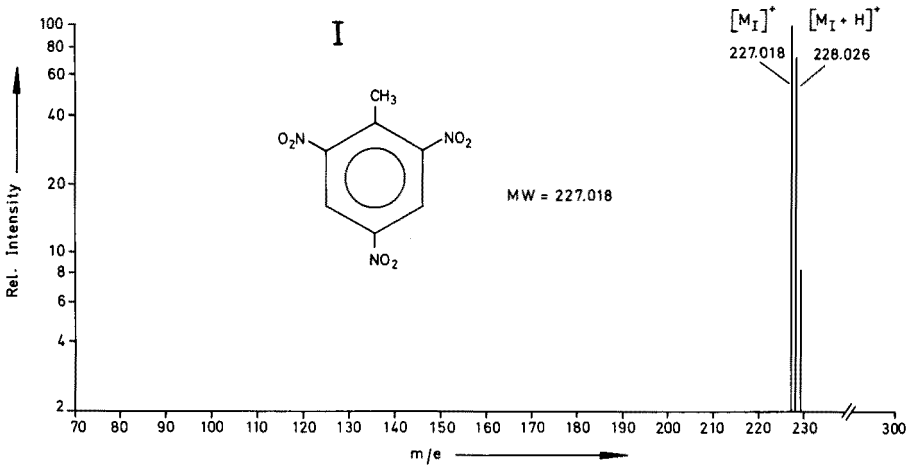

Fig. 2. F.d. mass spectrum of 2,4,6-trinitrotoluene (I).

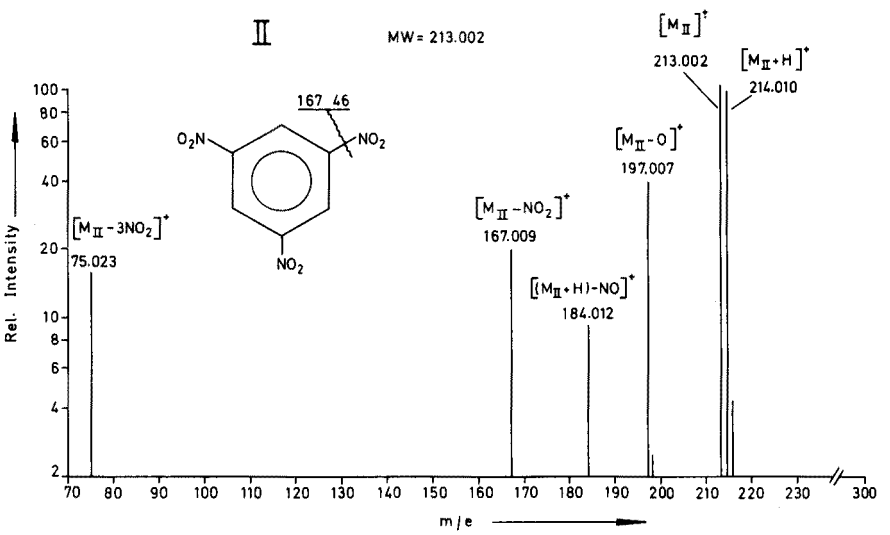

Fig. 3. F.d. mass spectrum of 1,3,5-trinitrobenzene (II).

from the loss of O, NO, and one or three nitro functions, are displayed. The elemental compositions of the f.d. fragments were evaluated by accurate mas measurements. This fragmentation is similar to e.i.m.s. where the base peak is *m/e* 75 for the ion $[M—3NO_2]^+$. This analogy between e.i. fragment ions and thermally induced f.d. fragments has been described previously [27]. The molecular ion at *m/e* 213 has a relative intensity of 31% in the e.i. mode [1] whereas c.i.m.s. gives the $[M + H]^+$ ion as base peak [8].

When the f.d. spectrum of *N*-methyl-*N*-2,4,6-tetranitroaniline (Tetryl, III) was recorded with 10 to 22 mA e.h.c. and all ions produced were detected photographically, the spectrum in Fig. 4 was obtained. The molecular ion

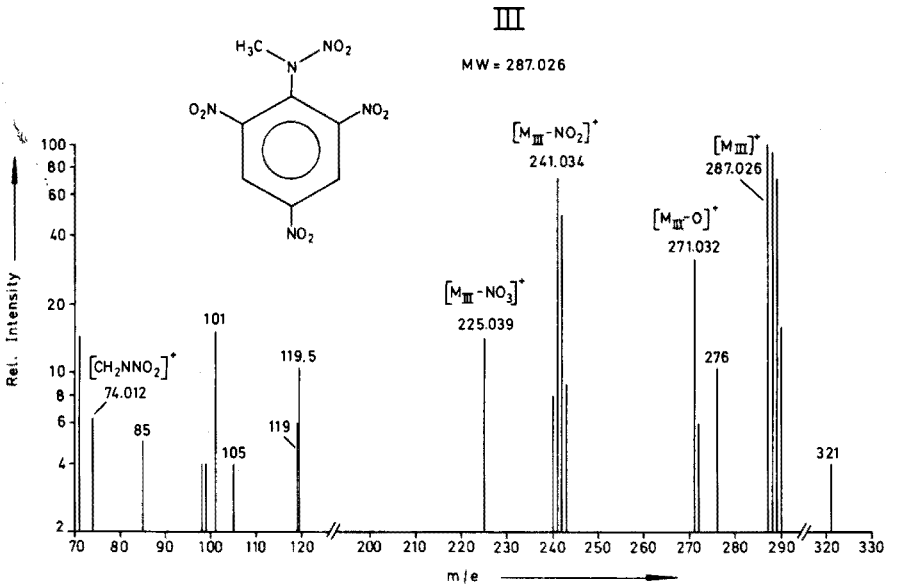

Fig. 4. F.d. mass spectrum of *N*-methyl-*N*-2,4,6-tetranitroaniline (III).

was the base peak. In addition, intense ions arising from the loss of oxygen, NO_2, and NO_3 were generated because of the relatively high emitter heating current. Some unidentified signals were registered at *m/e* 85, 98, 99, 101, 105, 119.5, 276, and 321. It could not be decided whether these ions were formed by a complex thermal decomposition or whether they indicate impurities in our sample of compound III which was of technical purity. For comparison with e.i.m.s., the molecular ion is of about 4% relative intensity and the spectrum is characterized by strong fragmentation. The base peak is at *m/e* 241 for the $[M—NO_2]^+$ ion [1, 8]. C.i.m.s. with isobutane as reagent gas gives no $[M]^{\cdot+}$ or $[M + H]^+$ ion [8]. The highest mass observed is the $[M + 1—0]^+$ ion at *m/e* 272 (11% rel. int.) and the base peak is the ion $[M + 1—CH_3NO]^+$ at *m/e* 243.

The results obtained from the f.d. spectra of aromatic explosives demonstrate that the emitter heating current has a decisive influence on the appearance of the spectra. Mass spectra that contain only the molecular ion group, the molecular ion group plus structurally significant fragment ions, or a large number of fragment ions including pyrolytic products can be generated by selecting the appropriate experimental parameters for desorption. In order to establish reproducible conditions, the use of an emitter current programmer [28] or a computer-controlled heating device [29] has been reported for electric detection of the f.d. spectra. For photographic detection the method of emission-controlled f.d.m.s. has been described [30, 31]. The advantages of the latter technique are illustrated by the investigation of a highly thermolabile tetranitrate.

Nitrates

Figure 5a shows the f.d. spectrum of pentaerythritol tetranitrate (PETN, IV). The protonated molecule has 58% relative intensity and allows unambiguous determination of the molecular weight. This is strongly supported by two complementary direct bond cleavages. The base peak is found at *m/e* 240.010 for the ion $[M—CH_2ONO_2]^+$, and for this ion species two complementary fragments at *m/e* 46 and *m/e* 194 are detected, underlining this typical feature in f.d. fragmentation. The thermogram (plot of e.h.c. versus time for a preselected emission-threshold) corresponding to the f.d. spectrum of compound (IV) is displayed in Fig. 5b. This thermogram gave

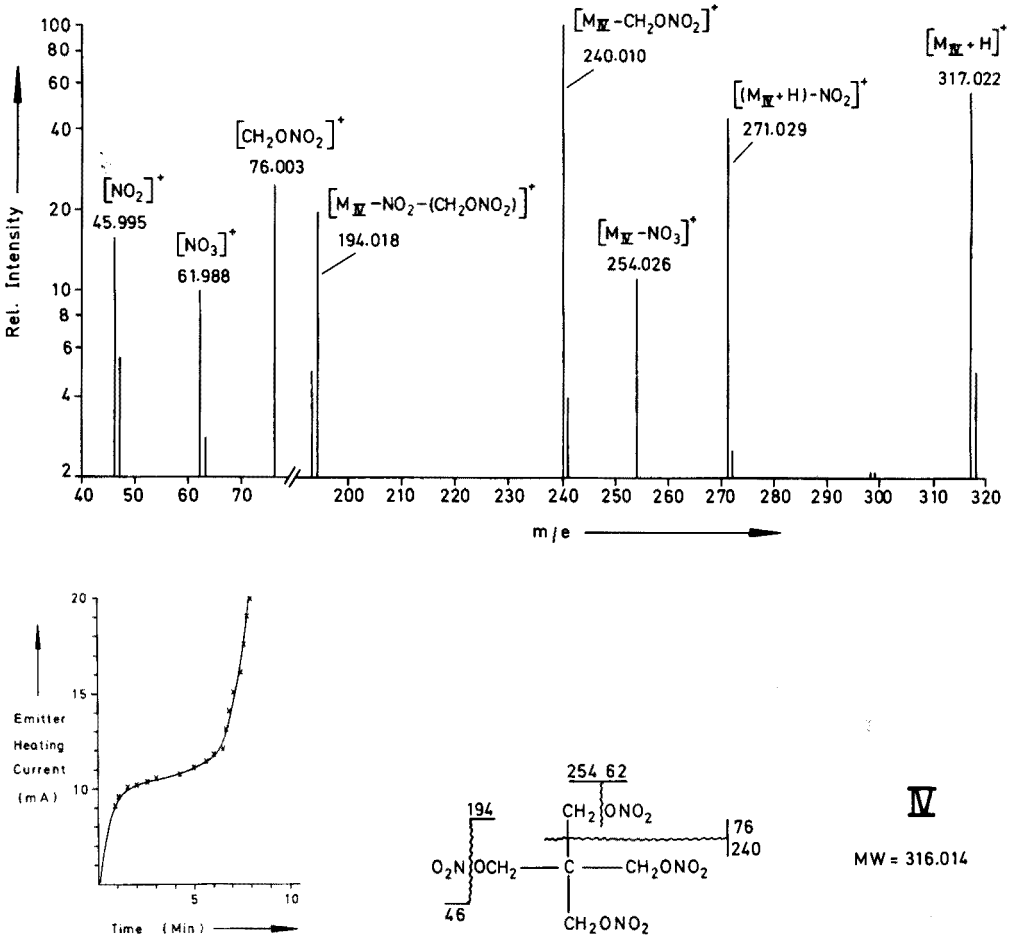

Fig. 5. (a) F.d. mass spectrum of pentaerythritol tetranitrate (IV). (b) Thermogram for the photographic recording of the f.d. spectrum in Fig. 5a. Background emission from residual gas in the ion source: 6.5×10^{-9} A. Selected emission threshold for emission-controlled desorption: 8×10^{-9} A. Desorption time for 1 μg of sample, 6 min; total exposure time in one track of the photoplate, 8 min; b.a.t., 8—10 mA.

an indication of the best anode temperature (here between 8 and 10 mA e.h.c.) and the desorption time of the whole sample (1 μg in ca. 5 min). The use of emission-controlled f.d.m.s. made it possible to regulate the desorption of the sample according to the physicochemical properties of the compound under investigation. For minimal fragmentation and high molecular ion intensities, the threshold current was set at the lowest value which produces a detectable ion current. The f.d. spectrum of compound (IV) (Fig. 5a) was recorded at a preset emission threshold of 8×10^{-9} Å. The resulting thermogram (Fig. 5b) showed a short, inclined plateau for the emitter heating current, indicating a thermolabile compound.

From the corresponding data for compound (IV) in the e.i. mode, the molecular ion is not detected and the base peak was at *m/e* 46 for the $[NO_2]^+$ ion [8]. Early studies by field ionization m.s. [32] revealed that (IV) gives the same base peak and a weak molecular ion of approximately 0.2% relative intensity. In c.i.m.s. with methane, the $[M + H]^+$ ion was also below 1% relative intensity [8]; the base peak was the same as in e.i.m.s. Only when water was used as reagent gas did the c.i. mass spectrum give an intense $[M + H]^+$ ion (68% rel. int. [10]). Comparing the mass spectra obtained with the different ionization modes, it becomes evident that f.d. is not only well suited for molecular weight determination but also provides relevant information about the structure of the compound in question.

Azacyclic compounds

Two widely used technical explosives are 1,3,5-triazacyclohexane (hexogen, R.D.X., (V)) and 1,3,5,7-tetranitro-1,3,5,7-tetrazacyclooctane (octogen, H.M.X., (VI)). In the f.d. spectrum of compound (V) (Fig. 6) the base peak was the $[M + H]^+$ ion. Further prominent fragment ions resulted from the loss of H_2O, NO_2 and $2HNO_2$ from the molecule and the protonated molecule respectively. Ring cleavage leads to the base peak at *m/e* 120.030 and the fragment ion at *m/e* 116.046 which were tentatively assigned to the $[M—NO_2—CH_2NCH_2NNO_2]^+$ ion and the $[M—NO_2—NNO_2]^+$ ion. No molecular ion [8] or a very low molecular ion intensity (0.04% [1]) have been reported in e.i. investigations of (V). Fragments of low mass were base peaks in these spectra (*m/e* 28, *m/e* 46 respectively). In c.i.m.s. the $[M + H]^+$ ion is found with methane [8] and water [10] with approximately 15% relative intensity.

The high thermolability of compound (VI) is reflected in the f.d. spectrum in Fig. 7, which displays an $[M + H]^+$ ion intensity of only 40%. By analogy with the f.d. spectrum of the structurally related compound (V), the base peak for (VI) is also represented by the ion at *m/e* 102.030. In addition, ring cleavages plus protonation lead to ions at *m/e* 74.019 and at *m/e* 149.031, (Fig. 7). Again no molecular ion [8] or a molecular ion of very low intensity (0.03% [1]) is observed in e.i.m.s. The base peak is the same as for (V). Neither methane nor isobutane gives $[M]^+$ or $[M + H]^+$ ions in c.i.m.s. [8]. However, when water is used as reagent gas the $[M + H]^+$ ion is of 6.5% relative intensity [10].

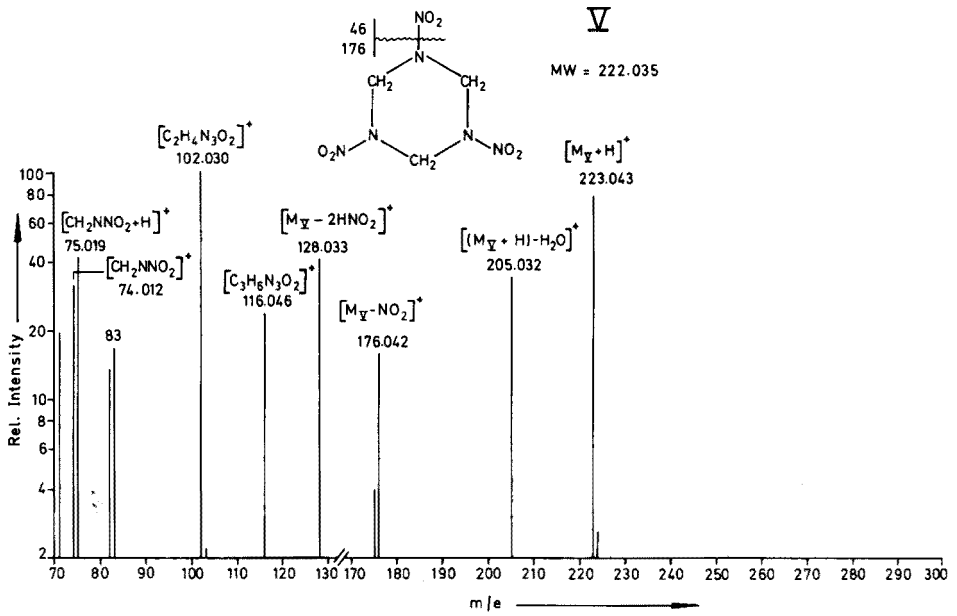

Fig. 6. F.d. mass spectrum of 1,3,5-trinitro-1,3,5-triazacyclohexane (V).

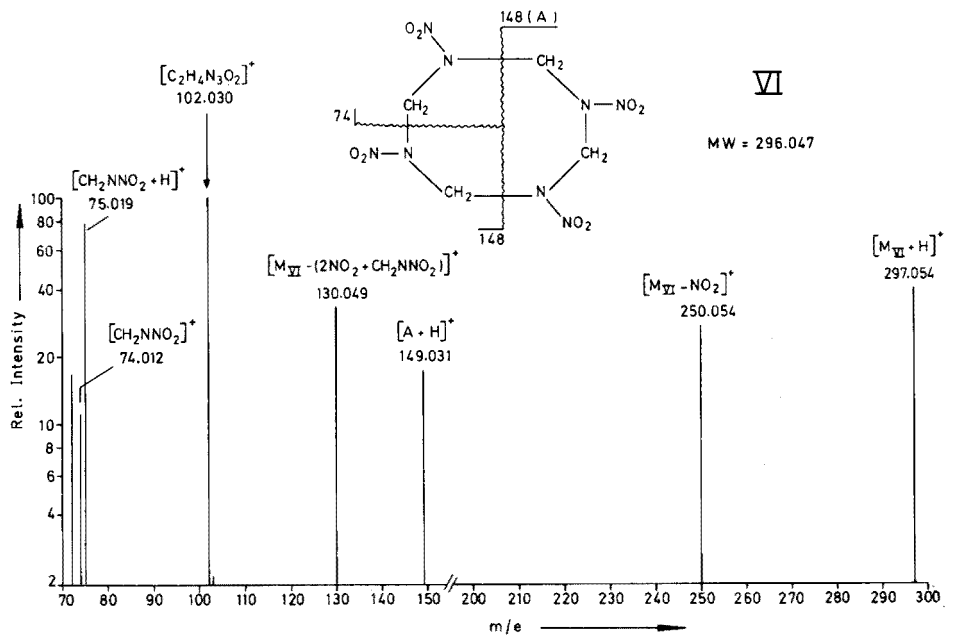

Fig. 7. F.d. mass spectrum of 1,3,5,7-tetranitro-1,3,5,7-tetrazacyclooctane (VI).

Explosive mixtures

The high intensities of the molecular ions or the protonated molecules of the standard explosives, as described above, are an essential prerequisite for the analysis of mixtures of these compounds. Moreover, f.d. at b.a.t., or slightly above b.a.t., produces a small number of fragments which are generated by simple reaction mechanisms, especially protonation and direct bond cleavages. Thus the possibility of superposition of fragment ions and molecular ions of other components is strongly reduced. Combined use of f.d. and accurate mass measurements offers a further advantage in the identification of mixture components. These facts prompted a study of some commercially available explosive mixtures.

When a mixture of hexogen (V) and octogen (VI) containing about 10% of (VI) was examined with f.d.m.s., the spectrum in Fig. 8 was obtained and the molecular ion and the protonated molecules of (V) and (VI) were easily recognized. With one exception (*m/e* 120.005) all fragment ions in the spectrum of the mixture were also found in the f.d. spectra of the individual components (Figs. 6 and 7). Under the experimental conditions selected, no products of a chemical interaction of compounds (V) and (VI) were detected. This is the first example of a successful mixture analysis of explosives by f.d.m.s.

Frequently, accompanying compounds are present in commercially available explosive mixtures. For analytical and forensic purposes it is of interest to identify and quantify these additives. To exploit the capacity of

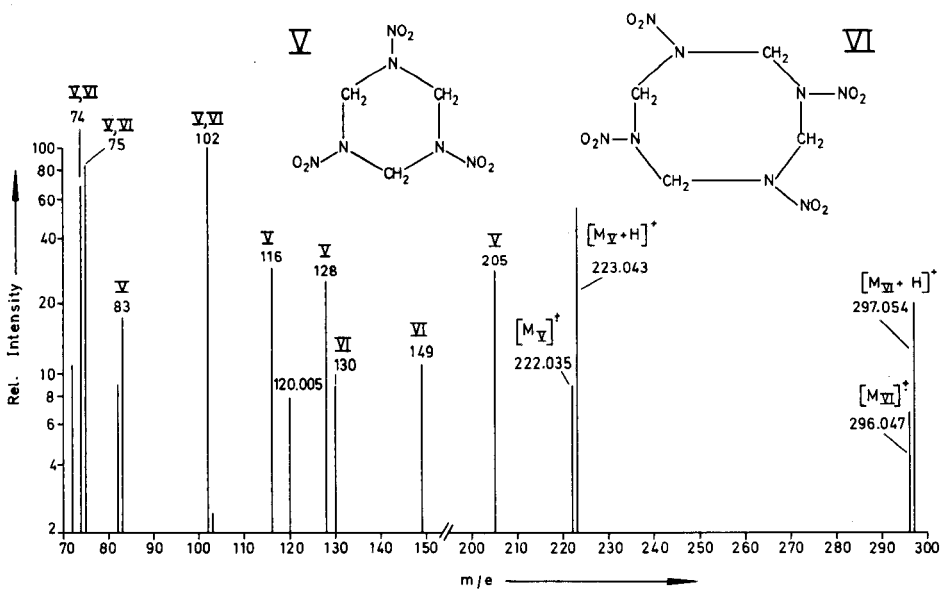

Fig. 8. F.d. mass spectrum of a technical explosive mixture of (V) and (VI) (2—10%). The prominent fragment at *m/e* 176.042 for the $[M_V—NO_2]^+$ ion is not included in the spectrum (15% relative intensity). Roman numerals assigned to fragment ions in the f.d. spectra of mixtures indicate their origin from the corresponding compounds.

f.d.m.s. for this purpose, a commercial mixture composed of compound (V) and stearic acid (VII) was studied. The f.d. spectrum of this mixture is shown in Fig. 9. Compared with the f.d. spectrum of the standard sample of (V) in Fig. 6, the protonated molecule is of 30% relative intensity only because of a faster rise of the emitter heating current and a shorter desorption time. The stronger thermal stress is also reflected in the enhanced fragmentation. Nevertheless, all fragment ions in the f.d. spectrum of the standard were also detected in the mixture and were again identified by accurate mass measurements. The desorption of the accompanying stearic acid resulted in a strong molecular ion at *m/e* 284.272 and no fragmentation. This is consistent with the f.d. mass spectrum of the pure stearic acid.

The utility of f.d.m.s. for quantification of derivatives of biogenic amines [33], antitumor drugs [30], and polycyclic hydrocarbons [34] by recording on photoplates has been reported. Electric detection by stable isotopic dilution and repetitive scan gave quantitative f.d. data for the determination of dopamine [35], cyclophosphamide [36], and glucose [37]. In this study, quantitative analysis was performed by stable isotope dilution of the mixture containing (V) and (VII) with stearic acid-d_{35} and recording of the molecular ion groups of (VII) and the deuterated internal standard by the double detector technique [38]. The amount of (VII) present in the explosive mixture was 2.2 ± 0.3%. This first estimation of a component in a technical mixture demonstrates the feasibility of f.d.m.s. for the qualitative and quantitative analysis of mixtures. An example of the analysis of an explosive mixture containing three compounds ((I), 39.5%; (V), 59.5%; and 1% wax) is also given.

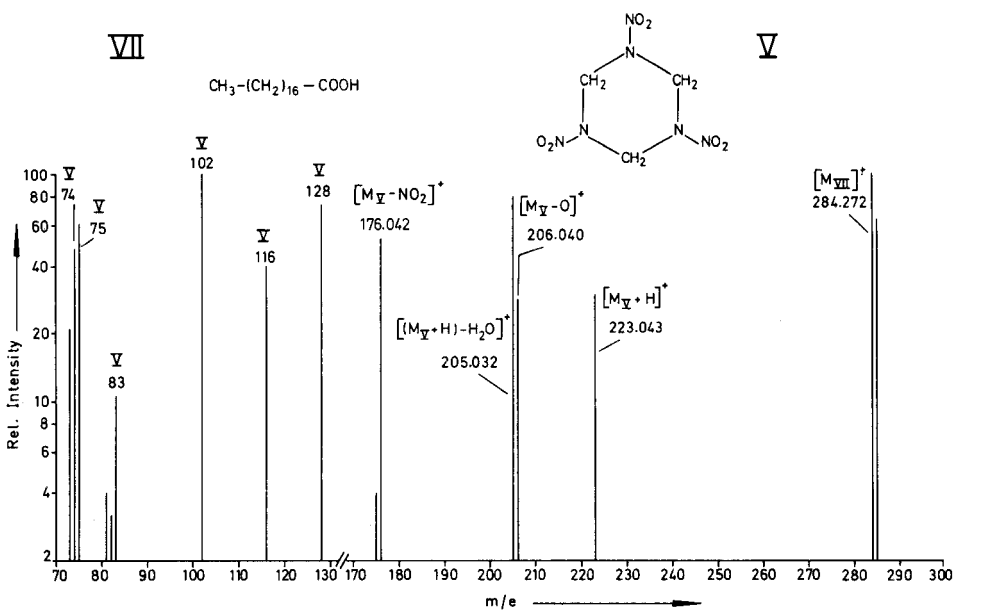

Fig. 9. F.d. mass spectrum of a technical explosive mixture of (V) and stearic acid (VII). The content of (VII) in the mixture was determined as described in the text.

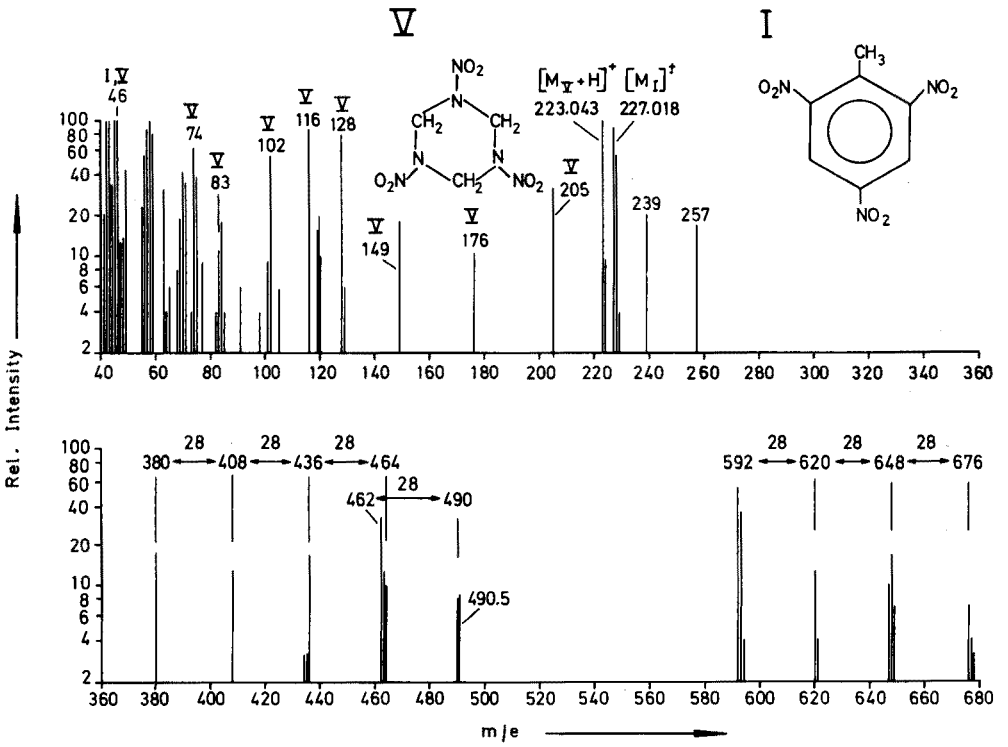

Fig. 10. F.d. mass spectrum of a technical explosive mixture of (I) (39.5%), (V) (59.5%), and 1% of a wax.

As shown in Fig. 10, (V) gave the $[M+H]^+$ ion at *m/e* 223.043 with 100% relative intensity; (I) gave a molecular ion at *m/e* 227.018 with 90% relative intensity, and thus the major components were easily identified. Apparently, the wax is composed of a number of fatty acids which vary by C_2H_4 units; the presence of a wax is clearly reflected in the f.d. spectrum in Fig. 10 by ion series differing by 28 mass units.

Conclusion

These results have shown that the method of emission-controlled desorption improves the experimental conditions in f.d.m.s., especially when photographic detection is employed. The explosives investigated gave intense molecular ions or protonated molecules and few structurally significant fragment ions. It is clearly demonstrated that f.d.m.s. is very well suited for the qualitative and quantitative analysis of technical explosive mixtures. The technique appears to be promising for quality control and the identification of explosives, and it might be useful as a complementary analytical tool in forensic investigations, e.g. extracts of debris after explosions as has been shown recently by c.i.m.s. [39, 40].

This work was supported by grants from the Deutsche Forschungsgemeinschaft, Fonds der Deutschen Chemischen Industrie, and Ministerium für Wissenschaft und Forschung des Landes Nordrhein-Westfalen. The authors thank Dr. J. Yinon (Weizmann Institute of Science, Rehovot, Israel) for preprints of the e.i. and c.i.m.s. articles on explosives [8—10, 40], and the Bundesinstitut für chemisch-technische Untersuchungen, Heimerzheim, West Germany (Dr. J. Zierath) for the generous gift of the compounds investigated and for valuable discussions.

REFERENCES

1 F. Volk and H. Schubert, Explosivstoffe, 16 (1968) 2.
2 R. T. M. Fraser and N. C. Paul, J. Chem. Soc., B, (1968) 659.
3 S. Bulusu, T. Axenrod and G. W. A. Milne, Org. Mass Spectrom., 3 (1970) 13.
4 J. Stals, Trans. Faraday Soc., 67 (1971) 1768.
5 J. Yinon and H. G. Boettger, Int. J. Mass Spectrom. Ion Phys., 10 (1972) 161.
6 J. Yinon, H. G. Boettger and W. P. Weber, Anal. Chem., 44 (1972) 2235.
7 S. Meyerson, R. W. Van der Haar and E. K. Fields, J. Org. Chem., 37 (1972) 4114.
8 S. Zitrin and J. Yinon, in A. Frigerio and N. Castagnoli (Eds.), Advances in Mass Spectrometry in Biochemistry and Medicine, Vol. I, Spectrum Publications, New York, 1976, p. 369.
9 S. Zitrin and J. Yinon, Org. Mass Spectrom., 11 (1976) 388.
10 J. Yinon, Biomed. Mass Spectrom., 1 (1974) 393.
11 H. D. Beckey, Field Ionization Mass Spectrometry, Pergamon Press, Oxford, 1971; 2nd edn., Principles of Field Ionization and Field Desorption Mass Spectrometry, Pergamon Press, Oxford, in press. H. D. Beckey and H.-R. Schulten, Angew. Chem., 87 (1975) 425; Angew. Chem. Int. Ed. Eng., 14 (1975) 403.
12 H.-R. Schulten in D. Glick (Ed.), Methods of Biochemical Analysis, J. Wiley, New York, Vol. 24 (1977) pp. 313—418.
13 K. L. Rinehart, Jr., C. Cook, Jr., K. H. Maurer and U. Rapp, J. Antibiot., 27 (1974) 1.
14 H. Adlercreutz, B. Soltmann and M. J. Tikkanen, J. Steroid Biochem., 5 (1974) 163.
15 H.-R. Schulten and D. Kümmler, Z. Anal. Chem., 278 (1976) 13.
16 H.-R. Schulten, J. Agric. Food Chem., 24 (1976) 743.
17 H.-R. Schulten, H. D. Beckey, A. J. H. Boerboom and H. L. C. Meuzelaar, Anal. Chem., 45 (1973) 2358.
18 H.-R. Schulten, Biomed. Mass Spectrom., 1 (1974) 223.
19 J. A. Sphon, P. A. Dreifuss and H.-R. Schulten, J. Assoc. Off. Anal. Chem., 60 (1977) 73.
20 H.-R. Schulten and B. Wittmann-Liebold, Anal. Biochem., 76 (1976) 300.
21 H. D. Beckey and H.-R. Schulten, in C. N. McEwen and C. Merritt (Eds.), Practical Spectroscopy Series, M. Dekker, New York, 1977.
22 H.-R. Schulten and H. D. Beckey, Org. Mass Spectrom., 7 (1973) 861.
23 H. D. Beckey, E. Hilt and H.-R. Schulten, J. Sci. Instrum., 6 (1973) 1043.
24 H.-R. Schulten and H. D. Beckey, Org. Mass Spectrom., 6 (1972) 885.
25 H. D. Beckey, A. Heindrichs and H. U. Winkler, Int. J. Mass Spectrom. Ion Phys., 3 (1970) App. 9 p. 11.
26 H. U. Winkler and H. D. Beckey, Org. Mass Spectrom., 6 (1972) 655.
27 D. A. Brent, P. de Miranda and H.-R. Schulten, J. Pharm. Sci., 63 (1974) 1370.
28 J. W. Maine, B. Soltmann, J. F. Holland, N. D. Young, J. N. Gerber and C. C. Sweeley, Anal. Chem., 48 (1976) 427.
29 H. U. Winkler, W. Neumann and H. D. Beckey, Int. J. Mass Spectrom. Ion Phys., 21 (1976) 57.

30 H.-R. Schulten, Cancer Treat. Rep., 60 (1976) 501.
31 H.-R. Schulten and N. M. M. Nibbering, Biomed. Mass Spectrom., 4 (1977) 55.
32 C. Brunnée, G. Kappus and K.-H. Maurer, Z. Anal. Chem., 232 (1967) 17.
33 W. D. Lehmann, H. D. Beckey and H.-R. Schulten, Anal. Chem., 48 (1976) 1572.
34 S. Pfeifer, H. D. Beckey and H.-R. Schulten, Z. Anal. Chem., 284 (1977) 193.
35 W. D. Lehmann, H. D. Beckey and H.-R. Schulten, in A. P. De Leenheer and R. R. Roncucci (Eds.), Quantitative Mass Spectrometry in Life Sciences, Elsevier, Amsterdam, 1977, p. 177.
36 H.-R. Schulten, W. D. Lehmann and M. Jarman, in A. P. De Leenheer and R. R. Roncucci (Eds.), Quantitative Mass Spectrometry in Life Sciences, Elsevier, Amsterdam, 1977, p. 187.
37 W. D. Lehmann and H.-R. Schulten, Angew. Chem., 89 (1977) 180; Angew. Chem. Int. Ed. Eng., 16 (1977) 184.
38 W. D. Lehmann and H.-R. Schulten, Biomed. Mass Spectrom., in press.
39 P. Vouros, B. A. Petersen, L. Colwell, B. L. Karger and H. Harris, Anal. Chem., 49 (1977) 1039.
40 J. Yinon and S. Zitrin, J. Forensic Sci., in press.

Analytica Chimica Acta, 93 (1977) 33—44
© Elsevier Scientific Publishing Company, Amsterdam — Printed in The Netherlands

CONTROLE ANALYTIQUE PAR SPECTROSCOPIE INFRAROUGE DE LA SYNTHÈSE ET DE LA PURETÉ DE SPIROPYRANNES ET MÉROCYANINES BENZOTHIAZOLINIQUES

M. GUILIANO, G. MILLE et J. CHOUTEAU*

Centre de Spectroscopie Infrarouge, Université de Droit, d'Economie et des Sciences d'Aix-Marseille, Centre Saint-Charles, 3, place Victor Hugo, 13331 Marseille (France)

J. KISTER et J. METZGER

Laboratoire de Chimie Organique A, Université de Droit, d'Economie et des Sciences d'Aix-Marseille, Centre Saint-Jérôme, Rue Henri Poincaré, 13397 Marseille (France)

(Reçu le 25 mars 1977)

RÉSUMÉ

Une méthode d'analyse par spectrométrie infrarouge de spiropyrannes et mérocyanines benzothiazoliniques est décrite. Elle permet de caractériser la structure des composés synthétisés (forme fermée ou forme ouverte), de contrôler leur pureté et également de mettre en évidence des produits de dégradation.

SUMMARY

Infrared spectroscopic studies of the synthesis and purity of benzothiazolinic spiropyrans and merocyanines.

An i.r. spectroscopic study of benzothiazolinic spiropyrans and merocyanines is described. The structures of the synthesized compounds (closed form or open form) can be characterized, their purity can be checked, and degradation products can be detected.

Dans le cadre d'une étude des spiropyrannes benzothiazoliniques photochromes [1—6] et de leur utilisation comme composés photo-sensibles dans un procédé photographique non argentique impliquant ou non un processus d'amplification du signal photonique primaire [4—7], nous avons synthétisé une série de dérivés substitués en positions 3, 6, 8 sur la partie benzopyrannique et 3′, 4′, 6′ sur la partie benzothiazolinique (I).

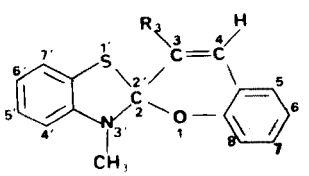

(I)

partie benzothiazolinique — partie benzopyrannique

Ces spiropyrannes ou formes fermées (FF) conduisent par irradiation dans l'ultra-violet et après rupture de la liaison $C_2—O_1$ à des formes ouvertes (FO) encore appelées photomérocyanines (schéma 1) hautement stabilisées thermiquement ($k = 10^3\ s^{-1}$ à 25°C dans le toluène [4—6, 8]

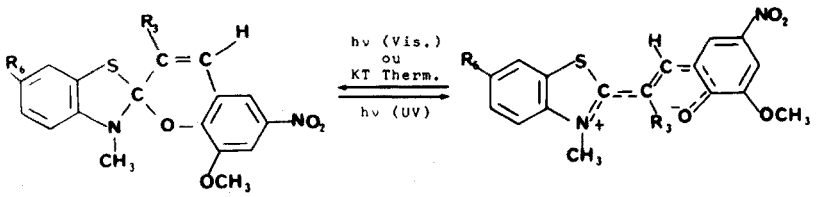

Schéma 1

Cette réaction est réversible et la vitesse de décoloration est liée aux paramètres structuraux de la molécule [9]. Dans le procédé photographique étudié, la photomérocyanine est stabilisée par adsorption sur un semi-conducteur avec lequel elle forme un complexe (schéma 2) et le cation résultant participe comme catalyseur au processus d'amplification [5—7, 10].

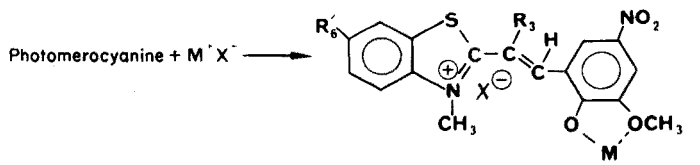

Schéma 2

Si de tels composés sont intéressants en vue de l'utilisation possible de ces spiropyrannes dans un ou des processus d'enregistrement photographique [5—7, 10], par contre leurs synthèses deviennent particulièrement complexes et délicates [4—6, 8].

Nous avons pensé que la spectrographie infrarouge pouvait à ce niveau, compétitivement à d'autres méthodes d'analyse (r.m.n., u.v., s.m.) permettre un bon contrôle réactionnel par l'identification rapide des structures intermédiaires et finales (FF ou FO), par le contrôle de la pureté des composés (FF dans FO, FO dans FF, produits de départ résiduels et produit de dégradation) et même simplifier des problèmes très difficiles à résoudre par les autres. Nous avions déjà entrevu dans le même genre de recherches [11] l'intérêt de la spectroscopie infrarouge.

En particulier la spectroscopie infrarouge permet des analyses á l'état solide, résolvant les problèmes posés par la non-solubilité des mérocyanines et par la technique a.t.r. (réflexion totale atténuée), leur étude sur support solide semi-conducteur.

Nous présentons dans la première partie la préparation des composés et leurs conditions d'isolement et dans la seconde leur analyse i.r.

SYNTHÈSES

Choix de structure

Le choix des composés étudiés a été guidé par le fait qu'ils doivent posséder, pour leur utilisation particulière en tant que produits photochromes, les propriétés suivantes: une bonne sensibilité, génératrice de bonnes propriétés photochromes [9]; une vitesse de décoloration thermique suffisamment lente [8, 9]; un groupe méthyle fixé sur l'azote en 3′ et qui sera rendu électrophile par la transformation du spiropyranne en mérocyanine [5, 6]; des propriétés correctes d'adhérence sur les supports solides semiconducteurs [5] et une dégradation faible lors du couchage du spiropyranne sur celui-ci (pas de background initial) [6]; pas de réaction de dégradation lors de l'ouverture en mérocyanine sur le support solide [6].

Les raisons du choix des différents substituants fixés sur le squelette spiropyrannique ont été précisées par ailleurs [4—6, 8]. Certains composés ne répondant pas à ces critères ont été plus spécialement préparés afin de constituer des séries homologues en vue de l'étude infrarouge.

Préparation des composés

La technique de préparation de ces composés a été amplement décrite [1, 4]. Toutes les synthèses ont été réalisées dans les mêmes conditions par chauffage en milieu éthanolique d'un mélange équimoléculaire de sel quaternaire hétérocyclique, de nitro-5 *o*-vanilline et de pipéridine. Les spiropyrannes sont le plus souvent obtenus sous leur forme ouverte, seule ou en mélange avec la forme fermée. Il reste alors à provoquer la fermeture et à recristalliser ces composés. Cette opération est réalisée en dissolvant le produit brut obtenu dans le toluène chaud [4—6]; après plusieurs heures de reflux, on déshydrate par distillation azéotropique, on filtre à chaud pour séparer la mérocyanine insoluble et on laisse précipiter à froid. On répète l'opération plusieurs fois. Parfois on peut effectuer un lavage à l'acétone anhydre. Dans d'autres cas la solution toluénique froide est jetée sur de l'éther de pétrole ou de pentane anhydre [4—6].

Il faut noter que pour des solutions toluéniques de concentration élevée en spiropyrannes (supérieure à 10^{-4} mol l^{-1} à 25°C) les FO peuvent précipiter après irradiation. Cette précipitation serait due à l'existence de photomérocyanine autoassociée sous forme dipole-dipole comme le suggèrent des effets de polarité, de solvant, de concentration et de température [8]. Le phénomène de photoprécipitation qui peut gêner dans certains cas la détermination des constantes de vitesse de refermeture thermique des mérocyanines, permet par contre de pouvoir isoler ces formes à l'état pur.

Le mode opératoire peut être résumé par la Fig. 1. Cette figure montre que l'on peut s'orienter soit vers une FF (étape I), soit vers une FO (étape II) posant un premier problème d'élucidation de structures. C'est le type de substitution intervenant sur le squelette du spiropyranne benzothiazolinique

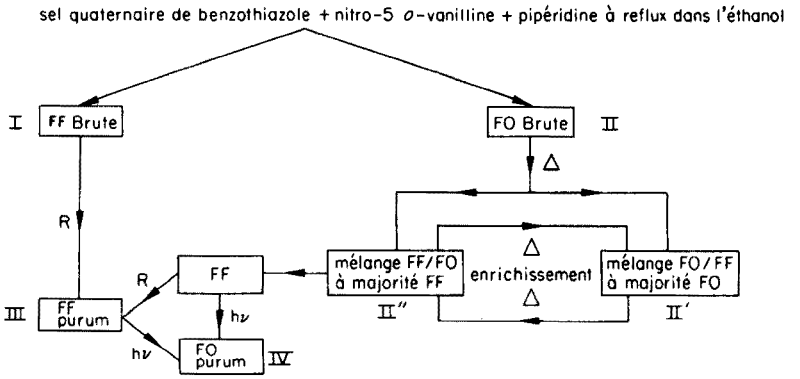

Fig. 1. Préparation des composés. △: refermeture thermique (reflux, toluène), *hν*: photoprécipitation. R: recristallisation.

qui oriente la réaction. Selon l'étape à laquelle les produits sont isolés (II, II', II'', III, IV) se pose en plus un double problème de structure (FF ou FO) et de pureté (FF dans FO, FO dans FF). En effet la fermeture de composés de plus en plus complexes dont les FO sont fortement stabilisées, devient particulièrement difficile, voire partielle ou impossible.

D'autres impuretés (autres que la FF dans FO et la FO dans FF) peuvent être rencontrées, notamment un intermédiaire de synthèse la nitro-5 *o*-vanilline.

Lors de l'étude des spiropyrannes sur support semi-conducteur de type TiO_2, ZnO, Al_2O_3, SiO_2, nous avons observé [5, 6] des dégradations lors du couchage photographique (background initial), et des dégradations après irradiation de la surface sensible avec formation de background orange.

Ces dégradations sont plus importantes sur support basique (ZnO, SiO_2) et moins prononcées avec un spiropyranne portant un groupement thiométhyl plutôt qu'un groupement méthoxy en 6' [6]. Ces phénomènes déjà observés en phase liquide [6] mais non expliqués sont délicats à étudier à cause de la non-solubilité des mérocyanines et de l'obligation de travailler sur support solide. La spectroscopie infrarouge semble être une technique de choix dans la mesure où l'on dispose des bases de comparaisons, c'est-à-dire des caractéristiques des produits couchés (FF et FO), des impuretés et des agents d'amplification [5, 6].

Composés synthétisés

La Tableau 1 donne la liste des composés synthétisés en indiquant la nature des différents substituants pour chacun des types de substitution et l'étape de la Fig. 1 à laquelle le composé a été isolé.

TABLEAU 1

Composés synthétisés

Substitution						Composés		Étape		Réf.
R'_3	R'_4	R'_6	R_3	R_6	R_8	FF	FO			
CH_3	H	OCH_3	OC_6H_5	NO_2	OCH_3	1a	1b	III	IV	[4, 5] [4, 5]
CH_3	H	SCH_3	OC_6H_5	NO_2	OCH_3	2a	2b	III	?	[4, 5] [4, 5]
CH_3	H	OCH_3	$O_\beta C_{10}H_7$	NO_2	OCH_3	3a	3b	II″	II, II′	[4, 5] [4, 5]
CH_3	SCH_3	OCH_3	OC_6H_5	NO_2	OCH_3	4a	4b	II″	II′	[4, 5] [4, 5]
CH_3	H	OCH_3	OC_6H_5	H	H	5a		III		[6]
CH_3	H	OCH_3	OC_6H_5	NO_2	H	6a	6b	III	IV	[6] [6]
CH_3	H	OCH_3	OC_6H_5	H	OCH_3	7a	7b	III	II′	[6] [6]
CH_3	H	H	CH_3	NO_2	CH_2OEt	8a	8b	III	IV	[6] [6]
CH_3	H	H	CH_3	NO_2	CH_2OH	9a	9b	II″	II, II′	[6] [6]
CH_3	H	OCH_3	OC_6H_5	NO_2	CH_2OEt	10a	10b	II″	II, II′	[6] [6]
CH_3	H	OCH_3	OC_6H_5	NO_2	CH_2OH	11a	11b	II″	II, II′	[6] [6]
CH_3	H	OCH_3	OCH_3	NO_2	OCH_3		12b		II	[6]
CH_3	H	H	OEt	NO_2	OCH_3	13a	13b	III	IV	[8][a] [8][a]
CH_3	H	mésityl	CH_3	NO_2	OCH_3	14a		I		[12]
CH_3	H	furyl	CH_3	NO_2	OCH_3	15a		I		[12]

[a]Le couple 13a, 13b nous a été fourni par A. Samat.

ANALYSE PAR SPECTROMÉTRIE INFRAROUGE

La spectrométrie infrarouge permet la détermination commode de structure de spiropyrannes ou mérocyanines benzothiazoliniques [11, 13] et également la caractérisation de la structure électronique de la molécule ouverte [11, 13, 14]. Disposant ici de plusieurs mérocyanines stables et de couples de composés FF—FO, il était intéressant d'étendre à ceux-ci une étude systématique du même type. Le but en est de vérifier les observations expérimentales décrites précédemment [11] relatives à un seul couple de composés FF—FO, et de les généraliser, constituant ainsi une méthode d'analyse des spiropyrannes et mérocyanines benzothiazoliniques. Nous avons appliqué cette méthode d'analyse à l'ensemble des composés et discuté les résultats en termes de structure, pureté et dégradation.

Conditions expérimentales

Les spectres infrarouges ont été enregistrés sur spectrographes Perkin-Elmer, modèles 125 et 225. Les échantillons ont été examinés sous forme de pastille de KBr (environ 1,50 mg de produit pour 150 mg de KBr). Seul le composé [4] a été examiné en solution dans $CDCl_3$.

Caractérisation des spiropyrannes benzothiazoliniques (FF)

Les attributions antérieurement proposées [11] pour les spiropyrannes benzothiazoliniques peuvent être étendues de façon systématique à l'ensemble des dérivés examinés ici (Tableau 2). Les spiropyrannes photochromiques possédent en général un substituant nitro, les vibrations de ce groupement sont utilisables au même titre que les mouvements de noyau pour les caractériser. La série de spiropyrannes homologues formée par les composés 5a, 6a, 7a et 1a, constitue une bonne base pour identifier les vibrations de noyau et pour caractériser les mouvements des substituants (Tableau 2).

Le spectre i.r. d'un spiropyranne benzothiazolinique peut être généralement caractérisé par la présence [11, 15] (cf. Figs. 2, 3):

(a) de quatre bandes, entre 1700 et 1550 cm^{-1}, correspondant aux quatre vibrations de plus haute fréquence du noyau spiropyrannique. Trois mouvements sont imputables au noyau benzopyrannique (dont la vibration de valence νC=C située vers 1650 cm^{-1}) et une au noyau benzothiazolinique. Le sommet i.r. correspondant au mode νC=C est souvent assez faible et même dans certains cas n'est pas observé. Deux des trois autres vibrations sont attendues au-dessous de 1600 cm^{-1} et donnent lieu parfois à des bandes superposées;

(b) d'une bande très forte vers 1515 cm^{-1} correspondant au mouvement $\nu_a NO_2$,

(c) d'un sommet intense vers 1480—1470 cm^{-1} dû au noyau benzothiazolinique [15],

(d) d'un maximum très intense à 1340 cm^{-1} ($\nu_s NO_2$);

(e) de bandes reliables aux mouvements ν CO intracyclique, ν(=C—OR) et à une vibration du noyau benzothiazolinique [15], entre 1300 et 1200 cm^{-1}

Caractérisation des mérocyanines benzothiazoliniques (FO)

Confirmation des attributions antérieures. Cette étude portant sur un nombre important de photomérocyanines nous a permis en premier de confirmer les attributions formulées antérieurement pour deux mérocyanines [11]. Nous retrouvons, en effet, dans cette nouvelle série de composés les mêmes perturbations entre les spectres de FF et de FO [11].

La comparaison des spectres des composés 8a et 8b permet de mettre en évidence de façon très nette le glissement de fréquences dans la région de 1350—1200 cm^{-1} (cf. Fig. 3). Les deux composés 8 ne possédant aucun motif structural =C—O autre que celui faisant intervenir l'oxygène intracyclique, on attend, entre 1300 et 1200 cm^{-1}, seulement la vibration νC—O et un mouvement du noyau benzothiazolinique [15]. Ceci permet de rattacher

TABLEAU 2

Fréquences infrarouges des spiropyrannes et mérocyanines benzothiazoliniques (1700—1150 cm^{-1}) (FF = très fort; F = fort; m = moyen; f = faible; e = épaulement; l = large)

Composés		Fréquences i.r. et attributions caractéristiques											
FF	FO	νCC éthylénique		νCC benzénique	$\nu_a NO_2$	ν noyau		νC⋯N?	$\nu_s NO_2$		νCO (cycle), ν = C—OR, ν noyau	?	
1a		1655m		1613f, 1587m, 1576m	1520F		1487F		1336F		~1250e, 1242F 1215m		
	1b		1588F	~1580e, ~1575e	1525F	1505F,		1392F		1288FF	1235FF (l)	~1200FF (l)	
2a		1650m		1614f, ~1585e, 1575m	1520F		1476F		1335F		~1250e, 1240F, ~1225e, 1200F		
	2b	1650m	1588F	~1595e	1520F	1490F	~1480e	1386m	~1335e	1285FF	~1250e (l), 1220FF	~1205e	
3a		1650f		1615f, ~1587e, 1580m	1520F		1487F		1337F		~1255e, 1240F, ~1230e		
	3b	1650m	1592F	~1622e, ~1577e, ~1558e	1517F	~1500e	1486F		1335F	1285F	~1265e, 1260F, 1233F (l)		
4		~1650m	~1596e	1605m, 1581m	1528F	~1500e	1490F		1340F	~1390e	1250F, 1225F		
5a		1645m		~1600e, 1587m, 1573m			1486FF				1243F, ~1230e, 1220F, 1207F		
6a		1645m		~1600e, 1588m, 1575m	1520F		1485FF		1337F		1262F, 1237F, ~1222e, 1202F		
	6b		1595FF	~1575e	1520F	1500F		1394F		1295FF	~1265e, 1245FF (l)	1192F	
7a		1645m		1604m, 1586m, 1575F			1485FF				1250m, 1225F, ~1213e, 1203F		
	7b		1588F	~1600e, 1572F			1485FF				~1260e (l), ~1225e, 1210F, ~1203e		
8a		1651f		1616f, 1583m	1525F		1470F		1340F		1233F, ~1220e		
	8b		1598FF	~1590e, 1575F, 1555F	1520F	1505F		1393F		1296FF	1245FF (l)	1194F	
9a		1650f		1613f, 1584m	1520F		1475F		1337F		1232F		
	9b	1650f?	1596FF	~1590e, ~1577e, 1555F	1520F	~1505e,	1485F	1393F	1337F,	1295F	1255FF (1), ~1232e	1196F	
10a		1652m		1590m	1522F		1485F		1340F		1238F, 1224F, 1216F, 1203F		
	10b		1598FF	~1595e, ~1575e, 1552F	1520F	1505F,	1482F	1390F	1337F,	1295FF	1250—1230FF (l)	1196F	
11a		1650m		1588m	1520m		1486F		1338F,	1295m	1272m, ~1245e, 1222F	~1200e	
	11b		1600FF	~1590e, ~1575e, 1555F	~1520m	1505F,	1485F	1393F	~1335e,	1297F	~1265e, 1245FF (l) ~1230e	1195F	

TABLEAU 2 (continué)

Composés		Fréquences i.r. et attributions caractéristiques										
FF	FO	νCC éthylénique		νCC benzénique	$\nu_a NO_2$	ν noyau		νC⋯N?	$\nu_s NO_2$		νCO (cycle), ν = C—OR, ν noyau	?
	12b		1590FF	~1580e, 1568F	1525F	1504F		1395F		1280FF	1245—1230FF (l)	1198F
13a		1645m		1612m, ~1583e, 1576m	1515F		1478F		1337F		1245F, ~1230e	
	13b		1588F	1575F, ~1567e, 1560F	1525F	1500F		1393F		1290FF	~1258e, 1245FF (1), ~1232e, ~1215e	1200F
14a		?		~1610e, 1596m, ~1580e	1523F		1475F		1337F		~1290m, 1245F	
15a		~1650e		1608m, 1582m	1523F		1478F		1337F		1290m, ~1260e, 1250F, 1238F, ~1220e	

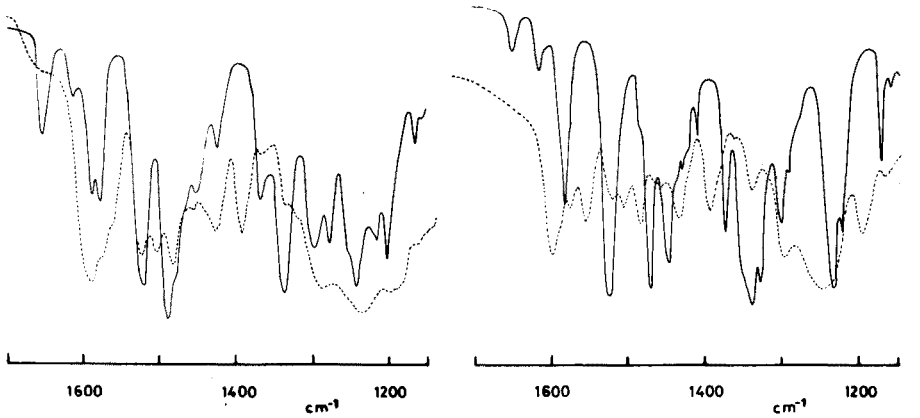

Fig. 2. Spectres infrarouges de 1700—1150 cm^{-1} des composés 1a FF (trait plein) et 1b FO (pointillés).

Fig. 3. Spectres infrarouges de 1700—1150 cm^{-1} des composés 8a FF (trait plein) et 8b FO (pointillés).

la forte bande à 1235 cm^{-1} du spectre de 8a (cf. Fig. 3) à la vibration de valence mettant en jeu la liaison C—O du cycle. Le spectre de 8b présente entre 1350 et 1200 cm^{-1} une bande forte à 1300 cm^{-1} et un sommet très large et très intense centré à 1245 cm^{-1}. La bande intense vers 1300 cm^{-1} également observée dans les spectres des FO 1b et 6b, est absente dans celui de la mérocyanine 7b qui ne possède pas de groupement NO_2. Ceci permet d'affirmer que le sommet νsNO_2 glisse bien de 1340 cm^{-1} pour les FF à 1300—1290 cm^{-1} pour les FO. Le maximum νCO glisse donc de 1235 à 1245 cm^{-1} lors de l'ouverture de la molécule 8a (cf. Fig. 3). Mieux que ce faible glissement de fréquence ($\Delta\nu C—O \sim 10$ cm^{-1}) ce sont l'intensification et l'élargissement très importants de la bande d'absorption qui apparaissent caractéristiques de l'ouverture de la molécule de spiropyranne.

Détermination de structure. Les modifications observées entre 1300 et 1200 cm^{-1} dans les spectres des mérocyanines par rapport à ceux des spiropyrannes correspondants peuvent être interprétées en envisageant une augmentation de la polarité de la liaison CO cyclique. Le glissement et l'exhaltation d'intensité du sommet $\nu C=C$ observés dans les spectres des FO (cf. Tableau 2) impliquent une délocalisation électronique. Ceci est en faveur d'une structure de type délocalisée pour l'ensemble des photo-mérocyanines benzothiazoliniques [11].

Caractérisation des mérocyanines. Le spectre infrarouge d'une mérocyanine benzothiazolinique est caractérisé par:

(a) la présence d'un massif intense au-dessous de 1600 cm^{-1} résultant du glissement des absorptions reliées à des vibrations du noyau benzopyrannique. Il est parfois difficile de distinguer dans ce massif les quatre absorptions théoriquement attendues;

(b) la position inchangée par rapport aux spectres des FF du mouvement νaNO_2 ;

(c) la bande forte à 1500 cm^{-1} correspondant au maximum observé vers 1480—1470 cm^{-1} dans les spectres des FF;

(d) l'apparition d'un sommet intense vers 1400 cm^{-1} qui peut être attribué à une vibration $\nu C{\cdots}N$;

(e) la présence d'un massif complexe composé de bandes larges et intenses entre 1300 et 1200 cm^{-1} . L'existence de ce massif s'explique facilement en admettant d'une part un abaissement de fréquence du mode νsNO_2 ($\Delta\nu \sim$ 50 cm^{-1}) et d'autre part une augmentation importante de l'intensité et de la largeur de la bande νC—O intracyclique. Ce massif comporte également les absorptions dues à ν(=C—OR) et à une vibration du noyau benzothiazolinique, ce qui augmente la complexité de cette région du spectre;

(f) la bande vers 1200 cm^{-1} , large et intense, non attribuée.

Application aux composés synthétisés

L'analyse des spectres entre 1700 et 1150 cm^{-1} des composés 1 à 15 est indiquée dans le Tableau 2.

Composés 1, 6, 8 et 13. Les spectres indiquent des FF et des FO pures (cf. Figs. 2 et 3) ce qui est en accord avec leurs origines "purum".

Composés 2. Le spectre de 2a implique une FF pure (origine "purum") tandis que celui de 2b montre la présence d'un mélange FO/FF. Il faut remarquer que le composé 2b peut être obtenu sous forme ouverte "purum". La présence d'un mélange semble donc indiquer que l'échantillon analysé ici n'a pas subi la photoprécipitation et n'est donc pas une FO "purum".

Composés 3. Ils se présentent sous forme de mélange FF/FO à prédominance FF pour 3a. L'examen des spectres de plusieurs échantillons permet de suivre l'évolution de ce mélange FF/FO. Les spectres des différents échantillons 3 montrent tous une bande vers 1740—1755 cm^{-1} attribuable à une vibration de valence νC=O d'une impureté de dégradation.

Composé 4. Il nécessite une synthèse en quatorze étapes dont le rendement global de 1% limite les produits disponibles, de ce fait il n'a pu être étudié qu'en solution dans le chloroforme deutérié sur les échantillons déjà utilisés en r.m.n. Fortement hygroscopique, il n'a pas été isolé sous forme fermée et ouverte. Son spectre montre surtout les bandes caractéristiques d'un spiropyranne (FF). Il présente également des bandes au-dessus de 1700 cm^{-1} , attribuables à des produits de dégradation.

Composé 5a. Il n'est pas photochrome (absence du groupement NO_2 en position 6), ce qui exclut l'obtention de la mérocyanine correspondante. Son spectre est caractéristique d'une FF pure.

Composés 7. Le spectre de 7a correspond à une FF pure. Dans celui de 7b on retrouve les mêmes bandes juxtaposées avec d'autres dues vraisemblablement à la présence de FO, les intensités respectives des deux types de bandes permettant de conclure à la prédominance de la FF. Le spiropyranne 7a est donc peu photochrome, ce qui est en accord avec l'absence d'un nitro en position 6.

Composés 9. Comme les composés 8 ils ne possèdent pas de motifs structuraux =C—O autre que celui mettant en jeu l'oxygène du cycle. Le spectre de 9a (cf. Fig. 4) montre par conséquent entre 1300 et 1200 cm^{-1} une seule bande forte à 1232 cm^{-1} attribuable au mouvement νC—O. Le spectre de 9b, dans la région 1350—1200 cm^{-1}, indique nettement que ce composé est en réalité un mélange FF/FO. On y distingue, en effet, la juxtaposition des bandes dues aux deux formes en présence respectivement, 1337 et 1295 cm^{-1} ($\nu_s NO_2$, FF et FO), 1255 et 1232 cm^{-1} (νC—O, FO et FF). Les spectres de 9a et de 9b montrent par ailleurs vers 1750 cm^{-1} une bande carbonyle pouvant être rattachée à un produit de dégradation.

Composés 10. Le spectre de 10b correspond à une FO pure ou à un mélange à forte majorité FO. Le spectre de 10a montre une nette prédominance de la FF, mais ce composé étant fortement hygroscopique son isolement est délicat [5, 6].

Composés 11. Ils sont également fortement hygroscopiques. Si le spectre de 11b correspond à une FO pure ou dominante, le spectre de 11a, en majorité caractérisé par la présence de bandes attribuables à une FF, présente également des absorptions à 1295 et 1245 cm^{-1} correspondant à la formation de FO. Précisément ce composé à l'état cristallin présente une évolution spontanée à la lumière. Nous avons d'ailleurs, dans un troisième échantillon de ce composé 11, trouvé la superpositon des caractéristiques spectrales d'une FF et d'une FO.

Composé 12b. C'est une mérocyanine permanente, la FF n'ayant jamais été isolée, ni étudiée. Effectivement le spectre ne montre aucune trace de FF.

Composé 14a. Son spectre présente principalement des maximums attribuables à une FF. Vers 1650 cm^{-1} on observe une bande large masquant le sommet C=C résultant vraisemblablement de la présence de nitro-5 orthovanilline comme impureté.

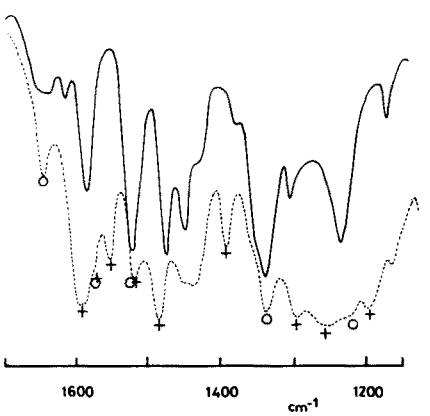

Fig. 4. Spectres infrarouges de 1700—1150 cm^{-1} des composés 9a FF (trait plein) et 9b FO (pointillés). Les sommets marqués ○ correspondent à une forme fermée (FF) et ceux marqués + à une forme ouverte (FO).

Composé 15a. Il correspond à une FF. Une faible bande vers 1650 cm^{-1} indique la présence de nitro-5 orthovanilline. Le spectre du composé que nous supposions être de la FO lors de la synthèse est très précisément la juxtaposition des spectres de la nitro-5 *o*-vanilline et de celui de 15a. Quelques bandes faibles interdisent toutefois d'exclure totalement la présence de faibles quantités de FO.

CONCLUSION

Cette étude spectroscopique i.r. des spiropyrannes benzothiazoliniques et des mérocyanines correspondantes, nous a conduit à mettre au point une méthode d'analyse permettant: (1) de préciser d'une manière simple et rapide la structure des différents produits synthétisés; (2) de contrôler la pureté des FF (fin de synthèse), des FO permanentes (absence de FF) et des FO obtenues par photoprécipitation; (3) de suivre les étapes successives de refermeture thermique et de suivre l'évolution d'un mélange FF/FO vers un composé à majorité FF ou à majorité FO; (4) de déterminer les impuretés (nitro-5 *o*-vanilline, FF dans FO, FO dans FF); (5) de déceler des dégradations en produit carbonylé et éventuellement d'identifier les dégradations sur support solide, ce qui est réalisable par la technique de réflexion totale atténuée (a.t.r.).

BIBLIOGRAPHIE

1 R. Guglielmetti et J. Metzger, Bull. Soc. Chim. Fr., (1967) 2824.
2 R. Guglielmetti, Thèse Sciences, Marseille, 1967.
3 A. Samat, Thèse spécialité, Marseille, 1972.
4 J. Kister, A. Blanc, E. Davin et J. Metzger, Bull. Soc. Chim. Fr., (1975) 2297.
5 J. Kister, Thèse spécialité, Marseille, 1974.
6 J. Kister, Travaux en cours.
7 J. Metzger dans R. J. Cox (Ed.), Non-Silver Photographic Processes, Academic Press, 1975, p. 155.
8 A. Samat, J. Kister, F. Garnier, J. Metzger et R. Guglielmetti, Bull. Soc. Chim. Fr., (1975) 2627.
9 F. Mentienne, A. Samat, R. Guglielmetti, F. Garnier, J. R. Dubois et J. Metzger, J. Chim. Phys., 70 (1973) 544.
10 J. Metzger, Brevet français no 7328538, (1973).
11 M. Guiliano, E. Davin-Pretelli, G. Mille, J. Chouteau et R. Guglielmetti, Helv. Chim. Acta, à paraître.
12 J. Kister, G. Vernin et J. Metzger, Helv. Chim. Acta, Sous presse.
13 E. Davin-Pretelli, Thèse spécialité, Marseille, 1975.
14 M. Guiliano, M. Maguet, G. Mille et R. Guglielmetti, C. R. Acad. Sci. Ser. B., 282 (1976) 13.
15 E. Davin-Pretelli, M. Guiliano, G. Mille, J. Chouteau et R. Guglielmetti, Helv. Chim. Acta, 60 (1977) 215.

Analytica Chimica Acta, 93 (1977) 45—52
©Elsevier Scientific Publishing Company, Amsterdam — Printed in The Netherlands

PRECONCENTRATION OF TRACE ELEMENTS FROM PURE MANGANESE AND MANGANESE COMPOUNDS WITH ACTIVATED CARBON AS COLLECTOR

H. BERNDT, E. JACKWERTH* and M. KIMURA§

Institut für Spektrochemie und angewandte Spektroskopie, Bunsen-Kirchoff-Straße 11, D-4600 Dortmund 1 (Federal Republic of Germany)

(Received 22 April 1977)

SUMMARY

A method is described for separation of traces of Bi, Cd, Co, Cu, Fe, In, Ni, Pb, Tl, and Zn from pure manganese and manganese compounds and their determination by flame a.a.s. After the metal or manganese dioxide samples have been dissolved in acid (and manganese salts in water) the trace elements are complexed with potassium xanthogenate. The solution is then filtered through a small filter paper covered with activated carbon, whereby complex compounds are separated from the matrix. When the charcoal is treated with acid, a trace concentrate is obtained which is nearly free of manganese. The detection limits for the analysis of 10-g samples of manganese metal are <0.5 p.p.m., and for 30-g samples of $MnCl_2 \cdot 4H_2O$ are ≤ 0.1 p.p.m. The relative standard deviation, in general, is lower than 5%.

Manganese metal of relatively pure grade is the basic material for a series of alloys with special electrical characteristics; the electrolytically produced metal is preferred. Impurities are generally in the range of p.p.m. or less. Of the different manganese compounds, MnO_2 and $Mn(NO_3)_2 \cdot 4H_2O$ are of particular technical importance. For the multielement analysis of pure manganese and its compounds, few methods have been described in the literature [1—6].

Without prior separation, the determination of trace elements by emission spectroscopy is difficult or even impossible, because of the large number of lines belonging to the matrix manganese. In flame a.a.s., a high background of non-atomic absorption with a simultaneous considerable decrease of trace signals occurs because of the high salt content of the sample solution. This results in poor sensitivity and detectability. Figure 1 shows the influence of manganese concentrations on the a.a.s. signals of traces of iron; curve I represents signal heights given by solutions of increasing $MnCl_2$ concentrations which contain a constant amount of iron (0.5 μg ml^{-1}). The absorption values of appropriate manganese solutions without measurable amounts of iron (i.e. the "non-atomic" part of the absorbance signals,

§ Present address: Nara Women's University, Department of Chemistry, Nara 630, Japan.

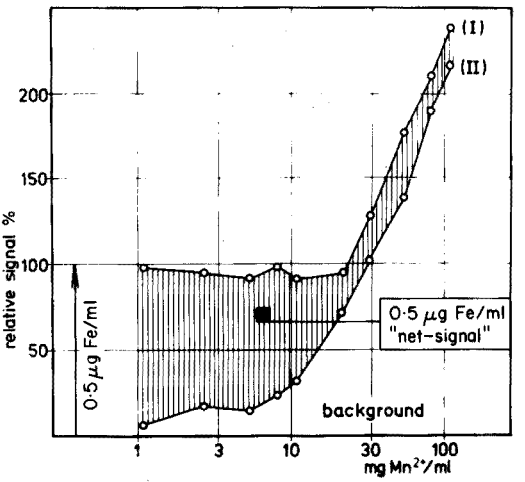

Fig. 1. Dependence of trace signal height (0.5 µg Fe ml^{-1}) on the manganese content of the solutions.

measured with a H_2 lamp) are shown in curve II. The "net signal" arising from the iron content at any manganese concentration can be calculated as the difference of the correlated data from curves I and II. Thus, even a manganese content of 15 mg ml^{-1} almost halves the iron signal. In this concentration range, the background signal (curve II) also begins to increase steeply. Behaviour similar to that for iron is obtained with traces of Bi, Cd, Ni, Pb, Tl, and Zn; the Cu signal is nearly independent of the manganese concentration of the sample solution. The different behaviour of the elements can be explained by the position of their analytical lines within the band spectrum of the matrix [7, 8]. Therefore, if small amounts of different metals have to be determined in samples of manganese, it is essential to transfer the elements into a trace concentrate separated from the matrix as far as possible.

INVESTIGATIONS OF TRACE PRECONCENTRATION

Potassium xanthogenate forms complex compounds with a number of metals which accompany the manganese during its production process. It was shown that the complexes are formed even with high matrix concentrations present in the solution. By sorption on activated carbon as collector, the trace complexes can be easily separated from the sample solutions. For the determination by flame a.a.s. the preconcentrated traces can be dissolved from the carbon by simple treatment with acid. The recovery data for preconcentration depend on the working conditions. Figure 2 shows the pH dependence of trace recovery for preconcentration from 10-g samples of manganese; the optimal working range is pH 6.5—7. At higher pH values manganese hydroxide is precipitated along with the traces and also removed

by the carbon collector causing a considerable decrease in the efficiency of separation from the matrix.

For pH adjustment bromothymol blue is a suitable indicator, its transition range being pH 6.0—7.6. In diluted sample solutions the indicator turns blue only somewhat above pH 7, but bromothymol blue can be used in this procedure for pH adjustment to 6.5—7.0, because its transition range is shifted by a negative salt error to lower pH values.

Figure 3 illustrates the dependence of trace preconcentration on the amount of xanthogenate added. When more than about 100 mg is added, almost all the elements tested are fully recovered. Therefore, in subsequent experiments a fixed amount of 120 mg of reagent was used for complexation of the trace elements. Before the preconcentration process, manganese metal and the insoluble compounds (e.g. MnO_2) must be converted to $MnCl_2$ by dissolution in hydrochloric acid. This is also necessary for $KMnO_4$; otherwise the reagent is oxidized. The surplus of acid is removed by evaporation.

The complexed traces are separated from the sample solution by filtration through a small filter paper covered with a layer of activated carbon. From 10-g samples of manganese, less than 5 mg Mn reaches the trace concentrate. If a nearly quantitative trace preconcentration is assumed, the enrichment factor is calculated to be about $2 \cdot 10^3$. Details of this technique as well as the specification for the activated carbon used have already been reported [9—11].

EXPERIMENTAL

Procedures

Manganese metal. Add 10 ml of water to 10 g of manganese. Add 50 ml of 38% (w/w) hydrochloric acid, and dissolve the metal by warming in a 600-ml glass beaker. Evaporate the sample solution to dryness, and bake the residual salt on a hot plate. [In this process, manganese dioxide is formed at the bottom of the beaker, the amount of which depends strongly on the drying temperature. MnO_2, however, causes a considerable delay in the

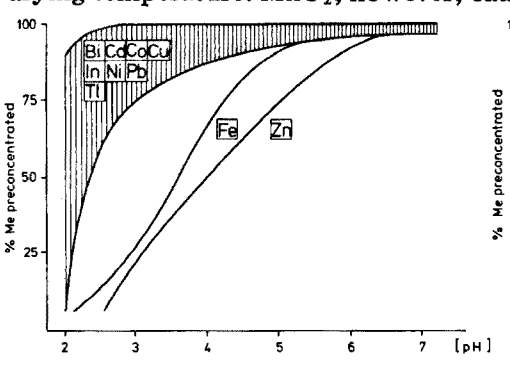

Fig. 2. Dependence of trace recovery on pH.

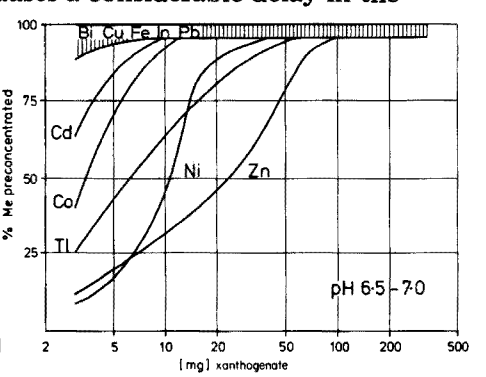

Fig. 3. Dependence of trace recovery on amount of xanthogenate at pH 6.5—7.0.

filtration and also reduces the separation effect. Therefore, it is important to achieve a complete evaporation of the hydrochloric acid without producing a disturbingly high amount of MnO_2. Heating of the salt residue at temperatures not above 150—200°C and allowing a drying time of 3—5 h is a convenient way of obtaining useful results.] Reduce the small amounts of MnO_2 which are inevitably formed by suspending the salt residue in 10 ml of water and 3 ml of 5% (w/v) sulphurous acid; volatilize the surplus of SO_2 by heating the suspension for about 10 min. Dissolve the salt in 250 ml of water; then add 0.2 ml of indicator solution (100 mg of bromothymol blue dissolved in 20 ml of ethanol and diluted to 50 ml with water). If the sample solution is not blue, adjust the pH by addition of some 0.1 M NH_3 solution. After addition of 120 mg of potassium xanthogenate, dissolved in 5 ml of water, set the sample solution aside for about 20 min. Then filter through a filter paper (25 mm in diameter) which is homogeneously covered with 50 mg of activated carbon, using a two-piece suction filter device.

To prepare homogeneously covered filter papers the following simple procedure is recommended: suspend 0.5 g of finely powdered activated carbon (analytical grade; Merck, Darmstadt, Art. No. 2186) in 100 ml of twice-distilled water; prevent sedimentation of the carbon by vigorous stirring. Pipette aliquot parts (10.0 ml) containing 50 mg of carbon, on to the filter placed in the suction device, and apply suction only after the pipette is empty. Thereafter, filter the sample solution with suction.

Dry the carbon filter containing the preconcentrated trace elements for 30 min at 110°C. Then scrape the carbon from the paper into a 25-ml glass beaker, add 1 ml of concentrated nitric acid, and evaporate to dryness. Suspend the residue in 10.0 ml of (1 + 3) HNO_3, and centrifuge. Determine the trace elements in the clear supernatant liquid by flame a.a.s.

For calibration, trace solutions in (1 + 3) HNO_3 are used. Table 1 shows the data for recovery, precision, and detection limits. For evaluation of the standard deviation, trace elements which were insufficient in the sample material applied, were added before dissolution of the samples, in amounts which yielded measurable analytical signals well above the a.a.s. background fluctuations.

Manganese dioxide. Samples (10 g) of MnO_2 are analyzed by the procedure given for manganese metal. The investigated calibration ranges and the trace recoveries are given in Table 2.

Potassium permanganate. Samples (10 g) of $KMnO_4$ are analyzed as described for manganese metal, but to dissolve the sample, 60 ml of 38% HCl is needed.

Because of the smaller salt error (10 g $KMnO_4$ = 3.48 g Mn), the indicator changes its colour at a pH value which is a little higher than observed for samples of 10 g of manganese metal. Therefore, the pH should be adjusted only to a green indicator colour and not to blue (see above). The investigated calibration ranges and the trace recoveries are given in Table 2.

TABLE 1

Analysis of manganese metal

Trace element	Calibration range (p.p.m.)	Recovery (%)	Trace content of the sample[a] (p.p.m.)	s_r (%)	Detection limit (3σ) (p.p.m.)
Bi	0.4—4	>95	4.0	1.7	0.2
Cd	0.05—1	>95	0.5	1.4	0.01
Co	0.1—7	>95	2.1	1.8	0.05
Cu	0.05—7	>95	5.9	3.7	0.02
Fe	2—30	95	12.1	2.2	0.4
In	0.3—5	>95	4.0	2.7	0.2
Ni	0.2—18	>95	4.8	3.9	0.03
Pb	0.3—3	>95	2.5	1.6	0.2
Tl	0.4—4	>95	4.0	4.0	0.2
Zn	0.5—6	>95	4.6	9.4	0.2

[a]Mean and relative standard deviation for $N = 15$.

TABLE 2

Analysis of manganese compounds

Trace element	MnO_2 (10-g samples)		$KMnO_4$ (10-g samples)		$Mn(NO_3)_2 \cdot 4H_2O$ (40-g samples)	
	Calibration range (p.p.m.)	Recovery (%)	Calibration range (p.p.m.)	Recovery (%)	Calibration range (p.p.m.)	Recovery (%)
Bi	0.4—16	>95	0.4—5	>95	0.1—2	92
Cd	0.05—1	>95	0.03—1	>95	0.02—4	>95
Co	0.2—3	⩾95	0.2—2	>95	0.05—2	>95
Cu	0.1—4	⩾95	0.3—4	>95	0.03—3	>95
Fe	40—100	85	1—15	>95	0.5—8	>95
In	0.3—5	>95	0.3—5	>95	0.2—2	>95
Ni	0.5—30	>95	0.2—2	>95	0.1—5	>95
Pb	0.4—4	⩾95	0.3—5	>95	0.1—3	95
Tl	0.4—4	>95	0.4—4	⩾95	0.1—1.5	>95
Zn	10—40	85...90	5—20	90	0.2—1.5	88

Manganese(II) chloride tetrahydrate. Samples (30 g) of $MnCl_2 \cdot 4H_2O$ are dissolved in 250 ml of water, 0.2 ml of bromothymol blue is added and the pH is adjusted (to a blue colour) with 0.1 M NH_3. The samples are analyzed as described for manganese metal. Table 3 contains values for recovery, precision, and detection limits.

Manganese(II) nitrate tetrahydrate. Samples (40 g) of $Mn(NO_3)_2 \cdot 4H_2O$ are analyzed by the procedure for manganese(II) chloride. The calibration ranges investigated and trace recoveries are given in Table 2.

TABLE 3

Analysis of $MnCl_2 \cdot 4H_2O$

Trace element	Calibration range (p.p.m.)	Recovery (%)	s_r (%)	Trace contents of the sample $N = 15$ (p.p.m.)	Detection limit (3σ) (p.p.m.)
Bi	0.1—2	>95	2.7	1.5	0.05
Cd	0.02—0.4	>95	4.3	0.1	0.003
Co	0.06—2	>95	2.8	0.3	0.02
Cu	0.03—3	>95	4.5	0.3	0.01
Fe	0.6—10	>95	3.5	2.0	0.1
In	0.2—2	>95	3.2	1.5	0.1
Ni	0.1—5	>95	3.6	0.5	0.02
Pb	0.1—3	>95	2.0	0.5	0.04
Tl	0.1—1.5	>95	4.1	1.0	0.05
Zn	0.2—1.5	⩾95	6.3	1.0	0.1

INVESTIGATION OF THE HOMOGENEITY OF TRACE DISTRIBUTION IN ELECTROLYTICALLY PRODUCED MANGANESE METAL

In cases of inhomogeneous distribution of trace elements, it is essential that the samples to be analyzed are representative of the whole material. In general, the probability of inhomogeneity increases with decreasing trace contents. During the development of the preconcentration technique reported above, the distribution of the metallic trace impurities in electrolytically produced manganese was found to be very inhomogeneous. The sample material was metal flakes (about 2 mm thick and 0.5—2 cm in diameter) from different sources. As an example, Fig. 4 shows the fluctuations of the a.a.s. signals when 10-g samples of metal flakes or of homogenized material (500 g of flakes powdered) were analyzed.

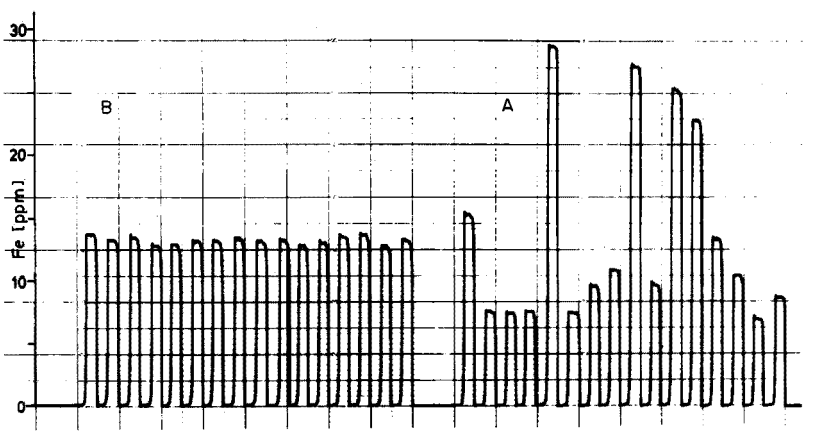

Fig. 4. Iron signal for 10-g samples of manganese flakes (A) and homogenized powdered material (B).

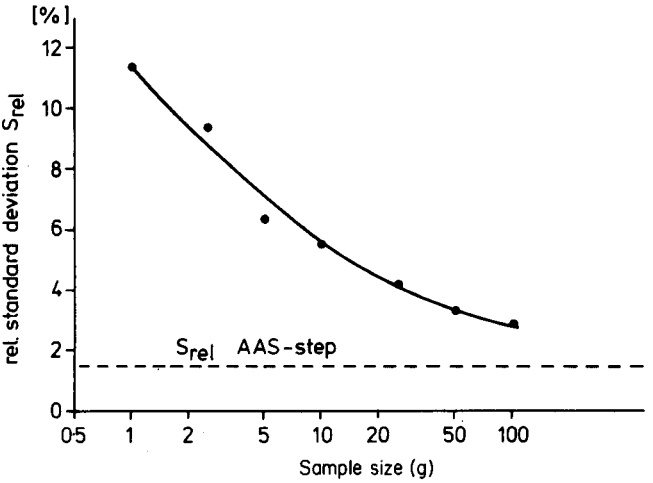

Fig. 5. Dependence of the standard deviation for the zinc determination on increasing size of manganese samples.

Table 4 lists the relative standard deviations for some elements analyzed by the recommended preconcentration and determination technique: the s_1 data relate to 10-g samples of flakes, and the s_2 data to equal sample amounts from material powdered in amounts of 500 g. According to the test for statistical significance, the standard deviations s_1 and s_2, for each of the elements investigated, are significantly different because of the inhomogeneous trace distribution in the flakes ($s_1/s_2 > 1.58$; 95% statistical probability $s_1/s_2 > 1.92$; 99%) [12].

Manganese flakes containing about 10 p.p.m. of zinc were used to examine the dependence of the standard deviation of the analytical method on the sample weights taken. The relatively high zinc content enabled a determination by flame a.a.s. without preconcentration. The standard deviation of this step was found to be $s_r = 1.5\%$ (10 μg Zn, 1 g Mn in 20 ml of sample solution; $N = 10$). Corresponding to the sample weights, the solutions were

TABLE 4

Standard deviations for the analysis of manganese flakes and homogenized material (For both types, the deviations were calculated from the results for fifteen 10-g samples).

Trace element	Flakes	Powdered material	s_1/s_2
	s_1	s_2	
Co	9.0	1.8	5.0
Cu	49	3.7	13.2
Fe	57	2.2	25.9
Ni	9.3	3.9	2.4
Pb	6.1	1.6	3.8
Zn	17	9.4	1.8

adjusted in volume to keep the manganese concentration constant within the whole series. The expected decrease in data fluctuations with increasing sample weights is illustrated in Fig. 5. It is interesting that for each zinc determination, samples of more than 100 g are necessary to ensure that the part of the standard deviation caused by the inhomogeneity of sample material can be neglected within the precision of the analytical results.

Investigations of this kind demonstrate that in the analysis of high-purity materials, even sample weights in the range of 10 g and higher should not be considered unchecked to be representative of the whole material.

The authors gratefully thank Miss E. Reiter for her comprehensive assistance.

REFERENCES

1 V. N. Muzgin and L. A. Gladysheva, Zavod. Lab., 34 (1968) 1076.
2 J. Lovasi and L. Zombory, Microchem. J., 11 (1966) 277.
3 T. Kawashima, M. Osawa, Y. Mochizuki and H. Hamaguchi, Bull. Chem. Soc. Jpn., 34 (1961) 701.
4 J. W. Mellichamp, Anal. Chem., 26 (1954) 977.
5 J. J. Vink, Analyst, 95 (1970) 399.
6 V. A. Job, S. B. Kartha, G. Krishnamurty and S. Gopal, Z. Anal. Chem., 271 (1974) 26.
7 R. Mavrodineanu and H. Boiteux, Flame Spectroscopy, Wiley, New York, 1965.
8 H. Berndt and E. Jackwerth, Z. Anal. Chem., 283 (1977) 15.
9 E. Jackwerth, J. Lohmar and G. Wittler, Z. Anal. Chem., 266 (1973) 1.
10 E. Jackwerth, Z. Anal. Chem., 271 (1974) 120.
11 E. Jackwerth and H. Berndt, Anal. Chim. Acta, 74 (1975) 299.
12 H. Kaiser and H. Specker, Z. Anal. Chem., 149 (1956) 46.

Analytica Chimica Acta, 93 (1977) 53—60
©Elsevier Scientific Publishing Company, Amsterdam — Printed in The Netherlands

FLAME-ATOMIC ABSORPTION ANALYSIS FOR TRACE METALS AFTER ELECTROCHEMICAL PRECONCENTRATION ON A WIRE FILAMENT

WALTER LUND*, YNGVAR THOMASSEN and PER DØVLE

Department of Chemistry, University of Oslo, Blindern, Oslo 3 (Norway)

(Received 4th April 1977)

SUMMARY

To avoid unspecific light losses in the atomic absorption analysis of trace metals in the presence of a high concentration of salts, electrochemical preconcentration on a wire filament is employed, prior to flame atomization. The elements in question are electrolyzed on to a platinum spiral filament which is then heated in an air—acetylene flame. A quartz tube is placed above the filament, to increase the sensitivity of the method. The separation technique is simple and non-destructive; a sample volume of 5—20 ml and an electrolysis time of 2—5 min are recommended. Because of the relatively low filament temperature, the method is limited to elements which are readily volatilized such as silver, bismuth, cadmium, mercury, lead, selenium, tellurium, thallium and zinc. For most elements, the detection limits are of the same order of magnitude as those of the "Delves cup" technique.

Electrochemical preconcentration techniques can be used in atomic absorption analysis of trace metals, to eliminate interferences from high concentrations of salts, which would otherwise give rise to unspecific light losses. In one version of the technique [1] the metal in question is deposited electrolytically on to a thin metal wire and is then atomized by electrical heating of the wire. This method has been applied successfully to the determination of cadmium in sea water [2] and urine [3]. In another approach, the metals are preconcentrated on a graphite rod, which is dried and ground, and a portion of the graphite powder is finally analyzed in a graphite furnace [4]. These techniques utilize flameless atomization of the metals, after the electrochemical preconcentration step. However, flameless atomization is not necessarily the technique of choice; the electrical heating of a wire filament within an unheated absorption cell results in a marked temperature gradient around the filament, and the use of a furnace to increase the temperature within the cell makes the construction of the flameless system more complicated and expensive.

As an alternative to flameless atomization, a normal flame can be used for this purpose. In a flame the sample will be efficiently atomized and maintained in the atomic state once it has been volatilized. In this paper the flame atomization of metals after electrochemical preconcentration on a

platinum spiral is described. The detection limits obtained are compared with those of the "Delves cup" technique.

EXPERIMENTAL

Apparatus

A double-beam atomic absorption spectrophotometer (Perkin-Elmer 400) equipped with a three-slot burner head and a Perkin-Elmer 159 recorder were used. The filament was made of a spiral-wound 0.5-mm platinum wire (99.999%, Koch-Light, Ltd); the design of the filament is shown in Fig. 1. The filament was mounted in a holder similar to that used for the Delves cup technique. A quartz absorption tube with nickel supports was placed in the optical path with the circular opening in the cylinder wall precisely above the filament wire. The diameter of the opening was slightly larger than that of the filament.

The electrochemical preconcentration was done by controlled-potential electrolysis with a home-made potentiostat. The platinum filament served as the working electrode, the reference electrode was a saturated silver/silver chloride electrode (Metrohm EA 427), and the counter electrode was a platinum coil. A Metrohm EA 880 vessel was used as electrolytic cell. The samples were stirred with a magnetic stirrer during the electrolysis.

Reagents and solutions

The metal solutions were prepared either from high-purity metals dissolved in nitric acid, or from analytical-grade nitrate, sulphate or phosphate salts. Solutions with a concentration below 10^{-3} M were prepared just before use. The potassium chloride used as supporting electrolyte, and the acids and sodium acetate used for adjusting the pH of the samples were of Suprapur quality (Merck). The water used was deionized with an ion-exchange resin and distilled.

Most of the experiments were carried out on spiked sea water samples. The sea water was collected from the Oslofjord, filtered through 0.45-μm Millipore filters, acidified to pH 2 with hydrochloric acid, and stored in a 5-l polythene bottle.

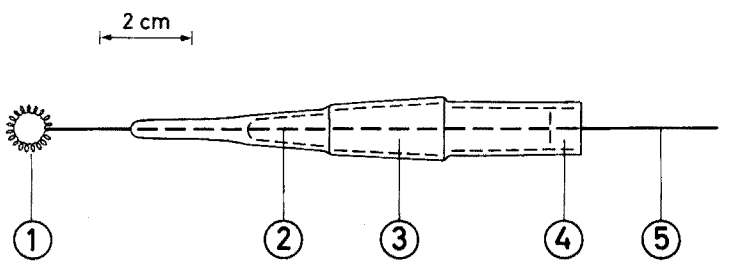

Fig. 1. Filament electrode. 1, Platinum spiral, made from a 0.5 mm wire; 2, point where the Pt and Cu wires are melted together; 3, B14 joint; 4, Teflon stopper; 5, copper wire.

Procedure

Adjust the pH of the sample solution to ca. 5 by adding an acetate buffer, and electrolyze a 25-ml aliquot for 2 min at −1.0 V vs. Ag/AgCl. At the end of the deposition period, remove the filament electrode from the electrolytic cell and then disconnect the electrical circuit. Rinse the electrode with distilled water and acetone, and let it dry in the air before placing it in the holder, which has been adjusted to give the optimal position of the filament relative to the burner head and the quartz absorption tube. Move the filament into its pre-adjusted position in a lean air—acetylene flame, and record the atomic absorption signal. Add a known amount of the element in question, repeat the deposition and atomization steps, and finally calculate the concentration according to the standard addition procedure.

RESULTS AND DISCUSSION

Design of the filament

In our previous work with wire filaments, the deposited metals were atomized by electrical heating of the wire. This flameless approach imposed severe restrictions on the dimensions of the filament wire; in order to obtain a sufficiently high filament temperature with a simple and cheap power supply (e.g. batteries) a wire diameter of ca. 0.2 mm had to be used. With such a thin wire the spiral must be relatively short to avoid deformation of the filament during its use [1]. In this work the diameter and length of the wire were increased significantly in order to obtain improved sensitivity; the amount of metal deposited is proportional to the area of the filament. A diameter of 0.5 mm was chosen to make a reasonably robust construction, which also had a relatively fast temperature response. With thicker wires the temperature of the filament increased slowly after the filament was moved into the flame. The shape and dimensions of the filament are such that it fits into commercial Delves cup microsampling equipment.

The choice of filament material warrants some comments. Metals like platinum, iridium, tungsten and tantalum have all been used as filament materials in atomic absorption analysis. Platinum has the disadvantage of a relatively low melting point (1769°C), but this metal is less susceptible to deactivation by mineral acids during electrolysis than tungsten [1, 3]. Tantalum was found to be similar to tungsten in this respect. The choice of iridium could have been a useful compromise, had this metal been less hard and brittle; repeated unsuccessful attempts were made to coil thin iridium wires.

A platinum filament of the type described here has a very long life, compared with the Delves cup and Sampling boat, which must be replaced after 20—50 determinations. The filament will also last longer than the thin tungsten or platinum spirals which are used for flameless atomization [1—3].

The purity of the platinum wire is of importance, inasmuch as low-purity wires may contain trace amounts of certain metals. Thus a 99.99% wire was found to contain significant amounts of silver and zinc. Therefore, only high-purity platinum wires are recommended for general use.

The preconcentration step

The choice of deposition potential depends on the metal which is of interest. The more negative the potential, the more elements are deposited on the filament. However, the accessible potential region is restricted on the cathodic side by hydrogen evolution, the rate of which becomes significant at potentials more negative than −1.0 V. Normally a potential of −1.0 V vs. Ag/AgCl (corresponding to −1.04 V vs. a saturated calomel electrode) was used in this work. If the solution is not well buffered, the pH around the working electrode may increase during electrolysis and eventually give rise to precipitation of metal hydroxides. The addition of an acetate buffer is therefore recommended.

The electrochemical preconcentration technique is of particular interest for the analysis of samples which contain a high concentration of non-volatile salts, like alkali and alkaline earth chlorides. Instead of being a source of interferences, these salts, which are not deposited at the electrode, have a beneficial effect on the preconcentration step; they serve as supporting electrolyte for the electrolysis. If the ionic strength of the sample is very low, as may be the case for fresh waters, a small amount of an electrochemically inactive salt or a buffer should be added to the sample. However, in such cases it may be better to use the Sampling boat or Delves cup technique. Most experiments in this work were carried out with spiked sea water samples.

The electrolysis was usually continued for 2—5 min; stirring was used to increase the mass transport to the electrode. The sensitivity of the method is increased when a longer deposition time is used; the analytical signal is approximately a linear function of the deposition time, provided that the sample volume is not too small. In the latter case a curved relationship is obtained.

The electrochemical preconcentration technique is essentially non-destructive when a short electrolysis time is used; the amount of metals deposited on the filament in a few minutes from a 25-ml sample is so small that it does not alter the composition of the sample significantly. This may be an advantage compared to for instance solvent extraction procedures. However, when a large filament area, a small sample volume and a long deposition time are used, the sample will be partially depleted during the electrolysis.

The rate of deposition of a given element is a function of many experimental parameters, some of which, like the surface conditions of the electrode and the chemical composition of the sample, are not easily controlled. Therefore, the standard addition procedure should always be

used for the determination of a given element in an unknown matrix. This procedure involves a second electrolysis after the addition of a standard to the electrolytic cell. The standard should be relatively concentrated and added in microlitre amounts, to avoid altering the composition of the sample and the total volume significantly; the effective electrode area depends on the volume of sample in the cell.

The method described here cannot handle micro-samples directly; because of the shape of the filament electrode a sample volume of at least 5 ml was normally needed to carry out the electrolysis. Smaller samples can, however, be diluted to a suitable volume for analysis, provided that the metal concentration is not too low. A sample volume of 50 ml was mostly employed in this work.

The atomization step

The electrolytic deposition step being completed, the filament electrode is mounted in a holder, and moved into the air—acetylene flame. The platinum spiral is positioned directly below the hole in the quartz absorption tube. The position of the light beam relative to the filament was found to be less critical than in the case of flameless atomization; in the latter case the position of the filament had to be adjusted very carefully [1]. A lean flame was used to avoid the deposition of carbon particles on the filament and the walls of the absorption tube. Obviously the temperature of the filament did not reach that of the flame, or the filament would have melted (flame temperature ca. 2450°C, melting point of platinum 1769°C). Attempts were made to use the hotter nitrous oxide—acetylene flame, but in this case the platinum filament did melt.

The atomization technique described here is in some ways similar to the Delves cup microsampling technique. Like this technique, the present method is limited to elements which are readily volatilized, because of the relatively low filament temperature obtained. The platinum spiral has a faster temperature response than the cup, and it probably also reaches a somewhat higher temperature. Ward et al. [5] claim that the temperature of the cup is ca. 1000°C in an air—acetylene flame, and 1500°C in a nitrous oxide—acetylene flame. However, we found that the platinum filament melted (m.p. 1769°C) in a nitrous oxide—acetylene flame; therefore, the temperature of the platinum spiral in the air—acetylene flame may also be somewhat higher than the 1000°C indicated above for the cup.

For a microsampling cup technique, the height of the atomization signal of a given element may be influenced by the composition of the sample matrix. At low filament temperatures, the peak height will depend on the rate of volatilization of the metal compounds which are formed in the cup during the drying step. For example, the lead halides will have a higher vaporization rate than lead oxide and lead metal [5]. This factor is also of interest when the electrochemical approach is used, although this technique gives deposits in which the metals are normally present in elemental

form. When the pure metals are less readily volatilized than the metal salts, the electrochemical technique may lead to decreased sensitivity compared to the microsampling technique.

No doubt it is the relatively low filament temperature, and thus the low rate of volatilization, which restricts the use of the flame-assisted techniques discussed here. Once the elements have been brought into the flame, they are efficiently atomized and maintained in the atomic state by the hot flame gases. In this respect the flame-assisted methods may be considered superior to the flameless techniques. The use of an absorption tube above the filament represents a further improvement; in this way the sample atoms are kept for a prolonged time in the optical path, thus improving the analytical sensitivities and detection limits of the flame-assisted techniques. For example, the peak height for lead was increased by a factor of six when the absorption tube was used.

In this work the following nine elements were studied: silver, bismuth, cadmium, mercury, lead, selenium, tellurium, thallium and zinc. The atomization signals for cadmium, mercury and zinc were very sharp and narrow, as illustrated in Fig. 2a. The other elements gave absorption peaks with some tailing at the end of the signal (Fig. 2b). The tailing may partly be explained by the diffusion of the sample vapour from the ends of the absorption tube; however, similar curves were observed even in the absence of an absorption tube.

Copper could not be detected by the present method. As pointed out by Ward et al. [5] this is probably explained by the slow vaporization of the metal from the filament, rather than by the poor atomization in the gas phase; this conclusion is supported by the fact that copper is easily determined in an air—acetylene flame when a direct nebulization system is used.

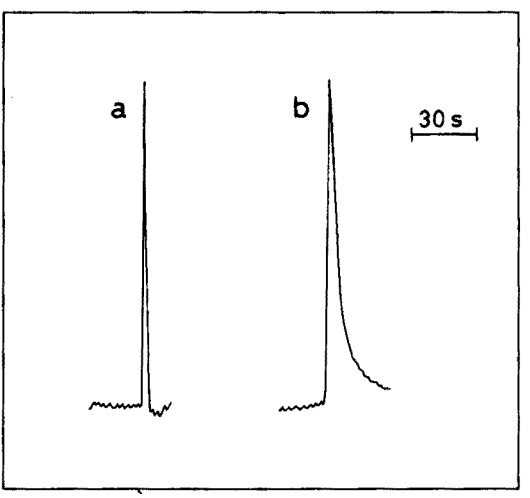

Fig. 2. Typical atomic absorption signals obtained with the platinum wire filament after electrochemical preconcentration.

When samples with a complex matrix are analyzed with a microsampling technique, background correction is usually essential, to compensate for unspecific light losses. The electrochemical approach eliminates the need for background correction, because the salts which normally give rise to unspecific absorption are not deposited on the filament electrode.

Detection limits

The detection limits (signal: noise, 2:1) for the nine elements which were examined are given in Table 1. All experiments were carried out with sea-water samples which were spiked with the elements in question. Each value refers to a 2-min electrolysis time. Obviously the detection limits can be further improved by using longer deposition times; if a sample volume of 25 ml is used, the detection limits may be lowered to one tenth of the values given in Table 1, if the electrolysis is continued for 20—30 min. The detections limits for the Delves cup technique, determined by Kerber and Fernandez [6], are also given in Table 1. These values refer to a sample volume of 100 μl, which is the maximum capacity of the cups; in practice, smaller volumes are normally employed (the Sampling boat, which can take a sample volume of up to 1 ml, will give better detection limits for some of the elements). The Delves cup values are valid only for simple aqueous solutions, whereas the detection limits for the present technique were determined in a sea-water matrix (salinity ca. 34 g l^{-1}). Even so, the values given for the electrochemical method compare favourably with the microsampling technique.

Superior detection limits were obtained for thallium, selenium and tellurium; the poor sensitivity for the last two elements in the Delves cup is probably explained by the formation of relatively non-volatile nickel selenide and nickel telluride in the cup and tube, which are both made of nickel. The stabilization of selenium and tellurium with nickel has recently been discussed by Ediger [7].

TABLE 1

Detection limits (in μg l^{-1}) of the present technique with a 2-min electrolysis, and of the Delves cup technique (from [6])

Element	Wavelength (nm)	This technique	Delves cup
Ag	328.1	1	1
Bi	223.1	150	20
Cd	228.8	0.1	0.05
Hg	253.7	100	100
Pb	283.3	5	1
Se	196.0	5	1000
Te	214.3	50	300
Tl	276.8	1	10
Zn	213.9	0.1	0.05

The electrochemical method appears to be slightly less sensitive to lead than the Delves cup technique. The reason for this difference is possibly explained by the lower vaporization rate of elemental lead compared to that of the lead salts, as discussed above.

The poorest sensitivity was found for bismuth; however, the analytical procedure was not optimized for this metal. Presumably the deposition rate of bismuth at a platinum electrode is relatively low, as indicated by the work of Lingane and Jones [8].

In general, the deposition rate, and thus the detection limit, of a given element may be influenced by the chemical composition of the sample. For instance, a fourfold increase in peak height was observed for cadmium, when an acetate buffer was added to the sea-water sample. Therefore detection limits differing from those given in Table 1 may be expected for certain types of samples.

Reproducibility

The reproducibility of the method is influenced by many experimental parameters which are related to the deposition and atomization steps, and it depends also on the sample composition. Normally a standard deviation of ca. 10% was obtained, although both higher and lower values were encountered. A reproducibility of this order of magnitude is usually to be expected when samples with a complex matrix are analyzed for trace metals at the p.p.b. level.

Applications

As already mentioned, the main advantage of the electrochemical preconcentration technique is the elimination of unspecific light losses when samples containing a high concentration of salts are analyzed. Typical samples in this category include sea water, urine, and biological as well as inorganic materials which are dissolved or decomposed in acids or fused-salt media. The method is limited to the more volatile elements; however, it can be seen from Table 1 that the list includes many of the toxic metals which are of particular concern in the present-day discussion of environmental pollution.

REFERENCES

1 W. Lund and B. V. Larsen, Anal. Chim. Acta, 70 (1974) 299.
2 W. Lund and B. V. Larsen, Anal. Chim. Acta, 72 (1974) 57.
3 W. Lund, B. V. Larsen and N. Gundersen, Anal. Chim. Acta, 81 (1976) 319.
4 Y. Thomassen, B. V. Larsen, F. J. Langmyhr and W. Lund, Anal. Chim. Acta, 83 (1976) 103.
5 A. F. Ward, D. G. Mitchell and K. M. Aldous, Anal. Chem., 47 (1975) 1656.
6 J. D. Kerber and F. J. Fernandez, At. Absorpt. Newsl., 10 (1971) 78.
7 R. D. Ediger, At. Absorpt. Newsl., 14 (1975) 127.
8 J. J. Lingane and S. L. Jones, Anal. Chem., 23 (1951) 1798.

Analytica Chimica Acta, 93 (1977) 61—67
©Elsevier Scientific Publishing Company, Amsterdam — Printed in The Netherlands

A SIMPLE AND RAPID HYDRIDE GENERATION—ATOMIC ABSORPTION METHOD FOR THE DETERMINATION OF ARSENIC IN BIOLOGICAL, ENVIRONMENTAL AND GEOLOGICAL SAMPLES

R. G. SMITH and J. C. VAN LOON*

Department of Geology, University of Toronto MSSIAI (Canada)

J. R. KNECHTEL and J. L. FRASER

Wastewater Technology Centre, Burlington (Canada)

A. E. PITTS and A. E. HODGES

Mineral Research Division, Ministry of Natural Resources, Toronto (Canada)

(Received 8th February 1977)

SUMMARY

An inexpensive 50-ml disposable (hypodermic) syringe is used as the arsine generation vessel. The arsine is passed into a 10-cm long, 10-mm i.d. electrically heated silica tube atomizer with nitrogen carrier gas. Excess of hydrogen is burned off in a hydrogen diffusion flame at the ends of the tube. Samples containing appreciable silica are fused with KOH—MgO, while organic samples are digested with H_2SO_4—H_2O_2. Parameters affecting the determination of arsenic as arsine have been investigated. Collaborative results on a variety of standard reference materials agree well with literature values. The advantages of the proposed method are that it is sensitive, selective, fast, simple, inexpensive, precise and accurate.

Numerous hydride generation—atomic absorption methods have been reported for the determination of arsenic. Most of these, including the automated procedures, are time-consuming and require expensive and relatively complex hydride generation apparatus. In manual methods, the equipment generally consists of a glass hydride generation flask connected to a gas reservoir, reagent delivery tubes and nebulization system by means of a number of stopcocks. Van Loon and Brooker [1] proposed a simplified method for arsine generation requiring only a disposal plastic syringe and some polyethylene tubing. The method outlined [1] gave good results for some samples but low values for those high in organic matter, e.g. NBS Orchard Leaves. An exhaustive study of the proposed arsine method with a syringe was therefore made by three independent laboratories working in the fields of geochemical, environmental and biological analyses. In this paper, procedures are outlined which will allow rapid and accurate analysis of a wide range of samples. Hydride generation and injection time per sample is 25—30 s, which is considerably faster than other published methods.

EXPERIMENTAL

Apparatus

Arsine was generated in a 50-ml, R-1314 (Becton and Dickinson) syringe fitted with a Yale no. 20 stainless steel needle. Each syringe lasts for 100—200 injections.

The procedure can be used with most atomic absorption (a.a.s.) equipment; Perkin-Elmer Models 305B, 503 and 603 and a Varian-Techtron Model AA6 were used here. Automated background correction was used in each case. In two of the three laboratories, output was obtained on a potentiometric recorder. The preferred line source was a Perkin-Elmer electrodeless discharge lamp, but arsenic hollow-cathode lamps may also be employed. The 193.7-nm As resonance line was used. Other instrument parameters were similar to those recommended by the manufacturer.

An electrically-heated silica absorption cell was employed. The preferred tube was 10 cm long by 10 mm i.d. wound with Chromel C resistance wire (0.7 ohm/ft.); windings must be close to, but not touching, each other. Asbestos insulation (8-mm thick) was applied over the windings. An ordinary Variac was used to power the furnace. The tube must be heated to 700—800°C for effective atomization of arsenic.

A silica inlet tube 10 cm long by 5 mm i.d. was joined at right angles to the center of the atomizer. Polyethylene tubing connected this tube to the nitrogen and hydrogen gas supplies. Nitrogen and hydrogen gases were passed through the tube at flow rates of 225 and 75 ml min^{-1}, respectively. Nitrogen is used as a carrier gas for AsH_3. Hydrogen is necessary to prevent sudden wide variations in conditions inside the tube during the injection of the H_2—AsH_3 mixture. The hydrogen burns quietly at the ends of the heated tube.

The absorption cell was fastened to the burner mount of the a.a.s. unit. This arrangement simplifies alignment of the tube in the optical beam.

An aluminum block (7.6-cm thick) with holes (2.54-cm diameter, 6.2-cm depth) was used to hold tubes for acid decomposition. Pyrex no. 7900 calibrated 50-ml Folin digestion tubes (O. H. Johns Scientific) were used.

Reagents and solutions

A 2% (w/v) solution of sodium borohydride was prepared by dissolving the appropriate weight in distilled water containing 1 pellet of KOH for every 100 ml of solution. The cloudy liquid was pressure-filtered through 0.45-μm porosity membranes. The solution could then be used for 1—2 weeks. It is important to purchase $NaBH_4$ supplied in glass containers (e.g. Fisher Certified); sodium borohydride supplied in metal containers was often contaminated with tin.

Commercially available hydrochloric acid contains varying amounts of arsenic; Fisher ACS reagent-grade was found to be best.

Arsenic standard and working solutions

To prepare the arsenic standard (1000 $\mu g\ ml^{-1}$), dissolve 1.320 g of primary standard arsenic(III) oxide in 25 ml of 20% (w/v) KOH solution, neutralize to a phenolphthalein end-point with 20% (v/v) H_2SO_4 solution, transfer to a 1-l flask, adding enough H_2SO_4 to give a final concentration of 1% (v/v), and dilute to the mark with distilled water. To produce a stable stock solution, transfer 100 ml of the arsenic(III) solution to a 1-l flask, add 10 ml of 15 M HNO_3, 2 ml of 18 M H_2SO_4 and 2 g of $K_2S_2O_8$, digest to white SO_3 fumes, cool and dilute to 1 l with water. This arsenic(V) stock solution (100 $\mu g\ ml^{-1}$) is stable for at least three months.

Working solutions of 1, 2, 5, 10, 20, 50, 75, and 100 $\mu g\ l^{-1}$ are prepared to contain 10% HCl; these are stable for at least one month.

Sample preparation

(A) Fusion method. This method should be used for samples containing appreciable siliceous material when total arsenic is required. The procedure is adapted from a method described by Lynch and Mihailov [2].

Place the sample (0.1—0.2 g) in a 30-ml nickel crucible. If the sample contains appreciable organic matter, add an equal weight of MgO. Add 1—2 drops of ethanol, mix to a slurry with several drops of water, and swirl to homogenize the mixture. Add about 10 KOH pellets (ca. 1 g) for each 0.1 g of sample, and dry the contents of the crucible at 100°C. Fuse the samples in a muffle furnace at 550°C for 15 min. After cooling, leach the fusion cake with small volumes of water, transferring the liquid to a 50-ml volumetric flask. Remove any adhering solid with a rubber policeman. After the crucible has been completely rinsed, add 11 M HCl to the solution to give a final acid concentration of 10% (v/v), dilute to volume and mix. Allow any sediment to settle before the hydride generation step. Filtration may be necessary for some persistently turbid samples. Nickel crucibles must be cleaned between runs with steel wool followed by soap and water.

(B) Acid digestion. This method should be used for organic samples without appreciable silica or when only mineral acid-extractable arsenic is required. The procedure is adapted from a method by Bishop et al. [3]. Several samples can be digested simultaneously.

Place the samples in 50-ml digestion tubes marked at the 25- and 50-ml levels. Moisten the samples with a few drops of ethanol. Place the tubes in the aluminum block and add 3 ml of 18 M H_2SO_4. Heat the block on a hot plate at 350°C, and run in 0.5-ml aliquots of H_2O_2 occasionally until the solutions clear. Cool the tubes and contents, add 5 ml of 11 M HCl and dilute the solutions to the 50-ml mark with water.

Hydride generation procedure

Draw standards and sample solutions containing 1—500 μg of arsenic in 10% hydrochloric acid into the syringe to the 5-ml mark, being careful to exclude air. Then dip the needle into a 2% $NaBH_4$ solution and withdraw

the plunger in one quick motion to the 50-ml mark; ca. 1.5 ml of $NaBH_4$ solution is drawn into the syringe. Invert the syringe; seal and hold the needle opening with a tissue. After shaking for 20 s, insert the needle through the tygon tubing at a point 5—8 cm from the end of the glass tube on the atomizer and inject the arsine into the furnace, slanting the syringe to prevent any solution from being injected into the heated tube. Place a 3.18-cm length of thick-walled rubber tubing (1.91-in diameter) on the ribs of the plunger to prevent the plunger from returning to the zero position; this permits an even injection rate without concern for solution entering the furnace. Monitor the arsenic peaks on a recorder. Remove the needle from the tygon tubing and discard the spent sample mixture. Rinse the syringe between determinations with 10% HCl. This latter step was found to be unnecessary for most samples.

RESULTS AND DISCUSSION

Sample preparation

The fusion and acid decomposition procedures given were subjected to exhaustive testing. They were preferred to several other methods [4—11] recommended in the literature. Most of the above procedural steps were established on the basis of extensive investigation, and should be adhered to very closely.

The fusion procedure decomposes most siliceous materials. It should be used when total arsenic is required even with samples containing only small amounts of silicate. Although nickel is a serious interference in the hydride generation step, nickel crucibles were employed. If fusion temperatures are kept to 550°C, quantitative decomposition is obtained without significant interference from nickel released from the crucible. The fusion should also be used on samples likely to contain large amounts of materials which form sulfate precipitates (e.g. Ba, Sr, Ca and Pb).

Steel wool must be used to clean crucibles. Other methods such as acid washes cause too much nickel to be released in the next fusion. If acid cleaning is periodically necessary, a blank fusion should be done before the crucible is re-used. Fusion time is not critical; 15 min is the optimum for decomposition at 550°C without excessive release of nickel.

The acid digestion procedure is faster and can be employed for organic samples devoid of siliceous material. This method is also useful when only mineral acid-extractable arsenic is required.

Hydride generation procedure

The hydride generation procedure might be suspected of being subject to large operator error, but the technique can easily be mastered with 1—2 h practice. Subsequently, a standard deviation of 2—5% is commonly obtained.

The borohydride—sample mixture in the syringe must be shaken for 20 s, to allow the hydride reaction to proceed to completion. Maximized arsenic signals, minimum interference and better reproducibility are thus obtained.

The arsenic signals for different nitrogen—hydrogen ratios and total flow rates were measured. Flow meters of good quality were required to reproduce and maintain uniform flame conditions. The hydrogen flow rate was set at 20, 75 and 250 ml min^{-1}. Nitrogen flow rates were adjusted to give 1:1. 3:1 and 10:1 nitrogen—hydrogen flow ratios. A low total flow rate yielded good sensitivity but noisy baselines, broader peaks and large reagent blank signals. Larger total flow rates yielded better linearity and flatter baselines but less sensitivity because of the cooling effect of the gas flow and the decreased residence time of the arsine in the furnace. Variation of the nitrogen—hydrogen ratio had little effect on the sensitivity and linearity. A hydrogen flow of 75 ml min^{-1} and a nitrogen flow of 225 ml min^{-1} were selected. Hydrogen was necessary to reduce the reagent blank signal to prevent an annoying "popping" produced by ignition of the injected hydrogen in the furnace.

Concentrations of 1, 2, 3, 4 and 5% $NaBH_4$ all yielded similar signals when pure arsenic solutions were analyzed. When interferences were present, 1—2% $NaBH_4$ was best. This concentration range was in excess of the amount required to react with arsenic and other constituents which consume reductant. Higher concentrations resulted in the reduction of some elements to the metal, so that arsenic could be trapped in the precipitate.

Peak heights as obtained on a potentiometric recorder were used by two of three participating laboratories. The other laboratory used digital readout. Peak area was found to give slightly better sensitivity but poorer precision.

Collaborative testing of the method

The proposed procedure was tested in the three cooperating laboratories on a wide range of sample types. Table 1 lists results obtained on available standard reference samples. The means represent the average of results from all laboratories. Each laboratory analyzed the samples at least three times.

Interferences

Extensive studies of interferences have been reported [6, 9, 12, 13], but these are not directly applicable to the sample solutions obtained by the proposed procedures. Hence, an interference study was undertaken.

Cations were added to arsenic solutions in the amounts shown in Table 2 before analysis. No interference was found for the amounts quoted. The values marked with an asterisk are threshold values above which an interference will occur. Concentrations higher than the tolerable levels given are unlikely to occur in water and vegetation samples. The severe interferences most likely to be encountered in real samples are Cu, Ni, Fe, Sb, and Se. Some soils and rocks may contain more than tolerance levels of these

TABLE 1

Results for arsenic in standard samples (ppm unless otherwise noted)

Sample	Digestion procedure	Mean value[a] (%)	Standard deviation %	Accepted value (%)
NBS 1571 (Orchard Leaves)	acid	10.2	±0.2	11.02 ± 2
NBS 1633 (Fly Ash)	fusion	59	±3.5	61.0 ± 6
Incinerated Sludge[b]	fusion	38	±4.2	34[c]
Sludge D[b]	fusion	15	±0.6	12[d]
USGS-W1	fusion	2.3	±0.2	2.4
GSC-SY2	fusion	19.4	±0.9	18[d]
GSC-SY3	fusion	19.3	±1.2	16[d]
GSC-SU1	fusion	524	±29.3	510[d]
GSC-MP1	fusion	0.83	±0.06	0.79

[a]This mean was calculated from the preferred value of each laboratory.
[b]From the Canada Center for Inland Waters, P.O. Box 5050, Burlington, Ontario, Canada.
[c]No accepted value. The value used is the average of results obtained from several laboratories.
[d]No accepted value. The value used is that obtained colorimetrically.

TABLE 2

Interference study (10 μg As l^{-1})

Cation	Concn. (μg ml^{-1})	Concn. in 1-g sample[a]	Cation	Concn. (μg ml^{-1})	Concn. in 1-g sample[a]
Ca^{2+}	4000	40%	Co^{2+}	100*	1%
Al^{3+}	4000	40%	Cd^{2+}	100*	1%
Mg^{2+}	4000	40%	Cu^{2+}	10*	1000 ppm
Na^{+}	1000	10%	Ni^{2+}	6*	600 ppm
K^{+}	1000	10%	Ag^{+}	5	500 ppm
Li^{+}	1000	10%	Ge^{4+}	1*	100 ppm
Fe^{3+}	750*	7.5%	Sb^{3+}	0.06*	6 ppm
Pb^{2+}	200*	2%	Sn^{2+}	0.8*	80 ppm
Zn^{2+}	200	2%	Bi^{3+}	0.6*	60 ppm
Mn^{2+}	200	2%	Se^{2+}	0.04*	4 ppm
Ba^{2+}	200	2%	Te^{2+}	0.3*	30 ppm
Cr^{3+}	100*	1%			

[a]The equivalent concentration for a 1-g sample in 100 ml of solution.
*Threshold values.

elements except possibly for selenium. The low detection limit of the proposed method offers an easy solution to interference problems. Dilution of samples with an automatic diluter will produce lower concomitant levels. When the arsenic level in the sample is too low for dilution, the method of standard addition can be used to evaluate the extent of any interference.

It is important to follow the recommended fusion procedure carefully. Failure to observe this precaution can result in nickel levels in the sample solution which exceed the threshold value.

By using a 1% solution of sodium borohydride, the tolerance levels for Cr, Cu, Ni, Co and Ag could be almost doubled. More serious depressions occurred with higher concentrations of sodium borohydride and coincided with increased visible formation of reduced metal in the case of Ag and Cu.

Conclusions

With this method, one arsenic determination can be made per minute. With duplicate measurements and standards, about 25 samples can be determined per hour. Arsine evolution involving a trapping stage followed by introduction into an atomic absorption spectrometer involves manipulation of various stopcocks, cleaning and pipetting. The proposed method eliminates many of these operations and is considerably simpler and less expensive than those using peristaltic pumping systems.

The detection limit, with flow rates of 225 and 75 ml min^{-1} for nitrogen and hydrogen, respectively, is 3 ng As.

Financial assistance for this work, to JCVL, was provided by the National Research Council of Canada.

REFERENCES

1 J. C. Van Loon and E. J. Brooker, Anal. Lett., 7 (1974) 502.
2 J. J. Lynch and G. Mihailov, Geol. Surv. Canada, Paper 63-8, (1963).
3 J. N. Bishop, L. A. Taylor and P. L. Diosady, High temperature acid digestion for the determination of mercury in environmental samples, Ministry of the Environment, Ontario, Report (March 1975).
4 F. E. Lichte and R. K. Skogerboe, Anal. Chem., 44 (1972) 1480.
5 R. M. Orheim and H. H. Bovee, Anal. Chem., 46 (1974) 1431.
6 P. N. Vijan and G. R. Wood, At. Absorpt. Newsl., 13 (1974) 33.
7 F. J. Schmidt and J. L. Royer, Anal. Lett., 6 (1973) 17.
8 R. C. Chu, G. P. Barron and P. A. E. Baumgarner, Anal. Chem., 44 (1972) 1476.
9 J. A. Fiorino, J. W. Jones and S. G. Capar, Anal. Chem., 48 (1976) 120.
10 D. D. Siemer, P. Koteel and V. Jariwala, Anal. Chem., 48 (1976) 836.
11 G. M. George, L. J. Frahm and J. P. McDonnell, J. Ass. Offic. Anal. Chem., 56 (1973) 1304.
12 A. E. Smith, Analyst, 100 (1975) 300.
13 F. D. Pierce and H. R. Brown, Anal. Chem., 48 (1976) 693.

Analytica Chimica Acta, 93 (1977) 69—75
© Elsevier Scientific Publishing Company, Amsterdam — Printed in The Netherlands

SYNERGIC EXTRACTION AND ATOMIC ABSORPTION SPECTROMETRIC DETERMINATION OF VANADIUM IN SILICATES

ISAO KOJIMA, TETSUO UCHIDA, MASAO NANBU, and CHUZO IIDA

Laboratory of Analytical Chemistry, Nagoya Institute of Technology, Showa-ku, Nagoya 466 (Japan)

(Received 31st March 1977)

SUMMARY

An atomic absorption spectrometric method for the determination of vanadium in silicates is proposed. Samples are digested with aqua regia and hydrofluoric acid in sealed Teflon vessels, iron is eliminated by anion exchange from 8 M hydrochloric acid, and vanadium is extracted synergically with β-isopropyltropolone into di-n-butyl ether in the presence of n-butanol from 0.5 M hydrochloric acid. The extract is aspirated into a nitrous oxide—acetylene flame. Less than 3 mg of iron in the organic extract (15 ml) does not interfere in the determination of 150 μg of vanadium. The results for vanadium in nine standard rock samples (USGS, GSJ and CSRM) agree well with earlier data. The recovery, reproducibility, and accuracy of the proposed method are satisfactory. Vanadium in new standard silicate rocks, GSJ-JB-2 and GSJ-JA-1, was also determined.

Numerous methods have been reported for the atomic absorption spectrometric determination of vanadium. In the case of direct atomization of aqueous solution, the sensitivity obtained is low and many interferences are possible. These defects can be improved by solvent extraction techniques or by the addition of aluminum [1]. The extraction systems which have been utilized in the determination of vanadium by atomic absorption spectrometry are: V(V)—cupferron with MIBK [2—4], di-n-butyl ether [4], and n-butyl acetate [5], V(V)—APDC with MIBK [6], and V(V)—5,7-dichloro-8-quinolinol with MIBK or n-butyl acetate [7]. In these cases, vanadium must be determined within a short time after extraction, because of the instability of the complex in the organic extract. In addition, extraction of the complex is either incomplete or is possible only in a narrow pH range, because of the low solubility of the complexes in the organic solvents.

Previous studies [8—11] have shown that vanadium can be synergically and completely extracted with monobasic and bidentate extraction agents, e.g. 8-quinolinol, BPHA, and β-isopropyltropolone (hinokitiol), in the presence of adduct-forming substances such as phenols, alcohols, and amines, and that the extracted complexes are very stable in organic solvents.

The present paper deals with the decomposition of silicates with aqua regia and hydrofluoric acid in a sealed Teflon vessel, separation of vanadium from iron on an anion-exchange resin from 8 M hydrochloric acid solution,

synergic extraction of the vanadium—β-isopropyltropolone complex into di-n-butyl ether in the presence of n-butanol, and atomic absorption spectrometric determination of vanadium. The proposed method has been successfully applied to the determination of vanadium in standard silicate samples.

EXPERIMENTAL

Apparatus

The Hitachi atomic absorption spectrophotometer, Model 207, was equipped with a nitrous oxide burner head (0.4 × 60 mm) and a vanadium hollow-cathode lamp (Westinghouse Products). Measurements were recorded on an Ohkura DR-2M stripchart recorder. The flow rates of nitrous oxide were controlled separately for nebulizer and auxiliary; the flow rate of auxiliary nitrous oxide was freely varied at a constant aspirating rate of sample solution. The pH of the aqueous solution was measured with a Radiometer PHM 22 pH meter. At high hydrogen ion concentration, the analytical concentration of hydrogen ion was also used. Extractions were done with an Iwaki mechanical shaker. Samples were digested in sealed Teflon vessels [12].

Ion-exchange resin. The anion-exchange resin Dowex 1-X8 (50-100 mesh; chloride form) was treated before use in the normal manner, packed into a glass column (8 × 80 mm; 1.5 g of wet resin) and finally conditioned with 8 M hydrochloric acid.

Reagents

Standard solution of vanadium (500 ppm, 1.0 M HCl). Dissolve 234.0 mg of NH_4VO_3 (G.R.; Wako Pure Chemicals Co.) in hydrochloric acid and dilute to 200 ml with distilled water.

β-Isopropyltropolone solution (0.02 M). Dissolve 1.642 g of β-isopropyltropolone (Takasago Perfumery Co.) and 50 ml of n-butanol in di-n-butyl ether and dilute to 500 ml with di-n-butyl ether.

Vanadium acetylacetonate solution (100 ppm V). Dissolve 52.1 mg of vanadyl acetylacetonate (Dojindo Laboratories, Kumamoto) and 5 ml of acetylacetone in ethanol and dilute to 100 ml with ethanol. Solutions of vanadium acetylacetonate (10 ppm V) in various solvents were prepared by diluting 10 ml of the 100-ppm solution to 100 ml with MIBK, acetone, di-isopropyl ether, di-n-butyl ether, ethyl acetate, n-butyl acetate, isoamyl acetate, n-hexane, and benzene.

All the reagents were of G.R. grade and used without purification.

Procedure

Into the Teflon decomposition vessel place 0.2—0.5 g of powdered sample, 4 ml of aqua regia, and 5 ml of 48% hydrofluoric acid. After sealing and digestion for 36 h at 25°C, transfer the contents to a polyethylene centrifuge tube with distilled water, centrifuge, and wash the residue with distilled

water. Evaporate the supernatant solution and the washing in a Teflon beaker, dissolve in 3 ml of 11 M hydrochloric acid, evaporate to dryness, and dissolve in 15 ml of 8 M hydrochloric acid. Pass the solution through the column at a flow rate of 3 ml min^{-1} and wash the beaker and the column three times with 5 ml of 8 M hydrochloric acid. Evaporate the effluent, dissolve the residue in 30 ml of 0.5 M hydrochloric acid, and shake the solution thus obtained for 10 min with 10 ml of 0.02 M β-isopropyltropolone solution. After complete phase separation, determine the concentration of vanadium in the organic extract by atomic absorption spectrometry.

The optimum operating conditions are: wavelength, 318.4 nm; flow rate of acetylene, 5.0 l min^{-1} (0.5 kg cm^{-2}); flow rates of nitrous oxide, 3.5 l min^{-1} (1.5 kg cm^{-2}) for nebulizer and 5.5 l min^{-1} (0.5 kg cm^{-2}) for auxiliary; burner height, position 1; lamp current, 12 mA; slit, No. 1 (0.18 nm).

RESULTS AND DISCUSSION

Operating conditions for atomic absorption spectrometry

In the atomic absorption spectrometric determination of vanadium, direct nebulization of aqueous sample solutions provides poor sensitivity and is very sensitive to interferences from other elements. As is well-known, the sensitivity obtained by nebulization of organic solutions is high in comparison. Organic solutions of vanadium acetylacetonate were used to study the effects of organic solvents, burner height (position, 0—3), and flow rates of acetylene (4.0—5.5 l min^{-1}) and auxiliary nitrous oxide (3.0—10.0 l min^{-1}) on the sensitivity, flame condition, flame noise, and deposition of carbon on the burner. Results typical of the many obtained are listed in Table 1 with the aspirating rate of the sample solution. Of the organic solvents studied, di-n-butyl ether, ethyl acetate, and n-butyl acetate are excellent, particularly with reference to the sensitivity, flame conditions, and deposition of carbon on the burner. Benzene provides high sensitivity but carbon deposits on the burner and clear flames are not obtained. Isoamyl acetate, acetone, and MIBK are unsuitable, because of low sensitivity. Isopropyl ether and n-hexane give high sensitivity but are unsuitable, owing to the high aspirating rate of the sample solution and the high flow rate of auxiliary nitrous oxide needed. Ethyl acetate and n-butyl acetate are unsuitable for the extraction of the vanadium—β-isopropyltropolone complex, because of the ready hydrolysis of the ester at high hydrogen ion concentrations. From these results, di-n-butyl ether was selected as the best solvent; the optimum operating conditions are listed in the Procedure.

Decomposition of silicates

Silicate rock ranging from acidic to basic can be completely digested by a mixture of aqua regia and hydrofluoric acid in a sealed Teflon vessel and all of the vanadium appears in the digested supernatent liquid. In contrast, ultrabasic rocks, PCC-1, DTS-1, and MRG-1, were incompletely digested by

TABLE 1

Effect of flow-rate of auxiliary nitrous oxide on absorption (mm)
(Vanadium acetylacetonate in organic solvent (10 ppm V); burner height, position 1; acetylene flow rate, 5.0 l min^{-1}; nitrous oxide flow rate for atomizer, 3.5 l min^{-1}.)

Organic solvent	N_2O (l min^{-1})								Sample flow rate (ml min^{-1})
	3	4	5	6	7	8	9	10	
MIBK		39[a]	40[a]	55[c]	31				2.4
Benzene			143[b]	146[b]	126[b]	74[c]	10		2.2
Bu_2O	80[b]	66[b]	55[c]	38	7				2.1
BuOAc	86[b]	72[b]	57[c]	35	5				2.0
n-Hexane				105[a]	112[c]	92	44	21	3.7
Acetone			50[a]	45[a]	25	12	3		3.7
Iso-Pr_2O			99[a]	87[a]	75[a]	36	10		3.7
EtOAc		131[a]	98[a]	61[c]	17	3			2.9
Iso-AmOAc	71[b]	55[c]	40[c]	19	2				1.7

[a] Luminous flame.
[b] Luminous flame and deposition of carbon on burner.
[c] Deposition of carbon on burner.

this method. Digestion was also incomplete even for acidic rocks with perchloric acid instead of aqua regia. To keep the procedure simple, the effect of decomposition at elevated temperatures was not examined.

Extraction of vanadium and iron

The percentage extraction of vanadium with β-isopropyltropolone into di-n-butyl ether in the absence and presence of n-butanol is given in Fig. 1. Vanadium is synergically and completely extracted into di-n-butyl ether at hydrogen ion concentrations of 0.02—1.2 M. At these acidities, the extracted vanadium complex is an ester, VOA_2OR, where A denotes the β-isopropyltropolone anion and R the butyl group. The synergy can be explained by the following equations

$$VO_2^+ + 2HA_{org} \rightleftharpoons VOA_2OH_{org} + H^+$$

$$VOA_2OH_{org} + ROH_{org} \rightleftharpoons VOA_2OR_{org} + H_2O_{org}$$

At acidities of 0.01—1.2 M, shaking for 10 min is sufficient for complete extraction of vanadium in the presence of 10% n-butanol. Prolonged extraction has no effect. The extract is stable on standing and the absorbance of the extract is constant for at least 4 h. Volume changes (25—40 ml) of the aqueous phase have no effect.

In contrast, irrespective of the addition of n-butanol, iron is completely extracted into di-n-butyl ether at hydrogen ion concentrations less than 1.5 M. The effect of iron concentration on the recovery of vanadium (150 μg) was tested by atomic absorption spectrometry. The results showed

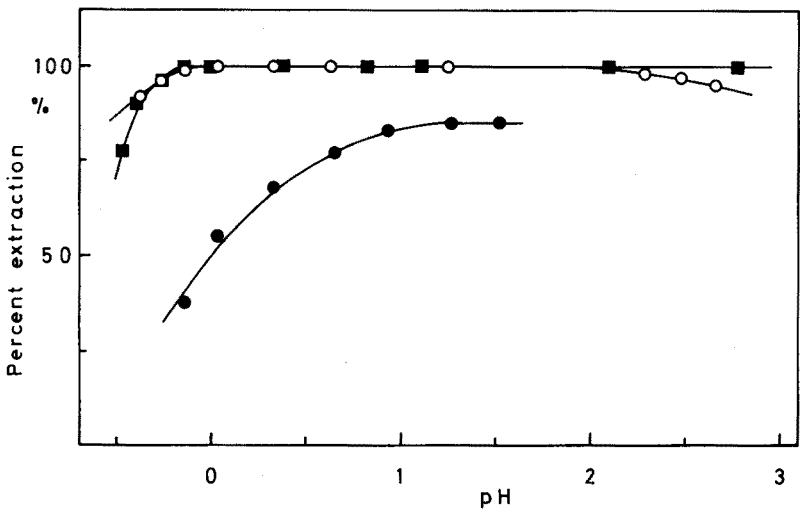

Fig. 1. Effect of pH on extraction of vanadium and iron in the absence and presence of n-butanol. Vanadium, 75 μg; aqueous phase, 25 ml; organic phase, 15 ml; extraction time, 10 min. ○ 10% butanol present. ● None. ■ 125 μg Fe with or without 10% butanol.

that the recovery of vanadium is lowered in the presence of more than 3 mg of iron, but remains quantitative for 0.5—3.0 mg of iron. As the viscosity of the organic extract increases with increasing amount of iron, the aspirating rate of the organic extract in the a.a.s. measurement decreases. Although vanadium is completely extracted, its recovery is lowered apparently. Therefore any iron present must be lowered to less than 3 mg by anion exchange.

Recovery of vanadium by anion-exchange separation

Vanadium can be separated from large amounts of iron by extraction of the iron from 8—9 M hydrochloric acid into di-iso-propyl ether [13], by elution of vanadium adsorbed on a cation [14] or anion [15] exchange resin with 1% hydrogen peroxide in 0.01—0.2 M sulfuric or perchloric acid, by adsorption of iron(III) on an anion-exchange resin from 8 M hydrochloric acid [16], or by the electrolysis at a mercury cathode [17, 18]. The anion-exchange separation technique seems to be most acceptable. Both vanadium(IV) and vanadium(V) can be completely separated from iron and completely recovered by passing through a suitable anion-exchange column at 8 M hydrochloric acid, for iron is completely adsorbed on the resin whereas vanadium is not (Table 2).

Calibration curve

A straight line with no intercept was obtained for vanadium concentrations up to 100 μg in 10 ml of organic solvent. The detection limit ($S/N = 2$) is 0.05 μg ml^{-1}. If organic extracts containing high concentrations of

TABLE 2

Recovery of vanadium in the presence of iron with anion-exchange resin

V(IV) taken (μg)	Fe present (mg)	Recovery (%)	V(V) taken (μg)	Fe present (mg)	Recovery (%)
20	0	101	20	0	101
	40	100		40	98
50	0	99	50	0	100
	10	98			
	40	99			

vanadium, e.g. 20 μg ml^{-1}, are diluted with 0.02 M hinokitiol solution, the same calibration curve is obtained. This dilution procedure is very convenient, and is one of the merits of the proposed method.

Analysis of standard rock samples

Results for vanadium in the JG-1, AGV-1, and BCR-1 standards are given in Table 3, which shows that reliable and reproducible results were obtained.

Results for vanadium in standard silicate rock samples are summarized in Table 4. These values are in reasonably good agreement with data reported by other workers. The results reported by Terashima were obtained by atomic absorption spectrometry and those by Donaldson, Kiss, Kojima, and Uchida by spectrophotometry. In the case of the ultrabasic rock samples, PCC-1, DTS-1, and MRG-1, the results for vanadium were rather low, because of incomplete digestion in the sealed Teflon vessel with aqua regia and hydrofluoric acid. However, the proposed method is successful for the determination of vanadium in acidic, neutral, and basic rock samples.

TABLE 3

Reproducibility and accuracy

Sample	JG-1	BCR-1	AGV-1
Sample weighed (mg)	500	200	250
No. of detns.	7	6	4
Mean ± *s* (ppm)	23.6 ± 0.1	413 ± 3	123 ± 4
Reported (ppm)	24	421	122
Accuracy (%)	98.3	98.1	100.8

TABLE 4

Results (ppm) for vanadium in geological standard silicates

USGS[a]					GSJ[b]				CSRM[c]		Ref.
W-1	BCR-1	GSP-1	AGV-1	G-2	JB-1	JB-2	JA-1	JG-1	SY-2	SY-3	
273	422	52.5	121	35.5	—	—	—	—	—	—	Donaldson [19]
264	399	52.9	125	35.4	—	—	—	—	—	—	Flanagan [20]
—	425	52.8	123	36.3	198	—	—	24.8	—	—	Kiss [21]
281	423	53	121	34	215	—	—	21	—	—	Terashima [1]
—	—	—	—	—	211	—	—	24	—	—	Ando et al. [22]
274	419	52	120	34	224	580[d]	102[d]	29	52	47	Kojima and Tanaka [8]
—	—	—	—	—	—	—	—	—	46	50	Abbey et al. [23]
284	417	—	—	—	249	—	—	—	—	—	Uchida et al. [24]
265	412	46	122	35.7	224	600	105	23.6	50	49	Present method

[a]USGS: United States Geological Survey.
[b]GSJ: Geological Survey of Japan, JA-1 and JB-2 are new samples.
[c]CSRM: Canadian Standard Reference Material.
[d]Unpublished data.

REFERENCES

1 S. Terashima, Bunseki Kagaku, 22 (1973) 1317.
2 H. J. Crump-Wiesner and W. C. Purdy, Talanta, 16 (1969) 124.
3 H. J. Crump-Wiesner, H. R. Feltz, and W. C. Purdy, Anal. Chim. Acta, 55 (1971) 29.
4 S. Shimomura, Y. Hayashi, H. Morita, and M. Kubo, Bunseki Kagaku, 25 (1976) 165.
5 D. C. G. Pearton, J. D. Taylor, P. K. Faure, and T. K. Steele, Anal. Chim. Acta, 44 (1969) 353.
6 T. Nakahara, S. Munemori, and S. Musha, Nippon Kagaku Zasshi, 90 (1969) 697.
7 Y. K. Chau and K. Lum-Shue-Chan, Anal. Chim. Acta, 50 (1970) 201.
8 I. Kojima and M. Tanaka, Anal. Chim. Acta, 75 (1975) 367.
9 I. Kojima and Y. Miwa, Anal. Chim. Acta, 83 (1976) 329.
10 I. Kojima and M. Tanaka, J. Inorg. Nucl. Chem., 29 (1967) 1769.
11 I. Kojima, T. Uchida, K. Ushida, and C. Iida, Bull. Nagoya Inst. Technol., 28 (1976) 109.
12 T. Uchida, M. Nagase, I. Kojima, and C. Iida, Anal. Chim. Acta, submitted.
13 G. A. Dean and J. F. Herringshaw, Analyst, 86 (1961) 106.
14 A. Janssen and F. Umland, Z. Anal. Chem., 254 (1971) 286.
15 L. Danielson, Acta Chem. Scand., 19 (1965) 670.
16 G. E. Janauer and J. Korkisch, Z. Anal. Chem., 179 (1961) 241.
17 R. Bock and S. Gorbach, Mikrochim. Acta (Wien), (1958) 593.
18 R. J. Nadalin and W. B. Brozda, Anal. Chem., 32 (1960) 1141.
19 E. M. Donaldson, Talanta, 17 (1973) 583.
20 F. J. Flanagan, Geochim. Cosmochim. Acta, 37 (1973) 1189.
21 E. Kiss, Anal. Chim. Acta, 77 (1975) 205.
22 A. Ando, H. Kurasawa, J. Ohmori, and E. Takeda, Geochem. J., 8 (1974) 175.
23 S. Abbey, A. H. Gillieson, and G. Rerrault, SY-2, SY-3, and MRG-1, A report on the collaborative analysis of three Canadian rock samples for use as certified reference materials, 1975, p. 49.
24 F. Uchida, S. Yamada, and M. Tanaka, Anal. Chim. Acta, 83 (1976) 427.

Analytica Chimica Acta, 93 (1977) 77—83
©Elsevier Scientific Publishing Company, Amsterdam — Printed in The Netherlands

DETERMINATION OF MANGANESE IN NATURAL WATERS BY FLAMELESS ATOMIC ABSORPTION SPECTROMETRY

J. M. McARTHUR

Department of Earth Science, The University, Leeds LS2 9JT (England)

(Received 16th February 1977)

SUMMARY

Manganese can be rapidly determined in natural waters by direct-injection flameless a.a.s. Interference caused by sea salts in waters of salinity 0—35°/$_{oo}$ can be eliminated by charring with ammonium nitrate and with a slow temperature rise. The sensitivity of the determination is depressed by the presence of nitric acid, the depression decreasing with graphite tube age. In saline water matrices, the detection limit is better than 0.002 ng and the sensitivity is better than 0.02 ng for 1% absorbance. Precision is better than 10% for manganese concentrations of 10 $\mu g\ l^{-1}$ in sea water.

The concentration of manganese in natural waters varies from about 0.2 $\mu g\ l^{-1}$ in open ocean water to over 10 000 $\mu g\ l^{-1}$ in pore water from some recent marine sediments; the concentrations in lakes, rivers, and estuaries lie between these extremes [1—4]. Methods developed for the determination of manganese in sea water by direct-injection flameless atomic absorption [5—9] can be applied to natural waters of any constant salinity. Their application to waters of variable salinity is not viable, however, because of a large salinity effect [8].

A new technique of direct injection analysis eliminates the interference of sea salts in the salinity range 0—35°/$_{oo}$; this allows sea water, and river, estuarine, and pore water to be analyzed rapidly. The factors which influence the operation of the salinity effect are discussed. As natural waters are usually acidified upon collection to prevent adsorption and precipitation losses, the effect of varying acid concentrations is also described.

EXPERIMENTAL

A Perkin-Elmer 306 atomic absorption spectrometer fitted with an HGA-74 flameless atomizer was used. Signals were recorded with a Tekman TE 200 chart recorder set to its fastest response time (<0.3 s full scale); peak heights were measured. The spectral source was a Perkin-Elmer Fe—Mn—Co—Cu—Mo hollow-cathode lamp, balanced to a deuterium-arc background corrector. Typical furnace conditions were: drying at ca. 100°C for 35 s; charring with either a rate programme, or a constant high-temperature char with cycle 2

for 15—20 s; atomization at 2400°C for 10 s and a heating-out stage at maximum temperature for 3—4 s. The Mini Flow gas mode was used throughout. Temperatures were measured with an optical pyrometer.

Solutions were prepared by diluting commercial atomic absorption standards with sea water and double distilled water containing 3 μg Mn l^{-1} and less than 0.1 μg Mn l^{-1}, respectively. Acidifications were made with UltraR nitric acid redistilled four times from glass, containing less than 0.1 μg Mn l^{-1}. Ammonium nitrate of the necessary purity was prepared by repeated crystallization. Additions of 20 μl of 30% (w/v) ammonium nitrate solution were made into the graphite tube before the sample was pipetted. A sample volume of 50 μl was used throughout. Micropipette tips were rinsed in dilute acid and sample, as appropriate, to eliminate contamination [10, 11].

The effects described are reproducible (within ±10%), at manganese concentrations of 10 μg l^{-1} and 100 μg l^{-1}, and under Mini Flow and Full Flow gas modes. The 10 μg l^{-1} Mini Flow results are therefore presented.

RESULTS

The effect of charring parameters

Charring losses from distilled water and sea-water matrices begin at about 1100°C. The addition of ammonium nitrate postpones the onset of such losses by at least 150°C; at a manganese concentration of 80 μg l^{-1}, charring with rate programme 8 (28° s^{-1}) causes little decrease in atomization peak heights below 1600°C.

Figure 1 shows that slower temperature programmes greatly increase the absorbance of manganese in a sea-water matrix, without much affecting the absorbance in a sea-water matrix modified by the addition of acid or ammonium nitrate.

The absorbance obtained for acidified sea water is about 40% lower than for equivalent concentrations of manganese in distilled water because a new graphite tube was used. The addition of ammonium nitrate decreases the absorbance of manganese by some 15% compared with equivalent distilled water standards, whilst the maximum for sea-water solutions is equal to them. Clearly, the use of a slow temperature rise for charring will eliminate the effect of sea-water concentrations of sea salts on manganese absorbance, probably because of the complete separation of matrix and analyte [12, 13]. High heating rates cause manganese to be lost by co-volatilization with salt, and result in lower sensitivities.

Manganese absorbance as a function of salinity

The interference of sea salt in the concentration range 0 to 35‰ salinity can be eliminated by charring with a slow rate programme (<28° s^{-1}) in the presence of either 1% nitric acid or an excess of ammonium nitrate (Fig. 2C). Charring with a slow rate programme alone considerably reduces the interference; charring with ammonium nitrate at too high a temperature re-introduces

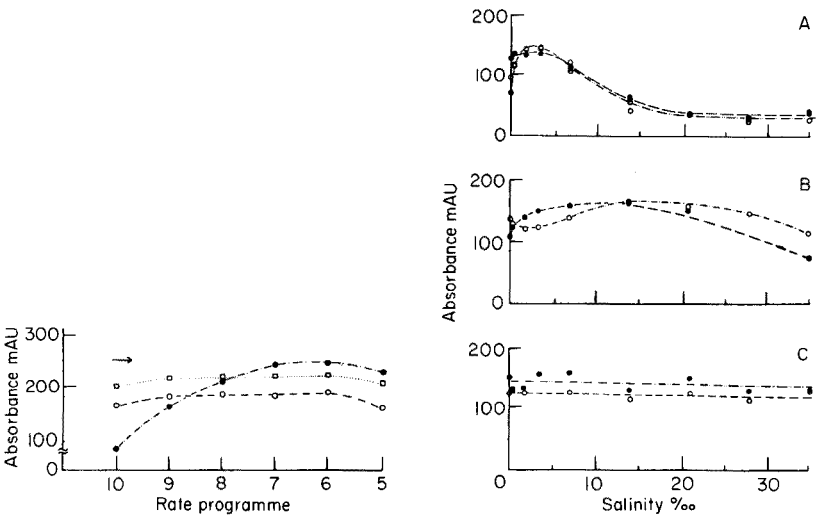

Fig. 1. Manganese absorbance as a function of the heating rate in the charring programme. Rate 10 refers to the rate of heating obtained with cycle 2. The arrow shows the absorbance of uncharred distilled water standards. • Sea water. □ Sea water plus ammonium nitrate. ○ Sea water plus 1% nitric acid. The decrease of absorbance at rate 5 is due to pre-atomization losses.

Fig. 2. Manganese absorbance as a function of salinity. A. Charring for 20 s at 1200°C. ○ Analyses 83—105. • Analyses 248—257. B. Charring with rate programme 8 to 1300°C. ○ With ammonium nitrate. • Without ammonium nitrate. C. Charring with rate programme 8. • Plus 1% nitric acid, charred to 1200°C. ○ Plus ammonium nitrate, charred to 950°C.

it (Fig. 2B). Charring at a fixed temperature results in an absorbance—salinity dependence very similar to that obtained by Segar and Cantillo [8] under similar conditions (Fig. 2A). The effect of salinity appears marginally greater in new tubes than in old, under these conditions.

The elimination of interference observed in Fig. 2C is probably the result of removal of chloride as hydrogen chloride or ammonium chloride [14, 15] and to a good separation of sublimation and vaporization products from manganese, because of the slow rise in temperature [12, 13]. According to Segar and Cantillo [8] the form of the curves in Fig. 2A probably arises from hot atom-cloud reactions. An alternative explanation may involve three competing effects, viz. retention of manganese on sea salts remaining after charring, co-volatilization losses with salt, and simple charring losses at very low salinities because of the high temperature required for salt vaporization. This last source of loss is possibly reduced in the presence of small amounts of salt (<5‰), giving rise to an initial absorbance increase, after which co-volatilization losses increasingly dominate, leading to a decrease in absorbances at higher salinities.

TABLE 1

Manganese absorbance as a function of graphite tube age for acidified and non-acidified distilled standards
(10 $\mu g\ l^{-1}$ Mn, 50 μl samples)

Injection No.	Unacidified (value/mean)	Acidified (1% HNO_3) (value/mean)	Difference of means
1		104	
2		95/99.7	76
3		100	
4	180		
5	165/176		
6	183		
29	198		
30	178		
31	/183.7	150	39
32		140/145	
33	175		
93	185		
94	184/184.5		
95		153	29
96		157/155	
299[a]		164	
300		165/164.5	0
7—298[b]	164.5		

[a]With a different tube.
[b]Mean of 24 control standards run during the tube lifetime ($s_r \pm 4\%$).

Manganese absorbance as a function of acid concentration

In both distilled water and sea-water solutions, nitric acid depresses the absorbance of manganese by an amount which is proportional to tube use. In well-used graphite tubes the effect is absent (Table 1). The depression is also linearly dependent on acid concentration for programmed rate charring but not for charring at a fixed temperature (Fig. 3). Too high a final charring temperature results in an increase in absorbance at higher acidities (Fig. 3); this indicates a slight increase in charring stability in the presence of nitric acid.

For stable calibration curves, the acidity of the sample must be kept to a minimum and the tube aged before the analysis. Alternatively, frequent calibration standards can be run.

The effect may be related to the differing viscosities or surface tensions of the acidified and non-acidified solutions. Peak shapes are different in new and old tubes; the measurement of peak area, rather than peak height, reduces the effect without eliminating it, so other factors play a part.

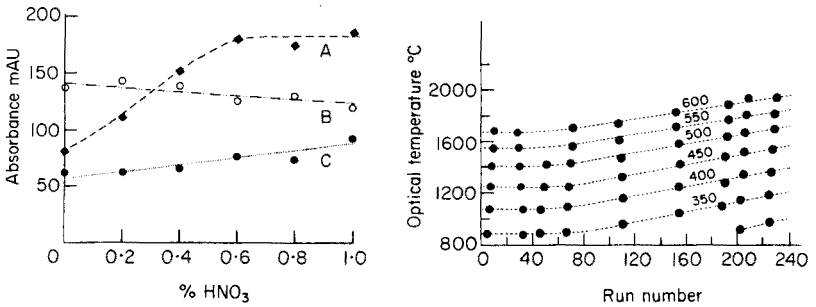

Fig. 3. Manganese absorbance in sea water as a function of nitric acid concentration. ○ Rate programme charring rate 8 to 1000°C, plus ammonium nitrate. • Rate programme charring, rate 8 to 1350°C. ♦ Cycle 2 char at a fixed temperature of 1200°.

Fig. 4. Optical temperature at fixed digital settings as a function of analysis number.

Manganese absorbance as a function of tube age

Under the conditions described, 250—300 analyses can be obtained with each graphite tube. The overall precision, calculated from up to 30 replicate distilled water standards run as controls during a tube lifetime, was usually between 4 and 6% relative standard deviation. In contrast, Segar and Cantillo [8] reported linear decreases of absorbance over a tube lifetime. Such decreases are almost certainly caused by increasing temperatures at fixed digital settings as the tube ages; gradually increasing charring losses, and therefore a gradual decrease in the atomization signal, take place. Figure 4 shows how the tube temperature at fixed digital settings can vary over a tube lifetime. The rate of the temperature drift, and tube life, is directly proportional to tube compression, and is obviously also influenced by the severity of the charring and atomization programmes, although these are of lesser importance.

In the absence of optical pyrometry, true tube temperatures can be kept roughly constant by continually altering the digital charring temperatures to maintain a constant sensitivity for a distilled water control standard.

Recommended method of analysis

The analysis for manganese of saline waters containing sea-salts in the concentration range 0 to 35‰ salinity is simple, rapid, and free of salt interference when the following procedure is used.

Inject 20 μl of 30% (w/v) ammonium nitrate into the tube, followed by 50 μl of sample. Dry without spitting, and char to 1100°C, from the drying temperature, at a temperature gradient of about 28°C s^{-1} (rate programme 8). Atomize for 8 s at 2400°C, and clean the tube by heating to maximum temperature for 5 s. Background correction is applied.

High manganese concentrations (>100 μg l^{-1}) are best analyzed at the less sensitive wavelength, 403.1 nm, at which non-specific absorption is very low and background correction is unnecessary.

Sensitivity, precision, accuracy and linear range

The sensitivity of the determinations is 0.01—0.02 ng for 1% absorption. This is ca. 5—10 times the claimed sensitivity [16]. The low sensitivity resulted from the use of wide slit settings, which were necessary to balance the hollow-cathode lamp output to that of the background corrector.

The recommended method has a detection limit (signal: noise = 2), for sea-water solutions, of 0.002 ng (0.04 $\mu g\ l^{-1}$ for a 50-μl sample). The observed limit is about ten times greater than that claimed for aqueous solutions [16]. This discrepancy is probably accounted for by the use of the background corrector, the presence of some salt "smoke" during atomization (even though this should be corrected by the deuterium arc) and the extreme age of the spectral source.

Both the short- and long-term precision of saline water analysis is poorer than those obtained for distilled water standards but both are below 10%, except at the lower extremes of a working range. Poor precision can arise from pipetting errors and from occasional incomplete mixing of the ammonium nitrate and the sample. Without ammonium nitrate, the precision is usually 4—6% for saline solutions.

In an examination of the accuracy, five samples of sediment pore water were analyzed by the recommended method (at 403.1 nm) and by the flame injection method of Sebastiani et al. [17]. Although the concentrations are close to the detection limit for the flame method and considerably lower than optimum for the 403.1 nm line, the results agree within the limits of error (Table 2).

At 279.5 nm, the calibration is linear up to ca. 0.20 absorbance units with a slit setting of 4 (0.7 nm). With the recommended slit setting of 3 (0.2 nm) linearly extends to ca. 0.25 absorbance units, equivalent to 0.45—1.15 ng of manganese for the Mini Flow gas mode. At 403.1 nm with recommended slit settings, calibration is linear up to at least 0.30 absorbance units, equivalent to ca. 8 ng of manganese with the Mini Flow

TABLE 2

Determination of manganese by flame and flameless atomic absorption methods (Sediment pore water; all concentrations are $\mu g\ l^{-1}$)

Sample	Flame[a]	s.d.	Flameless[b]	Max. dev. from mean
0—2	167[c]		153[d]	1
2—4	105	15	97	13
4—6	25	4	34	5
6—8	35	4	36	3
8—10	85	8	70	10

[a]Flame injection method [17]. Average of 7 determinations.
[b]Average of 5 determinations, recommended method, 50-μl sample, 403.1 nm.
[c]One determination.
[d]Two determinations.

gas mode. These limits may be increased by a factor of at least 3 by operating with the Full Flow gas mode.

This work was supported by Grant No. GR3/2180 from the Natural Environment Research Council.

REFERENCES

1 P. G. Brewer, in J. P. Riley and G. Skirrow (Eds.), Chemical Oceanography, Vol. 1, Academic Press, London, 2nd edn., 1975.
2 J. D. Hem, U.S. Geol. Surv. Water-Supply Paper, 1473, 2nd edn., 1970.
3 D. A. Livingstone, U.S. Geol. Surv. Prof. Paper, 440G (1963) 50.
4 S. E. Calvert and N. B. Price, Earth Planet. Sci. Lett., 16 (1972) 245.
5 P. E. Paus, Z. Anal. Chem., 264 (1973) 118.
6 D. A. Segar and J. G. Gonzalez, Anal. Chim. Acta, 58 (1972) 7.
7 T. H. Donnelly, J. Ferguson and A. J. Eccleston, Appl. Spectrosc., 29 (1975) 158.
8 D. A. Segar and A. Y. Cantillo, in Analytical Methods in Oceanography, Advances in Chemistry Series, 147, American Chemical Society, Washington D.C., 1975, pp. 56—81.
9 J. D. Willey, Mar. Chem., 3 (1975) 227.
10 M. R. Sommerfield, T. D. Love and R. D. Olsen, At. Absorpt. Newsl., 14 (1975) 31.
11 M. M. Benjamin and E. A. Jenne, At. Absorpt. Newsl., 15 (1976) 53.
12 J. Smeyers-Verbeke, Y. Michotte, P. Van den Winkel and D. L. Massart, Anal. Chem., 48 (1976) 125.
13 G. Baudin, M. Chaput and L. Feve, Spectrochim. Acta, 26 (1971) 425.
14 A. Le Bihan and J. Courtot-Coupez, Analusis, 3 (1975) 559.
15 R. D. Ediger, G. E. Petersen and J. D. Kerber, At. Absorpt. Newsl., 13 (1974) 61.
16 Perkin-Elmer Corporation (Bodenseewerk Perkin-Elmer and Co. GmbH). Methods for Flameless Atomic Absorption Spectroscopy with a Heated Graphite Atomiser, 1974.
17 E. Sebastiani, K. Ohls and G. Riemer, Z. Anal. Chem., 264 (1973) 105.

Analytica Chimica Acta, 93 (1977) 85—90
©Elsevier Scientific Publishing Company, Amsterdam — Printed in The Netherlands

DOSAGE PAR SPECTROPHOTOMÉTRIE D'ABSORPTION ATOMIQUE SANS FLAMME DE TRACES DE SÉLÉNIUM APRÈS EXTRACTION À L'AIDE DE 4-CHLORO-1,2-DIAMINOBENZÈNE. APPLICATION AUX MILIEUX BIOLOGIQUES

JEAN NEVE et MICHEL HANOCQ*

Université Libre de Bruxelles, Institut de Pharmacie, Laboratoire de Chimie Analytique et de Toxicologie, Campus Plaine, C.P. 205/1, Bd. du Triomphe, B 1050 Bruxelles (Belgique)

(Reçu le 4 Avril 1977)

RÉSUMÉ

Une nouvelle méthode de dosage du sélénium à l'état de traces par spectrophotométrie d'absorption atomique sans flamme est décrite. Mise au point à partir de solutions aqueuses, elle a été appliquée à certains milieux biologiques après minéralisation. Le sélénium(IV) est extrait, après réaction en milieu acide, avec la 4-chloro-1,2-diaminobenzène, dans le toluène. La limite de détection du sélénium est de 10 ng par ml d'échantillon biologique (plasma et globules rouges). La précision et la reproductibilité atteintes sont excellentes.

SUMMARY

The determination of traces of selenium after extraction with 4-chloro-1,2-diaminobenzene by graphite-furnace atomic absorption spectrometry. Application to biological samples.

A new method for the determination of very small amounts of selenium by flameless atomic absorption spectrometry is proposed. The procedure was checked with aqueous solutions of selenium and applied to mineralized biological fluids (red cells and plasma). Selenium(IV) is quantitatively extracted with toluene after reaction with 4-chloro-1,2-diaminobenzene. The sample detection limit for selenium is 10 ng ml^{-1}. Precision and reproducibility are excellent.

Sa participation dans la constitution d'un certain nombre d'enzymes parmi lesquelles la glutathione peroxydase, son rôle dans des maladies de carence chez l'animal et chez l'homme, ont fait du sélénium un des éléments dont la détermination à l'état de traces s'est avérée indispensable. A cette fin, plusieurs techniques faisant appel à une réaction du sélénium(IV) avec une *o*-diamine aromatique ont été proposées: il s'agit de la fluorimétrie [1—4] et de la chromatographie en phase gazeuse [5, 6]. La principale critique formulée vise la méthode fluorimétrique en raison de la valeur toujours élevée du blanc et la nécéssité d'une purification poussée des différents réactifs.

La spectrophotométrie d'absorption atomique avec flamme [7, 8] ou sans flamme est d'utilisation courante pour la détermination du sélénium; cette

dernière fait appel soit à une génération d'hydrure de sélénium [9, 10] soit à un four en graphite après séparation des ions à doser du milieu réactionnel par précipitation à l'aide d'acide ascorbique [11, 12] ou par passage de l'échantillon sur résines échangeuses d'ions [13].

Ces différentes techniques s'avèrent, dans certains cas, délicates, relativement peu sensibles, non reproductibles, voir même non quantitatives [9, 14].

Grâce à une extraction sélective en milieu acide du sélénium(IV) à l'aide de la 4-chloro-1,2-diaminobenzène après minéralisation éventuelle par une technique décrite précédemment [15], la méthode de spectrophotométrie d'absorption atomique sans flamme que nous proposons permet de doser cet élément dans les milieux biologiques à des doses physiologiques, toxicologiques ou subphysiologiques.

PARTIE EXPERIMENTALE

Appareillage

Un spectrophotomètre d'absorption atomique Varian-Techtron AA5 équipé du four en graphite modèle 63 (enregistreur Varian A25) est utilisé suivant les indications du constructeur: courant de lampe, 10 mA; longeur d'onde, 196,3 nm; fente, largeur 300 μm, hauteur 2 mm. Les conditions d'utilisation du four en graphite sont: déshydratation 30 s, 8 (1,1 V); minéralisation 20 s, 5,5 (1,7 V); atomisation 1 s, 8 (7,2 V). Débit d'azote dans le four: 6 l min^{-1}.

Toute la verrerie nécéssaire aux différentes opérations est lavée à l'aide d'eau régale et rincée plusieurs fois avec de l'eau distillée.

Réactifs

L'acide sulfurique (96%; Merck), l'acide nitrique (65%; Merck), l'ammoniaque (25%; Merck), l'acide perchlorique (71%; Baker) et le perhydrol (UCB) sont de qualités pour analyse.

Toluène (UVASOL Merck) préalablement saturé en eau tridistillée.

Solution standard de sélénium (1 p.p.m.) [3]. Une prise d'essai de 25,0 mg de sélénium élémentaire (Baker, p.a.) est dissoute dans 2 ml d'acide nitrique concentré en chauffant légèrement; on complète ensuite à 1 l à l'aide d'eau tridistillée. 10 ml de cette solution sont amenés à 250 ml à l'aide d'acide chlorhydrique 0,1 M. La solution étalon ainsi préparée s'est avérée stable pendant plusieurs mois, à température orindinaire.

Solution de 4-chloro-1,2-diaminobenzène. Une solution à 0,5% est préparée extemporanément par dissolution dans de l'eau tridistillée d'une prise d'essai de produit purifié suivant une technique décrite précédemment [16].

L'extraction du composé sélénié à partir de solutions aqueuses

Dans une ampoule à décanter de 50 ml, on introduit 25 ml d'une solution contenant de 0 à 1500 p.p.b. de sélénium(IV). Après avoir ajusté le pH entre 1 et 2 à l'aide d'acide chlorhydrique 4 M et d'ammoniaque 8 M, on ajoute

2 ml de la solution de 4-chloro-1,2-diaminobenzène et on laisse au repos pendant 2 h, à l'obscurité. On procède ensuite, pendant 5 min, à l'extraction du composé sélénié formé à l'aide de toluène (1 ml de solvant pour des doses comprises entre 150 et 1500 p.p.b.; 0,1 ml si les doses sont comprises entre 10 et 150 p.p.b.). Après séparation des phases, un volume de 2,5 μl de la couche organique est introduit dans le four en graphite, à l'aide d'une seringue (10 μl, Unimetrics).

Les calculs sont effectués par appréciation de la hauteur du signal d'absorption sur enregistrement graphique.

L'extraction du composé sélénié à partir de plasma et de globules rouges

Ce mode opératoire a été décrit par Ihnat [15]. Dans une fiole de Kjeldahl de 30 ml, on introduit 1 ml d'échantillon, 2 billes de verre et 10 ml d'acide nitrique concentré. Après un repos de quelque temps destiné à éviter la formation de mousse trop abondante, on chauffe prudemment sur bain électrique, en évitant tout charbonnement, de manière à réduire le volume de liquide à environ 3 ml. Après refroidissement, on ajoute 6 ml d'acide perchlorique (70%) et 3 ml d'acide sulfurique concentré; le mélange est alors chauffé à ébullition jusqu'à décoloration et apparition des fumées denses blanches. Au liquide légérement refroidi, on ajoute prudemment 1 ml de perhydrol destiné essentiellement à oxyder complètement le sélénium en Se(IV), seul succeptible de réagir avec l'*o*-diamine [13] et on chauffe à ébullition jusqu'à nouvelle apparition de fumées blanches. L'addition de perhydrol est alors répétée et le chauffage prolongé pendant quelques minutes jusqu'à obtention d'une solution parfaitement incolore.

Il s'est avéré important de chasser complètement l'acide perchlorique et l'acide nitrique afin d'éliminer du milieu réactionnel toute trace d'oxydant succeptible de provoquer l'oxydation de l'*o*-diamine qui se manifeste par l'apparition d'un précipité dont la présence entrave l'extraction par le toluène. C'est pourquoi après refroidissement, on ajoute 5 ml d'une solution aqueuse de chlorhydrate d'hydroxylamine (25% p/v). On dilue alors avec environ 10 ml d'eau et transvase quantitativement l'ensemble dans une ampoule à décanter de 50 ml. Après avoir amené le pH à 1—2 à l'aide d'ammoniaque concentré, on poursuit comme il est indiqué au mode opératoire précédent.

RESULTATS ET DISCUSSION

Choix des conditions pour l'extraction du composé sélénie

Parmi les *o*-diamines aromatiques réagissant quantitativement avec le sélénium(IV) [17, 18], notre choix s'est porté sur la 4-chloro-1,2-diaminobenzène, formant avec le sélénium(IV), à pH 0—2,5, un piazsélénol facilement soluble dans le toluène [19]. L'usage de ce solvant nous a permis d'effectuer des extractions totales en une seule opération et ce même pour des volumes de solvant organique de l'ordre de 0,1 ml; ceci explique le seuil de détection extrèmement bas de notre méthode: 10 ng Se ml^{-1}. D'autre

part, il va sans dire qu'une concentration suffisante en *o*-diamine est nécessaire en vue d'extraire complètement la totalité du sélénium, ce qui justifie la concentration de 0,5% choisie.

Enfin, la récolte de faibles volumes de solvant a été facilitée en réalisant de petites cuvettes coniques en verre s'adaptant parfaitement à l'extrémité des ampoules à décanter.

Etude de la précision et de la reproductibilité

En suivant le mode opératoire décrit ci-dessus, des tracés linéaires de l'absorption en fonction de la quantité de sélénium présente en solution aqueuse sont obtenus pour des doses de sélénium variant de 150—1500 p.p.b. lorsque l'extraction du composé sélénié se fait par 1 ml de toluène, et de 0—150 p.p.b. si elle se fait par 0,1 ml.

La limite de détection, définie comme la concentration minimale en sélénium donnant un signal net égal à deux fois la déviation standard des lectures du blanc, a été estimée à 100 ng ml^{-1} dans le premier cas et à 10 ng ml^{-1} dans le second.

Par comparaison à ces droites étalons, des analyses de différentes solutions aqueuses ont été effectuées; le Tableau 1 montre que la sensibilité et la reproductibilité sont excellentes.

TABLEAU 1

Dosage du sélénium par absorption atomique sans flamme après extraction

Se théorie (p.p.b.)	Toluène (ml)	Nombre de dosages	Se trouvé (p.p.b.)	*s* (p.p.b.)	Trouvé (%)
Solution aqueuse					
250	1	3	265	15	106
750	1	3	750	25	100
1250	1	3	1230	10	98,4
50	0,1	3	50	4	100
75	0,1	2	74	—	98,7
125	0,1	2	125	—	100
Liquide globulaire[a]					
250	1	3	255	9	102
750	1	3	765	18	102
1250	1	2	1240	—	101
Plasma[a]					
20	0,1	1	21	—	105
40	0,1	1	40	—	100
60	0,1	1	65	—	108

[a] Après minéralisation.

L'extraction du composé sélénié à partir de plasma et de globules rouges

Différents dosages de quantités de sélénium ajoutées préalablement à des globules rouges et à du plasma ont été effectués par comparaison à une droite étalon et en tenant compte de la valeur du "blanc réactif" et de la quantité de sélénium physiologiquement présente. Le Tableau 1 montre que, dans tous les cas envisagés, les moyennes sont proches des concentrations théoriques, même si le dosage n'a été effectué que sur une seule prise d'essai. Cette constatation nous parait importante, car l'analyste toxicologue, dans la pratique quotidienne, n'a très souvent à sa disposition qu'une quantité limitée d'échantillon.

D'autre part, la méthode a été appliquée à l'analyse de globules sanguins et de plasmas d'enfants africains atteints de la maladie du kwashiorkor, seule maladie humaine connue jusqu'à présent comme pouvant provoquer une diminution du taux de sélénium plasmatique [20, 21]. Ce dernier se situant entre 60 et 120 p.p.b., la technique analytique à mettre en oeuvre doit donc être suffisamment sensible.

Les résultats obtenus à l'aide de la méthode (Tableau 2) montrent que cette dernière est parfaitement adaptée au cas envisagé; la technique offre en outre l'avantage de pouvoir être appliquée sur 1 ml d'échantillon.

Il s'est àvéré important de tester, préalablement à toute analyse, la réponse du four en graphite: nous avons remarqué qu'un four neuf se révèle très souvent inefficace, ce n'est qu'après plusieurs dizaines de mises à feu qu'une réponse satisfaisante est obtenue. Ces observations confirment les constatations faites par Ihnat [11].

Nous adressons nos plus vifs remerciements au docteur P. Fondu (clinique pédiatrique de l'hôpital universitaire Saint-Pierre à Bruxelles — prof. H. Vis) pour nous avoir fourni les divers échantillons biologiques nécéssaires à cette étude.

TABLEAU 2

Dosage de sélénium plasmatique et globulaire chez des enfants atteints de kwashiorkor (Les taux sont exprimés en ng ml^{-1})

Sujets	Se plasmatique	Se globulaire
Non traités	A. 49 ± 1	A. 124 ± 6
	B. 61 ± 1	B. 100 ± 1
	C. 34 ± 5	C. 84 ± 1
Traités	A. 67 ± 4	A. 121 ± 9
	B. 82 ± 7	B. 113 ± 1
	C. 75 ± 1	C. 114 ± 5
Témoins	A. 67 ± 2	A. 119 ± 4
	B. 62 ± 6	B. 95 ± 4
	C. 52 ± 2	C. 93 ± 1

BIBLIOGRAPHIE

1 J. H. Watkinson, Anal. Chem., 38 (1966) 92.
2 P. R. Haddad et L. E. Smythe, Talanta, 21 (1974) 859.
3 O. E. Olson, I. S. Palmer et E. E. Cary, J. Ass. Offic. Anal. Chem., 58 (1975) 117.
4 C. C. Y. Chan, Anal. Chim. Acta, 82 (1976) 213.
5 J. W. Young et G. D. Christian, Anal. Chim. Acta, 65 (1973) 127.
6 J. A. Rodriguez-Vasquez, Anal. Chim. Acta, 73 (1974) 1.
7 S. Ng, M. Munroe et W. McSharry, J. Ass. Offic. Anal. Chem., 57 (1974) 1260.
8 B. C. Severne et R. R. Brooks, Anal. Chim. Acta, 58 (1972) 216.
9 M. Ihnat, J. Ass. Offic. Anal. Chem., 59 (1976) 4.
10 S. Ng et W. McSharry, J. Ass. Offic. Anal. Chem., 58 (1975) 987.
11 M. Ihnat, Anal. Chim. Acta, 82 (1976) 293.
12 M. Ihnat et R. J. Westerby, Anal. Lett., 7 (1974) 257.
13 E. L. Henn, Anal. Chem., 47 (1975) 428.
14 M. McDaniel, A. D. Shendrikar, K. D. Reizneir et P. W. West, Anal. Chem., 48 (1976) 2240.
15 M. Ihnat, J. Ass. Offic. Anal. Chem., 57 (1974) 368.
16 J. Nève et M. Hanocq, Anal. Lett., 10 (1977) 133.
17 M. Tanaka et T. Kawashima, Talanta, 12 (1965) 211.
18 T. Kawashima, Sci. Rep. Kagoshima Univ., 21 (1972) 57.
19 M. Akiba, Y. Shimoishi et K. Toei, Analyst (London), 100 (1975) 648.
20 R. F. Burk, W. V. Pearson, R. P. Wood et F. Viteri, Am. J. Clin. Nutr., 20 (1967) 723.
21 R. J. Levine et R. E. Olson, Proc. Soc. Exp. Biol. Med., (1970) 1030.

Analytica Chimica Acta, 93 (1977) 91—97
© Elsevier Scientific Publishing Company, Amsterdam — Printed in The Netherlands

THE POTENTIOMETRIC DETERMINATION OF INSECTICIDES
Part I. Organophosphorus insecticides inhibiting cholinesterase

W. N. DAHL, Å. M. R. HOLM and K. H. SCHRØDER*

University of Trondheim, Kjemisk institutt NLHT, N-7000 Trondheim (Norway)

(Received 22nd April 1977)

SUMMARY

A potentiometric method for the determination of organophosphorus insecticides based on the inhibition of cholinesterase is presented. The acetic acid formed by hydrolysis of acetylcholine is sensed by a glass electrode in a weakly buffered system. The insecticide is incubated with cholinesterase for 1 h at 25°C or 37°C before addition to the substrate. The effects of incubation time and temperature are discussed. The method is applied to the insecticides bromophos and dichlorvos. The detection limits are 2×10^{-8} M (7 ppb) for bromophos and 1×10^{-7} M (22 ppb) for dichlorvos. The initial rates of hydrolysis decrease linearly up to 2×10^{-7} M and 1×10^{-6} M, respectively.

One important group of insecticides is that which acts by inhibiting the enzyme cholinesterase. This enzyme controls the passage of impulses in the synaptic cleft of the nerve system by hydrolysing the transmitter substance acetylcholine [1]. Thus inhibition of cholinesterase leads to severe poisoning of the nerve system. The present paper reports a utilization of this effect in analyses of insecticides. Insecticide residues are mainly analysed by chromatographic techniques [2, 3]. The problems are the extremely small quantities of these residues and the heterogeneous materials in which they are found. Biochemical analysis of insecticides inhibiting cholinesterase has been studied by several workers [4—6], whose results indicate that biochemical assays can sometimes be comparable to gas—liquid chromatographic techniques.

Acetic acid and choline are the products formed in the reaction

$$CH_3COOCH_2CH_2N^+(CH_3)_3 + H_2O \rightleftharpoons CH_3COOH + HOCH_2CH_2N^+(CH_3)_3$$

and potentiometric methods of studying the hydrolysis have been reported previously [7—9]. In the present work, the method of Gibson and Guilbault [7] was used and extended for studies of inhibitory effects. The acetic acid formed is sensed by a glass electrode in a weakly buffered system. With pH values near the pK_a value of the buffer, there is a linear change of pH with time and the amount of acetic acid released. Therefore, measurement of the change in pH with time gives a value of the initial velocity of the reaction. To correlate the amount of acetic acid formed to the change in pH, the system is calibrated with aliquots of standard acetic acid.

Organophosphorus insecticides inhibit cholinesterase by blocking the esteratic site of the enzyme. The reaction can be described as

$$EH + PX \rightleftharpoons (EHPX) \overset{XH}{\rightarrow} EP$$

where EH is the enzyme and PX is the insecticide; EP is the phosphorylated enzyme which is hydrolysed extremely slowly. The reaction may be considered to be irreversible. In the present investigation, the inhibitory effects of the insecticides dichlorvos (I; 2,2-dichlorovinyldimethyl phosphate; Vapona; DDVP) and bromophos (II; 4-bromo-2,5-dichlorophenyl-diethyl phosphorothionate) were determined.

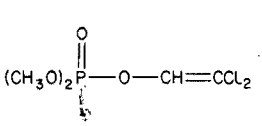

(I)

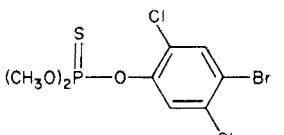

(II)

EXPERIMENTAL

Reagents and samples

Enzyme. Dissolve horse serum cholinesterase (Merck, Darmstadt) in redistilled water to give a 2.88 ± 0.02 mg ml^{-1} solution. The solution can be kept cold (4°C) for more than a week without significant loss in activity.

Insecticides (inhibitors). Stock solutions (3.92×10^{-3} M) of dichlorvos (Bayer, Leverkusen) were prepared in redistilled water. Stock solutions (1.0×10^{-3} M) of bromophos (CelaMerck, Ingelheim, W. Germany) were prepared in ethanol. The commercial products were not purified.

Buffer solutions. Dissolve 0.242 g of tris(hydroxymethyl)aminomethane (reagent grade; Merck, Darmstadt) and 9.00 g of reagent-grade sodium chloride in redistilled water and dilute to 1 l. Adjust the pH with hydrochloric acid; an initial pH of 8.30 is usually suitable for the reaction.

Substrate. Dissolve acetylcholine chloride (reagent grade; Merck) in the buffer solution to give a 9.0×10^{-3} M solution. Because of autohydrolysis of the acetylcholine, prepare this solution freshly.

Purified nitrogen is passed over the test solutions to avoid contamination by carbon dioxide.

Apparatus

The apparatus used is a modified version of that reported by Gibson and Guilbault [7]. The reaction cell is a Pyrex test tube of diameter 2.5 cm and height 6.0 cm, with a small hole half way down the side for injection of the enzyme. The cell has a tightly fitting polyethylene lid with tight holes for the glass (Radiometer G202C) and calomel (Radiometer K401) electrodes.

Nitrogen is introduced through a tube projecting just below the lid. The solution is stirred magnetically. A Radiometer pH meter PHM 64 was used.

The reaction cell is placed in a thermostatted water bath at 25.0°C. The enzyme and the inhibitor are added from Carlsberg micropipettes (accuracy, ± 1%).

Procedures

To oxidize bromophos to its active form, add 1.5 ml of water saturated with bromine to 10 ml of the stock solution of bromophos. Boil for 5 min in a water bath at 100°C and dilute to 10^{-4} M with redistilled water.

For the actual determination, mix equal volumes of insecticide (dichlorvos or oxidized bromophos) and enzyme (2.88 mg ml^{-1}) in a thermostatted water bath. Add 200 μl of this solution to 6.0 ml of acetylcholine chloride (1.54 mg ml^{-1}), thermostatted to 25.0°C. Measure the resulting initial rate of hydrolysis from the amount of acetic acid formed per minute by recording the change of potential for 2 min.

The concentrations of inhibitors, and the time and temperature of incubation were varied to improve the sensitivity of the method. All measurements were carried out with solutions in the pH range 7.9—8.2. In this narrow range, the change in pH is a linear function of the quantity of acetic acid formed by hydrolysis. This was confirmed from a calibration curve with μmol HAc/ΔpH = 6.8 for the buffer system used.

RESULTS

Figure 1 shows the results of the inhibition of cholinesterase with bromophos. The incubation time was 1 h at 25.0°C and the reaction time with substrate 2 min at the same temperature. The reaction rate decreases linearly with increasing concentration of bromophos, in that part of the curve which corresponds to the lowest concentration of the insecticide. This may be utilized for the determination of the compound. The straight line (with a slope of 0.01794 μmol HAc/min/mM bromophos) was found from a least-squares treatment of the data corresponding to the linear part of the curve. Figure 2 gives the results of the inhibition with dichlorvos at 25.0°C. Straight lines (slopes 0.0822 and 0.1990, respectively) were obtained for the lowest concentrations of the insecticide. Additional experiments were carried out similar to those reported in Fig. 2, but the temperature of incubation was increased from 25.0°C to 37.0°C. The results are presented in Fig. 3; the slope of the straight line is 0.4185.

The data presented in Figs. 1—3 result from several independent measurements and the plots are averages. The straight lines were calculated from all the individual data.

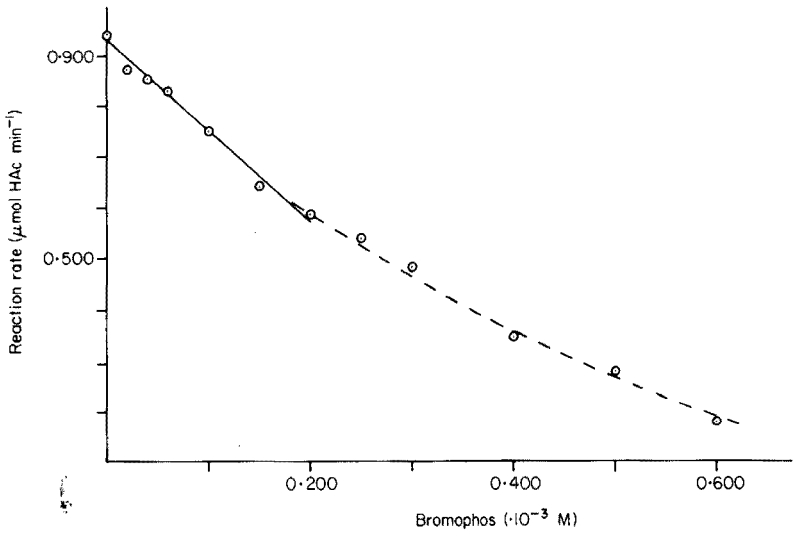

Fig. 1. Reaction rate (μmol HAc min^{-1}) as a function of the concentration of bromophos. Enzyme—bromophos solution (200 μl) was incubated for 1 h at 25.0°C before being added to 6.0 ml of substrate (9.0×10^{-3} M). The first part of the curve (full line) was linearized by the method of least squares.

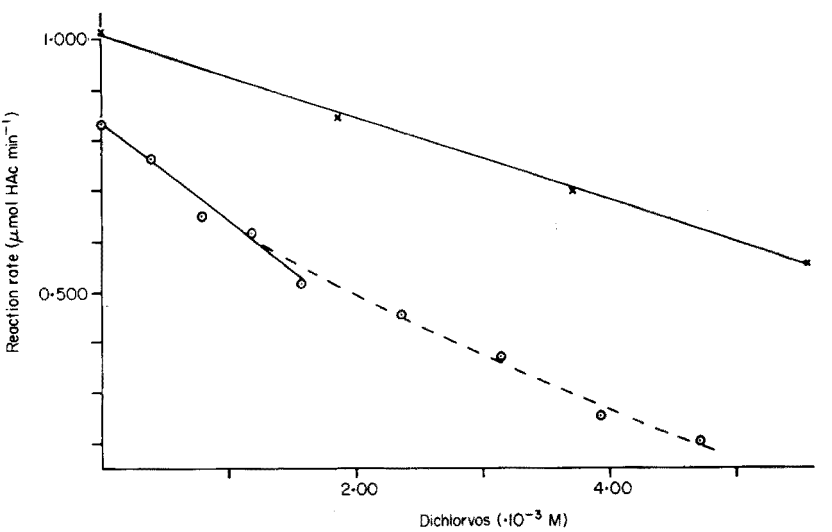

Fig. 2. Reaction rate (μmol HAc min^{-1}) as a function of the concentration of dichlorvos. Enzyme—dichlorvos solution (200 μl) was incubated for 1 h (○) or 15 min (×) at 25.0°C before being added to 6.0 ml of substrate (9.0×10^{-3} M). The curves were linearized (full lines) by the method of least squares.

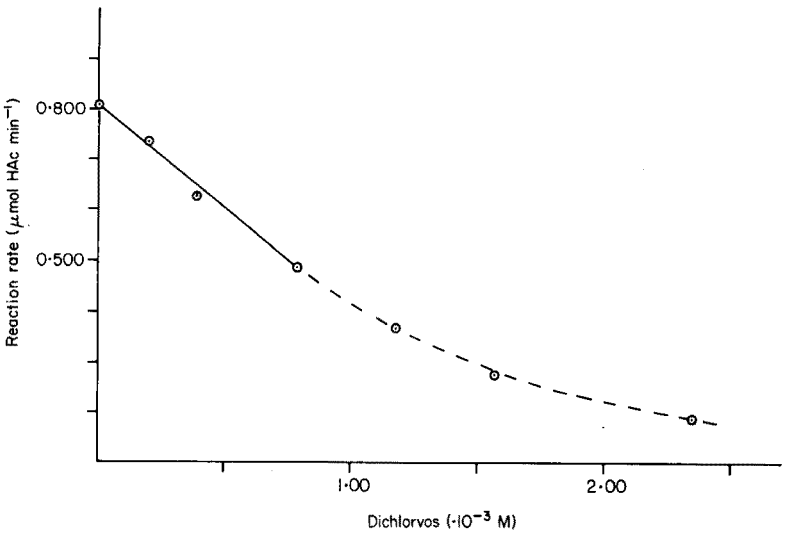

Fig. 3. Reaction rate (μmol HAc min^{-1}) as a function of the concentration of dichlorvos. Enzyme—dichlorvos solution (200 μl) was incubated for 1 h at 37.0°C before being added to 6.0 ml of substrate (9.0×10^{-3} M) at 25.0° C. The first part of the curve (full line) was linearized by the method of least squares.

DISCUSSION

Bromophos has an inhibitory effect in the oxidized form only. Amounts of bromine up to more than three times the amount recommended for the oxidation did not affect the inhibition. The inhibition was not changed by adding bromide. The time and temperature of oxidation did not affect the results when the oxidation was complete. Although it was proved to be unnecessary by these experiments, the excess of bromine was removed by boiling before further treatment of the insecticide.

The autohydrolysis of acetylcholine is the greatest limitation of the proposed method. Optimal results with acetylcholine were obtained at 25.0°C. The contribution from autohydrolysis was subtracted from all measurements. The rate of autohydrolysis was found to be 0.001 ΔpH min^{-1} at the given concentrations. At higher temperatures the autohydrolysis increased considerably. By using this procedure, no significant errors were caused by the hydrolysis.

Attempts were made to improve the method by varying the times of hydrolysis, but increasing this time did not affect the results.

The concentration of the substrate must be high enough to make the initial reaction rate independent of the amount of acetylcholine. A 9.0×10^{-3} M concentration of the substrate satisfied this requirement. Further increase in the concentration of acetylcholine was unfavourable.

Experiments were done to establish the best concentration of enzyme. According to Gibson and Guilbault [7] the quantity of acetic acid released per minute increases linearly with the amount of the enzyme up to 1 μmol of acetic acid per min. An amount of 2.88 mg ml^{-1} of the enzyme was found to be most satisfactory. This gave an initial reaction rate of about 0.9 μmol of acetic acid per min under the given conditions. However, the rate varied from one batch of enzyme to another.

The effect of the incubation time of enzyme with inhibitor was studied. For both bromophos and dichlorvos, the inhibitory effect increased with incubation time, and this increased the sensitivity of the analytical method. For practical reasons, incubation times of 1 h were used for most experiments. No significant improvements were found by using longer incubation times, except with higher concentrations of insecticides, so that there was no improvement in sensitivity. Figure 2 gives results with incubation times of 1 h and of 15 min. The line corresponding to 1 h is much steeper (slope 0.1990) than the other (slope 0.0822), corresponding to about a doubling of the sensitivity of the analysis. (The heights of the two series in Fig. 2 are not comparable, because two different batches of enzyme were used.)

The effect of incubation temperature seems to vary with the inhibitor. A pronounced improvement was obtained in the determination of dichlorvos by raising the temperature from 25.0°C to 37.0°C. Comparison of the results in Figs. 2 and 3 shows that an increase in the temperature from 25.0°C to 37.0°C more than doubles the sensitivity; the slope of the straight line increase from 0.1990 to 0.4185. With bromophos, sensitivity improvements with increasing temperature were slight. For this reason, the convenience of using only one temperature (25°C) for both the incubation and the reaction with the substrate, was preferred for the main experimental series (Fig. 1).

In conclusion, the best conditions for the analyses are those given in Fig. 1 for bromophos and in Fig. 3 for dichlorvos. The linear parts of the curves may be utilized as calibration curves in analysis. Reasonable linearities are obtained up to 70 ppb and 220 ppb, with detection limits of about 7 ppb and 22 ppb for bromophos and dichlorvos, respectively.

Winter and Ferrari [4] and Voss and Sachsse [6] have utilized the inhibitor effects of related insecticides on cholinesterase in colorimetric methods. Dichlorvos has been measured chromatographically [10, 11] with detection limits of about the same order of magnitude, or in some cases somewhat lower than those reported here.

The proposed potentiometric determination of insecticides by inhibition of cholinesterase, with bromophos and dichlorvos as examples, may be competitive with, or a valuable supplement to chromatographic methods. The analyses are simple to carry out and do not require expensive laboratory equipment or instruments. The inhibition of cholinesterase by the organophosphorus pesticides and the carbamates is highly selective. When the proposed method is used, the action of the insecticides in agriculture is the same as the action utilized in the analysis.

Experiments are now in progress to test immobilized systems on electrodes for this type of analysis.

REFERENCES

1 J. R. Corbett, The Biochemical Mode of Action of Pesticides, Academic Press, London, 1974, p. 107.
2 L. Fishbein, Chromatography of Environmental Hazards, Elsevier, Volume I, Amsterdam, 1972, p. 198.
3 L. Fishbein, Chromatography of Environmental Hazards, Elsevier, Volume III, Amsterdam, 1975, p. 509.
4 G. D. Winter and A. Ferrari, Residue Rev., 5 (1964) 139.
5 D. E. Ott and F. A. Gunther, J. Assoc. Off. Anal. Chem., 49 (1966) 669.
6 G. Voss and K. Sachsse, Toxicol. Appl. Pharmacol., 16 (1970) 764.
7 K. Gibson and G. G. Guilbault, Anal. Chim. Acta, 76 (1975) 245.
8 K. L. Crochet and J. G. Montalvo, Anal. Chim. Acta, 66 (1973) 259.
9 H. D. Michel, J. Lab. Clin. Med., 34 (1949) 1566.
10 M. C. Ivey and H. V. Claborn, J. Assoc. Off. Anal. Chem., 52 (1969) 1248.
11 G. Draeger, Pflanzenschutz-Nachr., 21 (1968) 373.

Analytica Chimica Acta, 93 (1977) 99—110
© Elsevier Scientific Publishing Company, Amsterdam — Printed in The Netherlands

THE FORMATION OF MIXED COPPER SULFIDE—SILVER SULFIDE MEMBRANES FOR COPPER(II)-SELECTIVE ELECTRODES†
Part II. Relation between Structure and Electrochemical Behaviour of the Electroactive Material

G. J. M. HEIJNE* and W. E. VAN DER LINDEN

Laboratory for Analytical Chemistry, University of Amsterdam, Nieuwe Achtergracht 166, Amsterdam (The Netherlands)

(Received 2nd May 1977)

SUMMARY

Mixed copper sulfide—silver sulfide precipitates used for copper-selective electrodes have been studied by x-ray powder diffractometry, scanning electron microscopy and solubility measurements, in order to find an explanation for the high limit of detection, measured in calibration experiments as well as in titrations. X-ray diffraction showed that some precipitates consisted of ternary sulfides (mainly jalpaite, $Ag_{1.5}Cu_{0.5}S$), while others were mixtures of the binary sulfides. The presence of ternary sulfides could be correlated with optimal electrochemical and mechanical characteristics. The solubility measurements showed extraordinarily high solubilities for these sulfides. Evidence is given that these high solubilities are caused by the oxidation of copper(I) present in the ternary compound, the reaction being $Cu_2S \rightleftarrows CuS + Cu^{2+} + 2e^-$. S.e.m. photographs gave some additional information about the structure and the particle size of several precipitates.

During the last decade much attention has been paid to the preparation and the use of copper(II)-selective electrodes. At least thirteen papers have been published describing a wide variety of techniques for the preparation [2—14]. Except for Sharp and Johansson [12], who used 7,7,8,8-tetracyanoquino-dimethane radical salts, all authors have applied copper chalcogenides as the electroactive material, obviously because the solubility products of these compounds are very low. It is generally assumed that the response of these electrodes is related to the dissolution process of the membrane material, and that the lower limit of detection of the electrode should correspond to the solubility of this material [5, 15, 16]. In spite of the low solubilities of the compounds used, about 10^{-13} mol l^{-1} at pH 5, all these electrodes showed linear response ranges only for copper concentrations between 10^{-1} and 10^{-7} M, when calibrated with copper(II) solutions. The supposition, made by Buck [17], that an unexpectedly high limit of detection might be caused by the occlusion of more soluble compounds, especially if sulfide precipitates are formed in alkaline medium, is not confirmed by

†Reference [1] forms Part I of this series.

the facts, because similar linear ranges have been found for single crystals [8, 18] and for materials obtained by a direct reaction of the elements [6, 7, 14].

In complexiметric titrations with EDTA, deviations were observed [1] between the experimental electrode response and the response expected from the copper concentration calculated on the basis of chemical equilibrium in the solution. The potentials were too high in the presence of an excess of ligand. As the free copper-ion concentration in the solution was well-buffered, the possible influence on the lower limit of detection of small amounts of copper from other chemicals in the solution or from desorption of the glassware used can be excluded.

Three other possible causes for the differences between the theoretically expected behaviour and the experimental results at low copper concentrations have been considered: (a) the compounds formed in the preparation of the electroactive materials are not those expected; (b) the literature values of the solubility constants are either incorrect or do not apply to the actual conditions during the measurements; and (c) the response is not merely based on dissolution equilibria of the compounds under consideration, but also depends on other processes.

In the present study, the first two points have been examined in more detail; the third point will be dealt with later. Measurements of the solubility showed that the amount of copper dissolved from the precipitates used for preparing electrodes, is much larger than can be expected from calculations based on the solubility products in the literature [19]. Since there was no certainty about the identity of the chemical compounds formed, x-ray powder diffraction was used for identification of the compounds present in the electroactive material. These experiments showed the formation of ternary copper—silver sulfides of well-defined composition. Apart from the relation between the method of preparation of the material and the electrochemical behaviour [1], there is also a correlation between the method of preparation of the material and its crystal structure. Scanning electron microscopy (s.e.m.) was applied to the materials as well as to pellets pressed from it, to obtain additional information about the particle size of the precipitates and about the surface morphology of the pellets, after exposing them to solutions under different conditions.

Solubility data from the literature

The literature contains data only for the solubility of the binary sulfides [19]. The solubility products, K_{so}, are about 10^{-35} for CuS, 10^{-48} for Cu_2S and 10^{-50} for Ag_2S. Thus at pH 5, at which calibrations were carried out, the solubilities of these compounds are about 10^{-13} mol l^{-1}, if $\alpha_{S(H)} = 10^{9.5}$ is used according to Ringbom [20]. Most solubility data, especially for CuS, have been obtained by thermodynamic calculations based on relatively few measurements of the heat of formation, ΔH_f^0, and the heat capacity, C_p. Nevertheless, these figures are probably at least of the right order of

magnitude, since in a recent study by Mathieu and Rickert [21] electrochemically obtained values for both copper(II) and copper(I) sulfide agreed reasonably well with the thermodynamic data given by the National Bureau of Standards [22]. Ravitz [23] and Trümpler [24] have given solubility products for Cu_2S based on electrochemical measurements in sulfide solutions, but their values are probably too low, because of the uncertainty of the dissociation constants of hydrogen sulfide used. CuS is unstable in concentrated sulfide solutions [24]: it is reduced to Cu_2S with simultaneous formation of yellow polysulfides in the adjacent solution.

For most of the solubility data, it is not clear whether the sulfide studied was a well specified crystalline material, e.g. covellite (CuS) or chalcocite (Cu_2S) [25], or an amorphous product. The degree of crystallization may affect the solubility, but there are no reliable data in the literature on this subject. The formation of mixed compounds of copper, silver and sulfur [26] cannot result in higher solubilities, because they would then be transformed to the binary sulfides when suspended in solution, if they were formed at all during the precipitation.

X-ray powder diffraction studies

X-ray powder diffraction has been applied only occasionally to materials used for the preparation of i.s.e. Gordievskii and co-workers [14] used it to determine the composition of copper selenides, and found that materials containing mixtures of compounds of different stoichiometry had similar electrochemical characteristics. Van de Leest [27] used x-ray diffraction in his study of membranes composed of pellets of silver salts with high ionic conductivity, which had been covered by a thin layer of another, less soluble, silver compound.

X-ray powder diffraction data are available for binary and ternary sulfides of copper and silver [28]. Apart from copper sulfides of different stoichiometry [25], one form of silver sulfide (acanthite) and three ternary sulfides are known at room temperature [26, 29—33]: these are stromeyerite [$Ag_{0.93}Cu_{1.07}S$], mckinstryite [$Ag_{1.2}Cu_{0.8}S$] and jalpaite [$Ag_{1.55}Cu_{0.45}S$ or $Ag_{1.5}Cu_{0.5}S$]. For all three, the naturally occurring minerals seem to have a certain composition range, but the composition can always be described as $(Ag, Cu)_2S$, indicating that only monovalent copper is present.

Scanning electron microscopy

Several authors have used s.e.m. to study electrode surfaces, especially in studies of the attack of solution components on the membrane material [34—36]. Some data on the particle size of CuS and Ag_2S gels have been presented by Rudnev et al. [37], but these precipitates were prepared in entirely different ways, and do not give comparable information.

EXPERIMENTAL

The precipitates used were prepared as described in Part I [1]. For the potentiometric measurements the same equipment was used, but the concentration of the acetate buffer was raised to 0.05 M. All chemicals were of analytical-reagent grade.

X-ray diffractograms were recorded with a Philips powder diffractometer PW 1050/25 with Cu Kα-radiation (λ = 1.5418 Å); tubing rate 40 kVp, 20 mA. Scanning electron micrographs were taken with a Cambridge Stereoscan Model 2A.

The solubilities of the copper—silver sulfides were measured by equilibrating the material in acidic solution, pH 1—3, and adjusting the ionic strength to 0.1 with potassium nitrate if necessary. In some cases, oxygen was removed from the solution by bubbling nitrogen before the precipitate was added; the vessel was then closed and kept under nitrogen. The vessels were shaken at intervals of several hours. After equilibration times of 7—90 h the solution was filtered under nitrogen to prevent oxidation of the wet sulfide. The copper content of the solution was determined in 0.05 M acetate buffer (pH 4.7) by titration with EDTA of suitable concentration. A copper i.s.e. was used for end-point indication; the equivalence points were obtained by linearization of the titration curve. The undisturbed functioning of the electrode indicated that no silver was present in this solution. Silver would strongly affect the response of the electrode [4, 5, 9]. The absence of silver was confirmed by titration with potassium iodide with a silver rod as indicator electrode. Nor could sulfide be detected when silver nitrate was added to the solution and back-titrated with iodide.

RESULTS

X-ray diffraction studies

Table 1 shows some results of x-ray powder diffraction analysis of several precipitates. The composition, the preparative conditions and the ratio of Ag_2S:CuS, are given in the notation reported earlier [1], to facilitate comparison with the electrochemical characteristics [1]. The mineral compounds found in the material are tabulated together with some anomalies; the last column of Table 1 gives the reference numbers according to the JCPDS-system [28]. Figure 1 shows some of the diffraction patterns obtained.

As discussed in Part I, two important properties can be defined for pellets pressed from the different electroactive materials: mechanical strength and electrochemical response. The former was shown to depend strongly on the nature of the precipitant and its concentration: in most cases, solution leaked through the membrane with mixed sulfides prepared with hydrogen sulfide or low concentrations of thioacetamide, and with copper sulfide alone. With these mixed sulfides, copper sulfide was precipitated after most of the silver sulfide had been formed, hence this leakage may be due to the unfavourable mechanical properties of copper sulfide.

TABLE 1

X-ray diffraction analysis of sulfide precipitates

No.	Composition and precipitating agent (% excess)			Observations	JCPDS[a] reference number
	Ag:Cu	Method 1 M solut. (excess)	Ag_2S:CuS[b]		
1	100:0	Na_2S (100%)		acanthite (Ag_2S)	14-27
2	100:0	TAA (100%)[c]		acanthite	
3	0:100	Na_2S (100%)		covellite (CuS) + large amt. of amorphous material[d]	6-464
4	0:100	TAA (100%)		covellite + bonattite ($CuSO_4 . 3H_2O$) + amorph. material	6-464; 22-249
5	67:33	Na_2S (80%)	50:50	jalpaite ($\sim Ag_{1.5}Cu_{0.5}S$) + trace of covellite, (some amorph. material)	12-207, 21-1336
6	67:33	0.1 TAA (100%)	50:50	acanthite + small amt. covellite + small amt. of amorph. material	
7	67:33	1 M TAA (100%)	50:50	acanthite + small amt. covellite (more than exp. 6) + amorph. mat.	
8	67:33	Na_2S (20%)	50:50	jalpaite + covellite (more than exp. 5)	
9	82:18	Na_2S (20%)	70:30	jalpaite + acanthite	
10	46:54	Na_2S (20%)	30:70	acanthite + covellite + amorphous material	
11	67:33	pellet, as 5	50:50	as 5, but two additional reflections at 6.32 Å and 3.18 Å	
12	82:18	pellet, as 9	70:30	as 9, reflections seem to be better	
13	67:33	pellet, as 7	50:50	as 7, refl. of covellite more pronounced	
14	67:33	as 5, under nitrogen	50:50	jalpaite + mckinstryite	12-152, 19-406
15	67:33	as 14	50:50	jalpaite + trace of mckinstryite	
16	67:33	pellet, as 14	50:50	as 14, no additional reflections	

[a]Joint Committee on Powder Diffraction Standards [28]. [b]Ratio Ag_2S:CuS corresponding to the indication used in part I [1]. [c]TAA: thioacetamide. [d]Amorphous material is indicated by the rise in the baseline.

The best electrochemical results were obtained with an Ag:Cu ratio of 67:33 and 80% excess of sodium sulfide. When 20% excess of sulfide or an Ag:Cu ratio of 82:18 was used, the characteristics were less favourable, but still acceptable. When the copper content was raised above 33% the response properties deteriorated markedly. Comparison of the electrochemical behaviour with the results of Table 1 shows that those materials containing jalpaite ($\approx Ag_{1.5}Cu_{0.5}S$) have good or acceptable properties (nos. 5, 8 and 9) while the other materials consist of mixtures of acanthite and covellite only. Of these latter sulfides, only no. 7 showed no leakage, but the response characteristics of the corresponding membranes were rather poor.

The best results were obtained with well crystallized jalpaite, which contains only small amounts of binary compounds, as was the case in the materials 5, 14 and 15. Mckinstryite ($Ag_{1.2}Cu_{0.8}S$) was found in material 14 and to a lesser extent in material 15, which were both prepared by a slower

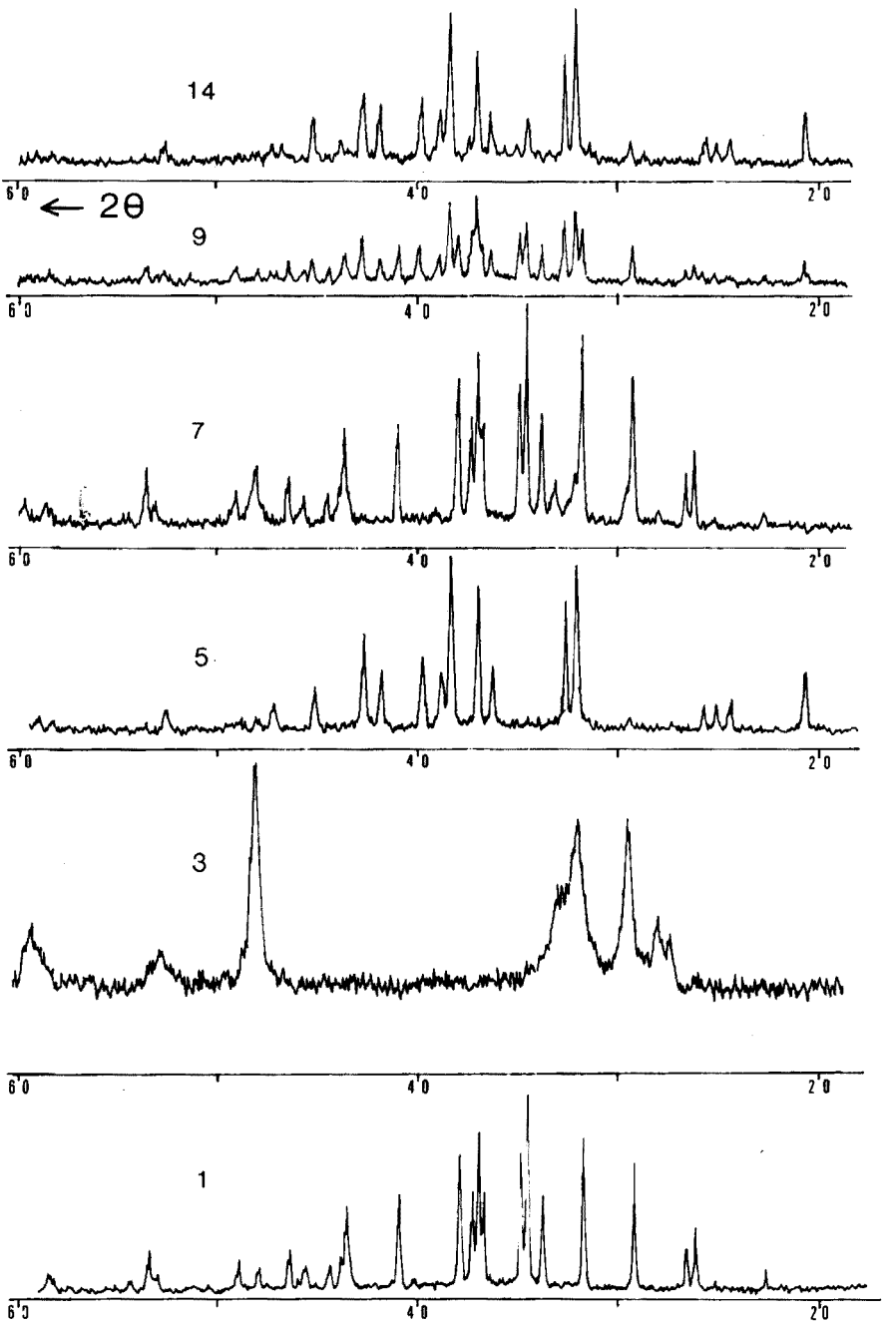

Fig. 1. X-ray powder diffraction patterns of some precipitates. The numbers correspond to those of Table 1. 1, Acanthite. 3, Covellite. 5, Jalpaite. 7, Acanthite + covellite (trace). 9, Jalpaite + acanthite. 14, Jalpaite + mckinstryite.

rate of addition of the metal solution and under nitrogen instead of under air. Both materials showed better response characteristics and seemed to be less sensitive to oxidation by air during long-term exposures (Fig. 2). The ill-defined shapes of the peaks and the increased background in the case of covellite (no. 3) in Fig. 1 indicate that it is not well crystallized and probably contains a lot of material amorphous with regard to x-ray diffraction. This rise in the base line was more or less pronounced in all materials containing copper. The copper sulfide probably crystallizes with difficulty, which may make it difficult to find clear proof of its presence. When it was certainly present, this is indicated in Table 1.

According to Skinner [30], the structures of ternary copper—silver sulfides are very susceptible to pressure and heat; and the reaction rates of the compounds are high on heating. Although all precipitates were dried for 17 h at about 80°C, except for a part of batch 14 and for batch 15, there was no indication that any change was brought about by heating. The influence of the pressure on the crystalline structure of the sulfides was checked by x-ray diffraction. The structure of pellets pressed at 7600 kg cm^{-2} generally did not differ from the original precipitate (see Table 1).

Solubility measurements

The data obtained from the solubility measurements are given in Table 2. For each determination, the conditions (pH of the solution, acid used, use of nitrogen, and equilibration time) are given in the first two columns. The fourth column gives the concentration of copper found in the solution after

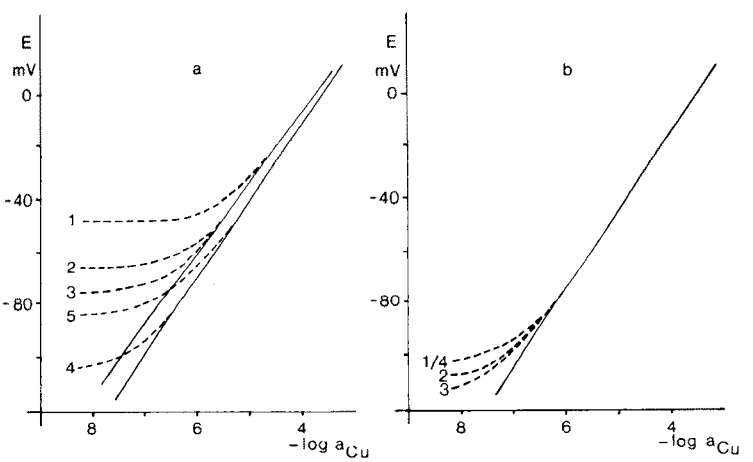

Fig. 2. Calibration curves of copper-i.s.e. made of differently prepared precipitates. A (prepared in air): 1—3, successive curves for new membrane; 4, after titration of 10^{-3} M copper(II) with EDTA; 5, after exposure to air for 27 days. B (prepared under nitrogen): 1 and 2, successive curves for new membrane; 3, after titration of 10^{-3} M copper(II) with EDTA; 4 (coincides with 1), after exposure to air for 13 days.

TABLE 2

Solubility data of sulfide precipitates.

No.	Medium[a] (M)	Equil. time (h)	Equil. concn. $[Cu^{2+}]_{eq.}$ (10^{-3} M)	Corrected $[Cu^{2+}]_{eq.}$ (10^{-3} M)	Expected equilibrium concn. calc. for		Remarks
					CuS[b] (10^{-10} M)	Cu_2S[b] (10^{-11} M)	
A. Copper(II) sulfide (covellite, Table 1, no. 3)							
1	0.01 HNO_3	5 min	1.99				36.6 mg 1.09×10^{-3} mol
2	0.01 HNO_3	5 min	3.86				71.7 mg Cu^{2+}/g CuS
3	0.01 HNO_3	117	1.91	0.54	1.78	1.85	
B. Copper—silver sulfide (jalpaite, Table 1, no. 5)							
1a	0.1 HCl	5 min	0.11				
b	0.1 HCl/N_2	5 min	0.11				av. of 2 detns. 4.3×10^{-5} mol
2a	0.1 HNO_3	20	5.80	5.09	17.8	8.58	
b	0.1 HNO_3	48	2.37	1.65	17.8	8.58	a and b are two
3a	0.01 HNO_3	20	0.85	0.78	1.78	1.85	separate series of
b	0.01 HNO_3	48	0.94	0.87	1.78	1.85	measurements
4a	0.001 HNO_3	20	0.07	0.06	0.18	0.40	
b	0.001 HNO_3	48	0.12	0.11	0.18	0.40	
5	0.1 HNO_3	7	1.36	0.93	17.8	8.58	
6	0.1 HNO_3	90	2.23	1.75	17.8	8.58	identical with 2b
7a	0.1 HNO_3	24	5.38	4.70	17.8	8.58	identical with 2a
b	0.1 HNO_3	72	8.24	8.24	17.8	8.58	material of 7a, directly re-u
8	0.1 HNO_3/N_2	21	0.65	0.43	17.8	8.58	
9	0.1 HNO_3	21	0.82	0.61	17.8	8.58	
10a	0.1 $HClO_4/N_2$	20	0.96	0.61	17.8	8.58	
b	0.1 $HClO_4/N_2$	72	0.22	0.22	17.8	8.58	material of 10a re-used
c	0.1 $HClO_4/N_2$	24	0.20	0.20	17.8	8.58	material of 10b re-used
11	0.01 $HClO_4$	72	0.40	0.26	1.78	1.85	KNO_3 present (0.1 M)
12a	0.1 HCl/N_2	21	0.41	0.19	17.8	8.58	
b	0.1 HCl/N_2	69	0.37	0.37	17.8	8.58	material of 12a re-used
13a	0.1 HCl/N_2	42	0.10	0.10	17.8	8.58	material of 1b re-used
b	0.1 HCl	42	0.29	0.29	17.8	8.58	material of 1a re-used

[a] The ionic strength was adjusted to 0.1 with potassium nitrate if necessary.
[b] Values used for the calculation: $K_{so}(CuS) = 10^{-35}$, $K_{so}(Cu_2S) = 10^{-48}$, $\beta^{H}_{HS} = 10^{12.6}$, $\beta^{2H}_{H_2S} = 10^{19.5}$.

filtration of the precipitate. Preliminary experiments showed that a certain amount of copper dissolved very easily during the first few minutes. Especially with older batches of copper sulfide large amounts of easily soluble copper were found ($1—2 \times 10^{-3}$ mol of copper per gram of sulfide). The solubility measurements were carried out with precipitate prepared as recommended in Part I. When it was stored over silica gel for two months, about 4×10^{-5} mol of copper per gram of material dissolved within the first 5 min. This value increased to 12×10^{-5} mol of copper per gram when the precipitate was stored without precautions for two weeks. Thus a slow oxidation may occur on exposure to humid air. X-ray diffraction of a batch of copper sulfide for which this value was 2×10^{-3} mol of copper per gram, revealed the presence of a large amount of $CuSO_4 \cdot 3H_2O$ (bonattite, Table 1,

no. 4). The loss of weight of about 40% found after washing the precipitate was in good agreement with the presence of about 2×10^{-3} mol $CuSO_4 \cdot 3H_2O$ per gram of copper sulfide material. These results prove that the precipitates are slowly oxidized by air. Storage over silica gel is therefore necessary, but it is probably even better to pellet the material directly after preparation to minimize the exposed surface.

The fifth column of Table 2 gives the copper concentration after correction for the amount of copper due to this air oxidation. Columns 6 and 7 show the copper concentrations calculated from the solubility products. The equilibrium constants used in these calculations were [19, 20]: $\log K_{so} = -35$ for CuS, $\log K_{so} = -48$ for Cu_2S, $\log \beta_{HS}^{H} = 12.6$ and $\log \beta_{H_2S}^{2H} = 19.5$. Although the results show rather poor reproducibility, the experimental values are clearly much higher than can be expected from the literature data. The high solubility found can be explained in several ways. First, hydrogen sulfide may volatilize from the solution. In view of the small amounts of copper dissolved and the good solubility of hydrogen sulfide in water, this influence should be small. Besides, the air volumes above the solution were small (25—100 ml). Secondly, sulfide may be oxidized by dissolved oxygen; but the short-term influence of oxygen seems to be of only limited importance (Table 2, B, nos. 8/9 and 13/14) even at these low concentrations of sulfide. Thirdly, there may be decomposition of the material, when copper(I) is present, as is the case in the ternary sulfides, according to the overall reaction

$$Cu_2S \rightleftarrows CuS + Cu^{2+} + 2e^-; E^0 = 0.54 \text{ V}$$

(The value of the normal potential was calculated from the solubility products.) For a ternary copper—silver sulfide, this reaction can be written

$$Ag_{2-x}Cu_xS \leftrightarrows (1 - \tfrac{1}{2}x)\,Ag_2S + \tfrac{1}{2}xCuS + \tfrac{1}{2}xCu^{2+} + xe^-$$

In prolonged solubility measurements, where the equilibrium solution was renewed every 24 h, decomposition of the ternary compound was found; after two weeks the solubility decreased to 2.3×10^{-6} M copper. X-ray diffraction at this stage showed the presence of acanthite and traces of covellite, but no reflections of jalpaite were found, in accordance with the reaction proposed. This process would also account for the absence of sulfide and silver ions in the solution, as mentioned under Experimental.

Although it is not clear which substances function as electron-acceptors, the amount of copper dissolved probably depends strongly on the presence of some electron-acceptors. As precautions with respect to redox-buffering of the solution were not taken, poor reproducibility of these solubility measurements was expected. To obtain additional evidence for the predominant role of oxidation of copper(I) in the dissolution process of these materials, precipitates containing jalpaite were equilibrated in solutions containing 10^{-3} M cyanoferrate(III) or a mixture of 10^{-3} M cyanoferrate(II) and 10^{-3} M cyanoferrate(III). The redox potential was measured at a platinum electrode versus SCE. In both solutions, the potential became

more negative, indicating that cyanoferrate(III) was reduced by the sulfide precipitate.

Scanning electron microscopy

S.e.m. photographs have been made both from the precipitates and the pellets. Pellets pressed from the standard precipitate were kept for two months in solutions of 0.1 M EDTA and Trien at pH 4.6. Spectrophotometry showed that 6—7 × 10^{-6} mol of copper had dissolved from these pellets, which is comparable to exhaustion of a surface layer of 1.5 μm when copper is distributed homogeneously throughout the pellet. Apart from the impression that the etched pellets had a slightly smoother surface, no clear difference was found between these pellets and others which had been in use occasionally for calibration curves or complexiметric titrations, or which had not been used at all.

Comparison of photographs made of four different types of precipitate (acanthite, covellite, jalpaite and a mixture of acanthite and covellite) (Fig. 3) shows a difference in particle size between covellite and the others. Covellite consists of rather regular spheres of about 60—100 nm in diameter,

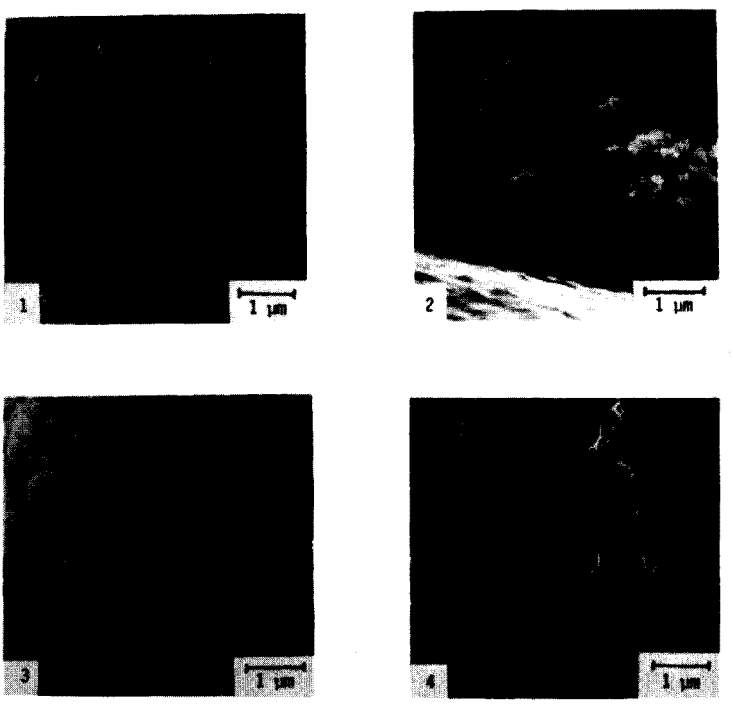

Fig. 3. Scanning electron microscope photographs of precipitates nos. 1, 3, 5 and 7 of Table 1. Magnification: 10 000 ×; 1, Acanthite. 2, Covellite. 3, Jalpaite. 4, Acanthite + covellite.

while those for the other compounds are about 200—600 nm and have less regular shapes. No clear crystalline structures can be distinguished with certainty. The mixture of both binary sulfides (Fig. 3, no. 4) seems to contain particles of the same size as acanthite, but covered with a layer of smaller particles, which might be covellite. In contrast, acanthite and jalpaite particles show rather smooth surfaces, which sometimes even look as if they had been molten.

DISCUSSION

The results found can explain the empirical correlation found between the method of preparation and the electrochemical properties of copper—silver sulfide precipitates used for copper-i.s.e. [1]. The formation of ternary sulfides, such as jalpaite, seems to be essential for obtaining electrodes with good electrochemical and mechanical properties. This formation requires the reduction of copper(II) during the preparation of the sulfide, and implies the presence of monovalent copper in the membrane. The reduction may be accompanied by oxidation of sulfide to sulfur, which forms polysulfides; the strong yellow of polysulfides was indeed observed. A similar color was observed by Trümpler [24] when CuS was in contact with a concentrated sulfide solution, which led to the formation of a layer of Cu_2S and of polysulfides in the solution. The same yellow was observed here in the formation of CuS alone. When this precipitate was equilibrated in solutions containing cyanoferrate(III) alone or mixed with cyanoferrate(II), the redox potential also became more negative, as happened with the material containing jalpaite. All these observations suggest that the copper(II) sulfide obtained under these conditions also contains a certain amount of copper(I). The presence of a surface layer of copper(I) sulfide would explain the relatively amorphous state of this material found with x-ray diffraction, as a very thin layer of copper(I) sulfide is unlikely to possess a crystalline structure, but may very well cause enhanced scattering. If decomposition of the ternary sulfide and formation of the binary sulfides occur, smoothing of the membrane surfaces on etching would be expected, but the s.e.m. studies did not give satisfactory confirmation on this point. The rather high concentrations of free copper(II) ions found with all types of copper-i.s.e.'s described in the literature might well be caused by this dissolution—oxidation process. Work on the response mechanism of the copper-i.s.e. from this point of view is in progress.

The authors express their gratitude to Dr. B. Koch and W. Molleman for their assistance with the recording and interpretation of the x-ray diffractograms and to C. Bakker for making the s.e.m. photographs. The advice of Prof. Dr. G. den Boef during the preparation of the manuscript is gratefully acknowledged.

REFERENCES

1 G. J. M. Heijne, W. E. van der Linden and G. den Boef, Anal. Chim. Acta, 89 (1977) 287.
2 T. Anfalt and D. Jagner, Anal. Chim. Acta, 56 (1971) 477.
3 J. D. Czaban and G. A. Rechnitz, Anal. Chem., 45 (1973) 471.
4 M. S. Frant and J. W. Ross, Ger. Offen. 1942379 (Cl. G. 01n) 12 Mar 1970.
5 E. H. Hansen, C. G. Lamm and J. Růžička, Anal. Chim. Acta, 59 (1972) 403.
6 H. Hirata and K. Date, Talanta, 17 (1970) 883.
7 H. Hirata, K. Higashiyama and K. Date, Anal. Chim. Acta, 51 (1970) 209.
8 A. Hulanicki, M. Trojanowicz and M. Cichy, Talanta, 23 (1976) 47.
9 M. Mascini and A. Liberti, Anal. Chim. Acta, 53 (1971) 202.
10 J. Pick, K. Tóth and E. Pungor, Anal. Chim. Acta, 61 (1972) 169.
11 N. I. Savvin, V. S. Shterman, O. A. Zemskaya, A. Ya. Sychenkov and A. V. Gordievskii, Zh. Anal. Khim., 26 (1974) 1281.
12 M. Sharp and G. Johansson, Anal. Chim. Acta, 54 (1971) 13.
13 H. Thompson and G. A. Rechnitz, Chem. Instrum., 4 (1972) 239.
14 A. F. Zhukov, A. V. Vishnyakov, Yu. I. Urusov and A. V. Gordievskii, Zh. Anal. Khim., 30 (1975) 1614.
15 M. Sato, Electrochim. Acta, 11 (1966) 361.
16 M. Koebel, Anal. Chem., 46 (1974) 1559.
17 R. Buck, Anal. Chem., 48 (1976) 23R.
18 J. Vesely, Collect. Czech. Chem. Commun., 36 (1971) 3364.
19 L. G. Sillén and A. E. Martell, Stability Constants, Spec. Publ. no. 17, The Chemical Society, London 1964; Supplement no. 1, Spec. Publ. no. 25, 1971.
20 A. Ringbom, Complexation in Analytical Chemistry, Interscience, New York, 1963.
21 H. J. Mathieu and H. Rickert, Z. Phys. Chem., NF 79 (1972) 315.
22 F. D. Rossini, D. D. Wagman, W. H. Evans, S. Levine and I. Jaffé, Nat. Bur. Stand., Circular 500, 1952.
23 S. F. Ravitz, J. Phys. Chem., 40 (1936) 61.
24 G. Trümpler, Z. Phys. Chem., 99 (1921) 9.
25 S. Djurle, Acta Chem. Scand., 12 (1958) 1415.
26 S. Djurle, Acta Chem. Scand., 12 (1958) 1427.
27 R. E. van de Leest, Analyst, 101 (1976) 433.
28 Powder Diffraction File, Joint Committee on Powder Diffraction Standards, Swarthmore, Penn., U.S.A.
29 D. Grybeck and J. J. Finney, Am. Mineral., 53 (1968) 1530.
30 B. J. Skinner, Econ. Geol., 61 (1966) 1.
31 B. J. Skinner, J. L. Jambor and M. Ross, Econ. Geol., 61 (1966) 1383.
32 B. W. Robinson and R. D. Morton, Econ. Geol., 66 (1971) 342.
33 A. J. Frueh, Z. Kristallogr. Kristallgeom. Kristallphys. Kristallchem., 106 (1956) 299.
34 M. H. Sorrentino and G. A. Rechnitz, Anal. Chem., 46 (1974) 943.
35 H. Malissa, M. Grasserbauer, E. Pungor, K. Tóth, M. K. Pápay and L. Pólos, Anal. Chim. Acta, 80 (1975) 223.
36 H. A. Klasens and J. Goossen, Anal. Chim. Acta, 88 (1977) 41.
37 N. A. Rudnev, A. M. Tuzova and G. I. Malofeeva, Zh. Anal. Khim., 26 (1971) 886; 28 (1973) 635; 31 (1976) 649.

Analytica Chimica Acta, 93 (1977) 111—120
©Elsevier Scientific Publishing Company, Amsterdam — Printed in The Netherlands

A STUDY OF THE BEHAVIOUR OF SOLID-STATE MEMBRANE ELECTRODES
Part III. A Model for the Response Time

J. BUFFLE* and N. PARTHASARATHY

Department of Inorganic and Analytical Chemistry, Sciences II. 30 quai E. Ansermet, 1211 Genève 4 (Switzerland)

(Received 10th January 1977)

SUMMARY

A model is proposed to explain the response time of solid-state membrane electrodes, in the range of potential—time curves corresponding to seconds or minutes. Several causes of slow response time are considered. In the range of milliseconds to seconds, diffusion seems to be the rate-determining factor, but for times exceeding about 10s, dissolution or crystallization and charge transfer at the membrane seem to be the predominant factors. A mathematical model is derived. The principle is applicable to any solid-state membrane electrode and takes into account the change in response time with changes in the nature or concentration of the test ion and in the surface electrochemical properties of the membrane.

In recent years there has been growing interest in the study of response time of ion-selective electrodes (i.s.e.). Theoretical as well as experimental studies [1—9] on the response rate of i.s.e. have been reported and mechanistic models have been proposed.

Most of the experimental studies have been done with automatic or continuous flow systems. However, the commonly used techniques in most laboratories are the immersion method, i.e. the electrodes are simply transferred from one solution to another for measurement, and the injection method in which known amounts of test ions are added to the solution and the potential is then measured. These methods were therefore used here for the investigation of response rates.

Some of the models proposed are summarized below.

(a) When the response time of the electrode is fast, i.e. of the order of milliseconds, the rate-determining process is diffusion [5, 10]. The following relationship between potential and time was derived by Rechnitz and Hameka [1]

$$E = E_{eq} - \frac{RT}{nF} \ln (1 - e^{-kt}) \qquad (1)$$

where E is the potential at time t and E_{eq} is the equilibrium potential.

(b) For response times of the order of seconds or minutes, a hyperbolic relationship between E and t has been established by Mertens et al. [9] for the fluoride electrode

$$E - E_i = t/(a + bt) \tag{2}$$

where E is the potential at time t; a and b are constants, and E_i is the potential at time $t = 0$. This is an empirical relationship and the response time behaviour is explained in terms of thin film diffusion. An equivalent electrical circuit and its RC constant were deduced from the results for the lanthanum fluoride membrane.

(c) For glass electrodes Rechnitz and Kugler [6] used another relation for the potential—time response

$$\log [(E - E_{eq})/E_{eq}] = kt^{\frac{1}{2}} \tag{3}$$

where k is a constant.

Models (a) and (c) were found to be inapplicable for our experimental conditions and though model (b) fitted the results, an attempt was made to interpret the results in terms of the physico—chemical properties of the system. Moreover, instead of the continuous analysis technique used by Mertens et al., the response times of electrodes were measured by the discontinuous methods commonly used.

EXPERIMENTAL

A Beckman chloride electrode (39604) coupled with a mercury(I) sulphate reference electrode with a 2 M sodium sulphate salt bridge was used for chloride measurements. Most of the fluoride measurements were made with a Beckman fluoride electrode (No. 39600). An Orion fluoride electrode (94-09 A) and a Beckman fluoride combination electrode (No. 39650) were used for comparison purposes. A saturated calomel reference electrode was used with the fluoride electrode. The potentials were recorded with a Metrohm recorder (E 478) to ± 0.1 mV to ensure a steady potential value. A Unicam SP 1900 atomic absorption spectrometer was used for the determination of silver(I). A PAR 170 electrochemical system was used as potentiostat. A Metrohm EA 125 conductivity cell (cell constant 0.56) and a WISS-Techn. conductimeter were used for conductivity measurements.

The solutions used were a 0.1 M stock solution of fluoride, 2 M $NaNO_3$, 0.1 M stock solution of potassium chloride, 0.1 M silver nitrate and 0.2 M KNO_3. All fluoride, chloride and silver solutions of varying concentrations were prepared by serial dilution with demineralized water. All working solutions of test ions were prepared by 1:1 dilution with the appropriate background electrolyte. For fluoride measurements, sodium nitrate was used as the background electrolyte; for chloride and silver measurements potassium nitrate was used.

Conductivity measurements were made in the absence of background electrolyte and under an atmosphere of nitrogen. All measurements were made by stirring the solution at 25 ± 0.1°C unless otherwise stated.

QUALITATIVE STUDIES OF THE RESPONSE TIME

Empirical relationship for potential—time response

Attempts to fit the experimental data to eqns. (1) and (3) were unsuccessful. Therefore, the results were used to formulate [11] an empirical relationship between E and t

$$E = E_{eq} - 1/(At + B) \tag{4}$$

where E is the potential at time t, E_{eq} is the equilibrium potential, and A and B are empirical constants. An empirical relation of similar type but without the constant term B has been reported [12].

Rearrangement of eqn. (4) gives

$$\frac{Et - E_i t_i}{E - E_i} = E_{eq} \cdot \frac{t - t_i}{E - E_i} - \frac{B}{A} \tag{5}$$

where E_i is the potential at a time t_i, arbitrarily chosen, but generally close to zero. Thus a plot of the left-hand side of eqn. (5) against $(t - t_i)/(E - E_i)$ should give a straight line of slope E_{eq}. A plot for the fluoride electrode is shown in Fig. 1B; the data used are shown in Fig. 1A. An excellent straight line is obtained, and eqn. (5) is valid for the entire portion of the E vs. t curve. Moreover, it was found that the value of E_{eq} is independent of the arbitrarily chosen value of t_i. Thus E_{eq} can be determined from eqn. (5) by simply recording a small portion of $E = f(t)$.

A good fit was also obtained by using eqn. (2) for the results of the addition technique. However, although eqn. (4) resembles eqn. (2), eqn. (4) is more practical for quick evaluation of the equilibrium potential, E_{eq}, by the immersion method, as a knowledge of potentials at three different times t at the beginning of the response time curve suffices [11].

Once E_{eq} is known, a plot of $1/(E - E_{eq})$ vs. t allows the parameters A and B to be determined and these are related to the kinetics of the system (see below).

The chief factors governing the response time

Several solid-state electrodes (e.g. F^-, Cu^{2+}, Cl^-, Pb^{2+} and Cd^{2+}) with different membrane compositions (LaF_3, AgCl, CuS, PbS/Ag_2S, CdS/Ag_2S, respectively) exhibit similar response time characteristics. Therefore, for explanation of the response time, one must seek a phenomenon (or several phenomena) fundamental to all these electrodes regardless of their chemical nature. Several possibilities were considered.

Formation of hydroxide film. Since the hydroxide ion interferes with most solid-state electrodes and in particular is the chief interference for the

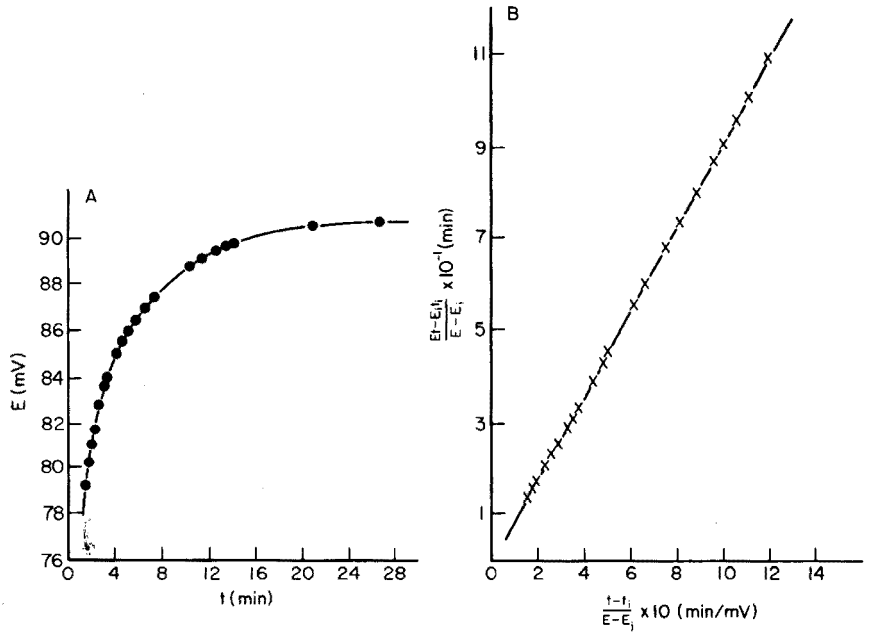

Fig. 1. A. E.m.f. vs. time curve for a fluoride electrode. Immersion technique. Concentration change from 10^{-2} to 10^{-4} M F^-. I = 1 M $NaNO_3$; T = 25°C. (The electrode used was old. Similar curves are obtained for new electrodes except that the time scale is reduced.) B. Verification of empirical relationship, with the experimental data of the curve given in A.

fluoride electrode, a possible reason for slow response might be a slow equilibrium between the test ion and a hydroxide film formed on the electrode. For the fluoride electrode, the equilibrium between La-OH [13] and fluoride ions can be written as La-OH + $F^-_{aq} \rightleftarrows$ LaF + OH^-_{aq}. However, the response characteristics of the electrode after pretreatment in acidic solution remain unchanged, which rules out this chemical process as a cause for slow response. Moreover, other solid-state electrodes whose constituents are less likely to form hydroxide films, e.g. the chloride electrode, exhibit the same potential—time dependence as the fluoride electrode. Thus, slow equilibration between La-OH and F^- ions is unlikely to be a controlling factor.

Response time of the circuitry. The response time of the electrodes may be limited by the response time of the electronic circuit used for the measurements (including the electrodes themselves). To measure the response time of the electronic circuit of the fluoride electrode, a potentiostat was inserted in series, in the circuit pH meter—electrodes. A step voltage of 117 mV was applied to the system and the resulting E vs. t curve was recorded. This was done with and without the electrodes in the system; the value 117 mV corresponds to a 100-fold step change in concentration, this change being one of the experimental conditions used in making response time measurements. The results showed that the response time of the circuitry alone or with fluoride electrode is much faster (less than 5s) than the response time of the electrode when it is subjected to step changes in concentrations.

The fact that the electronic circuit is not a chief factor in the response time was also checked by measuring the response time of a chloride electrode with potentiometers having different impedances. For this purpose, a Schneider voltmeter (resistance 10^8 ohm), a 10^{10}-ohm resistor connected in parallel to the Metrohm digital pH meter E-500, a portable Metrohm pH meter (resistance $\geqslant 2 \cdot 10^{11}$ ohm) and a Metrohm digital pH meter E-500 (resistance $\geqslant 10^{12}$ ohm) were used. These measurements were made by the addition technique with a step concentration of 2 (dilution experiment) or 10 (concentration experiment). The results showed that the impedance of the system does not influence the response time of the electrode. Furthermore, these results proved that the system indeed functioned at "zero" current for if current were drained through the electrode membrane because of insufficient impedance of the measuring device, distortion in potential would have been observed.

Diffusion and adsorption processes. At the electrode-solution interface, diffusion and adsorption can occur, and one of these steps might be the rate-determining step in the response kinetics of ion-selective electrodes. A simple diffusion model similar to that described by Rechnitz and Hameka [1], did not tally with the results observed here. The fluoride electrode crystal adsorbs fluoride ions [14], and since analogous adsorption of ions by other i.s.e. is not improbable, an attempt was made to explain the result of response time in terms of both diffusion and adsorption. An equation was derived on the basis that the test ion is adsorbed on the electrode surface with instantaneous attainment of the corresponding thermodynamic equilibrium; that the electrode responds to the non-adsorbed test ion; that the concentration gradient across the thin diffusion layer is linear; and that the surface of the electrode is plane. However, this equation did not fit the experimental data. Hence, it seems that adsorption and diffusion are not the primary processes determining the kinetics of the electrode.

Dissolution (or crystallization) of the electrode membrane. The membranes of all solid-state electrodes dissolve to some extent in test solutions, and the slow dissolution process might account for the observed potential—time relationship. Measurements were made with a chloride electrode to verify this hypothesis because of the fairly high solubility of the electrode crystal. The silver ion concentration resulting from the dissolution of electrode membrane in chloride solution was determined by atomic absorption spectrometry and conductimetry. Plots of logarithm of silver concentration vs. t (curves a, b), and of $(E - E_0)F/2.3RT$ vs. t (curve c) are shown in Fig. 2. Clearly, the time required to attain equilibrium is of the same order of magnitude as the response time of the electrode. Thus, the dissolution of the electrode membrane probably plays a vital role in the rate-determining step.

The above arguments show that a model for the response time must take into account the hyperbolic nature of the E—t relationships for $t \geqslant 1$ min, as well as the important role played by the dissolution process in this response time.

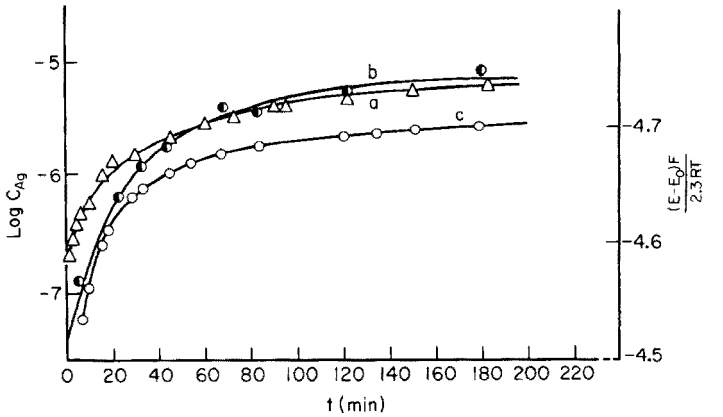

Fig. 2. Test of dissolution theory for a chloride electrode. Measurements made in 10^{-5} M chloride solution. T = 25°C; I = 0.1 M KNO_3. Curve (a), plot of log C_{Ag} vs. t C_{Ag} measured by conductimetry. Curve (b), plot of log C_{Ag} vs. t C_{Ag} measured by atomic absorption spectrometry. Curve (c), plot of $(E - E_0)F/2.3RT$ vs. t (E_0 = standard potential).

THEORETICAL DERIVATION OF POTENTIAL—TIME RELATIONSHIP

In general, the rate of growth or dissolution is given [15] by

$$R = d\Delta/dt = -kS\,\Delta^n \tag{6}$$

where R is the reaction rate, k is the rate constant, S is the surface area, and n is the order of the reaction. For a salt of the type $A_{z_M}M_{z_A}$, Δ is given by

$$\Delta = z_A\,|C_A - C_A^f| = z_M\,|C_M - C_M^f| \tag{7}$$

where C_A and C_M are the concentrations of the anion and cation, respectively, at time t. C_A^f and C_M^f are their equilibrium concentrations and are related by the solubility product (K_S, expressed in terms of concentration) of the salt

$$K_S = (C_A)^{z_M}\,(C_M)^{z_A} \tag{8}$$

C_A^f and C_M^f can also be written [15] as

$$C_A^f = (K_S z_A^{z_A} z_M^{z_M})^{1/(z_A + z_M)} \exp(-F\Psi^f/RT) = C_A \exp(-F\Psi/RT) \tag{9}$$

and

$$C_M^f = (K_S z_A^{z_A} z_M^{z_M})^{1/(z_A + z_M)} \exp(F\Psi^f/RT) = C_M \exp(F\Psi/RT) \tag{9'}$$

where Ψ^f and Ψ are the potential differences between the adsorbed layer and solution at equilibrium and at time t, respectively.

According to Davies and Jones [15], n is related to the stoichiometry of the salt and is frequently equal to

$$n = z_M + z_A \tag{10}$$

For silver chloride, n = 2 for crystal growth, but n = 1 for dissolution when

equivalent amounts of lattice ions are present in solution [16—18] and $n = 2$ when non-stoichiometric quantities of lattice ions are present [17]. In general, for symmetrical salts n is often found to be 2 [19—25], hence $n = 2$ is used below. Substitution of $n = 2$ in eqn. (6), integration and combination of the resulting equation with eqn. (7) gives

$$|(C_M/C_M^f) - 1| = 1/[C_M^f/|(C_M^i - C_M^f)| + z_M k S C_M^f t] \quad (11)$$

where C_M^i is the concentration of M^{+z_M} at $t = 0$.

Combining eqn. (11) with eqn. (8) or (9) gives, respectively,

$$|(C_M/C_M^f) - 1| = 1/[C_M^f/|(C_M^i - C_M^f)| + z_M k S\{K_S/(C_A^f)^{z_M}\}^{1/z_A} t] \quad (11a)$$

or:

$$|(C_M/C_M^f) - 1| = 1/[C_M^f/|(C_M^i - C_M^f)| + z_M k S\,(K_S z_A^{z_A} z_M^{z_M})^{1/(z_A + z_M)} \exp(F\Psi^f/RT)t] \quad (11b)$$

Analogous equations can be derived for anions.

Electrode potentials in non-equilibrium conditions

The activity of cation a_M at time t is also related to the current and the potential difference, $\Delta\phi$, at the interface by the Butler—Volmer equation [26]. If $\Delta\phi$ is measured relative to the equilibrium potential, $\Delta\phi_{eq}$, i.e. when $a_M = a_M^f$ = constant, and if the activity of the cation in the solid phase, $\bar{a}_M$, is independent of time, i.e. $\bar{a}_M = \bar{a}_M^f$, throughout the measurement, then the Butler—Volmer equation can be written as

$$i_M = k_M (a_M^f)^{1-\alpha} \left\{ \frac{a_M}{a_M^f} \exp\left[-\frac{\alpha z_M F}{RT} (\Delta\phi - \Delta\phi_{eq}) \right] - \exp\left[\frac{(1-\alpha)\cdot z_M F}{RT} (\Delta\phi - \Delta\phi_{eq}) \right] \right\} \quad (12)$$

where i_M is the current carried by the cation at the membrane-solution interface, α is the transfer coefficient for the cationic charge transfer and k_M is the rate constant for the charge transfer process. From the theory developed by Buck [27], it can be shown that

$$k_M = \frac{z_M F \bar{k} T}{h} (\bar{a}_M^f)^{\alpha} \exp\left[\frac{-\overleftarrow{\Delta G_M^*} + (1-\alpha) z_M F \Delta\phi_M^0}{RT} \right]$$

$$= \frac{z_M F \bar{k} T}{h} (\bar{a}_M^f)^{\alpha} \exp\left[-\frac{\overrightarrow{\Delta G_M^*} + \alpha z_M F \Delta\phi_M^0}{RT} \right] \quad (13)$$

where $\bar{k}$, h, $\overrightarrow{\Delta G_M^*}$, $\overleftarrow{\Delta G_M^*}$ and $\Delta\phi_M^0$ are as defined in ref. 27.

If the variation in potential with time depends solely on the reaction at the electrode—solution interface, then

$$E - E_{eq} = \Delta\phi - \Delta\phi_{eq} \quad (14)$$

provided that the liquid junction and reference potentials remains constant throughout the experiment.

An equation analogous to eqn. (12) can be obtained for the current carried by the anion; here α is replaced by β, the anionic charge transfer coefficient, the subscript A replaces subscript M throughout and $-Z_A$ replaces Z_M.

Since the total current, i, passing through the circuit is zero (see above),

$$i = i_A + i_M = 0 \tag{15}$$

Combining eqn. (12) corresponding to i_A and i_M, with eqns. (14) and (15), and taking into account eqn. (7) and the activity coefficients γ_M and γ_A of ions M and A, gives

$$\frac{a_M}{a_M^f} - 1 = \exp\left[\frac{z_M F}{RT}(E - E_{eq}) - 1\right] \cdot \left\{1 + \frac{k_A (a_A^f)^{1-\beta}}{k_M (a_M^f)^{1-\alpha}} F(E)\, R(E)\right\} \Big/$$

$$\left\{1 + \frac{k_A}{k_M} \frac{(a_M^f)^{\alpha}\, \gamma_A z_M}{(a_A^f)^{\beta}\, \gamma_M z_A} F(E)\right\} = \exp\left[\frac{z_M F}{RT}(E - E_{eq}) - 1\right] . \; G(E) \tag{16}$$

where $F(E) = \exp\,[(\alpha z_M + \beta z_A) F (E - E_{eq})/RT]$, and $R(E) = \{\exp\,[-z_A F (E - E_{eq})/RT] - 1\}/\{\exp\,[z_M F (E - E_{eq})/RT] - 1\}$.

Equation (16) can be simplified by making the following approximations. If we assume $|z_A(E - E_{eq})| \leqslant 10$ mV and $|z_M(E - E_{eq})| \leqslant 10$ mV, then $R(E) \simeq -z_A/z_M$ and $F(E) \simeq 1 + (\beta z_A + \alpha z_M) F (E - E_{eq})/RT$. This condition occurs near equilibrium where the variation in potential is small and the time taken to reach equilibrium is slow. Several limiting cases may then occur as follows.

(i) If $z_A = z_M = 1$, the term $(\beta z_A + \alpha z_M) F (E - E_{eq})/RT$ is never greater than 0.15 and the influence of $F(E)$ in eqn. (16) is weak. $G(E)$ is then almost independent of E, i.e. $G(E) \simeq$ constant $= K_G$. Thus

$$|(a_M/a_M^f) - 1| \simeq z_M F K_G |(E - E_{eq})|/RT. \tag{17}$$

(ii) If, simultaneously, $k_A/k_M \ll (a_M^f)^{1-\alpha}/(a_A^f)^{1-\beta}$ and $k_A/k_M \ll (a_A^f)^{\beta}/(a_M^f)^{\alpha}$, then $G(E) \simeq 1$, and

$$|(a_M/a_M^f) - 1| \simeq z_M F |E - E_{eq}|/RT. \tag{18}$$

(iii) Conversely, if $k_A/k_M \gg (a_M^f)^{1-\alpha}/(a_A^f)^{1-\beta}$, $\gamma_A = \gamma_M$ and $k_A/k_M \gg (a_A^f)^{\beta}/(a_M^f)^{\alpha}$ then $G(E) = -(z_A/z_M)^2 a_A^f/a_M^f$. Substitution of this relationship for $G(E)$ into eqn. (16) and application of eqn. (7) gives the same relationship as eqn. (18) with subscript A replacing subscript M throughout.

In practice, one of the these conditions is often satisfied. Condition (i) is valid for crystals whose anion and cation may both act as potential-determining ions, whereas conditions (ii) and (iii) are applicable when charge transfer is carried out only by cation or anion, respectively. For example, condition (iii) is satisfied in the case of the fluoride electrode which does not respond to lanthanum ions [28].

Potential—time relationship

If the activities are replaced by concentrations in eqns. (17) and (18) and in the analogous equation for condition (iii), and if each of these equations

are combined with eqn. (11), then for the limiting case (ii)

$$|E - E_{eq}| = 1 \Big/ \left\{ \frac{z_M F}{RT} \cdot \frac{C_M^f}{|C_M^i - C_M^f|} + kSC_M^f \frac{z_M^2 F}{RT} t \right\} \quad (19)$$

If A^{-z_A} is the potential-determining ion (limiting case iii), eqn. (19) is the same except that subscript A replaces subscript M throughout.

Equations (19) and (4) resemble each other, and A and B in eqn. (4) correspond to

$$A = kS\,(z_M^2 F/RT)\,C_M^f = kS\,(z_M^2 F/RT) \cdot (K_S z_A^{z_A} z_M^{z_M})^{1/(z_A + z_M)} \exp(F\Psi^f/RT) \quad (20)$$

and

$$B = (z_M F/RT) \cdot C_M^f / |C_M^i - C_M^f| \quad (21)$$

For the limiting case (i), A and B are multiplied by K_G. Similar equations for B and A are obtained if the anion is the potential-determining ion.

DISCUSSION

The proposed model can be verified [31] by studying the dependence of A and B/A on the concentration of the test ion, and the dependence of A on temperature and Ψ^f.

If the potential-determining ion, e.g. the anion, is the same as the test ion, then a plot of A vs. C_A^f should give a straight line; this would be expected for a fluoride electrode. In contrast, if the potential-determining ion, e.g. M^{+z_M}, is not the same as the test ion (A^{-z_A}), a hyperbolic relationship between A and C_A^f would be expected. This should happen for the chloride electrode if Ag^+ is the potential-determining ion and chloride the test ion. In this case, $A = kS\,(F/RT)\,(K_S/C_{Cl}^f)$.

Combining eqns. (20) and (21), and application of eqn. (7) gives

$$\frac{B}{A} = \frac{1}{kS} \cdot \frac{1}{z_M |C_M^i - C_M^f|} = \frac{1}{kS} \cdot \frac{1}{z_A |C_A^i - C_A^f|} \quad (22)$$

This equation is valid irrespective of whether the test ion is potential-determining ion or not.

Since $\ln k = C_1 - E^*/RT$ and $\ln K_S = C_2 - \Delta H_0/RT$ (where E^* and ΔH_0 are the activation energy for the crystallization (or dissolution) process and the standard heat of formation, respectively, and C_1 and C_2 are constants), combination with eqn. (20) gives

$$\ln(AT) = C - \left[\frac{E^* + \Delta H_0/(z_A + z_M) \pm F\Psi^f}{R} \right] \frac{1}{T} = C - E_t^*/RT \quad (23)$$

where C is a constant and the sign of the term $F\Psi^f$ is positive or negative depending on whether the cation or anion is the potential-determining ion.

In eqn. (23), Ψ^f is assumed to be independent of temperature. This is not rigorously correct. However, it can be shown that the change in Ψ^f with change in temperature is negligible. Moreover, in the limiting case (i), E_t^*

also depends on the temperature coefficient of K_G, E_G^*. Since K_G depends on the charge transfer rate constants, this coefficient may be high.

Thus, E_t^* is the sum of four different parameters; E^*, ΔH^0, $F\Psi^f$ and E_G^*. $E^* \geqslant 0$; ΔH^0, $F\Psi^f$ and E_G^* vary depending on the given compound. For silver chloride, ΔH^0 is positive (15.6 kcal [29]) and the sign of $F\Psi^f$ will be positive if silver ion determines the potential of the electrode [30]. Since ΔH^0 and E^* are constants, while Ψ^f and E_G^* depend on the nature and the concentration of the test ion, the experimental value of E_t^* should depend on these two factors.

The model proposed here should explain at least two important features of the response rate of solid-state ion-selective electrodes: the hyperbolic nature of the $E - t$ relationship and the change in the response rate with change in the test ion concentration. The principle should be applicable to most solid-state ion-selective electrodes.

We thank Orion Research Inc. and Beckman Instruments Inc. for providing the electrodes used in this work.

REFERENCES

1 G. A. Rechnitz and H. F. Hameka, Z. Anal. Chem., 214 (1965) 252.
2 G. Eisenman, Biophys. J., 2 (1962) 259.
3 G. Johansson and K. Norberg, J. Electroanal. Chem., 18 (1965) 239.
4 G. A. Rechnitz and M. R. Kresz, Anal. Chem., 38 (1966) 1789.
5 K. Tóth and E. Pungor, Anal. Chim. Acta, 64 (1973) 417.
6 G. A. Rechnitz and G. C. Kugler, Anal. Chem., 39 (1967) 1682.
7 R. P. Buck, J. Electroanal. Chem., 18 (1968) 363.
8 R. P. Buck, J. Electroanal. Chem., 18 (1968) 381.
9 J. Mertens, P. Van den Winkel and D. L. Massart, Anal. Chem., 48 (1976) 2.
10 R. Rangarajan and G. A. Rechnitz, Anal. Chem., 47 (1975) 324.
11 J. Buffle, J. C. Landry and W. Haerdi, Tech. Sci. Munic. - L'Eau, 11 (1974) 547.
12 Orion Newsletter, Orion Research Inc., Jan/Feb. (1971).
13 G. A. Rechnitz and M. J. D. Brand, Anal. Chem., 42 (1970) 478.
14 J. Buffle, N. Parthasarathy and W. Haerdi, Anal. Chim. Acta, 68 (1974) 253.
15 C. W. Davies and A. L. Jones, Trans. Faraday Soc., 51 (1955) 812.
16 A. L. Jones, Trans. Faraday Soc., 59 (1964) 2355.
17 C. W. Davies and C. H. Nancollas, Trans. Faraday Soc., 51 (1955) 818.
18 J. R. Howard, G. H. Nancollas and N. Purdie, Trans. Faraday Soc., 56 (1960) 280.
19 G. H. Nancollas, Croat. Chem. Acta, 45 (1973) 225.
20 C. H. Bovington and A. L. Jones, Trans. Faraday Soc., 66 (1970) 2088.
21 J. R. Campbell and C. H. Nancollas, J. Phys. Chem., 73 (1969) 1735.
22 S. T. Liu and G. H. Nancollas, J. Cryst. Growth, 6 (1970) 281.
23 G. H. Nancollas and S. T. Liu, Soc. Pet. Eng. J., 15 (1975) 509.
24 G. L. Gardner and G. H. Nancollas, J. Inorg. Nucl. Chem., 38 (1976) 523.
25 M. M. Reddy and G. H. Nancollas, Desalination, 12 (1973) 61.
26 K. J. Vetter, Electrochemical Kinetics, Academic Press, (1967).
27 R. P. Buck, Anal. Chem., 40 (1968) 1432.
28 N. Parthasarathy, Ph.D. Thesis (1975).
29 L. G. Sillen and A. E. Martell, Stability Constants, Spec. Publ., No. 17, Chemical Society, London, 1964.
30 R. P. Buck, in Physical Methods of Chemistry, Part IIA (A. Weissberger and B. E. Rossiter, Eds.), Wiley-Interscience, (1971) p. 138.
31 N. Parthasarathy, J. Buffle and W. Haerdi, Anal. Chim. Acta, 93 (1977) 115 (Part IV).

Analytica Chimica Acta, 93 (1977) 121—128
© Elsevier Scientific Publishing Company, Amsterdam — Printed in The Netherlands

A STUDY OF THE BEHAVIOUR OF SOLID-STATE MEMBRANE ELECTRODES
Part IV. Experimental Studies of the Response Time

N. PARTHASARATHY, J. BUFFLE* and W. HAERDI

Department of Inorganic and Analytical Chemistry, Sciences II, 30 quai E. Ansermet, 1211 Genève 4 (Switzerland)

(Received 10th February 1977)

SUMMARY

Some of the factors governing the response time of the fluoride-selective and chloride-selective electrodes have been investigated. The results of E—t and conductance measurements indicate that dissolution and charge-transfer processes control the ion-selective electrode kinetics. The temperature coefficients of the rate constants for dissolution of the chloride electrode membrane, determined by E—t curves and conductimetric measurements, are similar. The results, and the fact that the dissolution is a second-order process, indicate that surface processes play the predominant role in electrode kinetics near equilibrium.

In the previous report [1], various factors governing the response rate of ion-selective electrodes (i.s.e.) were discussed. An empirical relationship for the potential—time curve was established and a model based on dissolution kinetics of the electrode membrane was proposed. In this paper, experimental verification and a discussion of the validity of the model proposed are presented.

EXPERIMENTAL

All apparatus and reagents used were the same as those described in the preceding paper [1].

Potential—time curves

Two methods — immersion and injection (or addition) techniques — were used for recording potential—time curves.

Immersion method. The ion-selective and reference electrodes were dipped in the test solution and the potential E against time was recorded on a chart recorder; time t was taken as zero when the electrode touched the solution. Potential vs. time curves were recorded for concentrations in the range 10^{-2} — 8.10^{-6} M fluoride and 10^{-2}—10^{-5} M chloride.

Three series of measurements were made. In the first series, the response time was measured by going from a concentrated solution to a solution 100 times more dilute; this is referred to below as the dilution experiment.

In the second series, measurements were made by going from dilute to more concentrated solutions (concentration experiment); here, the step change in concentration varied from one measurement to another. In the third series, the initial concentration of the solution was kept constant (10^{-2} M) and the step change in concentration was varied. In the first two series, the chart scan rate was 100 cm s^{-1}, while in the third series the scan rate was 5 cm s^{-1}. In all cases the electrode surface was wiped with tissue paper between measurements.

E vs. time curves had the same profile as shown in Fig. 1 (Part III). Concentration experiments gave similar results but differed in that the potential decreased with increase in time. Similar $E = f(t)$ curves were observed for other ion-selective electrodes, e.g. the copper and lead electrodes, and similar behaviour has been reported for the cadmium electrode [2].

The influence of temperature on the response rate was studied by the procedures described above.

Injection method. In this method, the ion-selective and reference electrodes were dipped in the test solution of a given concentration, and potential vs. time was recorded until a steady potential was achieved. Then the concentration of the test ion was changed by adding a known amount of test ion or a known volume of supporting electrolyte, and the potential vs. time curve was recorded as before. These E vs. t curves had the same profiles as those observed in the immersion technique, but the time to reach equilibrium was much shorter than with the immersion technique. Fluoride, copper and lead electrodes gave similar results.

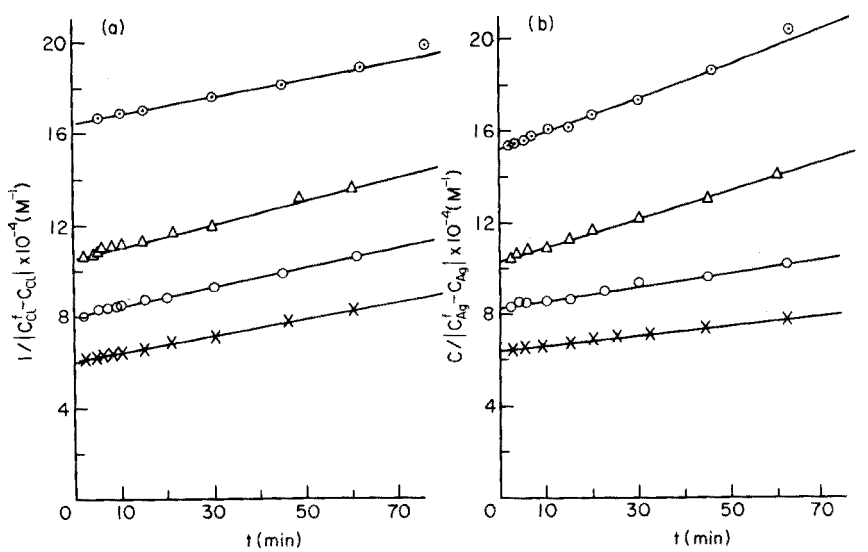

Fig. 1. Conductance measurements of dissolution of chloride crystal membrane. (a) In 10^{-5} M $AgNO_3$ solutions: ⊙ 19.3°C, △ 25.6°C, ○ 30.8°C, × 35.7°C. (b) In 10^{-5} M KCl solution: ⊙ 20.7°C, △ 25.2°C, ○ 30.0°C, × 35.0°C.

Kinetics of dissolution by conductimetry

The rate of dissolution of the chloride electrode crystal in the presence of silver or chloride ions was established by measuring the variation of conductance with time in water or 10^{-5} M silver nitrate or potassium chloride solutions. All measurements were made in stirred solutions and under a nitrogen atmosphere. Studies of the effect of temperature on dissolution rate were done similarly.

Mobility data for silver, chloride, potassium and nitrate ions at different temperatures were taken from the literature where reported [3], or were obtained by interpolation of the data [3] at 0, 18, 25, 35 and 45°C. The solubility of silver chloride at various temperatures was calculated by using the values of the solubility product, K_s, obtained by interpolation of a linear plot of log K_s vs. $1/T$ (T = Kelvin temperature) based on the data at 25, 35, 40 and 45°C [4].

The cell constant was assumed to be constant over the temperature range 19—45°C. For comparison purposes, potential—time curves were also recorded under the same conditions as those used for conductance measurements.

RESULTS AND DISCUSSION

Reproducibility of the results

Before the results obtained with the electrodes are discussed, it should be pointed out that there was a relatively large dispersion in the results, because the observed phenomena depend on several processes which are difficult to control, as discussed below. Consequently, only a semi-quantitative verification of the proposed relationships is possible. For example, even for simple systems such as dissolution of sparingly soluble salts in water, difficulties in obtaining identical crystal surfaces and achieving homogeneous stirring around the crystal area severely limit reproducibility [5] and, particularly when non-stoichiometric test solutions are used, factors such as adsorption [5] lead to irreproducibility. Unfortunately, ion-selective electrodes are used under such conditions. The methods used for measuring kinetics — the immersion and injection techniques — must also be considered. Response times by the immersion method are much slower; probably, during the transference of the electrodes from one solution to another, the electrode body becomes electrostatically charged and the subsequent dissipation of these charges accounts, at least partially, for the longer response time. Moreover, the amount of charge on the electrode may not be the same for all measurements, which would lead to uncertainties in the measurements. A further point is that the kinetics of dissolution (or growth) depends on the surface area and on the structure of the adsorbed layer of the two ions [6]; thus any impurities, particularly organic ones, in the background electrolyte might block the active sites by adsorption thereby modifying the kinetics [5]. Secondary reactions on the electrode surface may also affect the surface processes, e.g. the formation of

a lanthanum hydroxide film [7] on the electrode crystal. Photosensitive electrode membranes may pose problems since the kinetics of the surface processes may depend on illumination. Some types of chloride electrode provide examples of this [8]; such difficulties were avoided by carrying out experiments in the dark.

The rate law of dissolution of the silver chloride crystal

In Part III [1], the rate of dissolution of the membrane was assumed to be: $R = -\mathrm{d}|C^f - C|/\mathrm{d}t = k\,S|C^f - C|^n$, where n was assumed to be 2. Integration of this equation gives

$$1/|C^f - C| = [1/|C^i - C^f|] + k\,S\,t \qquad (1)$$

where C^f, C, k and S are as defined previously. A plot of $1/|C^f - C|$ vs. t should give a straight line of slope $k\,S$. Figure 1 shows typical results of kinetic runs obtained from conductance measurements. Obviously, eqn. (1) is obeyed throughout the observed dissolution time, which shows that the assumption $n = 2$ is valid for the conditions used.

Verification of the potential—time relationship

Concentration dependence of A. In Part III [1], the following empirical equation was proposed for the E—t curve:

$$E = E_{eq} - 1/(At + B) \qquad (2)$$

where E is the potential at time t, E_{eq} is the equilibrium potential, and A and B are constants. When the test ion is the potential-determining ion, then

$$A = k\,S\,C^f\,F/RT \qquad (3)$$

where C^f is the concentration of the test ion. In the case of the silver chloride electrode, silver is the potential-determining ion [9], and C^f must equal C_M^f, where C_M^f is the Ag^+ concentration. When the anion is the potential-determining ion, e.g. with the fluoride electrode, then $C^f = C_A^f$, where C_A^f is the anion concentration.

If the test ion is not the same as the potential-determining ion, e.g. when chloride is the test ion for potential measurements with the silver chloride electrode, then A can be related to C_A^f, the concentration of the anion, by

$$A = k\,S\,(K_s/C_A^f)\,(F/RT) \qquad (4)$$

Then A is inversely proportional to the anion concentration.

The dependence of A on equilibrium concentration is shown in Figs. 2 and 3 for the fluoride and chloride electrodes. Despite the dispersion in the experimental points caused by the above-mentioned experimental difficulties, it is clear that A is directly proportional to C_F^f for the fluoride electrode and inversely proportional to C_{Cl}^f for the chloride electrode, in the given concentration ranges. Thus the theory outlined earlier [1] seems verified: fluoride ions determine the potential of the fluoride electrode, and silver ion

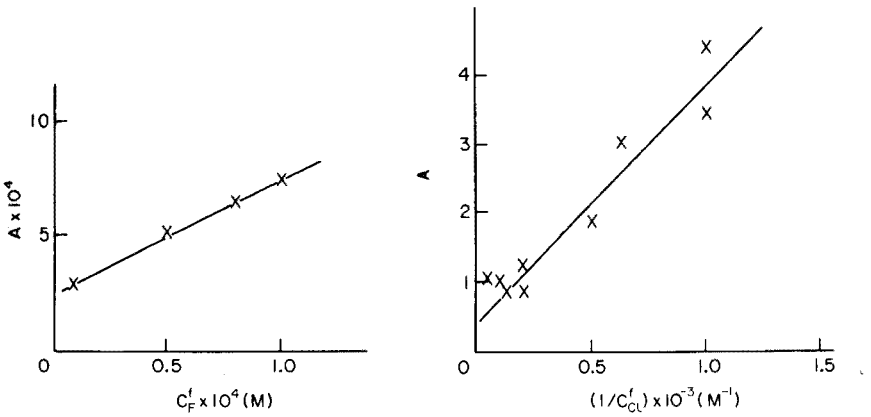

Fig. 2. Variation of A with fluoride concentration. T = 25°C; I = 1.0 M $NaNO_3$.

Fig. 3. Plot of A vs. $1/C_{Cl}^{f}$ for chloride electrode with chloride ion as the test ion. T = 25°C; I = 1.0 M $NaNO_3$.

the potential of the chloride electrode. Silver ions are, of course, also the mobile ions in many other electrodes, e.g. Cu, Pb, Cd, based on mixed precipitates [9].

Concentration dependence of B. In all the cases discussed above, B must be related to A for the chloride and fluoride electrodes (eqn. 22 [1]), by

$$B/A = 1/k\,S\,|C^{i} - C^{f}| \qquad (5)$$

Thus a plot of B/A vs. $1/|C^{i} - C^{f}|$ should give a straight line; the correlation found for the chloride electrode is shown in Fig. 4. Similar results were obtained with the fluoride electrode, thus confirming the form of eqn. (5).

Effect of temperature

Effect on potential–time curves. It has been shown (1) that

$$\ln (A\,T) = k' - E_t^*/RT \qquad (6)$$

where k' is a constant, E_t^* is the temperature coefficient [1], and T is the Kelvin temperature. Thus a plot of $\ln (A\,T)$ vs. $1/T$ should yield a straight line of slope E_t^*.

The effects of temperature on the response times of the fluoride and chloride electrodes are shown in Figs. 5 and 6. The immersion and injection methods yielded the same order of magnitude for the temperature coefficients, although the equilibrium was attained slowly in the immersion technique. For the fluoride electrode, a value of 9 ± 3 kcal was obtained for E_t^* from Fig. 5. Although the same order of magnitude was observed for E_t^* for any concentration of fluoride above 10^{-5} M, its value seemed to increase at lower concentrations. For the chloride electrode, Fig. 6 shows that when chloride is used as the test ion, A decreases with increase in temperature, which leads

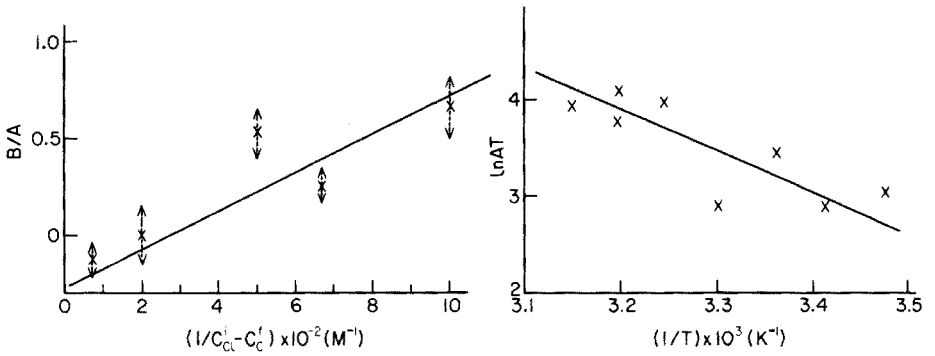

Fig. 4. Influence of chloride concentration on B/A with the chloride electrode. Dilution experiments with two-fold step change in concentration by the injection technique. I = 0.1 M KNO_3; T = 25°C.

Fig. 5. Plot of ln ($A\,T$) vs. $1/T$ for the fluoride electrode. Dilution experiment with a change in concentration from $5\cdot10^{-2}$ to $5\cdot10^{-4}$ M F^- in 1 M $NaNO_3$ (immersion technique).

to a value of E_t^* less than zero. E_t^* was found to be −15 ± 3 kcal. These results were obtained by the injection technique with dilution experiments ($4\cdot10^{-4}$—10^{-4} M Cl). Similar results were obtained by the immersion technique and by carrying out experiments at higher concentrations by the injection technique.

Effect on conductivity measurements. In these experiments, the slopes of the linear plots for $1/(C^f - C)$ vs. t give the value of $k\,S$, and the Arrhenius plots of ln ($k\,S$) versus $1/T$ can be compared with those obtained from potential—time curves. The conductivity experiments gave a value which was statistically the same as 0 kcal for the temperature coefficient with silver ions

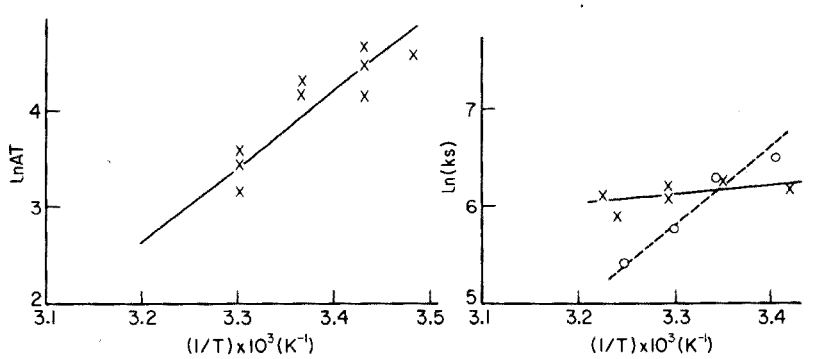

Fig. 6. Plot of ln ($A\,T$) vs. $1/T$ for the chloride electrode. Dilution experiments with a change in concentration from $4\cdot10^{-2}$ to 10^{-4} M Cl^- in 0.1 M KNO_3 (injection technique).

Fig. 7. Influence of temperature on the kinetics of dissolution of the chloride crystal membrane by conductance measurements. ×, $AgNO_3$ solution. ○, KCl solution.

in excess (Fig. 7). But when chloride was used as the test ion, a negative value of -16 ± 2 kcal was obtained for E_t^* (Fig. 7). This value is of the same order of magnitude as that obtained by potential–time curve measurements for chloride solution, made under exactly the same experimental conditions; the scatter of experimental points in the ln $(A\,T)$ vs. $1/T$ plot was high, because of the low concentration of electrolyte. These results are consistent with that reported in the preceding paragraph for slightly different concentrations of chloride.

These results may be explained as follows (cf. discussion of eqn. 23 [1]). The zero charge point of dispersed AgCl corresponds to $C_{Ag} = 10^{-4}$ M and $C_{Cl} = 10^{-5.7}$ M [10]. This point may be shifted to higher C_{Ag} values (and lower C_{Cl} values), for large crystals [10], but the charge at the electrode surface will be positive when silver ions are present in excess. Consequently, Ψ^f is negative in chloride solution, which facilitates the approach of potential-determining silver ions towards the electrode surface; this should result in a decrease in E_t^*.

For the fluoride electrode, an increase in E_t^* with a decrease in fluoride concentration may be explained analogously. Since fluoride is not only the test ion but the potential-determining ion, and since fluoride is adsorbed on the electrode crystal even at very low concentrations [11], the contribution of the term $\pm F\Psi^f$ to E_t^* is positive.

Conclusion

Under the experimental conditions used and within the experimental errors, the model presented seems to be consistent with the experimental data. The dependence of the experimental values of A and B/A on the equilibrium concentration of the test ion can be fitted by eqns. (3), (4) or (5). Moreover, the activation energy found is greater than the diffusional value (4.5 kcal mol^{-1} [12]), indicating that the observed results cannot be explained in terms of diffusion alone. The dependence of both A and B/A on the nature and concentration of the test ion emphasizes the importance of the contribution of surface phenomena (taken into account by the Ψ^f potential in our model).

However, the above model is probably too simplified. Apart from the mathematical approximations, some parameters have probably not been taken into account, as is indicated by the dispersion of the results. It is unlikely that the term $F\Psi^f$ would cause a change of about 15 kcal in E_t^* as observed for chloride electrode when the test ion is varied from Cl^- to Ag^+; indeed, this change would correspond to a change of about 0.65 V in Ψ^f. Some correction factors appear to be necessary, e.g., eqns. (9) and (9′) of Part III may be strictly applicable only near stoichiometric conditions. Moreover, if either of the ions is in excess, Ψ^f could be influenced by factors other than solubility, which could modify the relative weight of the last two parameters in eqn. (23) of Part III. However, the important role of Ψ^f was proved by preliminary studies on the electrode kinetics, when positive and negative

potentials were applied to the ion-selective electrode by means of a potentiostat in series; the response rate depended on the applied voltage.

In any case, the model formulated serves to explain semiquantitatively several of the experimental observations, and also indicates that surface reactions control the response rate near equilibrium. In general [6, 13], dissolution (or crystallization) kinetics is controlled by diffusion and surface processes; diffusion is rate-controlling when the system is considerably removed from equilibrium (i.e. $t \rightarrow 0$) whereas surface processes are rate-determining close to equilibrium. From the present results and those of refs. 5, 9, 10, of Part III, it can be concluded that diffusion is rate-determining at the beginning of the response time, whereas surface reactions control the final response rate of the electrode.

We thank Orion Research Inc. and Beckman Instruments Inc. for providing the electrodes used in this work.

REFERENCES

1 J. Buffle and N. Parthasarathy, Anal. Chim. Acta, 93 (1977) 109 (Part III).
2 Orion Newsletter, Orion Research Inc., Jan./Feb., 1971.
3 R. A. Robinson and R. H. Stokes, Electrolyte Solutions, Butterworths, London, 1959.
4 L. G. Sillen and A. E. Martell, Stability Constants of Metal Complexes, Spec. Publ. No. 17, The Chemical Society, London, 1964.
5 G. H. Nancollas, in A. J. Rubin (Ed.), Aqueous Environmental Chemistry of Metals, Ann Arbor Science Pub., Ann Arbor, Michigan, 1974.
6 C. W. Davies and G. H. Nancollas, Trans. Farad. Soc., 51 (1955) 818.
7 G. A. Rechnitz and M. J. D. Brand, Anal. Chem., 42 (1970) 478.
8 A. Marton and E. Pungor, Anal. Chim. Acta, 54 (1971) 209.
9 J. W. Ross, in R. A. Durst (Ed.) Ion-selective Electrodes, N.B.S. Spec. Publ. No. 314, 1969.
10 H. R. Kruyt, Colloid Science Vol. 1, Elsevier, Amsterdam, 4th edn., 1965, p. 231.
11 J. Buffle, N. Parthasarathy and W. Haerdi, Anal. Chim. Acta, 68 (1974) 253.
12 A. C. Riddiford, Q. Rev. Chem. Soc., 6 (1952) 157; Adv. Electrochem. Electrochem. Eng., 4 (1966) 47.
13 A. L. Jones, G. A. Madigan and I. R. Wilson, J. Cryst. Growth, 20 (1973) 93.

Analytica Chimica Acta, 93 (1977) 129—137
©Elsevier Scientific Publishing Company, Amsterdam — Printed in The Netherlands

A NEW ZERO-CURRENT CHRONOPOTENTIOMETRIC TECHNIQUE WITH ION-SELECTIVE ELECTRODES

I. SEKERKA* and J. F. LECHNER

Analytical Methods Research Section, Canada Centre for Inland Waters, Burlington, Ontario (Canada)

(Received 20th January 1977)

SUMMARY

The concept and application of zero-current chronopotentiometry with ion-selective electrodes are described. This technique utilizes sensors and gas-permeable membranes for measurements under non-equilibrium conditions. Measurements can be carried out in which the speed of the potential change is related to the concentration of the ion of interest in the sample. Instrumentation, procedure and interpretation of the results are simple and the measurement is fast. Very good sensitivities and selectivities are possible. The proposed technique is demonstrated for the determination of cyanide. Data on the accuracy and reproducibility of the method are given. Some potential applications of the technique are mentioned.

Recently, several potentiometric gas sensors, named gas-sensing electrodes [1], gas-sensing membrane probes [2, 3] or gas sensors [4—6], have been introduced into the expanding field of electrochemical sensors. These sensors, relatively simple to operate and with high selectivities, find wide application in laboratory and process analysis and are well suited to continuous analysis and research [7—15]. Thus sensors for ammonia, sulfur dioxide, carbon dioxide, and nitrogen dioxide are commercially available. Further extension to other species such as hydrogen sulfide, hydrogen cyanide, hydrogen fluoride, acetate and chlorine is possible [1]. The range of potentially useful application is very wide, as it is not only the gas which can be estimated but also those species in liquid or solid samples which can be selectively and quantitatively converted to a gas to be sensed [5]. Most of these electrodes are free of interferences and liquid junction-potential problems.

THEORY

All existing or proposed gas electrodes are in principle analogous to the carbon dioxide sensor [16—18]. A glass pH-sensing or an ion-selective electrode and a reference electrode are joined by a dilute electrolyte solution. The electrodes and electrolyte are separated from the sample solution by a

hydrophobic membrane (which is permeable to the gas but impermeable to the aqueous solution) [1—3] or by an air gap [4, 5]. The gas to be sensed diffuses through the gas-permeable membrane, or over an air gap into a film of electrolyte covering the active surface of the electrode and changes the activity of the ion being sensed by the electrode, until an equilibrium is established. Generally, the electrode potential is related to the investigated ion concentration by the conventional equation $E = K \pm RT \ln [X]/nF$, where E is the potential, X is the species sensed, and the other symbols have their usual meaning [4—7]. In comparison to ion-selective electrodes where the potential measured is an equilibrium potential, largely dependent on some suitable exchange mechanism, there is no membrane selectivity between different gaseous species in the case of gas-sensing electrodes. The characteristics of a gas sensor, particularly its time response, sensitivity and limit of detection, depend in a very complex way on the variables of geometry, membrane properties and the internal electrolyte used, and have been described by Ross et al. [1].

Provided that the geometry and membrane characteristics can be kept constant, the time response is a function of the concentration. When a gas sensor (a gas-permeable hydrophobic membrane, reference electrode and sensing electrode covered with a thin film of internal electrolyte) is immersed into a sample containing dissolved gas, the concentration gradient of the gas causes it to diffuse across the membrane. If the internal electrolyte dissolves the gas, or causes dissociation or chemical reaction, a properly selected sensing system monitors the concentration changes in a thin layer of the internal electrolyte on the surface of the sensing element. Assuming a constant concentration of the species in the external electrolyte and a constant zero concentration of this species in the internal electrolyte (because they react with the electrolyte), there is a constant concentration gradient which creates a constant flux of the diffusing species. This flux can be described by the expression ADC/m, where A is the electrode area, C is the concentration in external electrolyte, D is the diffusion coefficient and m is the membrane thickness. The rate of the concentration change of the ion being sensed in the internal electrolyte is related to the concentration of the species in the external electrolyte. Therefore, the speed of the electrode potential change over a certain fixed time period (ΔE) can be related to the concentration of the species in the external (sample) electrolyte and can be utilized for quantitative measurements.

For example, a given concentration of cyanide ion in a sample is converted at pH 5.5 to hydrogen cyanide which diffuses through the membrane, dissolves, dissociates and reacts in the film of the internal solution of silver nitrate buffered to pH 11.5. In this case, the potential of a silver-selective electrode immersed in the internal electrolyte is governed by the activity of silver ion. Diffusing hydrogen cyanide reacts with silver ion according to the equation: $Ag^+ + 2HCN = Ag(CN)_2^- + 2H^+$. This proceeds to the point where there is practically no silver ion present and the diffusing HCN dissociates to free

CN^- ions. Since the electrode is sensitive to cyanide ion as well as silver ion, the plot of potential (mV) vs. time (s) gives the curve A in Fig. 1. Higher or lower concentrations of cyanide in the external electrolyte produce curves B and C, or D and E, respectively. The internal electrolyte must be well buffered to prevent possible changes of pH caused by the reaction itself, or by interfering species such as CO_2, which may change the pH of the internal solution.

If the film of internal electrolyte covering the sensing element is renewed for each experiment, measurements of different cyanide concentrations give a set of curves, describing the dynamic behavior of the given system in terms of the potential vs. time. The potential change (ΔE) over a certain constant time period can be determined. This is illustrated by the vertical lines X and Y in Fig. 1. Plotting the ΔE values against the concentration of the cyanide gives a sigmoidal curve, which can be used as a calibration curve for the determination of cyanide by a given system. The Gran plot technique [19] of evaluating titration data is also applicable for this system. Figure 1 shows that the time necessary for the electrode to reach a certain potential corresponds to the concentration of the ion of interest in the sample (horizontal line Z). This offers another possibility for calibrating the system: plotting the time needed to reach a certain potential vs. concentration of the test ion gives a linear calibration curve. A similar approach for interpretation of the potential—time curves can be derived by using the equation for chronopotentiometry. The transition time (or equivalence point) depends on many factors, among which is the initial bulk concentration; if all other factors are kept constant, the transition time becomes a measure of bulk concentration. The diffusion across the membrane acts like a reagent transport titrating the ion at the electrode surface and the potential at the inflection in the potential—time curve is analogous to the equivalence point potential in a potentiometric titration curve.

The sensitivity of the technique depends on the geometry of the system, membrane and electrode characteristics, timing, and the concentration of internal electrolyte. With given geometry, membrane and electrode characteristics, the sensitivity can be altered by proper selection of the concentration of the sensed ion in the internal electrolyte and by proper timing of the ΔE reading. A decreasing concentration of the internal electrolyte increases the sensitivity, whereas decreasing time periods of the ΔE reading decreases the sensitivity (see below).

The selectivity of the technique is established by the chemistry of the internal electrolyte and by the sample pretreatment. Interferences can be limited, as will be shown in the description of practical applications. Water vapor transport can result in dilution of the internal electrolyte and represents a certain limitation for gas-sensing electrodes, demanding adjustment of the sample osmolality to that of the internal solution. Ambient humidity may become important, because for most membranes, changes in humidity could affect the permeability. With the proposed system, these effects are

not critical because measurements are accomplished in a closed system in a period of several seconds, and a fresh internal electrolyte is used for each measurement. The proposed technique should be useful for the determination of most species that can be converted to a gaseous form and for which a suitable sensing system is accessible.

EXPERIMENTAL

Equipment and chemicals

The sensor (Fig. 2) consists of a cylindrical Teflon body (1) (diam. 18 mm, length 120 mm) which accommodates the ion-selective (2) and reference electrodes (3). The bottom cap (4) provides the support (5) and seal (6) for the Fluoropore (1.0-μm pore size, 13-mm diameter; Millipore FALPO 1300) membrane (7). The internal space is filled with an internal solution (8). A top cap (9) fixes the position of the inner electrode body (10) and holds a lifting lever (11) which allows the inner electrode to be lifted and fresh electrolyte to be introduced to the surface of the sensing element. A constant pressure of the ion-selective electrode against the membrane, adjusting the thickness of the electrolyte film, is achieved by the "dead weight" principle

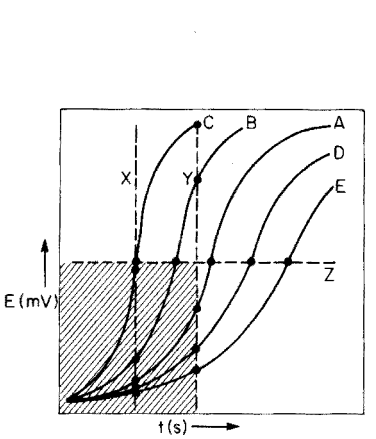

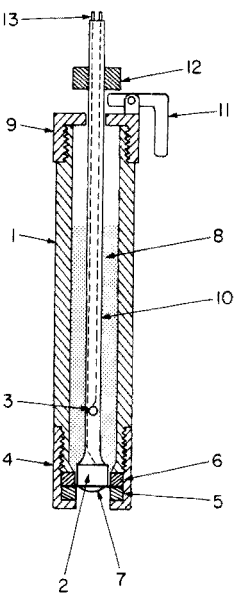

Fig. 1. Potential E(mV) vs. time (s) of a cyanide–silver(I) system. A, given concentration of CN^-. B and C, increasingly higher concentrations of CN^-. D and E, decreasingly lower concentrations of CN^-. X and Y, lines limiting the change of potential to a certain time period. Z, line indicating the time in which the system reaches a certain potential.

Fig. 2. Construction of the sensor. 1, Outer body. 2, Sensing element. 3. Reference element. 4, Bottom cap. 5, Spacer. 6, Seal. 7, Hydrophobic membrane. 8, Internal electrolyte. 9, Top cap. 10, Inner body. 11, Lifting lever. 12, Weight. 13, Terminals.

(12). This allows simple optimization of the adjustment and constancy of the electrolyte film on the surface of the sensing element. The terminals (13) connect the sensor to the millivoltmeter.

An Ionel Model S01A silver(I)-selective electrode and a chloridized silver disc were used as the electrode system. The diameter of a slightly convex sensing element was 6 mm. A Corning 101 millivoltmeter and a Hewlett-Packard 7004B recorder were used for measuring and recording the electrode response.

All chemicals used were of analytical-reagent grade. The stock solutions, prepared by weight, were standardized by appropriate standard analytical methods.

Measuring technique

Pipette an aliquot of sample solution into an Erlenmeyer flask, adjust the pH to 5.5 with a hexamine buffer, and stir the solution magnetically at a constant speed. Either immerse the sensor in the solution, or almost fill the flask and place the sensor in the air space near the solution surface, via a rubber stopper to form an air-tight system and to prevent losses of the gaseous species. The volume of the sample is limited only by the necessity of maintaining a constant concentration of the analyte during the measurement, i.e. losses of the analyte by evaporation and reaction with the internal electrolyte must be negligible. In the experimental arrangement used, the measurement of 5 ml of a $1 \cdot 10^{-8}$ M cyanide sample solution with a $1 \cdot 10^{-5}$ M Ag^+ internal electrolyte was performed five times successively with good reproducibility (±1 mV).

The internal electrolyte which is buffered to pH 11.5 (Tris—NaOH buffer), contains a known concentration of $AgNO_3$ ($1 \cdot 10^{-2}$—$1 \cdot 10^{-5}$ M). Lift the inner electrode body three times via the lifting lever to bring fresh electrolyte to the membrane and to flush away the "spent" electrolyte. Record the course of the potential change at this stage for a predetermined time period. All measurements can be repeated simply by lifting the inner electrode body up and down and by recording ΔE again. Repeat the same procedure for each sample. Factors affecting performance are discussed below.

RESULTS AND DISCUSSION

Basic function and calibration

To verify the theoretical conclusions, cyanide ion was selected as the analyte and silver ion was the species monitored by the electrode. Preliminary experiments showed an unstable potential of the electrode in $1 \cdot 10^{-3}$ M $AgNO_3$ solution buffered with Tris—NaOH buffer to pH 11.5. This was caused by an irregular and unstable layer of the internal electrolyte trapped between the polished surface of the electrode and the smooth side of the membrane. However, by grinding the electrode surface on 500 carbide paper or by placing the membrane with its reinforced mesh side towards the electrode

surface, a sufficiently stable potential was obtained. All reported results were obtained with the mesh side of the membrane facing the electrode surface. The pressure of the electrode against the membrane ("dead weight") did not affect the performance until some mechanical deformation of the membrane occurred. In the given system a "dead weight" of 300 g was used. The volume of internal electrolyte trapped between the electrode surface and the membrane, estimated by microscopic measurement, was ca. 1 μl.

The changes of potential with respect to time, for different concentrations of cyanide ion in the solution buffered to pH 5.5, were recorded when the sensor was immersed in the solution, as well as when the sensor was placed in the air gap over the solution. In both cases, the curves were in accordance with expectations (Fig. 1) and were analogous to the potentiometric titration curves of silver ion with cyanide. The immersion technique has the advantage of high sensitivity but suffers from the danger of gas bubbles being trapped on the membrane, which causes erratic results. Furthermore, it is difficult to detect possible leaks of internal electrolyte; and any wetting agents present in the samples would affect the hydrophobicity of the membrane, causing a malfunction of the sensor. For these reasons, a system where the sensor is not in direct contact with the solutions (air-gap principle [4]) is preferable for most applications. An exception must be made in the case of measurements at extremely low levels of analyte. Experiments showed that the size of the air gap has a definite influence on the response time and should be minimal. In the configuration used here, where the electrode was simply inserted through a rubber stopper into an Erlenmeyer flask almost filled with the sample solution, an air gap of 2 cm^3 was found to be the optimal compromise between practicality and retardation of measurements. If the electrode is exposed to the full concentration change, as illustrated in Fig. 1, a long time is needed to re-establish the starting potential after "rejuvenation" of the electrode, i.e. replacement of electrolyte layer.

It is not necessary to record the entire course of the "titration"; this would take a long time for successful measurement. It is adequate to use just the first part of the curve as indicated by the shaded area in Fig. 1. In this case, the electrode is exposed to the silver ion only, re-establishment of the potential is fast, and the time necessary for the measurement is short.

A set of different concentrations of cyanide was measured with the results given in Fig. 3, where potential (mV) is plotted against time (s). Figure 4 shows a plot of ΔE (mV) vs. the concentrations of cyanide. The values of ΔE were taken as the difference between the starting potential and the intersection of the vertical lines X and Y with the curves in Fig. 3. Curve A (Fig. 4) corresponds to a 15-s measurement whereas curve B was obtained for 30 s. Both curves can be used as calibration curves for the system. Figure 4 shows that decreasing the time period of the measurement causes a decrease in the sensitivity and an increase in the usable concentration range of measurement. An example of the recorder chart for the determination of cyanide in the concentration range 1—100 p.p.b. with a

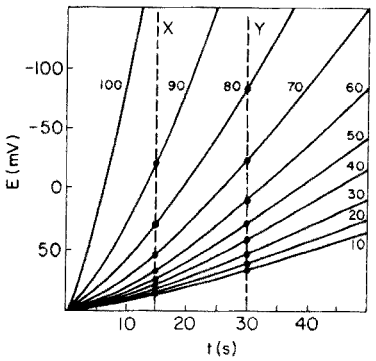

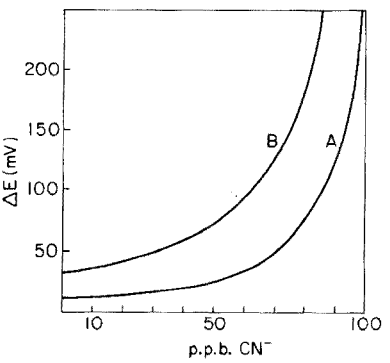

Fig. 3. The sensor response expressed as potential E(mV) vs. time (s) for increasing concentrations of cyanide (10—100 p.p.b. as indicated). The X and Y lines indicate the timing of the measurements.

Fig. 4. The sensor response expressed as change of potential ΔE (mV) vs. concentration (p.p.b.) of cyanide. A, The curve corresponding to a 15-s measurement period (points from line X in Fig. 3). B, The curve corresponding to a 30-s measurement (points from line Y in Fig. 3).

15-s measuring time and $1 \cdot 10^{-3}$ M Ag^+ internal electrolyte is given in Fig. 5. Under the given experimental conditions, the method is capable of covering the determination of concentrations over a range of two decades. With different timing and a different concentration of internal electrolyte, this concentration range can be shifted to higher or lower levels of the cyanide. The course of the potential changes corresponding to the concentration range 40—60 p.p.b. of cyanide is illustrated in Fig. 6.

Detection limits

Practically useful values of ΔE ($\Delta E > 2$ mV) were obtained down to $1 \cdot 10^{-8}$ M CN^- (0.26 p.p.b.) with a 10^{-5} M Ag^+ internal electrolyte and a 60-s measurement time. The upper detection limit was not established but determinations at $1 \cdot 10^{-1}$ M levels gave very good results.

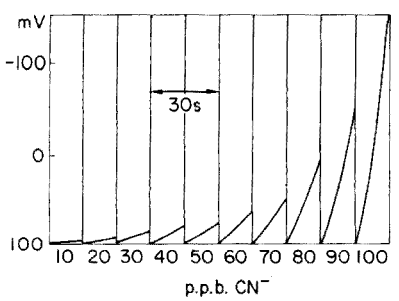

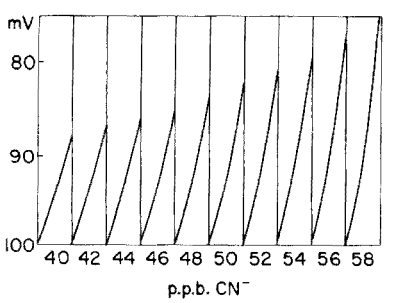

Fig. 5. Strip-chart record of measurements in the concentration range 10—100 p.p.b. CN^-.

Fig. 6. Strip-chart record in the concentration range 40—60 p.p.b. CN^-.

Selectivity

The proposed sensor suffers direct interference only from dissolved gaseous species in the sample that produce a change in the concentration of the sensed ion of the internal electrolyte. In the case of cyanide, only sulfide and some organic thio compounds are potential interferants. This interference can be eliminated by the addition of bismuth(III) to the sample [20]. The application of the sensor for the measurement of other species and elimination of the interferences is similar to the application of gas-sensing electrodes [2].

Practical applications

For the development of an analytical method by the proposed technique, various factors must be considered. First, the sample must be treated to convert the analyte quantitatively or partially [4, 5] to the gaseous state. Secondly, the sensing system must be selected according to the chemistry of the analyte and availability of sensors. It seems possible that all types of titrimetric analysis can be adapted, including acid—base, precipitation, complexiметric and redox titrations. From the practical viewpoint, the temperature of samples, standards, and sensor should be identical (±0.5°C) to keep the coefficient for Henry's law constant throughout the measurements and the samples, standards and internal electrolyte should be adjusted to have an equal total concentration of dissolved species. Direct interferences, i.e. species capable of being converted to gaseous forms and of affecting electrode potential and species capable of binding or reacting with the analyte during the sample treatment process, must be taken into consideration.

The timing of the measurement as well as the concentration of internal electrolyte must be matched to the expected level of the species of interest and to the sensitivity of the sensing system. Finally, the system must be properly calibrated and the treatment of the samples and standards should be identical.

The functioning of the proposed system was tested for the determination of cyanide. Experiments for the determination of sulfide and ammonia (with a silver-selective electrode) and sulfur and carbon dioxide, as well as nitrogen oxide (with a pH glass electrode), were successful and will be reported separately.

To test the precision, five replicate measurements were conducted on ten samples of synthetic lake water prepared with different cyanide concentrations; values of mean, standard deviation and relative standard deviations are given in Table 1. A very satisfactory precision, within 10% of content, is shown down to $1 \cdot 10^{-7}$ M level of cyanide.

Conclusion

The proposed zero-current chronopotentiometric method is fast, sensitive, relatively selective, and requires only simple and inexpensive instrumentation. It is capable of determining a variety of species and is adaptable for automatio

TABLE 1

Precision of cyanide determination

CN^- taken (p.p.b.)	Mean (n = 5) CN^- found (p.p.b.)	s (p.p.b.)	s_r (%)
0.26	0.31	0.08	25
0.52	0.58	0.09	17
1.04	1.09	0.14	13
2.6	2.56	0.3	12
5.2	5.36	0.6	11
10.4	10.7	0.9	9
26.0	25.2	2.6	10
52.0	53.4	3.1	6
104.0	104.2	3.8	4
260.0	252.0	13.0	5

and monitoring. Many chemical reactions allow the interconversion of the sample species to one which can be measured, e.g. the sulfide—sulfite—sulfate, cyanide—cyanate, and nitrite—nitrate—ammonia systems. Also, many reactions utilized in analytical chemistry produce gaseous species which may be detected by the system. The following reactions are a few examples

$H_2S_2O_8 + H_2C_2O_4 \rightarrow 2H_2SO_4 + 2CO_2$

$H_2C_2O_4 + 2Ce^{4+} \rightarrow 2CO_2 + 2Ce^{3+} + 2H^+$

$2KMnO_4 + 3HCOOK \rightarrow KHCO_3 + 2K_2CO_3 + 2MnO_2 + H_2O$

$2HNO_2 + CO(NH_2)_2 \rightarrow 2N_2 + CO_2 + 3H_2O$

$ClO_3^- + 6Br^- + 6H^+ \rightarrow Cl^- + 3Br_2 + 3H_2O$

$CO(NH_2)_2 + 3\,OBr^- \rightarrow N_2 + CO_2 + 3Br^- + 2H_2O$

$(NH_4)_3[PO_4 12MoO_3] + 26NaOH \rightarrow 12\,Na_2\,MoO_4 + Na_2HPO_4 + 3NH_3 + 14\,H_2O$

REFERENCES

1 J. W. Ross, J. H. Riseman and J. A. Krueger, Pure Appl. Chem., 36 (1973) 473.
2 P. L. Bailey and M. Riley, Analyst, 100 (1975) 145.
3 D. Midgley, Analyst, 100 (1975) 386.
4 J. Růžička and E. H. Hansen, Anal. Chim. Acta, 69 (1974) 129.
5 U. Fiedler, E. H. Hansen and J. Růžička, Anal. Chim. Acta, 74 (1975) 423.
6 T. Anfalt, A. Graneli and D. Jagner, Anal. Chim. Acta, 76 (1975) 253.
7 D. Midgley and K. Torrance, Analyst, 97 (1972) 626.
8 J. Mertens, D. Van den Winkel and D. L. Massart, Bull. Soc. Chim. Belg., 83 (1974) 19.
9 M. J. Beckett and A. L. Wilson, Water Res., 8 (1974) 333.
10 J. T. B. Sanders and W. Thornton, Clin. Chim. Acta, 46 (1973) 465.
11 N. J. Park and J. C. B. Fenton, J. Clin. Pathol., 26 (1973) 802.
12 P. M. Todd, J. Sci. Food Agr., 24 (1973) 988.
13 I. Sekerka and J. F. Lechner, Anal. Lett., 7 (1974) 463.
14 W. H. Evans and B. F. Partridge, Analyst, 99 (1974) 367.
15 M. L. Eagan and L. Dubois, Anal. Chim. Acta, 70 (1974) 157.
16 L. C. Clark, Trans. Am. Soc. Artif. Inter. Organs, 2 (1956) 41.
17 R. W. Stow, R. F. Baer and B. I. Randall, Arch. Phys. Med. Rehabil., 38 (1957) 676.
18 W. Severinghaus and A. I. Bradley, J. Appl. Physiol., 13 (1958) 515.
19 J. Gran, Acta Chem. Scand., 4 (1950) 559.
20 I. Sekerka and J. F. Lechner, Water Res., 10 (1976) 479.

Analytica Chimica Acta, 93 (1977) 139—144
© Elsevier Scientific Publishing Company, Amsterdam — Printed in The Netherlands

THE RESPONSE OF THE SULFIDE-SELECTIVE ELECTRODE TO SULFIDE, IODIDE AND CYANIDE

I. SEKERKA* and J. F. LECHNER

Canada Centre for Inland Waters, Burlington, Ontario (Canada)

(Received 14th February 1977)

SUMMARY

The responses of solid-state sulfide-selective electrodes in the presence of sulfide, iodide and cyanide are described. Linear near-Nernstian responses were obtained down to ca. 1×10^{-8} M solutions for these anions. Appropriate procedures of sample treatment limiting the interfering redox responses, adjusting pH and total ionic strength and preserving the ion of interest without contamination of the sample are described. These procedures improve the useful activity range as well as the reliability of the measurements.

The responses and detection limits of solid-state electrodes depend on the solubility product of the membrane [1—6], interference from supporting electrolytes [7—11], sensor surface contamination [12], and adsorption on container walls [13]. The response of sulfide-selective electrodes to different ions and ligands, and the observed apparent deviations from Nernstian responses which occur in dilute solutions are explained either by the activity of silver defects in the membrane [14], or by leaching of soluble metal ion salts from the electrode membrane [8, 15], or by production of metal ion by atmospheric oxidation [16—18]. The appearance of this effect has led some workers to question the theory which predicts an ultimate detection level determined by the solubility of the membrane material [6]. Because the solubility of silver sulfide is very small, it is not possible on thermodynamic grounds that pure Ag_2S membranes could respond to anions whose residual equilibrium silver ion activities are greater than those available from the membrane dissolution. However, responses are observed [19, 20] and experimental artefacts disappear when deaerated buffered solutions are used [19, 21—23].

This work describes practically applicable procedures for the measurements of sulfide, iodide, and cyanide ions. In these procedures the interfering redox responses of the electrode are limited, and the pH and ionic strength are adjusted without contaminating the sample while the ion of interest is preserved.

EXPERIMENTAL

The response profile of the Orion 94-16, Ionel SL-05 and home-made polycrystalline Ag_2S electrodes were studied with an Orion 90-02 double-junction reference electrode and a Corning 104 four-channel digital millivoltmeter coupled to a Hewlett-Packard 7004B recorder. All measurements were conducted in 250-cm^3 three-necked flasks, at a constant temperature (25 ± 0.1°C) with constant stirring. The electrodes were polished with wet alumina powder and conditioned in the proper buffered blank solution for 60 min. The same solution was used for the storage of the electrodes.

Solutions were prepared from demineralized double-distilled water and AR-grade L-ascorbic acid, potassium iodide, cyanide, nitrate, sodium hydroxic and sodium sulfide.

Calibration standards were prepared either by spiking from an Eppendorf Reagent Dispenser-5211 or by serial dilution.

Silver sulfide used for the preparation of the electrode was precipitated by slow addition of Na_2S solution to an acidified (acetic acid) and stirred solutio of silver nitrate. The precipitate was thoroughly washed with water and ethanol, filtered and dried at 80°C. The pellets were formed in a 6-mm die at 8000 kg cm^{-2} pressure and 150°C over a period of 20 min. The pellets were polished and mounted in heat shrinkable tubes. Internal electrical contact to a stainless-steel rod was achieved with a mercury pool [23].

RESULTS AND DISCUSSION

To record the calibration curves of the sulfide electrodes in the presence of sulfide and cyanide, the electrode assemblies were immersed in 10^{-2} M NaOH. The response to iodide was recorded at pH 3 (10^{-3} M HNO_3 plus 10^{-1} M KNO_3). Appropriate spikes of sulfide, iodide or cyanide were then introduced and the corresponding potentials were plotted. Figure 1 shows that the responses were near-Nernstian (57 mV for I^-, 28 mV for S^{2-} and 115 mV for CN^-). At lower concentrations, the response to sulfide increasingly deviated from the Nernstian response and meaningful calibration became impossible. This phenomenon was not observed in the case of cyanide and iodide, where the response remained useful down to 10^{-8} M. Cyanide was measured without addition of $Ag(CN)_2^-$ to the solution [20, 24], and the response of 115 mV compares favourably with the value of 118 mV per decade predicted by eqn. (35) given by Morf et al. [14] and with data published by Tseng and Gutknecht [19].

The considerable potential increase in the case of the response to sulfide has been attributed to crystal defects [14] or to oxidation effect by dissolved oxygen [17, 22]. Furthermore, heavy metal ions present as impurities in water and chemicals, can precipitate sulfide and contribute to the potential increase Also, the redox sensitivity of the sulfide electrode can play an important role.

To examine the oxidizing effect of dissolved oxygen, the potentials of the electrodes in 10^{-3} and 10^{-6} M sulfide, iodide and cyanide solutions, respective

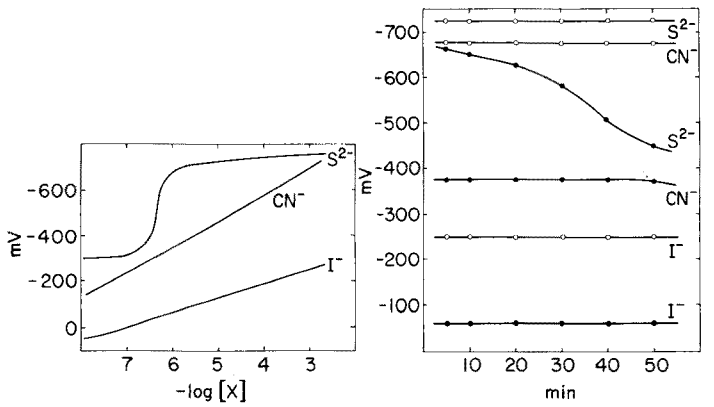

Fig. 1. E.m.f. responses of the sulfide electrode to sulfide, cyanide and iodide.

Fig. 2. Time stability of e.m.f. response of the sulfide electrode to sulfide, cyanide and iodide. ○ 10^{-3} M. ● 10^{-6} M solutions.

were recorded over a period of 1h. The results (Fig. 2) show stable readings at 10^{-3} M levels, whereas the potential at 10^{-6} M sulfide changed very quickly, indicating decreasing concentration. The potential changes of the electrode in 10^{-6} M cyanide and iodide solutions were much less pronounced. These results indicate that the prevention of losses of the ion of interest through oxidation with dissolved oxygen, by addition of an antioxidant or nitrogen saturation should extend the linear calibration range. However, continuous saturation with pure nitrogen did not eliminate the potential deviation and proved to be insufficient for sulfide measurement.

The addition of an antioxidant has two functions: it prevents the loss of sulfide by reaction with dissolved oxygen (or other oxidizing species); and as a redox buffer, the antioxidant extends the linear calibration range by keeping the total redox potential of the solution constant. To test the redox sensitivity effect, 100 ml of 10^{-4} M sulfide solution was titrated with 10^{-3} M bismuth(III) solution. The titration was monitored with the sulfide electrode and with a platinum redox electrode. Bismuth(III) was selected because it is not sensed by either electrode. The course of the titration is shown in Fig. 3. Both electrodes are capable of monitoring the titration. Even if the redox response of the sulfide electrode is not known clearly, it can contribute to the potential increase at low levels of sulfide. Figure 3 also shows the titration of 100 ml of 10^{-4} M sulfide solution with 10^{-3} M bismuth(III) in the presence of ascorbic acid. The total potential change during this titration is ca. 100 mV less than that obtained without ascorbic acid.

Any addition and sample treatment, however, may introduce interfering impurities. Adjustment of the ionic strength, pH and redox potential, and prevention of oxidation, requires relatively large additions. This is especially critical for the sulfide determination because of possible contamination of chemicals with heavy metals. Contrary to reports [24], the electrode response

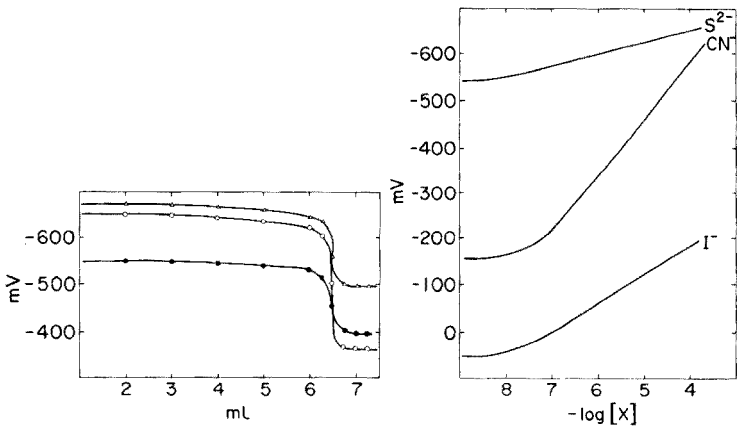

Fig. 3. Potentiometric titration of 100 ml of 10^{-4} M sulfide solution with 10^{-3} M bismuth(III). • Platinum electrode. ○ Sulfide electrode. △ Sulfide electrode in the presence of ascorbic acid.

Fig. 4. E.m.f. responses of the sulfide electrode to sulfide (antioxidant interference-free buffer), iodide (pH 3.5) and cyanide (pH 11.5).

was not improved by masking heavy metal ions with strong complexing agents (EDTA, CDTA, citrate and salicylate).

In an effort to minimize this effect, the sulfide electrode was immersed in 100 ml of deaerated stock solution containing NaOH (400 g l^{-1}) and ascorbic acid (500 g l^{-1}) and diluted to 1 l. This solution was titrated with 1-μl increments of 10^{-3} M sulfide solution. The titration was monitored with the sulfide electrode. The potentiometric titration curve obtained was well developed, allowing location of the equivalence point; this indicated the presence of heavy metals in the stock solution. The corresponding volume of sulfide solution necessary to reach the equivalence point was then added to the remaining stock solution. Standard solutions were prepared by mixing 90 ml of deoxygenated high-purity water with 10 ml of this treated stock solution, all under a nitrogen atmosphere, followed by spiking with appropriate amounts of 10^{-3} M sulfide solution. The calibration curve obtained (Fig. 4) showed a near-Nernstian response to sulfide ion down to 10^{-7} M. No increasing deviation was observed and the practical detection limit was extended to 10^{-8} M sulfide. Similar results were achieved with the use of an antioxidant buffer solution prepared from selected extra-pure chemicals. In this case, the sulfide treatment of the stock solution was unnecessary.

To test the antioxidant effectiveness of ascorbic acid, the potentials of the sulfide electrode were recorded in 10^{-6} M sulfide solution at pH 13 containing varying concentrations of ascorbic acid. The results (Fig. 5) show that a minimal concentration (40 g l^{-1}) of ascorbic acid in the sample solution was necessary. Lower concentrations of ascorbic acid did not protect the sulfide against oxidation sufficiently. Based on these results, the optimal stock

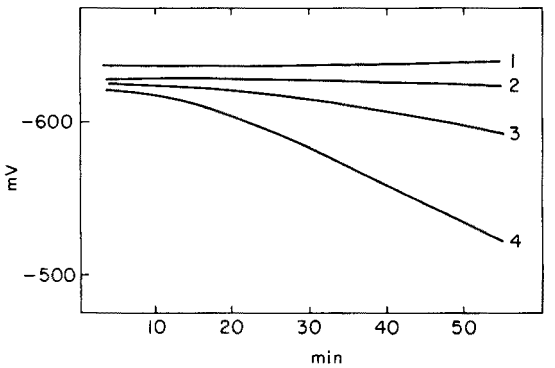

Fig. 5. Time stability of e.m.f. response of the sulfide electrode in 10^{-6} M solution containing varying concentration of ascorbic acid. 1, 40 g l^{-1}; 2, 20 g l^{-1}; 3, 10 g l^{-1}; 4, 5 g l^{-1} of ascorbic acid.

solution of antioxidant buffer contains 400 g of NaOH and 500 g of ascorbic acid (all components of highest purity) in 1 l of water. An aliquot of 100 ml of this solution is diluted to 1 l and titrated with 10^{-3} M sulfide solution as described above. If the titration is successful, the volume of sulfide solution corresponding to the equivalence point is added to the remaining stock buffer solution. If a sharp increase of the potential occurs immediately after the initial additions of the titrant (indicating sufficient purity of the stock solution), addition of sulfide to the stock solution is unnecessary. For practical determinations of sulfide, the stock buffer solution is mixed with the sample solution in a (1 + 10) ratio.

The electrode response to iodide and cyanide is practically unaffected by the redox potential, oxidation and contamination. Proper pH (3.0 for iodide and 11.0 for cyanide) and ionic strength (10^{-2} M) adjustment proved to be adequate, and gave practical detection limits in the 10^{-8} M range (Fig. 4). Three sets of different concentrations of sulfide, iodide and cyanide ions were analyzed; the precision data are given in Table 1.

TABLE 1

Precision of sulfide, iodide and cyanide determination

Taken (ppb)	Sulfide			Iodide			Cyanide		
	Mean (n = 5) found (ppb)	s (ppb)	s_r (%)	Mean (n = 5) found (ppb)	s (ppb)	s_r (%)	Mean (n = 5) found (ppb)	s (ppb)	s_r (%)
0.1	0.2	0.07	35	0.3	0.15	50	0.2	0.17	83
0.5	0.6	0.11	16	0.7	0.16	22	0.6	0.13	22
1.0	1.1	0.16	12	1.3	0.20	15	1.4	0.22	16
5.0	5.5	0.19	3	5.4	0.29	5	5.8	0.30	6
10.0	9.8	0.40	4	10.1	0.53	5	9.6	0.48	5
50.0	51.2	2.60	5	48.0	1.30	2	48.2	2.50	5
100.0	105.0	4.20	4	98.2	2.70	3	104.0	5.70	6

In conclusion, it is evident that the silver sulfide electrode responds to the activities of sulfide, iodide and cyanide with near-Nernstian (58, 29 and 115 mV, respectively) slopes down to 10^{-7} M solutions. Practical detection limits in the range of 10^{-8} M (0.5 ppb sulfide, 1.0 ppb iodide, 1.0 ppb cyanide) can be achieved, if the sample treatment is appropriate. The doubled Nernstian slope (115 mV) favors the sulfide electrode over the silver sulfide—silver iodide electrode normally used for the determination of cyanide ion [26].

All the electrodes tested behaved in an almost identical manner.

REFERENCES

1 M. S. Frant and J. W. Ross, Science, 154 (1966) 1553.
2 R. A. Durst (Ed.), Ion-Selective Electrodes, Nat. Bur. Stand. (U.S.) Spec. Publ. 314, Washington, D.C., 1969.
3 G. J. Moody and J. D. R. Thomas, Selective Ion Sensitive Electrodes, Merrow, Watford, Herts., England, 1971.
4 J. Koryta, Anal. Chim. Acta, 61 (1972) 329.
5 A. K. Covington, CRC Crit. Rev. Anal. Chem., 3 (1976) 355.
6 R. P. Buck, Anal. Chem., 48 (1976) 23R.
7 J. J. Lingane, Anal. Chem., 39 (1967) 881.
8 J. Růžička and C. G. Lamm, Anal. Chim. Acta, 54 (1971) 1.
9 N. Parthasarathy, J. Buffle and D. Monnier, Anal. Chim. Acta, 68 (1976) 185.
10 E. Mesmer, Anal. Chem., 40 (1968) 443.
11 I. Sekerka and J. F. Lechner, Talanta, 20 (1973) 1167.
12 J. Buffle, N. Parthasarathy and W. Haerdi, Anal. Chim. Acta, 68 (1974) 253.
13 R. A. Durst and B. T. Duhart, Anal. Chem., 42 (1970) 1002.
14 W. E. Morf, G. Kahr and W. Simon, Anal. Chem., 46 (1976) 1538.
15 J. Vesely, Collect. Czech. Chem. Commun., 39 (1976) 710.
16 W. J. Blaedel and D. E. Dinwiddie, Anal. Chem., 46 (1976) 873.
17 D. J. Crombie, G. J. Moody and J. D. R. Thomas, Anal. Chim. Acta, 80 (1975) 1.
18 M. J. Smith and S. E. Manahan, Anal. Chem., 45 (1973) 836.
19 P. K. C. Tseng and W. F. Gutknecht, Anal. Chem., 47 (1975) 2316.
20 M. S. Frant, J. W. Ross and J. H. Riseman, Anal. Chem., 44 (1972) 2227.
21 I. C. Popescu, C. Liteanu and L. Savici, Rev. Roum. Chim., 18 (1973) 1451.
22 J. Kontoyannakos, G. J. Moody and J. D. R. Thomas, Anal. Chim. Acta, 85 (1976) 47.
23 J. F. Lechner and I. Sekerka, J. Electroanal. Chem., 57 (1976) 317.
24 H. Clysters and F. Adams, Anal. Chim. Acta, 83 (1976) 27.
25 B. Fleet and H. von Storp, Anal. Chem., 43 (1971) 1575.
26 Orion Research Inc., Instruction Manual 94-06A Cyanide Ion Electrode, Cambridge, Mass.

Analytica Chimica Acta, 93 (1977) 145—151
© Elsevier Scientific Publishing Company, Amsterdam — Printed in The Netherlands

THE ADAPTATION OF COATED PIEZOELECTRIC DEVICES FOR USE IN THE DETECTION OF GASES IN AQUEOUS SOLUTIONS

LURANCE M. WEBBER and GEORGE G. GUILBAULT*

Department of Chemistry, University of New Orleans, New Orleans, Louisiana 70122 (U.S.A.)

(Received 25th April 1977)

SUMMARY

A method for the determination of ammonia and hydrogen sulfide in aqueous solution is presented. This method involves the use of a gas-permeable membrane which isolates the piezoelectric crystal device from the solution yet allows the desired gases to pass. Concentrations up to 0.45 M for NH_3 and $9 \cdot 10^{-4}$ M for H_2S give linear calibration curves of concentration vs. frequency change.

Piezoelectric crystals are very sensitive to the adsorption of a substance on their surface. This sensitivity is observed as a change in the resonance frequency of the crystal, which is proportional to the weight of the substance adsorbed on the crystal surface [1]. By coating the electrode surface of the crystal with a substance which will selectively adsorb a particular gas, it is possible to determine the concentration of that gas [2, 3]. Thus piezoelectric detectors are ideal for the determination of pollutants in the atmosphere. Several specific detectors of atmospheric pollutants at very low concentrations have been developed, including those for SO_2 [4—6], NH_3[7], and H_2S [8]. An awareness that even trace concentrations of noxious gases have a deleterious effect on the environment has made the development of these devices increasingly important.

The harmful effect of noxious gases is not limited to the atmosphere, however; water pollution by gases is also of importance. Thus, the adaptation of this sensitive piezoelectric method for use in aqueous solutions would be useful. The crystal itself cannot be immersed into the solution since the weight of water excessively dampens its resonance. However, the development of gas-permeable membranes has introduced a method of separating the crystal from the solution, while allowing the gas to pass through to be detected by the crystal. This paper reports the results of some experiments designed to adapt the piezoelectric method to water systems with such gas-permeable membranes. The feasibility of this method has been demonstrated for CO_2 [9].

EXPERIMENTAL

Cell design

The experimental cell is simple in design. A crystal holder was made by sealing two tungsten wires into the bottom of a standard taper male joint, and the crystal was attached to these wires. Close to the wires a small hole was blown to allow gases and water vapor to escape. This crystal holder was placed into a standard taper adapter, (24/40) with glass added to its bottom to inclose the crystal forming a crystal chamber when the membrane was in place. The added glass was shaped to retain an O-ring which held the gas-permeable membrane in position. Care was taken to ensure that the membrane was stretched across the bottom of the adapter in such a way that a good seal forms and there are no holes in the membrane. This was done so that water could not leak into the crystal chamber. The sample cells were simply standard taper female joints, 24/40, that were sealed off to contain about 150 ml of solution. One was equipped with capillary side-arms so that gases could be injected into the solution.

Membranes and crystal coatings

The membrane employed is one normally used for CO_2 electrodes (Instrumentation Laboratories, Inc.). A microporous Teflon membrane designed for NH_3 proved to be unsatisfactory for use with piezoelectric devices since it permits excessive water vapor to pass. Other membranes tried included the commercial food wraps, HandyWrap and SaranWrap, hydrophobic filters and waxed paper; the Instrumentation Laboratories membrane was the best.

The crystal coatings used were the nickel dimethylglyoxime (Ni—DMG) complex for NH_3, and the acetone extract of a chlorobenzoic acid soot for H_2S. Ni—DMG was chosen as the coating for NH_3 because of its low reactivity towards humidity; the more sensitive NH_3 coating, ascorbic acid—silver nitrate, reported previously [7], was unsatisfactory because it is sensitive to humidity. The Ni—DMG was prepared by mixing aqueous nickel nitrate and alcoholic dimethylglyoxime solutions and filtering the resultant precipitate. After drying in air, the precipitate was dissolved in chloroform and the saturated chloroform solution was applied to the electrode surface of the crystal. The preparation of the acetone extract of chlorobenzoic acid soot has been reported elsewhere [8].

Both solutions were applied to the crystal surface with a glass capillary. Solution was drawn into the capillary, and its tip was placed on the electrode of the crystal and held there as the solution evaporated. This method prevented the solution from spreading over the entire crystal surface since surface tension held the drop in place. This method was especially important in applying the very dilute Ni—DMG solution, since a large amount of solution was needed to build up a sufficient coating.

Piezoelectric crystals and instrumentation

The crystals were general-purpose devices with a normal resonant frequency of 9 mHz; they were of the smaller size, HC 25/U holders with the canister removed. Crystals for measuring NH_3 possessed gold electrodes, and were purchased from International Crystal Manufacturing Co. (Oklahoma); the H_2S crystals had silver electrodes and were obtained from Jan Crystals (Florida).

The instrumentation consisted of a low-frequency 1T transistor oscillator (International Crystal Mfg. Co.) powered by a Heathkit Model 28 power supply; the voltage used was a constant 9 V. The frequency output from the oscillator was measured by a Systron-Donner Model 8050 frequency meter which was modified by a digital-to-analog converter [7] so that the frequency could be recorded by a Bristol Model 570 Dynamaster recorder. Thus, data were obtained from both the frequency meter and the recorder.

The experimental procedures are described in the results section. The test solutions were obtained from C.P. ammonia or H_2S gases, or by using concentrated aqueous ammonia, either injected directly or diluted with distilled water.

RESULTS AND DISCUSSION

The crystal as an ammonia detector

Dissolved ammonia can be detected by a coated piezoelectric crystal that is separated from the aqueous solution by a gas-permeable membrane. This reaction is shown by a decrease in the frequency of the crystal caused by the adsorption of ammonia, over that caused by the adsorption of water alone. The frequency of the crystal was first measured with the crystal chamber dry and in air. After the crystal was placed into the sample cell with the membrane in contact with distilled water, and the frequency recorded, the frequency had dropped 550 Hz. After the distilled water was replaced with aqueous 1.5 M ammonia, the frequency dropped by 1150 Hz, giving a difference of 600 Hz due to ammonia. A concentration of aqueous ammonia of 0.15 M, produced a frequency difference of 135 Hz. In all cases the frequency drop was measured after a steady frequency reading was reached; this took considerable time.

To reduce the time necessary to perform the measurements, a new procedure was devised. The crystal was placed in position in the sample cell in contact with 150 ml of distilled water and the system was allowed to come to a steady frequency. Ammonia gas was then injected into the water through the capillary side arm and the frequency was again recorded after a steady frequency had been reached. In Fig. 1, the difference in frequency, ΔF, between that of distilled water and that after injection of ammonia, is plotted vs. the concentration of the solution resulting from the injection of ammonia. The concentration reported is total ammonia, i.e., corrections for equilibrium constants and solubilities were not considered. The plot in Fig. 1 shows that

there is a linear relationship between the concentration of ammonia and the frequency change (ΔF). The least-squares linear correlation coefficient was 0.956. Where two points are shown for a single concentration, the lower point resulted from a second injection of ammonia into the same solution. The crosses (+) refer to the sum of the two injections, i.e., the total concentration resulting from the two injections into the same solution. Both the second injection and the sums are on or near the linear calibration curve. Injections of room air had no effect on the frequency of the crystal exposed to distilled water.

The curve of Fig. 1 demonstrates that a linear relationship between ΔF and ammonia concentration can be obtained in solution. The experimental procedure, however, was not the best, since the diffusion of ammonia gas through the solution would have an effect, at least on the time necessary for the crystal to reach equilibrium. Hence, a different procedure was devised. A separate vessel, a round-bottom flask, containing distilled water was set up to allow the crystal to come to equilibrium with the aqueous environment. The crystal chamber, with crystal and membrane, was placed in the flask, but not in contact with the water, and was kept there except for measurements of ammonia solutions. To measure the ammonia test solution, the crystal chamber was transferred manually to the sample cell containing the test solution. The experimental results by this method are plotted in Fig. 2. The concentration vs. ΔF curve is linear to about 0.45 M with a least-squares linearity correlation coefficient of 0.971. After 0.45 M the curve levels off.

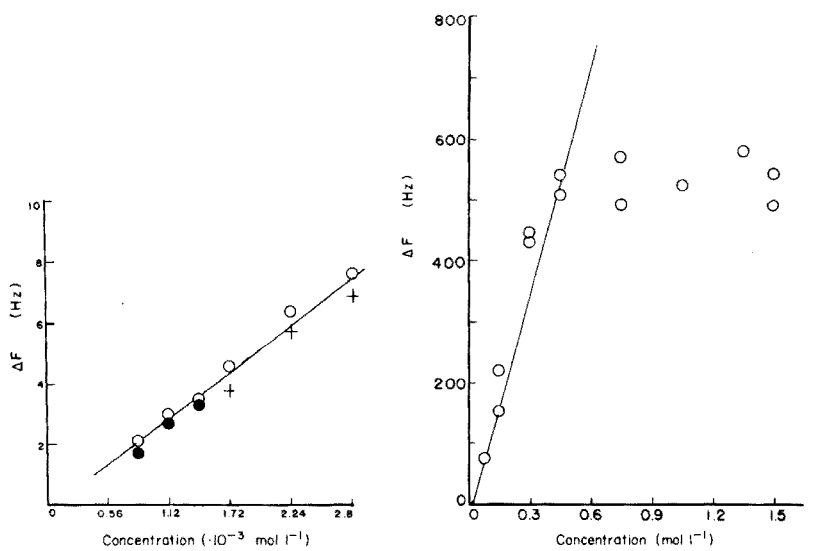

Fig. 1. A concentration vs. frequency change plot for ammonia injected into distilled water.

Fig. 2. A concentration vs. frequency change plot for ammonia in solution.

The transfer of the crystal and chamber to the sample cell containing only distilled water resulted in only a negligible frequency change. These results show, once again, that a linear relationship exists between ammonia concentration in water and the frequency of a coated piezoelectric crystal, and that an analytical method can be based on this principle. There is, however, a maximum concentration for which such a method can be useful.

Similar results were obtained with each different crystal preparation. After the crystal had been recoated with a fresh Ni—DMG solution, the frequency changes were reasonably near the same values and a similar calibration curve was obtained. A single crystal preparation lasted about two weeks, which is quite satisfactory.

The crystal as a hydrogen sulfide detector

Dissolved H_2S was also detected by a coated piezoelectric crystal separated from the solution by a gas-permeable membrane. In this case, the test solutions were prepared by injecting H_2S gas into a volumetric flask filled to the mark with distilled water. The gas was injected into the flask through a rubber septum placed over the flask opening. After injection the solution was shaken and allowed to stand. The experimental procedure was as previously described for NH_3 and a sample cell without side-arms was employed.

The relationship between concentration of H_2S and frequency change is shown in Fig. 3. Once again a linear relationship is demonstrated, this time up to $1.9 \cdot 10^{-4}$ M. The least-squares linearity correlation coefficient was 0.948. At concentrations above $1.9 \cdot 10^{-4}$ M the curve levels off to a relatively constant value. These results show that, as with NH_3, the concentration of H_2S in water has a linear relationship with the frequency change of a coated

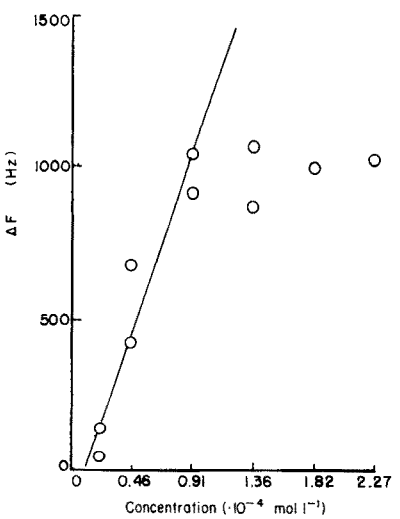

Fig. 3. A concentration vs. frequency difference plot for hydrogen sulfide.

piezoelectric crystal and that an analytical procedure based on this principle is possible.

The precision of the measurements was not good. This is especially true for the data of Figs. 2 and 3. Sufficient consecutive measurements were not made to make significant statistical calculations, but when two or more measurements were made at a particular concentration, the data were scattered. There are two possible causes for this scatter. First, the solutions were roughly prepared with no attempt made to buffer or stabilize them. Thus, reaction with CO_2 or other components of the air was possible. Secondly, the manual transfer of the crystal from one vessel to another must cause shock to the electronic system; this was usually shown as a spike on the recorder. The transfer of the crystal between vessels containing only distilled water showed little effect, but this may not have been so in each measurement.

The measurements were not particularly sensitive; the concentrations reported are not particularly low, especially for ammonia. However, equilibria were not considered; both H_2S and NH_3 have complex ionization and solubility equilibria. So the actual gas measured may be lower than reported, since only total concentrations are reported.

The sensitivity of the coating is greatly dependent on its reactivity. Thus, a coating which is more reactive toward the desired gas, or which adsorbs it more readily, would be more useful. The Ni—DMG coating for ammonia detection is not the most sensitive coating available, but it is the most sensitive coating found which is not too sensitive to humidity.

In the measurement of these gases in air [7, 8] meaningful data were obtained with low frequency differences. The instrumentation is capable of measuring and qualitatively distinguishing frequency differences below 10 Hz, and measuring accurately 1 Hz. Thus, with improved precision, concentrations much lower than those reported can be determined.

At higher concentrations, the time necessary to reach a stable change of frequency is somewhat slow. There is usually an initial drop, which takes 2—30 min, depending on concentration. This initial drop is followed by a period of much slower change of frequency. The data reported are for a complete change. This could take up to an hour, but might not be necessary for a good assay. The difficulty might be overcome by using a plot of rate of change (ΔF min^{-1}) in place of total frequency difference.

An experiment was performed to determine if it is necessary that the membrane be in contact with the solution. In this experiment, the crystal chamber was suspended over an H_2S solution in a closed cell. No frequency difference was noted. This shows that contact is necessary to obtain optimum results. In all experiments reported in this paper the membrane was in contact with the solution.

The preliminary data reported here show that a piezoelectric method for gases in solution is possible, but more research in necessary to improve the procedures, so that routine measurements can be performed. The potential is there, however. Work with gases in the atmosphere has shown that the

piezoelectic method is as sensitive as most methods and more sensitive than many. Concentrations down to 1 p.p.b. in air have been measured. The simplicity of the method and the potential for compact instrumentation are the greatest advantages. The method would be ideally suited for the monitoring of gases in solution as in pollution studies, and is potentially useful for many other systems.

REFERENCES

1 G. Z. Sauerbrey, Z. Phys., 155 (1959) 206.
2 W. H. King, Jr., Anal. Chem., 36 (1964) 1735.
3 W. H. King, Jr., Environ, Sci. Technol., 4 (1970) 1136.
4 K. H. Karmarkar and G. G. Guilbault, Anal. Chim. Acta, 71 (1974) 419.
5 K. H. Karmarkar, L. M. Webber and G. G. Guilbault, Environ. Lett., 8 (1975) 345; Anal. Chim. Acta, 81 (1976) 265.
6 J. L. Cheney, T. Norwood and J. Homolya, Anal. Lett., 9 (1976) 361.
7 L. M. Webber and G. G. Guilbault, Anal. Chem., 48 (1976) 2244.
8 L. M. Webber, K. H. Karmarkar and G. G. Guilbault, Anal. Chem., in preparation.
9 W. W. Fogleman and M. S. Shuman, Anal. Lett., 9 (1976) 751.

Analytica Chimica Acta, 93 (1977) 153—159
©Elsevier Scientific Publishing Company, Amsterdam — Printed in The Netherlands

COULOMETRIC TITRATION OF PENICILLINS AND PENICILLAMINE WITH MERCURY(II)

ULF FORSMAN

Institute of Chemistry, University of Uppsala, P.O.B. 531, S-751 21 Uppsala (Sweden)

(Received 14th April 1977)

SUMMARY

An absolute coulometric method based on the titration of hydrolysed penicillins with coulometrically generated mercury(II) is presented. An amalgamated gold plate is used as anode and the titration is performed in a pH 4.6 acetate buffer solution. The method gives values which deviate by less than 1% from values obtained by other absolute methods. The relative standard deviation for determination of penicillin G is 0.4%. The determinations of penicillamine and mixtures of penicillamine and penicilloate are also reported.

In earlier studies, titration techniques for penicillins [1] and 6-aminopenicillanic acid [2] with mercury(II) solutions were reported. These methods were based on volumetric titration of penicillins hydrolysed to the corresponding penicilloates with mercury(II) nitrate solution. Compensation for penicilloates initially present in the penicillins was made by titration of an unhydrolysed sample. For penicillamine, which is a break-down product of penicillins, volumetric titrations with mercury(II) solutions have also been published. Billabert et al. [3] used mercury(II) acetate for a titration at pH 6; two equivalence points were found, the first corresponding to formation of a sulphide and the second to formation of a chelate. Körbl and Vanicek [4] titrated penicillamine with mercury(II) perchlorate in a medium containing pyridine.

Coulometric generation of mercury(II) from the metal would serve as an alternative to these volumetric methods, and would have the advantage that no standardization is required. The use of coulometrically generated mercury (II) has been reported for several different substances. Vandenbalck et al. [5] determined aminopolycarboxylic acids with a mercury pool as anode; a back-titration procedure for metal ions was also presented. The titration of halides with electrolytically generated mercury(I and II) was reported by Przybylowicz and Rogers [6]. Three different anodes were investigated: a mercury pool, and mercury-coated silver and gold. The amalgamated gold anode was preferred and used in subsequent studies where sulphide [7] and cysteine [8] were titrated; errors of ±0.2% were reported for sulphide and <1% for cysteine. Mairesse-Ducarmois et al. [9] used coulometric mercury(II) titrations for thiols and reduced disulphides.

In this paper, the use of coulometrically generated mercury(II) for the titration of penicillins is reported. The effects of different buffer concentrations, pH, stirring efficiencies and types of anode, are discussed. Since penicillamine may be present as an impurity in the penicillins investigated, the determination of this substance in pure form and in mixtures with penicilloate has also been examined.

EXPERIMENTAL

Equipment

The generating current, 0—50 mA, was delivered by a simple transistorized current source with a maximum voltage output of 45 V. The voltage from a series resistor was converted to pulses by means of a V/F-converter (Burr-Brown VFC 12), calibrated to give 1, 10 or 100 pulses per mC. By feeding the pulses to the chart stepper motor of a recorder (Houston 3090 or Mettler GA 13), the number of coulombs generated was measured directly on the chart paper. The anode in the generating circuit was an amalgamated gold plate (working area, 8 cm^2). The platinum foil cathode was placed in a tube with a fritted disc (Metrohm EA247), containing the internal solution, 1 M HNO_3. A platinum foil indicator electrode was used with a saturated calomel reference electrode. Stirring was done magnetically.

Reagents

The samples were penicillins (Astra AB, Södertälje and Fermenta AB, Strängnäs) and penicillamine (Fluka AG, Buchs). A 0.8 M acetate buffer pH 4.6 was prepared by mixing equimolar amounts of sodium acetate and acetic acid. Other buffer concentrations were obtained by dilution of this solution. An aqueous 0.1% sodium thiosulphate solution was used to treat the indicator electrode.

Procedures

Titration of penicillins. The analysis involves titration of a hydrolysed sample, which gives the sum of intact and degraded penicillin in the sample, and titration of an unhydrolysed sample, which gives the amount of degradation of the substance. Intact penicillin corresponds to the difference.

For the first titration, dissolve 0.0800—0.1000 g of the penicillin in 250 ml of water, and hydrolyse a 10-ml aliquot with 5 ml of 1 M NaOH for 5—10 min. Then add 5 ml of 1 M HNO_3 and 60 ml of 0.4 M acetate buffer. Dip the indicator electrode into the thiosulphate solution for a few seconds before the titration to establish a low starting potential. Titrate at a generating current of 5 mA; decrease the current to 3 mA about 10% before the final end-point.

For the second titration, weigh accurately 0.02—0.2 g of sample and dissolve in 60 ml of 0.4 M acetate buffer. Titrate at a generating current of 3 mA, after pretreatment of the indicator electrode as above.

Titration of penicillamine. Titrate an appropriate amount of penicillamine (0.7—1.5 mg) directly in a 0.4 M acetate buffer solution at a generating current of 5 mA (3 mA before the second equivalence point).

RESULTS AND DISCUSSION

Titration of hydrolysed penicillin

A typical titration curve for the first titration is shown in Fig. 1, curve a. Well-defined potential jumps occur at molar ratios of 2:1 and 1:1 between penicilloate and Hg(II). The ratio between the number of coulombs generated up to the second equivalence point and up to the first one was 1.95, which is less than theoretical. Evaluation based on the first jump gave high results, whereas the second jump gave correct results; all determinations were therefore based on this jump. The use of a higher generating current at the first jump than at the second one, did not explain this effect.

Results of titrations of several hydrolysed penicillins are shown in Table 1. Values obtained with the volumetric titration technique and another absolute method [10] were in good agreement. Penicilloates initially present in the penicillins are accounted for in this comparison. Similar results were obtained for penicillinase-sensitive penicillins when the hydrolysis was done enzymatically as reported earlier [1]. Amounts of penicillin between 1.9 and 7.0 mg were analysed with accurate results. If the method outlined is followed an amount of about 3.5 mg is used. 6-Aminopenicillanic acid was acetylated before the titration as described earlier [2].

Titration of unhydrolysed penicillins

A titration curve obtained for the determination of penicilloate initially present in penicillin G is shown in Fig. 1, curve b. Results for penicilloate in different penicillins are shown in Table 2. The second jump was used for the evaluations. The coulometric method appears to give somewhat higher results

TABLE 1

Titration of hydrolysed penicillins

Penicillin	Assay (%)	No. of trials	s_r (%)	Alternative assays	
				Hg volumetric titration (%)	P.n. method (%)[a]
Penicillin G	99.2	10	0.4	99.5	99.3
Ampicillin	97.2	7	0.3	96.6	97.6
Penicillin V	99.1	3	0.3	100.0	—
Cloxacillin	100.0	5	0.4	99.9	—
6-Aminopenicillanic acid	96.5	10	0.5	96.9	—[b]

[a]Enzymatic hydrolysis followed by titration with NaOH [10].
[b]No other absolute method is available for this substance.

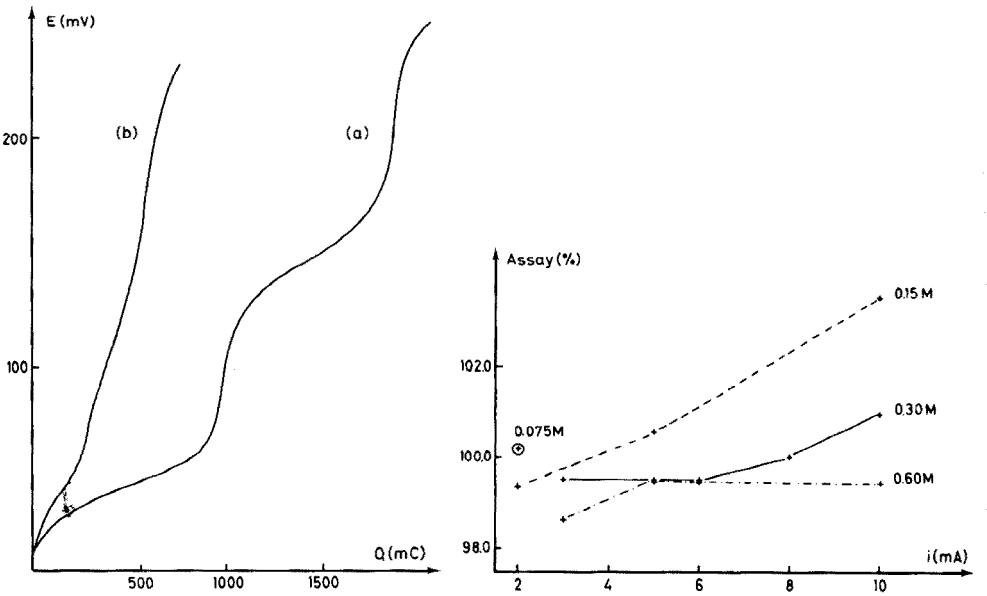

Fig. 1. Titration curves for (a) 3.5 mg of hydrolysed penicillin G and (b) 0.1 g of unhydrolysed penicillin G by the procedure described.

Fig. 2. Assay as a function of the generating current for titration of hydrolysed penicillin G in different buffer concentrations. The molarities of acetate in the titration media are shown in the figure.

TABLE 2

Titration of penicilloate in penicillins with mercury(II)

Penicillin	Assay (%)[a]	
	Coulometric titration	Volumetric titration
Penicillin G	0.58	0.50
Ampicillin	3.6	3.5
Penicillin V	0.20	0.19
Cloxacillin	0.15	0.12
6-Aminopenicillanic acid	1.3	1.2

[a]Mean of two determinations.

than the volumetric method (Table 2), but deviation is small and does not influence the penicillin assay.

The effect of different buffer concentrations

The concentration of the acetate buffer pH 4.6 in the titration media was of importance for accurate results. Figure 2 shows the assay of hydrolysed

penicillin G in different buffer concentrations with generating current of 2–10 mA. As can be seen, the assay was fairly constant when buffer concentrations of 0.3 and 0.6 M were used. At lower concentrations the penicillin assay rose over 100%, and still higher assays were found systematically when the current was increased. In all cases, the current was decreased to 2–3 mA before the second equivalence point. When 0.075 M or 0.15 M acetate was used, KNO_3 was added as supporting electrolyte. When high values were obtained, a black precipitate appeared on the anode. No precipitate was obtained when Hg(II) was generated in a blank titration medium or when EDTA was titrated; the black film was probably due to precipitation of the penicilloate–mercury(II) complex. Obviously 100% current efficiency was not obtained when the anode was covered with this precipitate. Since acetate clearly influences the rate of precipitation, enough acetate must be added to avoid this effect.

The sharpness of the two potential jumps was affected by the acetate concentration. When increasing amounts of acetate were used, the first jump became more distinct, while the second became flatter. Alternative systems, such as citrate, hydrogenphthalate, or phosphate buffers, are less attractive because of rather high complex formation constants with mercury(II).

Titrations should not be done at pH values above 5.5, because precipitation of the Hg–penicilloate complex makes titration difficult. However, if the pH value falls significantly below 4.0, results are erroneous, probably because of reduced stability of the Hg(II)–penicilloate complex. In titrations at pH 4.1, instead of 4.6, the shape of the titration curve changed in the same way when the acetate concentration was raised, i.e. the derivative at the first equivalence point increased while the second decreased. This effect also appeared when the temperature of the titration was raised.

The effect of stirring and different types of anode

The effect of different rates of stirring was investigated. Under the conditions specified in the procedure, a rotation speed of about 250 r.p.m. was sufficient. Doubling the velocity did not significantly increase the stirring efficiency. Higher generating currents could not be used without giving rise to precipitation on the anode.

When a rotating, gilded and amalgamated platinum net was used as anode, currents up to 15 mA could be applied for titrations in 0.3 M acetate buffer solutions. The much higher stirring efficiency obtained with this anode obviously prevented precipitation on the net, but certain drawbacks limited its practical usefulness. First, it had to be regilded and reamalgamated after about ten titrations; secondly, the first two titrations after reamalgamation gave low values although accurate results were obtained thereafter.

A mercury pool was also employed as anode; a magnetic stirrer was used on the surface of the mercury. However, efficient stirring was impossible, and the anode collected precipitate rather easily.

The use of the amalgamated gold plate in a vertical position in the solution

was found to be the most practical and reliable possibility. At least twenty titrations were possible with this anode without reamalgamation.

Treatment of the indicator electrode

When the indicator electrode was treated as recommended above, the potential was below +50 mV vs. SCE at the beginning of the titration, compared to +100—180 mV without treatment. In the latter case, the potential decreased during the titration until the first potential jump, but then the shape of curve was the same as when the outlined procedure was followed. Since the potential at the first equivalence point lies around +80 mV, this jump was reduced, and sometimes, especially for the titration of unhydrolysed penicillins, undetectable when the thiosulphate treatment was omitted.

Titration of penicillamine

When pure penicillamine was titrated, two equivalence points were obtained as for penicilloates and as reported previously [3]. Eight titrations by the recommended procedure gave an average of 98.2% recovery (s_r = 0.3%) on the basis of the second equivalence point. All the solutions were deaerated before use since penicillamine is easily oxidized in water. The results were not affected if the dissolved samples were left for up to 100 min, but thereafter, and when air-saturated water was used, low values were obtained.

Titration of mixtures of penicillamine and penicilloate

If penicillamine was present in a sample of penicillin which was hydrolysed and titrated with mercury(II), an initial jump appeared before the two usual ones. Figure 3 shows titration curves for two mixtures of penicillamine and penicilloate. The penicilloate was obtained by alkaline hydrolysis of penicillin G. The very negative initial potentials are due to the redox potential of penicillamine. The extra jump pertains to complex formation between penicillamine and Hg(II) at a molar ratio of 2:1. After this jump penicilloate reacts at the same molar ratio up to the next equivalence point; the transition to the 1:1 stoichiometry between Hg(II) and penicillamine and penicilloate then occurs simultaneously.

Mixtures of the two substances could be analysed since up to the first equivalence point only penicillamine was titrated. The difference between the second and first jump gave the amount of penicilloate, and the last equivalence point corresponded to the sum of the two substances. Results for two mixtures are shown in Table 3. The absolute standard deviation from theoretical values was less than 2.5% in all cases. Mixtures of this type were also titrated with 0.02 M $Hg(NO_3)_2$ solution [1]; good agreement between theoretical and observed values was again obtained.

The possibility of determining penicillamine in the presence of penicilloates and, of course, penicillins, is of interest in connection with stability investigations on penicillins where penicillamine and penicilloate are known degradation products.

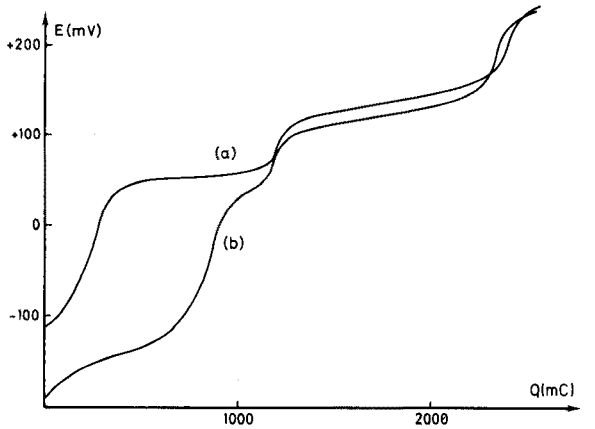

Fig. 3. Titration curves for mixtures of penicillamine and penicilloate. (a) Mixture 1. (b) Mixture 2 (see Table 3).

TABLE 3

Titration of mixtures of penicillamine and penicilloate

Mixture	Amount added		Amount found (molar %)
	mg	(molar %)	
1. Penicillamine	0.413	22.2	22.8, 21.6
Penicilloate	3.606	77.8	77.5, 79.1
(Total)	—	100.0	99.8, 99.8
2. Penicillamine	1.376	76.1	75.2, 73.7
Penicilloate	1.080	23.9	25.7, 24.7
(Total)	—	100.0	100.0, 98.7

The author thanks Dr. Bo Karlberg (Astra AB) for suggesting improvements on the manuscript, and Dr. Jörgen Lindquist (Astra AB) for valuable help with the equipment.

REFERENCES

1 B. Karlberg and U. Forsman, Anal. Chim. Acta, 83 (1976) 309.
2 U. Forsman and B. Karlberg, Anal. Chim. Acta, 86 (1976) 87.
3 A. Billabert, M. Callaquin and M. Hamon, Analusis, 3 (1975) 258.
4 J. Körbl and V. Vanicek, Czech. Patent No. 133, 383 (1969).
5 J. L. Vandenbalck, C. A. Mairesse-Ducarmois and G. J. Patriarche, Analusis, 3 (1975) 473.
6 E. P. Przybylowicz and L. B. Rogers, Anal. Chem., 28 (1956) 799.
7 E. P. Przybylowicz and L. B. Rogers, Anal. Chem., 30 (1958) 1064.
8 E. P. Przybylowicz and L. B. Rogers, Anal. Chim. Acta, 18 (1958) 596.
9 C. A. Mairesse-Ducarmois, J. L. Vandenbalck and G. J. Patriarche, J. Pharm. Belg., 28 (1973) 300.
10 Pharmacopea Nordica, Editio Svecia, Addendum, 1965, p. 229.

Analytica Chimica Acta, 93 (1977) 161—171
© Elsevier Scientific Publishing Company, Amsterdam — Printed in The Netherlands

ELECTROMETRIC TITRATIONS OF Cr(VI), Mn(IV), V(V), Co(III) AND U(VI) WITH A STANDARD IRON(II) SOLUTION IN ALKALINE MEDIA CONTAINING HEXITOLS

B. VELIKOV† and J. DOLEŽAL*

Department of Analytical Chemistry, Charles University, Albertov 2030, 128 40 Prague 2 (Czechoslovakia)

(Received 21st March 1977)

SUMMARY

Direct and indirect potentiometric, bipotentiometric and biamperometric titrations with a standard iron(II) solution are described for some inorganic compounds in alkaline media containing hexitols (mannitol, dulcitol and sorbitol). The optimal conditions for titrations based on the Cr(VI) → Cr(III), Mn(IV) → Mn(III) → Mn(II), V(V) → V(IV), Co(III) → Co(II) and U(VI) → U(IV) systems are discussed. Of the hexitols studied, sorbitol has the greatest effect on the value of the redox potential of the Fe(III)/Fe(II) system; the E_f^0 value is about −1.10 V vs. SCE.

Studies of the polarographic behaviour of many ions in electrolytes containing alditols [1, 2], inositols [3] and 1,6-anhydro-carbohydrates [4] as complexing agents have stimulated an extensive examination of the use of iron(II) solutions in titrimetric analysis. The formation of very stable iron(III) complexes with these reagents in alkaline solutions shifts the formal redox potential of the Fe(III)L/Fe(II)L systems to very negative potentials. The reagents thus obtained are very powerful reductants, similar to Ti(III), Cr(III) and V(III) in acidic solutions. Previous communications have dealt with titrations with iron(II) sulphate in alkaline solutions containing triethanolamine [5—7] (E_f^0 = −1.07 V vs. SCE) and mannitol [8, 9]. The present paper reports the use of mannitol, dulcitol and sorbitol as reagents forming strong complexes with iron(III) in alkaline solutions. To increase the sensitivity of the titrations, biamperometric and bipotentiometric techniques were used in addition to equilibrium potentiometric end-point detection.

EXPERIMENTAL

Reagents

A standard 0.05 M $FeSO_4$ solution was prepared by dissolving 6.950 g of $FeSO_4 \cdot 7H_2O$ (p.a; Lachema, Czechoslovakia) in 500 ml of 0.05 M H_2SO_4

† On leave from the Department of Analytical Chemistry, Sofia University, Bulgaria.

previously deaerated by passage of nitrogen for 30 min. The titre was checked weekly by titration of potassium dichromate in acidic medium. Other solutions 0.01—0.005 M, were prepared by suitable dilution.

A standard 0.05 N $K_2Cr_2O_7$ solution was prepared by accurate weighing of the p.a. substance (Lachema) and dissolution in redistilled water.

Solutions of manganese(II) ($MnSO_4 \cdot 5H_2O$) and cobalt ($CoSO_4 \cdot 7H_2O$) were standardized complexometrically. Uranium(VI) solutions ($UO_2(NO_3)_2 \cdot 6H_2O$ and $UO_2(CH_3COO)_2 \cdot 2H_2O$) were standardized by titration with iron(II) sulphate in 12 M H_3PO_4.

Sorbitol, mannitol and dulcitol (BDH, London) were recrystallized from ethanol, and stock solutions were prepared weekly. Blank determinations were done before each series of titrations with iron(II) sulphate.

Apparatus

The potentiometric, bipotentiometric and biamperometric titrations were carried out with a digital pH-meter (Seibold, Austria) and operational amplifier modular sets constructed in this laboratory and at the J. Heyrovský Institute of Physical Chemistry and Electrochemistry. The operational amplifier circuits were connected as described previously [10]. A three-way switch permitted rapid succession of potentiometric, bipotentiometric and biamperometric measurements. The measured signal is given in millivolts, even with biamperometric titrations. The abbreviations P, BP and BA in the Figures denote the potentiometric, bipotentiometric and biamperometric indication methods, respectively.

The titration vessels were 100-ml beakers which were tightly closed with lids carrying the platinum indicator and saturated calomel reference electrodes (potentiometry) or two platinum foil electrodes with active surface areas of 0.35 cm^2 (biamperometry and bipotentiometry). To improve the reproducibility of the measured potential or current values, the platinum electrodes were prepolarized at ca. 2 V in 1.8 M H_2SO_4 before each series of titrations; they were then immersed in an acidic 0.1 M $FeSO_4$ solution. The titrations were carried out in a nitrogen atmosphere. Traces of oxygen were removed from the nitrogen in traps containing an alkaline solution of sodium anthraquinone-β-sulphonate and an acidic solution of chromium(II) chloride. The solutions were stirred magnetically.

Polarization curves were recorded with a rotating platinum electrode with an active surface area of 0.40 cm^2 at 30 r.p.s., the rates of polarization being 440, 785 and 3750 mV min^{-1}. A three-electrode operational amplifier circuit and a Bryans 26000 A3 XY recorder were used.

Calibrated volumetric glassware was employed; the 10-ml burettes were graduated at 0.02-ml and the 1-ml burettes at 0.01-ml intervals.

RESULTS

Polarization curves of the Fe(III)/Fe(II) system in alkaline solutions containing hexitols

The reversibility of the Fe(III)/Fe(II) system in these media was examined by recording the polarization curves at a rotating platinum disk electrode. As the complexes of iron(III) are reduced at more negative potentials than those corresponding to hydrogen evolution, it was impossible to verify the degree of reversibility of the system, and the values of the applied voltage or current in biamperometric or bipotentiometric titrations had to be found experimentally.

Determination of chromium(VI)

The formal redox potentials of the hexitol complexes of the Fe(III)/Fe(II) system and the titre of the standard $FeSO_4$ solutions were determined in the titration of dichromate. In all titrations discussed in this paper, the dependence of the titration curves on the concentrations of KOH, hexitol and the test substance was examined.

The general procedure was as follows: to ca. 25 ml of a solution of KOH and a hexitol, previously deaerated with nitrogen, was added a certain amount of the test substance. Nitrogen was bubbled through the solution for 10 min, during which time the electrode potentials stabilized. Then the mixture was titrated with a 0.05, 0.01 or 0.005 M $FeSO_4$ solution.

The results of this determination of dichromate were compared with those of the titration in 0.7 M H_2SO_4 (Tables 1 and 2); the results were virtually identical and the reproducibility was very good. The slope $\Delta mV/\Delta ml$ indicates that the determination in alkaline hexitols is more sensitive, sorbitol yielding the best results. Sorbitol was therefore employed in most further experiments.

The effect of the reaction conditions on the course and precision of the titration of dichromate was studied (Table 3). The optimum conditions involve 2—4 M KOH and 0.25—0.50 M sorbitol. At lower sorbitol concentrations the potentials stabilized slowly, and precipitation sometimes occurred.

TABLE 1

Titration of 5 ml of 0.05 N Cr(VI) with iron(II) solution

Medium		Consumption (ml)[a]		Slope ($\Delta mV/\Delta ml$)		E_f (V)
		Range	Av.	P	BP	
0.7 M H_2SO_4		5.31—5.34	5.32_3	4500	62000	+450
0.5 M hexitol—2 M KOH	Sorb.	5.32—5.35	5.33_3	9000	66000	—1100
	Man.	5.33—5.38	5.35_0	6500	65000	—1065
	Dulc.	5.34—5.38	5.36_3	6000	65000	—1055

[a]Data for 6 titrations.

TABLE 2

Titration of 5 ml of 0.05 M Fe(II) with potassium dichromate

Medium		Consumption (ml)[a]	Slope (ΔmV/Δml)	
			P	BP
0.7 M H_2SO_4		4.69_3	5500	42000
0.5 M hexitol—2 M KOH	Sorbitol	4.64_3	7500	48000
	Mannitol	4.65_0	6000	46000
	Dulcitol	4.63_3	5500	46000

[a] Average of 6 titrations.

TABLE 3

The effect of the sorbitol and potassium hydroxide concentrations on the determination of 5 ml of 0.05 N Cr(VI) with iron(II) solution

Sorbitol (M)	KOH (M)	ΔmV/Δml	E_f (mV)	E_{eq} (mV)	Error (%)
0.1	0.1	1500	−670	−320	±4.5
	1	5500	−1050	−675	±3.4
	4	9500	−1090	−775	±2.6
0.25	0.1	2000	−705	−380	±2.8
	1	6500	−1053	−680	±1.5
	4	9000	−1118	−800	±1.5
0.5	0.1	3000	−726	−405	±0.85
	0.5	4200	−890	−580	±1.2
	1	5500	−1020	−665	±0.45
	2	9000	−1100	−780	±0.25
	3	12000	−1140	−830	±0.45
	4	14000	−1186	−880	±0.55
0.8	0.1	3000	−740	−415	±1.40
	4	10000	−1176	−860	±1.85

Under the optimum conditions, the slope ΔmV/Δml was 14000, and potential stabilization was practically instantaneous, except near the equivalence point when it required about 1 min. The solution changed from yellow to green after the equivalence point. Figure 1 shows the titration curves for various hexitols and various hydroxide concentrations. Amounts of 0.3—30 mg of chromium(VI) can be determined in 25 ml of solution (2 M KOH and 0.5 M sorbitol); the relative error is less than 1.6%.

In the reverse titration, i.e. the determination of iron(II) salts with dichromate, the maintenance of an inert atmosphere is more difficult, and

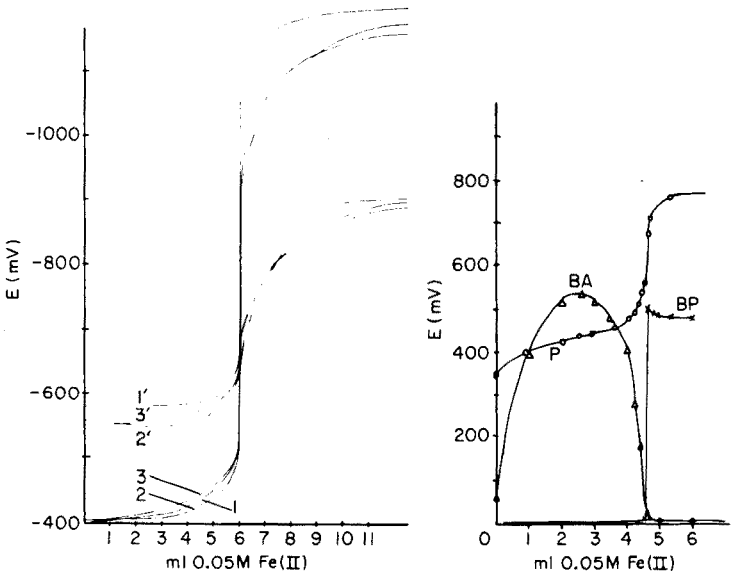

Fig. 1. Potentiometric titration of Cr(VI) by the iron(II) salt in alkaline hexitol solutions. Curves 1, 2, 3, 0.5 M sorbitol, 0.5 M dulcitol, 0.5 M mannitol, respectively, in 0.5 M KOH. Curves 1′, 2′, 3′, 0.5 M sorbitol, 0.5 M dulcitol, 0.5 M mannitol, respectively, in 4 M KOH.

Fig. 2. Potentiometric, bipotentiometric and biamperometric titration of Fe(II) with 0.05 N Cr(VI) in 0.7 M H_2SO_4.

consequently the results are subject to a larger error (Table 2). For biamperometric and bipotentiometric indication of these titrations, both in acidic solutions and alkaline hexitol media, the required values of the applied voltage and current were found empirically. The applied voltage in biamperometric titrations was varied from 100 to 1200 mV; the curves for titration of dichromate with iron(II) solution are given in Fig. 2 (acidic solution). The optimum applied voltage was 100 mV. In alkaline hexitol media, an applied voltage of at least 600 mV was required (Fig. 3). Generally, it can be seen that the biamperometric method is less suitable than equilibrium potentiometry, especially when small amounts of chromium(VI) are to be determined.

The current applied in the bipotentiometric titrations was varied from 1 to 5 μA, 3 μA being the most suitable. Bipotentiometry is more sensitive for this titration than equilibrium potentiometry, as down to 0.05 mg Cr can be determined in 25 ml. The slope ΔmV/Δml exceeded 60000, i.e. 4—5 times larger than in equilibrium potentiometry. A typical titration curve in an alkaline hexitol medium is shown in Fig. 4.

In contrast to the titration described earlier [5], vanadium interferes with the titration of chromium, because it is reduced to vanadium (IV) at similar potentials in alkaline hexitol solutions. The determination of dichromate in

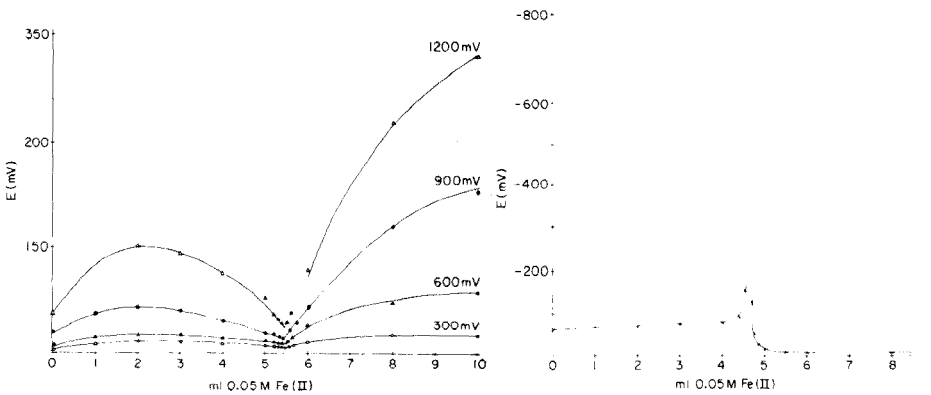

Fig. 3. The effect of the applied voltage on the shape of the biamperometric curves in titrations of Cr(VI) with 0.05 M Fe(II) in a solution of 0.25 M dulcitol in 2 M KOH.

Fig. 4. Bipotentiometric titration of Cr(VI) with 0.05 M Fe(II) in a solution of 0.5 M mannitol in 2 M KOH.

alkaline hexitol solutions is much more sensitive than the titration in acidic solutions, but the need for an inert atmosphere is a drawback.

Determination of manganese(IV) and (III)

Before the titration with iron(II) solution, manganese was oxidized by hexacyanoferrate(III), hydrogen peroxide or lead(IV) dioxide. The oxidation with hexacyanoferrate was monitored potentiometrically. When the equivalence point corresponding to the reaction Mn(III)—hexitol → Mn(IV)—hexitol was achieved, the oxidation was interrupted and the red-brown Mn(IV)—hexitol complex was immediately titrated with iron(II) solution. The reduction to the Mn(III)—hexitol complex was quantitative; the relative error did not exceed 1.82% in the potentiometric, bipotentiometric (3—8 μA current) and biamperometric (800—900 mV) titrations (Fig. 5). The titrant consumption corresponding to the Mn(III)—hexitol → Mn(II)—hexitol reduction was always subject to a positive error, which can be explained as discussed earlier [1]. The slope $\Delta mV/\Delta ml$ for 0.05 M $FeSO_4$ was 2500 for potentiometry and 7500 for bipotentiometry (Mn(IV)—sorbitol → Mn(III)—sorbitol). The most suitable medium for the determination of manganese was 0.5 M sorbitol in 1—3 M KOH (see Table 4). Amounts of 0.3—30 mg Mn can be determined potentiometrically and biamperometrically in 25 ml of solution, while bipotentiometry permits the determination of down to 0.04 mg Mn in 25 ml of solution.

Determination of vanadium(V)

The very negative value of the formal redox potential of the Fe(III)/Fe(II) system in alkaline hexitol solutions suggested the possibility of a sensitive determination of vanadate, which is reduced to the vanadyl cation. Like the

TABLE 4

The effect of the sorbitol and potassium hydroxide concentrations on the determination of 2.746 mg of Mn(IV) with iron(II) solution

Sorbitol (M)	KOH (M)	Found[a] (mg)	Error (%)	Found[b] (mg)	Error (%)
0.1	0.1	2.70	−1.70	2.84	+3.42
	1	2.72	−0.95	2.87	+4.51
	4	2.72	−0.95	2.81	+2.33
0.25	0.1	2.72	−0.95	2.81	+2.33
	1	2.72	−0.95	2.78	+1.23
	4	2.71	−1.31	2.79	+1.60
0.5	0.1	2.72	−0.95	2.86	+4.15
	0.5	2.73	−0.58	2.80	+1.97
	1	2.74	−0.22	2.79	+1.60
	2	2.735	−0.40	2.78	+1.23
	3	2.74	−0.22	2.79	+1.60
	4	2.70	−1.70	2.81	+2.33
0.75	0.1	2.72	−0.95	2.80	+1.97
	1	2.71	−1.31	2.81	+2.33
	4	2.70	−1.70	2.80	+1.97

[a]Calculated from the consumption for the Mn(IV)—sorbitol → Mn(III)—sorbitol reaction.
[b]Calculated from the consumption for the Mn(III)—sorbitol → Mn(II)—sorbitol reaction.

determinations of chromium and manganese, the titrations were not significantly affected by variations in the reaction conditions. The results indicated that the optimum medium was 0.5—0.7 M sorbitol in 2—3 M KOH. The potentials stabilized practically instantaneously in the potentiometric titration; the slope $\Delta mV/\Delta ml$ was 9500—15000 (0.5—4.0 M KOH, 0.5 M sorbitol) for 0.05 M iron(II).

The bipotentiometric (optimum current, 3—4 μA) and biamperometric (optimum voltage, 600—700 mV) methods gave results as precise as those of potentiometry; the relative error did not exceed 1.0%. Amounts of 0.1—3.0 mg V could be determined in 25 ml of solution. Figure 6 shows typical titration curves.

Determination of cobalt(III)

The sorbitol complex of cobalt(II) was oxidized in alkaline medium with hexacyanoferrate(III), hydrogen peroxide or lead(IV) dioxide [8]. Lead dioxide gave the best results. Appropriate amounts of KOH and sorbitol were pipetted into a 50-ml volumetric flask, followed by the cobalt(II) solution. The mixture was diluted with water to the mark and transferred to an Erlenmeyer flask, 1 g of PbO_2 was added, and the solution was stirred for

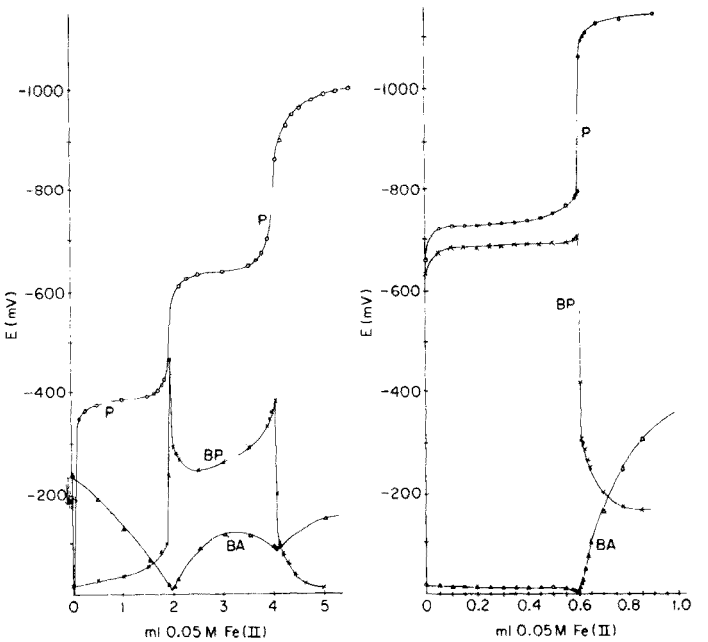

Fig. 5. Potentiometric, bipotentiometric and biamperometric titration of Mn(IV) with 0.05 M Fe(II) in a solution of 0.5 M sorbitol in 1 M KOH.

Fig. 6. Potentiometric, bipotentiometric and biamperometric titration of V(V) with 0.01 M Fe(II) in a solution of 0.6 M sorbitol in 2 M KOH.

15—20 min. After filtration through a G4 glass frit, an aliquot of the solution was titrated with 0.05 M $FeSO_4$.

Oxidation was proved by a colour change from the intense blue of the cobalt(II)—sorbitol complex to the green of the cobalt(III) complex. The oxidation was quantitative in solutions containing 0.5 M sorbitol in 3—4 M KOH. When less than 2 M hydroxide was present, the subsequent reduction with iron(II) was subject to large negative errors, probably because of auto-reduction of Co(III). The potentiometric titration proceeded best in 3—4 M KOH with 0.4—0.6 M sorbitol. Potential stabilization was almost instantaneous, and slope $\Delta mV/\Delta ml$ was 9000 for 0.05 M $FeSO_4$.

The end-point indication was equally successful when bipotentiometry (optimum current, 6—8 μA; $\Delta mV/\Delta ml$ = 20000 for 0.05 M Fe(II)) or biamperometry (optimum voltage, 700—800 mV) were employed (see Fig. 7). Amounts of 0.5—25 mg Co were determined in 25 ml with an error of 1.2%. When a large excess of iron(II) was added to the solution after the equivalence point, the solution gradually turned black and the electrodes became coated with a black-brown film. Partial reduction to cobalt metal probably occurred; this effect was not observed in an alkaline mannitol solution.

The slope values obtained in potentiometric and bipotentiometric titrations indicate that the alkaline sorbitol solution is more suitable for the determination of cobalt than an alkaline mannitol medium.

Determination of uranium(VI)

Preliminary experiments indicated that uranium(VI) is reduced to uranium(IV) by iron(II) sulphate in alkaline hexitol solutions. The end-points of titrations of 0.05—0.01 M uranyl nitrate or uranyl acetate with iron(II) solutions in 0.1—4 M KOH and 0.05—1 M sorbitol media were marked by a large change in the equilibrium potential. The optimum medium contained 0.2—0.5 M sorbitol in 1—2 M KOH (Table 5). The potentials stabilized instantaneously, and the slope $\Delta mV/\Delta ml$ was around 12000 for 0.05 M $FeSO_4$. Amounts of 0.5—50 mg of uranium could be determined in 25 ml of solution with an error not exceeding 1.7%.

When the hydroxide concentration was outside the 1—2 M range (0.5 M sorbitol), the potentials required 8—10 min to stabilize; this also happened when the sorbitol concentration was less than 0.1 M. The solution became turbid when 0.05 M sorbitol was used.

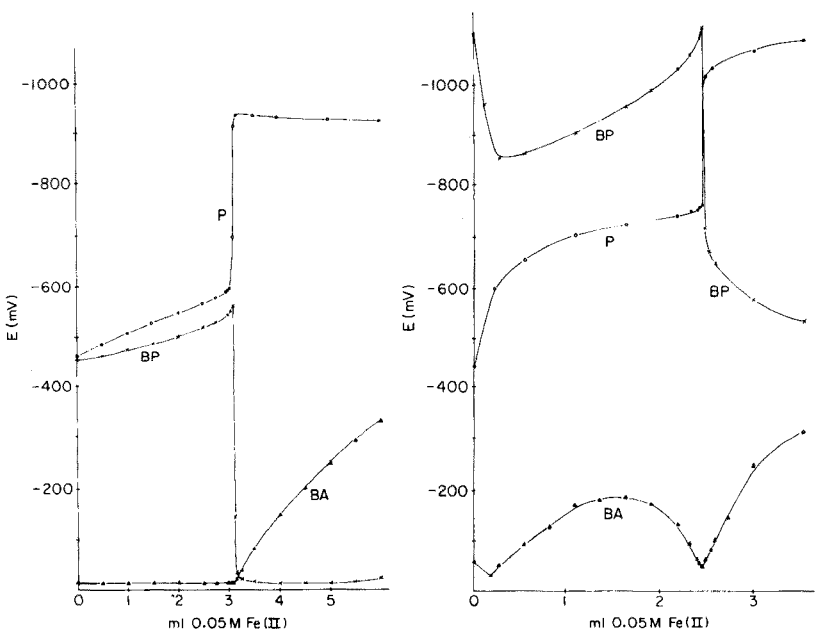

Fig. 7. Potentiometric, bipotentiometric and biamperometric titration of Co(III) with 0.05 M Fe(II) in a solution of 0.5 M sorbitol in 3 M KOH.

Fig. 8. Potentiometric, bipotentiometric and biamperometric titration of U(VI) with 0.05 M Fe(II) in a solution of 0.4 M sorbitol in 2 M KOH.

TABLE 5

The effect of the sorbitol and potassium hydroxide concentrations on the determination of 11.90 mg of uranium with a 0.05 M $FeSO_4$ solution

Sorbitol (M)	KOH (M)	Found (mg)	Error (%)	ΔmV/Δml P
0.05	0.1	11.66	−2.02	1500
	1	11.70	−1.68	4500
	4	11.64	−2.18	6000
0.10	0.1	11.61	−2.44	2500
	1	11.80	−0.84	6200
	4	11.85	−0.42	9000
0.20	0.1	11.82	−0.67	3200
	1	11.77	−1.09	10500
	4	11.86	−0.34	12500
0.50	0.1	11.85	−0.42	3500
	0.5	11.82	−0.67	7800
	1	11.91	+0.08	11600
	2	11.93	+0.25	12000
	3	11.96	+0.50	13200
	4	11.97	+0.59	13700
0.75	0.1	12.05	+1.26	4000
	2	11.98	+0.67	12500
	4	11.97	+0.59	14000
1.0	0.1	12.04	+1.18	4400
	2	11.98	+0.67	13000
	4	11.98	+0.67	15200

The bipotentiometric titration (optimum current, 10 μA) showed a slope ΔmV/Δml of 17500 for 0.05 M $FeSO_4$ (Fig. 8). The end-point could also be indicated biamperometrically, the optimum applied voltage being 1300 mV (Fig. 8).

This method should be applicable to the determination of uranium in various materials, especially in extracts obtained in the hydrometallurgical process of uranium mining.

DISCUSSION

The Fe(III)/Fe(II) formal redox potentials measured in sorbitol media (Fig. 1, Table 1) indicate that iron(II) sulphate is a very strong reductant in alkaline sorbitol solutions. The E_f^0 value of −1.10 V (SCE) in 0.5 M sorbitol−2 M KOH solutions is higher than the corresponding values for mannitol and dulcitol. This is in agreement, to a certain extent, with the values of the conditional

stability constants for the manganese(III) complexes with sorbitol, mannitol and dulcitol. The stability of these complexes from the point of view of their structure has been discussed [2].

The reducing properties of iron(II) salts in this medium are comparable with those of chromium(II), vanadium(II) and titanium(III) salts in acidic solutions. However, the latter reagents are unstable in air, their titre must be checked daily; their preparation and storage are much more complicated than those of iron(II) salts.

The interferences in the various titrations with iron(II) sulphate in alkaline hexitol solutions have not been studied in detail. It has been found that Ni(II), Zn(II), Cd(II), Cr(III), Fe(III) and Al(III) do not interfere when present in less than 10-fold (molar) amounts. Lead(II) is reduced by iron(II) to the metal, but the reaction is not quantitative, even if a sufficient excess of iron(II) sulphate is added. Among common anions, chloride, sulphate, nitrate and chlorate do not interfere.

Bipotentiometry was generally found to be a more sensitive end-point detection method than potentiometry, so that micro-titrations were usually possible. The bipotentiometric titration curves were considerably asymmetrical and indicated that the Fe(III)—sorbitol/Fe(II)—sorbitol system is virtually reversible at the platinum electrode, while the systems titrated are not. The end-point could be located precisely. Biamperometric indication showed no advantages over equilibrium potentiometry; moreover, variation in the applied voltage led to substantial changes in the shapes of the biamperometric titration curves. The bipotentiometric titration curves also changed their shapes on variation of the applied current. The biamperometric and bipotentiometric titration curves also depended on temperature (in the range 20—70°C).

Among the systems studied, the determination of uranium should be of the greatest practical importance.

REFERENCES

1 J. Doležal and O. Gürtler, Talanta, 15 (1968) 299.
2 B. Velikov and J. Doležal, J. Electroanal. Chem., 71 (1976) 91.
3 J. Doležal and H. Kekulová, J. Electroanal. Chem., 69 (1976) 239.
4 J. Doležal, E. Juláková, M. Černý and M. Kopanica, J. Electroanal. Chem., 52 (1974) 261.
5 J. Doležal, E. Lukšyte, V. Rybáček and J. Zýka, Collect. Czech. Chem. Commun., 29 (1964) 2597.
6 H. Alfaro, J. Doležal and J. Zýka, Chem. Anal., 55 (1964) 84.
7 J. Doležal, J. Rybáček and J. Zýka: Českosl. Farm., 14 (1965) 59.
8 J. Doležal and F. J. Langmyhr, Anal. Chim. Acta, 61 (1972) 73.
9 N. Chughtai, J. Doležal and J. Zýka, Microchem. J., (1975) 20.
10 R. Kalvoda, Operational Amplifiers in Chemical Instrumentation, E. Horwood, Chichester, 1975.

Analytica Chimica Acta, 93 (1977) 173—181
© Elsevier Scientific Publishing Company, Amsterdam — Printed in The Netherlands

ELECTROMETRIC TITRATIONS OF Bi(III), Cu(II), Pt(IV), Te(VI) AND Te(IV) WITH STANDARD IRON(II) SOLUTION IN ALKALINE MEDIA CONTAINING HEXITOLS

B. VELIKOV[§] and J. DOLEŽAL*

Department of Analytical Chemistry, Charles University, Albertov 2030, 128 40 Prague 2 (Czechoslovakia)

(Received 21st March 1977)

SUMMARY

Potentiometric, bipotentiometric and biamperometric titrations with an iron(II) salt in alkaline solutions containing sorbitol are reported. Suitable conditions are discussed for determinations based on the Bi(III) → Bi°, Cu(II) → Cu(I) → Cu°, Pt(IV) → Pt(II) → Pt° and Te(VI) → Te(IV) → Te° → telluride systems.

Potentiometric, bipotentiometric and biamperometric titrations of some inorganic systems with iron(II) solutions in alkaline hexitol media have been reported [1]. In these systems, the metal ions were reduced by iron(II) to a lower valence state, e.g. Cr(VI) → Cr(III), U(VI) → U(IV), etc. The present paper describes the utilization of the negative formal redox potential of the Fe(III)/Fe(II) system in alkaline hexitol (especially sorbitol) media for the titration of some systems involving reduction of various ions, e.g. Bi(III), Cu(II), Pt(IV), Te(VI) and Te(IV), to the metal.

EXPERIMENTAL

Standard 0.05 M solutions of $Bi(NO_3)_3$, $CuSO_4$, Na_2TeO_4, Na_2TeO_3, Na_2SeO_4 and Na_2SeO_3 were prepared from the p.a. substances (Lachema, Czechoslovakia) and 0.05 M solutions of $(NH_4)_2PtCl_6$, $PdCl_2$, $(NH_4)_2IrCl_6$ and $RhCl_4$ from the Specpure substances (Johnson Matthey Ltd., England). The other solutions employed were identical with those described previously [1]. Before each series of measurements, blanks were determined to check the hexitol purity.

The apparatus was the same as that described previously [1]. In the Figures, the abbreviations P, BP and BA denote the potentiometric, bipotentiometric and biamperometric methods, respectively. Unless otherwise mentioned, 25-ml volumes of test solution were taken.

[§]On leave from the Department of Analytical Chemistry, Sofia University, Bulgaria.

RESULTS

Determination of bismuth(III)

The strong reducing properties of the Fe(III)/Fe(II) system in alkaline solutions containing hexitols were used for the titration of bismuth based on the Bi(III)—hexitol → Bi^0 reaction. The colourless solution of the hexitol complexes of bismuth(III) gradually turned black during the titration, because elemental bismuth separated. Similarly to the previous determinations [1], the titrations were not greatly affected by the reaction conditions (Table 1); sorbitol again proved the best of the hexitols tested. The optimum conditions were 0.6 M sorbitol and 0.5—1.0 M KOH (Table 1). The potentials stabilized almost instantaneously, except near the equivalence point, where stabilization required about 1 min. The titration curves (Fig. 1) exhibited a sufficiently large potential break, the slope $\Delta mV/\Delta ml$ being 9500 for 0.05 M Fe(II) solutions. The end-point was also readily detected bipotentiometrically (applied current, 6 μA; slope, about 13500 mV for 0.05 M Fe(II)), but the biamperometric indication proved less suitable (the optimum applied voltage was about 850 mV).

Under the optimum conditions, 0.7—30 mg Bi could be determined in 25 ml of solution with a relative error not exceeding 1.45%.

Determination of copper(II) and (I)

In alkaline hexitol solutions, the potentiometric curve for titration of copper(II) with iron(II) solution exhibited two breaks, in contrast to the

TABLE 1

The effect of sorbitol and potassium hydroxide concentrations on the titration of bismuth (17.415 mg) with 0.05 M $FeSO_4$

Sorbitol (M)	KOH (M)	Found (mg)	Error (%)	$\Delta mV/\Delta$ ml P
0.3	1	16.95	−2.67	8000
	4	16.68	−4.22	8500
0.5	0.5	17.14	−1.58	8200
	1	17.24	−1.0	8700
	4	17.21	−1.18	9000
0.6	0.1	17.05	−2.09	8600
	0.5	17.38	−0.20	9500
	1	17.32	−0.54	9200
	2	17.27	−0.83	9500
	3	17.24	−1.0	9500
	4	17.14	−1.58	9800
0.75	0.5	17.30	−0.66	8500
	4	17.08	−1.92	9500

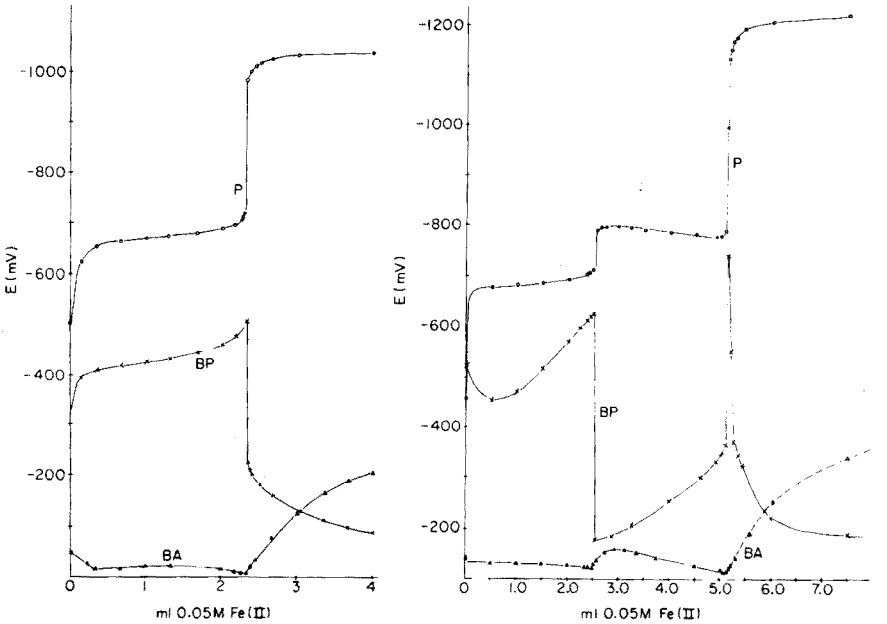

Fig. 1. Potentiometric, bipotentiometric and biamperometric titration of bismuth(III) with 0.05 M Fe(II) in a 0.6 M sorbitol—1 M KOH medium.

Fig. 2. Potentiometric, bipotentiometric and biamperometric titration of copper(II) with 0.05 M Fe(II) in a 0.4 M sorbitol—2M KOH medium.

reduction in the presence of triethanolamine (TEA) which proceeds in one step (Cu(II) → Cu°) [2]. The first step had a slope of 2750 mV for 0.05 M Fe(II) in 0.5 M hexitol—2 M KOH media, corresponding to the reduction of the Cu(II) complexes to the Cu(I) complexes. The second break was even steeper, with a slope of 11000 mV for 0.05 M Fe(II), corresponding to the reduction of the copper(I) complex to the metal (Fig. 2). Sorbitol gave the the best results; the use of mannitol and especially dulcitol led to smaller potential breaks.

Similarly to solutions containing TEA [2], the colour of the solution changed from intense blue, through orange-yellow (with a precipitate), to dark brown (Cu°). The potentials stabilized rapidly during the titration, but near the equivalence point it was necessary to wait for 2 min between titrant additions.

Table 2 summarizes the effects of variations in the sorbitol and KOH concentrations on the titration. The optimum medium composition involved 0.25—0.5 M sorbitol and 2—3M KOH. It must be pointed out that with 0.25—0.5 M sorbitol and 0.25—0.75 M KOH the potentials stabilized slowly (up to 10 min), but the first potential break had a larger slope than the second. With more than 10 mg of copper, the first potential break is more suitable for the determination, as the second break is not well defined. The

TABLE 2

The effect of the sorbitol and potassium hydroxide concentrations on the titration of copper (6.36 mg) with 0.05 M $FeSO_4$

Sorbitol (M)	KOH (M)	Found (mg)	Error (%)	ΔmV/Δml I[a]	ΔmV/Δml II
0.25	0.5	6.06	−4.72	3600	8500
	2	6.22	−2.20	3500	8600
0.5	0.1	5.93	−6.76	3200	7800
	0.25	5.97	−6.13	3500	8200
	0.5	6.02	−5.34	3800	8500
	0.75	6.18	−2.83	3800	8600
	1	6.23	−2.04	3400	9000
	2	6.32	−0.63	3500	10000
	3	6.31	−0.79	3500	11000
	4	6.29	−1.10	3600	11500
0.8	0.5	6.26	−1.17	2800	9500
	2	6.29	−1.10	3000	9800

[a]Δ mV/Δ ml I and II are the slopes of the first and the second potential breaks, respectively.

potential changes are more pronounced in alkaline hexitol (sorbitol) solutions than in alkaline TEA media.

The sensitivity of the method improved when the end-point was detected bipotentiometrically. With an applied current of 5 μA, the potential break at the Cu(II)—Cu(I)-sorbitol end-point had a slope of 25000 mV for 0.05 M Fe(II) solution. The second break was sharp with a slope of 20000 mV. In biamperometric titrations, an applied voltage of at least 900 mV was necessary; still, the break corresponding to the first end-point was poorly pronounced and difficult to use practically.

Under the optimum conditions, 0.6—25 mg Cu could be determined in 25 ml with a relative error of less than 1.0%.

Determination of platinum (IV) and (II)

Platinum(IV) is readily reduced to the metal in alkaline hexitol solutions and the potentiometric titration curve shows two breaks (Fig. 3). The first had a slope (Δ mV/Δml) of 20000 mV for 0.05 M Fe(II) solutions in 0.3 M sorbitol—0.3 M KOH media, corresponding to the reduction, Pt(IV)—hexitol → Pt(II)—hexitol. The second, corresponding to the reduction, Pt(II)—hexitol → Pt°, had a slope of 7000 mV. During the titration, the original light yellow of the solution became intense yellow and then suddenly black, because of platinum metal. Table 3 shows that the optimum medium contained 0.3—0.5 M sorbitol and 0.1—0.3 M KOH. With higher KOH concentrations and lower concentrations of sorbitol, the results were subject to large negative errors, probably owing to the formation of a precipitate immediately on mixing the complexing electrolyte with the sample solution. The titrant consumption

TABLE 3

The effect of the sorbitol and potassium hydroxide concentrations on the titration of platinum (9.76 mg) with 0.05 M $FeSO_4$

Sorbitol (M)	KOH (M)	Found[a] (mg)	Error (%)	Δ mV/Δ ml[b] *P*
0.1	0.05	9.25	−5.22	12500
	0.3	9.05	−7.27	14600
	1.0	8.95	−8.30	16200
	3.0	8.43	−13.62	17500
0.3	0.05	9.63	−1.33	18500
	0.3	9.68	−0.82	20000
	1.0	9.54	−2.25	21000
	3.0	9.12	−6.55	22300
0.5	0.05	9.66	−1.02	19000
	0.3	9.67	−0.92	20500
	1.0	9.48	−2.76	21600
	3.0	9.24	−5.32	23000
0.75	0.05	9.49	−2.77	18000
	0.3	9.55	−2.15	20000
	1.0	9.02	−7.58	22500

[a]Calculated from the consumption corresponding to the Pt(IV)—sorbitol → Pt(II)—sorbitol end-point.
[b]The slope of the first potential break.

corresponding to the second break was always 5—10% larger, even when an excess of iron(II) was added and back-titrated with potassium dichromate. Therefore, for very sensitive determinations of platinum, direct titrations are more suitable, provided that the first sharp potential break is used.

In the bipotentiometric (optimum current, 8 μA) and the biamperometric (optimum voltage, 900 mV) titrations the first break on the titration curve was also more pronounced. Under the optimum experimental conditions, 0.1—20 mg Pt could be precisely determined in a volume of 25 ml, with a relative error of less than 1%. The titration of platinum (IV) must, however, be carried out immediately after deaeration with nitrogen; after 2 h the results were 10% low, probably because of the reduction of platinum (IV) by sorbitol. This effect proved to be very rapid with rhodium, palladium and especially iridium, so that these cations were reduced to the metals during deaeration of the solution and did not consume any titrant. An attempt was made to determine hexitols (sorbitol) by titration with iridium(IV) standard solution in an alkaline medium, but the reaction was so complicated that the results could not be interpreted.

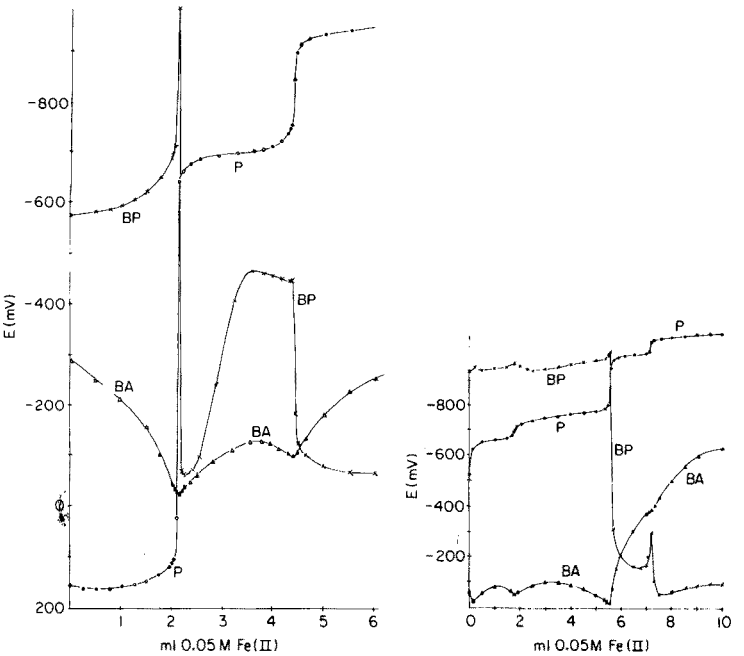

Fig. 3. Potentiometric, bipotentiometric and biamperometric titration of platinum(IV) with 0.05 M Fe(II) in a 0.3 M sorbitol—0.3 M KOH medium.

Fig. 4. Potentiometric, bipotentiometric and biamperometric titration of tellurium(VI) with 0.05 M Fe(II) in a 0.4 M sorbitol—3 M KOH medium.

Determination of tellurium(VI) and (IV)

Both tellurite and tellurate can be determined. During the titration of tellurate, a small amount of gray tellurium was temporarily formed, but redissolved quickly. This happened after each addition of titrant, the electrode potentials stabilizing very slowly; after the titrant addition the potential increased and then decreased for 4—5 min to about −720 mV. The tellurium metal was probably reoxidized by the remaining tellurate. The end of the Te(VI)—sorbitol → Te(IV)—sorbitol reaction could not be determined accurately, although there was a small potential break (Fig. 4), and the titrant consumption was 15—20% lower than the theoretical amount. On further addition of the titrant the solution turned black and the potentials stabilized faster. The end-point for the Te(VI)—sorbitol → Te° reduction was accompanie by a pronounced potential break, with a slope of 7500 mV for 0.05 M Fe(II) solution in 0.5 M sorbitol—3 M KOH media.

During the titration of tellurium(IV), the potentials stabilized rapidly from the beginning; gray-black tellurium was formed, and the end-point was marked by a sharp potential break with a slope of 10000 mV (Fig. 5). After the equivalence point, the titrations of Te(VI) and Te(IV) proceeded in the same

way. Further addition of iron(II) sulphate dissolved the tellurium and the solution became red-purple. The potentials stabilized within 2 min. Presumably, tellurium was reduced further to the telluride (Te(−II)), but the potential break was small (Δ mV/Δ ml about 200—250 mV) for 0.05 M Fe(II) solutions (see Figs. 4 and 5) and the reduction was not quantitative, the negative error being 10—15%.

On further addition of titrant the solution turned green. This sequence of the titrations for Te(VI) and Te(IV) was observed in a solution containing 0.4—0.5 M sorbitol and 3—4 M KOH, which was found to be most suitable (Table 4). When the KOH concentration was less than 0.5 M, the $Te^0 \rightarrow Te^{2-}$ reduction did not occur. When the test solution contained a mixture of hexavalent and tetravalent tellurium, the two forms were reduced together and the titrant consumption corresponded to the total tellurium content.

With bipotentiometric indication (optimum current, 10 μA), the $Te(VI) \rightarrow Te^0$ and $Te^0 \rightarrow Te^{2-}$ end-points were pronounced, whereas the $Te(VI) \rightarrow Te(IV)$ reduction gave only a poorly defined peak (Fig. 4). In the titration of tellurite, the $Te(IV) \rightarrow Te^0$ and $Te^0 \rightarrow Te^{2-}$ end-points gave sharp peaks. Similarly to some previous titrations, a poorly defined peak appeared at the start of the titration (at a consumption of 0.10—0.15 ml of 0.05 M Fe(II) solution) corresponding to a "blank". The biamperometric titration curves (optimum voltage, 1000 mV) showed breaks similar to those on the bipotentiometric titration curves, but the $Te^0 \rightarrow Te^{2-}$ end-point was poorly

TABLE 4

The effect of the sorbitol and potassium hydroxide concentrations on the titration of tellurium (4.25 mg Te(VI) or 6.38 mg Te(IV)) with 0.05 M $FeSO_4$

		Tellurium(VI)			Tellurium(IV)		
Sorbitol (M)	KOH (M)	Found (mg)	Error (%)	Δ mV/Δ ml *P*	Found (mg)	Error (%)	Δ mV/Δ ml *P*
0.1	0.5	4.53	+6.59	6000	6.48	+1.57	7500
	1.0	4.40	+3.53	6500	6.31	−1.09	8200
	4.0	4.42	+4.0	7300	6.28	−1.57	9000
0.25	0.5	4.36	+2.59	6300	6.42	+0.63	8500
	1.0	4.35	+2.35	6800	6.15	−3.60	9000
	4.0	4.45	+4.70	8000	6.41	+0.47	9500
0.5	0.5	4.43	+4.23	6500	6.48	+1.57	9000
	1.0	4.38	+3.05	7000	6.54	+2.51	9500
	2.0	4.31	+1.41	7200	6.40	+0.31	10000
	3.0	4.29	+0.94	7500	6.39	+0.16	10300
	4.0	4.33	+1.88	8000	6.40	+0.31	10500
0.75	0.5	4.45	+4.70	6500	6.27	−1.72	9000
	4.0	4.38	+3.05	8200	6.33	−0.78	10000

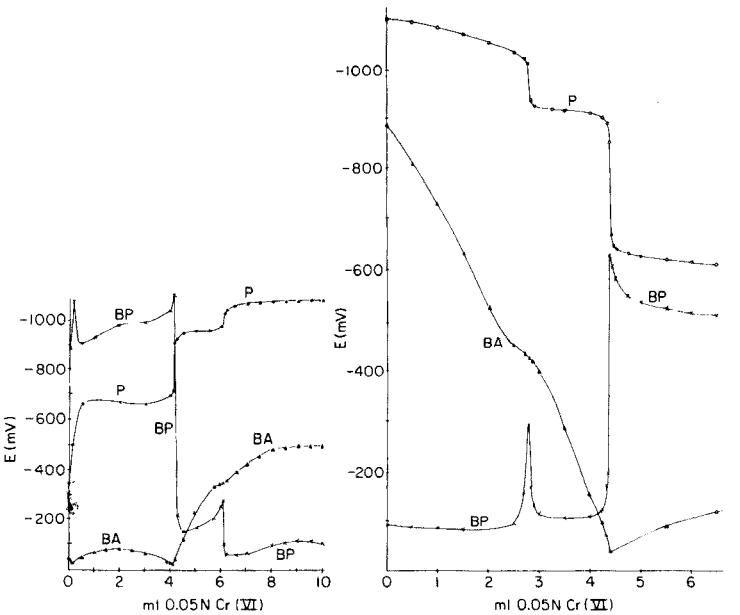

Fig. 5. Potentiometric, bipotentiometric and biamperometric titration of Te(IV) with 0.05 M Fe(II) in a 0.4 M sorbitol—3M KOH medium.

Fig. 6. Potentiometric, bipotentiometric and biamperometric titration of excess Fe(II) added to a solution of 0.05 N Te(VI) or Te(IV), with 0.05 N Cr(VI) in a 0.4 M sorbitol—3 M KOH medium.

defined. Amounts of 0.5—22 mg Te could be determined in 25 ml of solution potentiometrically, bipotentiometrically or biamperometrically with a relative error not exceeding 1.5%, by determining the titrant consumption for the Te(VI)—sorbitol → Te^0 or the Te(IV)—sorbitol → Te^0 reduction.

When excess of iron(II) sulphate was added to the test solution containing 3 M KOH, 0.5 M sorbitol and Na_2TeO_4 or Na_2TeO_3 in an inert atmosphere, a gray-black precipitate was formed immediately, but dissolved within about 10 min. During back-titration with 0.05 N $K_2Cr_2O_7$ solution, two breaks appeared on the potentiometric, bipotentiometric and biamperometric titration curves (Fig. 6), corresponding to the oxidation of the excess iron(II) (a slope of 400 mV for 0.05 N Cr(VI) with potentiometric indication) and to the oxidation, $Te^{2-} \rightarrow Te^0$ (the solution changed from red-purple to gray-black with, a slope of 9000 mV for potentiometric indication). The results obtained were virtually identical with those obtained in the direct titration.

The effect of selenite and selenate on the determination of Te(VI) and Te(IV) was also followed (Table 5). Selenium(IV) did not interfere up to Te(IV):Se(IV) molar ratios of 1:20 or Te(VI):Se(IV) ratios of 1:10. Selenium(VI) did not interfere up to Te(IV):Se(VI) molar ratios of 1:40 or Te(VI):Se(VI) ratios of 1:25. However, when excess of iron(II) was added

TABLE 5

The effect of selenate and selenite on the determination of 12.76 mg Te(IV) and 8.51 mg Te(VI) in a 0.5 M sorbitol—3 M KOH medium

Ratio	Te(IV) Found (mg)	Error (%)	Ratio	Te(VI) Found (mg)	Error (%)
Te(IV):Se(IV)			Te(VI):Se(IV)		
5:1	12.63	−1.02	5:1	8.49	−0.23
1:5	12.79	+0.23	1:1	8.43	−0.94
1:20	12.98	+1.72	1:5	8.58	+0.58
			1:10	8.67	+1.88
Te(IV):Se(VI)			Te(VI):Se(VI)		
1:1	12.82	+0.47	1:1	8.58	+0.58
1:10	12.71	−0.39	1:5	8.44	−1.52
1:40	12.95	+1.49	1:10	8.59	+0.94
			1:25	8.65	+1.64

to a solution containing selenate, partial reduction of the selenate occurred. Therefore, tellurium can be determined in the presence of selenium only by the direct titration.

Conclusion

The very negative formal redox potential of the iron(III)—sorbitol/iron(II)—sorbitol system in alkaline solutions has already been discussed [1]. Among the systems described, the determinations of platinum and tellurium are of special interest. The errors of the potentiometric and of the more sensitive bipotentiometric titrations do not exceed the usual permissible level. The methods will be studied further, especially from the point of view of the determination of some organic compounds.

REFERENCES

1 B. Velikov and J. Doležal, Anal. Chim. Acta, 00 (1977) 00.

2 J. Doležal, E. Lukšyte, V. Rybáček and J. Zýka, Collect Czech. Chem. Commun., 29 (1965) 2597.

Analytica Chimica Acta, 93 (1977) 183—189
© Elsevier Scientific Publishing Company, Amsterdam — Printed in The Netherlands

VOLTAMMÉTRIE DE L'ARGENT PAR REDISSOLUTION ANODIQUE SUR ÉLECTRODE DE CARBONE VITREUX ET APPLICATION AU DOSAGE DE L'ARGENT DANS L'URANIUM ET LE PLUTONIUM

B. HIRCQ et S. LAFONTAN

Commissariat à l'Énergié Atomique
BP no. 561, 92542 Montrouge Cedex (France)

(Reçu le 18 février 1977)

RÉSUMÉ

L'on décrit une méthode de dosage de l'argent par voltammétrie à redissolution anodique après avoir effectué un dépôt direct sur une électrode de carbone vitreux. Après l'étude des principaux paramètres, (temps de préélectrolyse, vitesse de balayage en potentiel, vitesse de rotation de l'électrode, molarité du milieu sulfurique utilisé), la méthode est appliquée à la détermination de l'argent dans l'uranium et le plutonium.

SUMMARY

Anodic stripping voltammetry of silver on a glassy carbon electrode, and application to the determination of silver in uranium and plutonium.

The use of a glassy carbon electrode for the anodic stripping voltammetry of silver, without deposition of a preliminary mercury film is described. The deposition time, scan rate, rotation speed and molarity of the sulfuric solution have been studied; the method is applied to the determination of silver in uranium and plutonium.

La voltammétrie à redissolution anodique (a.s.v.) est universellement reconnue comme une méthode d'analyse de traces. L'électrode utilisée est dans la plupart des cas l'électrode à goutte de mercure périodiquement renouvelée, le mercure formant un amalgame avec de nombreux métaux. Depuis quelques années, certains auteurs [1—4] utilisent une électrode de carbone vitreux ou de graphite recouverte d'un film de mercure, ce type d'électrode offrant une sensibilité accrue et une meilleure résolution. L'utilisation d'un film de mercure, par son oxydation, présente l'inconvénient de limiter le domaine d'exploration en potentiel et pratiquement, toutes les réactions électrochimiques dont le potentiel correspondant est supérieur à + 0,3 V/ECS ne peuvent être étudiées. Ceci explique dans bien des cas [5—11] l'utilisation directe d'une électrode de carbone vitreux, sans dépôt préalable d'un film de mercure. Dans notre cas, où nous avions à doser des traces d'argent dans les matériaux nucléaires uranium et plutonium, nous avons choisi cette méthode qui semblait bien adaptée par sa sensibilité et les moyens mis en oeuvre, après en avoir étudié les principaux paramètres expérimentaux.

PARTIE EXPÉRIMENTALE

Appareillage

Tous les essais ont été réalisés avec un polarographe Metrohm E261 à une température de 25±1°C. L'électrode de référence est une électrode à sulfate de potassium saturée (ESS) (K 6112 Radiometer).

L'électrode en carbone vitreux (Le Carbone Lorraine France, qualité V25) est préparée en découpant un disque d'épaisseur égale à 1 cm et en le scellant à l'intérieur et à l'extrémité d'un tube en verre pyrex, la surface du disque arasant le verre. Le contact électrique est assuré par un fil de platine plongeant dans du mercure préalablement versé au fond du tube et assurant la jonction électrique avec le carbone. La surface de l'électrode est d'abord polie avec du papier abrasif au carbure de silicium, puis avec de la pâte diamant ("DPS"; Struers, Copenhague, Danemark) en utilisant des grains de 15 μm pour terminer à 1 μm jusqu'à obtention d'un "poli miroir".

La rotation de l'électrode est assurée par un agitateur à variateur mécanique (Prolabo 0825112 France) permettant d'atteindre une vitesse ω maximale de 2000 r.p.m.

Tous les potentiels sont mesurés et donnés par rapport à ESS (ESS = + 0,650 V/EHN et ECS = + 0,246 V/EHN).

Réactifs

Les acides utilisés sont des produits supra-purs Merck. L'eau après permutation sur résines est bidistillée dans un appareillage en quartz. Les solutions d'Ag ont été préparées à partir d'un métal pur (Johnson Matthey, Londres). Les solutions dont la concentration est inférieure à 10^{-3} M sont fraîchement préparées. Les métaux U et Pu qui ont servi pour les solutions de synthèse ont été choisis après contrôle par spectrométrie de masse à étincelles, de telle façon que leur teneur en Ag soit inférieure à 0,05 p.p.m.

Mode opératoire

Tous les essais ont été effectués avec des solutions en milieu nitrique ou sulfurique. L'Ag est déposé pendant un temps t après polarisation de l'électrode sous un potentiel E_p de −0,750 V. Après une période de 20 s pour ajuster le potentiel à −1 V, le balayage en potentiel est alors effectué jusqu'à +1 V. Le courant i considéré est celui qui correspond au maximum du pic dont la hauteur est déterminée suivant la méthode de Barendrecht [13]. Le potentiel apparent correspondant au maximum est d'environ 0 V.

Pour une analyse d'U ou de Pu (dans le cas du Pu, toutes les opérations sont effectuées dans une boîte à gants sous balayage d'azote) l'échantillon après décapage sulfurique, lavage à l'eau et séchage, est pesé, et mis en solution par l'acide sulfurique concentré. Après évaporation à sec, le résidu refroidi est dissout en milieu sulfurique 0,1 N et l'enfiolage est réalisé de façon à obtenir une solution ayant une concentration d'environ 10 gl^{-1} en U

ou Pu. Une aliquote de cette solution (25 ml) est placée dans la cellule de mesure pour analyse suivant le processus noté plus haut. La teneur en Ag est calculée après extrapolation du signal de redissolution sur une droite d'étalonnage préalablement établie dans les mêmes conditions opératoires.

RÉSULTATS ET DISCUSSION

Influence du temps de préélectrolyse

Les essais ont été réalisés en milieu nitrique et sulfurique 0,1 N pour des valeurs de t allant de 1—18 min, avec les conditions suivantes: électrode stationnaire, E_p = —0,750 V; vitesse de balayage en potential, v = 2 V min^{-1}; diamètre de l'électrode, d = 5,3 mm; C_{Ag} = 0,2 μg ml^{-1} . Les résultats du Tableau 1 montrent qu'il n'y a pas proportionalité entre i et t et que le produit $i\,t^{-1}$ décroit en fonction de t. On remarque, d'autre part, une sensibilité légèrement supérieure en milieu sulfurique.

Influence de la vitesse de balayage en potentiel

Les essais ont été réalisés en milieu nitrique et sulfurique 0,1 N pour des valeurs de v allant de 0,17—2 V min^{-1}, avec les conditions suivantes: électrode stationnaire, E_p = —0,750 V, t = 3 min, d = 5,3 mm, 0,1 μg Ag ml^{-1}. Les résultats mettent en évidence une relation linéaire entre i et $v^{1/2}$ dans le domaine étudié, ce qui vérifié l'équation: $i = kn^{3/2}\,S\,C\,(D\,v)^{1/2}$ avec k = constante, S = surface de l'électrode, D = coefficient de diffusion de l'ion considéré dans le milieu, n = nombre d'électrons mis en jeu.

Influence de la vitesse de rotation de l'électrode (ω)

Les essais ont été réalisés en milieu nitrique et sulfurique 0,1 N pour des valeurs de ω comprises entre 400 et 2000 r.p.m., avec les conditions suivantes: E_p = —0,750 V, t = 1 min, d = 3,2 mm, 1 μg Ag ml^{-1} , v = 2 V min^{-1}. Les résultats montrent que i croit linéairement en fonction de $\omega^{1/2}$, ce qui vérifie le critère de Levich que l'on peut exprimer par la relation: $i = K\,\omega^{1/2}$ avec K une constante. Dans les deux milieux considérés, K est égal à environ 30 nA (r.p.m.)$^{-1/2}$.

TABLEAU 1

Variation du courant de redissolution en fonction du temps de préélectrolyse

t (min)	1	3	6	9	12	15	18
i (μA) (HNO_3 0,1 N)	0,28	0,75	1,20	1,56	1,80	2,08	2,36
$i\,t^{-1}$ (μA min^{-1})	0,28	0,25	0,20	0,17	0,15	0,14	0,13
i (μA) (H_2SO_4 0,1 N)	0,33	0,78	1,32	1,78	2,10	2,38	2,66
$i\,t^{-1}$ (μA min^{-1})	0,33	0,26	0,22	0,20	0,18	0,16	0,15

Influence de la normalité du milieu

Les essais ont été réalisés en milieu sulfurique pour des normalités allant de 0,07 — 3,6 N, avec les conditions suivantes: E_p = —0,75 V, t = 1 min, d = 3,2 mm, v = 2 V min^{-1}, 1 μg Ag ml^{-1}, ω = 2000 r.p.m. Les résultats indiquent une chute de sensibilité pour des normalités supérieures à 1 N et l'on remarque une déformation des pics pour les normalités supérieures à 2 N.

D'autre part, quelques essais en milieu nitrique nous montrent que les pics de redissolution sont plus larges qu'en milieu sulfurique, pour une même normalité. Ces constations, identiques à celles d'autres auteurs [9] nous ont conduit à choisir le milieu sulfurique 0,1 N.

Application au dosage de Ag dans U et Pu

Des étalonnages ont été réalisés en présence des matrices U et Pu pour des concentrations en Ag comprises entre 0,01 et 0,15 μg ml^{-1} et une concentration en matrice de 10 g l^{-1}. Tous les essais ont été réalisés en milieu sulfurique 0,2 N, avec les conditions suivantes: E_p = —0,9 V, t = 20 min, d = 3,2 mm, v = 2 V min^{-1}, ω = 2000 r.p.m.

Les droites obtenues (Fig. 1) confirment la validité de la méthode en présence des matrices où nous avions à doser Ag dans cette gamme de concentration. Nous observons une sensibilité accrue en absence de matrice. Par contre, la présence d'une matrice U ou Pu n'a pas d'influence significative sur la pente et l'écart observé sur la Fig. 1 est dû à l'utilisation pour chaque étalonnage d'une électrode différente et par conséquent d'une "surface active" différente.

L'ensemble des résultats obtenus nous montre l'avantage de l'électrode tournante sur une électrode stationnaire, qui ne permet pas, comme le signalent Petăk et Vydra [9], d'obtenir une linéarité et une aussi bonne reproductibilité.

Des analyses comparatives ont été effectuées en utilisant la spectrophotométrie d'absorption atomique, et les résultats mentionnés dans le Tableau 2 indiquent une bonne concordance (chaque résultat pour une même référence d'échantillon est relatif à une nouvelle mise en solution).

Reproductibilité de la méthode

Dix essais ont été effectués sur 2 solutions exemptes de matrice, ayant des concentrations de 0,1 et 2 μg Ag ml^{-1}, en utilisant les conditions suivantes: E_p = —0,750 V, ω = 2000 r.p.m., v = 1 V min^{-1}, t = 3 min; milieu H_2SO_4 0,1 N, d = 5,3 mm pour 0,1 μg Ag ml^{-1}, d = 3,2 mm pour 2 μg Ag ml^{-1}. Les resultats du Tableau 3 nous montrent que l'écart type moyen relatif n'excède pas 2%.

Des essais complémentaires portant sur 8 mesures ont été effectués en présence des matrices U et Pu avec une concentration 0,01 μg Ag ml^{-1} et une concentration en matrice de 10 g l^{-1}. Les conditions expérimentales sont les suivantes: milieu H_2SO_4 0,2 N, E_p = —0,750 V, ω = 2000 r.p.m., v = 2 V min^{-1}, d = 3,2 mm, t = 25 min.

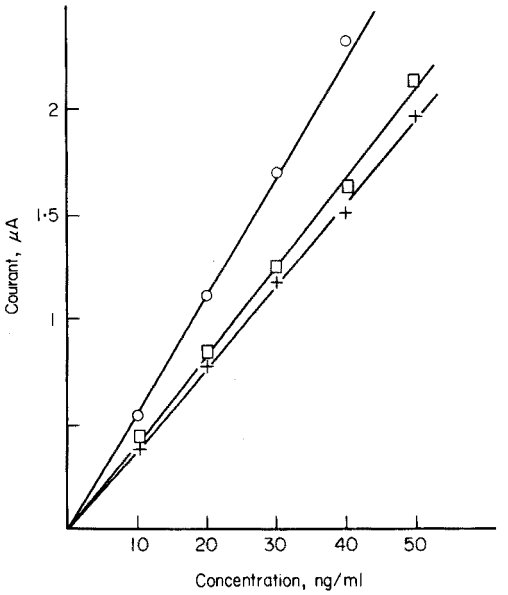

Fig. 1. Courant de redissolution en fonction de la concentration en argent: ○ argent seul, □ argent en présence d'uranium à 10 g l^{-1}. + argent en présence de plutonium à 10 g l^{-1}.

Pour les matrices U et Pu, nous obtenons respectivement un courant *i* moyen de 0,62 et 0,64 μA et un écart-type moyen relatif de 1,7 et 4,7%. La dispersion plus importante dans le cas du Pu est inhérente au travail en boîte à gants où la précision des manipulations est moins bonne. En ce qui concerne la matrice U, nous ne notons pas une influence sur la reproductibilité de la méthode.

TABLEAU 2

Analyses comparatives par spectrophotométrie d'absorption atomique

Référence échantillon	Matrice	Résultat (p.p.m.) A.s.v.	A.a.s.
1	U	0,2	< 1
2	U	0,08	< 1
3	U	1,3	1,1
4	U	3,6—3,1	3,6
5	U	25—28—29	26—27—28
6	Pu	1,1	1,0

TABLEAU 3

Reproductibilité du courant de redissolution pour 10 mesures

Ag (μg ml^{-1})	0,1	2
i moyen (μA) (N = 10)	2,06	6,95
Ecart-type moyen	0,042	0,055
Ecart-type moyen relatif (%)	2,0	0,8

Interférences

Les interférences éventuelles dans les milieux étudiés sont le mercure, l'or et les chlorures. L'interférence du mercure n'a pas été étudiée, cet élément n'étant jamais présent dans U ou Pu à des niveaux supérieurs à 0,05 p.p.m. L'une des solutions possibles serait le cas échéant, comme le signalent certains auteurs [12], de séparer le mercure en chauffant à 500°C environ le résidu obtenu après mise en solution et évaporation.

L'or n'est pas gênant dans la mesure où sa concentration n'excède pas celle de l'argent d'un facteur 5, ce qui est pratiquement toujours le cas. Dans ces conditions, le dosage simultané des deux éléments est possible.

L'"interférence" des chlorures a été plus particulièrement étudiée à cause des risques de pollution en boîte à gants, et par suite, d'une précipitation de chlorure d'argent. Nous avons noté dans le Tableau 4, les valeurs de i pour 1 μg Ag ml^{-1} ($9{,}25 \cdot 10^{-6}$ M) et pour des ajouts de $4 \cdot 10^{-7}$ à $4 \cdot 10^{-6}$ M. Les essais ont été réalisés en milieu sulfurique 0,2 N avec les conditions suivantes: E_p = —0,75 V, ω = 2000 r.p.m., v = 2 V min^{-1}, d = 3,2 mm, t = 1 min.

Pour les concentrations en chlorures inférieures à $1{,}4 \cdot 10^{-6}$ M, i reste constant et reproductible. Par contre, au delà de cette valeur, i n'est plus reproductible et croît au fur et à mesure des essais par suite d'une accumulation en chlorure d'argent sur la surface de l'électrode. A noter que le produit des concentrations en ions argent et chlorures correspondant à l'apparition de l'interférence est de $1{,}34 \cdot 10^{-11}$, valeur nettement inférieure au produit de solubilité de AgCl à 25°C, soit $1{,}56 \cdot 10^{-10}$. Ce phénomène s'explique par une augmentation de C_{Ag} au niveau de l'électrode, lors de la période de préélectrolyse, ce qui entraîne une précipitation de AgCl sur la surface de l'électrode.

TABLEAU 4

Influence de la concentration en chlorures sur le courant de redissolution, C = 1 μg ml^{-1}

Concentration en chlorures (10^{-6} M)	0,4—0,6—0,8—1—1,2—1,4—1,6	2	2,4	3	3,5	4
Courant, i (μA)						
1er essai	1,44	1,56	2,22	2,70	3,36	3,90
2e essai	1,44	1,68	2,36	2,90	3,54	4.20
3e essai		1,80			3,68	

BIBLIOGRAPHIE

1 T. M. Florence, J. Electroanal. Chem., 27 (1970) 273.
2 W. Lund et M. Salberg, Anal. Chim. Acta, 76 (1975) 131.
3 D. N. Hume et J. N. Carter, Chem. Anal. (Warsaw), 17 (1972) 747.
4 A. H. Miguel et C. M. Jankowski, Anal. Chem., 46 (1974) 1832.
5 F. Vydra et P. Petăk, J. Electroanal. Chem., 24 (1970) 379.
6 M. Kopanica et F. Vydra, J. Electroanal. Chem., 31 (1971) 175.
7 H. E. Zittel et F. J. Miller, Anal. Chem., 37 (1965) 200.
8 A. M. Bond, T. A. O'Donnell et R. J. Taylor, Anal. Chem., 46 (1974) 1063.
9 P. Petăk et F. Vydra, Anal. Chim. Acta, 65 (1973) 171.
10 V. Eisner et H. B. Mark, J. Electroanal. Chem, 24 (1970) 345.
11 D. C. Johnson et R. E. Allen, Talanta, 20 (1973) 305.
12 E. Temmerman et F. Verbeek, Anal. Chim. Acta, 58 (1972) 263.
13 E. Barendrecht dans A. J. Bard (Ed.), Electroanalytical Chemistry, Vol. 2, M. Dekker, New York, 1967, p. 94, Fig. 16 (b).

Analytica Chimica Acta, 93 (1977) 191—201
© Elsevier Scientific Publishing Company, Amsterdam — Printed in The Netherlands

POLYURETHANE—PYRIDYLAZONAPHTHOL FOAMS IN THE PRECONCENTRATION AND SEPARATION OF TRACE ELEMENTS

T. BRAUN*, A.B. FARAG† and M. P. MALONEY**

Institute of Inorganic and Analytical Chemistry, L. Eötvös University, P. O. Box 123,1443 Budapest (Hungary)

(Received 14th April 1977)

SUMMARY

The feasibility of using PAN—polyether and polyester polyurethane foams in batch and column operations has been examined. The effects of pH, plasticizer and various anions present in the aqueous solution on the extraction behaviour of cobalt, iron and manganese have been investigated. In dynamic systems, the effect of flow rate on the extraction efficiencies of these metal ions has been investigated. The uptake of cobalt(III) and manganese(II) on PAN—polyester foam columns is quantitative at flow rates up to 10 ml min^{-1} and 2 ml min^{-1}, respectively. The retention of iron(III) by the foam column is not quantitative even at a flow rate of 1 ml min^{-1}. Preconcentration of cobalt and its separation from various concentrations of manganese are successful..

Considerable attention has been directed in recent years to the use of cellular and foamed plastics after special treatment with a suitable reagent for simple and rapid separation and preconcentration processes [1]. The advantages of using chelating agents supported on polyurethane foam have been emphasized [2—4]. In general, chelating agents immobilized on polyurethane foam have potential for separations owing to the homogeneous distribution of the organic reagent on the relatively high surface area of the foam which allows reasonable, adequate contact between the metal ion in solution and the chelating agent on the foam. This was proved by the fast, quantitative collection of very small amounts of metal ion in high volumes of aqueous solution on reagent foams by means of batch or column techniques. The reagents studied include dithizone [2, 3, 5], 1-nitroso-2-naphthol [4], diethylammoniumdiethyldithiocarbamate [3] and dimethylglyoxime [6].

Since the observation by Liu [7] in 1951, that PAN (1-(2-pyridylazo-2-naphthol)) forms chelates with many heavy metals, this reagent and its analogues have found extensive use in analytical work [8]. The stability of PAN, its low solubility in water (over pH 2—11), and its ability to react with a large number of metals all suggest that it may have a promising role if it is immobilized on polyurethane foam in a new reagent foam system.

†Present address: National Research Centre, Dokki, Cairo, Egypt.
**Present address: Chemistry Department, University of Wales Institute of Science and Technology, Cardiff, Wales.

The aim of the present study was to assess the performance of PAN as a foam-supported reagent and to determine which parameters were of greatest importance. The extraction of cobalt, iron and manganese was investigated for this purpose.

EXPERIMENTAL

Reagents and materials

Except where otherwise mentioned, all chemicals used were of analytical-reagent grade. α-Dinonyl phthalate (phthalic acid di-3,5,5-trimethylhexylester pure grade) was used without further purification. The polyurethane foam was a polyether of open-cell type (Greiner K.G.Schaumstoffwerk-Kremsmunster, Austria). Open-cell polyester polyurethane foam (PPI-80 nFR) was supplied by Eurofoam (9200 Wetteren, Belgium).

Polyether polyurethane foam was cut into small pieces of less than 5 mm edge, soaked in 2 M hydrochloric acid, washed with distilled water and acetone and then dried in an oven at 80°C. An identical procedure was applied for the polyester foam except that 0.2 M hydrochloric acid was used instead of 2 M to prevent hydrolysis.

PAN solution was prepared by dissolving 1 g of the reagent in 100 ml of α-dinonyl phthalate. This solution was used to prepare [2] plasticized PAN—polyether and polyester foams, which contained 55% and 35% (w/w) of the PAN solution, respectively. For lower PAN loadings, the solution was diluted before use.

Unplasticized PAN—polyether and polyester foams were prepared by dissolving a suitable amount of PAN in acetone, stirring the foam into the solution and evaporating off the acetone.

Stock cobalt(II), iron(III) and manganese(II) solutions (about 10 mg ml^{-1}) were prepared from analytical-grade cobalt(II) chloride, iron(III) chloride and manganese(II) sulphate, respectively. All solutions were standardized by conventional methods [9]. Solutions containing microgram amounts of cobalt, iron or manganese were prepared by diluting the stock solution of these elements with water. A little hydroxylammonium chloride solution was added to all manganese solutions to keep them as manganese(II). Cobalt, iron and manganese solutions were then spiked with radioactive cobalt-58, iron-59 and manganese-54, respectively, and radiometric detection method used in all the subsequent experiments.

Instrumentation

For activity measurements, an NaI(Tl) well-crystal and an energy-selective counting device (type NK-107/B, Gamma, Budapest) were employed.

Methods

Effect of pH. To each of a number of 100-ml flasks were added 0.1 g of plasticized PAN—polyether foam (containing 0.55% PAN by weight), and

10 ml of aqueous solution containing 0.2 μg of cobalt, or 2 μg of iron or manganese. The pH of the aqueous solution was adjusted to various values with hydrochloric acid and potassium hydroxide solutions. Extraction was done by shaking for 2 h in a mechanical shaker. The pH of the aqueous solution was checked again, the radioactivity of a 2-ml sample was measured and the percentage extraction calculated.

Effect of various anions on the extraction efficiency. The effect of 23 anions was examined. In each case 10 ml of 0.1 M potassium bromide solution containing 0.2 μg of cobalt, 2 μg of iron or 2 μg of manganese was shaken with 0.1 g of plasticized PAN—polyether foam (0.55% PAN, w/w) for 2 h. For each metal ion, the pH of the aqueous solution was fixed at the optimal value before extraction. The final activity of the aqueous solution was compared with the initial value and the percentage extraction calculated.

Kinetic studies. To study the effect of plasticizer on the foam and anion in the aqueous solution, 0.1 g of PAN-loaded foam (plasticized or unplasticized) and 8 ml of aqueous solution, adjusted to the optimum pH for the metal ion under investigation, were shaken for 10 min to wet the foam. Then 2 ml of the spiked metal ion solution were added to each flask and the shaking continued. Samples were taken at 1, 3, 5, 10, 20, 40 and 60 min after addition of the spiked solution for radioactivity counting.

Absorption isotherm and capacity measurements. A series of flasks containing 0.1 g of PAN-foam (0.55% PAN, w/w) and 20 ml of 0.125 M sodium bromide solution, containing various amounts of spiked cobalt, were shaken for 2 h and the amount extracted was determined. Plasticized and unplasticized PAN—polyether foams were used.

Distribution ratios. These were determined for 2 μg of the element in 10 ml of aqueous solution, adjusted to the optimum pH for extraction, and 0.1 g of PAN-foam containing different amounts of PAN. After equilibration for 6 h at room temperature in a mechanical shaker, the activity of the solution was measured, and the percentage extraction calculated. The distribution ratios were calculated from

$$D = \frac{\text{amount of element on foam}}{\text{amount of element in solution}} \cdot \frac{\text{ml of solution}}{\text{g of PAN-foam}}$$

Flow experiments. PAN-foam (5 g) was packed into glass columns of diameter 2.5 cm, by the vacuum packing technique [10]. The effects of flow-rate, presence or absence of plasticizer, and metal ion concentration on the recovery of metal ions from aqueous solution were investigated. Also some separations were tried.

RESULTS AND DISCUSSION

PAN is an extremely sensitive and comparatively selective reagent that can be used for the extraction and determination of microgram amounts of various heavy metals. Generally, extraction with PAN is controlled by

adjusting the pH of the aqueous solution and/or by adding inorganic or organic salts to the aqueous phase.

In the present work on PAN-foam, the dependence of extraction of cobalt, iron and manganese on the pH of the aqueous solution, the effect of different anions and the role of other parameters on the extraction process were investigated.

Effect of pH on the extraction efficiency of cobalt, iron and manganese with plasticized PAN-foam

The pH of the aqueous solution was adjusted with dilute hydrochloric acid and sodium hydroxide, to eliminate any probable effect of buffers on the retention of the metal ions. The curves of Fig. 1 show the percentage of metal ion extracted as a function of pH. As can be seen, the collection of cobalt and iron is quite complete from aqueous solutions of pH 4—9. However, manganese is completely extracted only above pH 9; below pH 6 the extraction of manganese is negligible. Generally, these results are in good agreement with those reported [11—13] for the liquid—liquid extraction technique.

Effect of various anions on the extraction of cobalt, iron and manganese with plasticized PAN-foam

Cobalt(II) is known to form a red-coloured complex with PAN, which changes to the greyish-green cobalt(III) complex in contact with air [11]. The metal to PAN ratio in the PAN chelates of cobalt(III), iron(III) and manganese(II) is 1:2 [11, 14], i.e. cationic cobalt(III)— and iron(III)—PAN complexes and an electrically neutral manganese(II)—PAN chelate are formed. Obviously, the cobalt and iron—PAN chelates will form ion association complexes with an anion to yield species extractable by PAN-foam. However, the electrically neutral manganese—PAN complex can be extracted directly with the plasticized PAN-foam.

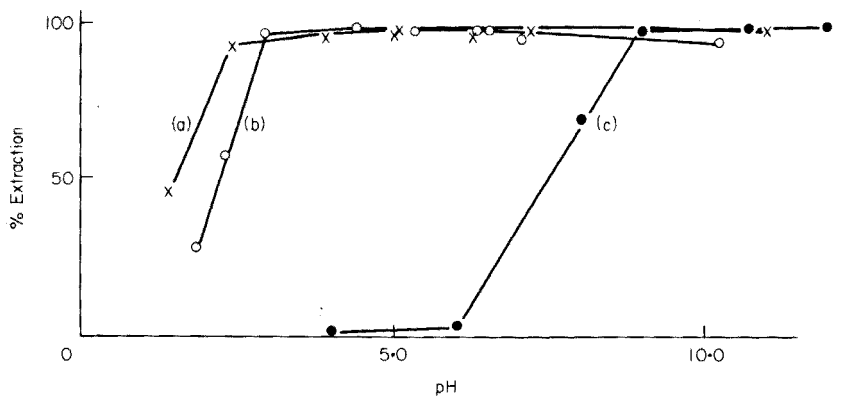

Fig. 1. Extraction of cobalt, iron and manganese as a function of pH. (a) Iron. (b) Cobalt. (c) Manganese.

Because the presence of anions in the aqueous solution can affect the extractions, the effects of 23 anions were studied. The aqueous solution containing cobalt, iron or manganese was adjusted to the optimum pH for extraction of each metal ion (cf. Fig. 1). Table 1 shows that cyanide, peroxide, periodate and citrate mask quite strongly the three metal ions. Borate, fluoride, phosphate and tartrate mask iron more than cobalt, but have no effect on manganese. The complete extraction of cobalt in the presence of thiocyanate is interesting, for thiocyanate has been reported [11] to mask the green colour of the cobalt(III) complex.

The anions which gave the highest percentage extraction were studied in more detail for each metal ion. A series of kinetic experiments was carried out for the extraction of cobalt from aqueous 0.1 M solutions of thiocyanate, oxalate, phthalate, bromide, iodide and nitrate. In this set of experiments PAN—polyether polyurethane foam was used.

Figure 2 shows that the rate of extraction of cobalt from the above-mentioned aqueous solutions decreases in the order thiocyanate > oxalate, phthalate > iodide > bromide, nitrate. In a parallel experiment, the extraction of cobalt from aqueous solutions containing these different anions onto unloaded polyether polyurethane foam (i.e. without PAN) was determined under identical conditions. The extraction of cobalt by the unloaded foam was quite negligible from all these solutions, except from thiocyanate solution in which the extraction was highly significant. The extraction observed with PAN—polyethe foam from thiocyanate medium can be attributed to the interaction of the thiocyanate complex of cobalt with the polyether foam itself. In this connection Bowen [15] has reported that polyether-type polyurethane foam extracts thiocyanate complexes. To eliminate this factor, while keeping the cobalt thiocyanate—PAN-foam system, PAN—polyester polyurethane foam

TABLE 1

Effect of various salts (0.1 M) on the extraction of cobalt, iron and manganese with PAN—foam

Salts	% Extraction			Salts	% Extraction		
	Co	Fe	Mn		Co	Fe	Mn
NH_4-oxalate	98.0	98.7	98.6	Na-acetate	85.8	97.3	97.5
KSCN	98.6	98.3	97.3	$KBrO_3$	93.7	99.7	99.4
KH-phthalate	99.2	94.6	98.1	Na_2SO_4	70.5	99.5	98.8
NaBr	98.0	98.5	98.6	$(NH_4)_2SO_4$	58.6	99.2	98.9
NaI	99.0	100.0	99.1	Na_2HPO_4	56.5	16.4	100.0
$NaNO_3$	98.8	99.0	98.9	KIO_3	70.2	97.1	98.5
KCl	94.4	99.2	98.4	KH-tartrate	86.2	22.0	96.1
NaCl	95.2	99.6	99.0	$NaIO_4$[a]	10.0	42.9	0.0
NH_4Cl	94.7	97.8	98.7	H_2O_2(1%)	52.5	7.3	—
$Na_2S_2O_3$	94.6	99.3	99.1	Citric acid	18.9	72.4	81.6
H_3BO_3	90.6	15.4	98.5	KCN	1.2	25.3	21.3
NaF	89.8	31.6	96.2	H_2O	30.0	99.2	99.2

[a]Saturated solution.

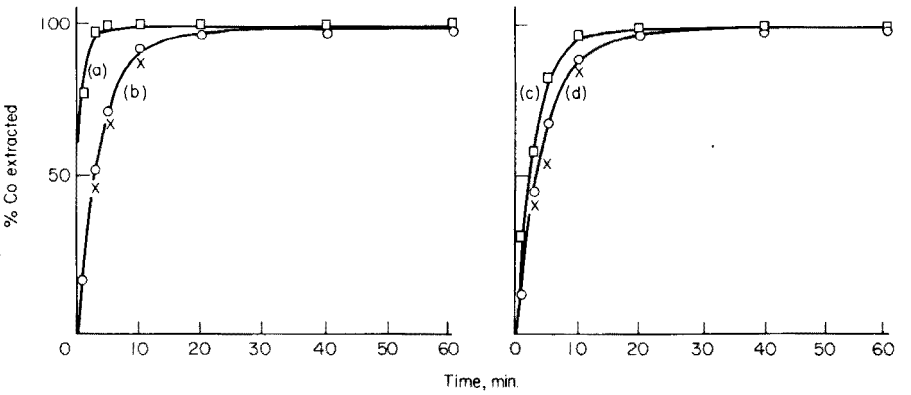

Fig. 2. Rate of extraction of cobalt from various anion solutions (pH 5) onto plasticized PAN—polyether foam. (a) Potassium thiocyanate. (b) Potassium hydrogenphthalate, ammonium oxalate. (c) Sodium iodide. (d) Sodium bromide, sodium nitrate.

was employed, as cobalt is not extracted by the unloaded polyester foam from thiocyanate medium. Figure 3 shows the extraction rate curve of cobalt on to PAN—polyester foam from thiocyanate solution.

Although the extraction rate on PAN—polyester foam is slower than that on PAN—polyether foam, the extraction of cobalt from this thiocyanate solution is still higher than from oxalate, phthalate, iodide, bromide or nitrate solutions; thus the thiocyanate ion promotes the extraction of cobalt onto PAN—foam. However, the extraction of iron(III) onto PAN—polyester foam is affected by the presence of any of the anions examined. The highest extraction rate is obtained from water. More or less complete extraction is attained after shaking for about 20 min. These results disagree with those reported [11] for a liquid—liquid extraction system with chloroform. As expected, anions which do not mask manganese(II) do not affect its extraction rate on PAN—polyester foam. The extraction rate for manganese with PAN-foam is slower than that for cobalt, but it is still slightly better than that for iron (Fig. 3).

Effect of plasticizer on the extraction rate and isotherm of cobalt on PAN-foam

Since cobalt is not extracted from aqueous bromide solution with unloaded polyether polyurethane foam, PAN—polyether foam could be used in studying the effect of plasticizer on the extraction rate of cobalt in that medium. The rate of extraction of 0.2 μg of cobalt from 0.1 M sodium bromide solution (10 ml) onto plasticized and unplasticized 0.35% (w/w) PAN—polyether foam is presented in Fig. 4. The curves indicate that the rate of extraction for cobalt on the plasticized foam is slightly better. Further, the extraction isotherms (Fig. 5) show that the plasticized PAN—foam is slightly superior to the unplasticized one. This can be explained by the fact that the permeability of the plasticized foam is better than that of the unplasticized one [2, 3].

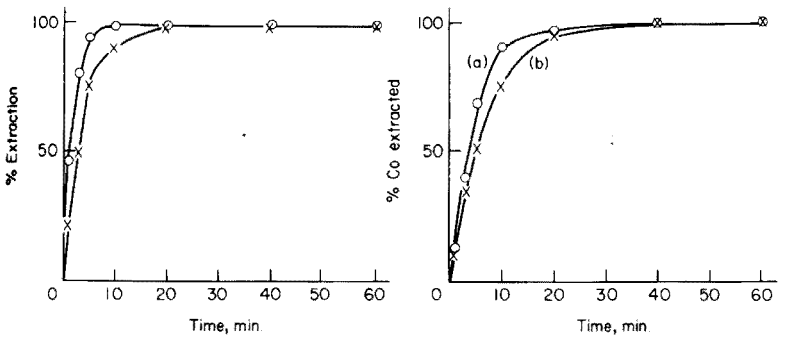

Fig. 3. Rate of extraction onto plasticized PAN–polyester foam. (○) Extraction of cobalt from 0.1 M thiocyanate solution (pH 5). (×) Extraction of manganese from aqueous solution (pH 10).

Fig. 4. Rate of extraction of cobalt from 0.1 M sodium bromide solution (pH 5) onto plasticized PAN–polyether foam. (a) Plasticized. (b) Unplasticized.

The capacities of the plasticized and unplasticized PAN-foams were determined by batch experiments. From the capacity, the complex was calculated to have a cobalt:PAN ratio of 1:2, which agrees with the theoretical capacity of the PAN-foam used and the composition of the complex reported [11]. This was further confirmed by plotting the logarithm of the distribution ratio of cobalt, iron and manganese vs. the logarithm of the PAN concentration on the foam (Fig. 6). Generally, the three curves are linear with slopes of 2.

Recovery of cobalt from plasticized and unplasticized PAN-foams was tested with 20 ml of acetic acid, citric acid, hydrochloric acid, EDTA or potassium cyanide solution. The results were very poor, particularly in the case of potassium cyanide. This is surprising because cyanide completely masks the extraction of cobalt by PAN-foam. The first three solutions were quite acidic and showed slightly higher recoveries. It may be that kinetic factors influence the recovery unfavourably although the flasks were shaken for 2 h before sampling.

Column experiments

Preliminary experiments on the extraction of cobalt with PAN-foam columns offered some interesting features. Initially, bromide solution was used but this gave poor recoveries even at flow rates of 5 ml min^{-1}. Subsequent experiments were therefore done with 0.2 M potassium thiocyanate solution and PAN-polyester foam columns containing 5 g of loaded foam. Table 2 shows the effect of flow-rate on the extraction of 2 μg of cobalt on to plasticized and unplasticized columns. Both types give more or less quantitative recovery up to flow rates of 10 ml min^{-1}, but higher flow rates decrease their efficiency. The plasticized foam columns are usually slightly better.

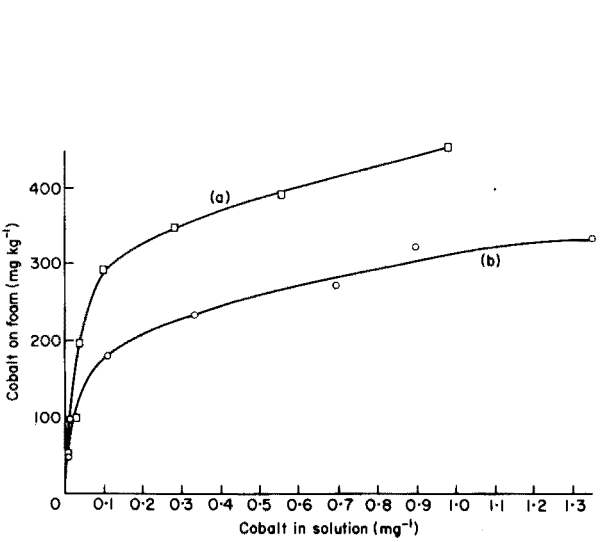

Fig. 5. Absorption isotherms of cobalt from 0.1 M aqueous sodium bromide solution (pH 5) on plasticized and unplasticized PAN—polyether foam. (a) Plasticized. (b) Unplasticized.

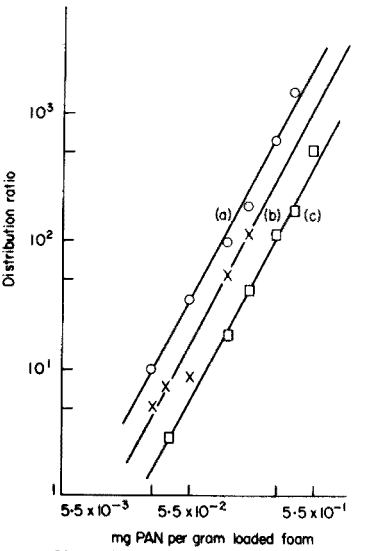

Fig. 6. Distribution ratios of cobalt, manganese and iron as a function of PAN concentration of the foam. (a) Cobalt. (b) Manganese. (c) Iron.

In contrast, 2 μg of cobalt in 0.2 M thiocyanate solution is retained quantitatively by plasticized and unplasticized PAN—polyether foam columns at flow rates up to at least 40 ml min^{-1}. This high efficiency of the polyether foam columns is clearly due to the proved extra interaction between the thiocyanate complex of cobalt and the polyether foam itself. A detailed study of the retention efficiency of unloaded polyether type polyurethane foam for various metal—thiocyanate complexes will be described elsewhere.

The uptake of various amounts of cobalt by plasticized and unplasticized PAN—polyester foam columns was investigated for flow rates of 8—10 ml min^{-1} and 5—7 ml min^{-1}, respectively. Both types of foam give satisfactory recoveries for carrier-free cobalt-58 solution and for solutions containing up to 200 μg of cobalt (Table 3). These results offer attractive possibilities for the application of PAN—polyester foam columns in preconcentration processes.

As a practical example, preconcentration of 0.5 μg of cobalt in 1 l of aqueous thiocyanate solution (0.2 M) was examined with plasticized and unplasticized PAN—polyester foam columns. The results were satisfactory (Table 4). In these experiments, 100 ml of acetone was applied at 3 ml min^{-1} for the recovery of cobalt from both types of column and was found to be more than enough. Obviously, PAN is completely leached from the column with this amount of acetone, and the remaining unloaded foam can be loaded again for further use.

The effect of flow rate on the extraction efficiency for 2 μg of manganese(II of iron(III) from aqueous solutions adjusted to pH 5 and 10, respectively, on

TABLE 2

Effect of flow rate on the uptake of 2 μg of cobalt or manganese on plasticized and unplasticized PAN—polyester polyurethane foam columns

Flow rate (ml min^{-1})	Average metal extracted ($\bar{X}$, %)	Relative accuracy of mean (%)	Standard deviation (s)	Confidence limit $\bar{X} \pm ts/n^{\frac{1}{2}}$, $t = 0.95$
Cobalt				
5	99.6[a]	−0.4	0.123	99.6 ± 0.2
	98.6[b]	−1.4	0.142	98.6 ± 0.2
10	98.8[a]	−1.2	0.464	98.8 ± 0.6
	96.7[b]	−3.3	0.562	96.7 ± 0.7
15	94.8[a]	−5.2	0.686	94.8 ± 0.9
	91.8[b]	−8.2	0.710	91.8 ± 0.9
20	92.1[a]	−7.9	0.387	92.1 ± 1.1
	86.4[b]	−13.6	2.690	86.4 ± 3.3
Manganese				
1	98.4[a]	−1.6	0.254	98.4 ± 0.3
3	96.4[a]	−3.6	0.591	96.4 ± 0.7
5	89.1[a]	−10.9	0.695	89.1 ± 0.9

[a]Plasticized. [b]Unplasticized.

to PAN—polyester foam columns was also investigated. Satisfactory recovery of manganese by the PAN-foam columns was obtained only at flow rates up to 3 ml min^{-1} (Table 2). For iron(III), however, the extraction is not quantitative even at flow rates as low as 1 ml min^{-1}, probably because of kinetic factors. This result was not unexpected because extraction of iron is slower than that of cobalt or manganese.

Collection of various concentrations of manganese(II) on PAN—polyester foam columns was examined at a flow rate of 1 ml min^{-1}. Table 3 shows complete recovery of 0.2—200 μg of manganese.

Obviously, the separation of different metal ions with PAN-foam columns can offer the definite advantage of increased selectivity by pH control alone or in combination with masking agents. The differences in the rates of extraction of some metal ions may also be applicable for selective separations.

In the present study, the separation of cobalt from various concentrations of manganese affords a practical application of the pH approach. An aqueous 0.2 M thiocyanate solution containing manganese and cobalt in various ratios and adjusted to pH 4—5, was allowed to pass through a PAN—polyester foam column at a flow rate of 1—2 ml min^{-1}. Under such conditions, cobalt is quantitatively extracted on the foam while manganese moves with the solvent front. An aqueous 0.2 M thiocyanate solution adjusted to pH 4—5 was used

TABLE 3

Collection of various concentrations of cobalt or manganese on plasticized and unplasticized PAN—polyester polyurethane foam columns

Amount of metal taken (μg)	Average extracted ($\bar{X}$, %)	Relative accuracy of mean (%)	Standard deviation (s)	Confidence limit $\bar{X} \pm ts/n^{\frac{1}{2}}$, $t = 0.95$
Cobalt				
Carrier-free	98.6[a]	−1.4	0.235	98.6 ± 0.3
	98.7[b]	−1.3	0.497	98.7 ± 0.6
0.2	98.6[a]	−1.4	0.273	98.6 ± 0.4
	98.6[b]	−1.4	0.187	98.6 ± 0.2
2.0	98.8[a]	−1.2	0.464	98.8 ± 0.6
	98.6[b]	−1.4	0.141	98.6 ± 0.2
20.0	99.2[a]	−0.8	0.212	99.2 ± 0.2
	98.7[b]	−1.3	0.570	98.7 ± 0.7
200.0	95.8[a]	−4.2	1.868	95.8 ± 2.0
	97.1[b]	−2.9	0.540	97.1 ± 0.7
Manganese				
0.2	98.5[a]	−1.5	0.700	98.5 ± 0.4
2.0	98.4[a]	−1.6	0.510	98.4 ± 0.3
20.0	98.2[a]	−1.8	0.866	98.2 ± 0.5
200.0	96.7[a]	−3.3	1.520	96.7 ± 0.9

[a]Plasticized. [b]Unplasticized.

TABLE 4

Preconcentration of 0.5 μg Co l^{-1} on 5-g plasticized and unplasticized PAN—polyester polyurethane foam columns

Average Co extracted ($\bar{X}$%)	Relative accuracy of the mean (%)	Standard deviation (s)	Confidence limit $\bar{X} \pm ts/n^{\frac{1}{2}}$, $t = 0.95$
100.7[a]	+0.3	1.911	100.7 ± 2.3
98.7[b]	−1.3	1.594	98.7 ± 2.0

[a]Plasticized. [b]Unplasticized.

to remove manganese(II) ions. Acetone was then used for the elution of cobalt. The results (Table 5) show good separations, and suggest attractive possibilities for using PAN in different separation and preconcentration processes with the advantageous column technique.

TABLE 5

Separation of cobalt from various concentrations of manganese with PAN-foam columns

Ions separated (μg)		Co:Mn	% Mn in effluent	Average	%Co in effluent	Average
Co	Mn					
2	2	1:1	102.3		100.5	
			98.9	100.8	99.3	99.6
			101.1		98.9	
2	20	1:10	97.7		101.2	
			99.0	98.4	99.8	99.9
			98.5		98.7	
2	200	1:100	98.3		103.0	
			102.0	99.8	101.7	102.3
			99.1		102.3	
0.2	200	1:1000	96.2		99.8	
			95.9	96.4	102.9	101.0
			97.0		100.2	

REFERENCES

1 T. Braun and A. B. Farag, Talanta, 22 (1975) 699.
2 T. Braun and A. B. Farag, Anal. Chim. Acta, 69 (1974) 85.
3 T. Braun and A. B. Farag, Anal. Chim. Acta, 71, (1974) 133.
4 T. Braun and A. B. Farag, Anal. Chim. Acta, 76 (1975) 107.
5 A. Chow and D. Buksak, Can. J. Chem., 53 (1975) 1373.
6 A. Chow and D. G. Gregoire, Talanta, 22 (1975) 453.
7 J. C. I. Liu, Ph.D. Thesis, University of Illinois, 1951.
8 H. Flaschka and A. J. Barnard (Eds.), Chelates in Analytical Chemistry Vol. 4, Dekker, New York, 1972.
9 A. I. Vogel, Quantitative Inorganic Analysis, Longmans, London, 3rd edn., 1961.
10 T. Braun and A. B. Farag, Anal. Chim. Acta, 62 (1972) 476.
11 A. Galik and A. Vinourova, Anal. Chim. Acta, 46 (1969) 113.
12 S. Shibata, Anal. Chim. Acta, 23 (1960) 367.
13 S. Shibata, Anal. Chim. Acta, 25 (1961) 348.
14 D. Betteridge, Q. Fernando and H. Freiser, Anal. Chem., 35 (1963) 294.
15 H. J. M. Bowen, J. Chem. Soc. A, (1970) 1082.

Analytica Chimica Acta, 93 (1977) 203—210
©Elsevier Scientific Publishing Company, Amsterdam — Printed in The Netherlands

SYNTHESIS OPTIMIZATION AND THE PROPERTIES OF 8-HYDROXYQUINOLINE ION-EXCHANGE RESINS

F. VERNON* and K. M. NYO

Department of Chemistry and Applied Chemistry, University of Salford, Salford M5 4WT Lancashire (U.K.)

(Received 14th April 1977)

SUMMARY

The preparation of oxine-containing ion-exchange resins has been treated rigorously. The reactant ratios, nature of cure, degree of cross-linking and hydrophilicity have been evaluated in terms of metal capacity and kinetics of metal uptake. The preparation of a bead polymer with good physical properties is described; stability tests show that the gel polymers must never be allowed to dry, otherwise their advantageous properties are destroyed. Stability towards acids in re-cycling procedures is excellent in terms of metal capacity, but there is some loss in water regain which equates to a slower equilibration rate with constant use.

It is now over 20 years since Von Lillin [1] described a chelating ion-exchanger, produced by the copolymerization of resorcinol and 8-hydroxyquinoline (oxine) with formaldehyde; the resin was selective for heavy metals. Parrish [2] produced a resorcinol—oxine—formaldehyde resin with chelating properties similar to oxine itself. Pennington and Williams [3] made a resorcinol: oxine (1:1) resin with a copper capacity of 7.9 meq g^{-1} at pH 8; as the theoretical capacity is 7.6 meq g^{-1} for 1 : 1 complexes of copper ions and oxine groups, the high capacity may have resulted from copper adsorption within the resin after hydrolysis of copper salts at pH 8. Hale [4] suggested that steric factors may prevent the combination of a metal ion with more than one chelating group, so that only 1:1 complexes are formed. Vernon and Eccles [5] attempted to reproduce several resins but found very low capacities; although Pennington and Williams [3] had not given details of the polymerization technique, Parrish [6] pointed out that a resin cure (sealed container) produced a swollen resin gel of high capacity.

De Geiso et al. [7] prepared both acid- and base-catalyzed resorcinol—oxine—formaldehyde polymers; the acid-catalyzed versions, of low molecular weight, were soluble in dimethylformamide. They also studied the variation of capacity with cross-linking; but only one set of results showed a significant decrease in capacity for cross-linked polymers compared with a linear polymer. Parrish and Stevenson [8] produced oxine exchangers with high capacities; they attempted to show that the water regain depended upon original water content, molar ratios of resorcinol: oxine:formaldehyde, and

the curing temperature, but more than one parameter at a time was changed in the preparations. The results are therefore rather ambiguous but the theoretical capacity for copper was achieved. These authors [8] also pointed out that inadequate swelling is the reason for low capacities in this type of resin; a study of the kinetics of metal uptake correlated the equilibration rates (measured by $t_{\frac{1}{2}}$) with the water regain for a series of resins. Davies et al. [9] prepared oxine–resorcinol–formaldehyde resins incorporating sodium phenol sulphonate; the incorporation of ionic groups improved the rate of equilibration and they were probably the first authors to recognize that modification of resin hydrophilicity is possible independently of the chelating functional groups. However, such modification of an oxine–resorcinol resin is not necessary as the equilibration rate can be sufficiently fast if the correct preparative conditions are used. Parrish [10] said that oxine–resorcinol resins without sulphonic groups were unsatisfactory in the regeneration step and that the recovery of metals was not quantitative in the elution time allowed.

The purpose of this paper is to optimize the conditions for the preparation of oxine–resorcinol ion exchangers. The merits of open- against sealed-cure techniques are evaluated. The influences of changing the water content of the resin mix, varying the molar ratios of reactants, varying the degree of cross-linking and hydrophilicity of the resin are examined in terms of the capacity, kinetics, and physical toughness of the resin. The stability of the resin to acidic and basic eluants and to heat is also studied.

EXPERIMENTAL

Preparation of the resin mix

(a) 8-Hydroxyquinoline, G.P.R. grade, ground to a fine powder, was stirred into sodium hydroxide solution to give a suspension. Formalin (37% w/w formaldehyde solution) was added with stirring and warming on a water-bath until solution was effected; a predetermined quantity of water was then added.

(b) Resorcinol or cresols were added to sodium hydroxide solution and warmed until dissolved. This solution was added to the oxine–formaldehyde solution with stirring; a deep red solution resulted.

Curing of the resin, grinding and washing procedures

A resin mix, prepared as described above, was divided into two equal parts; one part was cured in an open beaker and the other in a sealed glass tube (3 × 25 cm) for 60 h at 100°C. After curing, the resins were crushed and soaked in water for at least 2 d to convert them to the fully swollen state. They were then sieved, the fraction passing 22-mesh but retained by 60-mesh was used for subsequent determinations. Before use, the resins were washed with water for several days until the supernatant solution remained colourless. They were then equilibrated with 4 M hydrochloric acid for at least 2 d and

washed with deionized water until the washings were chloride-free. To convert them to the neutral form, the resins were equilibrated with 0.1 M sodium acetate solution for 2 d and were finally washed thoroughly with deionized water. The final wash water was usually ca. pH 4.5.

1st Series

The molar ratios of oxine : resorcinol : formaldehyde were 1:1:2.5. Only the water content of each resin mix was varied, from 67% to 75%, by the addition of deionized water in (a). Three batches of resin were prepared, each being divided into 2 portions for dry-cure and sealed-cure techniques.

2nd Series

To study the effects of changing the cross-linking, 3 batches of resin were initially prepared with the cross-linking resorcinol gradually replaced, mole for mole, by *p*-cresol. The molar proportions of the mix were again 1:1:2.5 in terms of total phenols : oxine : formaldehyde. Three further batches were prepared with the concentrations of resorcinol and oxine held constant; part of the resorcinol was replaced by *m*-cresol. Through this set of resins the cross-linking *m*-cresol was gradually replaced by non-crosslinking *p*-cresol to give a set of resins of constant hydrophilicity and decreasing cross-linking. All resins in this series were cured by the sealed-tube method.

3rd Series

The resorcinol:oxine ratio was varied from 1:1 to 1:4 in four batches of resin. Although the total weight of water in each mix was constant, the percentage of water present increased from 67% (1:1 resorcinol : oxine resin) to 73% (1:4 resin).

Preparation of a bead resin

A bead resin was prepared by the method of Parrish [8]. Oxine (0.1 mol) was added to 47.5 ml of 2 M sodium hydroxide and stirred to give a yellow paste. Formaldehyde (0.25 mol, as 37% formalin) was added and stirred until a red solution was obtained; 10 ml of deionized water were added. A solution of resorcinol (0.1 mol) in 15 ml of 2 M sodium hydroxide was added to the oxine—formaldehyde solution. The mixture was heated on a water bath, with stirring, until a viscous solution was obtained. The resin mix was poured into 250 ml of liquid paraffin at 80°C and stirred sufficiently quickly to produce small droplets of aqueous phase. Stirring was continued for 4 h by which time the droplets had gelled to resin beads. The resin—paraffin mixture was then sealed and cured at 100°C for 60 h. The resin beads were filtered from the liquid paraffin, rinsed with chloroform, washed thoroughly with soap solution to remove all paraffin, then with water. The washing procedure previously described was then carried out.

Evaluation of resin properties

Water regain. The resin, which had been soaked in water for at least 2 d, was filtered under slightly reduced pressure, the filtration being continued for exactly 1 min after the disappearance of surface water. The resin was lightly pressed between 2 filter papers to remove surface moisture then transferred rapidly to a watch glass and the weight determined. After drying at 100°C for 48 h the dry weight was determined and the weight of water associated with 1 g of dry resin was calculated.

Equilibration rate. The procedure is basically as described previously [5]. An amount of fully swollen resin corresponding to 1 g of dry resin was equilibrated with 0.05 M copper sulphate solution containing sodium acetate–acetic acid buffer, pH 5.0. The amount of copper sulphate solution used, determined from total capacity studies, was that volume which contained an amount of copper equal to twice the capacity of the resin. Sets of equilibrations were carried out; the resin was removed by filtration at 5-min intervals for the first hour, then at 2-h intervals to 12 h. The final determinations had equilibration times of 24 and 48 h. From the graph of copper capacity against time, the time taken to occupy half of the resin sites ($t_{\frac{1}{2}}$) was found.

Metal capacities. The procedure for metal capacity determination has been given in previous work [5, 11, 12]. Acetate buffer (ca. 1 M) was used and the ion whose capacity was to be determined was 0.1 M. Capacities for copper, aluminium and iron(III) were determined at pH 5.0, 4.0, and 2.8, respectively. Aluminium was determined spectrophotometrically as the oxine complex. Copper and iron were determined by a.a.s.

Resin stability tests. Resin stability towards acids and bases was tested by leaving samples of the resin in contact with 4 M hydrochloric acid, 1 M sodium hydroxide and 1 M ammonia for 7 d.

Stability towards the metal uptake—elution cycle was tested by immersion in a buffer solution (pH 5) for 24 h, then eluting the copper with 2 M hydrochloric acid for 24 h. This cycle was repeated 10 times. The copper capacity and water regain of the resin were then determined.

The effect of drying the resin was studied by determining the copper capacity and water regain before and after drying a batch of resin (i) at 100°C for 48 h, (ii) at room temperature in air for 48 h.

RESULTS AND DISCUSSION

A comparison of open-cure and sealed-cure methods for identical resin mixes is given in Table 1. The sealed-cure technique gives a vastly superior product both in terms of metal total capacity and kinetics of metal uptake. Theoretical values for copper uptake, assuming that only 1:1 complexes are formed, are easily achieved. Table 1 also shows the effect of increasing the original water content of the sealed cure resin mix. The equilibration ratio and water regains are markedly effected by relatively small variations in

TABLE 1

Influence of (a) the curing method and (b) the water content of the resin mix on the properties of a 1:1:2.5 oxine : resorcinol : formaldehyde ion exchange resin

1st Series	Original water content of resin mix (%)	Water regain ($g\ g^{-1}$)	Equilibration rate ($t_{\frac{1}{2}}$)	Metal capacities[a] ($mmol\ g^{-1}$)		
				Cu(II)	Fe(III)	Al(III)
			pH	5.0	2.8	4.0
Batch 1						
Dry cure	67	0.67	6 h	0.70	0.04	0.32
Sealed cure		1.8	25 min	3.24	1.96	1.17
Batch 2						
Dry cure	70	0.70	5.5 h	1.40	0.06	0.33
Sealed cure		5.2	8.5 min	3.15	2.05	1.11
Batch 3						
Dry cure	75	1.0	1.5 h	1.41	0.08	0.52
Sealed cure		7.8	4 min	3.10	2.05	1.39

[a]Theoretical metal capacity from nitrogen contents of the resins is 3.2 to 3.3 $mmol\ g^{-1}$ assuming 1:1 complex formation.

water content, in good agreement with Jakubovic [13]. Although equilibration rates, in terms of time to 50% resin saturation, are given here, such measurements are dependent upon resin particle size and distribution. The particle size range used (22—60-mesh fraction) is so wide that it can be argued that variation in equilibration rates, particularly in Table 2 where such variations are small, may be determined by differences in resin particle size rather than in the parameter being varied. As Parrish [8] has demonstrated and others have discussed [14, 15], the water regain values can give

TABLE 2

The effects of changing the hydrophilicity and the degree of cross-linking of an oxine-containing ion-exchange resin

2nd Series	Resorcinol	*m*-Cresol	*p*-Cresol	Oxine	Cross linking (%)	Water regain ($g\ g^{-1}$)	Equilibration rate ($t_{\frac{1}{2}}$) (min)	Copp capac
Batch 1	4		0	4	50	4.8	4.7	3.5
Batch 2	3		1	4	37.5	2.9	6.0	3.4
Batch 3	2		2	4	25	2.4	6.5	3.2
Batch 4	2	2	0	4	50	1.6		2.8
Batch 5	2	1	1	4	37.5	2.2		3.1
Batch 6	2	0	2	4	25	2.5		2.8

[a]Theoretical copper capacity, from nitrogen contents, is 3.3—3.4 $mmol\ g^{-1}$.

comparable values of rates of equilibration for series of similar resins such as are compared here. The water regain, being a bulk resin property, is not dependent on particle size so that fluctuations in this parameter will accurately reflect the changes in equilibration rates which would be obtained for series of resins of identical particle size. Batch 3, sealed cure resin in Table 1, had ideal properties of high metal capacity and fast kinetics, but the material was a rather soft gel. Both this material and batch 2 were not sufficiently tough and attrition-resistant to withstand the rigors of indefinite column operation. Batch 1, with a water regain of 1.8 g g^{-1}, was suitable for this purpose. Subsequent series of resins were prepared by the sealed-cure method.

Of the second series, batches 1, 2 and 3 were prepared in an attempt to show the improvement in equilibration rate as the cross-linking decreased. For this purpose, resorcinol was replaced, mole for mole, by the non-cross-linking *p*-cresol. The results were the opposite of what was expected; the equilibration rate (as reflected in water regain) decreased as the cross-linking decreased. Obviously another over-riding factor was involved; this proved to be the substitution of the hydrophobic $-CH_3$ group in *p*-cresol for the hydrophilic —OH group in resorcinol. Batches 4, 5 and 6 were formulated to keep the hydrophilicity constant by replacing the cross-linking *m*-cresol with its non-cross-linking isomer; the water regain increased, and the kinetics improved as the cross-linking decreased, as would be expected. There is a marginal but significant change in copper capacity between the two sets; the more hydrophilic materials have higher copper capacities.

Table 3 shows the effects of changing the degree of cross-linking in a quite different way by simply varying the ratio of oxine to cross-linking agent. Unfortunately, the nature of the preparation made it impossible to hold the water content of the resin mix constant — this increased regularly although no additional water was added because the weight of resorcinol decreased. Batches 1 of the first and third series were identical formulations and, in terms of capacity and water regain, the reproduction of resin properties was good. To assess the effects of reducing the resorcinol content at constant water content, compare batch 2 of the first series with batch 3 of the third, each having an initial 70% water content. A decrease in the cross-linking by

TABLE 3

Effects of changing the cross-linking by varying the oxine:resorcinol ratio in an oxine-containing ion-exchange resin

3rd Series	Molar ratios of ingredients		Original water content (%)	Water regain (g g^{-1})	Copper capacity	
	Resorcinol	Oxine			Found	Calc. from % N
Batch 1	4	4	67	1.7	3.2	3.2
Batch 2	3	4	69	1.7	3.4	3.8
Batch 3	2	4	70	2.3	3.8	4.2
Batch 4	1	4	73	3.7	4.0	4.8

replacing resorcinol by oxine produces a worse resin kinetically because of the decrease in hydrophilicity. This change is more than offset, however, in Table 3 by increasing the original water content of the mixture. As this series had a varying oxine content, it was necessary to calculate a copper capacity from the nitrogen content of the resins. As the oxine:resorcinol ratio increases, oxine sites become unavailable to copper through over-crowding. An alternative explanation is that as the oxine content increases, there are statistically more oxine groups in suitable positions for 1:2 metal: oxine complex formation.

The microbead resin produced was from a 1:1 oxine:resorcinol mix containing 67.4% of water. Stirring the polymer gel in liquid paraffin for less than 1 h at 80°C gave beads which tended to coagulate; stirring for 4 h gave a very good, tough bead resin. The water regain of this resin was 4.1 g g^{-1}; the time to 50% equilibration with the 0.05 M copper solution was 4 min. From the nitrogen content of the dried resin (N 4.67%), the estimated total capacity for copper, assuming 1:1 complexes, was 3.3 mmol g^{-1}. The copper capacity at pH 5 was 3.2 mmol g^{-1}. This exchanger is therefore a good resin with fast kinetics, high metal capacity, and good physical characteristics.

Resin stability was tested towards acids, bases, metal recycling, and heat. After 4 d in 4 M hydrochloric acid the solution was slightly yellow. The depth of colour intensified gradually for 7 d, after which the copper capacity of the resin was 2.87 mmol g^{-1}. The batch of resin used for all the stability tests had initial water regain 2.6 g g^{-1}; initial copper capacity at pH 5, 2.9 mmol g^{-1}. Loss of functionality is therefore negligible in 4 M hydrochloric acid. The acid probably removes a small amount of very low molecular weight polymer which is present; protonation of the basic nitrogens would render it soluble. Sodium hydroxide and ammonia have large effects upon the resin, leaching yellow material quickly so that an intensely yellow coloured solution results within 1 h. As the resin washing step did not include an alkaline wash, this is not unusual, but the resins described here are obviously limited in use to acidic and neutral solutions. The preparation of an alkali-stable resin was not explored. The results of the stability to metal uptake—elution cycling were interesting. After the cycles, involving a total of contact for 10 d with pH 5 buffer and a further 10 d with 2 M hydrochloric acid, the copper capacity was still 2.90 mmol g^{-1}, but the water regain had decreased from 2.6 to 1.54 g g^{-1}. Parrish [10] found that an oxine resin water regain was reduced by 25%, and countered this tendency by the inclusion of hydrophilic sulphonic acid groups. In other work, where the oxine resin was in contact with sea-water for up to two months, no subsequent decrease in copper capacity was found.

These swollen gel polymers are not capable of being dried then re-swollen to the same extent because more methylene bridges are formed as the methylol groups and active sites approach each other as water is expelled. Thus, on air-drying at 20°C for 48 h, the water regain decreased from 2.6 to

0.56 g g^{-1} and the copper content of the re-swollen resin to 0.15 mmol g^{-1}. A much more rigorous treatment, drying at 100°C for 48 h, made surprisingly little difference; the water regain decreased to 0.43 g g^{-1} and the copper capacity to 0.13 mmol g^{-1} after re-swelling.

Successful oxine-containing chelating ion exchangers can therefore be made reproducibly in the laboratory. Resorcinol is the recommended cross-linking agent; a sealed cure technique is essential, and attention must be paid to the water content of the resin mix. With the ability to produce a tough gel bead with excellent kinetic properties and high metal capacity, it may be at last that the remarkable separating powers of oxine ion exchangers will be fully used in the analytical laboratory.

REFERENCES

1 H. Von Lillin, Angew. Chem., 66 (1954) 649.
2 J. R. Parrish, Chem. Ind., (1955) 386.
3 L. D. Pennington and M. B. Williams, Ind. Eng. Chem., 51 (1959) 759.
4 D. K. Hale, Research, 9 (1956) 104.
5 F. Vernon and H. Eccles, Anal. Chim. Acta, 63 (1973) 403.
6 J. R. Parrish, private communication.
7 R. C. De Geiso, L. G. Donaruma and E. A. Tomic, J. Appl. Polym. Sci., 9 (1965) 411.
8 J. R. Parrish and R. Stevenson, Anal. Chim. Acta, 70 (1974) 189.
9 R. V. Davies, J. Kennedy, E. S. Lane and J. L. Williams, J. Appl. Chem., (1959) 368.
10 J. R. Parrish, Lab. Pract., 24 (1975) 399.
11 F. Vernon and H. Eccles, Anal. Chim. Acta, 77 (1975) 145.
12 F. Vernon and H. Eccles, Anal. Chim. Acta, 79 (1975) 229.
13 A. O. Jakubovic, J. Chem. Soc., (1960) 4820.
14 J. P. De Villiers and J. R. Parrish, J. Polym. Sci., 42 (1964) 1331.
15 K. M. Saldadze and B. Kelman, Khim. Aktiv. Polim., Ikh. Primen., (1969) 236.

Analytica Chimica Acta, 93 (1977) 211—219
© Elsevier Scientific Publishing Company, Amsterdam — Printed in The Netherlands

SIMPLEX OPTIMIZATION OF THE SEPARATION OF PHOSPHOLIPIDS BY HIGH-PRESSURE LIQUID CHROMATOGRAPHY

M. LOUISE RAINEY** and WILLIAM C. PURDY*

Department of Chemistry, University of Maryland, College Park, MD 20742 (U.S.A.)

(Received 23rd March 1977)

SUMMARY

A simplex procedure is shown to be an efficient approach for solving separation problems. The best solvent ratio for the separation of phosphatidylcholine and sphingomyelin has been found by means of a two-dimensional simplex capable of expansion and contraction. A successful high-pressure liquid chromatography separation of lysophosphatidylcholine, phosphatidylethanolamine, phosphatidylinositol, phosphatidylserine, phosphatidylcholine, sphingomyelin and phosphatidic acid was achieved with a 180-cm column packed with Corasil II and a solvent mixture of chloroform—methanol—ammonia (50.0:35.9:7.0, v/v/v).

Phospholipids are important components of cell membranes and account for about 30% of the mass of erythrocyte membranes [1]. Phospholipids are believed to perform a large variety of functions in cell membranes and to be important indicators of many disease states [2—4].

The commonest method of analysis for phospholipids is by thin-layer chromatography (t.l.c.) [5]; the method involves solvent development in two directions, scraping the spots off the plate, digesting the spot, and phosphorus color development [6]. A high-pressure liquid chromatography (h.p.l.c.) method for phospholipids could present significant advantages over t.l.c. in terms of speed and ease of analysis.

Although t.l.c. may be an important indicator of the proper solvent for separation by h.p.l.c., the process of finding the proper solvent for a system involving more than one solvent is often "hit-or-miss". A 'simplex' procedure, which is a statistical design for finding the optimum of a response surface, has been used quite frequently in analytical chemistry.

In undertaking this work, it was hoped to demonstrate that the simplex method could be used to find the separation conditions, in particular the ratio of solvents, which would result in the best separation of phospholipids.

---

*Present address: Department of Chemistry, McGill University, Montreal, Quebec, H3A 2K6, Canada.

**Present address: Dow Chemical Company, Midland, Michigan.

The mixture of phospholipids to be separated was relatively complex and included phosphatidylethanolamine (PE), phosphatidylserine (PS), phosphatidylinositol (PI), phosphatidylcholine (PC), phosphatidic acid (PA), sphingomyelin (SM), and lysophosphatidylcholine (LPC).

One problem with the column chromatography of phospholipids has involved detection, since the phospholipids do not absorb in the region 250—380 nm. It was believed when this work was begun that the moving-wire detector would be a sensitive detector for phospholipids.

Simplex optimization

The optimization of a chemical system is the process of adjusting a set of controlling variables to achieve optimal results. This often means maximum absorbance, maximum separation, or highest yield, but it may also mean lowest overall cost in an industrial setting or improved stability of a product. If the variables affecting the measured result do not interact, each one may be optimized independently of the others, usually by holding all but one variable constant and changing one variable until the maximum result is obtained. In fact, this is the most commonly used method even when the variables do interact. This one-factor-at-a-time approach will not usually result in an optimum set of conditions.

There are many different methods of optimization [7] but none is as simple and easy to apply as the simplex method. One optimization method which has several features in common with the simplex method, including the simultaneous variation of several variables, has been developed by Box and Draper [8]. This method is called "evolutionary operation" and is especially useful in industrial processes.

The simplex method is a very powerful method for finding that set of conditions which will result in the most desirable response from a chemical system. Variables which interact can be optimized; the method, developed by Spendley et al. [9], was applied to analytical chemistry by Long [10]. A review by Deming and Morgan [11] helped to clarify the attractiveness of the simplex method for analytical problems.

The rules which govern a decision regarding the change of variables for a system are simple and can, in principle, be applied to any number of variables. The easiest system to visualize is a set of two variables, since the movement of the simplex can be graphed in two dimensions. In general terms a simplex is a geometrical figure with one vertex more than the number of dimensions involved. A simplex in two dimensions is a triangle; a simplex in three dimensions is a tetrahedron and so on to higher dimensions for which no easily visualized model can be given. In the basic form of optimization, the simplexes are regular figures, e.g. equilateral triangles in two dimensions, but the method is perfectly capable of generalization. The movement of the simplex has been described and the rules governing movement, contraction and expansion of the simplex, and treatment of local maxima have been given [11].

EXPERIMENTAL

Chemicals

Methanol, chloroform, and ammonia liquor were reagent grade (Fisher Scientific Co.). PE and PC were synthetic dipalmitoyl phospholipids (Calbiochem, lot 300020, and Sigma Chemical Co. lot 122 C-2790, respectively). PA (Sigma, lot 122 C-2250) and LPC (Sigma, lot 113 C-8120) were commercially prepared from egg lecithin. SM (Sigma, lot 92 C-0890) and PS (Calbiochem, lot 300546) were commercially prepared from bovine brain. PA, PE, PC, SM, and LPC were received in powder form. PS and PI (Applied Science Laboratories, lot 1819) were obtained dissolved in chloroform. Phospholipids were stored at −25°C when dissolved, and in a desiccator in a refrigerator when in solid form.

The following reagents were prepared. Chloroform was distilled in glass from bulk reagent-grade; 0.75% methanol (v/v) and ca. 0.1 mg l^{-1} of butylated hydroxytoluene (BHT) were added to prevent oxidation. PE, PC, LPC, and PA were all dissolved in chloroform; SM was dissolved in chloroform/methanol, 1:1 (v/v).

Apparatus

Solvent was contained in a round-bottom flask fitted with a heating mantle and a specially constructed condenser. The round-bottom flask, heating mantle, and condenser were placed on top of an LCM2 cabinet (Pye Unicam, Cambridge, England) ca. 5 ft. above the pump to give the solvent a positive pressure. The purpose of the heating mantle was to deaerate and heat the solvent before it entered the pump, to avoid vaporization of the solvent when it reached the pump, which was warm because of the motor. The pump was a Milton Roy Minipump capable of 5000 psi. Every effort was made to keep the pump on continuously. It was kept on overnight either by recycling methanol through the waste valve or by dialing a very low stroke setting and pumping solvent through the column to condition it when the solvent mixture was being changed.

Columns were 30-cm, 60-cm, and 90-cm lengths of 316 stainless steel tubing (i.d. 3/16 in., o.d. 1/4 in.). When all three columns were used to make a 180-cm column, the 30- and 60-cm lengths were connected by a Swagelok union drilled out and the two 90-cm lengths were then connected by a short piece of capillary-bore stainless steel tubing. The pressure gauges were brass Bourdon tubes isolated from the solvent system by isolator pistons (Scientific Systems, Inc.). The system was provided with a stopped-flow injector.

The detector was a moving-wire (Pye Unicam, Cambridge, England). Gas lines were fitted with molecular sieves (Chemical Research Services, Inc.). A Unicam AR25 linear recorder was used and an Autolab 6300 digital integrator (VIDAR) was connected between the detector and the recorder for quantitative area measurements.

Procedures

Column preparation. Before packing, all columns were cleaned as recommended by Majors [12]. The column was washed with 1:1 (v/v) nitric acid, distilled water, acetone, chloroform, and acetone and dried in a stream of dry nitrogen. The detector end of the column was fitted with a frit of stainless steel mesh and porous Teflon.

Column packing. Corasil II (Waters Associates) was dried overnight at 110°C and then placed in a plastic container with a narrow spout from which it could flow easily into the column. A dry packing technique was used. Packing material was squeezed from the plastic container in ca. 0.5-ml increments, after which the column was tapped on a solid surface and tapped gently a few times at the level of the filling material. After filling, the column was tapped for 5 min. Another frit was placed at the top of the column.

Integrator setting. When the integrator was used, the baseline corrector was switched off and the electrometer back-off was used to zero the integrator. This was necessary because the integrator baseline corrector would "see" some of the broad flat peaks as baseline drift. To prevent the integrator from stopping integration at the top of the broad flat peaks, the integrator noise adjust was turned to maximum. Filtering and slope sensitivity were also set at maximum.

Detector. Oxidizer oven temperature was always 720°C; optimum evaporator oven temperature varied according to wire speed and solvent mixture. Whenever the wire spools were changed, the oxidizer and evaporator glassware were cleaned by soaking in cleaning solution. Occasionally, small pieces of wire were found piled around the restrictor and these were removed by vacuum.

RESULTS AND DISCUSSION

Separation of PC and SM

A 60-cm column packed with Corasil II was used. The chloroform—methanol—ammonia solvent system was used since the presence of only two independent variables allowed the movement of the simplex to be represented graphically. The volumes (ml) of methanol and ammonia were the two independent variables; the volume of chloroform was held constant at 50 ml.

The data for the optimization of the separation of PC and SM are shown in Table 1. The response is the resolution of the two peaks, determined by comparing the chromatograms with the set of standard peaks given by Snyder [13]. Several applications of the modified simplex optimization technique should be noted. At vertex 4, the response was the best response in the simplex and so the simplex was expanded using $\gamma = 2$. However, the response at the expanded vertex, 4.1, was worse than at vertex 4 so the expanded vertex was dropped. The measurement of the response at vertex 4.1 is probably in error (considering the location of the eventual optimum) but the simplex method does not require replications and the eventual

TABLE 1

Simplex steps for the separation of PC and SM (chloroform, 50 ml)

Vertex	Retained vertices[a]	Methanol (ml)	Ammonia (ml)	Response
1		25.0	5.0	0.4
2		25.0	7.0	0.4
3		33.7	6.0	0.4
4	2, 3	33.7	8.0	0.8
4.1	$\gamma = 2$	38.1	9.5	0.4
5	3, 4	42.4	7.0	0.4
6	4, 5	42.4	9.0	0.5
7	4, 6	33.7	10.0	0.4
7.1	$\beta = 1/2$	35.9	9.3	1.0
8	4, 7.1	27.2	8.3	0.4
8.1	$\alpha = -1/3$	37.3	8.8	0.9
9	7.1, 8.1	39.5	10.1	0.8
9.1	$\beta = 1/3$	37.6	9.4	0.8
10	7.1, 9.1	36.2	9.9	1.0

[a] α, β, and γ are factors used in calculating new vertices when it is desirable to contract or expand the simplex.

progress of the simplex toward the optimum illustrates that replication is not necessary. At vertex 7, the response was the worst in the new simplex but not worse than the worst response in the previous simplex, so the simplex was contracted but its direction was not reversed. At vertex 8, the response was the worst in the new simplex and also worse than the worst response in the previous simplex, so the simplex was contracted and its direction was reversed. The simplex was stopped when the next calculation indicated a step size of less than 5% of the domain of both variables. The four best responses 7.1, 8.1, 9.1, and 10 have ratios of methanol to ammonia of 3.7:4.2 and very little difference between these chromatograms can be noted.

Separation of more complex mixtures

With the solvent mixture chloroform—methanol—ammonia (50:35.9:9.3, v/v/v), a flow rate of 0.38 ml min^{-1}, and a 60-cm column packed with Corasil II, a mixture of PE, PC, and SM was separated. When PA was added to the mixture, it was not adequately separated from SM. A mixture of PI, PC, and SM could not be separated with the same solvent mixture. Following the suggestions of Snyder [14], an increase in column length seemed advisable. A 30-cm column packed with Corasil II was added to the 60-cm column but little improvement in the separation of PI, PC, and SM was noted. It was therefore decided to change to a chloroform—methanol—acetone—acetic acid—water system.

Table 2 shows the simplex steps for the attempt to optimize the separation of PI, PA, PC, PS, and PE with the chloroform—methanol—acetone—acetic

TABLE 2

Simplex steps for the separation of PI, PA, PC, PS, and PE (chloroform, 50 ml)

Vertex	Retained vertices	Acetone	Methanol	HAc	H_2O
1		40.0	7.5	15.0	5.0
2		35.0	1.9	21.3	4.8
3		35.0	5.0	15.0	3.0
4		30.0	12.0	15.0	4.0
5		50.0	10.0	10.0	5.0
6	1, 3, 4, 5	42.5	15.4	6.2	3.7
6.1	$\alpha = -1/2$	35.9	10.7	13.3	4.1
7	1, 3, 4, 6.1	50.5	4.6	11.7	4.6
8	1, 3, 6.1, 7	30.7	3.9	17.5	3.4
8.1	$\alpha = -1/2$	45.2	8.5	11.9	4.6
9	3, 6.1, 7, 8.1	43.3	6.9	11.0	3.2
10	3, 6.1, 7, 9	37.2	5.1	13.6	2.9
10.1	$\gamma = 2$	33.1	3.4	14.5	2.0
11	3, 6.1, 9, 10.1	23.2	8.4	15.2	1.6
12	3, 9, 10.1, 11	31.4	1.2	14.6	0.8
13	3, 10.1, 11, 12	18.1	2.1	18.7	0.5
14	10.1, 11, 12, 13	17.9	2.6	16.5	0.5
14.1	$\alpha = -1/2$	30.7	4.4	15.4	2.1
15	10.1, 12, 13, 14.1	33.5	2.9	16.4	1.1
16	10.1, 13, 14.1, 15	22.5	6.6	17.5	2.3
16.1	$\alpha = -1/2$	29.2	2.5	15.3	1.2
17	10.1, 14.1, 15, 16.1	41.3	6.8	15.8	2.6
17.1	$\alpha = -1/2$	23.9	3.0	13.7	1.1
18	10.1, 15, 16.1, 17.1	25.3	2.9	14.1	0.8
10.1	repeat	33.1	3.4	14.5	2.0

acid—water solvent system. The prime difficulty was the quantitative assessment of the "goodness" of separation. One attempt [15] to define a quantity called the "informing power of a chromatographic method" was deemed to be insufficiently specific. Since the simplex method does not require a quantitative evaluation of the response at each vertex but only that the responses be ordered, the simplex method still presented a reasonable choice of approach to the separation problem. However, it was found in practice that the evaluation of the chromatograms, particularly attempts to rank order two or three chromatograms which closely resembled each other, was very difficult. Frequently, several criteria had to be applied simultaneously such as the degree of separation of two or three early eluting peaks versus excessive band broadening and flattening of late eluting peaks.

A second and more difficult problem involved the determination of the direction in which the simplex was moving and when, or if, it was circling. If only two independent variables had been involved and the simplex could have been graphed, then the problem of not being able to evaluate each

chromatogram quantitatively would have been lessened. If the simplex began retracing a previous path, then this would have been apparent from the graph and the chromatograms could have been re-evaluated to ascertain whether or not an error had been made. The simplex was therefore discontinued since it did not appear to be progressing toward an acceptable separation.

At this juncture, the chromatograms with the chloroform—methanol—ammonia system were re-investigated. The sample now contained PE, PS, PI, PC, PA, SM, and LPC and the column length was extended to 180 cm. A new simplex was constructed and ranked in terms of PC band spreading. Five steps were required to obtain separation; these steps are shown in Table 3. Vertex 5 may not represent the optimum separation of these seven phospholipids but it does give a separation. A summary of the instrumental conditions is given in Table 4.

One possible method of calculating peak area is to inject varying amounts of the same standard solution and measure the area variation. An analysis of variance was performed with PE and three different injection volumes; variation in area was significant at the 0.01 level.

With the solvent mixture of vertex 5 (Table 3), standard curves, area vs. μg of phospholipid, were constructed for each of the seven phospholipids. The injection volume was 10μl. Each graph point represented the average of at least four counts. For points close to the detection limit, the data point represented the average of 7—10 area counts. Table 5 shows the slopes of these standard curves and gives the detection limits for the seven phospholipids. The detection limit is defined as the amount of phospholipid that gives a signal twice the noise level under the separation conditions described. The detection limits for SM and LPC are higher than for the other phospholipids because band spreading is much greater for these phospholipids, and on reaching the coating block of the moving-wire detector they are more dilute than others. Table 6 shows the retention times for the seven phospholipids.

A mixture of PE, PI, PC, PA, SM, and LPC was analyzed by means of the standard curves. PS was excluded as commercial samples were found to contain other phospholipid impurities. The relative proportions of the phospholipids to each other were chosen to approximate the relative proportions in blood samples [16]. Table 7 shows the average areas of the respective peaks

TABLE 3

Simplex for separation of PE, PS, PI, PC, PA, SM, LPC (chloroform, 50 ml.)

Vertex	Retained vertices	Methanol (ml)	Ammonia (ml)
1		35.9	5.0
2		25.0	5.0
3		35.0	3.0
4	1,2	25.0	7.0
5	1,4	35.9	7.0

TABLE 4

Summary of conditions for separation of PE, PS, PI, PC, PA, SM, LPC

Column: 180 cm × 3/16 in. i.d.
Column packing: Corasil II
Solvent: chloroform—methanol—ammonia (50:35.9:7.0, v/v/v)
Flow rate: 2.78 ml min^{-1}
Pressure: 50 kg cm^{-2}
Wire speed: X6 = 18 cm s^{-1}
Evaporator temperature: 100°C
Oxidizer temperature: 720°C
Chart speed: 5 min cm^{-1}
Current, full scale: 1.6 × 10^{-2} A

TABLE 5

Slopes and detection limits for phospholipids

Phospholipid	Slope	Detection limit (μg)
PE	1.3×10^3	10
PS	1.7×10^3	10
PI	1.9×10^3	5
PC	1.1×10^3	15
SM	1.5×10^3	50
LPC	1.1×10^3	90
PA	9.1×10^2	20

TABLE 6

Reproducibility of retention times for phospholipids
(Solvent, chloroform—methanol—ammonia (50.0: 35.9:7.0). Flow rate, 2.78 ml min^{-1})

	PE	PS	PI	PC	PA	SM	LPC
Average retention time (min)	5.2	6.7	7.4	11.5	15.3	16.5	31.2
Standard deviation	0.4	0.4	0.5	0.5	—	0.4	1.9
Relative standard deviation	7.4	6.0	7.1	0.5	—	2.3	6.0
N	10	4	9	8	2	7	3

from 10 injections of 10 μl of the same prepared mixture, and also shows the amount of each phospholipid which each area represents according to the standard curves. The last column compared the amount of phospholipid injected with the amount of phospholipid alleged to be present according to the standard curve.

The difference of PE from the injected amount may be due to impurities in the other phospholipids by implication from experience with PS. The

TABLE 7

Analysis of prepared mixture of PE, PI, PC, PA, SM, LPC

	Concentration (mg ml^{-1})	μg PPL in 10-μl injection	Area of peak $\times 10^{-4}$	S.d. $\times 10^{-4}$ ($N = 10$)	S.d. (%)	Found (μg)	Recovery (% of PPL injected)
PE	16.0	160	23.5	0.94	4.0	188	117
PI	4.5	45	11.0	1.7	15.5	46	102
PC	25.0	250	26.4	1.4	5.3	248	99
PA	2.0	20	1.6	0.10	6.2	26	130
SM	16.8	168	20.0	1.7	8.3	176	105
LPC	2.0	20					

amount of PA is near the detection limit and less reliable on that basis. In addition, the PA peak, although separated from PC, is not as well separated as other phospholipids. This, together with the fact that it appears next to PC (which is very much more concentrated), may account for the difference.

This paper was taken in part from the Ph.D. dissertation of M. Louise Rainey, University of Maryland, 1974.

REFERENCES

1 G. Nelson, Blood Lipids and Lipoproteins: Quantitation, Composition and Metabolism, Wiley-Interscience, New York, 1972, p. 320.
2 E. Ball, R. McKee, C. Anfinsen, W. Curz, and Q. Geiman, J. Biol. Chem., 175 (1948) 547.
3 D. Morrison and H. Jeskey, Fed. Proc., 6 (1947) 279.
4 M. Angus, K. Fletcher, and B. Maegraith, Ann. Trop. Med. Parasitol., 65 (1971) 429.
5 G. Nelson, Blood Lipids and Lipoproteins: Quantitation, Composition and Metabolism, Wiley-Interscience, New York, 1972, pp. 51—73.
6 S. McClean, W. C. Purdy, A. Kabat, J. Sampugna, R. DeZeeuw, and G. McCormick, Anal. Chim. Acta, 82 (1976) 175.
7 G. S. G. Beveridge and R. S. Schechter, Optimization: Theory and Practice, McGraw-Hill, New York, 1970.
8 G. E. P. Box and N. R. Draper, Evolutionary Operation, Wiley, New York, 1969.
9 W. Spendley, G. R. Hext, and F. R. Himsworth, Technometrics, 4 (1962) 441.
10 D. E. Long, Anal. Chim. Acta, 46 (1969) 193.
11 S. Deming and S. L. Morgan, Anal. Chem., 45 (1973) 278A.
12 R. E. Majors in M. Hadden, F. Bauman, F. MacDonald, M. Munk, S. Stevenson, D. Gere, F. Zamaroni, and R. Majors, Basic Liquid Chromatography, Varian Aerograph, Walnut Creek, Calif., 1971, pp. 5—7.
13 L. R. Snyder, J. Chrom. Sci., 10 (1972) 200.
14 L. R. Snyder, J. Chrom. Sci., 10 (1972) 369.
15 D. L. Massart and R. Smits, Anal. Chem., 46 (1974) 283.
16 G. Nelson, Blood Lipids and Lipoproteins: Quantitation, Composition and Metabolism, Wiley-Interscience, New York, 1972, p. 331.

Analytica Chimica Acta, 93 (1977) 221—226
© Elsevier Scientific Publishing Company, Amsterdam — Printed in The Netherlands

THE DETERMINATION OF HYDRAZINE AND 1,1-DIMETHYLHYDRAZINE, SEPARATELY OR IN MIXTURES, BY HIGH-PRESSURE LIQUID CHROMATOGRAPHY

HAMED M. ABDOU, THOMAS MEDWICK and LEONARD C. BAILEY

College of Pharmacy, Rutgers University, P.O. Box 789, Piscataway, N.J. 08854 (U.S.A.)

(Received 23rd March 1977)

SUMMARY

A rapid, sensitive liquid chromatographic method for the determination of hydrazine and 1,1-dimethylhydrazine, separately or in mixtures of varying proportions, is described. The procedure involves salicylaldehyde derivative formation followed by chromatography on a reversed phase (octadecylsilane) column with acetonitrile (52%)—0.14 M potassium dihydrogenphosphate (48%) as a mobile phase and u.v. (254 nm) detection. This system is sensitive to 2 $\mu g\ ml^{-1}$ of hydrazine and 5 $\mu g\ ml^{-1}$ of 1,1-dimethylhydrazine and has a relative standard deviation of less than 1%. Monomethylhydrazine forms an unstable salicylaldehyde hydrazone; although it cannot be determined, it can be detected (sensitivity 5 $\mu g\ ml^{-1}$) and does not interfere with quantitative measurement of either hydrazine or 1,1-dimethylhydrazine.

In recent years the detection and determination of hydrazine (H) and its derivatives has received considerable attention because of their uses as rocket fuels, industrial chemicals, and pharmacological agents. The excellent monograph by Malone [1] treats many of the approaches to this analytical problem.

The various titrimetric procedures based on the acid—base and electron transfer behavior of these compounds are limited by a lack of sensitivity. The more sensitive spectrophotometric and gas chromatographic procedures are useful if preliminary derivatization steps are completed. Earlier work [2] described a spectrophotometric procedure for hydrazine and asymmetric dimethylhydrazine (UDMH) after salicylaldehyde derivatives with useful u.v. spectra were formed. Derivatization to produce decafluorobenzaldazine, followed by tritium electron-capture detection, was suggested by Lin et al. [3]. Dee [4] reported enhanced detector response when substituted pyrazoles were formed from hydrazines before chromatography.

This paper describes the determination of H and UDMH by preparation of their salicylaldehyde derivatives and their subsequent separation and determination by high-pressure liquid chromatography (h.p.l.c.). These derivatives, studied extensively by Bailey and Medwick [2], are useful since their high molar absorptivities permit detection of low levels of H and UDMH by u.v. absorption. The method is rapid, sensitive, accurate, and precise.

EXPERIMENTAL

Apparatus

The liquid chromatograph consisted of a Laboratory Data Control model 2396 minipump, LDC model 709 pulse dampener, and LDC model 1285 u.v. monitor operated at 254 nm. A Chromatronix HPSV-20 sample injection valve (fixed volume, 20 μl) was used to introduce the samples onto the chromatograph. The detector output was displayed on a recorder (full scale range, 10 mv). The column was a stainless steel tube, 30 cm long by 4 mm i.d., filled with a microparticulate reverse-phase packing material (μBondapak C18, Waters Associates). The mobile phase, at 800—900 p.s.i.g., gave a flow rate of 1.2—1.4 ml min^{-1}.

Reagents and chemicals

Anhydrous hydrazine, (97%) (Matheson, Coleman and Bell) and 1,1-dimethylhydrazine (95%) and 1-methylhydrazine (98%) (Aldrich Chemicals) were used as obtained. Reagent-grade glacial acetic acid (Fisher Scientific) was redistilled twice before use. Salicylaldehyde (from the bisulfite compound Eastman Kodak) was redistilled immediately before use. Analytical-grade potassium dihydrogenphosphate (Mallinckrodt) was used.

Spectranalyzed-grade methanol, chloroform, isopropanol, and acetonitrile (99 mole %, Fisher Scientific) were used as received.

Sampling of hydrazines

Because of the tendency of the hydrazines to be oxidized by atmospheric oxygen, to absorb carbon dioxide, and to fume in air, a special sampling technique was used. An amount of the hydrazine in excess of that required for the analysis was drawn into an all-glass syringe which was then weighed accurately. The approximate amount of the hydrazine required was transferred to a 100-ml volumetric flask containing about 40 ml of chilled isopropanol. The syringe was then reweighed.

Mobile phase

The mobile phase consisted of acetonitrile (52 ± 2% by volume) and aqueous 0.14 M potassium dihydrogenphosphate (48 ∓ 2% by volume). The mobile phase was filtered and degassed under vacuum before use.

Standard preparation

Into a 50-ml low-actinic volumetric flask seated in an ice bath and containing about 25 ml of isopropanol, weigh accurately the required amount of the hydrazine standard or sample. A sample representing ca. 0.5 g of hydrazine or 0.7 g of 1,1-dimethylhydrazine should be weighed.

Mix well by swirling; while the flask is in the ice bath, add 5 ml of glacial acetic acid in small portions, mixing well after each addition. Dilute to volume with isopropanol. Transfer 2.0 ml to a 50-ml low-actinic volumetric

flask and add 0.5 ml of salicylaldehyde reagent solution (45 ml of salicylaldehyde diluted to 100 ml with isopropanol). Stopper the flask securely and place in a water bath at 60°C for 20 min. Remove the flask from the bath, cool to room temperature, and dilute to volume with chloroform. Transfer 3.0 ml of this solution to a 10-ml low-actinic volumetric flask, and dilute to the mark with methanol.

Sample preparation

Prepare the sample solution in a manner exactly analogous to the preparation of the standard solution. In the analysis of an unknown mixture, a sample representing 0.5 g of total hydrazines should be weighed.

Chromatographic procedure

Via the sample injection valve, introduce 20 μl of the final methanolic solution of the standard into the liquid chromatograph. From the retention times, identify each peak; measure the peak heights (or areas). Treat the sample solution in the same manner. Calculate the quantity (g) of each hydrazine present in the original sample from $(Hu/Hs) \times Ws \times P$, where Hu is the height of a specific component in the unknown solution, Hs is the height of the corresponding peak in the standard chromatogram, Ws is the weight (g) of the standard component initially taken, and P is the % purity of the standard hydrazine or 1,1-dimethylhydrazine.

System suitability test

To check the reproducibility of the chromatographic system before each analysis, introduce 3 injections of the working standard solution onto the column. Calculate the reproducibility of the peak heights in terms of the relative standard deviation, which should not exceed 2%.

RESULTS AND DISCUSSION

The procedure developed earlier [2] for the preparation of salicylaldehyde derivatives of H and UDMH was followed with minor modification. In the reported procedure, the amount of salicylaldehyde was about 50% in excess of that required for complete reaction even if the sample were entirely hydrazine, whose reaction stoichiometry involves 2 molecules of salicylaldehyde. This excess of salicylaldehyde was added to ensure rapid reaction completion and did not interfere with the separation and measurement.

The solvent for the standard and sample solutions was chosen to facilitate dissolution of the derivatives and subsequent miscibility with the aqueous mobile phase. Both derivatives, salicylaldazine, a yellow crystalline solid, and salicyl-1,1-dimethylhydrazone, a yellow liquid, dissolved easily in chloroform. A second dilution with methanol ensures that the system is compatible with the chromatographic mobile phase.

The chromatographic behavior of the salicylaldehyde derivatives of H and UDMH is shown in Fig. 1. The retention times are listed in Table 1. The retention time for salicylaldehyde is 3 min. The separations are excellent and clearly indicate that excess of salicylaldehyde does not interfere.

To monitor reaction completeness and test the linearity of the chromatographic response, the behavior of different levels of compounds was studied. Four different concentrations of H and UDMH, of ca. 25, 50, 100, 125% of the working standard levels, were treated separately with salicylaldehyde and chromatographed (see Experimental). The response was expressed in terms of Response Ratios. The mean values (Table 1, column 5) did not vary by more than 1%, indicating reproductibility of response. Furthermore, in both cases linear regression analysis of each set of four concentrations and the matching chromatographic peak heights (Table 1, column 6) showed the response to be linear, with correlation coefficients very close to unity. The minimum level of detection, taken for convenience as a peak 2 cm higher than the noise level, is ca. 2 μg ml^{-1} for H and 5 μg ml^{-1} for UDMH in the solutions to be chromatographed.

It was not possible to measure monomethylhydrazine (MMH) successfully by this procedure. In agreement with earlier experience [2], the salicylaldehyde monomethylhydrazone was unstable, yielding analytical recoveries of 83—95% of the expected quantities. This instability, particularly evident when H and UDMH were present, did not interfere with the quantitative measurement of H and UDMH since no azine or salicylaldehyde dimethylhydrazone resulted from the salicylaldehyde monomethylhydrazone instability. The recovery data for H and UDMH were independent of the amount of MMH present. If present, MMH would have a retention time of about 4 min, very close to that of the salicylaldehyde peak. Complete resolution of the monomethylhydrazone from salicylaldehyde may be accomplished with a different mobile phase, 37% acetonitrile—53% aqueous 0.14 M potassium dihydrogenphosphate, and a flow rate of 2 ml min^{-1}. Under these conditions

TABLE 1

Chromatographic behavior of salicylaldazine and salicylaldehyde-1,1-dimethylhydrazone

1 Compound	2 Concentration range (mg ml^{-1})	3 Retention time (min)	4 Peak height, range (cm)	5[a] Response ratios (cm mg^{-1})	6[b] Least squares parameters
Salicylaldazine	0.154—0.328	14	5.21—11.05	33.75 (s_r = 0.17%)	R = 0.99999 S = 33.62 i = 0.0297
Salicylaldehyde-1,1-dimethylhydrazone	0.138—0.634	6	4.68—21.37	34.03 (s_r = 0.71%)	R = 0.9999 S = 33.82 i = 0.081

[a]The response ratio in terms of peak height per mg is a useful expression of sensitivity.
[b]The least squares parameters are: correlation coefficient, R; slope, S (cm ml mg^{-1}); intercept, i (cm).

elution of all compounds is retarded as shown in Fig. 2. The retention times were: salicylaldehyde, 6 min; salicylaldehyde monomethylhydrazone, 8.5 min; salicylaldehyde-1,1-dimethylhydrazone, 20 min; salicylaldazine, more than 1 h. Since the azine did not elute within 1 h, it was washed from the column with methanol. Thus, although MMH cannot be measured quantitatively in an acceptable fashion, it is possible to detect its presence reliably with the 37% acetonitrile mobile phase. The minimum level of detection for MMH is ca. 5 μg ml^{-1} of the solution to be chromatographed.

After systems suitability tests proved that the chromatographic system was satisfactory with a relative standard deviation of less than 2%, twelve samples containing variable proportions of accurately weighed quantities of H and UDMH were analyzed; the results are shown in Table 2. The average recovery

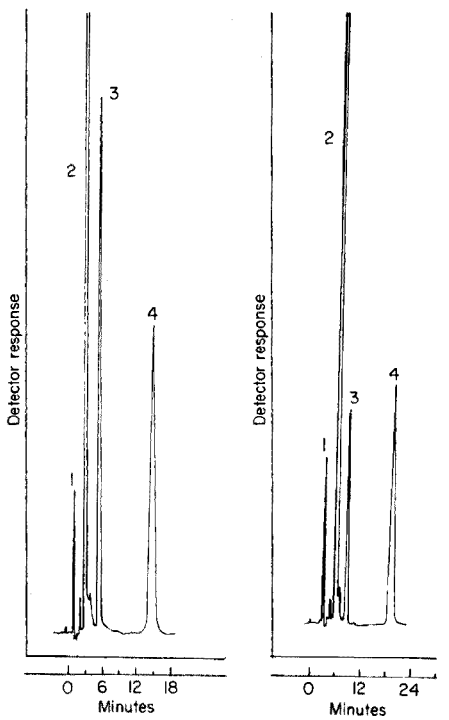

Fig. 1. Chromatogram for a mixture of H and UDMH. Mobile phase: acetonitrile (52%)—0.14 M aqueous potassium dihydrogenphosphate (48%). Chart speed, 6 in. per h. Peaks are:— (1) solvent, (2) salicylaldehyde, (3) salicylaldehyde-1,1-dimethylhydrazone, (4) salicylaldazine.

Fig. 2. Chromatogram for identification of MMH. Mobile phase: acetonitrile (37%)—0.14 M aqueous potassium dihydrogenphosphate (63%). Chart speed, 3 in. per h. Peaks are:— (1) solvent, (2) salicylaldehyde, (3) salicylaldehyde monomethylhydrazone, (4) salicylaldehyde-1,1-dimethylhydrazone. Salicylaldazine under these conditions elutes after 1 h and is not shown.

TABLE 2

Analysis of hydrazine-1,1-dimethylhydrazine mixtures by h.p.l.c.

Taken (g)		Found (g)		Recovery (%)	
H	UDMH	H	UDMH	H	UDMH
0.5145	0.9410	0.5130	0.9525	99.71	101.22
0.6388	0.8610	0.6468	0.8668	101.25	100.67
0.4160	0.8622	0.4142	0.8608	99.58	99.83
0.3395	0.6562	0.3402	0.6502	100.22	99.09
0.4155	0.6038	0.4145	0.5962	99.76	98.76
0.2912	0.6158	0.2945	0.6178	101.12	100.32
0.2682	0.5442	0.2685	0.5450	100.09	100.14
0.2415	0.4900	0.2410	0.4880	99.79	99.59
0.2038	0.3938	0.2035	0.3980	99.88	101.08
0.2770	0.3622	0.2750	0.3662	99.28	101.10
0.1598	0.2152	0.1580	0.2128	98.91	98.84
0.1285	0.2352	0.1292	0.2350	100.58	99.89
			Mean	100.01	100.04
			s_r	0.69	0.87

is 100.1% (s_r = 0.7%) for H; 100.0% (s_r = 0.9%) for UDMH. The results are accurate and precise and are obtained rapidly with this simple, convenient chromatographic procedure.

The sample sizes are limited by the dilution pattern and the capability of the instrument to produce a signal without excessive noise. Thus, it is possible to have samples whose initial concentrations are 10% of those presented in Table 2 if more sensitive detector attenuations are used. In addition, variations in the dilution patterns may be introduced to increase sensitivity.

The detector was operated at 254 nm, which is the most commonly available wavelength. However, the absorption maxima of both salicylaldehyde derivatives of H and UDMH occur at 293 nm [2] and they absorb much more strongly at this wavelength. Presumably a significant increase in sensitivity could be attained if a variable wavelength detector were to be used at 293 nm.

This work was abstracted from a Ph.D. thesis submitted by H. Abdou to the Graduate School, Rutgers University, May 1977.

REFERENCES

1 H. E. Malone, The Determination of Hydrazino—Hydrazide Groups, Pergamon, New York, 1970.
2 L. C. Bailey and T. Medwick, Anal. Chim. Acta, 35 (1966) 330.
3 Y. Lin, I. Schmeltz and D. Hoffmann, Anal. Chem., 46 (1974) 885.
4 L. A. Dee, Anal. Chem., 43 (1971) 1416.

Analytica Chimica Acta, 93 (1977) 227—237
©Elsevier Scientific Publishing Company, Amsterdam — Printed in The Netherlands

ÉTUDE PAR SPECTROSCOPIE D'ABSORPTION DE LA COMPLEXATION DES LANTHANIDES TRIVALENTS PAR LES ACIDES AMINO-CARBOXYLIQUES

E. MERCINY, J. M. GATEZ et G. DUYCKAERTS

Institut de Chimie, Université de Liège au Sart Tilman, B-4000, Liège (Belgique)

(Reçu le 11 mai 1977)

RÉSUMÉ

La complexation des lanthanides par les acides aminoacétiques est accompagnée d'un glissement de certaines bandes d'absorption du cation vers les plus grandes longueurs d'ondes. En choisissant judicieusement le milieu — pH et concentrations — il est possible d'obtenir une valeur caractéristique du glissement pour chaque espèce complexe. Cette étude a été faite à 20°C dans KCl M et elle a porté sur les complexes 1:1, 1:2 et 1:3 ou mixtes du praséodyme, du holmium et du thulium avec divers acides aminoacétiques: glycine (G), acide iminodiacétique (IMDA), acide nitrilotriacétique (NTA), acide hydroxyéthyléthylènediaminotriacétique (HEDTA), acide éthylènediaminotétraacétique (EDTA), acide diaminocyclohexanetétraacétique (DCTA), acide diéthylènetriaminopentaacétique (DTPA). Ces glissements chimiques ont été discutés en fonction du nombre de sites de coordination des agents chélatants concernés. Une modification importante, probablement dans la structure du complexe, se manifeste lorsque le nombre de sites de coordination dépasse neuf pour les terres rares cériques on huit pour les terres yttriques.

ABSTRACT

An absorption spectrophotometric study of the complexation of trivalent lanthanides by aminocarboxylic acids

Complexation of the lanthanides by aminoacetic acids shows a shift in some absorption bands of the cation towards higher wavelengths. By choosing the medium — pH and concentrations — adequately, each complex species can be characterized by a certain shift. This study has been carried out at 20°C in M KCl and concerns the 1:1, 1:2, 1:3 and mixed complexes of praseodymium, holmium and thulium with G, NTA, HEDTA, EDTA, DCTA and DTPA. The characteristic shifts are correlated with the number of coordinating sites of the chelating agents. It seems that a significant change occurs in the structure of the complex when the number of coordinating sites exceeds nine for the cerium rare earths or eight for the yttrium elements.

Pour évaluer le nombre de coordination d'un acide aminopolycarboxylique dans un complexe 1:1 avec les lanthanides trivalents, on se contente souvent de faire la somme des atomes d'azote et des groupements carboxyliques du chélatant. Si cette façon de procéder s'applique parfaitement aux complexants de petite taille (IMDA = 3, NTA = 4, EDTA = 6 · · ·) elle est mise en défaut dans le cas de molécules plus volumineuses. C'est ainsi que le

DTPA, dont le nombre de sites actifs est égal à huit, est considéré par certains auteurs [1] comme heptacoordiné, par d'autres [2] comme octocoordiné; le TTHA (acide triéthylènetétraaminohexaacétique), dont le nombre de sites coordinants est égal à 10, semble se comporter comme un ligand octocoordiné dans ses complexes 1:1 monoprotonés et hexacoordinés dans ses complexes 1:1 non protonés avec les lanthanides [2]. Enfin, il subsiste toujours un désaccord concernant la valeur exacte du nombre de coordination du HEDTA, dans Ln(HEDTA), les uns considérant que le groupement hydroxyle participe à la coordination (hexacoordinè) [2], les autres estimant que le ligand est hexacoordiné pour certains lanthanides et pentacoordiné lorsque le nombre atomique du lanthanide considéré augmente [3].

La situation se complique encore si l'on considère les complexes 1:2, 1:3 et mixtes que forment ces acides avec les terres rares; on obtient des complexes dont l'encombrement stérique est très important. Quel est, dans ce cas, le nombre de sites réellement impliqués dans la coordination.

On trouve dans la littérature, quelques tentatives d'approche de ce problème. Certains auteurs tentent, par exemple, d'établir une corrélation entre la constante de formation du complexe et le nombre de sites disponibles dans le chélatant [4]. D'autres attribuent à chaque cycle formé (CO$\diagdown\!\!\diagup$Me$\diagdown$ / $\diagdown$CH$_2$—CH$_2\diagup$N) une contribution à la valeur de la constante de formation globale du complexe: connaissant la valeur de la constante, ils en déduisent le nombre de cycles formés et par conséquent le nombre de coordination [5].

On peut également songer à rechercher l'influence de la complexation sur la position de certaines bandes d'absorption électronique du cation: même si l'on n'est pas toujours d'accord sur le nombre exact de molécules d'eau de solvatation dans la première sphère de coordination des ions Ln^{3+}, on s'accorde pour admettre que la complexation par les acides polyaminopolycarboxyliques s'accompagne d'une élimination partielle ou totale des molécules d'eau. On modifie ainsi l'environnement du cation conduisant à un déplacement de certaines bandes d'absorption de l'ion central concerné.

En étudiant le glissement de la bande d'absorption correspondant à la transition $^4I_{9/2} \rightarrow {}^2P_{1/2}$ du néodyme en fonction de la concentration en ion acétate en solution aqueuse, Choppin et al. [6] arrive à la conclusion qu'il est proportionnel au nombre de molécules d'eau remplacées par des groupements acétates. Cette méthode a également été utilisée pour obtenir des informations sur le nombre de coordination dans les complexes des lanthanides avec le TTHA [2].

Nous nous proposons, dans ce travail, d'explorer les possibilités de cette méthode pour une série de complexes 1:1, 1:2, 1:3 et mixtes formés entre trois lanthanides (praséodyme, holmium et thulium) d'une part et divers acides aminoacétiques d'autre part.

PARTIE EXPÉRIMENTALE

Des solutions 0,2 M en Pr^{3+}, Ho^{3+} ou Tm^{3+} sont préparées par attaque, par HCl concentré, des oxydes correspondants préalablement calcinés à 1200°C pendant 3—4 h. Les solutions 0.02 M en complexes 1:1, 1:2, 1:3 ou mixtes dans KCl M sont préparées en introduisant dans des jaugés de 100 ml, 10 ml d'une de ces solutions de lanthanide, 0.1 môle de KCl et une quantité stoechiométrique d'un ou de plusieurs complexants; le pH est ajusté par ajout de KOH exempt de carbonate.

Comme nous le verrons plus loin le choix du pH peut être très critique dans certains cas; il est recherché par ordinateur grâce au programme REPA, adaptation du programme COMICS [7] dont il sera question dans le prochain chapitre.

Les spectres sont enregistrés à 20°C, au moyen d'un spectrophotomètre CARY 17 en utilisant des cellules de 50 mm. La largeur spectrale est, dans tous les cas, égale ou inférieure à 0.02 nm; l'étalement spectral et la fidélité du tracé sont ajustés de façon à pouvoir mesurer la position exacte du maximum de la bande d'absorption avec une précision de l'ordre de 0.02 nm.

Recherche du milieu adequat (pH et concentrations)

Pour obtenir des données significatives, il est évidemment primordial de choisir des conditions expérimentales, c'est à dire pH et concentrations en lanthanide et en chélatants, de façon à n'avoir en solution qu'une seule espèce complexe. Considérons, dans un premier stade, les complexes 1:1, 1:2, 1:3 et mixtes non-protonés, c'est à dire des espèces pour lesquelles tous les sites sont disponsibles pour la coordination. Le choix du pH est relativement aisé lorsqu'il s'agit de complexes 1:1 non-protonés avec des ligands formant des complexes stables comme c'est le cas pour l'EDTA, le DCTA ou le DTPA; les choses sont nettement plus compliquées dans le cas des complexes 1:1 de chélatants plus faibles (IMDA) et surtout dans tous les cas des complexes 1:2, 1:3 ou mixtes où plusieurs espèces différentes peuvent exister simultanément en proportions variables suivant le pH.

Prenons, comme exemple, le cas en apparence simple des complexes $Pr(IMDA)_x$ avec $x = 1$, 2 ou 3, pour lesquels les courbes de répartition des différentes espèces sont représentées sur la Fig. 1. Si l'on désire que le spectre corresponde au complexe 1:1, on peut voir que pour une composition correspondant au rapport métal/complexant = 1/1, il est nécessaire de choisir un pH de 6.5: en dessous de ce pH, on est gêné par une quantité non négligeable de Pr^{3+} libre et de $Pr(IMDA)H^{2+}$; au dessus de cette valeur, la formation de composés hydroxylés et de complexes 1:2 et 1:3 devient importante.

Si l'on a en vue le spectre du complexe $Pr(IMDA)_2^-$, le rapport métal/complexant égal à 1/3 et un pH égal à 7.5 constituent des conditions satisfaisantes: en effet, en choisissant un rapport de 1:2, le pH le plus favorable se situerait à 8.0 mais on serait déjà gêné par des proportions non négligeables

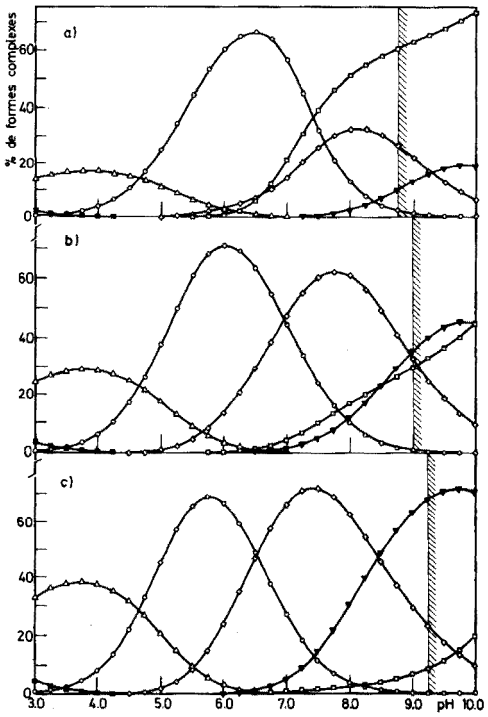

Fig. 1. Calcul et représentation graphique, par le programme REPA de la répartition, en fonction du pH, du praséodyme entre ses différents complexes avec l'acide iminodiacétique pour différentes valeurs du rapport [Métal]/[Complexant]. a. Rapport 1/1. b. Rapport 1/2. c. Rapport 1/3. △ $Pr(IMDA)H^{2+}$; □ $Pr(OH)_2^+$; ▼ $Pr(IMDA)_3^{3-}$; ○ $PrIMDA^+$; ◇ $Pr(IMDA)_2^-$. L'espèce non complexée Pr^{3+} n'est pas représentée. Les lignes verticaux indiquent le début de précipitation de $Pr(OH)_3$.

des complexes 1:1, 1:3 et hydroxylés; de plus, expérimentalement, on observe dans ces conditions, une précipitation de $Pr(OH)_3$. Pour l'obtention du spectre du complexe 1:3, $Pr(IMDA)_3^{3-}$, on choisira la composition 1/3 et un pH égal à 9.5.

Il s'agit encore ici d'un cas relativement simple si on le compare, par exemple, au système PrEDTA—HEDTA où plus de dix espèces complexes différentes peuvent coexister en proportions variables suivant le pH: PrEDTAH $PrEDTA^-$, PrHEDTA, $PrHEDTAOH^-$, PrEDTA—HEDTA-H_2^{2-}, PrEDTA—HEDTA-H^{3-}, PrEDTA—$HEDTA^{4-}$, $Pr(EDTA)_2^{5-}$, $Pr(EDTA)_2H^{4-}$, $Pr_2(EDTA)_3^{6-}$, $Pr(HEDTA)_2^{3-}$ · · · etc.

Dans ces conditions, nous avons établi un programme sur ordinateur intitulé REPA, dérivé de COMICS [7], qui permet d'obtenir les courbes de répartition en fonction de pH et des concentrations en lanthanide et en complexants, si l'on connaît les différentes constantes d'équilibre.

Choix des bandes d'absorption

Nous avons évidemment choisi, pour cette étude, des lanthanides absorbant dans le visible.

Le praséodyme possède trois bandes d'absorption dans ce domaine ($^3H_4 \rightarrow {}^3P_2$, $^3H_4 \rightarrow {}^3P_1$, $^3H_4 \rightarrow {}^3P_0$) qui se situent pour l'ion solvaté respectivement à 444.39 nm, 486.93 nm et 481.85 nm, la première étant une transition hypersensible ($\Delta j = 2$). Nous n'avons finalement considéré que la première bande: les deux autres peuvent subir, pour certains complexes, des déformations qui rendent parfois difficile le localisation exacte du maximum d'absorption. De plus, la sensibilité à la structure du complexe est beaucoup plus faible que pour la première bande en question.

Le holmium est un cas peu favorable: il possède deux transitions situées dans le visible ($^5I_8 \rightarrow {}^5G_6$ et $^5I_8 \rightarrow {}^5F_1$) respectivement à 450.90 nm et 485.39 nm pour l'ion solvaté. Pour les même raisons que précédemment, nous n'avons considéré que la première transition encore que, même dans ce cas, des épaulements et des dédoublements importants se manifestent dans certains cas et que la position du maximum de la bande est très difficile à apprécier. Le holmium a cependant été retenu parce que c'est le seul élément dans cette partie de la famille des lanthanides, à donner des résultats plus ou moins exploitables.

Dans le cas du thulium, enfin, on observe une transition intéressante située pour l'ion solvaté à 683.60 nm: la bande reste simple et bien définie dans tous les cas étudiés avec un glissement relativement important suivant la nature des complexants étudiés.

RÉSULTATS ET DISCUSSION

Les résultats du glissement $\Delta\lambda$ de la bande d'absorption en fonction du nombre de sites de coordination (NC), sont groupés dans les Tableaux 1—3 et représentés graphiquement sur les Figs. 2, 3. Ils sont intéressants à plus d'un point de vue: si l'on examine, dans le cas du praséodyme tout d'abord, l'allure générale du graphique, on observe une augmentation continue de $\Delta\lambda$ en fonction de NC suivie d'une discontinuité très marquée et d'une nouvelle augmentation entre NC = 10 et 12. Cette valeur de neuf est celle généralement avancée pour le nombre de valences coordinatives des terres cériques ou encore pour le nombre de molécules d'eau dans la première sphère de coordination de l'ion solvaté: l'augmentation régulière de $\Delta\lambda$ observée entre NC = 3 et 9 semble donc en rapport direct avec le remplacement progressif des molécules d'eau de solvatation par les groupes actifs des chélatants comme le signale Choppin et al. [6]. Au delà de NC = 9 on se serait plutôt attendu à trouver un plateau dans l'allure de l'évolution, l'accroissement du nombre de sites coordinants ne conduisant plus à une coordination supplémentaire en sphère interne. Au lieu de celà, on obtient une brusque discontinuité suivie d'une nouvelle augmentation de $\Delta\lambda$; cela signifie que l'ajout d'un coordinant supplémentaire continue d'affecter l'environnement direct

TABLEAU 1

Complexes du praséodyme. Transition $^3H_4 \rightarrow {}^3P_2$ (444.5 nm)
(Milieu KCl 1 M; t = 20°C)

Espèce étudiée	Rapport Métal/Complexant	pH	λ_{max} (nm)	$\Delta\lambda$ (nm)[a]
$PrCl_3$	—	2.00	444.39	—
PrIMDA	1/1	6.10	444.43	0.04
PrNTA	1/1	6.04	445.00	0.61
PrHEDTA	1/1	6.28	445.40	1.01
PrEDTA	1/1	5.99	445.60	1.21
PrDCTA	1/1	6.33	445.90	1.51
PrDTPA	1/1	6.06	444.14	−0.25
$Pr(IMDA)_2$	1/3	7.50	447.07	2.68
$Pr(IMDA)_3$	1/3	9.08	450.80	6.41
$Pr(NTA)_2$	1/2	8.01	449.50	5.11
PrNTA—IMDA	1/1/1	7.85	448.42	4.03
PrHEDTA—Glycine	1/1/1	9.88	445.74	1.35
PrHEDTA—IMDA	1/1/1	9.50	448.20	3.81
$Pr(HEDTA)_2$	1/2	9.94	446.57	2.18
PrEDTA—IMDA	1/1/1	9.85	449.00	4.61
PrEDTA—NTA	1/1/1	10.05	446.78	2.39
PrEDTA—HEDTA	1/1/1	10.35	447.35	2.96
$Pr(EDTA)_2$	1/2	7.33	447.82	3.43

[a]Déplacement par rapport à la position de la bande dans l'ion aqueux.

du cation métallique et à jouer un rôle dans la chélation. La valeur de neuf ne semble donc pas constituer une limite infranchissable pour la coordination des terres cériques en solution; il semble plutôt que lorsqu'on le dépasse, dans le cas des acides aminoacétiques en tout cas, tous les sites continuent à se lier mais probablement dans une structure moléculaire différente, en déplaçant éventuellement des molécules d'eau de la seconde sphère de coordination.

Si l'on examine à présent ce graphique de façon plus détaillée, on observe que les points expérimentaux se groupent sur trois droites d'après le type de complexes concernés: droite a: complexes 1:1, 1:2, 1:3 et mixtes avec des chélatants monoazotées; droite b: complexes 1:1 et mixtes avec un chélatant biazoté; droite c: complexes 1:2 ou mixtes avec, en général, deux chélatants biazotés.

Cette classification est peut-être le reflet d'une structure moléculaire particulaire à chaque type de complexes.

Remarquons enfin que les pentes des droites a et b conduisent à une augmentation moyenne de $\Delta\lambda$ de 1.1 unité pour une augmentation de 1 unité dans NC. Il nous semble que l'on peut, sur base de ces remarques, lever l'indétermination en ce qui concerne le nombre de valences coordinatives dans les complexes des lanthanides avec le HEDTA: en effet, la différence de $\Delta\lambda$ pour les complexes PrEDTA et PrDCTA due vraisemblablement à

TABLEAU 2

Complexes du holmium. Transition $^5I_8 \rightarrow {}^5G_6$ (450.8 nm)
(Milieu KCl 1 M; t = 20°C)

Espèce étudiée	Rapport Métal/Complexant	pH	λ_{max} (nm)	$\Delta\lambda$ (nm)[a]
$HoCl_3$	—	2.00	450.90	—
HoIMDA	1/1	5.33	451.40	0.50
HoNTA	1/1	5.65	452.05	1.15
HoHEDTA	1/1	6.02	entre 451.2 et 451.7	0.80 et 0.30
HoEDTA	1/1	6.15	452.20	1.30
HoDCTA	1/1	6.12	451.80	0.90
HoDTPA	1/1	6.07	451.85	0.95
$Ho(IMDA)_2$	1/3	7.32	452.55	1.65
$Ho(IMDA)_3$	1/3	9.00	entre 452 et 453	2.1 et 1.1
$Ho(NTA)_2$	1/2	7.42	453.51	2.61
HoNTA · IMDA	1/1/1	8.00	453.00	2.10
HoHEDTA—Glycine	1/1/1	9.00	452.50	1.60
HoHEDTA—IMDA	1/1/1	7.90	453.35	2.45
$Ho(HEDTA)_2$	1/2	8.78	453.3	2.40
HoEDTA—IMDA	1/1/1	9.23	entre 451.6 et 452.1	1.20 et 0.70
HoEDTA—NTA	1/1/1	9.23	entre 453 et 453.5	2.60 et 2.10
HoEDTA—HEDTA	1/1/1	10.37	453.5	2.50
$Ho(EDTA)_2$	1/2	7.27	entre 453.7 et 454	3.10 et 2.80

[a]Déplacement par rapport à la position de la bande dans l'ion aqueux.

une différence de structure liée à la rigidité plus grande du DCTA est de 0.30 nm. Entre PrEDTA et PrHEDTA, cette différence n'est que de 0.20 nm; Or, il faut rappeler qu'une augmentation du NC d'une unité provoque, dans tous les autres cas, une augmentation moyenne de 1.1 unité de $\Delta\lambda$. La faible différence que l'on observe entre PrEDTA et PrHEDTA semble donc plutôt due à la différence de structure moléculaire des deux chélatants plutôt qu'à une différence dans le nombre de valences coordinatives. Avec les terres rares cériques, le HEDTA semble donc hexacoordonné dans les complexes 1:1.

Dans les complexes doubles et mixtes, par contre, le HEDTA comparé à l'EDTA, paraît être pentacoordiné: contrairement aux conclusions de Mackey et Powell [8], la fonction hydroxyle semble moins active que les fonctions carboxyliques ou aminées dans la complexation des lanthanides.

Pour terminer, signalons la situation très particulière qu'occupe le complexe PrDTPA.

Nous ne nous attarderons guère au cas du holmium: le repérage précis du maximum d'absorption est souvent rendu difficile par les déformations que subit la bande. L'allure générale du graphique se traduit néanmoins par une

TABLEAU 3

Complexes du thulium. Transition $^3H_6 \rightarrow {}^3H_4$ (682.5 nm)
(Milieu KCl 1 M; t = 20°C)

Espèce étudiée	Rapport Métal/Complexant	pH	λ_{max} (nm)	$\Delta\lambda$ (nm)[a]
$TmCl_3$	—	2.00	683.50	—
TmIMDA	1/1	5.75	685.34	1.84
TmNTA	1/1	6.25	687.04	3.54
TmHEDTA	1/1	5.87	689.15	5.65
TmEDTA	1/1	5.65	690.28	6.78
TmDCTA	1/1	5.80	685.54	2.04
TmDTPA	1/1	6.50	690.18	6.68
$Tm(IMDA)_2$	1/3	6.58	688.83	5.33
$Tm(NTA)_2$	1/2	7.63	689.12	5.62
TmNTA—IMDA	1/1/1	7.82	689.89	6.39
TmHEDTA—Glycine	1/1/1	9.04	689.51	6.01
TmHEDTA—IMDA	1/1/1	9.04	691.13	7.63
TmHEDTA—NTA	1/1/1	10.60	690.24	6.74
$Tm(HEDTA)_2$	1/2	9.15	688.05	4.55
TmEDTA—IMDA	1/1/1	9.85	690.00	6.50
TmEDTA—NTA	1/1/1	10.00	690.29	6.79
TmEDTA—HEDTA	1/1/1	10.30	688.44	4.94
$Tm(EDTA)_2$	1/4	7.66	688.74	5.24

[a]Déplacement par rapport à la position de la bande dans l'ion aqueux.

augmentation continue de $\Delta\lambda$ avec NC entre 3 et 8 suivie d'une discontinuité et d'une nouvelle augmentation pour NC compris entre 9 et 12. On notera également la position du complexe HoHEDTA comparée à celle de HoEDTA et enfin le fait que le déplacement provoqué par HoDCTA est inférieur à celui provoqué par HoEDTA à l'inverse de ce que l'on observe dans le cas du praséodyme.

Le thulium se présente de façon beaucoup plus favorable et si l'on commenc par examiner l'allure générale du graphique, on peut constater que $\Delta\lambda$ augmente régulièrement en fonction de NC mais cette fois, comme pour le holmium et contrairement au praséodyme, cette augmentation continue s'arrête à NC = 8. Elle est suivie d'une discontinuité et d'une nouvelle augmentation entre NC = 9 et 12. La pente des droites pour NC > 9 est cependant nettement plus faible que celle observée pour le praséodyme.

En suivant le même raisonnement que précédemment, il semble que la valence coordinative de huit constitue une limite pour une structure donnée mais de nouveau, cette valeur de huit ne semble pas constituer une limite absolue puisque, au delà de cette valeur, on observe une nouvelle augmentation de $\Delta\lambda$ en fonction de NC.

Notons également que la discontinuité est beaucoup plus importante pour les complexes contenant deux chélatants biazotés que pour les complexes mixtes où un seul chélatant biazoté.

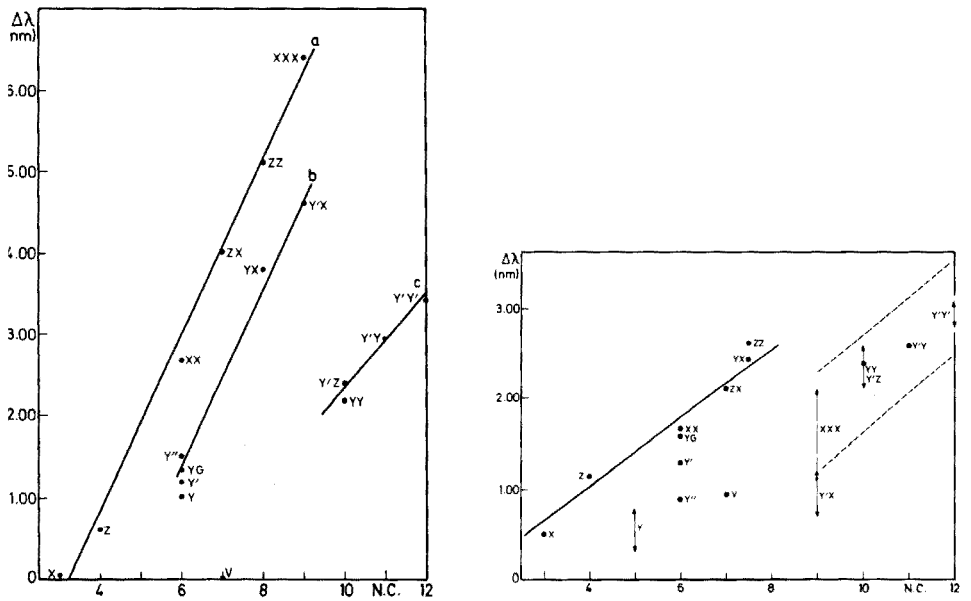

Fig. 2. Complexes du praséodyme. Transition $^3H_4 \rightarrow {}^3P_2$. Déplacement, par rapport à sa position dans l'ion solvaté, du maximum de la bande d'absorption pour différentes entités complexes 1:1, 1:2, 1:3 et mixtes formées entre le cation métallique et certains acides aminoacétiques en fonction du nombre de sites de coordination (NC). X = IMDA (acide iminodiacétique), Z = NTA (acide nitrilotriacétique), Y = HEDTA (acide hydroxyéthyléthylènediaminetriacétique), Y′ = EDTA (acide éthylènediaminetétraacétique), Y″ = DCTA (acide diaminecyclohexanetétraacétique), G = Glycine, V = DTPA (acide diéthylènetriaminepentaacétique).

Fig. 3. Complexes du holmium. Transition $^5I_8 \rightarrow {}^5G_6$. Même légende et conventions que la Fig. 2.

Qu'en est-il du comportement de HEDTA vis à vis des terres yttriques? On peut se rendre compte (Fig. 4) que le glissement provoqué par la formation du complexe du thulium avec l'EDTA est cette fois beaucoup plus important que celui observé avec le HEDTA. La droite qui joint les points correspondant à ces deux complexes a d'ailleurs exactement la même pente que celle qui joint tous les autres points correspondant aux complexes avec NC $\leqslant$ 8. Il semble donc cette fois que contrairement à ce que nous avons observé pour le praséodyme, pour des raisons d'encombrement stérique plus important, HEDTA est pentacoordiné, la fonction hydroxyle ne paraissant pas suffisamment liante pour déplacer une molécule d'eau de la sphère interne du thulium.

Nous terminerons cet examen en signalant la position très particulière occupée par le DCTA: alors que le praséodyme subit un glissement légèrement supérieur à celui de l'EDTA, que la situation du holmium est inversée, le cas du thulium est totalement différent: la contraction du rayon ionique ne permet plus à la molécule de DCTA d'envelopper suffisamment l'ion central par suite de la plus grande rigidité du DCTA comparé à l'EDTA.

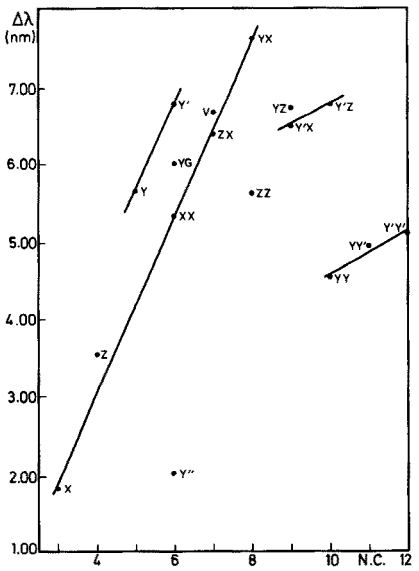

Fig. 4. Complexes du thulium. Transition $^3H_6 \rightarrow {}^3H_4$. Même légende et conventions que la Fig. 2.

On peut sans doute se demander, si dans l'examen des résultats, il n'est pas préférable de suivre la démarche inverse, à l'instar de certains auteurs, à savoir porter le déplacement pour un complexe donné sur la droite obtenue pour NC $\leqslant$ 9 ou 8 suivant le cas et, en déduire le nombre de sites intervenant dans la chélation.

Cette démarche exige que l'on connaisse avec certitude le nombre de coordination dans les complexes choisis pour tracer la droite de référence; d'autre part, elle postule que le glissement du maximum d'absorption dépend uniquement du nombre de coordination fixé par les chélatants et en aucune façon de la structure et en particulier de la symétrie et des distances entre ion central et sites de coordination. Par ailleurs, comment expliquer qu'en passant du complexe 1:2 du HEDTA (NC = 10) au complexe mixte EDTA—HEDTA (NC = 11) puis au complexe 1:2 de l'EDTA (NC = 12) on continue à observer un accroissement important du $\Delta\lambda$, sans admettre que le nombre de sites coordinés à l'ion central est supérieur à neuf.

Enfin, si l'on applique ce raisonnement au thulium, on trouve pour les complexes $Tm(HEDTA)_2$, TmEDTA—HEDTA et $Tm(EDTA)_2$ des nombres de coordination de 4, 4.3, 4.5 c'est à dire des valeurs inférieures à celles observées pour les complexes 1:1 correspondants à savoir TmEDTA et TmHEDTA.

Il semble donc certain que du point de vue spectroscopique la structure du complexe joue un rôle non moins important que le nombre de sites de liaison.

BIBLIOGRAPHIE

1 G. R. Choppin, Pure Appl. Chem., 27 (1971) 23.
2 R. B. Gayhart et T. Moeller, J. Inorg. Nucl. Chem., 39 (1977) 49.
3 E. Merciny, B. Gilbert et G. Duyckaerts, Bull. Soc. Chim. Belg., 80 (1971) 617.
4 J. M. Gatez, E. Merciny et G. Duyckaerts, Anal. Chim. Acta, à paraître.
5 A. B. Shalinets, Radiokhimiya, 14 (1972) 20.
6 G. R. Choppin, D. E. Henrie et K. Buijs, Inorg. Chem., 5 (1966) 1743.
7 D. D. Perrin et I. G. Sayce, Talanta, 14 (1967) 833.
8 J. L. Mackey et J. E. Powell, Proc. 2nd Conf. Rare Earth Res., Gorden et Breach, New York, 1962, p. 47.

Analytica Chimica Acta, 93 (1977) 239—247
© Elsevier Scientific Publishing Company, Amsterdam — Printed in The Netherlands

VARIATIONS OF FLUORESCENCE EFFICIENCIES OF 9-(10H)-ACRIDONE AND ITS 4-METHOXY DERIVATIVE WITH pH. EXCITED-STATE PROTON TRANSFER IN VERY WEAK ACIDS AND BASES

STEPHEN G. SCHULMAN* and ROY J. STURGEON§

College of Pharmacy, University of Florida, Gainesville, Florida 32610 (U.S.A.)

(Received 23rd March 1977)

SUMMARY

Acridone and its 4-methoxy derivative behave as very weak acids in their lowest excited singlet states. This behavior is shown to account for the pH dependences of their fluorescence spectra in alkaline solutions. 4-Methoxyacridone is also a very weak base in its lowest excited singlet state, which results in a pH dependence of its fluorescence spectrum in dilute acidic media. Acridone, although functioning as a very weak base in its lowest excited singlet state, in acidic ethanolic water, does not demonstrate excited-state proton exchange in acidic "pure" water. This suggests selective solvation by ethanol in the mixed solvent.

The electronic excitation of an aromatic acid may be followed by protolytic dissociation during the lifetime of the lowest excited singlet state of the acid [1]. Moreover, if the lifetime of the excited conjugate base of the excited acid is sufficiently long, reprotonation of the excited base may also occur [2]. These processes cause the fluorescence intensity of the directly excited acid to demonstrate a dependence on pH which differs from the way that it varies with pH, as a result of ground-state ionization [2].

For a dilute acid HA, the fluorescence intensity is given (provided that the fluorescence of the conjugate base does not overlap that of the conjugate acid at the emission wavelength) by

$$F_{HA} = 2.3\ \phi^0_{HA}\ I_0\ \epsilon_{HA}[HA]l \qquad (1)$$

where ϕ^0_{HA} is the fluorescence efficiency of HA, ϵ_{HA} is its molar absorptivity at the wavelength of excitation, [HA] is its equilibrium concentration (in the ground state), I_0 is the intensity of exciting light at the wavelength of excitation and l is the optical depth of the sample. Ground-state ionization of the acid causes [HA] to vary according to

$$[HA] = C_A\ [H_3O^+]/([H_3O^+] + K_a) \qquad (2)$$

§Present address: College of Pharmacy, University of South Carolina, Columbia, South Carolina 29206, U.S.A.

where C_A is the formal concentration of the acid, K_a is its dissociation constant, in the ground state, and $[H_3O^+]$ is the hydrogen ion concentration (or, more appropriately, activity) at which F_{HA} is measured. Then

$$F_{HA} = 2.3\,\phi^0_{HA}\,I_0\,\epsilon_{HA}\,C_A\,[H_3O^+]l/([H_3O^+] + K_a) \tag{3}$$

When $[H_3O^+] \gg K_a$ ($pH \leqslant pK_a - 2$), F_A depends only on C_A, according to

$$F^0_{HA} = 2.3\,\phi^0_{HA}\,I_0\,\epsilon_{HA}\,C_A\,l \tag{4}$$

where F^0_{HA} is the pH-independent fluorescence intensity of HA. If HA* (the excited acid) is a stronger acid than HA, F_{HA} will depend on pH but, in this case, it is the fluorescence efficiency ϕ_{HA} which varies with pH;

$$F_{HA} = 2.3\,\phi_{HA}\,I_0\,\epsilon_{HA}\,C_A\,l \tag{5}$$

In this case, $\phi_{HA} = \phi^0_{HA}$ and $F_{HA} = F^0_{HA}$ only when the rate of reprotonation of the excited conjugate base is much greater than the rate of dissociation of HA*. Dividing eqn. (5) by eqn. (4) gives

$$F_{HA}/F^0_{HA} = \phi_{HA}/\phi^0_{HA} \tag{6}$$

The actual form of the pH dependence of ϕ_{HA} depends on the mechanism of proton-transfer in the lowest excited singlet state (provided that equilibrium is not fully established). In aqueous solutions of pH 0—14, in the absence of buffer ions, two mechanisms of proton-transfer are possible when the acid is directly excited [3].

(a) H_2O is the proton-acceptor and H_3O^+ is the proton-donor

$$HA^* + H_2O \underset{\overleftarrow{k}_A}{\overrightarrow{k}_A} A^{-}* + H_3O^+$$

In this case, it has been shown [2] that ϕ_{HA} varies with $[H_3O^+]$ according to

$$\frac{\phi_{HA}}{\phi^0_{HA}} = \frac{1 + \overleftarrow{k}_A\,\tau_0'\,[H_3O^+]}{1 + \overrightarrow{k}_A\,\tau_0 + \overleftarrow{k}_A\,\tau_0'\,[H_3O^+]} \tag{7}$$

where τ_0 and τ_0' are the lifetimes of the lowest excited singlet states of HA* and its conjugate base A^-*, respectively, and $\vec{k}_A$ and $\overleftarrow{k}_A$ are, in this case, the rate constants for dissociation of directly excited HA* (pseudo-first order) and reprotonation of A^-* (second order). It should be noted that mechanism (a) corresponds to moderately strong acids where H_2O is a strong enough base to effect deprotonation of HA*. Moreover, if mechanism (a) is operative, excited-state proton-transfer will be observed only if HA* dissociates during a time which is similar to, or much faster than, deactivation of HA* by fluorescence and non-radiative decay (i.e., $\vec{k}_A^{-1} \leqslant \tau_0$). However, if this condition is fulfilled, the back-reaction need not occur during τ_0' for the effect of excited-state dissociation to be apparent in the fluorimetric pH titration

of HA*. In the latter circumstance, ϕ_{HA}/ϕ^0_{HA} will be independent of pH but will not be equal to 1

$$(\phi_{HA}/\phi^0_{HA})_{const.} = 1/(1 + \vec{k}_A \tau_0) \tag{8}$$

The conjugate base A^-* will show a dependence of its relative fluorescence efficiency ($\phi_{A^-}/\phi^0_{A^-}$) on $[H_3O^+]$ according to

$$\phi_{A^-}/\phi^0_{A^-} = \vec{k}_A \tau_0/(1 + \vec{k}_A \tau_0 + \overleftarrow{k}_A \tau_0' [H_3O^+]) \tag{9}$$

and if the rate of reprotonation of A^-* is very slow,

$$(\phi_{A^-}/\phi^0_{A^-})_{const.} = \vec{k}_A \tau_0/(1 + \vec{k}_A \tau_0) \tag{10}$$

(b) OH^- is the proton-acceptor and H_2O is the proton-donor

Very weak acids which, in water, are deprotonated by OH^- and undergo proton-exchange according to

$$HA^* + OH^- \underset{\overleftarrow{k}_A}{\overset{\vec{k}_A}{\rightleftharpoons}} A^-* + H_2O$$

demonstrate a different dependence on pH than in the case represented by mechanism (a). If k_f and k_f' are the rate constants for fluorescence of HA* and A^-*, k_d and k_d' are the unimolecular rate constants for non-radiative deactivation of HA* and A^-*, and $\vec{k}_A$ and $\overleftarrow{k}_A$ are now the bimolecular rate constant for deprotonation of HA* by OH^- and the pseudo-first-order rate constant for protonation of A^-* by water, respectively; if no processes other than these occur during the lifetimes of HA* and A^-*, the rates of disappearance of HA* and A^-* from the excited state are, under steady-state conditions

$$-\mathrm{d}\,[HA^*]/\mathrm{d}t = (k_f + k_d + \vec{k}_A [OH^-])\,[HA^*] - \overleftarrow{k}_A [A^-*] \tag{11}$$

and

$$-\mathrm{d}\,[A^-*]/\mathrm{d}t = (k_f' + k_d' + \overleftarrow{k}_A)\,[A^-*] - \vec{k}_A\,[HA^*]\,[OH^-] \tag{12}$$

But $k_f + k_d = 1/\tau_0$ and $k_f' + k_d' = 1/\tau_0'$ where τ_0 and τ_0' are the mean lifetimes of HA* and A^-*, respectively, so that

$$-\mathrm{d}\,[HA^*]/\mathrm{d}t = (1/\tau_0 + \vec{k}_A [OH^-])\,[HA^*] - \overleftarrow{k}_A [A^-*] \tag{13}$$

$$-\mathrm{d}\,[A^-*]/\mathrm{d}t = (1/\tau_0' + \overleftarrow{k}_A)\,[A^-*] - \vec{k}_A [HA^*]\,[OH^-] \tag{14}$$

If only HA is directly excited, we may, at time $t = 0$, set $[HA^*] = 1$ and $[A^-*] = 0$ and at time $t = \infty$, $[HA^*] = 0$ and $[A^-*] = 0$, then

$$\int_1^0 -\mathrm{d}\,[HA^*] = (1/\tau_0 + \vec{k}_A [OH^-]) \int_0^\infty [HA^*(t)]\,\mathrm{d}t - \overleftarrow{k}_A \int_0^\infty [A^-*(t)]\,\mathrm{d}t \tag{15}$$

$$\int_0^0 -\mathrm{d}\,[A^{-}*] = (1/\tau_0' + \overleftarrow{k}_A) \int_0^\infty [A^{-}*(t)]\,\mathrm{d}t - \vec{k}_A\,[OH^-] \int_0^\infty [HA*(t)]\,\mathrm{d}t \tag{16}$$

with the substitutions [2]

$$\int_0^\infty [HA*(t)]\,\mathrm{d}t = \tau_0\,\phi_{HA}/\phi^0_{HA} \tag{17}$$

and

$$\int_0^\infty [A^{-}*(t)]\,\mathrm{d}t = \tau_0'\,\phi_{A^-}/\phi^0_{A^-} \tag{18}$$

eqns. (15) and (16) can be integrated and rearranged to

$$\phi_{HA}/\phi^0_{HA} = [1 + \overleftarrow{k}_A\,\tau_0'\,(\phi_{A^-}/\phi^0_{A^-})]/(1 + \vec{k}_A\,\tau_0\,[OH^-]) \tag{19}$$

$$\phi_{A^-}/\phi^0_{A^-} = (1 + \overleftarrow{k}_A\,\tau_0')\,(\phi_{A^-}/\phi^0_{A^-})/\vec{k}_A\,\tau_0\,[OH^-] \tag{20}$$

respectively. Finally, combination of eqns. [19] and [20] gives

$$\phi_{HA}/\phi^0_{HA} = (1 + \overleftarrow{k}_A\,\tau_0')/(1 + \vec{k}_A\,\tau_0\,[OH^-] + \overleftarrow{k}_A\,\tau_0') \tag{21}$$

and

$$\phi_{A^-}/\phi^0_{A^-} = \vec{k}_A\,\tau_0\,[OH^-]/(1 + \vec{k}_A\,\tau_0\,[OH^-] + \overleftarrow{k}_A\,\tau_0') \tag{22}$$

In this case, excited-state proton-transfer will be observed only if $\vec{k}_A\,[OH^-]$ is comparable to or much greater than $1/\tau_0$. Since this depends always on $[OH^-]$ there will never be a flat, pH-independent region in the fluorimetric titration curve such as that in the case of a moderately strong excited acid (eqn. 8). Moreover, if the rate of the back-reaction (protonation by water) is very slow ($1/\tau_0' \gg \overleftarrow{k}_A$) by comparison with $1 + \vec{k}_A\,\tau_0\,[OH^-]$, eqn. (21) reduces to

$$\phi_{HA}/\phi^0_{HA} = 1/(1 + \vec{k}_A\,\tau_0\,[OH^-]) \tag{23}$$

which is the Stern—Volmer equation for dynamic quenching of the fluorescence of HA* by OH^-.

A rather interesting contrast between mechanisms (a) and (b) can be made, in that eqns. (7) and (8) permit the explicit determination, by graphical and analytical methods, of the rate constants $\vec{k}_A$ and $\overleftarrow{k}_A$ and therefore, allow the calculation of the excited-state equilibrium constant $K_a^* = \vec{k}_A/\overleftarrow{k}_A$. However, eqn. (21), if rearranged to

$$\frac{1 - \phi_{HA}/\phi^0_{HA}}{\phi_{HA}/\phi^0_{HA}} = \frac{\vec{k}_A\,\tau_0\,[OH^-]}{(1 + \overleftarrow{k}_A\,\tau_0')} \tag{24}$$

permits evaluation of $\vec{k}_A\,\tau_0/(1 + \overleftarrow{k}_A\,\tau_0')$, but $\vec{k}_A$ and $\overleftarrow{k}_A$ cannot be explicitly determined unless one of the two or the value K_a^* is determined independently

It should be noted that excited-state proton-exchange in bases can be described fluorimetrically by equations similar to (7—10) and (21) and (22).

Thus, the hydrolysis of a moderately strong base [4], according to

$$B^* + H_2O \underset{\overleftarrow{k}_B}{\overset{\vec{k}_B}{\rightleftharpoons}} BH^{+*} + OH^-$$

shows a dependence of the fluorescence efficiencies of B and BH^+ upon OH^-,

$$\phi_B/\phi_B^0 = (1 + \overleftarrow{k}_B \tau_0' [OH^-])/(1 + \vec{k}_B \tau_0 + \overleftarrow{k}_B \tau_0' [OH^-]) \quad (25)$$

and

$$\phi_{BH^+}/\phi_{BH^+}^0 = \vec{k}_B \tau_0/(1 + \vec{k}_B \tau_0 + \overleftarrow{k}_B \tau_0' [OH^-]) \quad (26)$$

where τ_0 and τ_0' now correspond to B* and BH^{+*} and $\vec{k}_B$ is the pseudo-first order rate constant for hydrolysis of B* while $\overleftarrow{k}_B$ is the second-order rate constant for deprotonation of BH^{+*}. When $\overleftarrow{k}_B [OH^-] \ll 1/\tau_0'$, eqns. (25) and (26) reduce to

$$(\phi_B/\phi_B^0)_{const.} = 1/(1 + \vec{k}_B \tau_0) \quad (27)$$

and

$$(\phi_{BH^+}/\phi_{BH^+}^0)_{const.} = \vec{k}_B \tau_0/(1 + \vec{k}_B \tau_0') \quad (28)$$

in which case the fluorescence efficiencies of B* and BH^{+*} are independent of pH.

The protonation of a very weak base by H_3O^+ and dissociation of its conjugate acid, BH^+ by H_2O, demonstrate variations of fluorescence efficiencies with $[H_3O^+]$ according to

$$\phi_B/\phi_B^0 = (1 + \overleftarrow{k}_B \tau_0')/(1 + \vec{k}_B \tau_0 [H_3O^+] + \overleftarrow{k}_B \tau_0') \quad (29)$$

and

$$\phi_{BH^+}/\phi_{BH^+}^0 = \vec{k}_B \tau_0 [H_3O^+]/(1 + \vec{k}_B \tau_0 [H_3O^+] + \overleftarrow{k}_B \tau_0') \quad (30)$$

from which $\vec{k}_B \tau_0/(1 + \overleftarrow{k}_B \tau_0')$ can be evaluated but not $\vec{k}_B$ and $\overleftarrow{k}_B$ explicitly. In eqns. (29) and (30), $\vec{k}_B$ is the bimolecular rate constant for protonation by H_3O^+ and $\overleftarrow{k}_B$ the psuedo-first order rate constant for deprotonation by H_2O. When $\overleftarrow{k}_B \tau_0'$ is very small, eqn. (29) becomes

$$\phi_B/\phi_B^0 = 1/(1 + \vec{k}_B \tau_0 [H_3O^+]) \quad (31)$$

which is the Stern—Volmer equation for quenching of the fluorescence of B* by H_3O^+.

In the present study, the pH dependences of the fluorescence spectra of acridone, a very weak acid, and 4-methoxyacridone, a very weak ampholyte, in their lowest excited singlet states, were examined.

EXPERIMENTAL

Chemicals

9-(10H)-Acridone and 4-methoxy-9-(10H)-acridone (Aldrich Chemical Company, Milwaukee, Wisconsin) were recrystallized several times from absolute ethanol.

The solutions for measurement of fluorescence and absorption spectra were 1×10^{-5} M in 9-(10H)-acridone or its 4-methoxy derivative and had their pH adjusted with $HClO_4$ or NaOH solution. The use of standard buffer solutions was avoided because high concentrations of buffer ions complicate the kinetic treatment of the fluorimetric titration data [3].

Apparatus

Fluorescence spectra were taken on a Perkin-Elmer MPF-2A fluorescence spectrophotometer whose monochromators were calibrated against the xenon line emission spectrum and whose output was corrected for instrumental response by means of a rhodamine-B quantum counter. A Beckman DB-GT spectrophotometer and an Orion 801 pH meter with a Corning silver—silver chloride—glass combination electrode were also used. Lifetimes of the lowest excited singlet states (fluorescence lifetimes) were measured on nitrogen-purged solutions, on a TRW nanosecond decay-time fluorimeter, with an 18-W pulsed deuterium lamp (pulse time, 1.6 ns), interfaced with a Tektronix 556 dual-beam oscilloscope by means of two 1A1 plug-in, dual-channel amplifiers. With this apparatus fluorescence lifetimes of duration $\geqslant 1.7$ ns, could be measured.

RESULTS AND DISCUSSION

The spectral features, including fluorescence decay times, of the cations, neutral molecules and anions derived from 9-(10H)-acridone and 4-methoxy-9-(10H)-acridone (hereafter called acridone and 4-methoxyacridone, respectively) are presented in Table 1. The fluorimetric pH titrations of acridone and 4-methoxyacridone are shown in Fig. 1. Also presented in Table 1 are the ground-state dissociation constants of acridone [5, 6] and 4-methoxyacridone (this work).

The inflection point of the fluorimetric pH titration of acridone, in acidic solution (H_0-0.4), nearly coincides with the pK_a value for the ground-state equilibrium between the cation and neutral molecule (pK_{CN}) of acridone [5]. Consequently, it may be concluded that protonation of acridone by H_3O^+ is too slow to occur during the lifetime of its excited singlet state. Interestingly, it was found by Kokobun [7] that in 50% aqueous ethanol, protonation of acridone did occur during the lifetime of the excited state. This may indicate that selective solvation by ethanol, which is a weaker hydrogen bond donor than water, may enhance the basicity, and hence the rate of protonation of excited acridone.

TABLE 1

Long wavelength absorption ($\bar{\nu}_a$), fluorescence maxima ($\bar{\nu}_f$) and fluorescent decay times (τ_0) of acridone, 4-methoxyacridone and their corresponding cations and anions

	$\bar{\nu}_a$ ($cm^{-1} \times 10^{-4}$)	$\bar{\nu}_f$ ($cm^{-1} \times 10^{-4}$)	τ_0 (sec $\times 10^9$)
Acridone			
Cation	2.39 (O—O band)	2.30 (O—O band)	33.8 ± 0.3
$pK_{CN} = -0.3$	2.51 (max.)[a]	2.19 (max.)[a]	
Neutral molecule	2.49 (O—O band)	2.40 (O—O band)	12.3 ± 0.4
$pK_{NA} = 12.8$	2.61 (max.)[a]	2.27 (max.)[a]	
Anion	2.32 (O—O band)	2.25 (O—O band)	15.8 ± 0.3
	2.46 (max.)[a]	2.14 (max.)[a]	
4-Methoxyacridone			
Cation	2.32 (O—O band)		8.9 ± 0.3
$pK_{CN} = -0.8$	2.42 (max.)[a]	2.00 (max.)[b]	
Neutral molecule	2.48 (O—O band)		27.3 ± 0.7
$pK_{NA} = 12.7$	2.58 (max.)[a]	2.22 (max.)[b]	
Anion	2.34 (O—O band)	2.25 (O—O band)	33.6 ± 0.5
	2.46 (max.)[a]	2.14 (max.)[a]	

[a]In the species demonstrating vibrationally structured spectral bands, the maximum occurred, in each case, at the second vibronic sub-band.
[b]The cation and neutral molecule derived from 4-methoxyacridone demonstrate unstructured fluorescence bands.

In alkaline solutions, the inflection regions of the fluorimetric titration curves of acridone and 4-methoxyacridone occur at pH lower than pH = pK_{NA}. Moreover, in acidic solutions, the inflection region of the fluorimetric titration curve of 4-methoxyacridone occurs at about 4 pH units higher than pH = pK_{CN}. Both observations indicate excited-state proton-transfer with 4-methoxyacridone acting as a very weak base in acidic solutions and both compounds acting as very weak acids in alkaline solutions. Eight points taken from each

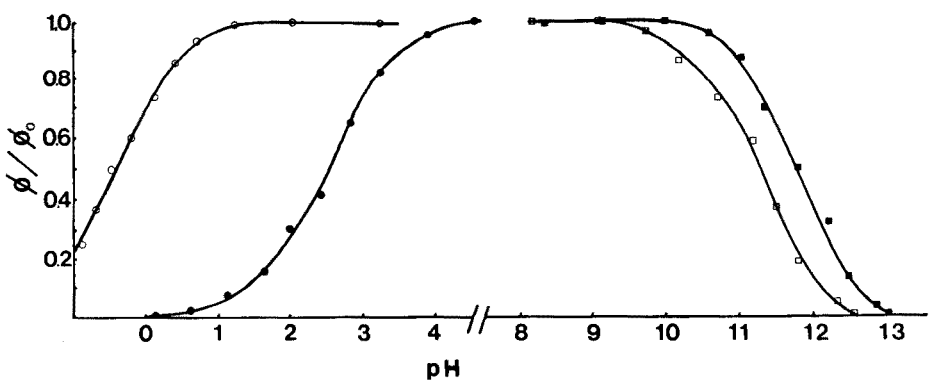

Fig. 1. Variations of relative fluorescence efficiencies of 1.0×10^{-5} M solutions of acridone in aqueous acidic (—○—) and alkaline (—□—) solutions and 4-methoxyacridone in aqueous acidic (—●—) and alkaline (—■—) solutions.

of the fluorimetric titration curves represented in Fig. 1 were used to calculate $\vec{k}_A\tau_0/(1 + \overleftarrow{k}_A\tau_0')$ for acridone and 4-methoxyacridone (from eqn. 24) and $\vec{k}_B\tau_0/(1 + \overleftarrow{k}_B\tau_0')$ for 4-methoxyacridone (from eqn. 29). These results are presented in Table 2.

At prototropic equilibrium, in the lowest excited singlet state, for acridone and 4-methoxyacridone

$$\vec{k}_A/\overleftarrow{k}_A = [A^-{}^*]/[HA^*][OH^-] = K_{NA}{}^*/K_W \quad (32)$$

where $K_W = 1.00 \times 10^{-14}$ (the ion-product of water); and for 4-methoxyacridone

$$\overleftarrow{k}_B/\vec{k}_B = [B^*][H_3O^+]/[BH^+{}^*] = K_{CN}{}^* \quad (33)$$

$pK_{NA}{}^*$ and $pK_{CN}{}^*$ can be estimated from the shifting of the absorption and fluorescence spectral maxima accompanying protonation or dissociation (even when proton-exchange in the excited state does not occur) and pK_{NA} and pK_{CN}, the respective ground state dissociation constants [1]. At 25°C, for acridone and 4-methoxyacridone, in alkaline solutions

$$pK_{NA} - pK_{NA}{}^* = 2.10 \times 10^{-3}\,(\bar{\nu}_N - \bar{\nu}_A) \quad (34)$$

where $\bar{\nu}_N$ and $\bar{\nu}_A$ are the averages of the absorption and fluorescence maxima of the neutral and anionic species, and for 4-methoxyacridone, in acidic solutions

$$pK_{CN} - pK_{CN}{}^* = 2.10 \times 10^{-3}\,(\bar{\nu}_C - \bar{\nu}_N) \quad (35)$$

where $\bar{\nu}_C$ is the average of the absorption and fluorescence maxima of the cation. The values of $pK_{NA}{}^*$ and $pK_{CA}{}^*$ calculated from eqns. (34) and (35), are presented in Table 2. From these values $K_{NA}{}^*$ for acridone and 4-methoxyacridone were found to be 1.3×10^{-10} and 3.2×10^{-10}, respectively, and $K_{CN}{}^*$ was found to be 6.3×10^{-4} for 4-methoxyacridone. Substitution of these values of $K_{NA}{}^*$ into eqns. (32) and (24), and of $K_{CN}{}^*$ into eqns. (33) and (29), gave the values of $\vec{k}_A$, $\overleftarrow{k}_A$, $\vec{k}_B$ and $\overleftarrow{k}_B$ in Table 2.

According to Table 2, the rate of proton abstraction, by OH^-, from excited acridone, is diffusion-controlled [8]. However, the rate constant for this

TABLE 2

Parameters of prototropic reactivity of excited acridone and 4-methoxyacridone

	Acridone	4-Methoxyacridone		Acridone	4-Methoxyacrido
$\bar{\nu}_C$ ($cm^{-1} \times 10^{-4}$)	2.35	2.21	$\overleftarrow{k}_B$ (s^{-1})	—[a]	7.4×10^6
$\bar{\nu}_N$ ($cm^{-1} \times 10^{-4}$)	2.44	2.40	pK_{NA}^*	9.9	9.5
$\bar{\nu}_A$ ($cm^{-1} \times 10^{-4}$)	2.30	2.25	$\vec{k}_A\tau_0/(1 + \overleftarrow{k}_A\tau_0')$	5.5 ± 0.4	1.7 ± 0.1
pK_{CN}^*	1.6	3.2	$\vec{k}_A$ (M^{-1} s^{-1})	4.8×10^{10}	6.4×10^9
$\vec{k}_B\tau_0/(1 + \overleftarrow{k}_B\tau_0')$	—[a]	3.0 ± 0.3	$\overleftarrow{k}_A$ (s^{-1})	3.7×10^6	2.0×10^5
$\vec{k}_B$ (M^{-1} s^{-1})	—[a]	1.2×10^{10}			

[a]Excited-state proton-exchange in acridone was observed, only between the neutral molecule and anion.

process ($\vec{k}_A$) in 4-methoxyacridone is almost an order of magnitude smaller, reflecting the acidity-weakening influence of the 4-methoxy group in the excited state. It should be noted that $\overleftarrow{k}_A$ for the 4-methoxy derivative is also considerably smaller than that for acridone. This suggests that the electron-donating electromeric effect of the 4-methoxy group may be insignificant in the excited anionic species, a hypothesis which is supported by the fact that the spectral maxima of the anions are almost identical in acridone and its 4-methoxy derivative. It is possible that the inductive or field effect (electron-withdrawing) of the oxygen atom of the 4-methoxy group is responsible for diminishing the basicity of the nitrogen atom of the 4-methoxyacridone anion relative to that of the nitrogen atom of the acridone anion.

The protonation of excited 4-methoxyacridone is characterized by a $\vec{k}_B$ which is almost large enough to indicate a diffusion-limited process [8]. No doubt the failure of acridone to become protonated, in the excited state, while 4-methoxyacridone does, is due predominantly to a small $\vec{k}_B$, a conclusion which is suggested by the small value of K_{CN}* of acridone compared to that of 4-methoxyacridone.

The authors express their appreciation to Ms. Rebecca McKinley for typing the manuscript.

REFERENCES

1 T. Förster, Z. Phys. Chem. N.F., 54 (1952) 42.
2 A. Weller, Z. Elektrochem., 56 (1952) 662.
3 S. G. Schulman and A. C. Capomacchia, J. Phys. Chem., 79 (1975) 1337.
4 A. Weller, Z. Elektrochem., 61 (1957) 956.
5 A. Albert and J. N. Phillips, J. Chem. Soc., (1956) 1294.
6 E. Kalatzis, J. Chem. Soc. B, (1969) 96.
7 H. Kokobun, Z. Elektrochem., 62 (1958) 599.
8 M. V. Smoluchowski, Z. Phys. Chem., 92 (1917) 129.

Analytica Chimica Acta, 93 (1977) 249—253
©Elsevier Scientific Publishing Company, Amsterdam — Printed in The Netherlands

EXTRACTION—SPECTROPHOTOMETRIC DETERMINATION OF RHENIUM WITH 5,6-DIPHENYL-2,3-DIHYDRO(ASYM)TRIAZINE-3-THIONE

A. K. MAJUMDAR*, S. K. BHOWAL and B. DATTA

Department of Chemistry, Jadavpur University, Calcutta-700032 (India)

(Received 30th March 1977)

SUMMARY

The reagent 5,6-diphenyl-2,3-dihydro(asym)triazine-3-thione produces a green complex with perrhenate in hydrochloric acid medium in presence of stannous chloride. The complex on extraction in chloroform shows a peak at 685 nm. The system obeys Beer's law from 2—10 p.p.m. of rhenium and its molar absorptivity is $1.53 \cdot 10^{-4}$. It tolerates the presence of a large number of ions, including Mo^{6+} and W^{6+}. Job's and molar ratio methods suggest that rhenium and the reagent are present in the ratio 1:2 and the isolated complex is of the same composition, i.e. $ReO(C_{15}H_{10}N_3S)_2$.

Of the many spectrophotometric methods for rhenium, those utilizing thiocyanate, some sulphur-bearing organic reagents and some oximes are of particular importance [1—16]. Some of these reagents suffer from lack of sensitivity [9—13] and/or have narrow acidity ranges [1—8]. Although a few oxime derivatives [5—8, 14, 15] are sensitive in their colour reactions towards rhenium, the amount of reagent required for full colour development may be very large [6] and the methods lack selectivity. In the methods based on the use of thiocyanate [16] (the commonest reagent for rhenium), oximes and most of the other reagents mentioned above, prior separation of molybdenum, a metal usually associated with rhenium, by ion-exchange or solvent extraction is essential. Moreover, data regarding the composition and stability constants of the complexes are conspicuous by their absence in several earlier publications [1—3, 5—7, 10].

The present paper describes the use of 5,6-diphenyl-2,3-dihydro(asym)-triazine-3-thione as a sensitive, selective reagent for the spectrophotometric determination of rhenium. The reagent, which has previously been used for the gravimetric determination of palladium [17], reacts with perrhenate in 0.5—2.5 M hydrochloric acid in the presence of tin(II) chloride to produce a green complex. The complex is extractable by solvents such as chloroform, benzene, isoamyl alcohol, ethyl acetate, amyl acetate and ether. Extraction with chloroform is preferred because of the higher stability of the colour in this medium. The chloroform extract of the complex, which has a metal to reagent ratio of 1:2, shows a peak at 685 nm, where the reagent does not

absorb. Beer's law is obeyed over a useful range of concentrations. The method is superior to many of those proposed earlier, because of its broad acidity range, high sensitivity and selectivity. Here, 27-fold ratios of molybdenum and 35-fold ratios of tungsten can be tolerated in the absence of any masking agent. For molybdenum, this limit increases to 32-fold in the presence of tartaric acid.

EXPERIMENTAL

Apparatus and solutions

A Unicam SP 600 spectrophotometer with 10-mm glass cells was used.

An accurately weighed quantity of potassium perrhenate (Johnson-Matthey) was dissolved in doubly distilled water; the solution was standardized by the internal electrolytic method of Majumdar and Bhowal [18].

The reagent, 5,6-diphenyl-2,3-dihydro(asym)triazine-3-thione was prepared by the method of Polonvski and Pesson [19], and used as a 0.1% (w/v) solution of the reagent in acetone. A 1.0 M solution of tin(II) chloride (GR, Merck) was prepared in 6 M hydrochloric acid. Solutions of diverse cations were prepared from their chlorides or sulfates and of anions from their sodium, potassium or ammonium salts, and were standardized by conventional procedures.

General procedure

Add 2.5 ml of the reagent solution to a solution of perrhenate in a separatory funnel, followed by 1.75 ml of 1 M tin(II) chloride solution and hydrochloric acid to maintain the final acidity between 0.5 and 2.5 M. Dilute to 10 ml with water and mix thoroughly. Extract with one 10-ml and two 5-ml portions of chloroform for 30 s each time. Dry the combined extracts over anhydrous sodium sulfate, transfer to a 25-ml volumetric flask, and dilute to the mark with chloroform. Measure the absorbance of the green complex at 685 nm against a reagent blank similarly prepared.

RESULTS AND DISCUSSION

Optimum reaction conditions

The complex showed a peak at 685 nm (Fig. 1).

Complete extraction of the complex in chloroform took only 30 s, and the extract was stable for 20 min. The addition of 1.5 ml of the 0.1% reagent solution in acetone produced full colour intensity with 10 p.p.m. of rhenium. Addition of more reagent had no adverse effect, so 2.5 ml of the reagent solution were used in all further tests. The optimum acid concentration required for maximum colour development was 0.5—2.5 M in hydrochloric acid. Addition of 1.25 ml of 1 M tin(II) chloride solution sufficed for 250 μg of rhenium in 25 ml. Change in the concentration of the $SnCl_2$ solution from 1 M to 2 M had a negligible effect. For further tests, 1.75 ml of 1 M tin(II) chloride in 6 M hydrochloric acid was used.

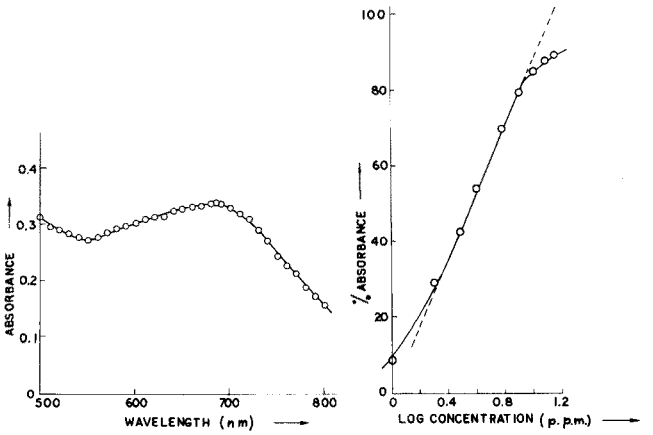

Fig. 1. Absorption spectrum for 4 p.p.m. of rhenium (general procedure).

Fig. 2. Ringbom plot.

The coloured complex was not formed if a chloroform solution of the reagent were used. The complex was therefore first formed in aqueous acetone medium and then extracted into chloroform. Addition of acetone up to 5 ml had no adverse effect on the colour intensity, but more acetone reduced the intensity.

The order of addition of reagents given in the procedure must be strictly maintained. The addition of $SnCl_2$ before the reagent lowered the colour intensity considerably.

Beer's law, optimum range, relative error, sensitivity and molar absorptivity

The colour system obeyed Beer's law for 2—10 p.p.m. of rhenium at 685 nm. The optimum range evaluated from Ringbom's curve [20] (Fig. 2) was 2.3—8.5 p.p.m. The relative error per 1% absolute photometric error [21] was 2.72%. With 4 p.p.m. of rhenium the relative standard deviation was ±1%. The Sandell sensitivity and the molar absorptivity (calculated from Beer's law values) were 0.012 μg Re cm^{-2} and $1.53 \cdot 10^4$ l mol^{-1} cm^{-1}, respectively.

Composition of the complex

The composition of the coloured complex was determined by Job's method of continuous variations [22] and by the mole ratio method [23]. For Job's method, mixtures (12 ml total) of equimolar solutions ($0.5 \cdot 10^{-3}$ M) of the perrhenate and the reagent were treated as in the general procedure. The curve (Fig. 3) indicates that the complex contains rhenium and the reagent in the ratio 1:2. This result was confirmed by the mole ratio method, for 2 ml of $0.5 \cdot 10^{-3}$ M perrhenate solution (Fig. 4). The same 1:2 composition was also found in the complex isolated as follows. About 0.078 g of $KReO_4$ (i.e. 0.050 g Re) dissolved in 40 ml of 2 M hydrochloric acid was

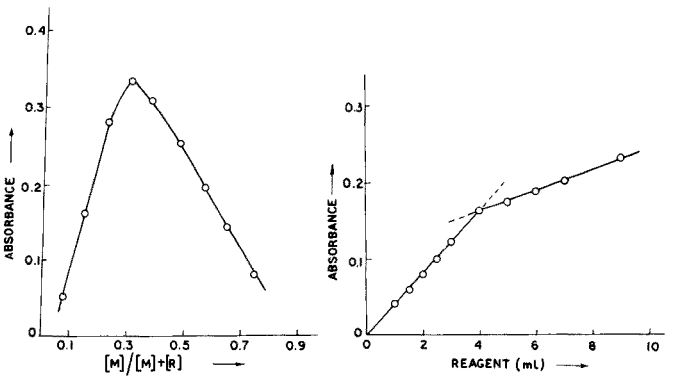

Fig. 3. Job's method. Rhenium = reagent = $0.5 \cdot 10^{-3}$ M.

Fig. 4. Molar ratio method. Rhenium = reagent = $0.5 \cdot 10^{-3}$ M.

mixed with a solution of about 0.370 g of reagent in 40 ml of dimethylformamide, and 20 ml of tin(II) chloride solution (1 M in 2 M hydrochloric acid) was added; the final acidity was thus about 1.5 M. The green precipitate was filtered, washed first with about 50 ml of 1:1 water—dimethylformamide and then with water and dried in vacuo.

Analysis: found, 48.85% C, 3.1% H, 8.9% S, 11.3% N; calculated for $ReO(C_{15}H_{10}N_3S)_2$, 49.2% C, 2.8% H, 8.8% S, 11.5% N.

Degree of dissociation and stability constant

The value of α, the degree of dissociation, was calculated from Harvey and Manning's equation [24] and the instability constant K' was evaluated from the equation $K' = (m\alpha c)^m (n\alpha c)^n / c(1 - \alpha)$, where $m = 1$, $n = 2$, in this case. Then, the stability constant K was calculated as $1/K'$. The stability constant K and stepwise formation constants k_1 and k_2 of the 1:2 complex were evaluated by Leden's method [25] and by the method of Rossotti and Rossotti [26]. All the values were calculated for 685 nm (Table 1).

Effect of foreign ions

With 4 p.p.m. of rhenium, the tolerance limits for foreign ions were as

TABLE 1

Stability constant and stepwise formation constants of the complex by different methods

Harvey and Manning [24]					Leden [25]		Rossotti—Rossotti [26]	
Em	*Es*	*c*	α	*K*	*K*		*K*	
0.620	0.167	$4.0 \cdot 10^{-5}$	0.7338	$10.5 \cdot 10^7$	$4.4 \cdot 10^7$		$9.3 \cdot 10^7$	
					k_1	k_2	k_1	k_2
					$3.8 \cdot 10^3$	$1.2 \cdot 10^4$	$9.1 \cdot 10^3$	$1.0 \cdot 10^4$

follows (p.p.m. in parentheses): W^{6+} (140), V^{5+} (50), Mn^{2+} (200), Fe^{3+} (100), Zn^{2+} (30), Zr^{4+} (70), Mo^{6+} (110), Hg^{2+} (10), Pb^{2+} (10), Tl^{+} (20), UO_2^{2+} (10), Pt^{4+} (10), Ru^{3+} (8), As^{3+} (80), Sb^{3+} (15). Citrate, oxalate, tartrate and EDTA (disodium salt) in 300-fold amounts and relatively large amounts of Nb^{5+} (in the presence of tartaric acid), Ta^{5+} (in the presence of tartaric acid), Al^{3+}, Be^{2+}, Ni^{2+}, Cd^{2+} did not interfere. Rhenium could be determined in the presence of Hg^{2+} (50 p.p.m.) and Mo^{6+} (130 p.p.m.) when tartaric acid was used as masking agent, and in the presence of UO_2^{2+} (40 p.p.m.) with oxalic acid. However, Cr^{3+}, Co^{2+}, Cu^{2+}, Os^{8+}, Pd^{2+} and Ag^{+} interfered with the determination. The oxidation states of the ions given above were those of the ions before the addition of tin(II) chloride.

REFERENCES

1 A. I. Busev, V. M. Byr'ko and G. K. Kondakova, Zh. Anal. Khim., 22 (1967) 1028.
2 L. L. Talipova, E. L. Abramova, N. A. Parpiev and S. B. Lyapin, Zh. Anal. Khim., 27 (1972) 1305.
3 V. K. Akimov, L. Ya. Kliot and A. I. Busev, Zh. Anal. Khim., 28 (1973) 118.
4 L. V. Borisova, E. I. Plastinina and A. N. Ermakov, Zh. Anal. Khim., 29 (1974) 743.
5 J. L. Kassner, S. F. Ting and E. L. Grove, Talanta, 7 (1961) 269.
6 A. Narayanan and P. R. Subbaraman, Indian J. Chem., 5 (1967) 436.
7 F. Trusell and R. J. Thompson, Anal. Chem., 36 (1964) 1870.
8 V. W. Meloche, R. L. Martin and W. H. Webb, Anal. Chem., 29 (1957) 527.
9 J. Bankovskis and E. Labauova, Latv. PSR Zinātr. Akad. Véstis, 1 (1960) 97; C.A., 54 (1960) 15067c.
10 E. N. Pollock and L. P. Zopatti, Anal. Chim. Acta, 32 (1965) 418.
11 A. I. Lazarev and V. I. Lazarev, Opred. Mikroprimesei, No. 1 (1968) 90; C.A., 71 (1969) 108808z.
12 L. V. Borisova, E. I. Plastinina and A. N. Ermakav, Zh. Anal. Khim., 29 (1974) 1362.
13 M. Kozlicka, M. Wojtowiez and I. Adamiec, Chem. Anal., 15 (1970) 701.
14 J. L. Kassner and Shih-Fau Ting, U.S. Dept. Com., Office Tech. Serv., P.B. Rept. 154,908 (1960) 14; C.A., 57 (1962) 12088h.
15 D. Thierig and F. Umland, Fresenius' Z. Anal. Chem., 240 (1968) 19.
16 E. B. Sandell, Colorimetric Determination of Traces of Metals, 3rd edn., Interscience, N.Y., 1959, p. 754.
17 M. Edrissi, A. Massoumi and I. Lalezari, Talanta, 19 (1972) 814.
18 A. K. Majumdar and G. Bhowal, Anal. Chim. Acta, 48 (1969) 192.
19 M. Polonovski and M. Pesson, Compt. Rend., 232 (1951) 1260.
20 A. Ringbom, Z. Anal. Chem., 115 (1938/39) 332.
21 G. H. Ayres, Anal. Chem., 21 (1949) 652.
22 P. Job, Compt. Rend., 180 (1925) 928; Ann. Chim. (Paris), 9 (1928) 113.
23 J. H. Yoe and A. L. Jones, Ind. Eng. Chem., Anal. Ed., 16 (1944) 111.
24 A. E. Harvey and D. L. Manning, J. Am. Chem. Soc., 72 (1950) 4488; 74 (1952) 4744.
25 I. Leden, Z. Phys. Chem., 188A (1941) 160.
26 F. J. Rossotti and H. Rossotti, The Determination of Stability Constants, McGraw-Hill, 1961, p. 275.

Analytica Chimica Acta, 93 (1977) 255—259
© Elsevier Scientific Publishing Company, Amsterdam — Printed in The Netherlands

A POTENTIOMETRIC AND SPECTROPHOTOMETRIC STUDY OF GALLIUM—BENZOHYDROXAMIC ACID COMPLEX FORMATION

PIERRE BIANCO*, JEAN HALADJIAN and RAYMONDE PILARD

Laboratoire de Chimie et Electrochimie des Complexes, Université de Provence, Place Victor Hugo, 13331 Marseille Cedex 3 (France)

(Received 29th March 1977)

SUMMARY

The complex formation of gallium with benzohydroxamic acid has been studied by potentiometry and spectrophotometry. Three successive complexes, GaL^{2+}, GaL_2^{+}, and GaL_3, are formed. The stability constants, $\log \beta_1$, β_2 and β_3, are 9.2 ± 0.1, 18.0 ± 0.1 and 25.3 ± 0.1, respectively, in 3 M $NaClO_4$ at 25°C.

Hydroxamic acids are good chelating agents of metal cations, particularly iron(III) and some other trivalent elements. Moreover, there is renewed biochemical interest in hydroxamic acids because they have been found in natural products such as antibiotics and bacterial growth factors. Iron compounds have been studied extensively because iron has a unique position in many biological systems, but no study is known of the complexation of gallium by hydroxamic acids. Stability constants of the iron(III) and aluminium(III) complexes of aceto- or benzo-hydroxamic acid have been determined [1—3]; the iron(III) is more stable. Because of the similar behaviour of aluminium and gallium, and in some cases of iron(III) and gallium, it was of interest to study the complexation of gallium by hydroxamic acids. In this paper, the stability constants of gallium complexes with benzohydroxamic acid are determined by potentiometry and u.v. spectrophotometry.

EXPERIMENTAL

Hydrated gallium(III) perchlorate was recrystallized from a solution of hydroxide dissolved in perchloric acid (60%). Benzohydroxamic acid (Aldrich) was used without further purification. Other reagents were analytical-grade products.

Gallium was determined by titration with acid in the presence of excess of oxalate [4] after decomposition of the benzohydroxamic group by hot nitric acid.

The potentiometric procedure has been described previously [5]. The experiments were done at 25 ± 0.05°C with a glass electrode in 3 M $NaClO_4$ medium. For all titrations the gallium concentration, (m) remained constant at 10^{-3} M, and the ratio $r = [\text{ligand}]_{\text{total}} / [\text{Ga}]_{\text{total}} = 1/m$ was varied between

0 and 10. Solutions were acidified with perchloric acid to obtain the lowest pH values, and then titrated with sodium hydroxide.

In the spectrophotometric study, absorbances were measured with a Cary 14 spectrophotometer in 1-mm Hellma quartz cells. Solutions with a constant ratio $r = 1$ at various pH values were measured.

POTENTIOMETRIC STUDY

The titration curves $pH = f(x)_r$ for several ratios r, where $x = ([OH^-]_{added} - [H^+]_{added})/m$, are shown in Fig. 1. The complex formation is observed on decreasing pH and by the absence of the undulations which usually appear in the gallium titration curve for $r = 0$ [6]. Precipitates are formed at increased pH values. Analysis showed that the % gallium in these precipitates was lower (12—13%) than the theoretical for the 1:3 chelate (14.6%).

For the interpretation of experimental results, complex formation was assumed to take place by stepwise association of the benzohydroxamate anion (L^-) around the gallium cation and so the following equilibria were taken into account: $HL \overset{K}{\rightleftharpoons} H^+ + L^-$; $Ga^{3+} + L^- \overset{\beta_1}{\rightleftharpoons} GaL^{2+}$; $Ga^{3+} + 2L^- \overset{\beta_2}{\rightleftharpoons} GaL_2^+$; $Ga^{3+} + 3\,L^- \overset{\beta_3}{\rightleftharpoons} GaL_3$, where K is the dissociation constant of the acid and $\beta_1, \beta_2, \beta_3$ are the stability constants of the complexes. Hydroxo complex formation is assumed to be negligible in the pH range investigated [7].

The classical mass-balance equations were used to calculate the formation curve $pl_1 = -\log l_1 = f(\bar{n})$, where l_1 and $\bar{n}$ designate respectively the benzohydroxamate anion concentration and the average number of ligands bound to one gallium atom (Fig. 2). Within the limits of experimental error the data relate to points gathered on a single curve between $\bar{n} = 0.2$ and $\bar{n} = 2.5$. This curve provided values of the three stability constants $\beta_1, \beta_2, \beta_3$, which were refined after comparisons between the experimental data and the calculated titration curves (Fig. 1). The values found were: $\log \beta_1 = 9.2 \pm 0.1$;

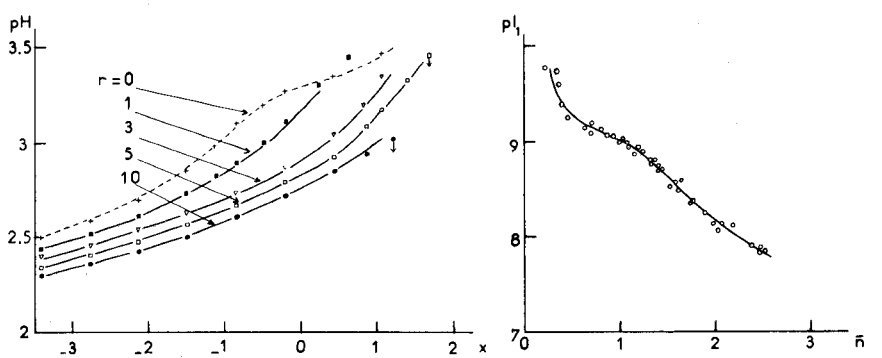

Fig. 1. Titration curves $pH = f(x)_r$ with $m = l \times 10^{-3}$ M for different r values. The points correspond to experimental data, the curves are calculated. The arrows (↓) indicate the beginning of precipitation.

Fig. 2. Formation curve $pl_1 = f(\bar{n})$.

$\log \beta_2 = 18.0 \pm 0.1$; $\log \beta_3 = 25.3 \pm 0.1$; $pK = 9.03 \pm 0.02$ (3 M $NaClO_4$; $25 \pm 0.05°C$).

These results confirm the existence of three successive complexes, GaL^{2+}, GaL_2^+, GaL_3, the distribution of which as a function of pH is plotted in Fig. 3.

SPECTROPHOTOMETRIC STUDY

The electronic absorption spectra of benzohydroxamic acid were studied by Exner and Kabac [8] to determine the structure of the acid and its anion. In acidic and neutral media one band is found at ca. 228 nm and two bands appear at 226 and 264 nm in alkaline solutions. Solutions of Ga^{3+} do not give an absorption band.

The following study was based on a method tested previously [5]. The classical mass-balance equations give the relation

$$y = [\epsilon l - (\epsilon_0 l_0 + \epsilon_1 l_1)]/m = \beta_1 l_1 (\epsilon_{11} - y) + \cdots + \beta_n l_1^n (\epsilon_{1n} - y)$$

where ϵ is the molar absorptivity of the solution, and ϵ_0 and ϵ_1 the molar absorptivities of the undissociated molecule (concentration = l_0) and of the anion (concentration = l_1). ϵ_{11} (or more generally ϵ_{1n}) designates the molar absorptivity of GaL^{2+} (or GaL_n^{3-n}).

If y is divided by $\beta_1 l_1$, neglecting terms where the power of $l_1 \geqslant 1$, the following expression is obtained: $y = \epsilon_{11} - (y/\beta_1 l_1)$. Thus the curve $y = f(y/l_1)$ must be a straight line of slope $(-1/\beta_1)$; ϵ_{11} is the extrapolated value when $y/l_1 \to 0$. More generally, for several successive complexes, the equation becomes

$$y = \epsilon_{1n} - \frac{1}{\beta_n}\left[\frac{y - \sum_2^n \beta_{n-1}\, l_1^{n-1} (\epsilon_{1,n-1} - y)}{l_1^n}\right]$$

and this theoretically enables β_n and ϵ_{1n} to be calculated. ϵ, ϵ_0, ϵ_1 are experimental data; l_0 and l_1 can be computed for a given pH value from the formation curve. This method was applied for the ratio $r = 1$ within the range pH 2.38 — 3.02; the determination of ϵ_1 was unnecessary as the contribution of the term $\epsilon_1 l_1$ is negligible in this pH range.

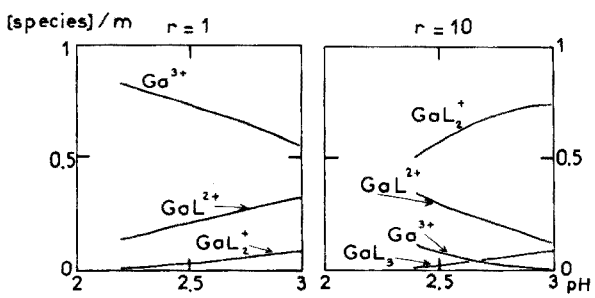

Fig. 3. Species distribution diagrams as function of pH. ($r = 1$ and $r = 10$).

The dissociation constant of benzohydroxamic acid, calculated from spectrophotometric data (Fig. 4), was pK = 9.03 ± 0.05, which agrees with the potentiometric result. In Fig. 4 the absorption spectra are also plotted at various pH values for the ratio r = 1. The absorption band at ca. 260 nm increases with increasing pH values, and the proportion of complex also increases. In Fig. 5, the best-fit straight line gives for the first stability constant $\log \beta_1 = 9.4 \pm 0.2$, which agrees with the potentiometric value. The other complexes GaL_2^+ and GaL_3 are present in smaller proportion over the pH range examined here; their stability constants could not be measured.

The ϵ_{11} values of the GaL^{2+} complex were obtained by extrapolation of the simple equation $y = \epsilon_{11} - (y/\beta_1 l_1)$ for various wavelengths. The calculated absorption spectrum of this species, assumed to be in an isolated state, shows a high absorption maximum at 262 nm (Fig. 4). The presence of isosbestic points is explained by the existence of an equilibrium between two preponderant species: the undissociated benzohydroxamic acid and GaL^{2+}.

DISCUSSION

The complex formation between gallium and benzohydroxamic acid takes place by successive steps and leads to a very stable 1 : 3 chelate (I),

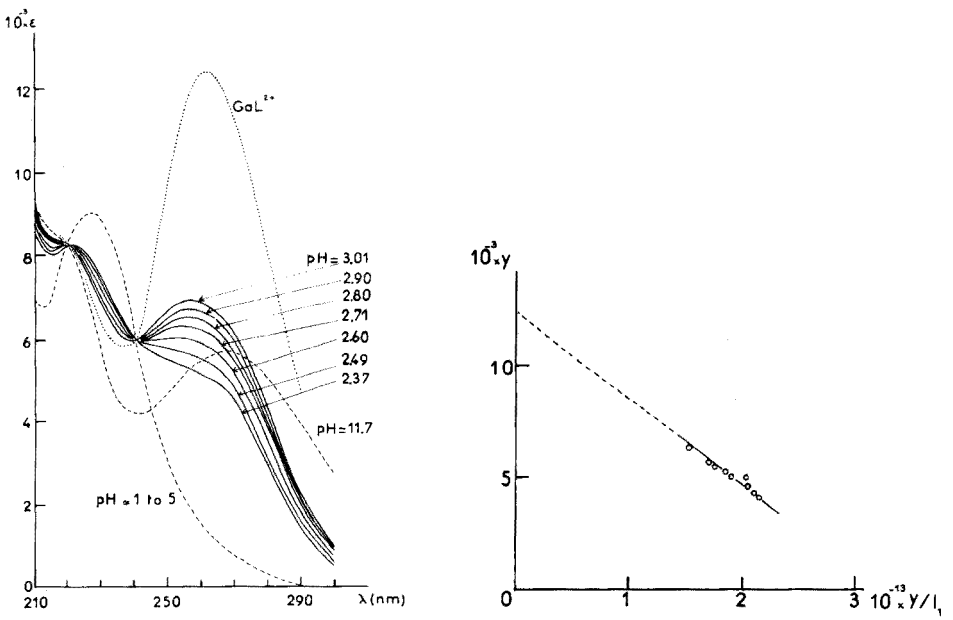

Fig. 4. Absorption spectra at various pH values ($m = l = 1 \times 10^{-3}$ M). The dashed lines represent absorption spectra of benzohydroxamic acid in acidic (pH 1.8—5.8) or alkaline (pH 11.7) medium. The dotted line represents the extrapolated absorption spectrum of the 1:1 complex.

Fig. 5. Relation $y = f(y/l_1)$ for the calculation of ϵ_1 and β_1. (λ = 260 nm).

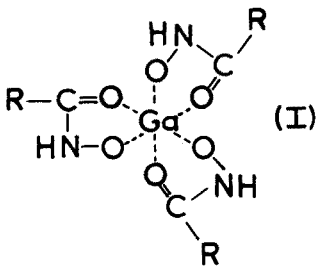

(I)

similar to an acetylacetonate complex, and to the iron(III)—benzohydroxamic acid complex [3]. One of the most interesting features is the very high value of the stability constant β_3. A comparison with the stability constants for the iron(III) and aluminium(III) complexes of benzo- and aceto-hydroxamic acid (which have similar chelating abilities) shows that gallium has a position intermediate between these two trivalent cations (see Table 1). This tendency was predicted by Emery [9], but no proof has been put forward previously. The small difference between the stability constants for $Ga(BH)_3$ and $Ga(acac)_3$ should also be noted; the iron(III) complexes differ similarly [3].

The present work has shown that complexation produces a band ($\simeq$ 255 nm) which characterizes the 1:1 complex. Some analytical applications could be obtained from these observations. Although some solid metallic benzohydroxamates have been prepared for analytical purposes [10], the gallium compounds must be regarded with some caution, as their composition depends on the mode of precipitation.

TABLE 1

Comparison between the stability constants, β_3, for some complexes (acac = acetylacetonate anion; AH = acetohydroxamate anion; BH = benzohydroxamate anion.)

Medium	0.1 M $NaClO_4$		3 M $NaClO_4$		0.1 M $NaNO_3$
Temperature (°C)	20	20	25	25	20
Ref.	[1]	[1]	present work	[5]	[2]
Complex	$Fe(BH)_3$	$Fe(AH)_3$	$Ga(BH)_3$	$Ga(acac)_3$	$Al(AH)_3$
log β_3	27.8	28.3	25.3	24.3	21.5

REFERENCES

1 G. Schwarzenbach and K. Schwarzenbach, Helv. Chim. Acta, 46 (1963) 1390.
2 G. Anderegg, F. L'Eplattenier and G. Schwarzenbach, Helv. Chim. Acta, 46 (1963) 1400.
3 G. Anderegg, F. L'Eplattenier and G. Schwarzenbach, Helv. Chim. Acta 46 (1963) 1409.
4 S. Lacroix, Ann. Chim., 4 (1949) 5.
5 J. Haladjian, P. Bianco and R. Pilard, J. Chim. Phys., 71 (1974) 1251.
6 H. Gamsjager, K. Aeberhard and P. Schindler, Helv. Chim. Acta, 52 (1969) 2315.
7 P. Bianco, J. Haladjian and R. Pilard, J. Less-Common Met., 42 (1975) 127.
8 O. Exner and B. Kabac, Collect. Czech. Chem. Commun., 28 (1963) 165.
9 T. Emery, Adv. Enzym., 35 (1971) 135.
10 L. Lapatnik, J. Hazel and W. McNabb, Anal. Chim. Acta, 36 (1966) 366.

Analytica Chimica Acta, 93 (1977) 261—266
© Elsevier Scientific Publishing Company, Amsterdam — Printed in The Netherlands

FAST DETERMINATION OF MOLYBDENUM AND TELLURIUM BY NEUTRON ACTIVATION ANALYSIS

MIRKO DIKSIC*

Department of Chemistry, McGill University, 801 Sherbrooke St. West, Montreal, Quebec, H3A 2K6 (Canada)

TOME F. COLE

Environmental Trace Substances Research Center, University of Missouri, Columbia, Mo. 65201 (U.S.A.)

(Received 4th February 1977)

SUMMARY

The utilization of 14.6-min ^{101}Mo and 25-min ^{131g}Te for the determination of molybdenum and tellurium in biological materials by radiochemical neutron activation analysis is described for the first time. Radioisotopes were separated from the samples activated in a thermal neutron flux of about 10^{14}n cm^{-2} s^{-1}. The radiochemical procedure for molybdenum involves extraction of Mo^{6+} from 6 M HCl into diethylether, re-extraction into water, precipitation as oximate, and measurement of the gamma activity of ^{101}Tc. The tellurium was separated by reduction to the element with SO_2 in 3 M HCl, dissolution in HNO_3, and reprecipitation as the element for the measurement of radioactivity. The sensitivity was estimated at ca. 10 ng at the level of confidence of 95%. The methods were tested by analyzing NBS-standard Bovine Liver and Orchard Leaves for molybdenum; the concentrations found were 3.2 ± 0.1 μg g^{-1} and 300 ± 60 ng g^{-1}, respectively. The tellurium content of bovine liver was estimated at 90 ± 15 ng g^{-1}.

It has been known for some time that molybdenum is an essential element for all organisms, except perhaps for some green algae [1, 2]. Tellurium is generally accepted as moderately toxic to plants [3] and highly toxic to mammals [4] even at trace levels. The normal dietary level is usually less than 1 p.p.m.

The recognition of the importance of trace elements in nutrition and pollution has led to the determination of these elements at very low levels; several analytical methods, e.g. emission spectroscopy, flame spectrophotometry, colorimetry, and neutron activation are generally used. Neutron activation appears to be most suitable for the determination of such low quantities of molybdenum and tellurium.

The ^{98}Mo (n, γ) ^{99}Mo ($t_{1/2}$ = 66.6 h) reaction [5] has been most frequently used in the determination of molybdenum. After irradiation, molybdenum is separated and the radioactivity of ^{99m}Tc ($t_{1/2}$ = 6.0 h) [5] is measured. The determination of molybdenum by this procedure offers several advantages,

one of them being that there is ample time for the radiochemical separation. A major disadvantage, however, lies in the fact that relatively long irradiation and cooling periods are required to obtain a good detection sensitivity and to ensure safe handling of the samples, since the matrix is also subject to substantial activation.

Fukai and Meinke [6] introduced the ^{100}Mo (n, γ) ^{101}Mo($t_{1/2}$ = 14.6 min) [5] $\xrightarrow{\beta^-}$ ^{101}Tc($t_{1/2}$ = 14.2 min) [5] determination. Technetium was separated from irradiated marine samples after equilibrium was reached. In this procedure the authors assumed that the same chemical yield for technetium applied to all determinations and was equal to that determined in an independent run. This assumption could introduce rather large errors in the final results.

Tellurium determinations in a variety of matrices have been carried out by means of the following reactions [7—11]: ^{122}Te(n, γ) ^{123m}Te ($t_{1/2}$ = 117 d) [5], ^{126}Te(n, γ) ^{127m}Te($t_{1/2}$ = 107 d) [5] or ^{127}Te($t_{1/2}$ = 9.4 h) [5] and ^{130}Te(n, $^{131m/g}$Te $\xrightarrow{\beta^-}$ ^{131}I($t_{1/2}$ = 8 d) [5]. All of these methods have the same advantages and disadvantages as mentioned earlier for molybdenum. The tellurium determination via ^{131}I may prove to be difficult because losses of elementary iodine could occur in the early stage of a fusion [14]. A great fraction of the iodine formed in the β^--decay of tellurium appears as elemental iodine [12, 13] and some could be lost after the quartz vial is broken.

In order to avoid these difficulties, a fast and accurate method is proposed for the determination of these elements in biological materials.

The separation of the products of the following reactions, ^{130}Te(n, γ) ^{131g}Te($t_{1/2}$ = 25 min) [5] and ^{100}Mo (n, γ) ^{101}Mo ($t_{1/2}$ = 14.6 min) [5] was used in the procedures for tellurium and molybdenum respectively. These have been tested by assaying Bovine Liver and Orchard Leaves (NBS-standards for molybdenum, and Bovine Liver and spiked Bovine Liver for tellurium and they were applied to different biological materials afterwards. The sensitivity of the procedures is ca. 10 ng at the confidence level of 95%.

EXPERIMENTAL

Reagents and standards

The molybdenum and tellurium standards were prepared by dissolution of a known amount of the element in distilled HNO_3 and dilution to give a concentration of 0.5 mg ml^{-1}. This solution was later diluted to 0.1 mg ml^{-1}. The volume of standard solution used was 5 or 10 μl.

Irradiation

Samples of biological material (200—300 mg) were irradiated for 15 or 20 min at a thermal neutron flux of ca. 10^{14} n cm^{-2} s^{-1} in the University of Missouri Research Reactor. The samples and the standards were packaged in high density polyethylene vials and encapsulated in high density polyethylene rabbits. The standards were irradiated during separate runs. The average activity obtained with three standards irradiated between samples was used

in calculations. A negative pressure pneumatic system was used for transferring the rabbits into and out of the reactor. The same radiochemical procedure was used for both samples and standards.

Radiochemical procedure

The samples were transferred into Pyrex flasks which contained 10 mg of carrier. The inside of the vials was washed with digestion solution consisting of a mixture of HNO_3 + $HClO_4$ (4:1). The entire content of a vial was digested in the case of a standard sample. Ten ml of the digestion mixture were used in order to destroy the organic matrix. This was achieved in a microwave oven where the digestions were carried almost to dryness. After the digestion had taken place, the precipitate was dissolved in 6 M NaOH (1 ml).

Molybdenum separation

The procedure was derived from that of Wiles and Coryell [15]. After digestion, the solution was made 6 M in HCl and two drops of 2 M $NaBrO_3$ were added if molybdenum blue (Mo^{5+}) was present to ensure the presence of Mo^{6+}. The molybdenum was extracted into two 30-ml portions of diethyl ether equilibrated with 6 M HCl, and re-extracted into two 10-ml portions of water. About 2 mg of Fe^{3+} were added; $Fe(OH)_3$ was precipitated by adding 6 M ammonia solution and then discarded. The solution was made just acid to methyl orange with 6 M HCl. Five ml of 5% sodium acetate were added and the solution was heated nearly to boiling. The molybdenum oxinate was precipitated by adding 1 ml of 5% 8-hydroxyquinoline solution in 1 M HCl. The molybdenum oxinate was filtered and washed with 5-ml portions of water, ethanol and diethyl ether, dried for 10 min at 110°C, and weighed for chemical yield determination. The time of precipitation was recorded and used as the moment of Mo—Tc separation. The technetium does not precipitate under these conditions [16]. Typical chemical yields were 50—60%; the radiochemical purity was very good. The total time required for a separation is 15—20 min.

Tellurium separation

Tellurium was separated by adapting the procedure of Glendenin [17]. Prior to filtration the final precipitate of tellurium was washed twice with hot water in a centrifuge tube, and then sequentially rinsed with water, alcohol and ether on the filter paper. The precipitate was dried for 5—7 min at 110°C and weighed. A typical chemical yield was 70%.

Activity measurements

Radioactivity was measured with a Ge(Li)-detector of 10% relative efficiency. The efficiency was defined as the ratio of the area under the 1.333-MeV full-energy peak (FEP) for 7.5 cm × 7.5 cm NaI(Tl) crystal to that of the Ge(Li) detector at a source-to-detector distance of 25 cm. The full width at half-maximum [FWHM] resolution of the system was 2.6 KeV at 1.33 MeV with

a peak-to-Compton ratio of 30:1. The spectra were acquired for 1000 or 2000 s in the live mode. The area of the FEP-s was calculated by subtracting a straight-line background from the total FEP area. The area of a FEP was corrected for decay and, if necessary, acquiring [18] time prior to the concentration of the corresponding element was estimated.

RESULTS AND DISCUSSION

The nuclear data and the relative sensitivities for molybdenum and tellurium are given in Table 1. The relative sensitivities were calculated by using an irradiation time of 24 h or one half-life for radioisotopes with half-life less than 30 min, a "cooling" period of 4 d for samples irradiated for 24 h, and the most intense γ-ray.

The determination of molybdenum via $^{101}Mo \xrightarrow{\beta^-} {}^{101}Tc$ has approximately the same sensitivity as given by the $^{99}Mo \xrightarrow{\beta^-} {}^{99m}Tc$ pair (Table 1). It is faster and the activation of the matrix is smaller. In this case the Mo—Tc separation time should be recorded, as mentioned earlier. The radioactivity of ^{101}Mo at the end of the bombardment (EOB) was estimated from the area under the 307-keV FEP of ^{101}Tc, the Mo—Tc separation time, and the equation derived from the relationship between parent and daughter decay

$$A_2(t_D) = A_1^\circ \cdot e^{-\lambda_1 t_c} \cdot \lambda_2 \cdot t_D \cdot \left[1 - \frac{\epsilon \cdot \lambda_2}{1+\epsilon} \cdot \frac{t_D}{2}\right]$$

where $\epsilon = t_1 - t_2/t_2$ and t_1 and t_2 are the half-lives of molybdenum and technetium respectively; A_1° is the radioactivity of ^{101}Mo at the end of irradiation; $A_2(t_D)$ is the radioactivity of ^{101}Tc at the time t_d after Mo—Tc separation; t_c is the time between EOB and the beginning of counting; and λ are radioactive constants.

TABLE 1

Nuclear data and relative sensitivities for tellurium and molybdenum isotopes

Radioisotope produced	Natural abundance (%)	σ[barn]	$t_{1/2}$	E_γ (keV)	I_γ (%)	Relative sensitivity	Ref.
^{121m}Te	0.089	0.34	150 d	212.2	89.1	$4.79 \cdot 10^{-5}$	[5]
^{121}Te	0.089	2.0	17 d	573.1	79.1	$8.07 \cdot 10^{-4}$	[5]
^{123m}Te	2.46	2.0	117 d	158.8	84	$1.04 \cdot 10^{-2}$	[5]
^{125m}Te	4.61	0.05	58 d	109.3	3	$2.79 \cdot 10^{-5}$	[5]
^{127m}Te	18.71	0.13	109 d	417.9	0.27	$8.3 \cdot 10^{-6}$	[5]
^{127}Te	18.71	0.9	9.3 h	417.9	0.27	$7.7 \cdot 10^{-3}$	[5]
^{129m}Te	31.79	0.016	34.1 d	459.6	8.5	$2.8 \cdot 10^{-4}$	[5]
^{129}Te	31.79	0.9	69 h	459.6	13.2	$1.5 \cdot 10^{-1}$	[5]
^{131m}Te	34.48	0.02	30 h	149.7	17	$2.6 \cdot 10^{-2}$	[23]
^{131}Te	34.48	0.2	25 min	149.7	68	1	[5]
^{99}Mo	23.78	0.14	66.6 h	142	90	0.95	[5]
^{101}Mo	9.63	0.2	14.6 min	307	88.9	1	[5]

The concentration of tellurium was estimated by measuring the area under the 149.7-keV FEP.

The results are given in Table 2. Each result represents the weighted average of eight independent determinations. The error in each determination was estimated as the square root of the sum of squares of individual errors at a 95% confidence level, including uncertainties in peak integration, weighing (1%), and pipeting (2%). The uncertainty in A_i° was estimated as the total differential of the above equation. Three standards of each element, irradiated separately, were used.

From Table 1, it is obvious that ^{131g}Te and ^{101}Mo provide a very sensitive means of determination of tellurium and molybdenum. A possible interference in the determination of these elements can come from the ^{235}U (n, f) reaction with fission yields of (5.1 ± 0.3)% and (2.97 ± 0.06)% for molybdenum and tellurium respectively [19]. The uranium content in the NBS standards [20] and in biological materials is, in general, very low and does not represent any possibility of interference. The overall precision is ca. 10—20%, which is reasonable for the determination of nanogram amounts of the elements concerned.

Our results agree well with those obtained by other means [21, 22] for molybdenum (see Table 2) in both NBS standards. With the exception of this work, no value has been published for tellurium as yet.

The sensitivity, measured by using samples with known concentrations of Mo or Te, was estimated at about 10 ng at the confidence level of 95%.

We thank the staff of the University of Missouri Research Reactor for their assistance in performing irradiations.

TABLE 2

Molybdenum and tellurium results for NBS standards

Material	Concentration of Mo (ng g^{-1})	Concentration of Te (ng g^{-1})
Bovine Liver, NBS-1577	3200 ± 100 3200 ± 120 [22] 3200[a]	90 ± 15
Orchard Leaves, NBS-1571	300 ± 60 300 ± 30 [21] 260 ± 10 [22] 300 ± 100[b]	

[a]NBS certified value
[b]NBS not certified value

REFERENCES

1 H. J. M. Bowen, Trace Elements in Biochemistry, Academic Press, N.Y., 1966.
2 E. J. Underwood, Trace Elements in Human and Animal Nutrition, Academic Press, N.Y. and London, 1971.
3 K. Scharrer and W. Schropp, Z. Pfl. Ernahr. Dung. Bodenk., 50 (1950) 187.
4 E. Cerwenka and W. C. Cooper, Arch. Environ. Health., 3 (1961) 189.
5 C. M. Lederer, J. M. Hollander and I. Perlman, Table of Isotopes, 6th edn., J. Wiley, N.Y., 1967.
6 R. Fukai and W. W. Meinke, Limnol. Oceanogr., 7 (1962) 186.
7 O. E. Zyagintsev and V. I. Shamaev, Zh. Anal. Khim., 14 (1959) 503.
8 A. E. Williams, Analyst, 86 (1961) 172.
9 D. F. C. Morris and R. A. Killick, Talanta, 10 (1963) 279.
10 C. Baloanx, R. Dams and J. Hoste, Anal. Chim. Acta, 41 (1968) 147.
11 R. C. Koch and J. Roesmer, J. Food. Sci., 27 (1962) 309.
12 C. H. W. Jones and J. L. Warren, J. Inorg. Nucl. Chem., 30 (1968) 2289.
13 R. M. Gordon, J. Inorg. Nucl. Chem., 29 (1967) 287.
14 H. J. M. Bowen, Anal. Chem., 40 (1968) 969.
15 D. Wiles and C. Coryell, Phys. Rev., 96 (1954) 696.
16 C. Perrier and E. Segre, J. Chem. Phys., 7 (1939) 155; E. Jacobi, Helv. Chim. Acta, 31 (1948) 2118.
17 L. E. Glendenin, in C. D. Coryell and N. Sugarman (Eds.), Radiochemical Studies; The Fission Products; McGraw-Hill, N.Y. 1951, Book 3, p. 1613.
18 J. B. Cumming, Application of Computers to Nuclear and Radiochemistry, National Academy of Sciences, National Research Council, Nuclear Science Series, 1967, p. 25.
19 A. C. Wahl, A. E. Norris, R. A. Rouse and J. C. Williams, 2nd IAEA Symposium on Physics and Chemistry of Fission, Vienna (1969) p. 813.
20 NBS-Certificate, SRM-1577 and SRM-1571.
21 V. P. Guinn, M. D. Casa, J. J. M. de Goeij and D. R. Young, Proc. 2nd Int. Conf. Nuclear Methods in Environmental Research, University of Missouri, Col., Mo., 1974, p. 24.
22 A. Abu-Samra, J. S. Morris, S. R. Koirtyohann, and J. R. Vogt, Proc. 2nd Int. Conf. Nuclear Methods in Environmental Research, University of Missouri, Col., Mo., 1974, p. 206.
23 M. Diksic, D. K. McMillan and L. Yaffe, J. Inorg. Nucl. Chem., 36 (1974) 7.

Analytica Chimica Acta, 93 (1977) 267—273
© Elsevier Scientific Publishing Company, Amsterdam — Printed in The Netherlands

ACID—BASE TITRATIONS IN AQUEOUS MICELLAR SYSTEMS

A. L. UNDERWOOD

Department of Chemistry, Emory University, Atlanta, Georgia, 30322 (U.S.A.)

(Received 13th April 1977)

SUMMARY

Some water-insoluble carboxylic acids and amines have been titrated in aqueous surfactant solutions to demonstrate that solubilization in micelles provides a useful solvent system for certain acid—base titrations. Potentiometric titrations can be very slow because of electrode drift in these solutions, but visual titrations are convenient. Observed pK shifts are generally interpretable in terms of the influence of micellar charge on the work of proton removal.

Surfactant micelles display the phenomenon of solubilization, whereby water-insoluble substances are dispersed in a medium which is, overall, an aqueous one [1]. Although ambiguities still exist regarding the sizes and shapes of micelles and the details of their hospitality toward "guest" molecules, not a great deal more can be said about many other solvent—solute interactions and it is reasonable to investigate solubilization in micelles as an alternative to nonaqueous solvents in a variety of analytical situations. A few examples already exist. Skoog and Focht solubilized lead soaps in aqueous dodecylamine acetate for the polarographic determination of lead in paint driers [2]. More recently, in a polarographic study of azobenzene in aqueous surfactant solutions [3], excellent polarograms were found, as was the case in less extensive studies of solubilized menadione, progesterone, lumiflavin, carbon tetrachloride, and several aromatic nitro and carbonyl compounds [4]. Fujihira et al. have employed detergent-solubilized mediator-titrants in spectroelectrochemical studies of heme proteins [5]. In the present work, it is shown that weak acids and bases of very low water solubility can be titrated in aqueous surfactant solutions. The micellar systems not only provide solvents but also induce interesting pK shifts in the solubilized acids and bases.

EXPERIMENTAL

Apparatus

pH measurements were performed with a Radiometer Type PHM 26 instrument and a GK 2301B combination electrode. Readability in the expanded scale mode was about 0.002 pH. Potentiometric titrations were done at room

temperature, which was controlled at 22 ± 1°C. Carbon dioxide was excluded from all solutions. The microburet could be read to 0.002 ml.

Reagents

Sodium dodecyl sulfate (SDS, Fisher Scientific Co., U.S.P.) was recrystallized twice from ethanol and dried in vacuo at 60°C [6] (m.p. 183—193°C, decompn.). Dodecyltrimethylammonium chloride (DTAC, General Mills Chemicals, Inc.) was obtained as an aqueous 50% solution called Aliquat 4. The solution was lyophilized and the solid residue was recrystallized from acetone and dried in vacuo at 70°C (m.p. 252—255°C, decompn.). This material is very hygroscopic [7]; rough weighings can be done in the open, but accurate ones require a dry box. Dodecylammonium chloride (DAC, Eastman Kodak Co. reagent chemical) and hexadecyltrimethylammonium bromide (HTAB, J. T. Baker Co. analyzed reagent) were used as obtained.

Dodecanoic (lauric, Eastman Kodak Co. reagent chemical), hexadecanoic (palmitic, Matheson Co., Inc.), and octadecanoic (stearic, Fisher Scientific Co. reagent grade) acids were purified via their molecular compounds with acetamide by the method of Magne et al. [8]; they were finally recrystallized from 1:1 aqueous ethanol and dried in vacuo at 40°C. The respective melting points were 44.5—45.5, 62.0—62.5, 68.5—69.5°C (lit.: 44, 63—64, 69—70°C [9]). Purities calculated from titrations were 99.7, 98.5, and 99.1%, respectively. Other acids and bases were used as obtained from Eastman Kodak Co.

Procedures

The desired quantities of the acids and bases were fully solubilized in the aqueous surfactant solutions at room temperature. However, the dissolution rate was slow, and it was convenient to warm the solutions to 60 or 70°C to achieve solubilization in a few minutes. For a typical visual titration, 20—100 mg of an acid was dissolved in 50 ml of 0.05 M HTAB, 0.2 ml of 0.5% (w/v) phenolphthalein in 50% ethanol was added, and the solution was titrated rapidly with 0.1 M sodium hydroxide. The system equilibrated rapidly and there were no problems such as premature end-points. The bases were titrated similarly in 0.1 M SDS with 0.1 M hydrochloric acid, in the presence of 0.1 ml of aqueous 0.1% phenol red. With this two-color indicator, it was helpful to titrate to a color match with a buffered solution (0.01 M phosphate buffer pH 7 in 0.1 M SDS). The surfactant solutions were well above the critical micelle concentrations. These values vary somewhat with measurement metho surfactant purity, and solution conditions, but 8×10^{-3} M can be taken as the c.m.c. for SDS and 9×10^{-4} M for HTAB, as guidelines [10]. HTAB was preferred to other cationic surfactants for the titration of acids simply because of the commercial availability of a pure grade which was conveniently handled

Potentiometric titrations were performed in a conventional manner. Although they were useful in selecting indicators for the visual titrations and for obtaining pK values, they are not recommended for routine analytical applications where high accuracy is required. When the pH values of surfactant

solutions were changed, the electrode system responded sluggishly. Drifting for 30 min was not uncommon, and in some cases a complete titration required 3—4 h. This was confirmed with several different electrodes. It must be emphasized that the acid—base reactions themselves are not slow; rapid equilibration was seen in both visual and photometric titrations, and drift was still troublesome when thoroughly aged solutions were presented to the electrode system. The sluggish response has been observed by others [11]. The drift in pH involves only the second and third decimal places and would not preclude potentiometric titrations where the highest accuracy was not required.

RESULTS AND DISCUSSION

Visual titrations

Results of visual titrations (Tables 1 and 2) suggest that micellar solubilization provides practical solvent systems for titrating amines and carboxylic acids. The "taken" values in the Tables were obtained by conventional titrations of the acids and bases in ethanol. The K_b enhancement for the amines in SDS solution (see below) is translated into a subjectively sharper end-point than is observed in aqueous ethanol.

pK Shifts

The most striking (albeit expected) results are the large pK shifts induced by the incorporation of acids and bases into charged micelles. Figures 1 and 2 show typical titration curves for dodecanoic acid and tetradecylamine solubilized in both anionic and cationic micelles. Also shown are calculated points for hypothetical titrations in water based on an "intrinsic" pK_b of 3.38 for tetradecylamine, obtained from a literature value for the pK_a of tetradecylammonium chloride [12] and a pK_a of 4.80 for dodecanoic acid. The latter value is a reasonable one estimated from literature values for lower carboxylic acids, for there is little change from one member of the homologous series to the next; e.g., pK_a for butyric acid is 4.81 and for hexanoic acid 4.80 [13].

Qualitatively, in most cases the pK shifts are readily understood in terms of the contemporary model of a micelle as suggested schematically for SDS in Fig. 3. The number of monomer units per micelle (aggregation number, n) is roughly 100 for SDS in water, although values as low as 62 [14] and as high as 131[15] may be found. A core comprising the hydrocarbon chains of the surfactant and the guest, is surmounted by the Stern layer containing the polar head groups and about 80% of the counter-ions. (A convenient compilation of literature values for α, the degree of dissociation, of a number of micelles has been presented [16].) The remaining counter-ions are found in a much more diffuse Guoy—Chapman layer which, for many purposes, need not be considered a part of the micelle. The net charge on the micelle, then, is the difference between the "native" charge, n, contributed by the head groups and the charge of opposite sign, $(1 - \alpha)n$, provided by the bound counter-ions.

TABLE 1

Results of visual titrations of carboxylic acids

Acid	Amount (mg)			Acid	Amount (mg)		
	Taken	Found	Error		Taken	Found	Error
Dodecanoic	15.4	15.1	0.3	Decanedioic	16.9	16.8	0.1
	16.2	16.1	0.1		31.8	31.8	0.0
	34.4	34.4	0.0		44.5	44.4	0.1
	52.4	52.5	0.1		59.7	59.6	0.1
	81.8	81.8	0.0		82.4	82.7	0.3
	87.4	86.9	0.5				
	105.0	105.5	0.5	Dodecanedioic	22.3	21.9	0.4
					41.3	41.2	0.1
Hexadecanoic	16.3	16.1	0.2		68.6	68.5	0.1
	18.4	18.5	0.1		82.0	82.2	0.2
	31.2	31.0	0.2				
	52.6	52.7	0.1	2-Naphthoic	27.0	26.6	0.4
	70.1	70.0	0.1		39.9	39.4	0.5
	85.1	85.3	0.2		60.5	60.3	0.2
	97.0	97.7	0.7		73.0	73.0	0.0
					83.1	83.3	0.2
Octadecanoic	19.3	18.9	0.4				
	29.4	28.8	0.6	1-Naphthylacetic	20.7	20.5	0.2
	48.7	48.5	0.2		42.2	42.2	0.0
	50.3	50.2	0.1		59.7	59.7	0.0
	72.5	72.9	0.4		70.7	70.8	0.1
	101.0	100.9	0.1		82.2	82.0	0.2
					90.0	90.0	0.0

TABLE 2

Results of visual titrations of amines

Amine	Amount (mg)			Amine	Amount(mg)		
	Taken	Found	Error		Taken	Found	Error
Dodecyl	23.1	22.8	0.3	Hexadecyl	23.5	23.2	0.3
	44.0	44.2	0.2		39.8	39.7	0.1
	57.7	57.8	0.1		56.9	57.1	0.2
	78.2	77.6	0.6		73.7	73.7	0.0
	87.7	87.8	0.1		88.0	87.8	0.2
Tetradecyl	21.7	21.4	0.3	Octadecyl	20.8	19.6	1.2
	40.0	40.4	0.4		28.4	28.9	0.5
	57.1	57.0	0.1		36.5	36.9	0.4
	79.5	80.4	0.9		42.1	41.4	0.7
	92.2	91.6	0.6		49.1	49.4	0.3
					60.4	62.6	2.2

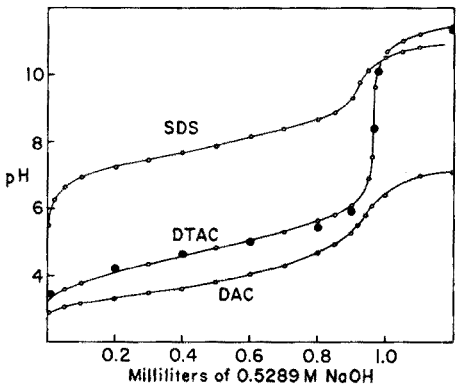

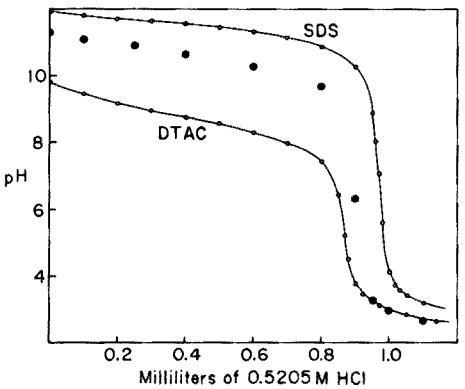

Fig. 1. Potentiometric titrations of dodecanoic acid. Top curve: 98.9 mg of acid in 50 ml of 0.1 M SDS. Middle curve: 102.6 mg of acid in 50 ml of 0.1 M DTAC. Bottom curve: 100.4 mg of acid in 50 ml of 0.1 M DAC. Solid circles: calculated points for 102.6 mg of acid of $pK_a = 4.80$ in 50 ml of water.

Fig. 2. Potentiometric titrations of tetradecylamine. Upper curve: 111.1 mg of amine in 50 ml of 0.1 M SDS. Lower curve: 101.1 mg of amine in 50 ml of 0.1 M DTAC. Solid circles: calculated points for 99.97 mg of amine of $pK_b = 3.38$ in 50 ml of water.

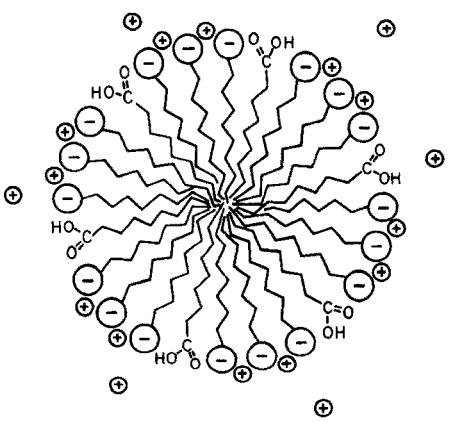

Fig. 3. Schematic section of an SDS micelle containing solubilized carboxylic acid showing hydrocarbon interior, polar head groups, and bound and dissociated counter-ions.

It may be supposed that an acid solubilized in SDS as depicted in Fig. 3 possesses an "intrinsic" pK_a, i.e., the value which would be observed if the carboxyl group were in the surface of a sphere of zero charge. The best estimate for this value is probably the pK_a value for the acid in an ordinary aqueous solution. Now, the observed pK_a in an anionic micellar system should also reflect the work required to remove a proton from a negatively charged surface, i.e., the pK_a should be higher than the usual value for a carboxylic acid. That this is the case, and that the effect is large, may be seen in Fig. 1; the pK_a value is about 3 units above the intrinsic one.

By the same argument, the pK_a should be lowered if the acid is incorporated in a cationic micelle. Surprisingly, as shown in Fig. 1, little change from the intrinsic value was observed with DTAC. The explanation for this is not completely clear. Perhaps the model of an ionizable group in the surface of a uniformly charged sphere is too simple and the microscopic structure of the micelle must be considered. Possibly the carboxyl group of the solubilized acid is not readily accommodated among the head groups in DTAC micelles and lies partly outside the Stern layer. It is reasonable to suppose that the carboxyl experiences a stronger interaction in SDS, where the charge resides largely on the oxygen atoms, than in DTAC, where the charge is carried by the central nitrogen atom. If this be an important aspect, then replacing the bulky methyl groups of DTAC with hydrogen atoms should enhance the acidity of the solubilized acid. Figure 1 shows that this is indeed the case; the pK_a value in DAC solution is more than one unit below the intrinsic one. (DAC micelles do not provide a good titration medium, however, because their own acidity — $pK_a = 8.3$ — limits the "break" for the carboxyl end-point.)

Figure 2 shows the expected result that the basicity of the amine is enhanced by incorporation into a negatively charged micelle and diminished with the cationic micelle. It may be noted that the effect of DTAC on the amine is much greater than that on the acid. The smaller size of the amino group compared with the carboxyl seems relevant.

Analogous pK shifts have been observed by others in different contexts. Rosano and co-workers titrated sodium and potassium soaps with hydrochloric acid both above and below their c.m.c. values [17, 18]. Interesting pH effects associated with self-micellization were observed, but the titrations were complicated by the formation of precipitates. Tokiwa and Ohki studied the effect of micelle formation on the protonation of dimethyldodecylamine oxide [19] and on the acid—base equilibria of the amphoteric surfactants *N*-dodecyl-β-aminopropionic acid and *N*-dodecyl-β-iminodipropionic acid [20]. Behme and Cordes reported pK shifts for the Schiff base *p*-chlorobenzylidene-1,1-dimethylethylamine on incorporation in charged micelles [21]. Finally, titrations of globular proteins exemplified by Tanford's study of ribonuclease [22] show that the overall charge on a macromolecule influences the observed pK of an ionizable group in a manner analogous to the effect of micellar charge.

REFERENCES

1 M. E. L. McBain and E. Hutchinson, Solubilization and Related Phenomena, Academic Press, New York, 1955.
2 D. A. Skoog and R. L. Focht, Anal. Chem., 25 (1953) 1922.
3 P. G. Westmoreland, R. A. Day, Jr., and A. L. Underwood, Anal. Chem., 44 (1972) 737.
4 R. A. Day, Jr., N. Kamiya, S. A. Santoro, Jr., V. Z. Shih, and A. L. Underwood, unpublished observations.
5 Y. Fujihira, T. Kuwana, and C. R. Hartzell, Biochem. Biophys. Res. Commun., 61 (1974) 538.

6 E. F. J. Duynstee and E. Grunwald, J. Am. Chem. Soc., 81 (1959) 4540.
7 M. F. Emerson and A. Holtzer, J. Phys. Chem., 71 (1967) 1898.
8 F. C. Magne, R. R. Mod, and E. L. Skau, J. Am. Oil Chem. Soc., 34 (1957) 127.
9 The Merck Index, 9th edn., Merck, Rahway, N. J., 1976, pp. 707, 907, 1136.
10 P. Mukerjee and K. J. Mysels, Critical Micelle Concentrations of Aqueous Surfactant Systems, NSRDS-NBS 36, U.S. Dept. of Commerce, Washington, 1971, pp. 51, 107.
11 F. M. Menger, personal communication.
12 Handbook of Chemistry and Physics, 55th edn., CRC Press, Cleveland, 1974, p. D-128.
13 Stability Constants of Metal-ion Complexes, 2nd edn., Special Publication No. 17, The Chemical Society, London, 1964, pp. 415, 485.
14 K. J. Mysels and L. H. Princen, J. Phys. Chem., 63 (1959) 1696.
15 P. Schmidt and H. Sucker, Z. Anal. Chem., 250 (1970) 384.
16 L. Romsted, Ph.D. Thesis, Indiana University, 1975.
17 H. L. Rosano, K. Breindel, J. H. Schulman, and A. J. Eydt, J. Colloid Interface Sci., 22 (1966) 58.
18 M. E. Feinstein and H. L. Rosano, J. Phys. Chem., 73 (1969) 601.
19 F. Tokiwa and K. Ohki, J. Phys. Chem., 70 (1966) 3437.
20 F. Tokiwa and K. Ohki, J. Phys. Chem., 71 (1967) 1824.
21 M. T. Behme and E. H. Cordes, J. Am. Chem. Soc., 87 (1965) 260.
22 C. Tanford and J. D. Hauenstein, J. Am. Chem. Soc., 78 (1956) 5287.

Analytica Chimica Acta, 93 (1977) 275—279
© Elsevier Scientific Publishing Company, Amsterdam — Printed in The Netherlands

A STUDY OF THE MOLAR ABSORPTIVITY OF ASCORBIC ACID AT DIFFERENT WAVELENGTHS AND pH VALUES

M. I. KARAYANNIS, D. N. SAMIOS and CH. P. GOUSETIS

Laboratory of Analytical Chemistry, University of Athens, Athens (Greece)

(Received 1st March 1977)

SUMMARY

A spectral study of ascorbic acid was made in buffer solutions of different pH. The molar absorptivities of the unionized (ϵ_{HA}) and ionized (ϵ_{A^-}) forms of ascorbic acid were determined at six wavelengths. An isosbestic point occurs at 250.7 nm; the molar absorptivity at this wavelength is 8250 ± 150 l mol^{-1} cm^{-1}. The spectral information presented is of importance for the spectrophotometric assay of samples containing vitamin C.

Ascorbic acid is a constituent of many chemical and biological systems and mixtures of biological or pharmaceutical origin. In such systems ascorbic acid can be determined spectrophotometrically, but many parameters may affect such determinations. Kinetic studies of the reaction of ascorbic acid with different reactants, or studies of the stability of chemical systems containing vitamin C require a knowledge of the molar absorptivity of ascorbic acid at different wavelengths and pH values [1, 2].

The u.v. spectrum of ascorbic acid in aqueous solutions shows a peak at 243 nm; the molar absorptivity at this wavelength is 9560 l mol^{-1} cm^{-1} [3]. This band has a width of 37 nm and its maximum is pH-dependent. Ascorbic acid coexists frequently with dehydroascorbic acid, which absorbs at 223 nm. A full study of the molar absorptivities of ascorbic acid at wavelengths outside the range of absorption of dehydroascorbic acid has therefore been made.

EXPERIMENTAL

Apparatus

The pH of ascorbic acid solutions was measured to within ± 0.02 units at 25°C with a carefully standardized null point pH-meter (Beckman research model). All absorbance measurements and the spectra of the ascorbic acid solutions were taken at 25°C with a double-beam spectrophotometer (Beckman Model DK) calibrated carefully for wavelength and absorbance with a standard solution of K_2CrO_4 [4]. At elevated pH values, where prolonged exposure of the ascorbic acid solutions causes its autoxidation, absorbances

were measured with a stopped flow spectrophotometer (Durrum Model D-131); absorbances were read immediately after the mixing of the reagents.

Reagents

All solutions were prepared in doubly distilled water. Solutions of ascorbic acid in buffers were prepared from a stock solution 0.1 M in water. Sodium sulfate—sodium hydrogensulfate buffers were used for the range pH 1.6—3.4, sodium acetate—acetic acid buffers for the range pH 3.0—5.5, and the borate—NaOH system for pH values greater than 6. These buffers were chosen for their absorption characteristics over the range of wavelengths studied.

Procedure

Ascorbic acid has two dissociation constants, $K_1 = 6.17 \cdot 10^{-5}$ and $K_2 = 1.65 \cdot 10^{-12}$ ($pK_1 = 4.21$, $pK_2 = 11.79$) at 20 and 16°C, respectively [5, 6]. For the pH range considered, the contribution of the second dissociation step is negligible. In the following discussion, ascorbic acid will be symbolized as HA. In solutions of a weak acid, the relationship of Flexer, Hammett and Dingwall [7] for the spectrophotometric titration of weak acids is valid:

$$pH = pK_1' + \log [(\epsilon - \epsilon_{HA})/(\epsilon_{A^-} - \epsilon)] \quad (1)$$

where K_1' is the apparent dissociation constant, ϵ_{HA} and ϵ_{A^-} are the molar absorptivities of the unionized and ionized forms of the acid, respectively, and ϵ is the observed absorptivity of their mixture. ϵ_{HA} and ϵ_{A^-} can thus be calculated from measurements of ϵ at two pH values. If the only absorbing species in the solution are the two forms of ascorbic acid, then for each pH

$$\epsilon bC = \epsilon_{HA} bC_{HA} + \epsilon_{A^-}\ bC_{A^-} \quad (2)$$

where C_{HA} and C_{A^-} are the concentrations of the acidic and alkaline form of the ascorbic acid and b is the light path in cm. If the observed absorbance, A_{obs}, is plotted against C for a series of concentrations of ascorbic acid at constant pH, ϵ can be determined from the slope of the plot. By measuring ϵ for two pH values, above and below pK_1', ϵ_{HA} and ϵ_{A^-} can be estimated at the wavelength considered. ϵ can be calculated by rearrangement of eqn. (1):

$$\epsilon = (\epsilon_{A^-} 10^{(pH - pK_1')} + \epsilon_{HA})/(10^{(pH - pK_1')} + 1) \quad (3)$$

at any pH for the specific wavelength λ.

RESULTS AND DISCUSSION

Table 1 shows experimental data for 223, 243, 265, 270, 275 and 290 nm. The values of ϵ shown were determined from diagrams $A_{obs} = f(C)$ for each pH. The experimental data of Table 1 were evaluated by the following procedures. At 265 nm, values of ϵ_{HA} and ϵ_{A^-} were measured at pH 1.50 and 8.00. The means of five such pairs of values were $\bar{\epsilon}_{HA} = 2550$ and $\bar{\epsilon}_{A^-} =$

TABLE 1

Molar absorptivities of ascorbic acid at different wavelengths and pH values

pH	ϵ(l mol^{-1} cm^{-1})					
	λ = 223	λ = 243	λ =265	λ = 270	λ = 275	λ = 290 nm
1.27	4200	—	2600	—	—	—
1.50	4100	9400	2200	—	350	0
2.00	—	9650	—	1300	550	—
2.20	—	—	—	1350	650	—
2.65	—	9600	3000	—	—	—
3.00	—	9100	—	2000	1250	270
3.50	—	9000	—	—	—	—
3.65	—	—	5450	4198	3000	—
3.85	—	8600	—	—	—	—
4.05	2800	—	8050	—	—	—
4.30	—	—	9900	—	—	2050
4.40	—	—	10800	—	—	—
4.50	—	6900	—	9800	—	2300
4.75	1700	—	—	—	8500	—
5.00	—	6130	12600	—	—	—
5.40	—	—	13800	—	—	—
5.50	—	5800	—	12850	10300	—
5.95	—	—	—	—	—	3300
6.20	—	5650	—	—	—	—
6.50	—	5600	—	13130	—	—
7.50	—	—	—	13800	—	—
7.70	—	—	14500	—	—	—
8.00	—	—	14560	13300	—	—

14560 l mol^{-1} cm^{-1}. Application of these values to eqn. (1) for different pairs of pH and ϵ at 265 nm in Table 1 gave a mean value of $K_1' = 7.94 \cdot 10^{-5}$ ($pK_1' = 4.10$). The pH range used for this calculation was 2.65—4.50. From this value of K_1', in connection with eqn. (3), the theoretical curve for λ = 265 nm (curve 1, Fig. 1) was constructed. The agreement between the experimental data and the theoretical curve is very good. The value pK_1' = 4.10 deviates from the literature value, pK_1 = 4.21, because the elevated ionic strength of the solution has a positive effect on the value of the thermodynamic dissociation constant, according to the Debye—Hückel theory. The temperature might also have a small effect.

For further evaluation, values of ϵ_{HA} and ϵ_{A^-} were calculated from the data of Table 1 for all the wavelengths, by solving simultaneous equations for two pairs of pH and ϵ values in eqn. (1). Solution of the simultaneous equations gives

$$\epsilon_{HA} = \{\epsilon_1(K_1 + [H^+]_1) - \epsilon_2(K_1' + [H^+]_2)\}/\{[H^+]_1 - [H^+]_2\} \quad (4)$$

$$\epsilon_{A^-} = \{\epsilon_1 [H^+]_2(K_1' + [H^+]_1) + \epsilon_2 [H^+]_1(K_1' + [H^+]_2)\}/\{K_1'([H^+]_1 - [H^+]_2)\} \quad (5)$$

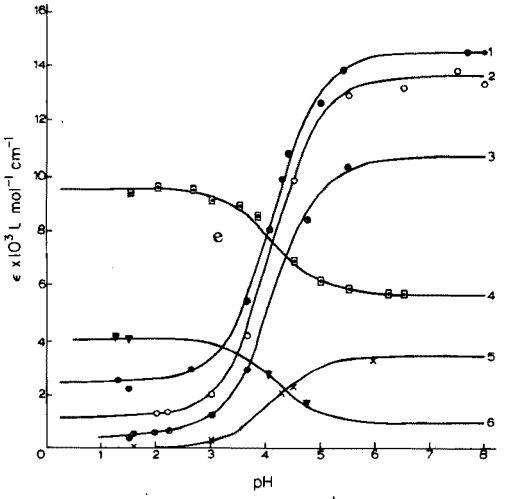

Fig. 1. Spectrophotometric titration of ascorbic acid in buffers at 25°C. The curves were calculated from eqn. (3) with $pK_1' = 4.10$ and ϵ_{HA} and ϵ_{A^-} as given in Table 2 for different wavelengths; λ: (1) 265 nm; (2) 270 nm; (3) 275 nm; (4) 243 nm; (5) 290 nm; (6) 223 nm. The symbols show the experimental data.

where $[H^+]_1$ and $[H^+]_2$ are given by the measured pH, and ϵ_1 and ϵ_2 are the corresponding molar absorptivities. For each pairs of pH and ϵ values, one value was selected in the range pH 2.50—4.00 and the other in the range pH 4.00—5.00. The value of K_1' used for this calculation was $7.94 \cdot 10^{-5}$. The values of ϵ_{HA} and ϵ_{A^-} thus calculated are listed in Table 2. The theoretical curves, constructed for all the wavelengths, are shown in Fig. 1; in all cases they fit the experimental data well.

Figure 2 shows a group of spectra of ascorbic acid for different pH values. The exact wavelength of the isosbestic point at ca. 250 nm was found as follows. The absorbances of $5 \cdot 10^{-5}$ M ascorbic acid were measured at pH 3.20 and 8.00 at 248, 249, 250, 251, and 252 nm; the absorbances were measured

TABLE 2

Molar absorptivities (l mol^{-1} cm^{-1}) of the unionized ϵ_{HA} and the ionized ϵ_{A^-} forms of ascorbic acid at different wavelengths

λ (nm)	ϵ_{HA}	ϵ_{A^-}
223	4150 ± 200	950 ± 50
243	9600 ± 350	5625 ± 200
265	2550 ± 100	14560 ± 450
270	1150 ± 50	13550 ± 400
275	477 ± 25	10630 ± 300
290	0	3460 ± 150

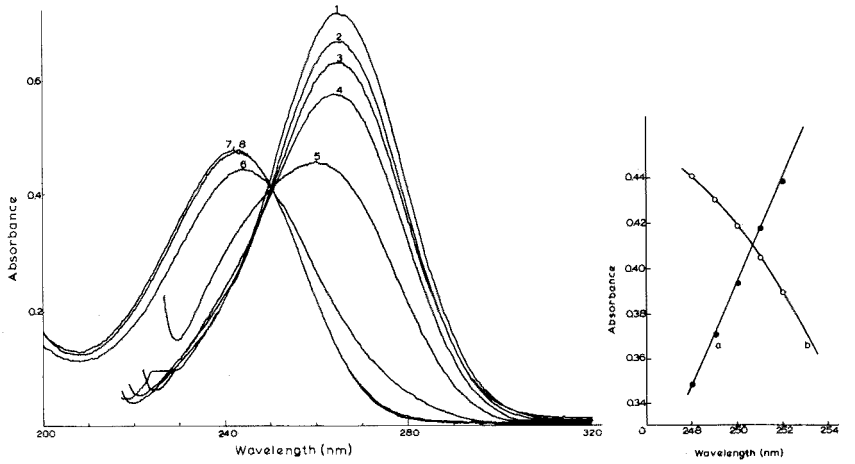

Fig. 2. Absorption spectra of $5 \cdot 10^{-5}$ M ascorbic acid in buffers of different pH: (1) 6.0; (2) 5.5; (3) 5.0; (4) 4.5; (5) 4.0; (6) 3.0; (7) 2.0; (8) 1.5.

Fig. 3. Absorbance of a $5 \cdot 10^{-5}$ M absorbic acid in the region of the isosbestic point for (a) pH 8.0; (b) pH 3.2.

against buffers. The results are shown in Fig. 3; the two lines cross at 250.7 nm, the isosbestic point of the spectrum of ascorbic acid. The molar absorptivity at this point, evaluated from eight measurements in acidic and alkaline solutions was $\bar{\epsilon} = 8250 \pm 150$ l mol^{-1} cm^{-1}. The error quoted is the standard deviation of the mean calculated conventionally; the difference of the means in the two groups of data for the acidic and alkaline solutions was statistically insignificant (t-Test).

The author acknowledges the assistance of Miss Lela Nanou and Miss Dina Athanasopoulou during the experimental work and the contribution of Miss Yuli Tsoutsoura in preparing the figures.

REFERENCES

1 M. I. Karayannis, Anal. Chim. Acta, 76 (1975) 121.
2 M. I. Karayannis, Talanta, 23 (1976) 27.
3 M. Roth, Fluorometric assay of Bilirubin and of Vitamin C, in M. Roth (Ed), Methods of Clinical Chemistry, University Park Press, Baltimore, Maryland, 1970, p. 61.
4 G. W. Haupt, J. Res. Nat. Bur. Std., 48 (1952) 414.
5 E. G. Ball, J. Biol. Chem., 118 (1937) 219.
6 P. Karrer and G. Schwarzenbach, Helv. Chim. Acta, 17 (1934) 58.
7 L. A. Flexer, L. P. Hammett and A. Dingwall, J. Am. Chem. Soc., 57 (1935) 2103.

Analytica Chimica Acta, 93 (1977) 281—285
©Elsevier Scientific Publishing Company, Amsterdam — Printed in The Netherlands

Short Communication

ÉTUDE DE L'ÉQUILIBRE PLOMB-HYDROXYDE PAR ÉLECTRODES SÉLECTIVES

C. BIRRAUX, J. CL. LANDRY et W. HAERDI*

Département de Chimie Minérale et Analytique, Université de Genève, Sciences II, CH-1211 Genève 4 (Suisse)

(Reçu le 7 février 1977)

L'application des électrodes sélectives à l'étude d'équilibres chimiques en milieu naturel implique à priori, la connaissance de l'influence de complexants sur la réponse de ces électrodes. Les effets des ions halogénures sur la réponse de l'électrode sélective au plomb, ont été étudiés dans un travail précédent [1]. Les effets du pH sur la réponse de l'électrode font l'objet de cette étude.

Théorie

La précipitation de l'hydroxyde de plomb se fait selon l'équilibre: $Pb^{2+} + 2\ OH^- \rightleftarrows Pb(OH)_2$, qui est régi par l'équation du produit ionique: $K_i = [Pb^{2+}]\,[OH^-]^2$. Or l'électrode sélective répond aux activités du plomb libre selon l'équation de Nernst

$$E = E_0 + S \log a_{Pb} \qquad (1)$$

(où E = potentiel mesuré; E_0 = potentiel standard de l'électrode sélective; S = pente de l'électrode; et a_{Pb} = activité des ions Pb^{2+}). Or $a_{Pb} = \gamma_{Pb}\,[Pb^{2+}]$, et en milieu de force ionique constante, γ_{Pb} est constante. En tirant $[Pb^{2+}]$ des équations ci-dessus et en l'introduisant dans l'éqn. 1, celle-ci devient après réarrangement

$$E = E_0' + S \log (K_i/K_e^2) - 2\,S\ pH \qquad (2)$$

E_0' inclut le terme γ_{Pb}. Lorsque l'équilibre de précipitation est atteint, le potentiel de l'électrode sélective au plomb et le pH sont dans une relation linéaire. L'ordonnée à l'origine permet de calculer K_i.

Complexes mononucléaires. Avant de précipiter le plomb, les ions hydroxyles peuvent le complexer. On ne considérera que l'influence des complexes $PbOH^+$ et $Pb(OH)_2$ soluble, estimant que le complexe $Pb(OH)_3^-$ n'a qu'une influence négligeable avant la précipitation de l'hydroxyde. Les constantes de stabilité apparentes sont données par $\beta_1 = [PbOH^+]/[Pb^{2+}]\,[OH^-]$ et $\beta_2 = [Pb(OH)_2]/[Pb^{2+}]\,[OH^-]^2$. La relation habituelle, faisant le bilan des particules, s'applique:

$$[Pb'] = [Pb^{2+}] + [PbOH^+] + [Pb(OH)_2] \quad (3)$$

où $[Pb']$ = concentration totale du plomb soluble, et $[Pb^{2+}]$ = concentration du plomb libre.

En introduisant β_1 et β_2 dans l'éqn. (3), on obtient après réarrangement

$$(\alpha - 1)/[OH^-] = \beta_1 + \beta_2 [OH^-] \quad (4)$$

où $\alpha = [Pb']/[Pb^{2+}]$. α et OH^- sont calculé ou mesurés directement avec les électrodes sélectives. La relation (4) est linéaire; β_1 est obtenu par l'ordonnée à l'origine, β_2 par la pente.

Complexes polynucleaires. L'expérience montre (Fig. 1) que pour des concentrations variables en plomb total et pour un même pH, α varie. Cela signifie qu'il se forme des complexes polynucléaires. Compte tenu de nos conditions expérimentales force ionique en particulier, les seuls équilibres pris en considération sont ceux du dimère et du tétramère.

Pour retrouver la même terminologie que la littérature [2], dans les constantes de complexes polynucléaires, les équilibres d'hydrolyse sont considérés comme suit

$$Pb^{2+} + 2\,H_2O \leftrightarrows Pb(OH)^+ + H_3O^+;\ \beta'_1 = [Pb(OH)^+]\,[H_3O^+]/[Pb^{2+}] \quad (5)$$

$$Pb^{2+} + 4\,H_2O \leftrightarrows Pb(OH)_2 + 2\,H_3O^+;\ \beta'_2 = [Pb(OH)_2]\,[H_3O^+]^2/[Pb^{2+}] \quad (6)$$

$$2\,Pb^{2+} + 4\,H_2O \leftrightarrows Pb_2(OH)_2^{2+} + 2\,H_3O^+;\ \beta_{22} = [Pb_2(OH)_2^{2+}]\,[H_3O^+]^2/[Pb^{2+}]^2 \quad (7)$$

$$4\,Pb^{2+} + 8\,H_2O \leftrightarrows Pb_4(OH)_4^{4+} + 4\,H_3O^+;\ \beta_{44} = [Pb_4(OH)_4^{4+}]\,[H_3O^+]^4/[Pb^{2+}]^4 \quad (8)$$

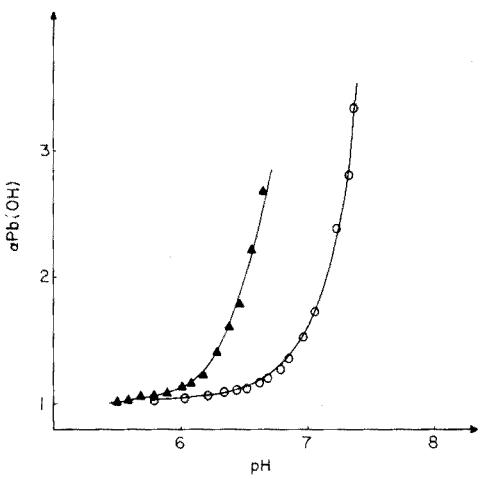

Fig. 1. Variation de $\alpha_{Pb(OH)}$ expérimental en fonction du pH. (○) 10^{-3} M Pb^{2+}; (▲) 10^{-2} M Pb^{2+}.

Le bilan des particules devient

$$[Pb'] = [Pb^{2+}] + [PbOH^+] + [Pb(OH)_2] + 2[Pb_2(OH)_2^{2+}] + 4[Pb_4(OH)_4^{4+}] \quad (9)$$

En introduisant les éqns. (5–8) dans l'éqn. (9), on obtient après réarrangement

$$\frac{1}{[Pb^{2+}]}\{[(\alpha - 1)\,[H_3O^+] - \beta_1'][H_3O^+] - \beta_2'\} = 2\,\beta_{22} + 4\,\beta_{44}\,\frac{[Pb^{2+}]^2}{[H_3O^+]^2} \quad (10)$$

α, $[Pb^{2+}]$, $[H_3O^+]$, β_1', β_2' sont connus ou peuvent être déterminés expérimentalement. Le graphe du membre de gauche de l'éqn. (10) en fonction de $[Pb^{2+}]^2/[H_3O^+]^2$ permet de déterminer β_{22} et β_{44}.

Réactifs et appareillage

Les réactifs sont Merck p.a. L'électrode sélective au plomb Orion No 94—82 et l'électrode de pH Metrohm E.A. 120 sont utilisés. Les millivoltmètres digitaux sont du type Metrohm E 500, les enregistreurs graphiques du type Metrohm E 478. Les calculs ont été effectués sur Hewlett Packard HP 9100 et sur CDC 3.800.

Conditions expérimentales

Les caractéristiques de l'électrode, E_0' et S, sont déterminées à partir d'une droite d'étalonnage, établie par mesure directe. Le pH mètre est également étalonné avec l'électrode de pH, à l'aide de solutions tampons (Merck). Les solutions de Pb^{2+}, sont en milieu de force ionique constante (0,1 M KNO_3). Les mesures se font en cellule thermostatisée à 25 ± 0,2°C. Dans la cellule de mesure les solutions sont d'abord acidifiées au pH 3—4, par HNO_3. Un courant d'azote barbotte dans la cellule pour éliminer CO_2. Ce courant est maintenu tout au long de l'expérience.

Quand le potentiel de l'électrode au plomb est stable et quand le pH est stable, on fait des ajouts de NaOH. Les solutions de NaOH sont préparées à partir de Titrisol (Merck) avec de l'eau déminéralisée, bouillie et dégazée.

Conditions particulières pour la détermination de constantes de complexes polynucléaires. Les solutions de plomb ont des concentrations variant de 10^{-2} M à 10^{-1} M par 0,5 unité. Pour chaque concentration, on effectue les mesures aux pH 5,5 — 5,7 — 5,9 — 6,1 — 6,3 — 6,5.

Résultats des mesures de produit ionique et des constantes de complexes Pb—OH. Discussion

Les valeurs de β_1 et β_2 calculées selon l'éqn. (4), sont données dans le Tableau 1 pour différentes concentrations totales de plomb.

La Figure 2 donne le graphe de l'éqn. (4), pour une concentration totale en plomb de 10^{-5} M. La Figure 3 donne le graphe du potentiel de l'électrode au plomb en fonction du pH. Pour $[Pb'] = 10^{-3}$ M et 10^{-2} M et des pH respectivement supérieurs à 7,3 et 6,7, la relation est linéaire. Le produit ionique calculé vaut: $K_i = (1{,}7 \pm 0{,}4)\,10^{-19}$. Les résultats montrent que la

TABLEAU 1

Valeurs de β_1 et β_2 obtenues pour différentes concentrations totales de plomb (0,1 KNO_3, $T = 25°C$)

Concentration de plomb (M)	β_1	β_2
10^{-5}	$(5{,}95 \pm 0{,}07)\ 10^6$	$(1{,}11 \pm 0{,}07)\ 10^{12}$
10^{-4}	$(5{,}1 \pm 0{,}2)\ 10^6$	$(2{,}2 \pm 0{,}2)\ 10^{12}$
10^{-3}	$(2{,}1 \pm 0{,}1)\ 10^6$	$(3{,}5 \pm 0{,}2)\ 10^{13}$
10^{-2}	$(1{,}4 \pm 0{,}4)\ 10^6$	$(8{,}2 \pm 0{,}4)\ 10^{14}$

valeur de β_1 est indépendante de la concentration totale de plomb, mais pas celle de β_2. La concentration totale de plomb augmentant, les autres espèces complexes commencent à intervenir sur les équilibres et ne sont plus aussi négligeables.

Cette hypothèse est confirmée par la valeur de β_2 obtenue pour une concentration totale en plomb de 10^{-5} M, valeur proche de celles citées dans la littérature [2].

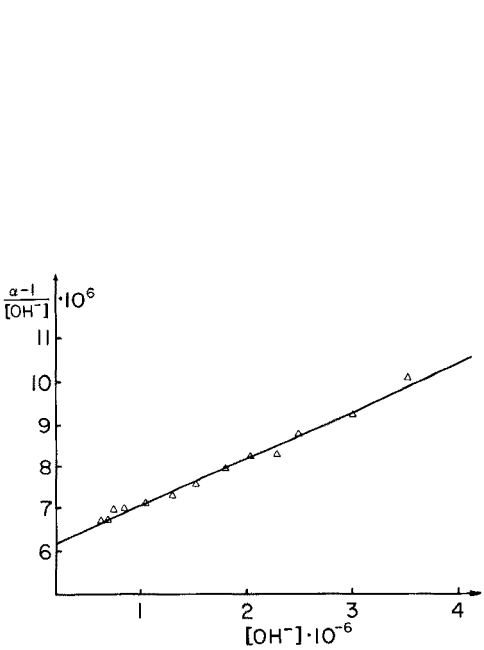

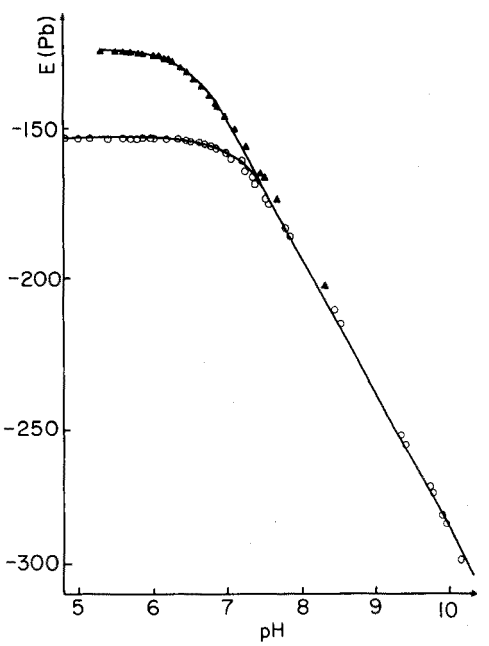

Fig. 2. Graphe de $(\alpha - 1)/[OH^-]$ en fonction de la concentration en OH^-, pour une concentration totale de plomb de 10^{-5} M.

Fig. 3. Graphe du potentiel de l'électrode au plomb en fonction du pH. (○) 10^{-3} M Pb^{2+}; (▲) 10^{-2} M Pb^{2+}.

TABLEAU 2

Valeurs de β_{44} obtenues à partir de l'éqn. (10). (La série 1 se rapporte aux concentrations totales de plomb variant de 10^{-2} à $4 \cdot 10^{-2}$ M; la série 2 à celles variant de $4{,}5 \cdot 10^{-2}$ à $7{,}5 \cdot 10^{-2}$ M; la série 3 à celles variant de $8 \cdot 10^{-2}$ M à 10^{-1} M. Dans chaque série les concentrations vont croissant par 0,5 unité; force ionique 0,1 M KNO_3, T = 25°C.)

pH	série	β_{44}
5,5	1	$(7 \pm 2) \cdot 10^{-19}$
	2	$(3{,}6 \pm 0{,}3) \cdot 10^{-20}$
	3	
5,7	1	$(5 \pm 1) \cdot 10^{-19}$
	2	$(5{,}2 \pm 0{,}2) \cdot 10^{-20}$
	3	$(3{,}7 \pm 0{,}5) \cdot 10^{-20}$
5,9	1	$(3{,}8 \pm 0{,}7) \cdot 10^{-19}$
	2	$(1{,}02 \pm 0{,}04) \cdot 10^{-19}$
	3	$(1{,}11 \pm 0{,}02) \cdot 10^{-19}$
6,1	1	
	2	$(2{,}12 \pm 0{,}04) \cdot 10^{-19}$
	3	$(8 \pm 2) \cdot 10^{-20}$
6,3	1	$(4{,}1 \pm 0{,}5) \cdot 10^{-19}$
	2	$(5{,}9 \pm 0{,}4) \cdot 10^{-19}$
	3	$(5{,}33 \pm 0{,}03) \cdot 10^{-19}$
6,5	1	$(6{,}1 \pm 0{,}5) \cdot 10^{-19}$
	2	$(1{,}4 \pm 0{,}1) \cdot 10^{-18}$
	3	$(1{,}2 \pm 0{,}0) \cdot 10^{-18}$

Résultats des mesures de constantes de complexes polynucléaires

Les valeurs de β_{44} obtenues à partir de l'éqn. (10) sont reportées dans le Tableau 2. Les calculs donnent des valeurs négatives pour β_{22}. Elles ne peuvent donc pas être prises en considération. Cela signifie que le dimère ne se forme pas ou que son influence est négligeable devant celle du tétramère.

En ce qui concerne le tétramère, les valeurs obtenues sont en bonne corrélation avec celle de la littérature [2]. Elles sont en particulier semblables à celles déterminées par Olin [3, 4] tant par électrochimie que par thermochimie. Olin ne signale pas la présence de complexes de type dimère. Il note la présence de complexes polynucléaires autres, 2:1, 3:4, 6:8, mais dans des conditions expérimentales différentes de celles présentement utilisées (force ionique élevée). En conclusion, l'électrode au plomb s'applique bien à l'étude des équilibres plomb-hydroxyde. Elle permet de suivre de manière satisfaisante, l'évolution des phénomènes de complexation et de précipitation en fonction du pH.

BIBLIOGRAPHIE

1 J. Cl. Landry, C. Birraux et W. Haerdi, Anal. Chim. Acta, 90 (1977) 51.
2 L. B. Sillen et A. E. Martell, Stability constants, Spec. publ. No 17, Chemical Society, London, 1964.
3 A. Olin. Acta Chem. Scand., 14 (1960) 126, 814.
4 B. Carell et A. Olin. Acta Chem. Scand., 16 (1962) 2350.

Analytica Chimica Acta, 93 (1977) 287—290
© Elsevier Scientific Publishing Company, Amsterdam — Printed in the Netherlands

Short Communication

THE COULOMETRIC GENERATION OF TUNGSTATE ION FROM A TUNGSTEN ELECTRODE IN AQUEOUS BASE SOLUTIONS

G. STEPHEN KELSEY

Department of Chemistry, University of Missouri—Columbia, Columbia, Missouri 65201 (U.S.A.)

(Received 28th January 1977)

As a continuation of the study of the anodic oxidation of Group VI metals in aqueous solution [1], the conditions of current density, basicity, and temperature conducive to quantitative generation of tungsten(VI) were determined. These results are part of a study of the electrode kinetics of tungsten in aqueous base solutions.

Experimental

Apparatus. A PAR 173 Potentiostat/Galvanostat (Princeton Applied Research Corp., Princeton, N.J.) equipped with a Model 179 digital coulometer was used. The cells were Metrohm EA 880 Universal Titration Vessels of 20-ml initial volume, jacketed for temperature control. Tungsten electrodes were 0.25 in. diameter rods, fixed in a demountable holder, suitable for weighing before and after polarization. Platinum foil counter electrodes of about 1.5 cm^2 area were used inside isolation tubes inserted in the cell cap. A saturated calomel reference electrode (s.c.e.) of the high impedance type was used with a salt bridge, in connection with a PAR Model 178 Electrometer Probe which was connected to the potentiostat and completed the three-electrode cell circuit.

Solutions were thermostatted to ± 0.02°C.

Reagents. Tungsten metal was obtained 99.95% pure (0.25-in. diameter rod; A. D. Mackay, Inc., New York). Electrolytes were all reagent-grade chemicals. Solutions were prepared from distilled deionized water and were purged with prepurified nitrogen before all experiments.

Procedures. Anodic current—potential data were obtained under galvanostatic conditions, i.e., $E = f(i)$. Currents of ca. $1 \cdot 10^{-5}$—$5 \cdot 10^{-1}$ A were applied to the working/counter electrode pair and the potential of the tungsten electrode (vs. s.c.e.) was recorded after it had stabilized (a period not exceeding 30 s, except for the first several measurements).

Coulometric current efficiency data were obtained both potentiostatically and galvanostatically. Between 50 and 300 coulombs of charge were passed. The electrode was again weighed after careful rinsing and drying, the coulometric efficiency being calculated as the observed change in mass divided by

that calculated on the basis of accumulated coulombs and Faraday's Law, for a 6e oxidation. The net anodic coulombs were read from the Model 179 coulometer.

The constant-current experiments were run in order to test the feasibility of constant-current generation of tungstate, a process requiring less sophisticated equipment for current integration. In this case, a constant current was applied to the cell for a time sufficient to pass a number of coulombs comparable to that of the potentiostatic experiments.

Current densities were calculated from the applied current and the geometric area of the immersed portion of the electrode, without regard for surface roughness. The technique used to obtain current—potential data (see above) was such as to minimize area changes during an experiment except at very high applied currents.

Tungsten rods were clamped in a chuck and rotated by an electric motor, while wet-sanded with 240-grit SiC paper, followed by 400-grit and finally wet polished with 600-grit SiC paper; pretreatment was completed by thorough rinsing with distilled deionized water [2] and oven-drying at 110°C for 5 min before weighing.

The electrolyte solutions contained $NaNO_3$ for ionic strength adjustment. Their compositions were:

Soln.	NaOH (M)	Na_2WO_4 (M)	$NaNO_3$ (M)
1	0.10	0.00	5.90
2	1.00	0.00	5.00
3	5.00	0.20	0.40

Results and discussion

Current—potential characteristics. The potentials in Fig. 1 were plotted against log current density to reveal the potential region wherein the linear Tafel relationship holds. In general, it extends for about two decades of current density. The solid lines are drawn with a slope of 4.606 *RT/F*.

It is not uncommon for the electrochemical oxidation of a metal to proceed with a non-stoichiometric number of electrons consumed [3, 4]. The possible formation of an initial oxidation state less than +6 for tungsten metal was investigated during the present work by the weight method (see above). Potentiodynamic polarizations [5] in these solutions did not reveal active regions where oxidation to a state less than +6 would be expected, as was observed for chromium [6]. Coulometric "*n*" determination showed a 6e oxidation in all solutions at potentials in the Tafel region and even at more positive potentials, where concentration polarization was evident. Indeed, the overall stoichiometry of the equation $W + 8OH^- \rightarrow WO_4^{2-} + 6e + 4H_2O$, was observed.

Current efficiency. Table 1 contains current efficiency data for the production of tungstate ion. Potentiostatic generation proceeds at essentially

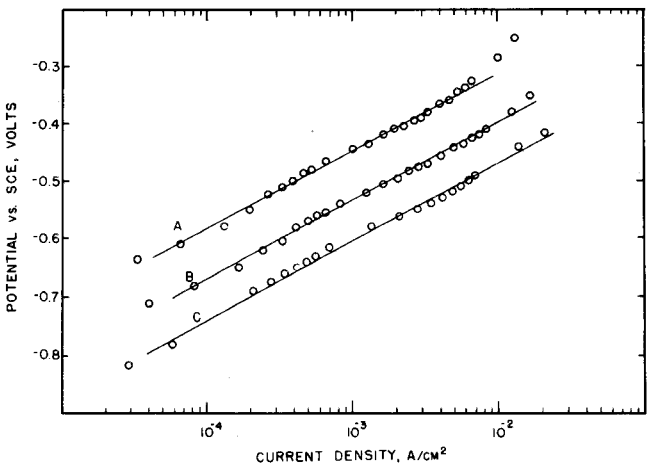

Fig. 1. Anodic Tafel diagram for tungsten metal in aqueous sodium hydroxide solutions. A, 0.10 M; B, 1.00 M; C, 5.00 M.

TABLE 1

Current efficiencies (%) at different potentials, current densities and temperatures

Solution			E_{app} (V vs. s.c.e.)	Applied current density (mA cm^{-2})	T (°C)
1	2	3			
Potentiostatic method					
104 ± 2	100.7 ± 0.5	100.0 ± 0.4		—	15.00
101.3 ± 1.0	100.5 ± 1.0	100.0 ± 0.6	−0.500	—	25.00
100.5 ± 2.0	100.0 ± 0.6	100.0 ± 0.7		—	45.00
100.8 ± 0.5	100.3 ± 0.3	100.1 ± 0.2		—	15.00
100.3 ± 0.5	100.5 ± 0.6	100.0 ± 0.0	+0.000	—	25.00
100.5 ± 0.5	100.0 ± 0.5	100.2 ± 0.5		—	45.00
100.4 ± 0.2	100.0 ± 0.2	100.2 ± 0.2		—	15.00
100.2 ± 0.4	100.7 ± 0.5	100.0 ± 0.3	+0.500	—	25.00
100.0 ± 0.5	100.3 ± 0.5	100.7 ± 0.5		—	45.00
Galvanostatic method					
100.7 ± 0.6	100.2 ± 0.5	100.0 ± 0.7	—	8.5	25
44.3 ± 0.7	100.3 ± 0.6	100.3 ± 0.6	—	46	25
36.0 ± 0.7	100.8 ± 0.9	100.3 ± 0.3	—	90	25

100% efficiency. The data for an applied potential of —0.500 V vs. s.c.e. in 0.10 M NaOH are less precise than the others because of the extended time periods (>24 h) required to accumulate 60 coulombs. The weight loss determination was thus less significant than those at 120 coulombs (corresponding to ca. 0.1 g W).

The galvanostatic efficiency data (Table 1) illustrate the necessity of knowing the current—potential characteristics of the system before attempting to generate tungstate ion at constant current. In the most dilute base, the applied currents above 40 mA cm^{-2} fall in the limiting current region of the *i—E* curve. During these experiments profuse gas evolution was observed at the electrode surface, as well as the formation of a translucent coating on the tungsten surface. This would seem to indicate that perhaps an insoluble or slightly soluble oxide forms in the concentration polarization region, where it cannot diffuse away or dissolve fast enough to support the applied current. The potential of the anode rose to a value over +5 V in a matter of seconds, after which evolution of oxygen began. The other seven galvanostatic experiments (Table 1) were well below the limiting current density, and the measured anode potentials corresponded almost exactly to those observed in the linear Tafel plots.

Conclusions. The production of tungstate ion from anodic oxidation of the parent metal proceeds with 100% current efficiency over a wide range of current densities and temperatures in basic solutions. Although passivity prohibits applications requiring in situ generation in acidic media, the method lends itself to coulometric titrations with externally generated tungstate; it also suggests a method for the preparation of standard tungstate solutions of low concentration, where gravimetric methods would not suffice.

REFERENCES

1 G. S. Kelsey and H. W. Safford, Anal. Chem., 46 (1974) 1585.
2 American Society for Testing and Materials G 5-72, Standard Reference Method for Making Potentiostatic and Potentiodynamic Anodic Polarization Measurements, ASTM, 1916 Race St., Philadelphia, PA 19103.
3 M. E. Straumanis and M. Dutta, Inorg. Chem., 3,(1966) 992.
4 M. L. Rumpel, A. W. Davidson and J. Kleinberg, Inorg. Chem., 3 (1964) 935; 2 (1963) 81
5 M. Pourbaix, Lectures on Electrochemical Corrosion, Plenum Press, New York, 1973, p. 2
6 A. I. Kostromin, A. A. Akhmetov and V. V. Mosolov, Zh. Anal. Khim., 25 (1970) 847.

Analytica Chimica Acta, 93 (1977) 291—295
© Elsevier Scientific Publishing Company, Amsterdam — Printed in The Netherlands

Short Communication

THE DETERMINATION OF TOTAL MERCURY IN COAL AND ORGANIC MATTER WITH MINIMAL RISK OF EXTERNAL CONTAMINATION

D. GARDNER*

Department of Oceanography, University of Liverpool, Liverpool L69 3BX (England)

(Received 30th March 1977)

The use of coal as a domestic and industrial fuel, and as an energy source increases annually. Besides concern about public health from volatile materials released into the atmosphere, environmental pollution by trace elements, especially mercury, is a problem. It appears that increased levels of mercury found along the jet stream belt in the Northern Hemisphere are the result of this type of industrial and domestic activity [1], so that analysis of environmental samples for mercury will continue to be of interest. This communication describes a wet oxidation method that can be used to determine mercury in samples, such as coal, that have a high percentage of organic matter. The technique minimizes possible errors from atmospheric mercury contamination, incomplete sample oxidation and retention of mercury by acid-insoluble matter.

Experimental

Reagents. Reagents were prepared with mercury-free water obtained by all-glass distillation followed by passage through a cation-exchange resin (Dowex AG50W-X8) in the hydrogen form. Analytical-grade reagents were employed and were tested for mercury contamination.

Nitric acid was distilled twice from an all-silica apparatus and stored in glass Winchesters. (Polythene containers were avoided as atmospheric mercury diffused through the container walls.)

Tin(II) chloride reagent was prepared as required by dissolving tin(II) chloride dihydrate (30 g) in 30 ml of 5 M HCl which had been purified by passage through a column of DeAcidite FF anion-exchange resin (50-100 mesh). The solution was then diluted to 50 ml with distilled water, and purified by bubbling nitrogen through it to remove mercury.

Hydroxylammonium chloride solution (20% w/v) was purified by repeated extraction with 0.05% dithizone in redistilled carbon tetrachloride.

*Present address: CSIRO Division of Fisheries and Oceanography, P.O. Box 21, Cronulla, N.S.W. 2230, Australia.

A standard mercury solution (1 mg ml^{-1}) was prepared by dissolving 0.1354 g of mercury(II) chloride in 100 ml of 5 M HCl. A standard solution (100 ng ml^{-1}) was prepared daily by dilution.

Apparatus. All glassware was cleaned with a mixture of concentrated nitric and hydrochloric acids (1 + 1) and rinsed with mercury-free water before use.

The all-glass, modified Bethge [2] apparatus (Fig. 1) used to digest the sample consists of a 250-ml three-necked flask (A) into which protrudes a thermometer well (B). The flask is surmounted by a bulb device which allows refluxing or distilling without exposing the digest to external contaminants. This consists of a three-way tap (C), an asbestos lagged by-pass tube (D), and a long side arm (E) which finally delivers the selected distilled fractions into a graduated cylinder (F). A condenser (G) with a trap (H) is fitted above the bulb. This trap contains mercury-free 15 M HNO_3 to prevent mercury-contaminated air entering the apparatus.

The mercury extracted was measured with a Unicam SP90A Series 2 atomic absorption spectrometer by the cold-vapour technique (Fig. 2). The mercury vapour liberated when tin(II) chloride is added to the 25-ml measuring cylinder (A), is pumped through a short drying column (B) of magnesium perchlorate, and then into the 15-cm fused silica cell (C) in the light path of the spectrometer by a peristaltic pump (D) (flow rate 130 ml min^{-1}). Dead space is kept to a minimum by making all connecting tubing as short and narrow as possible.

Procedure for coal. Set up the apparatus as shown in Fig. 1. Weigh out 1 g of coal dust and place on a cold sand bath overnight with 25 ml of mercury-

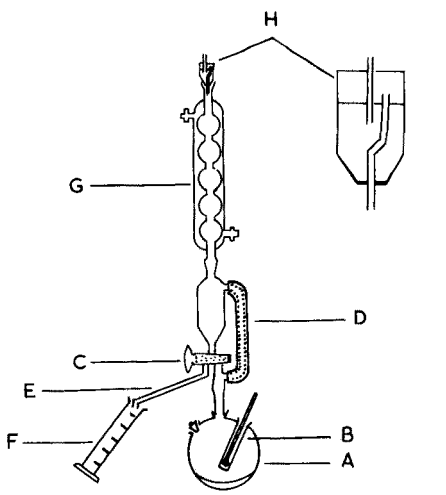

Fig. 1. The apparatus for digesting samples.

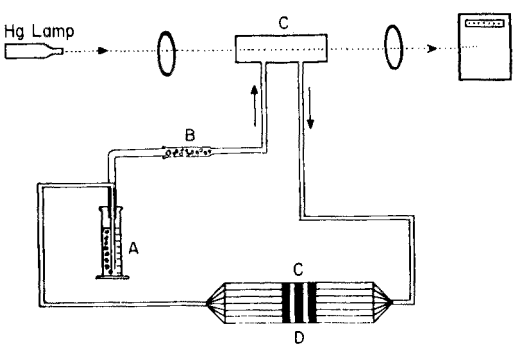

Fig. 2. The mercury detection apparatus.

free HNO_3 and 1.5 ml of H_2SO_4. Then reflux until the digest becomes pale yellow. Add 10 ml of 45% perchloric acid (care: only when the digest is yellow) and approximately 0.40 g of aminoacetic acid (glycine). Using a Meker burner, distil off into a measuring cylinder and discard the HNO_3 at $< 130°C$ until about 5 ml of HNO_3 remains. Distil the residue up to a temperature of 340°C (at which point the sulphuric acid starts to fume), and collect the $HClO_4$ and remaining HNO_3 in the 25-ml measuring cylinder. Quickly stopper the cylinder. (It is advisable to do the digestion and separation with safety screens in place.) Make the collected fraction up to about 22.5 ml with mercury-free water. Before the final analysis add 0.5 ml of freshly prepared 7% iron(II) ammonium sulphate (to eliminate nitrogen dioxide interference from the nitric acid present) and 1 ml of 10% hydroxylammonium chloride. After at least 15 min add 1 ml of 30% tin(II) chloride solution, fit the bubbling head on the cylinder immediately, and pass air through the closed circuit with the peristaltic pump. Measure the absorbance at 253.7 nm; a steady state should be attained after 30 s. Measure a blank value for the reagents and prepare a calibration graph for standard mercury solutions.

The levels of atmospheric mercury contamination should be checked regularly [3] throughout the procedure, to prevent accidental contamination of the sample. If contamination does exist, keep extractor fans full on, never expose samples or reagents to the atmosphere, always be sure the HNO_3 trap is in place, use Pyrex glass for reagent storage and clean the glassware immediately before use.

Results and discussion

Methods used to determine mercury in coal [4, 5] and in other materials of high organic content [6—9] have been reported. Such techniques have been reviewed [10—12]. In this laboratory, a suitable a.a.s. method was needed to analyse very low mercury concentrations in coal and similar materials in a mercury-contaminated atmosphere. Such a method is required by many laboratories which do not have adequate facilities to prevent mercury vapour being present in the air in quantities that might contaminate samples and reagents [3, 13].

For development of the technique, ^{203}Hg tracer was used, but standard additions of natural mercury were used to test the method under optimum conditions. Finally, a set of coal samples was analysed independently by a different method by the National Coal Board laboratory. Good agreement of results was obtained.

Early experiments showed that decomposition of coal in furnaces of varying length was accompanied by emission of dense gases that quickly condensed on cooler transmission tubing. Mercury determinations were rapid, however, and the technique was ideal for samples with little or no organic content, but for coal samples the tarry deposits retained a large percentage of the mercury. Consequently, for coal analysis, a wet chemical technique was chosen for further development.

Preliminary tests showed that when digestions were done in open or partially enclosed vessels, samples became contaminated by mercury present in the surrounding air. The Bethge apparatus with a HNO_3 trap [3, 12] to prevent this was finally selected. The present technique is a development of the work reported by Gorsuch [2], who showed that volatile chloro complexes were formed when glycine was added to an acid digest containing perchloric acid, and mercury could be distilled from the residue.

In the present experiments, the recovery of mercury in the perchloric acid distillate depended critically on the volume of H_2SO_4 with 3 ml of H_2SO_4 only 55—65% was recovered. No more than 1.5 ml of H_2SO_4; should be used for > 97% recovery, and the distillation should proceed until copious white fumes fill the system.

The volume of nitric acid allowed to remain in the digestion flask was also critical. If more than 10 ml remained, the final atomic absorption measurement was affected. If less than 3 ml was left behind, a small fraction of the total mercury would have been discarded, as it would have started to distil over with the last few ml of the nitric acid. The volume left was assessed by collecting the HNO_3 to be discarded in a measuring cylinder. About 5 ml was the optimum volume to be allowed to distil over with the 10 ml of perchloric acid.

The technique was used to determine mercury in many coal samples, fish tissue, including seals' liver, filter papers, organic mercury complexes, sediments and oil. This wide range of different materials could be analysed accurately because all organic matter was completely oxidized before the mercury was distilled. Selected results are presented in Table 1. Generally, standard deviations for quadruplicate analyses of coal were 6 and 16% at the 2.0 and 0.2-ppm levels, respectively. For replicate analyses of seals' liver at 360 ppm, the standard deviation was ca. 10%. This increase was probably due to the difficulty of obtaining a representative sample from incompletely homogenized fibrous material.

Normally the complete analysis will take a maximum of 24 h for coal and about half a day for other materials. This is because it is necessary to leave samples overnight with the HNO_3—H_2SO_4 before heating. This eliminates

TABLE 1

Replicate analyses of coal samples and a sample of seals' liver with mean and standard deviations of mercury concentrations

Sample	Mercury concentrations from replicate analyses (ppm)						Mean	Standard deviation
Coal A	0.15	0.16	0.19	0.19	0.22		0.18	0.03
Coal B	0.39	0.36	0.33	0.35			0.36	0.03
Coal C	2.00	1.95	2.06	2.24			2.06	0.13
Coal D	0.64	0.50	0.50	0.50	0.53		0.53	0.06
Seals' liver	374	314	380	319	404	372	360	36

frothing during the initial decomposition stages. The output can be increased by digesting the samples in batches of 10, of which at least one is a blank (early experiments showed that unless reagent batches were changed, one blank was sufficient).

The absolute detection limit of the method was 5 ng. Optimum measurements were done between 20 and 100 ng. This was achieved by varying the amount of material digested or by dilution before the final measurement.

I thank Professor J. P. Riley for helpful comments, NERC for financial support, and the National Coal Board for supplying samples.

REFERENCES

1 D. Gardner, Mar. Pollut. Bull., 6 (3) (1975) 43.
2 T. T. Gorsuch, Analyst, 84 (1959) 135.
3 D. Gardner, Anal. Chim. Acta, 82 (1976) 321.
4 M. E. Hinkle, U.S. Geol. Surv. Prof. Pap. No. 750B (1971) 171.
5 G. W. Kalb, Am. Chem. Soc., Div. Fuel Chem. Prepr., 16 (3) (1972) 1.
6 E. Orvini, T. E. Gills and P. D. LaFleur, Anal. Chem., 46 (1974) 1447.
7 E. S. Peck, Anal. Chim. Acta, 80 (1975) 75.
8 Y. Kuwae, T. Hasegawa and T. Sheno, Anal. Chim. Acta, 48 (1975) 185.
9 A. M. Ure and C. A. Shand, Anal. Chim. Acta, 72 (1974) 63.
10 D. J. Von Lehmden, R. H. Jungers and R. E. Lee, Jr., Anal. Chem., 46 (1974) 238.
11 M. D. Schlesinger and H. Schultz, U.S. Bur. Mines Rep. Invest., (1972) 7609.
12 Mercury Analysis Working Party of the Bureau International Technique du Chlore, Anal. Chim. Acta, 84 (1976) 231.
13 T. Gunther, Talanta, 19 (1972) 1489.

Analytica Chimica Acta, 93 (1977) 297—299
© Elsevier Scientific Publishing Company, Amsterdam — Printed in The Netherlands

Short Communication

X-RAY FLUORESCENCE SPECTROMETRIC DETERMINATION OF TECHNETIUM IN NUCLEAR FUELS PROCESSING WASTES

S. G. METCALF

Atlantic Richfield Hanford Company, Richland, Washington 99352 (U.S.A.)

(Received 11th January 1977)

Technetium is formed in greater than 6% yield by thermal neutron fission of ^{235}U [1]. The long half-life of ^{99}Tc ($2.12 \cdot 10^5$ y) makes the rapid and accurate determination of technetium in processing wastes important from the standpoint of waste storage and handling. Technetium was first determined by its radioactivity [2]. It is most often determined by β-counting techniques, which require a prior separation from all other β-emitting isotopes. Nuclear fuels processing wastes contain large amounts of such isotopes and relatively small amounts of technetium. Separation factors greater than 10^8 may be routinely required, which may be difficult to achieve; thus there is a need for alternative methods of analysis. Technetium has been determined by spectrophotometric [3—5], polarographic [6], and neutron activation [7] methods. Extraction of technetium from basic solutions with quaternary amines has been reported [8, 9]. The low detection limits, selectivity, and simplicity of operation generally offered by x-ray spectrometric methods coupled with the apparent ease of separation of technetium from basic media suggested that this combination would provide a functional method for the determination of technetium in nuclear fuels processing wastes.

Experimental

Apparatus. The spectrometer used was a Spectratrace 440, equipped with a tungsten target transmission x-ray tube. The x-radiation from the tube was filtered with a $5.5 \cdot 10^{-2}$-mm thick lead filter. A 0.1-mm beryllium filter was placed over the detector collimator to eliminate the technetium β-radiation. The data were accumulated, analyzed, and stored on a Northern Scientific Model 750 Multichannel Analyzer coupled to a Northern Scientific Model 111 magnetic tape system. The instrument operating parameters were as follows: x-ray tube potential, 50 kV; x-ray tube current, 0.80 mA; time (dead time corrected), 500 s; number of analyzer channels, 1024; energy per channel, 40 eV.

Reagents. A stock solution of methyltricaprylammonium chloride (MTC; Chemical Division, General Mills) was prepared by diluting 30 ml of MTC to

100 ml with reagent-grade xylene (J. T. Baker). A stock solution of rhenium (1 g Re l^{-1}) in 1 M HNO_3 was prepared from the metal. Working solutions of NaOH (12 M), $NaNO_2$ (5 M), and $NaNO_3$ (7 M) were prepared. A working solution of $NaAlO_2$ was prepared by dissolving reagent-grade $NaAlO_2$ in 12 M NaOH and diluting with deionized water to give a $NaAlO_2$ concentration of 4 M and NaOH concentration of 1.7 M. Stock solutions of As, Bi, Co, Cu, Ga, Y, Pb, Hg, Nb, Ni, Ru, Zr and Mo were made by dissolving the metal or oxide in 15 M HNO_3 and diluting to give a nominal metal concentration of 1 g l^{-1} and a HNO_3 concentration of 1 M. NH_4TcO_4 solution (Battelle Northwest Laboratories, Richland, Washington) was diluted to give a technetium concentration of 1.179 g l^{-1} in 1 M HNO_3.

Procedure. During the investigation of possible chemical interferences of ions common to nuclear fuels processing waste, the following procedure was used. All tests except the NaOH tests were done in 4 M NaOH solutions. The following were added to a 35-ml glass screw-cap vial, containing ca. 10 ml of deionized water, in the order listed; 12 M NaOH (6.7 ml), compound under study, stock solutions of Re and Tc (500 μl and 75 μl, respectively). The resulting solution was stirred and diluted to 20 ± 0.1 ml with deionized water. Exactly 1.00 ml of MTC stock solution was added and stirred for 10 min at a speed providing a good emulsion. The phases were allowed to separate by standing for 5 min. The MTC phase (upper) was transferred as quantitatively as possible to a 2-dram glass screw-cap vial. None of the aqueous phase was transferred. Two aliquots (250 μl) of the technetium-containing MTC were added dropwise to a filter pad and dried under an i.r. lamp for 20 min. The pad was placed on a "spectrocup" (31.75-mm o.d., Somar Inc., New York) and covered with three layers of Mylar. The mounts were then counted with the instrument operating parameters given above and compared with standards prepared by taking known amounts of Tc through the procedure. Test samples of actual waste solutions were run by the same procedure except that no Tc or NaOH was added.

Results and discussion

The detection limit (C_l, the minimum concentration of analyte detectable to a specified confidence level) is considered to be given by $C_l = T\alpha\sigma_{s=0}/MN^{\frac{1}{2}}$, where $T\alpha$ is the test statistic; $\sigma_{s=0}$ is the standard deviation in signal at zero analyte concentration; M is the slope of the calibration curve; and N is the number of measurements.

Assuming $N = 1$, $\sigma_{s=0} = 40$ cps and $M = 284$ cps/μg (typical values) a 20-ml sample size and using the 97.5% confidence level, the detection limit is 90 μg Tc l^{-1} of sample.

The following ions, at the indicated levels common to nuclear fuels processing wastes, have no significant effect on the proposed method: 2—8 M NaOH, 0—4.6 M $NaNO_3$, 0—3 M $NaNO_2$, and 0—2.5 M $NaAlO_2$. Cations that could potentially cause a spectral interference with either Tc or Re were tested by adding a 10:1 (weight) amount to a solution containing 92 μg Tc

and 500 μg Re and taking through the procedure. The following did not prevent essentially quantitative technetium recovery and were not coextracted: As, Bi, Co, Cu, Ga, Y, Pb, Nb, Ni, Ru, Zr, and Mo. Under the test conditions, mercury was coextracted; a 10:1 ratio caused only a 91% technetium recovery. The average technetium recovery for 92 μg Tc was 102 ± 2% at the 95% confidence level for 12 data points. For 5.9 μg Tc with six trials and the 95% confidence limit, the recovery was 101 ± 9%. Tests indicated quantitative recovery of 92 μg Tc from solutions of 10—100 ml (with 4 M NaOH in all cases), showing that volume control during the extraction step is not critical.

The method was tested by analyzing a number of actual waste samples. The following result was typical. A solution (4-ml aliquots) was analyzed five times. The technetium value found was 7.7 ± 0.1 mg Tc l^{-1} at the 95% confidence level. The Re recovery was quantitative. The exposure dose rate of radiation from the pad containing the technetium was less than $7 \cdot 10^{-5}$ Ci kg^{-1} s^{-1} (1 mrad h^{-1}). The radiation from the same volume of sample without separation of the technetium from other isotopes present was $1.9 \cdot 10^{-2}$ Ci kg^{-1} s^{-1} (240 mrad h^{-1}). Thus a significant reduction in personnel exposure to ionizing radiation results from the separation. At least 12 samples can be analyzed in an 8-h working day.

In summary, the method provides for rapid, simple, accurate and safe analyses of nuclear fuels reprocessing wastes for technetium.

REFERENCES

1 R. Colton, The Chemistry of Rhenium and Technetium, Interscience, New York, 1965, p. 5.
2 C. Perrier and G. Segre, J. Chem. Phys., 5 (1937) 712.
3 O. H. Howard and C. W. Weber, Anal. Chem., 34 (1962) 530.
4 F. J. Miller and P. F. Thomason, Anal. Chem., 33 (1961) 404.
5 F. J. Miller and H. E. Zittel, Anal. Chem., 34 (1962) 1349.
6 L. Astheimer and K. Schwochare, J. Electroanal. Chem., 15 (1967) 61.
7 G. E. Boyd and Q. V. Larson, J. Phys. Chem., 60 (1956) 707.
8 W. J. Maeck, G. L. Booman, M. E. Kussy and J. E. Rein, Anal. Chem., 33 (1967) 1775.
9 G. B. S. Salaria, C. L. Rulfs, and P. J. Elving, Anal. Chem., 35 (1963) 983.

Analytica Chimica Acta, 93 (1977) 301—305
© Elsevier Scientific Publishing Company, Amsterdam — Printed in The Netherlands

Short Communication

SUBSTOICHIOMETRIC RADIOISOTOPE DILUTION ANALYSIS FOR TRACES OF MERCURY BY SOLVENT EXTRACTION WITH SILVER DIETHYLDITHIOCARBAMATE

J. M. LO, J. C. WEI, and S. J. YEH

Institute of Nuclear Science, National Tsing Hua University, Hsinchu 300 (Taiwan)

(Received 3rd January 1977)

Many metal ions form complexes with the diethyldithiocarbamate anion, $(C_2H_5)_2NCS_2^-$ (DDC), and can be extracted into organic solvents. Extraction coefficients for metal ions with DDC under some conditions have been reported by several authors [1—6]. For analytical extractions, some complexes, $Me(DDC)_n$, in the organic solvent are often preferred as reagents to HDDC and NaDDC, which are less stable and easily decomposed in acidic solution [1, 2, 7—9]. Moreover, a certain $Me(DDC)_n$ in a suitable organic solvent can be chosen to extract metal ions selectively, in accordance with the order of the extraction coefficients [1]. For example, in 0.05 M H_2SO_4 media, the order suggested by Wyttenbach and Bajo [1] is Hg^{2+}, Ag^+, Ni^{2+}, Cu^{2+}, Bi^{3+}, Sb^{3+}, Te^{4+}, Mo^{6+}, Se^{4+}, In^{3+}, As^{3+}, Cd^{2+}, and Zn^{2+}. The extraction coefficient for Ag^+ is higher than those for other metals except Hg^{2+}, hence none of these metal ions should be extracted if AgDDC is used as the reagent. The extraction coefficient for Ag^+, 10^{12}, is 3 orders of magnitude less than that for Hg^{2+}, 10^{15} [2, 6]. Accordingly, mercury in water should be readily and selectively extracted into a solution of AgDDC in an organic solvent.

In this study, substoichiometric isotope dilution analysis, as developed by Suzuki and Kudo [10, 11] and Růžička and Stary [12], was applied for the determination of traces of mercury in aqueous solution, by solvent extraction of Hg^{2+} with AgDDC in chloroform. The same quantities of AgDDC in chloroform are used to extract the same quantities of mercury to be partly separated in the standard and test solutions. The standard solution contains only the mercury radioisotope and the test solution is a mixture of test sample and a known amount of standard solution. Theoretically, the radioactivity of each extract should be inversely proportional to the initial total mass of mercury in both solutions; and the general formula for the calculation of substoichiometric isotope dilution analysis is

$$M_x = M[(A/A')-1] \quad (1)$$

where A and A' are the activities extracted from the standard and test solutions, respectively, and M and M_x are the masses of mercury in the standard and sample, respectively.

It is shown below that eqn. (1) requires determination of very small amounts of mercury ($\leqslant 1\ \mu g$) in solution.

Experimental

Reagents. AgDDC was prepared by precipitation of 0.5 g of $AgNO_3$ in water with 2 g of $NaDDC \cdot 2H_2O$ in ethanol. The precipitate was filtered, washed with water, dried at 60—70°C, then dissolved in as little chloroform as possible and the same volume of ethanol was added. AgDDC was recrystallized by slow evaporation of chloroform at 70—80°C. The filtered crystals were washed repeatedly with pure water until no silver(I) was detected then dried at 60—70°C for at least 10 h.

AgDDC solutions in chloroform were obtained by accurate weighing and dissolution in chloroform with appropriate dilution.

Aqueous mercury(II) solutions were prepared by dissolution of HgO in dilute perchloric acid, and suitable dilution.

$^{197,203}Hg$ and ^{110m}Ag were produced by irradiating pure HgO and $AgNO_3$ in the Tsing Hua Open-Pool Reactor at a thermal neutron flux of about $2 \cdot 10^{12}$ n cm^{-2} s^{-1} for 30 h and 90 h, respectively.

The chemicals used were Suprapur grade (E. Merck). The water used was distilled, passed through an ion-exchange column and further purified by the sub-boiling distillation method suggested by Kuehner et al. [13].

Treatment of containers. All containers were cleaned by immersing in (1 + 1) HNO_3 for 1 d, washing with distilled water several times and then with the sub-boiled distilled water. Before each series of experiments, the cleaned vessels were washed with AgDDC—$CHCl_3$ solution. The last traces of AgDDC were removed with chloroform.

Solvent extraction and activity measurements. Glass-stoppered Erlenmeyer flasks (50 ml) were used as extraction vessels. The solutions were mechanically shaken for 2 min at room temperature (amplitude, 2.5 cm; frequency, 3 s^{-1}). Increased shaking times did not affect the extraction rates.

Aliquots of the organic and aqueous phases were taken from the extraction flasks, and the activity was measured with a well-type NaI crystal connected to a single-channel analyzer.

Results and discussion

Stability of AgDDC in chloroform during storage. A $3.0 \cdot 10^{-5}$ M solution of AgDDC in chloroform was divided, and one part was stored at 5°C in the dark and the other at 20°C in daylight. A mercury(II) solution (5 ml) of pH 0.5 ($HClO_4$) labelled with $^{197,203}Hg$ was extracted with 5 ml of the initial AgDDC solution; 65% of the radioactivity was extracted. Similar tests were carried out over a period of 3 weeks with the stored AgDDC solutions. The radioactive Hg^{2+} solution of pH 0.5 was proved to be stable for several weeks. The percentage extraction of the radioactivity by the AgDDC solution stored at 5°C in the dark remained constant (65%) for 3 weeks, whereas the extraction with the reagent, stored at 20°C in the light decreased gradually to ca. 55% during that time.

Stability of AgDDC in chloroform during extraction with acidic solutions. AgDDC labelled with ^{110m}Ag was used for these tests. Solutions (10 ml) of HCl, HNO_3, $HClO_4$ and H_2SO_4 at different concentrations were shaken with 10 ml of the labelled $5.0 \cdot 10^{-5}$ M AgDDC solution in chloroform. The percentage of AgDDC remaining in the organic phase was measured by its radioactivity after shaking. HCl and HNO_3 decomposed AgDDC rapidly as the acidity increased up to 2 M, whereas $HClO_4$ and H_2SO_4 had no effect on the stability of AgDDC even at acidities of 5—6 M. The mercury(II) sample solutions must be adjusted with $HClO_4$ or H_2SO_4 to pH < 1, to ensure the presence of only the Hg^{2+} form in the solution [14], and to prevent losses of mercury by adsorption on the container [15].

Extraction of metal ions other than mercury(II). Metal ion solutions (10 ml, 50 p.p.m.) at pH 0.5 ($HClO_4$) were shaken with 10 ml of the labelled $5.0 \cdot 10^{-5}$ M AgDDC solution in chloroform. At these concentrations, silver ion would be released quantitatively into the aqueous phase, if the other metal ion were extracted. Aliquots (2 ml) of aqueous phase were taken for ^{110m}Ag radioactivity measurement, and the percentage of the activity in the aqueous phases after extraction was calculated. When Ba^{2+}, Ni^{2+}, Bi^{3+}, Mg^{2+}, Sn^{2+}, Zn^{2+}, Fe^{3+}, Mn^{2+}, Tl^{3+}, Co^{2+}, and Pt^{4+} were tested, less than 0.2% of the ^{110m}Ag activity appeared in the aqueous phase, with Cu^{2+} and Cd^{2+}; the values were about 1.5%. Thus none of these metal ions are extracted, which agrees with the theoretical predictions [1]. Unfortunately, Au^{3+} and Pd^{2+} were extracted strongly and seriously affected the substoichiometric determination of mercury. When Au^{3+} and Pd^{2+} were tested, the percentages of ^{110m}Ag activity found in the aqueous phase were 94% and 90%, respectively. Clearly, the extraction coefficients for Au^{3+} and Pd^{2+} are higher than that for Ag^{+}.

Substoichiometric radioisotope dilution analysis for mercury. The preceding experiments showed that for a successful analysis, the reagent solution must be stored at 5°C in the dark, the aqueous solution must be acidified with $HClO_4$ to pH < 1, and Au^{3+} and Pd^{2+} must be absent. To investigate the applicability of this method for the determination of traces of mercury in water, a series of mercury(II) solutions (20 ml) containing 12—40 p.p.b., were extracted with 5 ml of unlabelled $1.7 \cdot 10^{-7}$ M AgDDC in chloroform. The total mass of mercury in these solutions was in the range 0.24—0.80 μg, and each solution contained the same amount of $^{197,203}Hg$ activity. The same mass of mercury should be extracted into the organic phase from each solution. The percentages of radioactive mercury extracted were between 20% and 80%.

The reciprocal activity extracted from each solution was plotted against the total initial mass of mercury in each solution as a straight line (Fig. 1), but this line did not pass through the origin, which is at variance with the theory. As indicated geometrically in Fig. 1, $(M + M_x)/M \neq A/A'$ so that eqn. (1) could not be used for the calculation of the present experimental results. These experiments were checked repeatedly and the same results were always obtained.

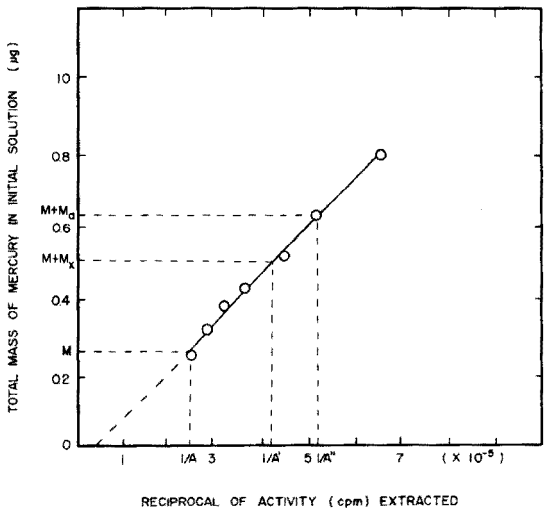

Fig. 1. Relationship between total mass of mercury in initial solution and reciprocal of ^{197,203}Hg activity extracted by AgDDC in chloroform.

Deviation of experimental results from theory is often inevitable. For example, the mercury in the standard solution containing only radioactive mercury could not be determined accurately because of the very small amount of radioisotope available. A modification of eqn. (1) is suggested for the calculation of the practical results. As indicated in Fig. 1, another standard solution with mercury mass = M_a but containing no radioisotope, was added to the standard solution with mass = M containing only radioisotope. The amount of mercury, M_a, was known accurately by dilution from a large amount of mercury (e.g. 100 mg) to a trace mercury solution. The activity extracted from the mixture ($M + M_a$) was determined as A'', and the activity extracted from ($M + M_x$) was A'. From Fig. 1, the relationship found is

$$M_x/M_a = \left(\frac{1}{A'} - \frac{1}{A}\right) \Big/ \left(\frac{1}{A''} - \frac{1}{A}\right) \qquad (2)$$

from which the mass of mercury in the sample (M_x) can be determined. It is to be noted that M, the mass of mercury in the standard solution containing only radioisotope, is not involved in eqn. (2). This modification is practical in analysis for traces of mercury in water. Trace amounts of mercury can be determined accurately through calculation by the modified formula (eqn. 2) instead of the conventional formula, (eqn. 1), as shown in Table 1.

TABLE 1

Substoichiometric isotope dilution analysis for mercury by solvent extraction with AgDDC
M = not analyzed, M_a = 1.48 μg, A = 33012, A'' = 21345

A'	M_x (μg)	
	Taken	Found
27610	0.48	0.53
24330	0.94	0.96
19528	1.86	1.86
16110	2.78	2.84
13538	3.71	3.89
11963	4.63	4.75

We are indebted to Dr. Vianney K. C. Cheng for helpful advice.

REFERENCES

1 A. Wyttenbach and S. Bajo, Anal. Chem., 47 (1975) 1813.
2 A. Wyttenbach and S. Bajo, Anal. Chem., 47 (1975) 2.
3 H. Bode and K. J. Tusche, Z. Anal. Chem., 157 (1975) 414.
4 R. Wickbold, Z. Anal. Chem., 152 (1956) 259.
5 G. Eckert, Z. Anal. Chem., 155 (1957) 23.
6 J. Stary and K. Kratzer, Anal. Chim. Acta, 40 (1968) 93.
7 J. Kucera, Radiochem. Radioanal. Lett., 24 (1976) 215.
8 P. A. Schubiger and O. Muller, Radiochem. Radioanal. Lett., 24 (1976) 353.
9 J. W. Mitchell, Radiochem. Radioanal. Lett., 24 (1976) 123.
10 N. Suzuki, Proc. 2nd Conf. Radioisotopes (Japan), 1958.
11 N. Suzuki and K. Kudo, Anal. Chim. Acta, 32 (1965) 456.
12 J. Růžička and J. Stary, Talanta, 10 (1963) 287.
13 E. C. Kuehner, R. Alvarez, P. J. Paulsen, and T. J. Murphy, Anal. Chem., 44 (1972) 2050.
14 R. de Levie, J. Chem. Educ., 47 (1970) 187.
15 J. M. Lo and C. M. Wai, Anal. Chem., 47 (1975) 1869.

Analytica Chimica Acta, 93 (1977) 307—310
© Elsevier Scientific Publishing Company, Amsterdam — Printed in The Netherlands

Short Communication

L'UTILISATION DU 2,2'-BIPYRIDINE POUR LA SÉPARATION FER(II)—FER(III) AU MOYEN DES RÉSINES ÉCHANGEUSES D'IONS

GRIGORE POPA, LUMINITA VLĂDESCU et ELENA PREDA

Laboratoire de Chimie Analytique, l'Institut de Chimie, I.P.B. Splaiul Independenţei 202, Bucarest 7000 (Roumanie)

(Reçu le 21 decembre 1976)

La séparation de certains ions présentant divers degrés d'oxydation, peut être realisée en bonnes conditions, d'une manière rapide et simple, en faisant appel à la technique de l'échange ionique. On a proposé quelques procédés de séparation pour le système Fe^{2+}—Fe^{3+}, par exemple sur des résines échangeuses d'ions en présence d'acide chlorhydrique comme agent de compléxation [1—3], sur des résines échangeuses de cations par l'élution des ions Fe^{3+} à l'aide de l'acide oxalique et des ions Fe^{2+} à l'acide chlorhydrique [4], et en milieu de solvents mixtes en éluant le cationit avec un mélange de benzène—*n*-butanol—HCl (33%)[5]. L'utilisation de l'acide chlorhydrique comme agent de compléxation présente le désavantage de favoriser l'oxidation des ions $Fe^{2+} \rightarrow Fe^{3+}$, ce qui peut introduire des erreurs jusqu'à 20%. Les ions Fe^{2+}—Fe^{3+} ont été séparés efficacement, sur des résines échangeuses d'ions, en présence de certains agents de compléxation comme l'1,10-phénanthroline, le sulfocyanure de potassium et l'acide chlorhydrique [6], ou le phosphat, le tartrat, le citrat, et l'EDTA [7].

Dans le présent travail, on propose la séparation du fer (Fe^{2+} et Fe^{3+}), basée sur la formation des combinaisons complexes stables à charge électrique différente, sélectivement retenues par les résines échangeuses d'ions et qui ne permettent pas l'oxydo—réduction des ions présents dans l'échantillon. L'ion Fe^{2+} compléxé par le 2,2'-bipyridine, est fortement retenue par les résines échangeuses de cations, pendant que les ions Fe^{3+} peuvent être élués à l'acide chlorhydrique. En utilisant les résines échangeuses d'anions, les ions Fe^{3+} sont fixés comme anion complexe $[FeCl_4]^-$, tandis que la combinaison complexe $[Fe(bip)_3]^{2+}$ passe dans l'effluent et le Fe(II) est directement déterminé spectrophotométriquement.

Partie éxperimentale

Les matières premières étaient: résines échangeuses de cations Dowex-50W-X8 et Vionit CS-3, et d'anions Amberlite IRA-400 et Vionit AT-1. Solution aqueuses: 10^{-2} M de sel Mohr à titre connu; 10^{-2} M de $FeCl_3 \cdot 6H_2O$ à titre connu; $FeSO_4$; 20% d'ácetate d'ammonium; 0,5% du 2,2'-bipyridine (Reanal).

La détermination des ions à été réalisée par titration compléximétrique à l'EDTA en présence d'acide sulfosalicylique pour le Fe^{3+} [8] et spéctrophotométriquement au 2,2′-bipyridine pour le Fe^{2+} [9].

Résultats et discussions

Afin d'établir les conditions optimaux de travail, on a fait des études spéctrophotométriques pour déterminer les facteurs qui influencent la stabilité du complexe $[Fe(bip)_3]^{2+}$ et des études concernant le rétention des ions $[Fe(bip)_3]^{2+}$ et $[FeCl_4]^-$ sur des résines échangeuses d'ions. On a observé une diminution de l'absorbances des solutions du complexe $[Fe(bip)_3]^{2+}$ pour des teneurs en HCl > 4 M.

La combinaison complexe du Fe(II) avec le 2,2′-bipyridine est fortement retenue sur une résine échangeuse de cations, de sorte que les ions sont extraits seulement en petite quantité avec l'acide chlorhydrique 7 M, probablement à cause de l'échange ionique $[Fe(bip)_3]^{2+} \rightleftharpoons H^+$. La plus grande partie des ions Fe^{2+} reste fixée dans le cationit sous forme de complexe et est éluée avec un mélange de H_2SO_4—H_2O_2. Pour une concentration de 4 M de l'acide chlorhydrique, toute la quantité (0.56 mg) de fer(II) reste dans la résine sous forme de complexe. Pour expliquer ce comportement, il faut accepter l'existence [10] du complexe $[Fe(bip)_3H^+]^{3+}$ dans des solutions acides, ainsi que dans la résine trouvée dans la forme ionique H^+. Dans les mêmes conditions, les ions Fe^{3+} sont complètement élués par l'acide chlorhydrique 4 M. Pour des concentrations plus fortes en acide, le volume de l'éluant peut êtreidiminué. Donc, ces conditions permettent la séparation complète des ions Fe^{3+} et Fe^{2+}.

Dans le cas de l'utilisation des résines échangeuses d'anions, on passe par la colonne des échantillons contenant la même quantité d'ions Fe^{3+} en présence de HCl de différentes concentrations. Les résultats montrent une rétention maximum pour des concentrations plus fortes que 5 M et minimum pour des concentrations plus faibles que 1 M; les résultats concordent avec les valeurs déterminées pour les coefficients de partage [11, 12]. En partant des résultats expérimentaux obtenus, on a séparé des mélanges synthétiques, contenant des quantités connues d'ions Fe^{2+} et Fe^{3+}. On a travaillé aussi bien avec des résines échangeuses de cations, qu'avec des résines échangeuses d'anions.

La séparation Fe^{3+}—Fe^{2+} avec des résines échangeuses d'anions. On introduit 4 g de Amberlite IRA-400 ou Vionit AT-1, dans une colonne de 25 × 1 cm, qu'on lave à HCl 7 M. L'échantillon constitué de quantités connues de Fe(II), 2,2′-bipyridine 0,5%, HCl 6 M et Fe(III), est passé avec une vitesse de 1,5 ml min^{-1}. Les ions Fe^{3+} sont fixés dans la résine sous la forme d'anions $[FeCl_4]^-$, tandis que les ions complexes du Fe^{2+} passent dans l'effluent. La colonne est lavée avec de l'acide chlorhydrique 6 M. Finalement les ions Fe^{3+} ont été élués à l'àcide chlorhydrique 0,1 M. On a travaillé avec des échantillons contenant du Fe^{2+}(0,56—5,6 mg) et du Fe^{3+} (0,56—5,6 mg) dans des rapports 10:1 à 1:10.

La méthode permet une séparation rapide et quantitative du fer dans les deux degrés d'oxydation. L'effluent contenant le complexe coloré du Fe(II) avec le bipyridine sert pour la détermination spectrophotométrique de l'ion séparé.

La séparation Fe^{2+}—Fe^{3+} avec des résines échangeuses de cations. On introduit 4 g de résine Dowex-50W-X8, ou Vionit CS-3 dans une colonne en verre de 25 × 1 cm. L'échantillon contenant des quantités connues d'ions Fe^{2+} et Fe^{3+} et du 2,2'-bipyridine est passé avec une vitesse de 0,5 ml min^{-1}, de sorte que les deux cations sont fixés dans la résine. Les ions Fe^{3+} ont été élués avec HCl 4 M. Le Fe^{2+} est extrait en détruisant les cations complexes sous l'action d'un mélange de H_2SO_4 et H_2O_2(1 + 1). On a appliqué ce procedure sur des mélanges synthétiques contenants les ions Fe^{2+} (0,56—5,6 mg) et Fe^{3+} (0,56—5,6 mg) trouvés dans des rapports 10:1 à 1:10. Tous les types de résines utilisées ont conduit aux résultats semblables.

La méthode de séparation mise au point et verifiée sur des mélanges synthétiques, a été appliquée sur des solutions de $FeSO_4$, sel Mohr et $FeCl_3$ d'âges différents. Les résultats obtenus se trouvent dans le Tableau 1.

Conclusions

L'utilisation des cationits est recommandée lorsque les ions Fe(III) prédominent dans l'èchantillon et l'utilisation des anionits lorsque prédominent les ions Fe(II). L'application de la méthode sur des mélanges synthétiques, ainsi que sur des combinaisons simples du Fe(II) et Fe(III), a donné de bons résultats.

TABLEAU 1

Les résultats d'application de la méthode de séparation sur des sels

Sel	Solution conc. (M)	âge	Introduit (mg)	Quantité de fer Fe(II) trouvé (mg)	(%)	Fe(III) trouvé (mg)	(%)
$FeSO_4$	10^{-2}	1 jour	0,84	0,72	85,7	0,11	12,5
	10^{-2}	7 jours	1,12	0,95	84,0	0,16	14,2
Sel	10^{-2}	1 jour	1,12	0,94	83,9	0,21	18,7
Mohr	10^{-2}	2 jours	1,12	0,93	83,0	0,22	19,6
	10^{-2}	1½ année	1,68	1,19	70,8	0,43	26,1
	10^{-2}	1½ année	1,12	0,79	70,2	0,29	25,8
	10^{-2}	1½ année	1,68	1,18	70,2	0,44	26,1
$FeCl_3$	—	—	1,6	—	—	1,6	100

BIBLIOGRAPHIE

1 K. A. Kraus et G. E. Moore, J. Am. Chem. Soc., 72 (1950) 5792.
2 F. H. Pollard, J. F. McOmie, A. S. Banister et G. Nickless, Analyst, 82 (1957) 790.
3 F. H. Pollard, J. F. McOmie, G. Nickless et H. W. Hanson, J. Chromatogr., 4 (1960) 108.
4 B. Zagorchev et B. Balusev, C. R. Acad. Bulgare Sci., 14 (1961) 479.
5 H. Ladzinska-Kulinska, Zeszyty Nonkowe Politechniki Lodzkiey, Chemia z., 10 (1961) 36, 67.
6 A. Rusi et S. Ionescu, Stud. cerc. fiz., 2 (1963) 127.
7 B. Zagorchev, Chem. Anal. (Warsaw), 17 (1972) 973.
8 C. Liteanu, Chimie Analitică Cantitativă — Volumetria, Ed. Didactică şi Pedagogică, Bucuresti, 1969, p. 608.
9 J. T. Woods et M. G. Mellon, Ind. Eng. Chem., Anal. Ed., 13 (1941) 551.
10 P. Krumholz, J. Chem. Soc., 60 (1956) 87.
11 F. W. E. Strelow, Anal. Chem., 32 (1960) 1185.
12 K. A. Kraus et F. Nelson, Proc. Ist. Intern. Conf. Peaceful Uses At. Energy, Genève, Session 9 B1, P/837, vol. 7 (1956) p. 113.

Analytica Chimica Acta, 93 (1977) 311—315
© Elsevier Scientific Publishing Company, Amsterdam — Printed in The Netherlands

Short Communication

THE DETERMINATION OF TOTAL OXYGEN AND NITROGEN IN STEELS AND WELD METALS

D. B. RATCLIFFE* and C. S. BYFORD

Central Electricity Generating Board, Marchwood Engineering Laboratories, Marchwood, Southampton SO4 4ZB (England)

(Received 19th March 1977)

The mechanical properties of steels and weld metals are influenced by their oxygen and nitrogen content. Particles of oxides and nitrides are hard and are claimed by Kotecki and Moll [1] to act as void initiators, reducing the ductility of the metal. A suitable analytical method should determine these two elements in both the dissolved and combined states. Oxygen in steels has been determined by Fassel et al. [2] using a vacuum fusion method, and by Hancart and Marot [3], Goldbeck et al. [4] using an inert gas fusion method. However, doubts have been expressed and summarized by Goward [5], that nitrogen is not completely evolved and measured from certain steels, particularly at the lower temperatures used in the vacuum fusion method.

Before the nitrogen can be evolved or an oxide reduced, sufficient energy has to be applied to break the metal—element bond. The stability of a metal nitride or metal oxide is usually expressed in terms of the free energy of formation, ΔG^0, at a particular temperature. In the weld metals investigated, the most stable nitride likely to be present was titanium nitride, TiN (at 2000 K, $\Delta G^0{}_T = -297$ kJ mol^{-1} N_2). The most stable oxide thought to be present was calcium oxide (at 2000 K, $\Delta G^0{}_T = -811$ kJ mol^{-1} O_2). The equilibrium dissociation pressures for titanium nitride, calculated from the ΔG^0 data, were about $1 \cdot 10^{-8}$ atmospheres of nitrogen at 2000 K and about $1 \cdot 10^{-2}$ at 3000 K. Thus, to extract nitrogen from the pure titanium nitride, low partial pressures and high temperatures are needed. If the sample of the nitride is mixed with an iron or nickel flux, as is the case with a molten steel sample, the nitrogen dissociation pressure is higher, because of the free energy contribution to the total reaction of the solution of the liberated metal in the molten flux. These data indicate that it should be thermodynamically feasible to decompose the nitrides of the usual alloying elements present in the weld metal at the temperature (2800 K) attainable with an inert gas fusion procedure. The decomposition of an oxide follows reduction with carbon to form carbon monoxide with solution of the released metal into the molten steel sample. The temperatures at which the oxides are

reduced by the carbon are lower than those needed to decompose the nitrides; and if the partial pressure of the carbon monoxide is lowered, e.g. by displacing it with an inert gas, then the metal oxide will be reduced at even lower temperatures. Calculations of the free energy of carbon reduction of various oxides with various equilibrium carbon monoxide pressures show that calcium oxide is reduced to calcium by carbon at 2600 K when the carbon monoxide partial pressure is one atmosphere. If the partial pressure is lowered to $1 \cdot 10^{-3}$ atmospheres then reduction occurs at 2100 K. Thus, whilst the lower fusion temperature (2300 K) of the vacuum method is adequate for the oxygen determination, the higher (2800 K) temperature of the inert gas fusion method is more suitable for determining the nitrogen in weld metals.

An experimental study was made to test whether oxygen and nitrogen could be determined by the inert gas fusion method irrespective of their state of combination. Various metal oxides and nitrides, covering a wide stability range, were fused in either an iron or nickel flux and the gases evolved were measured quantitatively. It was shown that complete evolution and measurement of nitrogen from titanium nitride and several less stable nitrides, and complete evolution and measurement of oxygen from calcium oxide and several less stable oxides, can be achieved by an inert gas fusion procedure.

Experimental

Apparatus. A Laboratory Equipment Company Limited Model TC30 oxygen and nitrogen analyzer was used for the helium gas fusion procedure.

Reagents. Vanadium nitride, 99% VN; silicon nitride, 99.9% Si_3N_4; niobium nitride, 99.5% NbN; tantalum nitride, 99.0% TaN; aluminium nitride, AlN, and titanium nitride, 99.0% TiN, were obtained from Koch-Light Laboratories, Colnbrook, Bucks, England. Boron nitride, ca. 98% BN, was obtained from BDH Limited, Poole, Dorset, England.

Nickel oxide, iron(III) oxide, chromium sesquioxide, silicon dioxide, titanium dioxide, magnesium oxide, aluminium oxide, zirconium dioxide, and calcium oxide (obtained by heating calcium carbonate) were obtained as the Specpure reagents (Johnson Matthey and Company Limited, London).

British Chemical Standard Steel Nos. 265/2, 237/2, 264/1, 204/4 and 318B; National Bureau of Standards SRMs 346, 1092, 1090 and 356; Analytica AB, Sollentuna SKF Nos. 200S-1, 300-1 and 100-1 certified steels and alloys containing known amounts of oxygen and nitrogen were used in preparing the calibration curves.

Calibration. Several methods were used to calibrate the apparatus. Steel and alloy samples containing known amounts of oxygen and nitrogen were fused and the instrument responses to the evolved amount of gas noted. Known volumes of carbon dioxide and nitrogen, simulating the gases evolved from a fused steel sample, were injected and the instrument responses noted. Finally known weights of oxygen, added as a measured aliquot of a standard solution of potassium hydrogenphthalate and dried at 105°C, were

fused in a tin capsule and again the instrument responses noted. There was no significant difference between the various methods of calibration; a straight line calibration was found over the ranges 0—750 μg of oxygen and 0—2000 μg of nitrogen with a constant blank value of about 1—2 μg of each element. The precisions of the calibration determinations were such that over the range 100—750 μg, the relative standard deviation for oxygen was between 2.5% and 4%, whilst that for nitrogen was between 1.3% and 2.5%.

Procedure. Known amounts (1—5 mg) of the dried oxides and nitrides, weighed to the nearest microgram, were placed in 0.5-g pure nickel or 0.5-g stainless steel capsules and sealed by crimping. The sample capsules were placed in a previously outgassed graphite crucible which was clamped between two copper electrodes within a sealed compartment and any residual air was flushed out by helium. The crucible acted as the primary resistance to current flow in the secondary circuit of a transformer which was briefly overloaded, and a series of heating pulses raised the temperature of the crucible and contents to about 2800 K for 25 s. The oxygen (evolved as carbon monoxide and subsequently oxidized to carbon dioxide), and nitrogen were separated chromatographically on a silica gel column, and measured with a thermistor detector coupled with an integrator. The instrument does not record the actual fusion temperature but displays the current flowing through the graphite crucible. A reading of 0.6 kA coincided with the melting point of molybdenum within the crucible, indicating that a temperature of approximately 2800 K was reached; this current reading was selected as confirmation that the set operating temperature had been reached.

Discussion and results

Recovery of nitrogen from metal nitrides. Seven nitrides were selected which varied in thermal stability (expressed as the standard free energy of formation, ΔG^0_T, for the reaction of 1 g-mol of nitrogen at 1 atmosphere pressure with the pure metal to form the nitride at T K) from vanadium nitride to titanium nitride (Table 1). After fusion of the weighed nitride in either a 0.5-g nickel or steel capsule, the actual amount of nitrogen evolved was compared with the theoretically possible recovery (after correcting for the crucible and capsule blank value). The results (Table 1) show clearly that within experimental error, complete recovery of nitrogen was obtained when the nitrides were fused in a nickel fusion bath. Complete recovery of nitrogen from the nitrides of vanadium, silicon, boron, tantalum and aluminium was also achieved when a steel fusion bath was used, but low recoveries were obtained for the very stable nitrides of niobium and titanium. When nickel was added to the steel fusion bath so that the ratio of nickel to iron exceeded 1:1, complete recovery of nitrogen was achieved from these two nitrides. It proved experimentally difficult to determine the nitrogen recovery from boron and aluminium nitride as these sublimed; only by weighing out very small amounts (ca. 0.2 mg) was it possible to achieve decomposition rather than sublimation, hence the results for these determinations

TABLE 1

Percentage recovery of nitrogen from metal nitrides

Nitride	VN	Si_3N_4	BN	NbN	TaN	AlN	TiN
ΔG^0_T at 2000K (kJ mol^{-1} N_2)	2VN −17	$\frac{1}{3}Si_3N_4$ −29	2BN −150	2NbN −159	2TaN −205	2AlN −272	2TiN −297
Recovery from 0.5-g steel capsule (%)	95 96 95	104 91 99	98 97	87 76 76	93 101 100	90 101 100	65 40 59
Recovery from 0.5-g Ni capsule (%)	99 99 100 96	98 106 99 97	88 106 105 97 108	95 95 95 97	101 99 99 100	87 103	98 97 1 103
Recovery from 0.25-g Ni—0.25-g steel capsule (%)				94 97 92			97 1 99

are less precise than the other five series. The temperature of the fusion for the above series of tests for both iron and nickel bath fusions was fixed at 2800 K or greater. Some tests were made at lower fusion temperatures (2300 K) and low recoveries of nitrogen from niobium and titanium occurred even with a nickel fusion bath. It is, therefore, essential to ensure that the fusion bath temperature is not less than 2800 K. This, combined with the use of a nickel metal addition to the weld metal sample, should result in the determination of total nitrogen.

Recovery of oxygen from oxides. Tests, similar to those made on the metal nitrides, were carried out on a number of metal oxides of different thermal stability (Table 2). After fusion of the oxide in either a nickel or steel fusion bath, the recovered oxygen value, after correction for any blank value, was compared with the theoretical recovery value. The results (Table 2) show that within experimental error, complete recovery of oxygen was achieved from all oxides when either a nickel or a steel fusion bath was used. The temperature of the fusion bath was fixed at 2800 K by the need to recover nitrogen: complete recovery of oxygen appeared to be achieved at lower temperatures (2300 K) but a detailed study of this was not made.

At the conclusion of these tests a series of steels was analyzed. Samples were cut into approximately 0.5-g lumps, cleaned with a file, etched with hydrochloric acid and rinsed with water, acetone and finally ether. The samples were then weighed and fused and the oxygen and nitrogen content noted. The precision of the method was such that for oxygen the standard deviation about the mean of ten results was 2.3 p.p.m. at the 39-p.p.m. level, 2.6 p.p.m. at the 89-p.p.m. level and 19 p.p.m. at the 501-p.p.m. level. The precision for nitrogen was such that the standard deviation about the mean of ten results was 2.2 p.p.m. at the 40-p.p.m. level, 4.7 p.p.m. at the 340-p.p. level and 106 p.p.m. at the 4400-p.p.m. level. The inert gas fusion method will therefore determine the oxygen and nitrogen content of steels and weld

TABLE 2

Percentage recovery of oxygen from metal oxides

Oxide	NiO	Fe_2O_3	Cr_2O_3	SiO_2	TiO_2	MgO	Al_2O_3	ZrO_2	CaO
ΔG^0_T at 2000K (kJ mol^{-1} O_2)	2NiO −104	$\frac{2}{3}Fe_2O_3$ −205	$\frac{2}{3}Cr_2O_3$ −397	SiO_2 −548	TiO_2 −581	2MgO −635	$\frac{2}{3}Al_2O_3$ −690	ZrO_2 −723	2CaO −811
Recovery from 0.5-g steel capsule	100 98 100	104 106 102	106 105 105	103 101 98	105 97 104	100 93 103	87 96	96 97 101	96 98 95
Recovery from 0.5-g nickel capsule	104 99 96 101	97 102 100	99 100 104 99	96 99 100	98 97 99 99	93 95 99 95	95 94 95	101 96 99 102	98 98 95

metals, whether in the dissolved or combined state, mainly because of the high fusion temperatures possible. It is rapid, sensitive and precise, a determination taking about 10 min per prepared sample.

This work is published by permission of the Central Electricity Generating Board.

REFERENCES

1 D. J. Kotecki and R. A. Moll, Weld. J. (New York), 49 (1970) 157.
2 V. A. Fassel, F. M. Evans and C. C. Hill, Anal. Chem., 36 (1964) 2115.
3 J. Hancart and J. Marot, Rev. Met., 57 (1960) 911.
4 C. G. Goldbeck, S. P. Turel and C. J. Rodden, Anal. Chem., 40 (1968) 1393.
5 G. W. Goward, Anal. Chem., 37 (1965) 177.

Analytica Chimica Acta, 93 (1977) 317—322
© Elsevier Scientific Publishing Company, Amsterdam — Printed in The Netherlands

Short Communication

ION EXCHANGE OF 36 ELEMENTS WITH DIAION PA306

EIKO AKATSU* and HIROMICHI WATANABE§

Nuclear Engineering School, Tokai Establishment, Japan Atomic Energy Research Institute, Tokai-mura, Ibaraki-ken (Japan)

(Received 8th February 1977)

Ion-exchange resins are widely used as demineralizers in nuclear reactors, and in chemical and boiler plants. For obvious reasons, ion-exchange behavior is usually studied in acidic media where the chemical species of most metal ions are well defined, and rarely in water or alkaline solution where many metal ions are hydrolyzed. Thus, a survey in alkaline solution was considered to give some useful information. In this communication, the ion-exchange behavior of some elements at a tracer level was studied radiochemically in 0.1—2.0 M sodium chloride, 0.1—2.0 M sodium carbonate and 0.05—1.0 M sodium sulfate with the porous anion-exchange resin Diaion PA306, which was selected from the practical point of view.

Experimental

Materials. The anion-exchange resin selected was Diaion PA306, which is a porous resin with quaternary alkylammonium groups. The bead diameter was 1190—297 μm, and the divinyl benzene content 3%. The resin was conditioned by the ordinary method [1]. The difference in volume between the OH and Cl forms was 3.5%. The resin was converted to the chloride, carbonate or sulfate form, and dried in air. The water contents, measured by drying to constant weight at 110°C, were 24.02 ± 0.096% for the chloride form, 18.21 ± 0.032% for the carbonate form, and 16.21 ± 0.028% for the sulfate form. These values are the averages of 4 or 5 measurements made over the period of the experiments. Ion-exchange capacities, determined by acid—base titration [2], for the chloride form were 3.2 ± 0.11 meq g^{-1} for the air-dried resin and 0.85 ± 0.025 meq ml^{-1} for the wet resin.

The radioactive nuclides used are shown in Table 1 together with specific activity. The tracers were used below 0.1 mCi l^{-1}, and were added as chloride to the chloride and carbonate systems, and as sulfate to the sulfate system. When a visible precipitate was formed, the supernate was used.

The aqueous phases were prepared from JIS special-grade reagents. The pH values, measured with a Horiba pH meter Type M-7, were 5.5 for 0.1, 0.2, 0.5, 1.0 and 2.0 M sodium chloride; 11.6 for 0.1, 0.2 and 0.5 M sodium

§ Present address: Ibaraki General Vocational Training Centre, Mito-shi, Ibaraki-ken, Japan.

TABLE 1

Radioactive nuclide and specific activity

Nuclide	Specific activity ($Ci\ g^{-1}$)		Nuclide	Specific activity ($Ci\ g^{-1}$)	
^{24}Na	$2 \cdot 10^{-2}$	a	^{95}Nb	$CF(4 \cdot 10^{4})$	d
^{32}P	$CF(3 \cdot 10^{5})$	b	^{99}Mo	$2 \cdot 10^{-4}$	a
^{35}S	$CF(4 \cdot 10^{4})$	b	^{99m}Tc	$CF(10^{9})$	d
^{38}Cl	$4 \cdot 10^{-2}$	a	^{106}Ru	not CF	c
^{42}K	$8 \cdot 10^{-3}$	a	$^{109,111}Pd$	$3 \cdot 10^{-1}$	a
^{45}Ca	$1.4 \cdot 10^{-3}$	b	^{110m}Ag	$5.6 \cdot 10^{-1}$	b
^{46}Sc	not CF	a	^{124}Sb	$1.1 \cdot 10^{-2}$	b
^{51}Cr	$2.5 \cdot 10^{2}$	b	^{131}I	$5 \cdot 10^{-2}$	c
^{56}Mn	2	a	^{137}Cs	$CF(9 \cdot 10^{1})$	c
$^{55,59}Fe$	not CF	c	^{139}Ba	$2 \cdot 10^{-1}$	a
^{60}Co	9.6	c	^{144}Ce	$CF(3 \cdot 10^{3})$	c
^{64}Cu	$6 \cdot 10^{-2}$	a	^{152}Eu	not CF	c
^{65}Zn	$2 \cdot 10^{-4}$	a	^{177}Lu	$6 \cdot 10^{-2}$	a
^{65}Ni	$1 \cdot 10^{-2}$	a	^{198}Au	$2 \cdot 10^{-1}$	a
$^{80,80m}Br$	$2 \cdot 10^{-1}$	a	^{234}Th	$CF(2 \cdot 10^{4})$	d
^{90}Sr	$CF(1.4 \cdot 10^{2})$	c	^{233}Pa	$CF(2 \cdot 10^{3})$	d
^{90}Y	$CF(5 \cdot 10^{5})$	d	^{237}U	not CF	e
^{95}Zr	$CF(2 \cdot 10^{4})$	c	^{239}Np	$CF(2 \cdot 10^{5})$	d

[a] Carbonate, nitrate or metal was irradiated in JRR-2 or -4.
[b] Obtained from Radioisotope Centre, JAERI
[c] Imported.
[d] Separated from the parent nuclide.
[e] Separated from UO_2 irradiated in LINAC, JAERI [3].

carbonate; 12.2 for 0.8 and 2.0 M sodium carbonate; and 5.8 for 0.05, 0.1, 0.2, 0.5 and 1.0 M sodium sulfate solutions. Distribution ratios were determined with the above solutions; 4.00 ± 0.08 ml was used in each determinatic

Determination of distribution ratio. Distribution ratios were determined by batch equilibration [4]. The resins (0.2000 ± 0.0005 g) in the chloride, carbonate or sulfate form were used in chloride, carbonate or sulfate systems, respectively. Distribution ratios were calculated from the eqn.

$$K_d(\text{ml g}^{-1}) = \frac{\text{volume of aqueous phase(ml)}}{\text{weight of dried resin(g)}} \times \frac{\text{initial count—final count}}{\text{final count}}$$

where the count rates (in cpm ml^{-1}) refer to the initial solution before additio of resin, and the final solution obtained after shaking for 30 min with the resin. Weights of dried resin were obtained from the weights of air-dried resin and the water contents. The shaking time, 30 min, was determined by preliminary testing with ^{99m}Tc, ^{131}I and ^{152}Eu in different media (Fig. 1).

Gamma-ray activities of most muclides were measured with a well-type 1.5 × 2-in. NaI(Tl)counter. Radioactivities of ^{32}P, ^{35}S, ^{45}Ca, ^{90}Y and ^{234}Th were measured with a liquid scintillation system (Aloka LSC—651); the

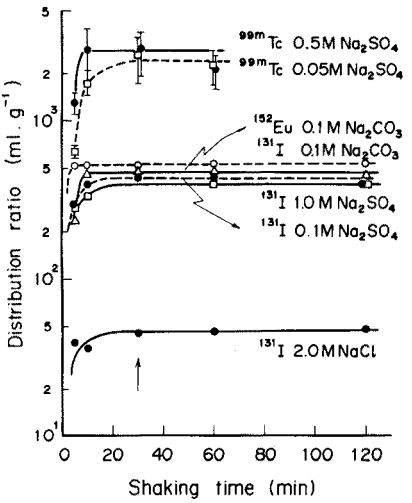

Fig. 1. Effect of shaking time.

scintillator was a 1:1 mixture of Insta gel and ordinary scintillator (4g DPO + 100mg POPOP in 1 l of toluene). Radioactivities of ^{95}Zr and ^{95}Nb were measured from their γ-ray spectra obtained with an ND 2200 with Ge(Li) detector.

Results and discussion

The distribution ratios are shown in Figs. 2—4. The elements showing "no adsorption" were considered not to form anionic species with chloride, sulfate, carbonate or hydroxide [5]. Some of the adsorbable elements gave fluctuating values, e.g. gold and antimony(V) in the chloride system, palladium in the carbonate system, and antimony(V) and thorium in the sulfate system. However, most adsorbable elements showed systematic changes of distribution ratio, though radiocolloid formation was expected in some cases, e.g. ^{90}Y, ^{95}Zr, ^{95}Nb, ^{233}Pa and ^{234}Th [6], under the conditions used.

When the influence on distribution ratio of imbibition of electrolyte by the resin can be neglected, the slope of a plot of log K_d vs. log a gives the average charge of ions according to the Marcus—Coryell treatment [7], where a is the activity of electrolyte in the aqueous phase. As an approximation, activity and molarity were considered equal. This was permissible for chloride and bromide in the sodium chloride system, which showed a slope of —1 despite the activity coefficient of sodium chloride changing from 0.1 to 2.0 M [8]. Pertechnetate and iodide also showed slopes of nearly —1, and chromate a slope of nearly —2 in the sodium chloride system.

Zinc was expected to be present as Zn^{2+} in sodium chloride solution by calculation from the pH values, specific activity and hydroxide formation constant [5]; the equilibrium shifts to the left in the reaction $Zn^{2+} + 3Cl^-$

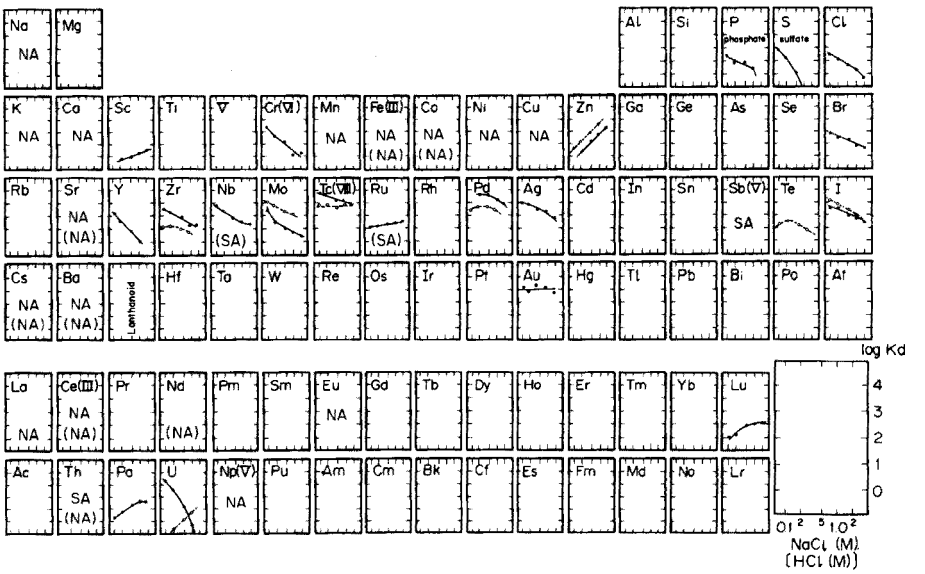

Fig. 2. Distribution ratios of elements between Diaion PA306 and NaCl solution. Data in brackets or denoted by —○— refer to the Diaion PA316—HCl system. SA=slight adsorption. NA=no adsorption. A=adsorbable.

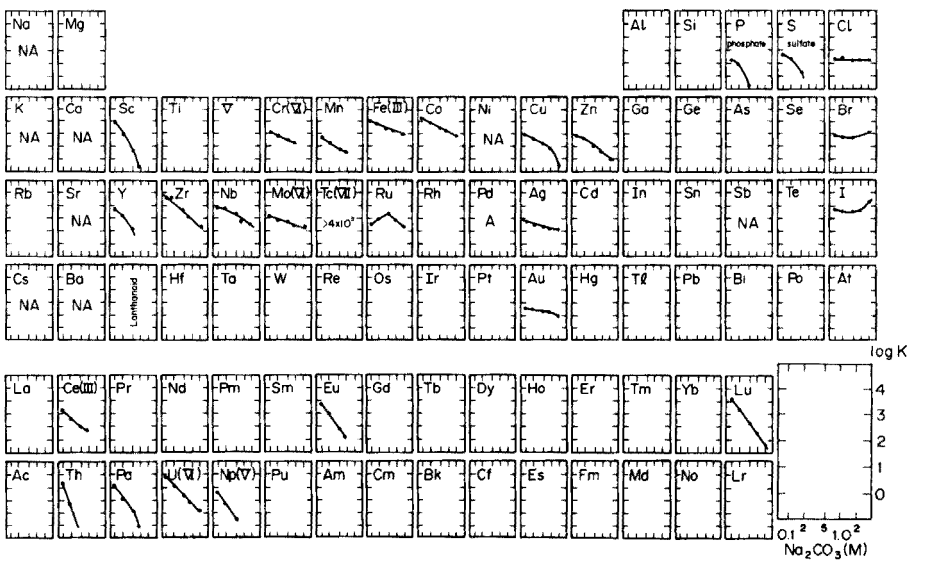

Fig. 3. Distribution ratios of elements between Diaion PA306 and Na_2CO_3 solution. For symbols, see Fig. 1.

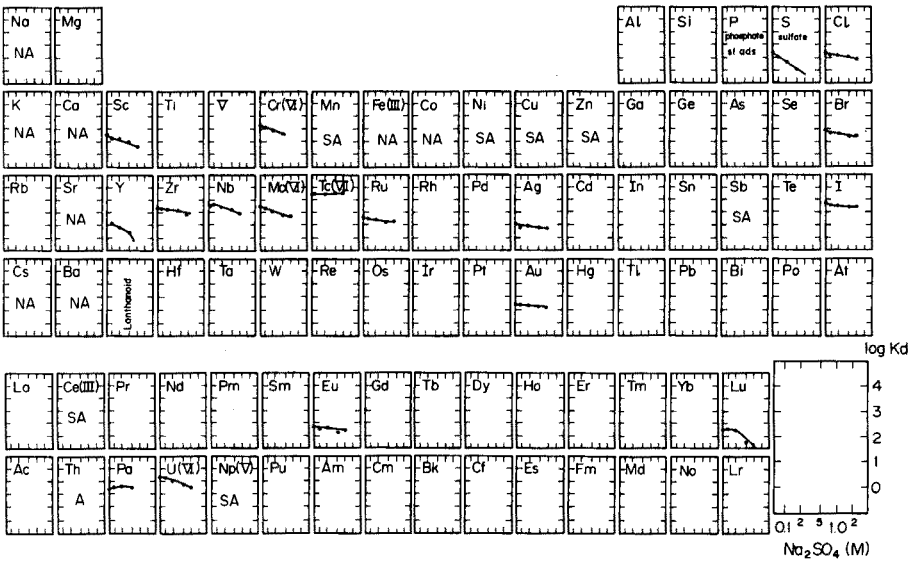

Fig. 4. Distribution ratios of elements between Diaion PA306 and Na_2SO_4 solution. For symbols, see Fig. 1.

$\rightleftharpoons ZnCl_3^-$ [5]. This agreed with the experimental results (Fig. 2) as zinc showed a slope of +2. The distribution ratio of zinc was about 10^2 for 2 M sodium chloride solution, therefore, the equilibrium constant for adsorption should be over 10^6 if the adsorbed species is $ZnCl_3^-$. A similar result was obtained for the Diaion PA316—hydrochloric acid system [10].

Silver showed a negative slope in sodium chloride systems. Calculations similar to the above showed the possible formation of negative chloro complexes in 0.1 M sodium chloride [5]. Figure 2 shows anionic species of yttrium and cationic species of scandium; this does not agree with the reported results in a hydrochloric acid system [9], but repeated experiments on yttrium agreed within experimental error. In this case, hydroxide or radiocolloid formation might have some effect. Uranium(VI) showed a negative slope for the distribution ratio in sodium chloride solution, contrary to that in hydrochloric acid solution, and the slope was too steep to be explained by simple chlorocomplex formation only [5]. Zirconium was considered to be a hydrolyzed species, as in the Diaion PA316—hydrochloric acid system [10].

In the carbonate system negative slopes of −1.7 to −3.3 for rare earth elements, −2 for uranium(VI), −1 for copper and −4 for thorium, were expected from the reported complex formation data with carbonate and hydroxide [5], though the change of activity coefficient is large [11]. However, the behavior of halides could not be explained. Iron(III), cobalt and zinc were adsorbed; the distribution ratios showed negative slope. Carbonate complexes or mixed carbonate—hydroxide complexes may be formed.

On the whole, the behavior in carbonate and sulfate systems was similar to that in solvent extraction systems containing quaternary alkylammonium chloride and ammonium carbonate or sulfate [12]. Chloride in the chloride system and sulfate in the sulfate system showed distribution ratios correspondi to the quotient of exchange capacity divided by the electrolyte concentration of the aqueous phase.

REFERENCES

1 M. Honda, H. Kakihana and Y. Yoshino, Ion Exchange Resins, (in Japanese), Hirokawa Shoten, Tokyo, 1963, p. 25.
2 Mitsubishi Chemical Industry Co. Ltd., Diaion, Manual of Ion Exchange, (in Japanese) Tokyo, 1971.
3 E. Akatsu, T. Kuroyanagi and T. Ishimori, Radiochim. Acta, 2 (1963) 1.
4 S. Yokotsuka, E. Akatsu and K. Ueno, J. Nucl. Sci. Technol., 8 (1971) 622.
5 L. G. Sillen and A. E. Martell, Stability Constants, Spec. Pubs. Nos. 17 and 25, Chemical Society, London, 1964 and 1971.
6 T. Sasaki, Jikken-kagaku-koza, (in Japanese), No. 12, Maruzen, Tokyo, 1956, p. 339.
7 Y. Marcus and A. S. Kertes, Ion Exchange and Solvent Extraction of Metal Complexes, Wiley—Interscience, London, 1969, p. 370.
8 H. S. Harned and B. B. Owen, Physical Chemistry of Electrolytic Solutions, Reinhold, New York, 1958, p. 731.
9 K. A. Kraus, F. Nelson and G. W. Smith, J. Phys. Chem., 58 (1954) 11.
10 E. Akatsu, Y. Aratono and C. Y. Bahk, J. Nucl. Sci. Technol., 10 (1973) 453.
11 C. E. Taylor, J. Phys. Chem., 59 (1955) 653.
12 K. Ueno and A. Saito, Anal. Chim. Acta, 56 (1971) 427.

Analytica Chimica Acta, 93 (1977) 323—326
©Elsevier Scientific Publishing Company, Amsterdam — Printed in The Netherlands

Short Communication

THE CALCIUM AND SODIUM CONTENTS OF BISAZOCHROMOTROPIC ACID DERIVATIVES AND THEIR REMOVAL

MICHIO ZENKI

Department of Chemistry, Okayama College of Science, 1-1, Ridai-cho, Okayama, 700 (Japan)

(Received 10th January 1977)

Since Savvin [1] reported the synthesis and applications of arsenazo III, many bisazochromotropic acid derivatives have been synthesized and investigated as sensitive spectrophotometric reagents.

For proper investigation of their properties, the pure bisazo compounds are essential. The bisazo derivatives are commonly synthesized in alkaline media containing a large amount of calcium ion; impurities such as monoazo compounds, other by-products and calcium ion are removed by washing with hydrochloric acid solution or by recrystallization [1, 2]. However, trace amounts of calcium(II) may remain because the calcium complexes of bisazo derivatives are stable [2]. Thus a small amount of calcium in the bisazo compounds may affect the subsequent analytical procedure. As well as calcium, some sodium ion also remains; to establish accurately the molecular weight of the bisazo compound, the sodium content must be determined. A few reports concerning the purity of the bisazo derivatives have been published [3—5], but these deal with colored substances.

Several bisazo derivatives are now produced commercially, and are used widely for analytical purposes without further purification. In this communication, the determination of calcium and sodium remaining in the commercially available bisazo compounds by atomic absorption spectrometry (a.a.s.) is reported, and a new method for the removal of calcium and sodium is proposed. This method is more effective and convenient than the cation-exchange method.

Experimental

Bisazochromotropic acid derivatives. As representative bisazo derivatives having different functional groups, six commercially available reagents (arsenazo III, carboxyarsenazo, sulfonazo III, dimethylsulfonazo III, chlorophosphonazo III and sulfochlorophenol S) were used. They were dissolved in water directly to prepare $2 \cdot 10^{-4}$ M solutions; the molecular weights employed were those given by the suppliers.

Calcium and sodium stock solutions. Calcium carbonate or sodium chloride which had previously dried at 105°C for 6 h, was dissolved in

0.1 M hydrochloric acid or water, respectively. Deionized distilled water was used in all dilutions.

Apparatus. A Nippon Jarrel-Ash model AA-782C atomic absorption/emission spectrometer fitted with a conventional 100-mm slit burner was used with an air—acetylene flame. The signal was recorded on a Yanaco YR-110 recorder (10 mV full-scale deflection). The signal was expanded with the concentration mode of the spectrometer. The calcium and sodium hollow-cathode lamps (Hamamatsu TV Co.) were operated at 10 mA.

Results and discussion

Determination of calcium. The bisazo derivative solution was sprayed directly into the air—acetylene burner and the absorbance at 422.7 nm measured. Calibration curves and standard additions were used to evaluate the accuracy and precision; the difference between the values obtained by these methods was negligibly small within experimental error. The results for the six bisazo derivatives are shown in Table 1.

The calcium contents vary with the structure and supplier. They probably depend on the manner of purification, but also on the differences in the stabilities of the calcium complexes. The calcium complexes of arsenazo III, carboxyarsenazo and chlorophosphonazo III are stable and have molar absorptivities of more than 10^4 l mol^{-1} cm^{-1} under optimal conditions, whereas the calcium complexes of sulfonazo III and dimethylsulfonazo III have molar absorptivities of only 10^3—10^2 l mol^{-1} cm^{-1} [1, 2, 6].

Determination of sodium in the bisazo derivatives. Commercially available bisazo derivatives are supplied in various salt forms. The derivatives recrystallized from hydrochloric acid solutions are generally mono- or

TABLE 1

Determination of calcium in bisazochromotropic acid derivatives

Derivative	Supplier	Concn. in solution (g l^{-1})	Calcium found in solution[a] (p.p.m.)	Calcium content	
				(%)	Mole ratio [Ca]/[R]
Arsenazo III	A	0.1550	1.53	0.99	0.19
	B	0.1676	4.70	2.80	0.55
Carboxyarsenazo	A	0.1401	0.188	0.13	0.02[4]
Sulfonazo III	A	0.1558	0.055	0.03[5]	0.00[7]
Dimethylsulfonazo III	A	0.1522	0.035	0.02[3]	0.00[4]
	B	0.1628	0.025	0.01[5]	0.00[3]
Chlorophosphonazo III	A	0.1606	1.13	0.70	0.14
Sulfochlorophenol S	A	0.1784	6.63	3.72	0.85

[a]The mean values obtained by the use of calibration curves and standard additions.
[b][R] : The molar concentration of the bisazo derivative solution, regarded as $2.0 \cdot 10^{-4}$ M.

di-sodium salts. It is very difficult to obtain a sodium salt of strictly stoichiometric composition, because the sodium content depends strongly on the acidity of the mother liquor during recrystallization.

Sodium was determined at 589.0 nm by a.a.s. in the same manner as calcium. The results for the six derivatives (Table 2) show that the sodium contents vary widely and differ greatly from the values given by the suppliers.

Purification by solvent extraction. For many analytical purposes, the reagent must be pure and in the case of the bisazo derivatives the best form is the free acid. To remove calcium and sodium ions, a strongly acidic ion-exchange resin (Dowex 50W or Amberlite IR-120) has been used [2]. Though this method is useful, the solution must be very dilute and the concentration of hydrogen ion must be adjusted carefully.

Taketatsu et al. [7] and Yamamoto [8] have reported the extraction—photometric determination of rare earths and thorium, respectively, with chlorophosphonazo III using 1-butanol or 3-methyl-1-butanol as the solvent; both the metal chelate and the reagent are extracted into the organic solvent from acidic media. However, it was established here that the alkaline earth metal and alkali metal chelates of the bisazo derivatives are not extracted, and that the reagent alone is extracted from aqueous phases below pH 2. This phenomenon is applicable to the purification of these derivatives. The method is as follows.

About 0.5 g of the derivative (commercially available or synthesized) is dissolved in 200 ml of 1 M hydrochloric acid. The solution is transferred to a 500-ml separatory funnel and 200 ml of 1-butanol or 2-methylpropanol is added. The bisazo derivatives are extracted into the butanol phase by shaking vigorously for a few minutes. After phase separation, the aqueous phase is transferred to another separatory funnel, and the extraction is repeated. The combined extracts are washed with 1 M hydrochloric acid, concentrated by rotary evaporation, and then evaporated to dryness on a water bath or hot plate.

TABLE 2

Determination of sodium in bisazochromotropic acid derivatives

Derivative[a]	Composition indicated by supplier	Sodium found in solution[b] (p.p.m.)	Sodium content	
			(%)	Mole ratio [Na]/[R][c]
Arsenazo III	H	1.3	0.84	0.29
	2-Na	6.5	3.88	1.40
Carboxyarsenazo	H	1.5	1.07	0.33
Sulfonazo III	4-Na	17.2	11.0	3.75
Dimethylsulfonazo III	2-Na	3.5	2.30	0.75
	4-Na	13.6	8.35	2.95
Chlorophosphonazo III	2-Na	0.6	0.37	0.13
Sulfochlorophenol S	4-Na	6.5	3.64	1.40

[a]The concentrations of the derivatives and the suppliers are the same as in Table 1.
[b,c]See footnotes a and b of Table 1.

Bisazo derivatives purified by the above method were dissolved in distilled water to give a $2 \cdot 10^{-4}$ M solution. Tests with the a.a.s. method showed that all the derivatives were free from calcium and sodium ions. Accordingly, the derivatives were obtained as their free acids.

Chromatographic investigation of the colored substances. The commercially available and the purified bisazo derivatives were examined by paper chromatography and thin-layer chromatography (silica gel); a 2 M ammonia solution saturated with 2-methylpropanol was used as the developing solvent [9]. The chromatograms obtained were the same. Thus, the purification is not useful for the elimination of the monoazo compounds or other colored by-products, though it is effective for the removal of calcium and sodium ions. The colored substances can be removed by activated charcoal, followed by recrystallization from hydrochloric acid solution [1, 2, 6].

The author is indebted to Professor Kyoji Tôei of Okayama University for valuable advice and discussion.

REFERENCES

1 S. B. Savvin, Talanta, 8 (1961) 673; 11 (1964) 1; 11 (1964) 7.
2 B. Budesinsky, Chelates in Analytical Chemistry, Vol. 2, M. Dekker, New York, 1969, p. 1.
3 A. A. Nemodruk, Zh. Anal. Khim., 22 (1967) 629.
4 S. B. Savvin, T. G. Akimova, E. P. Krysin and M. M. Davydova, Zh. Anal. Khim., 25 (1970) 430.
5 S. Shibata, K. Goto and Y. Ishiguro, Anal. Chim. Acta, 62 (1972) 305.
6 M. Zenki, Anal. Chim. Acta, 83 (1976) 267.
7 T. Taketatsu, M. Kaneko and N. Kono, Talanta, 21 (1974) 87.
8 T. Yamamoto, Anal. Chim. Acta, 63 (1973) 65.
9 B. Budesinsky and L. Krumlova, Anal. Chim. Acta, 39 (1967) 375.

Analytica Chimica Acta, 93 (1977) 327—330
© Elsevier Scientific Publishing Company, Amsterdam — Printed in The Netherlands

Short Communication

SPECTROPHOTOMETRIC DETERMINATION OF LANTHANIDES IN THE PRESENCE OF THORIUM WITH CHLOROPHOSPHONAZO III

TOMITSUGU TAKETATSU* and ATSUKO SATO

College of General Education, Kyushu University, Ropponmatsu, Nishi-ku, Fukuoka 810 (Japan)

HIRONDO KURIHARA and SATOKO MAEDA

Department of Chemistry, Faculty of Science, Fukuoka University, Nanakuma, Nishi-ku, Fukuoka 814 (Japan)

(Received 12th January 1977)

Many analytical investigations for mixtures of lanthanides and thorium have been reported, because these metals possess similar chemical behavior and coexist in minerals and ores.

Micro and macro amounts of thorium in the presence of large amounts of lanthanides can be easily determined by colorimetric [1] and chelate titration [2] methods, respectively, because the stability constants between thorium and various chelating reagents are considerably larger than those for the corresponding lanthanide complexes. Macro amounts of thorium and lanthanides in mixtures can also be titrated sequentially with complexones by adjusting the pH of the solution [3]. However, it is difficult to determine micro amounts of lanthanides coexisting with large amounts of thorium colorimetrically. Chlorophosphonazo III (2,7-bis(4-chloro-2-phosphonophenylazo)-1,8-dihydroxy naphthalene-3,6-disulphonic acid), which is a chromotropic acid derivative, has been proposed by O'Laughlin and Jensen [4] and Taketatsu et al. [5], as a sensitive reagent for lanthanides. The present communication reports a spectrophotometric determination of lanthanides with the reagent in the presence of larger amounts of thorium, by using EDTA (ethylenediaminetetraacetic acid), DTPA (diethylenetriamine-*N,N,N',N'',N''*-pentaacetic acid) and TTHA (triethylenetriamine-*N,N,N',N'',N''',N'''*-hexaacetic acid) as masking agents.

Experimental

Reagents and apparatus. Standard solutions of the metal ions were prepared by dissolving the 99.9% pure oxides (for lanthanides except cerium) and chlorides (cerium(III) and thorium) in dilute hydrochloric acid. The solutions were standardized by titration with EDTA and xylenol orange indicator.

A standard solution of chlorophosphonazo III (Dojindo Co.) was used without further purification. The concentration represents 76% of the amount weighed as reported earlier [6].

Standard solutions of EDTA, DTPA and TTHA were prepared by dissolving known amounts of the reagents (Dojindo Co.) in dilute sodium hydroxide solution. All other chemicals used were analytical reagent grade.

Hitachi EPS-3T automatic recording and a 101 manual spectrophotometer were used.

Procedure. Transfer a dilute hydrochloric acid solution containing less than 40 μg of lanthanide and less than 2 mg of thorium to a beaker. Add 2 ml of 0.02 M TTHA solution, adjust the pH to 3.1—3.4 with dilute hydrochloric acid and sodium hydroxide solutions, and transfer the solution to a 20-ml volumetric flask. Add 5 ml of $4.5 \cdot 10^{-4}$ M chlorophosphonazo III solution and dilute to volume with water. Measure the absorbance in 1-cm cells at 677 nm against a reagent blank solution within 1 h of preparation. All experiments were done at 20—25°C.

Results and discussion

Absorption spectra. Figure 1 shows the absorption spectra of the lanthanum and thorium chlorophosphonazo III chelates in the presence and absence of TTHA. Though the spectrum of the lanthanum chelate is not affected by the addition of TTHA, that of the thorium chelate is scarcely visible in the range 600—700 nm.

Figure 2 shows the variation of absorbance at 677 nm in the thorium—chlorophosphonazo III—TTHA, —DTPA and —EDTA systems and also in the lanthanum—chlorophosphonazo III—TTHA system as a function of pH. The absorbance in the thorium systems is not affected by EDTA, but decreases with increasing pH value in the case of DTPA and TTHA. The absorbance approaches zero in the presence of TTHA beyond pH 3.2. However, the

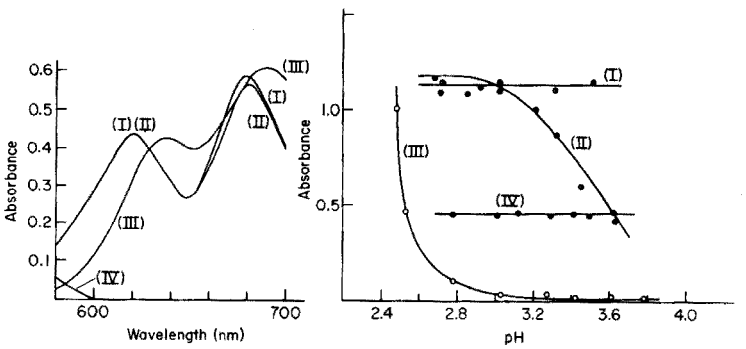

Fig. 1. Absorption spectra of lanthanum and thorium chlorophosphonazo III chelates in the absence and presence of TTHA. (I) La—chlorophosphonazo III (CPA III). (II) La—CPA III—TTHA. (III) Th—CPA III. (IV) Th—CPA III—TTHA. La, $1.54 \cdot 10^{-5}$ M; Th, $1.55 \cdot 10^{-5}$ M; CPA III, $1.24 \cdot 10^{-4}$ M; pH, 3.1—3.2; reference, reagent blank.

Fig. 2. Variation of absorbance with pH for the lanthanum and thorium chlorophosphonazo III chelates at 677 nm in the presence of EDTA, DTPA and TTHA. (I) Th—EDTA. (II) Th—DTPA. (III) Th—TTHA. (IV) La—TTHA. La, $1.25 \cdot 10^{-5}$ M; Th, $1.85 \cdot 10^{-4}$ M; EDTA, $9.88 \cdot 10^{-4}$ M; DTPA, $1.59 \cdot 10^{-3}$ M; TTHA, $1.39 \cdot 10^{-3}$ M.

absorbance for the lanthanum chelate is unaffected by the presence of TTHA in the pH range 2.0—4.0. Of course, the absorbance is not affected by EDTA and DTPA because the order of the stability constants of lanthanum with these complexones is TTHA—DTPA—EDTA.

Figure 3 shows the variation of absorbance at 677 nm for the lanthanide and thorium chlorophosphonazo III chelates as a function of mole ratio of TTHA/metal. The absorbance for the thorium chelate decreases remarkably with increase in the concentration of TTHA, and approaches zero beyond the mole ratio 2:1. In contrast, the absorbances for the lighter lanthanide chelates are constant even in the presence of large excesses of TTHA, although the absorbances for the heavier lanthanide chelates are somewhat affected by such large excesses.

Figure 4 shows the variation of absorbance at 677 nm for the lanthanide and thorium chlorophosphonazo III chelates in the presence of TTHA as a function of time. The absorbance in the lanthanide systems is not affected by time, but the absorbance of the thorium system increases. Possibly chlorophosphonazo III replaces TTHA in the thorium chelate. Therefore, it is necessary to add TTHA to the sample solution before addition of chlorophosphonazo III, and to measure as soon as possible after the solution has been prepared.

Determination of lanthanides. Beer's law is obeyed up to 2 μg ml^{-1} of each lanthanide in the presence of TTHA.

Several lanthanides in the presence of various amounts of thorium were determined by the recommended procedure. Accurate results can be obtained even when a 50-fold amount of thorium is present (Table 1).

Since thorium is used for collecting micro amounts of lanthanides by coprecipitation as the hydroxides, the following procedure was examined. A solution containing a known amount of thorium and a small amount of

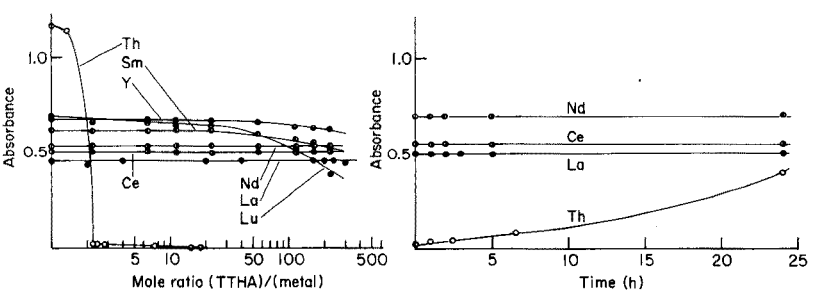

Fig. 3. Variation of absorbance of lanthanide and thorium chlorophosphonazo III chelates at 677 nm as a function of mole ratio, (TTHA)/(metal). Lanthanide, $1.25 \cdot 10^{-5}$ M; Th, $1.85 \cdot 10^{-4}$ M; CPA III, $1.25 \cdot 10^{-4}$ M; pH, 3.1—3.3.

Fig. 4. Variation of absorbance of lanthanide and thorium chlorophosphonazo III chelates at 677 nm in the presence of TTHA as a function of time. Lanthanide, $1.25 \cdot 10^{-5}$ M; Th, $1.85 \cdot 10^{-4}$ M; CPA III, $1.11 \cdot 10^{-4}$ M; TTHA, $6.95 \cdot 10^{-4}$ M; pH, 3.2—3.3.

TABLE 1

Determination of lanthanides in the presence of thorium
(All data are given as $\mu g\ ml^{-1}$)

	Ln taken	Th added	Ln found	Error		Ln taken	Th added	Ln found	Erro
La	1.74	10.8	1.74	0.00	Ce	1.75	107.5	1.88	+0.0
La	1.74	21.5	1.78	+0.04	Nd	1.80	21.5	1.81	+0.0
La	1.74	43.0	1.76	+0.02	Nd	1.80	107.6	1.92	+0.1
La	1.74	107.6	1.88	+0.14	Gd	1.97	21.5	1.92	−0.0
La	1.74	215.0	1.90	+0.16	Gd	1.97	107.6	2.01	+0.0
La	1.74	322.8	1.99	+0.25	Lu	2.19	21.5	2.19	0.0
Ce	1.75	21.6	1.75	0.00	Lu	2.19	107.6	1.94	−0.2

TABLE 2

Determination of lanthanum after coprecipitation with thorium hydroxide
(All data are given as $\mu g\ ml^{-1}$. The amount of Th used was 42.9 $\mu g\ ml^{-1}$ in each case.)

La taken	La found[a]	Error[a]	La found[b]	Error[b]
1.74	2.58	+0.84	1.72	−0.02
1.74	2.58	+0.84	1.72	−0.02
1.74	2.59	+0.85	1.72	−0.02
0.87	1.66	+0.79	0.80	−0.07

[a]Reagent blank was used as reference.
[b]Chlorophosphonazo III solution containing thorium was used as reference.

lanthanum was treated with a known amount of sodium hydroxide solution. The precipitate was filtered on paper and dissolved in a constant volume of a dilute hydrochloric acid solution, and lanthanum was determined by the recommended procedure. The results (Table 2) show a constant positive error regardless of the lanthanum concentration. To establish the cause, an amount of thorium equivalent to that added to lanthanum, was precipitated, filtered and dissolved by the same procedure, and a reference solution was prepared by adding chlorophosphonazo III to this solution. When this reference solution was used instead of the reagent blank solution for the determination of lanthanum, reasonable values were obtained (Table 2). The error is probably caused by diverse metals, e.g. calcium, originating from glass vessels or reagents such as sodium hydroxide.

REFERENCES

1 T. Yamamoto, Anal. Chim. Acta, 63 (1973) 65.
2 J. S. Fritz and J. J. Ford, Anal. Chem., 25 (1953) 1640.
3 R. Pribil and V. Vesely, Talanta, 10 (1963) 899; 19 (1972) 1448.
4 J. W. O'Laughlin and D. F. Jensen, Talanta, 17 (1970) 329.
5 T. Taketatsu, M. Kaneko and N. Kono, Talanta, 2 (1974) 87.
6 T. Taketatsu, M. Noda and M. Takasugi, Bunseki Kagaku, 25 (1976) 134.

Analytica Chimica Acta, 93 (1977) 331—333
© Elsevier Scientific Publishing Company, Amsterdam — Printed in The Netherlands

Short Communication

ROOM-TEMPERATURE PHOSPHORESCENCE OF FOLIC ACID, *p*-HYDROXYBENZOIC ACID AND BENZOCAINE

R. M. A. von WANDRUSZKA and R. J. HURTUBISE*

Department of Chemistry, University of Wyoming, Laramie, Wyoming 82071 (U.S.A.)

(Received 11th January 1977)

Room-temperature phosphorescence of adsorbed ionic organic molecules was first reported by Roth [1] and later by other workers [2, 3]. Wellons et al. [4] have reported on room-temperature phosphorimetry of biologically important compounds. Seybold and White [5] used the external heavy-atom effect to enhance the signal of 2-naphthalene sulfonate adsorbed on filter paper. A novel method for the determination of *p*-aminobenzoic acid in vitamin tablets was recently reported [6]: *p*-aminobenzoic acid was adsorbed on a sodium acetate solid surface from ethanolic solution, the solvent was evaporated and the phosphorescence signal was measured with a spectrodensitometer. This method has great sensitivity and selectivity, is relatively insensitive to moisture, and does not require a prior separation from the complex vitamin tablets. In this communication analytical findings for folic acid, *p*-hydroxybenzoic acid and benzocaine are described.

Experimental

Folic acid (ICN Pharmaceuticals Inc., Cleveland, Ohio) was recrystallized from benzene; *p*-hydroxybenzoic acid (99+%, Aldrich, Milwaukee, Wis.) and benzocaine (98%, Aldrich) were used without purification. Absolute ethanol was purified by distillation as described by Winefordner and Tin [7]. Benzocaine was hydrolyzed to *p*-aminobenzoic acid by refluxing for 15 min in 0.1 M HCl. The molecules were adsorbed on sodium acetate and phosphorescence measurements were made as described previously [6].

Results and discussion

The room-temperature phosphorescence excitation and emission maxima for folic acid adsorbed on sodium acetate were 320 nm and 465 nm, respectively. The maxima for *p*-hydroxybenzoic acid were 285 nm and 420 nm, respectively. Preliminary results indicated a 340-nm excitation maximum and a 404-nm emission maximum for *p*-hydroxybenzoic acid [6]. These wavelengths resulted either from an impurity or from the high concentration of *p*-hydroxybenzoic acid used. The excitation and emission wavelengths reported here were obtained from a very pure sample and were reproducible.

The calibration curves for both compounds showed the characteristic linear region, followed by a reproducible curved region, as was found earlier for *p*-aminobenzoic acid [6]. The calibration curve for folic acid (Fig. 1, curve A) had a linear range from 0—120 ng and a limit of detection of 4 ng of folic acid per sample spot. For *p*-hydroxybenzoic acid (Fig. 1, curve B), the linear range was 0—140 ng and the limit of detection was 20 ng. The amount of sodium acetate used was 11 mg in all cases.

Benzocaine (ethyl-*p*-aminobenzoate) did not show room-temperature phosphorescence when adsorbed on sodium acetate. However, it was found that benzocaine could be readily hydrolyzed by refluxing in dilute acid. The hydrolyzed solution was subsequently neutralized with aqueous alkali. Small amounts of this solution, when applied to sodium acetate and evaporated to dryness, showed the characteristic *p*-aminobenzoic acid phosphorescence on excitation with a u.v. lamp. No quantitative data were gathered for benzocaine, but it appears that there would be little difficulty in developing a sensitive method for its determination.

Wellons et al. [4] have commented on the advantages of room-temperature phosphorimetry with filter paper as the adsorbing medium. One disadvantage found with filter paper is the sensitivity of the phosphorescence signal to moisture. With sodium acetate as the adsorbing medium no serious moisture problems were noted. The main disadvantage of sodium acetate is that fewer molecules phosphoresce when adsorbed on it. However, this makes sodium acetate more selective than filter paper. Interestingly, folic acid is phosphorescent at room temperature when adsorbed on sodium acetate, but not when adsorbed on filter paper [4]. With a better understanding of the adsorption process, probably several additional surfaces could be used to induce room-temperature phosphorescence.

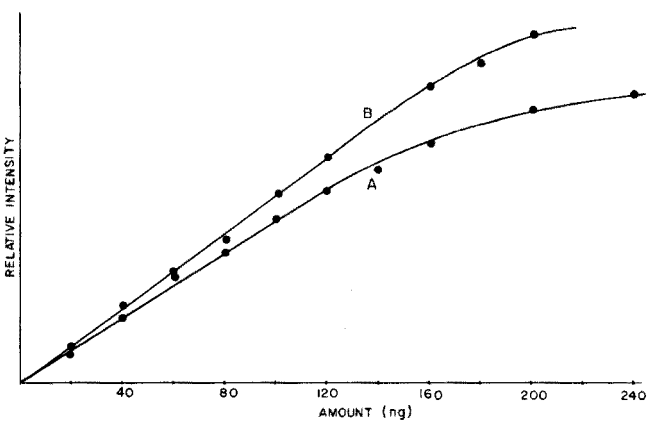

Fig. 1. Calibration curves. A, folic acid; B, *p*-hydroxybenzoic acid.

REFERENCES

1 M. Roth, J. Chromatogr., 30 (1967) 276.
2 E. M. Schulman and C. Walling, Science, 178 (1972) 53; J. Phys. Chem., 77 (1973) 902.
3 R. A. Paynter, S. L. Wellons and J. D. Winefordner, Anal. Chem., 46 (1974) 736.
4 S. L. Wellons, R. A. Paynter and J. D. Winefordner, Spectrochim. Acta, Part A, 30 (1974) 2133.
5 P. G. Seybold and W. White, Anal. Chem., 47 (1975) 1199.
6 R. M. A. von Wandruszka and R. J. Hurtubise, Anal. Chem., 48 (1976) 1784.
7 J. D. Winefordner and M. Tin, Anal. Chim. Acta, 31 (1964) 239.

Analytica Chimica Acta, 93 (1977) 335—339
© Elsevier Scientific Publishing Company, Amsterdam — Printed in The Netherlands

Short Communication

EXTRACTIVE SPECTROPHOTOMETRIC DETERMINATION OF NICKEL(II) AND SIMULTANEOUS DETERMINATION OF COBALT(II) AND NICKEL(II) WITH 6-NITROQUINOXALINE-2,3-DITHIOL

CHANDRAKANT K. BHASKARE and USHA D. JAGADALE

Department of Chemistry, Shivaji University, Kolhapur 416 004 (India)

(Received 15th March 1977)

The simultaneous determination of cobalt and nickel under various experimental conditions by non-extractive methods with quinoxaline-2,3-dithiol (QDT) has been reported by several workers [1—5]. Recently, a new derivative of QDT, 6-nitroquinoxaline-2,3-dithiol (NQDT), has been synthesized and applied to the extractive photometric determination of cobalt [6]. Nickel forms a blue complex with NQDT in alkaline medium; on acidification with hydrochloric acid, the complex can be extracted with methyl iso-butyl ketone (MIBK).

In this communication, an extractive method for the simultaneous determination of nickel and cobalt and the photometric determination of nickel with NQDT are reported. Comparison of the data in Table 1 clearly indicates the superiority of NQDT over QDT. The extractive method also has the advantage that the enrichment of the constituents allows application even to small traces of the two elements. The electrophilic nitro group in NQDT makes the two —SH groups more easily ionized (ionization constants 4.45 and 6.00; cf.6.84 and 9.95 for QDT), which facilitates complexation. The molar absorptivities of the NQDT complexes indicate the better sensitivity for cobalt and nickel available with NQDT.

Experimental

Reagents. NQDT was obtained by hydrolysis of 6-nitro-S-2(3-mercaptoquinoxalinyl)thiuronium chloride [6], with ammonia liquor. A stock 0.5% solution in ammonia liquor was prepared. Standard solutions of nickel and cobalt were prepared from analytical-grade sulphates.

Apparatus. A Beckman DU2 spectrophotometer, with matched 10-mm cells, and a Philips pH meter PR9405L with a glass/calomel combined electrode were used.

Procedure for nickel. To an aliquot of solution containing 4—27 μg of Ni(II), add 2.5 ml of reagent solution and make strongly alkaline with ammonia liquor. Adjust to pH 2.1 and extract with two 4-ml portions of MIBK. Dry the extracts with anhydrous sodium sulphate and transfer to

TABLE 1

Comparison of methods reported for cobalt and nickel with QDT and NQDT

	pH	Solvent	λ_{max} (nm)	ϵ (l mol^{-1} cm^{-1})	Ref.
Ni	(Ammoniacal)	aqueous	520	19 000	1
Ni	(Acidic)	80%	650	15 870	2
Co		DMF	505	36 817	
Ni	3.0	80%	656	17 270	3
Co		C_2H_5OH	510	34 660	
Ni	10.0	8%	472	20 820	4
Co		C_2H_5OH	520	35 550	
Ni	2.6	DMF	665	18 100	5
Co			510	37 400	
Ni	2.1	extracted	710	20 700	Present
Co		in MIBK	530	40 000	method

a 10-ml volumetric flask. Dilute to volume and measure the absorbance at 710 nm, against a reagent blank prepared in a similar way.

Procedure for cobalt and nickel. To a solution containing cobalt (3—15 μg) and nickel (4—27 μg), add about 5 ml of reagent solution and enough ammonia liquor to make it strongly alkaline. Adjust to pH 2.1 and extract with two 4-ml portions of MIBK. Dry the extracts with anhydrous sodium sulphate, transfer to a 10-ml volumetric flask, and dilute to volume. Measure the absorbances at 530 and 710 nm, against an appropriate reagent blank. Calculate the molar concentrations of cobalt and nickel from the simultaneous equations: $[Co] \times 10^5 = 2.497 \times A_{530} - 1.355 \times A_{710}$, and $[Ni] \times 10^5 = 4.822 \times A_{710}$.

Analysis of iron-base alloys. Solutions of NBS standard reference samples were prepared, and iron and copper were removed as reported by Burke and Yoe [3]. Suitable aliquots were analyzed as outlined above.

The results obtained for mixtures and NBS standard reference samples are shown in Tables 2 and 3.

Results and discussion

Absorption spectra and experimental conditions. The absorption spectra of the reagent, nickel complex and cobalt complex, all at pH 2.1, are shown in Fig. 1. The nickel complex has absorption maxima at 640 and 710 nm. The absorbance is higher at 710 nm where the contribution of the reagent absorption is less, therefore 710 nm was selected as the analytical wavelength for nickel.

TABLE 2

Simultaneous determination of cobalt and nickel in synthetic mixtures[a]

Sample No.	Co/Ni ratio	Cobalt (p.p.m.)			Nickel (p.p.m.)		
		Taken	Found	Diff.	Taken	Found	Diff.
1	0.25	0.60	0.57	0.03	2.40	2.36	0.04
2	0.50	0.87	0.85	0.02	1.74	1.73	0.01
3	0.75	1.00	1.04	0.04	1.34	1.34	0.00
4	1.00	1.25	1.25	0.00	1.25	1.22	0.03

[a]Each result is a mean of 3 separate determinations.

TABLE 3

Analysis of NBS standard reference materials

Sample	Cobalt (%)		Nickel (%)	
	Present	Found	Present	Found
55e Ingot	0.007	0.0069	0.038	0.036
466 Ingot iron	0.046	0.045	0.051	0.051
33b Iron-base alloy	—	—	2.24	2.24
33d Iron-base alloy	—	—	2.38	2.37

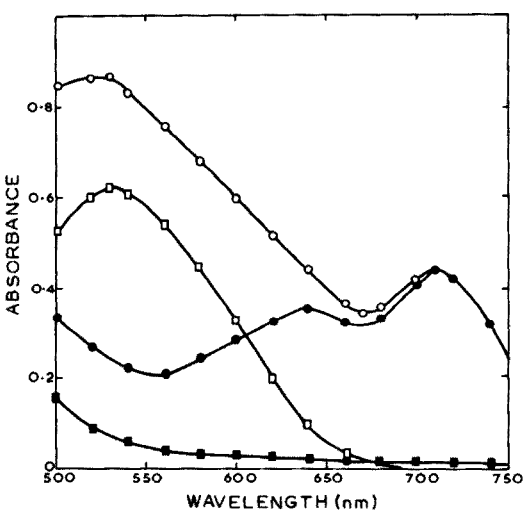

Fig. 1. Absorption spectra at pH 2.1. (□) Co(II)—NQDT complex (0.9 p.p.m. Co); (●) Ni(II)—NQDT complex (1.25 p.p.m. Ni); (○) (Ni + Co)—NQDT complexes; all measured against reagent blanks. (■) $4.0 \cdot 10^{-3}$ M NQDT alone.

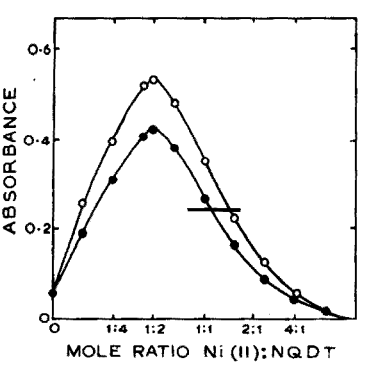

Fig. 2. Job's method of continuous variations.

Extractions carried out from solutions at varying pH values, indicated the optimum pH range giving constant and maximum absorbance to be 1.8 to 2.4. The complex is not extracted from basic medium, but is quantitatively extracted from solutions at pH 2.1. The extracts show constant absorbance for several hours.

Beer's law is obeyed over the range 0.15—3 p.p.m. of Ni(II). The optimum analytical range, from a Ringbom plot [7], is 0.4—2.7 p.p.m. of Ni(II).

Composition of the complex and dissociation constant. The composition of the Ni(II)—NQDT complex was determined by Job's continuous variations method [8]; Fig. 2 shows the formation of a 1:2 Ni(II): NQDT complex. This was confirmed by the mole ratio [9] and slope ratio methods. The degree of dissociation, α, and the dissociation constant, K, obtained by the method of Harvey and Manning [10], were $\alpha = 0.1072$ and $K = 6.05 \cdot 10^{-12}$.

Sensitivity and accuracy. The molar absorptivity of the nickel complex at 710 nm is $2.07 \cdot 10^4$ l mol^{-1} cm^{-1}, which corresponds to a sensitivity of 0.0028 μg cm^{-2} (for $A = 0.001$). The relative standard deviation of the calculated absorptivities for 10 samples in the optimum concentration range was 2.0%.

Simultaneous determination of cobalt and nickel. The molar absorptivity reported earlier [1] for the cobalt—NQDT complex was $1.93 \cdot 10^4$ l mol^{-1} cm^{-1}. By changing the reaction conditions and following the procedure recommended above, the molar absorptivity was enhanced to $4.00 \cdot 10^4$ l mol^{-1} cm^{-1}. Since the reaction conditions for cobalt and nickel are the same, both elements can be extracted with MIBK as complexes of NQDT from solutions at pH 2.1. The spectra for the individual species and for a mixture (Fig. 1) show that the absorbances are additive, so that simultaneous equations can be developed. The cobalt complex does not absorb at 710 nm.

Effect of foreign ions. Various ions were added to the sample containing a fixed amount of nickel (2 p.p.m.). The complexes were extracted as in the recommended procedure and the absorbances measured. Interference was considered to occur if the error in the absorbance exceeded 2%. Cu(II), Pd(II), Pt(IV) and Os(VIII) interfered seriously and require prior separation. Mg(II), Ti(IV), Tl(I), In(III), Ce(IV), Ga (III), Te(IV), Ag(I), Au(III), Al(III), As(IV) and rare earths did not interfere, nor did common anions such as chloride, sulphate, carbonate and hydrogencarbonate. The tolerance limits for the other ions tested were (in p.p.m.): Fe(III), 2; Mn(II), 6; Zn(II), 10; Pb (II), 12; Hg(II), 14; Zr(IV), 16; Mo(IV), 4; W(VI), 4; Cd(II), 18; Th(IV), 40; U(VI), 10; PO_4^{3-}, 60; acetate, 100; citrate, 100; tartrate, 80.

One of the authors (U.D.J.) thanks the U.G.C. (India) for the award of a junior research fellowship.

REFERENCES

1 D. A. Skoog, M. Lai and A. Furst, Anal. Chem., 30 (1958) 365.
2 G. H. Ayres and R. R. Anand, Anal. Chem., 35 (1963) 33.
3 R. W. Burke and J. H. Yoe, Anal. Chem., 34 (1962) 1379.
4 J. A. W. Dalziel and A. K. Slawinski, Talanta, 15 (1968) 367.
5 R. W. Burke and E. R. Deardroff, Talanta, 17 (1970) 255.
6 C. K. Bhaskare and U. D. Jagadale, Z. Anal. Chem., 278 (1976) 127.
7 A. Ringbom, Z. Anal. Chem., 115 (1938) 332.
8 P. Job, Ann. Chim. Phys., 9 (1928) 113.
9 J. H. Yoe and A. I. Jones, Ind. Eng. Chem. Anal. Ed., 16 (1944) 111.
10 J. R. Harvey and D. L. Manning, J. Am. Chem. Soc., 72 (1950) 4488.

Analytica Chimica Acta, 93 (1977) 341—344
© Elsevier Scientific Publishing Company, Amsterdam — Printed in The Netherlands

Short Communication

A COLORIMETRIC MODIFICATION OF THE WICKBOLD PROCEDURE FOR THE DETERMINATION OF NON-IONIC SURFACTANTS IN BIODEGRADATION TEST LIQUORS

J. WATERS* and G. F. LONGMAN

Unilever Research Port Sunlight Laboratory, Port Sunlight, Wirral, Merseyside L62 4XN (England)

(Received 14th April 1977)

The Wickbold procedure [1—4] has been adopted for the determination of non-ionic surfactants in biodegradation test liquors in the German [3], French [5] and U.K. [6] methods. The lengthy procedure requires three separate analytical stages: first, non-ionic surfactant is concentrated from dilute samples by solvent sublation [1, 2], then the isolated material is precipitated from aqueous solution with a modified Dragendorff reagent (barium chloride—potassium tetraiodobismuth(III)); finally, the non-ionic surfactant—complex precipitate is dissolved and the liberated bismuth ion is titrated potentiometrically with pyrrolidine dithiocarbamate complexone.

This communication describes a modified procedure which uses a final colorimetric determination to give a comparatively simple and quick analysis. The proposed end-determination is based on a method reported by West and Coll [7] for determining bismuth ion by the ultraviolet absorptivity of its EDTA complex.

Experimental

Reagents and apparatus. Prepare the reagents in de-ionized water from analytical reagent-grade materials. De-ionized water was used throughout. A Unicam SP 1800 spectrophotometer was used with matched 20-mm quartz optical cells.

Concentration of non-ionic surfactant. Use the Wickbold solvent sublation technique [2, 3] to concentrate 250—1000 μg of non-ionic surfactant from an appropriate volume of test liquor. Treat similarly an equivalent volume of control solution, if available.

Modified precipitation step. Dissolve the non-ionic residue, contained in a 400-ml beaker, in 5 ml of methanol. Add 40 ml of water and 3—5 drops of bromocresol purple solution (0.1% in methanol) and adjust the pH with dilute (0.2 M) hydrochloric acid until the indicator just turns yellow. Add 30 ml of modified Dragendorff reagent [2, 3], occasionally stir the solution with a glass rod over a period of 10 min, and leave the precipitate to stand for about 10 min. Filter the mixture through a G4 crucible fitted with a new GF/C glass fibre pad cut to fit the base exactly. Wash successively the beaker

and crucible with three 10-ml portions of glacial acetic acid to ensure removal of excess Dragendorff reagent. Drain the beaker and filter of glacial acetic acid as completely as possible. Carefully wipe the crucible base to remove any splashed reagent and position it on a clean filter flask.

Colorimetric procedure. Use 15 ml of freshly prepared hot aqueous ammonium tartrate solution (1.77% w/v) to dissolve the precipitate in the crucible. Use a further 15 ml of hot tartrate solution to rinse the sides of the sample beaker before passing it through the crucible. Finally, wash the crucible with another 15 ml of tartrate solution followed by 10 ml of water. Return the contents of the filter flask to the original beaker. Rinse the flask with two 10-ml portions of water (the total volume of sample should be about 75 ml). Add 4 ml of 0.02 M EDTA solution, mix, and transfer to a 100-ml volumetric flask. Wash the beaker with water to bring the sample up to volume. Read the absorbance in a 20-mm quartz optical cell at 263.5 nm against a water reference. Correct the sample absorbance for the control value, and determine the amount of non-ionic surfactant by reference to a previously prepared calibration graph.

After use, clean the crucibles by placing them overnight in a 1% potassium permanganate solution (acidified with a few drops of 18 M sulphuric acid) and then immersing them in 10-vol. hydrogen peroxide solution for several hours. Finally, wash well with water before use.

Preparation of calibration graph. Add from a burette 0, 2, 4, 6, 8 and 10 ml (0—1000 μg) of a 100 mg l^{-1} non-ionic surfactant solution to a series of 250-ml beakers and dilute to 40 ml with water. Add 5 ml of methanol and 30 ml of Dragendorff reagent and proceed as above. Construct a calibration of absorbance against the concentration (μg) of non-ionic surfactant.

Scope of the method

Colorimetric conditions. West and Coll [7] indicated that the molar absorptivity (ϵ_{max}, $9.35 \cdot 10^3$) of the highly stable bismuth—EDTA complex at 363.5 nm remains constant over the pH range 2—9. Since the final pH of sample solutions was generally in the range 4—5, no pH control in the colorimetric estimation was required. A 10-fold or greater excess of EDTA (4 ml of 0.02 M EDTA solution) over the bismuth in samples was used. Linear Beer's Law plots were obtained over the range 100—1000 μg for all the non-ionic surfactants examined, with the exception of the shorter ethoxylate chain compounds, i.e. those containing 6 or less ethylene oxide (EO) units.

The colorimetric responses of two typical series of non-ionic surfactants are given in Table 1. The estimated limit of detection of the colorimetric modification is about 25 μg (0.025 mg l^{-1} for a 1-l sample) of an average 10 (EO) alkylphenol ethoxylate.

Interferences. Heavy metal ions result in positive interferences in the colorimetric determination as they do in the original titrimetric determination. In particular, iron(III) and copper(II) form stable EDTA complexes that absorb strongly at the λ_{max} of the bismuth complex. However, the use of analytical-grade reagents and high-quality de-ionized water generally results in acceptable

TABLE 1

Colorimetric response of two series of non-ionic surfactants

Surfactant type	Hydrophobe	Average (EO) chain length	Absorbance for 1000 μg surfactant[a]
Alcohol ethoxylate	C_{13}—C_{15} alkyl chain	6	0.606
		10	0.650
		13	0.745
		18	0.790
		25	0.830
		30	0.881
		50	0.960
Nonylphenol ethoxylate	C_9 alkyl chain	6	0.546
		10	0.676
		30	0.856

[a]At 263.5 nm in 20-mm cells.

reagent blanks. Both the tartrate ion and EDTA absorb slightly at 263.5 nm and contribute to the absorption reading for the reagent blank (typical readings are 0.03—0.040 absorbance). Nitrate ion which also absorbs strongly in the ultraviolet, should be absent at the final stage.

Results

The original Wickbold method and the modified procedure were compared for a range of ring-test samples from the Organisation for Economic Cooperation

TABLE 2

Determination of non-ionic surfactants — comparison of the modified and Wickbold procedures

Test situation	Surfactant	Nominal level[a] (mg l^{-1})	Level found (mg l^{-1}) Wickbold method	Colorimetric modification
Distilled Water	Nonylphenol ethoxylate (NPE)	0.11	0.10	0.09
		0.28	0.30	0.27
		0.55	0.51	0.57
		0.83	0.77	0.76
'Detergent Free' Sewage Effluent	Alcohol ethoxylate	0.10	0.11	0.09
		0.50	0.53	0.50
		2.00	2.16	2.14
		0.30	0.40	0.36

[a]1-l sample.

TABLE 3

Determination of non-ionic surfactant in distilled water, OECD synthetic sewage [8] and secondary effluent by the modified procedure

Nominal NPE concentration added[a] ($mg\ l^{-1}$)	NPE found ($mg\ l^{-1}$)		
	Distilled water	Synthetic sewage	Secondary effluent[b]
0.25	0.21	0.34	0.23
	0.25	0.26	0.26
0.38	0.41	0.36	0.39
	0.36	0.36	0.41
0.50	0.48	0.49	0.55
	0.53	0.50	0.51

[a] 1-l sample.
[b] Result corrected for a background level of non-ionic surfactant in sample.

and Development (OECD) and found to be in good agreement (Table 2). The applicability of the modified procedure to a range of test liquors is further demonstrated in Table 3.

REFERENCES

1 R. Wickbold, Tenside Deterg., 8 (1971) 61.
2 R. Wickbold, Tenside Deterg., 9 (1972) 173.
3 German Federal Law Gazette, part 1, Bonn, 23rd August 1975, page 1.
4 EEC draft directive No. XI/315/76-E, Annex, Chapter 6, Brussels, February 1976.
5 Determination of the Biodegradability of Non-ionic Surfactants, T 73-270, L'Association Francaise de Normalisation, Paris, 1974.
6 Standing Technical Committee on Synthetic Detergents, Supplement to 8th Progress Report, HMSO, London, 1966.
7 P. W. West and H. Coll, Anal. Chem., 27 (1955) 1221.
8 Pollution by Detergents. Determination of the Biodegradability of Anionic Synthetic Surface-Active Agents, Organisation for Economic Cooperation and Development, Paris, 1972.

Analytica Chimica Acta, 93 (1977) 345—348
© Elsevier Scientific Publishing Company, Amsterdam — Printed in The Netherlands

Short Communication

FLUORESCENCE QUENCHING OF THE ε-ADP— A SIMPLE SENSITIVE METHOD FOR THE DETERMINATION OF COPPER(II)

W. E. HÖHNE* and H. WESSNER

Institut für Physiologische und Biologische Chemie der Humboldt-Universität, 104-Berlin (D.D.R.)

(Received 14th April 1977)

Adenosine phosphates form complexes with several divalent metal ions. The stability of the complexes decreases in the order ATP>ADP≫AMP [1]. Fluorescent 1, N^6-etheno derivatives of adenosine mono-, di-, and tri-phosphates (ε-AMP, ε-ADP and ε-ATP) were first described by Secrist et al. [2, 3]. The intense fluorescence of these compounds (Q = 0.56) permits measurements down to a concentration range below 10^{-7} M. Some divalent metal ions, especially Co^{2+} and Cu^{2+}, drastically quench the fluorescence of the etheno—adenosine phosphates [4]. The complex formation constants are similar to those of the unmodified adenosine phosphates.

The present communication reports a simple sensitive method for determination of copper(II) based on the fluorescence quenching caused by complex formation with ε-ADP. ε-ADP is preferred to ε-ATP, because of its higher stability against hydrolysis in solution. The method can be applied to other metal ions with comparable quenching effects, such as Co^{2+}, Fe^{2+}, and Fe^{3+} at higher concentrations.

Experimental

ε-ADP was prepared as described by Secrist et al. [2]. The product, characterized by its absorption spectrum and by phosphate determination after acid hydrolysis, was more than 95% pure and was used without further purification. Solutions of divalent metal ions were made up from the following salts: $CuSO_4 \cdot 6H_2O$, $FeSO_4 \cdot 7H_2O$, $Fe(NO_3)_3 \cdot 9H_2O$, $MnSO_4 \cdot 4H_2O$, $ZnSO_4 \cdot 7H_2O$, $MgSO_4 \cdot 7H_2O$, and $CaCO_3$, and were of reagent grade (VEB Laborchemie, Apolda). If not indicated otherwise, all measurements were performed in HEPES buffer (FERAK, Berlin), pH 7.2, 0.01 M, at 25°C, although the pH can be varied [4] between 5.5 and 10.

A Hitachi fluorescence spectrophotometer MPF-2A was used with a 10-nm bandwidth, 315-nm excitation wavelength and 405-nm emission wavelength.

The complex formation constants were calculated by linear regression analysis from the equation $1/L = M_t \cdot K/(L_t - L) - K$, which is a linearization of the binding equation (L_t = total ε-ADP concentration; L = free ε-ADP

concentration, calculated from the difference between the fluorescence intensity at a given total metal ion concentration and the maximal decrease of the fluorescence intensity; M_t = total metal ion concentration; K = formation constant). K is derived from the slope or the intercept of the lines plotting $1/L$ versus $M_t/(L_t - L)$. It was assumed that a 1:1 stoichiometry applies [4].

A typical determination involves 1 ml of the reagent solution (0.01 mM ϵ-ADP in 10 mM HEPES buffer, pH 7.2) and addition of 20 μl of a neutralized sample solution containing 0.1—0.6 μg Cu^{2+}, with immediate measurement of the fluorescence quenching.

Results and discussion

Figure 1 shows the dependence of the fluorescence quenching on Cu^{2+} concentration for two ϵ-ADP concentrations. The calibration curve is reasonably linear for Cu^{2+} concentrations below, or comparable with, the ϵ-ADP concentration provided that the latter is higher than the corresponding reciprocal complex formation constant. With ϵ-ADP concentrations in the range of the reciprocal binding constant (about $1.2 \cdot 10^{-6}$ M), much lower Cu^{2+} concentration can be determined, but the calibration curves become nonlinear.

Fluorescence quenching comparable to that of Cu^{2+} is caused by Fe^{2+} and Co^{2+} (Fig. 2). In principle, these ions could also be determined, but the procedures would be less sensitive because of the weaker binding of these ions to ϵ-ADP, and because of incomplete fluorescence quenching (see Table 1 and [4]). In these cases, ϵ-ATP would be a better reagent.

As expected, the formation constant depends on ionic strength (Table 1). Therefore, the ionic strengths must be identical for the calibration curve and the assays.

The interferences of metal ions which form complexes with ϵ-ADP, were checked for the Cu^{2+} determination. Table 2 shows the ratios at which the

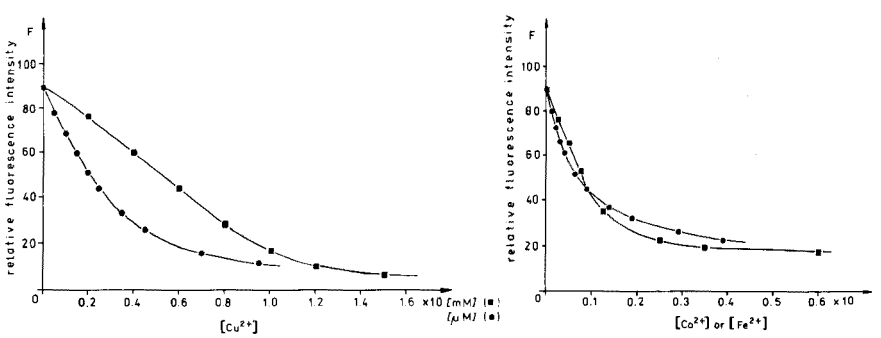

Fig. 1. Dependence of the ϵ-ADP fluorescence quenching on the Cu^{2+} concentration: (■) 0.1 mM ϵ-ADP; (●) 4 μM ϵ-ADP. The curves are normalized to identical initial fluorescence.

Fig. 2. Dependence of the ϵ-ADP fluorescence quenching on the Co^{2+} and Fe^{2+} concentration (●) Co^{2+} dependence with 0.1 mM ϵ-ADP; (■) Fe^{2+} dependence with 4 μM ϵ-ADP. The curves are normalized to identical initial fluorescence.

TABLE 1

Complex formation constants for the ϵ-ADP complexes of copper(II), iron(II) and cobalt(II)

(Cu^{2+} and Fe^{2+} binding studies: 0.01 M HEPES buffer, 4 μM ϵ-ADP. Co^{2+} binding studies: 0.1 M HEPES buffer, 0.1 mM ϵ-ADP. The constants are given for pH 7.2 and 25°C.)

Metal	KNO_3(M)	K(M^{-1})
Cu^{2+}	—	$(8.5 \pm 0.44) \cdot 10^5$
Cu^{2+}	0.1	$4.5 \cdot 10^5$
Cu^{2+}	0.2	$2.7 \cdot 10^5$
Cu^{2+}	0.5	$1.1 \cdot 10^5$
Fe^{2+}	—	ca. $3 \cdot 10^5$
Co^{2+}	0.1	$1.1 \cdot 10^4$ [4]

TABLE 2

Interference of selected metal ions with the fluorimetric determination of copper(II)[a]

Ion	Me/Cu(II)	ΔF	Ion	Me/Cu(II)	ΔF
Mg^{2+}	160	+	Co^{2+}	5.0	—
Ca^{2+}	300	+	Fe^{2+}	0.24	—
Mn^{2+}	117	+	Fe^{3+}	5.3	—
Zn^{2+}	267	+			

[a]At the concentration ratio indicated, a 10% error in fluorescence was observed. Positive ΔF means increase of fluorescence; ΔF negative means decrease of fluorescence. In these tests, 4 μM ϵ-ADP and 3 μM Cu^{2+} were used.

fluorescence deviation reached 10%. Errors can arise when the interfering component itself quenches the ϵ-ADP fluorescence, e.g. Fe^{2+} and Co^{2+}, or when the fluorescence quenching is decreased by complex formation (e.g. Mg^{2+}). The interferences of Co^{2+} and Fe^{2+} are in line with the complex formation constants (Table 1).

The method described here is suitable for simple sensitive Cu^{2+} determinations in solutions of known composition. The detection limit estimated from a 10% fluorescence decrease is about 1 μM for Cu^{2+}, corresponding to 19 ng Cu if 300 μl microcuvettes are employed.

The method may be applied for the measurement of Cu^{2+} after dialysis, ultrafiltration or other methods related to binding studies with macromolecules. The ϵ-ADP reagent is stable even in solution for long times if kept at 4°C, and is commercially available or easy to prepare.

The authors are indebted to Prof. Dr. Dr. S. Rapoport for critical reading of the manuscript.

REFERENCES

1 A. E. Martell and L. G. Sillen, Stability Constants of Metal-Ion Complexes, The Chemical Society, Burlington House, London, 1964.
2 J. A. Secrist, J. R. Barrio, N. J. Leonard and G. Weber, Biochemistry, 11 (1972) 3499.
3 J. R. Barrio, J. A. Secrist and N. J. Leonard, Proc. Nat. Acad. Sci. U.S.A., 69 (1972) 2039.
4 W. E. Höhne and P. Heitmann, Anal. Biochem., 69 (1975) 607.

Analytica Chimica Acta, 93 (1977) 349—352
© Elsevier Scientific Publishing Company, Amsterdam — Printed in The Netherlands

Short Communication

COLORIMETRIC DETERMINATION OF AMINES AND AMINO ACIDS

JOHN ELLIS*, ANTHONY M. HOLLAND and RHONDA A. HOLLAND
Department of Chemistry, University of Wollongong, N.S.W. 2500 (Australia)
(Received 30th March 1977)

Nitrous acid reacts rapidly to convert the amino group of amino acids to a hydroxyl group; the volume of nitrogen liberated is used in the Van Slyke method [1] to estimate the number of primary amino groups present. This reaction was extended to the determination of primary amino groups in aromatic amines, amides and sulphonamides [2]. Nitrous acid also reacts with secondary amines and *N*-monosubstituted amides to give *N*-nitroso derivatives, but without evolution of nitrogen.

By treating the amino compound with a much smaller excess of nitrous acid than that normally used, the unreacted nitrite can be determined colorimetrically and hence the amino compound determined by difference. The two major potential sources of error are loss of nitrogen oxides to the atmosphere, and disproportionation of nitrous acid to nitric oxide and nitric acid with further aerial oxidation of nitric oxide to nitrogen dioxide. Both these sources of error may be eliminated by conducting the reaction in a sealed system under reduced pressure and absorbing the evolved fumes in sodium hydroxide solution; the apparatus involved has been described [3]. Any nitrate ion formed by aerial oxidation is reduced to nitrite ion with copperized cadmium and the total excess of nitrite ion is determined colorimetrically by reaction with sulphanilamide and *N*-(1-naphthyl)-ethylenediamine [4].

Experimental

Compounds. Commercially available amines and amino acids were checked for purity by g.c.—mass spectrometry. All reagents were analytical-reagent grade. Sodium nitrite solution was prepared by dilution of a stock solution prepared weekly by dissolving 7.500 g of sodium nitrite in 100 ml of distilled deionized water. Copperized cadmium was prepared from Merck coarse cadmium powder [5].

Equipment. Volumetric glassware was all Grade A. The diazotization apparatus consisted of a glass-stoppered (B24) 5 × 2-cm test tube with the extended ends of two 10-ml burettes sealed through the glass stopper; the tips of the burettes were angled away from each other. The vessel is similar to that described previously [3] but without the side-arm. A Cary spectrophotometer was used.

Procedure. Place an aqueous solution of the amino compound (0.5 ml; ca. 0.03 mmol), prepared by successive dilution of a 2 mg ml^{-1} stock solution in 1 M HCl, in the reaction vessel. Add hydrochloric acid—sodium acetate buffer (1 ml; pH 3.6), close the burette stopcocks and insert the burette assembly into the reaction vessel. Place sodium nitrite solution (1.0 ml; 6 mg ml^{-1}) in one burette and create a partial vacuum by cooling the reaction vessel in ice. Open the burette tap briefly to admit the nitrite solution. Then place sodium hydroxide solution (1.5 ml; 8 M) in the other burette. Keep the mixture at 0—4°C for 45—60 min, depending on the amino compound used, and then warm to ca. 40°C by immersion in hot water for 10—15 min to complete the reaction. Again cool the vessel in ice and admit small portions of sodium hydroxide solution from the second burette. When all the alkali has been added, shake the contents of the vessel to absorb acidic nitrogen oxides. Then wash residual sodium nitrite solution from the first burette into the reaction vessel with small portions of dilute sodium hydroxide solution. Transfer the alkaline solution to a volumetric flask, add citric acid solution (5 M; 4 ml) to adjust the pH to 7—8, and EDTA solution (4 ml; 0.1 M), and dilute the solution to the mark.

Allow a 50-ml aliquot of this solution to percolate slowly through a column (20 cm × 1 cm) of copperized cadmium, and wash through with 3 × 50-ml portions of distilled water into a 250-ml volumetric flask. Dilute to the mark with distilled water, and analyze a 10-ml aliquot colorimetrically by the sulphanilamide—*N*-(1-napthyl)-ethylenediamine method [4]. After suitable dilution, measure the absorbance at 543 nm with a sodium nitrite blank worked up in exactly the same way as reference.

Results and discussion

Scope and limitations of method. The method is applicable to primary and secondary amines and amino acids (Table 1). Primary and secondary amines are not distinguished but the method could be used in conjunction with the direct spectrophotometric determination of secondary amines as their nitroso derivatives [6].

The optimum pH for the diazotization of amines has been studied [7]; the reaction rate declines markedly below pH 3. At the low pH necessary to achieve rapid diazotization of amides (6 M sulphuric acid [8]), amines are fully protonated and therefore unreactive. Hence, by appropriate adjustment of the pH used for the diazotization step, the procedure can be used to determine amines in the presence of amides and vice versa.

The reaction is not seriously affected by steric hindrance and gives better results than the Van Slyke procedure for "anomalous" amino acids; for example, glycine gives a quantitative result whereas the Van Slyke method leads to the formation of nitrous oxide and nitrogen [9, 10]. The production of nitrous oxide has been attributed to the formation of a nitrolic acid intermediate [11], especially at high temperature and high nitrite concentration. The present method uses a low sample concentration and only a moderate

TABLE 1

Analysis of amines and amino acids

Amino compound[a]	Reaction time (min)	Sample mass (mg)	Recovery[b] (%)
n-Butylamine	40	1.8	96.7—101.6
i-Butylamine	60	3.7	98.3—100.5
t-Butylamine	60	1.7	97.7— 99.4
Piperidine	60	2.1	97.7—106.5
Dicyclopentylamine	60	3.2	98.4—100.9
Glycine	40	3.0	99.8—101.0
		1.0	99.7—103.0
Glycylglycine	50	4.0	98.8—102.0
Phenylalanine	50	2.0	100.5—103.5
Leucine	50	4.0	96.3—102.0
Tyrosine	45	4.0	99.5—101.0
t-Butylamine (+ 4 mg isobutyramide)	60	1.7	98.8— 99.4
Isobutyramide (+ 1.7 mg t-butylamine)	15	1.0	98.0—103.0

[a]Amines and amino acids diazotized at pH 3.5—4, and amide groups in 6 M sulphuric acid.
[b]Three determinations of each amino compound.

excess of nitrous acid; the probability of reaction of the intermediate with water is therefore enhanced relative to its reaction with nitrous acid.

The principal classes of interfering substances are as for the Van Slyke procedure [12]. Positive interference may be expected from isonitroso and active methylene groups and from monohalogenocarboxylic acids, phenols, sulphur compounds oxidizable by nitrous acid, indoles and oxindoles, and lactams. Negative errors will arise for amines which are difficult to diazotize or dissolve. The Van Slyke procedure has two additional sources of negative error: amines which give relatively stable diazonium salts and side-reactions of the intermediate diazonium salt. Bromine—acetic acid has been used to block the interference of active methylene compounds, phenols and sulphur compounds [12]. Treatment of a tyrosine solution with a few drops of bromine water before the diazotization gives quantitative results (Table 1).

Inorganic ions which can reduce nitrite interfere, but minor concentrations of oxidizing inorganic ions do not: any nitrate produced is reduced to nitrite by the cadmium column. High concentrations of metal ions could interfere with the function of the EDTA, which complexes the Cd^{2+} released by oxidation of the cadmium [5].

Sensitivity and precision. The precision was studied by performing five replicate determinations at each of two different concentration levels with phenylalanine and t-butylamine (Table 2). When all the manipulations of

TABLE 2

Effect of sample mass on precision

Phenylalanine (mg)	2	0.2	t-Butylamine (mg)	2	0.2
s_r (%, n = 5)	2.1	2.7	s_r (%, n = 5)	1.1	5.0

the procedure are taken into account, solutions containing as little as 0.017 mg of amino nitrogen can be determined with a relative standard deviation of 2.7% Because the method is based on comparison with the absorption of a blank subjected to the entire procedure, errors associated with nitrate impurities in the nitrite reagent and uptake of nitrogen oxides from the atmosphere are minimized. The sensitivity depends on the absorptivity of the azo dye used to measure nitrite concentration. With 10-cm cells, nitrite concentrations as low as 14 μg N l^{-1} have been measured [5] with a relative standard deviation of 4%.

Conclusions. This procedure affords a sensitive and accurate method for determining primary and secondary amines and amino acids. The apparatus is simpler to construct and use than the Van Slyke apparatus. It avoids the chromophoric substituent effects associated with direct spectrophotometric determination of the derivatives formed by 2,4-dinitrofluorobenzene [13] or 2,4,6-trinitrobenzenesulphonic acid [14] and gives a stable colour in contrast to that given by ninhydrin [15].

One of us (A.M.H.) acknowledges the support of a Commonwealth Postgraduate Award.

REFERENCES

1 D. D. Van Slyke, J. Biol. Chem., 12 (1911) 275.
2 G. Kainz, Mikrochim. Acta, (1953) 349.
3 J. Ellis and A. M. Holland, Analyst, 101 (1976) 996.
4 M. B. Shinn, Ind. Eng. Chem. Anal. Ed., 13 (1941) 33.
5 E. D. Wood, I. A. J. Armstrong and I. A. Richards, J. Mar. Biol. Ass. U.K., 47 (1967) 23.
6 S. J. Clark and D. J. Morgan, Mikrochim. Acta, (1956) 966.
7 E. D. Hughes, C. K. Ingold and J. H. Ridd, J. Chem. Soc., (1958) 88.
8 T. A. Turney and G. A. Wright, Chem. Rev., 59 (1959) 497.
9 A. T. Austin, J. Chem. Soc., (1950) 149.
10 G. Kainz, F. Kasler and H. Huber, Mikrochim. Acta, (1959) 883.
11 G. Kainz and F. Kasler, Mikrochim. Acta, (1960) 62.
12 G. Kainz, H. Huber and F. Kasler, Mikrochim. Acta, (1957) 744.
13 G. Koch and W. Weidel, Z. Physiol., 303 (1956) 213.
14 R. Fields, Biochem. J., 124 (1971) 581.
15 S. Moore, P. H. Spackman and W. H. Stein, Anal. Chem., 30 (1958) 1185.

Analytica Chimica Acta, 93 (1977) 353—356
© Elsevier Scientific Publishing Company, Amsterdam — Printed in The Netherlands

Short Communication

THE DETERMINATION OF GLUCOSE WITH IMMOBILIZED GLUCOSE OXIDASE AND PEROXIDASE

J. N. MILLER, B. F. ROCKS and D. THORBURN BURNS

Department of Chemistry, Loughborough University of Technology, Loughborough, Leics. LE11 3TU (England)

(Received 14th April 1977)

During the continuing rapid development of analytical methods based on immobilized enzymes, several techniques have been described for the determination of glucose. For example, glucose oxidase (E.C.1.1.3.4) entrapped in polyacrylamide gel was used by Updike and Hicks in two methods. In one case [1], the hydrogen peroxide produced during the oxidation of glucose was detected by measuring the increase in absorbance of an oxidized dye in the presence of a second enzyme, horseradish peroxidase (E.C.1.11.1.7): the limit of detection was approximately 10 μg ml^{-1}. In the second method [2] a layer of immobilized glucose oxidase was wrapped round the plastic membrane of a polarographic oxygen electrode, which measured the oxygen consumed during the oxidation of glucose. Weibel et al. [3] immobilized glucose oxidase on porous glass and measured oxygen consumption with a separate Clark electrode. Hornby et al. attached glucose oxidase covalently to the inner surfaces of polystyrene [4] or nylon [5] tubes and used a colorimetric method to monitor the concentrations of glucose solutions in the range 0—6 mM.

The present authors have recently described [6] the use of diazotized polyaminostyrene beads for the immobilization of enzymes. When packed into glass coils, the enzyme beads are suitable for use in rapid automatic analysis systems. Horseradish peroxidase immobilized in this way was used in the determination of hydrogen peroxide. The activity of the immobilized enzyme was only a few per cent of that of the soluble peroxidase, but nanogram detection limits were achieved by using a fluorimetric method, and the relatively hydrophobic nature of the beads permitted rapid equilibration and high sample throughput. The present communication describes the use of immobilized peroxidase to determine the peroxide produced in the oxidation of glucose by immobilized glucose oxidase. This application of two immobilized enzymes permits the rapid and simple determination of glucose at microgram levels.

Experimental

Glucose oxidase (Sigma Chemical Co. Ltd., Type V, 1250 units ml^{-1}) was immobilized by reaction with diazotized polyaminostyrene beads (Dow Chemical Company, 20-35 mesh) for 2 h at 0°C in 0.1 M Tris—HCl buffer pH 8.5, containing 0.75 M sucrose (Tris = tris(hydroxymethyl)aminomethane). (This preparation of glucose oxidase contained relatively low levels of the contaminating enzyme catalase — ca. 32 units ml^{-1}. Other preparations containing proportionately larger quantities of catalase were found to be unsuitable). Horseradish peroxidase (Sigma Chemical Co. Ltd., Type 1) was attached to diazotized polyaminostyrene beads as previously described [6]. Beads with both glucose oxidase and peroxidase simultaneously immobilized were prepared by the same method. Enzyme beads were packed into glass coils and incorporated into the simple automatic analysis system already described [6], which was used with a flow rate of 2 ml min^{-1}. Hydrogen peroxide, derived from the oxidation of glucose, was determined with homovanillic acid (Whatman Biochemicals Ltd.) as a substrate, the product 2,2′-dihydroxy-3,3′-dimethoxyphenyl-5,5′-diacetic acid being determined fluorimetrically (excitation wavelength 315 nm; emission wavelength 425 nm; Baird-Atomic "Fluoripoint" spectrofluorimeter). All reagents were AnalaR or equivalent grade, and triply distilled water was used throughout.

Results and discussion

Figure 1 shows the effect of storage on the activity of the glucose oxidase beads. Even after 40 days storage at 2°C, the immobilized enzyme retained over 60% of its initial activity. Peroxidase is markedly less stable when immobilized by the same method, losing 90% of its activity within 30 days [6]

To investigate the effects of pH on the sensitivity of the combined glucose oxidase—peroxidase system, solutions containing 10 $\mu g\ ml^{-1}$ glucose, 10 $\mu g\ ml^{-1}$ peroxidase and 85 $\mu g\ ml^{-1}$ homovanillic acid in Tris—HCl at various pH values were passed through a coil containing glucose oxidase beads. In

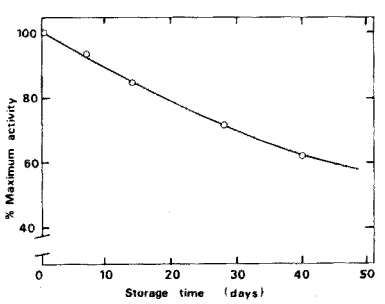

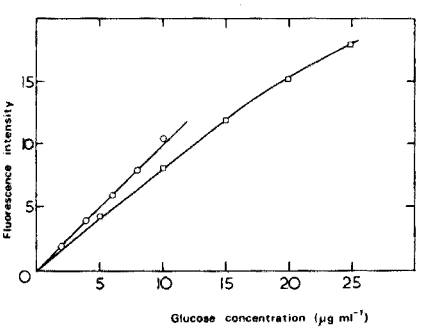

Fig. 1. Stability of immobilized glucose oxidase on storage at 2°C.

Fig. 2. Use of immobilized glucose oxidase and peroxidase in the determination of glucose Analytical curves obtained with (a) glucose oxidase beads and peroxidase beads in consecutive coils (○) and (b) mixed glucose oxidase beads and peroxidase beads (□).

TABLE 1

Effect of pH on the glucose oxidase—peroxidase system

pH	7.0	7.5	8.0	8.5	9.0
Fluorescence (arbitrary units)	8	42	79	100	84

principle, the variations observed in the resulting fluorescence intensity might have been caused by the effects of pH on the activity of one or both of the enzymes, or on the fluorescence intensity of the oxidation product of homovanillic acid. The results (Table 1) show that the maximum fluorescence intensity was observed at pH 8.5. This is close to the value previously obtained in studies of peroxidase alone [6], and probably represents a compromise between the optimum pH of this enzyme, and the optimum pH for the fluorescence of 2,2′-dihydroxy-3,3′-dimethoxyphenyl-5,5′-diacetic acid [7]. The optimum pH for soluble glucose oxidase is reported to be 5.6 [8]. An approximately 8-fold increase in fluorescence (compared with that found when pH 8.5 was used throughout) was obtained by passing the sample through the glucose beads at pH 6.0 (potassium dihydrogenphosphate buffer) and adjusting its pH to 8.5 with 0.05 M alkali before passing it through the peroxidase beads. Since the sensitivity of the system used at a constant pH of 8.5 was more than adequate (see below), this modification, which increased the complexity of the automatic analysis system, was not used routinely.

The best disposition of the immobilized enzymes in the automatic analysis system was studied in a separate series of experiments, with solutions containing 10 μg ml^{-1} glucose and 85 μg ml^{-1} homovanillic acid in Tris—HCl buffer, pH 8.5, as samples: the results are given in Table 2. Passing the sample solution through separate coils of glucose oxidase and peroxidase beads arranged in series produced nearly as intense a fluorescence signal as did passing a sample containing soluble peroxidase through the same coil of glucose oxidase beads. This suggests that most of the hydrogen peroxide produced by the glucose oxidase-catalyzed reaction was being

TABLE 2

Methods of utilizing immobilized glucose oxidase and peroxidase

Experimental system	Fluorescence (arbitrary units)
1 Glucose oxidase beads with sample containing soluble peroxidase	100
2 Glucose oxidase and peroxidase beads in consecutive glass coils	87
3 Glucose oxidase and peroxidase beads from 2 mixed and repacked in glass coils	52
4 Glucose oxidase + peroxidase beads containing same weights of enzymes as in 2 and 3	95

consumed in the indicator reaction involving peroxidase. When the glucose oxidase beads and peroxidase beads were intimately mixed and replaced into two glass coils in series, the resultant fluorescence was almost halved, presumably because some of the hydrogen peroxide produced was not consumed in this case. Beads containing the same weights of two enzymes immobilized simultaneously were far more active than the mixture of glucose oxidase beads and peroxidase beads. Similar increases in efficiency in matrix-bound multi-enzyme systems have been found by other authors [9, 10] and may be due to the spatial proximity of the immobilized enzymes leading to a higher local concentration of hydrogen peroxide around the immobilized peroxidase. Nevertheless, the system based on two separate coils containing glucose oxidase and peroxidase beads, respectively, would be the most flexible for general use, in view of the differing stabilities of the immobilized enzymes on storage.

Figure 2 shows the calibration plots obtained when immobilized enzymes were used in the analysis of standard solutions of glucose. It is evident that glucose can readily be determined at the p.p.m. level, i.e. at a concentration corresponding to an approximately 100-fold dilution of normal human blood plasma. The sensitivity of the method is due to the use of the fluorimetric determination procedure.

The successful use of polystyrene-bound peroxidase in the analysis of glucose foreshadows further applications in cases where the substrate under study is oxidized in a reaction in which hydrogen peroxide is also produced. Preliminary experiments with immobilized xanthine oxidase (E.C.1.2.3.2) have shown that microgram concentrations of xanthine can be determined in this way, and immobilized uricase (E.C.1.7.3.3.) has been prepared and used in the analysis of uric acid.

REFERENCES

1 G. P. Hicks and S. J. Updike, Anal. Chem., 38 (1966) 726.
2 S. J. Updike and G. P. Hicks, Nature, 214 (1967) 986.
3 M. K. Weibel, W. Dritschilo, H. J. Bright and A. E. Humphrey, Anal. Biochem., 52 (1973) 402.
4 W. E. Hornby, H. Filipusson and A. McDonald, FEBS Lett., 20 (1971) 291.
5 D. J. Inman and W. E. Hornby, Biochem. J., 129 (1972) 255.
6 J. N. Miller, B. F. Rocks and D. T. Burns, Anal. Chim. Acta, 86 (1976) 93.
7 G. G. Guilbault, P. Brignac and M. Zimmer, Anal. Chem., 40 (1968) 190.
8 R. Bentley, in P. D. Boyer, H. Lardy and K. Myrback (Eds.), The Enzymes, Vol. 7, p. 572, Academic Press, London, 1963.
9 K. Mosbach and B. Mattiasson, Acta Chem. Scand., 24 (1970) 2093.
10 B. Mattiasson and K. Mosbach, Biochem. Biophys. Acta, 235 (1971) 253.

Analytica Chimica Acta, 93 (1977) 357—358
© Elsevier Scientific Publishing Company, Amsterdam — Printed in the Netherlands

Short Communication

DETERMINATION OF QUATERNARY AMMONIUM SALTS BY ION-PAIR EXTRACTION-TITRATIONS WITH TETRABROMOPHENOLPHTHALEIN ETHYL ESTER AS INDICATOR

TADAO SAKAI*

Department of Chemistry, Gifu College of Dentistry, Takano 1851, Hozumi, Motosu, Gifu (Japan)

MASAHIRO TSUBOUCHI, MOTOHIRO NAKAGAWA and MASAYA TANAKA

Faculty of General Education, Tottori University, Koyama, Tottori (Japan)

(Received 3rd February 1977)

Various reports [1—5] have appeared regarding the two-phase titration of quaternary ammonium salts with dyes as indicators. End-point detection is based on movement of the dye from one phase to the other, but accurate detection is difficult.

In the two-phase titration proposed here, sodium tetraphenylborate is used as titrant with tetrabromophenolphthalein ethyl ester as indicator in the presence of 1,2-dichloroethane. This procedure gives sharp end-points, as the organic layer changes from blue to yellow, and there is less likelihood of error. Tetrabromophenolphthalein ethyl ester (Ind) is insoluble in water, but gives a yellow solution in 1,2-dichloroethane. The quaternary ammonium ion is extracted as a blue ion-pair with the dye from the aqueous phase to the 1,2-dichloroethane phase. When the quarternary ammonium ion (NR_4^+) is titrated with sodium tetraphenylborate (TPB) solution, the $[NR_4^+ \cdot TPB^-]$ is formed in the organic layer, and the reaction followed at the end-point is

$$\underset{\text{blue}}{[NR_4^+ \cdot Ind^-]_{org}} + H^+ + [TPB^-]_{aq} \rightarrow [NR_4^+ \cdot TPB^-]_{org} + \underset{\text{yellow}}{[Ind]_{org}}$$

Experimental

Tetrabromophenolphthalein ethyl ester potassium salt was dissolved in ethanol. Quaternary ammonium salts were dried under reduced pressure. The phosphate buffer pH 8 solution was prepared from 0.3 M disodium hydrogenphosphate solution with several drops of dilute sulfuric acid.

Zephiramine (tetradecyldimethylbenzylammonium chloride) solution (10 ml of 0.005 M), 5 ml of the phosphate buffer solution, 5 ml of 1,2-dichloroethane, and 2—3 drops of tetrabromophenolphthalein ethyl ester solution (0.1%) were placed in an Erlenmeyer flask. The mixture was titrated with 0.005 M sodium tetraphenylborate solution with shaking by hand.

Results and discussion

Quantitative titrations were obtained in the pH range 5—9 when 1—5 drops of the 0.1% indicator solution were added. Larger amounts of buffer solution

had no influence on the titration, but when less than 1 ml was added, phase separation was poor. Various water-immiscible solvents were tested: nitrobenzene, methyl isobutyl ketone, butyl acetate, isoamyl alcohol, 1,2-dichloroethane, chlorobenzene, chloroform, toluene, benzene, carbon tetrachloride, and n-hexane. Of these, 1,2-dichloroethane and chloroform were suitable for the titration of tetrabutylammonium salts, and nitrobenzene, butylacetate, 1,2-dichloroethane, chlorobenzene, chloroform, toluene and benzene were suitable for the titration of zephiramine.

Table 1 shows the effect of concentration of the titrant on the titration of zephiramine.

The proposed method was applied to the determination of cationic surfactants such as benzethonium, cetyltrimethylammonium, trimethylphenylammonium and benzyltriethylammonium salts, in the same way as for zephiramine. Titration with 0.02—0.002 M tetraphenylborate was suitable for the determination of tetrabutylammonium, tetraphenylphosphonium, tetraphenylarsonium, and sparteine salts. Tetraethylammonium salts could be titrated only when the concentration of the titrant was 0.02 M. The accuracy was 0.3% or better. Tetramethylammonium salts did not give sharp end-points in any range of the concentration. It is reasonable to consider that a large quaternary ammonium ion is more readily extractable as an ion-pair into 1,2-dichloroethane than a small one.

The effect of other species on the titration process was studied for 10 ml of $2 \cdot 10^{-6}$ M tetrabutylammonium bromide solution. The following ions did not interfere at the 10^{-2} M level: sodium, calcium, magnesium, nitrate, acetate, sulfate, carbonate, citrate, bromide, chloride, iodide and phosphate. Ammonium ion caused positive errors, and the maximum permissible amount was 10^{-3} M.

TABLE 1

Effect of concentration of tetraphenylborate as a titrant

Tetraphenylborate (M)	Zephiramine added (mg/10ml)	Zephiramine found (mg/10ml)
0.02	73.80	73.80
0.01	36.91	36.90
0.005	18.45	18.43
0.002	7.38	7.38
0.001	3.69	3.67
0.0005	1.85	1.80

REFERENCES

1 S. R. Epton, Nature, 160 (1947) 795.
2 P. Mukerjee, Anal. Chem., 28 (1956) 870.
3 D. M. Patel and R. A. Anderson, Drug Standards, 26 (1958) 189.
4 J. T. Cross, Analyst, 90 (1965) 315.
5 P. J. Cooper and P. W. Hammond, Analyst, 92 (1967) 180.

Analytica Chimica Acta, 93 (1977) 359—362
©Elsevier Scientific Publishing Company, Amsterdam — Printed in The Netherlands

Short Communication

ÉTUDE D'ÉQUILIBRES EN SOLUTION À L'AIDE DES ÉCHANGEURS D'IONS
III. Détermination des constantes de dissociation du chlorure de césium et du nitrate de sodium dans les mélanges eau—acide acétique

A. R. RODRIGUEZ* and C. POITRENAUD

Institut National des Sciences et Techniques Nucléaires de Saclay, B.P. n° 6, 91190 Gif-sur-Yvette (France)

(Reçu le 29 mars 1977)

Une expression théorique du coefficient de partage d'un élément monovalent entre une résine échangeuse de cations et une solution acide d'un sel métallique de cet élément dans un mélange hydro—organique en fonction des paramètres dont il dépend (concentration de l'acide en solution, constantes de dissociation de l'acide et du sel, coefficient de sélectivité des ions échangés) a été établie précédemment [1]. Nous avons appliqué cette expression à la détermination des constantes de dissociation du chlorure de césium et du nitrate de sodium dans les mélanges eau—acide acétique à partir de mesures des coefficients de partage de ces éléments dans ces milieux.

Partie expérimentale

L'échangeur utilisé était la résine Bio Rad AG 50W-X8, 50-100 mesh, mise sous forme H^+ après plusieurs cycles d'échange H^+—Na^+. L'acide acétique (contenant 0,05—0,3% d'eau), les acides chlorhydrique et nitrique et le nitrate de sodium étaient des produits R.P. Prolabo, l'acétate de césium était un produit Merck. Les mélanges hydro—organiques ont été préparés par pesée. Le dosage des éléments à l'aide de traceurs radioactifs et la mesure des coefficients de partage ont été réalisés comme nous l'avons décrit précédemment [1, 2].

Résultats et discussion

Nous avons déterminé les coefficients de partage du césium et du sodium en fonction du pourcentage d'eau des mélanges hydro—acétiques. La Fig. 1 montre les résultats obtenus pour le césium dans les mélanges eau—acide acétique—acide chlorhydrique 0,1 M et pour le sodium dans les mélanges eau—acide acétique—acide nitrique 0,1 M.

Nous avons aussi étudié la variation du coefficient de partage du césium en fonction de l'inverse de la concentration totale de l'acide chlorhydrique

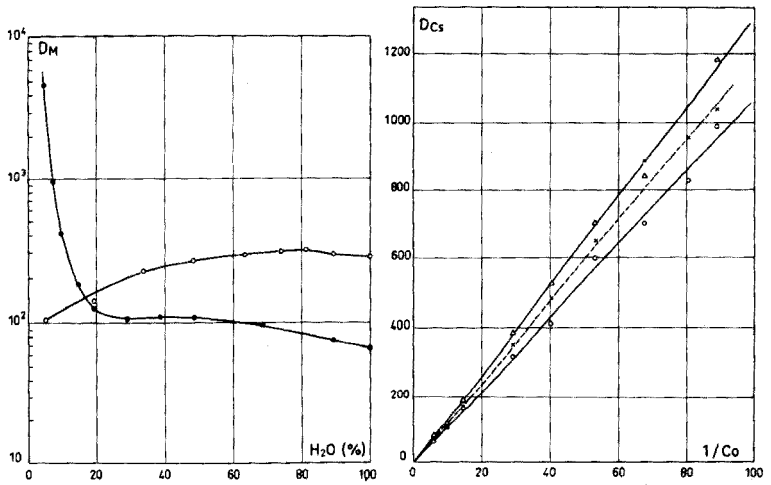

Fig. 1. Variation de D_M en fonction du pourcentage d'eau des solutions. (○) D_{Cs} dans les mélanges eau—acide acétique—acide chlorhydrique 0,1 M. (●) D_{Na} dans les mélanges eau—acide acétique—acide nitrique 0,1 M.

Fig. 2. Variation de D_{Cs} en fonction de l'inverse de la concentration d'acide chlorhydrique. Mélanges eau—acide acétique à: (○) 4,8% d'eau, (×) 9,6% d'eau et (△) 14,4% d'eau.

en solution, C_0. La Fig. 2 montre les courbes expérimentales obtenues dans les mélanges hydro—organiques de teneur en eau constante et inférieure à 15%. On remarque que D_{Cs} présente une variation linéaire avec $1/C_0$ à tous les pourcentages d'eau étudiés. On peut donc prévoir [1] que les constantes de dissociation de l'acide chlorhydrique et du chlorure de césium sont voisines dans ces mélanges.

Chlorure de césium. Pour déterminer les constantes de dissociation du chlorure de césium, il est nécessaire de connaître les constantes de dissociation de l'acide chlorhydrique dans les mélanges eau—acide acétique. Le Ber [3] a déterminé ces constantes dans les mêmes mélanges par potentiométrie en faisant certaines hypothèses simplificatrices relatives à la force ionique et aux coefficients d'activité des espèces. Nous avons repris ses résultats et nous les avons exploités d'une manière plus rigoureuse comme nous l'avons déjà fait dans le cas de l'acide perchlorique [4]. Les résultats que nous avons obtenus (voir Fig. 4) ont été utilisés par la suite dans nos calculs.

Connaissant les constantes de dissociation de l'acide chlorhydrique, nous avons déduit les constantes de dissociation du chlorure de césium des mesures du coefficient de partage. Nous avons exploité nos résultats expérimentaux à l'aide de l'expression établie précédemment [1]

$$Z' = \frac{1+u}{DC_0} C_E = \frac{1}{K^*}\left[\frac{K_{0D}^{HX}}{K_{0D}^{MX}} + \frac{y_{H^+(S)}}{y_{M^+(S)}} u\right]$$

avec (1)

$$u = 2 \Big/ \left[\left(1 + \frac{4C_0 y_{H^+(S)} y_{X^-(S)}}{K_{0D}^{HX}} \right)^{1/2} - 1 \right]$$

où D est le coefficient de partage de l'élément M, K_{0D}^{HX} et K_{0D}^{MX} sont les constantes de dissociation de l'acide et du sel, respectivement, C_0 est la concentration totale d'acide HX en solution, C_E est la capacité d'échange de la résine, y_{i^+} le coefficient d'activité de l'espèce i, en solution; K^* peut être considéré comme un coefficient de sélectivité des ions M^+ et H^+.

Dans chaque mélange étudié D, K_{0D}^{HX}, C_E et C_0 sont connus. On peut tracer, pour un solvant donné, les coubes de variation de Z' en fonction de $u \cdot y_{H^+(S)}/y_{M^+(S)}$. Ce sont des droites dont la pente $(1/K^*)$ et l'ordonnée à l'origine $(1/K^*) \cdot (K_{0D}^{HX}/K_{0D}^{MX})$ nous ont servi à calculer les coefficients de sélectivité des ions (K^*) et la constante de dissociation du sel (K_{0D}^{MX}).

Nous avons obtenu des variations linéaires de Z' en fonction de $u \cdot y_{H^+(S)}/y_{Cs^+(S)}$ (Fig. 3). Les valeurs trouvées du coefficient de sélectivité relatif à l'échange entre Cs^+ et H^+ sont égales à 1,86; 2,47 et 2,57, dans des mélanges à 4,8; 9,6 et 14,4% d'eau, respectivement. Si l'on compare ces résultats à la valeur trouvée par Bonner et Smith [5] dans l'eau égale à 2,56, on observe que le coefficient de sélectivité de ces ions varie peu avec la composition du mélange.

Les pK de dissociation du chlorure de césium sont représentés sur la Fig. 4, où nous avons fait aussi figurer le pK de dissociation de l'acide chlorhydrique dans les mêmes mélanges hydro—acétiques. On remarque que les valeurs des pK de dissociation de l'acide et du sel sont voisines.

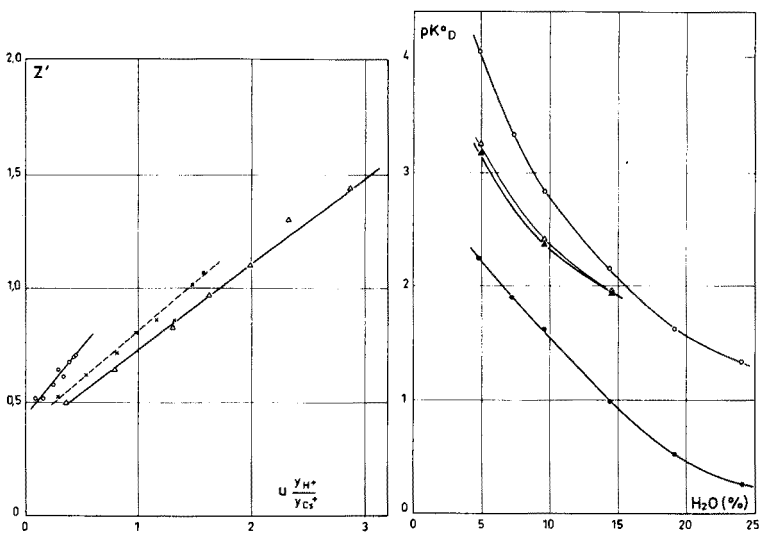

Fig. 3. Variation de Z' en fonction de $u\, y_{H^+}/y_{Cs^+}$. Mélanges eau—acide acétique à: (○) 4,8% d'eau, (×) à 9,6% d'eau et (△) 14,4% d'eau.

Fig. 4. Variation de pK_{0D} en fonction du pourcentage d'eau des solutions. Mélanges eau—acide acétique: (△) HCl, (▲) CsCl, (○) HNO_3 (●) $NaNO_3$.

Nitrate de sodium. Pour exploiter les mesures expérimentales concernant le nitrate de sodium, nous avons supposé, en nous basant sur les résultats obtenus pour le césium, que la valeur du coefficient de sélectivité, K^*, relatif à l'échange entre Na^+ et H^+, était indépendante de la teneur en eau des mélanges et égale à 1,56, valeur trouvée dans l'eau [5], aussi bien que dans les mélanges eau—acide acétique—acide perchlorique [2]. Dans ce cas, C_0, C_E, $K_{0D}^{HNO_3}$ et K^* sont connus et nous avons calculé, à l'aide de l'expression (1), les constantes de dissociation du nitrate de sodium (4—25% d'eau) à partir des mesures du coefficient de partage du sodium en fonction du pourcentage d'eau des mélanges eau—acide acétique—acide nitrique 0,1 M. Les valeurs obtenues sont représentées sur la Fig. 4. On voit que dans les mélanges eau—acide acétique les constantes de dissociation de l'acide nitrique et du nitrate de sodium sont très différentes.

BIBLIOGRAPHIE

1 A. R. Rodriguez et C. Poitrenaud, Anal. Chim. Acta, 87 (1976) 125.
2 A. R. Rodriguez et C. Poitrenaud, Anal. Chim. Acta, 87 (1976) 141.
3 F. Le Ber, Thèse, Paris, 1970.
4 A. R. Rodriguez et C. Poitrenaud, Analusis, 3 (1975) 491.
5 O. D. Bonner et L. L. Smith, J. Phys. Chem., 61 (1957) 326.

Analytica Chimica Acta, 93 (1977) 363—369
© Elsevier Scientific Publishing Company, Amsterdam — Printed in the Netherlands

Book Reviews

G. Svehla (Ed.), *Comprehensive Analytical Chemistry, Volume VII, Thermal Methods in Analytical Chemistry, Substoichiometric Analytical Methods*, Elsevier, Amsterdam, 1976, 322 pp., price Dfl. 125.00.

This latest addition to Wilson and Wilson's volumes on analytical chemistry deals with two major analytical methods — thermal analysis and substoichiometric analysis. The chapter (205 pages) on thermal analysis has been contributed by Clement Duval. (Regrettably, this has appeared posthumously, the author having died in March 1976.) Duval's eminence in this field is very well known and his own work over many years on thermogravimetric analysis has done much to popularise the technique. The present account is a worthwhile condensation of the vast literature which now threatens to overwhelm the guileless reader, anxious to know more about the applications of TG, DTA and DSC. Although greatest emphasis is placed on TG in the present volume, the differential thermal techniques are also given suitable treatment (less so for DSC).

The second chapter (92 pages) contributed by J. Stary and J. Růžička deals with the principles and applications of their well-known substoichiometric radiochemical method of analysis. The basic theory of neutron activation analysis and isotope dilution analysis is followed by a brief account of instrumentation and experimental procedures. The applications of the substoichiometric technique to the determination of some fifty elements are then described.

This volume maintains the standards set by earlier volumes in the series and is a most useful addition to this valuable reference work.

W. I. Stephen

R. W. B. Pearse and A. G. Gaydon, *The Identification of Molecular Spectra*, Chapman and Hall, London, 4th edn., 1976, viii + 407 pp., price £20.00.

The significance of gas-phase molecular emission and absorption in analytical flame spectroscopy and related fields has greatly increased over the last decade. For instance, extensive applications of emissions from molecules such as S_2, PHO and InCl have been reported, and the important effects of molecular absorption on atomic absorption signals from flames and electrothermal atomizers have been increasingly recognized. Thus the appearance of this fourth edition of "Pearse and Gaydon" is particularly to be welcomed by analytical spectroscopists, as well as those engaged in more fundamental studies.

This fourth edition has been expanded and updated to list wavelengths, relative intensities, etc., for the band spectra from some 490 diatomic and 127 polyatomic molecules, organized, as previously, in alphabetical order of elemental symbol. The tables of persistent head wavelengths have been appreciably rationalized and a separate section on the spectra of deuterides has been incorporated. The table of the most persistent atomic lines, the spectrograms and the chapter on practical procedure and precautions are retained, together with subject and author indexes.

A. Townshend

M. Mehring, *High Resolution NMR Spectroscopy in Solids (NMR — Basic Principles and Progress, Vol. 11*, P. Diehl, E. Fluck and R. Kosfeld (Eds.)), Springer-Verlag, Berlin, 1976, x + 246 pp., price DM 68.

The present volume is a valuable addition to this well-established series, originally devoted to theoretical and physical aspects of n.m.r. spectroscopy, but now also describing problems and developments on the applied side. With a few exceptions, solid samples absorb energy over too wide a range of frequencies to provide sharply resolved spectra for solving analytical chemical problems. Techniques now available for overcoming the natural line-broadening mechanisms in solids are reviewed in this monograph. Multiple-pulse experiments aimed at repressing dipolar and quadrupolar interactions which mask shift interactions and scalar couplings, and double-resonance experiments on different types of rare spins aimed at achieving high resolution spectra, are discussed in detail. Applications of the techniques that include the investigation of dynamic problems in molecular and solid-state physics are described

Study of this text should prove profitable to most n.m.r. spectroscopists faced with the problem of obtaining high-resolution spectra from solid-state samples. Since the vast majority of chemists who employ n.m.r. spectroscopy deal with liquid samples (where nature has usually performed the manipulations and removed the anisotropic interactions!), the range of appeal of the book within the chemical fraternity is likely to be strictly limited.

B. D. Flockhart

B. Lindman and S. Forsén, *Chlorine, Bromine and Iodine NMR. Physico-Chemical and Biological Applications (NMR — Basic Principles and Progress, Vol. 12*, P. Diehl, E. Fluck and R. Kosfeld (Eds.)) Springer-Verlag, Berlin, 1976. xiii + 368 pp., price DM 96.

This volume contains an account of the n.m.r. spectroscopy of one set of related quadrupolar nuclei: chlorine (^{35}Cl and ^{37}Cl), bromine (^{79}Br and ^{81}Br) and iodine (^{127} I). Fluorine is excluded because the only stable isotope, ^{19}F,

has a spherically symmetric distribution of nuclear charge. A brief introduction to the parameters that characterize the n.m.r. spectra of quadrupolar nuclei is followed by detailed discussion of specific aspects of halogen n.m.r.: quadrupole relaxation of covalently bonded chlorine, bromine and iodine, and of chloride, bromide and iodide ions; halogen relaxation rates in paramagnetic systems; shielding effects in covalent halogen compounds; halide ion shieldings; halogen spin coupling constants; chemical exchange of halide ions. Applications of halogen n.m.r. surveyed in detail include quadrupole splitting in liquid crystals and halide ion quadrupole relaxation in biological and non-biological systems. Halogen quadrupole splitting studies are being increasingly applied to obtain information on, for example, molecular geometry and electric field gradients. Biochemical applications of the quadrupolar relaxation method made to date have involved studies of the relaxation of aqueous ions taking part in chemical exchange with a protein, polypeptide or other molecule of biological interest, e.g. humic acids.

A judgment based on published papers suggests that most chemists and biologists who regularly use n.m.r. in their investigations have been reluctant to study nuclei with large electric quadrupole moments, doubtless because in non-symmetric environments the observed n.m.r. spectra are usually broad and cannot be studied by ordinary high-resolution techniques. Problems associated with less familiar experimental procedures and spectral parameters are certainly encountered when investigating quadrupolar nuclei, but the authors of this monograph show clearly that the study of quadrupolar halogen nuclei can provide unique and valuable information on a variety of physico-chemical and biological systems. The authors have also included a comprehensive literature citation, which affords a ready access to further information.

In summary, this is a valuable book for workers in the field of halogen n.m.r. spectroscopy, for those with a potential interest in the field, and for n.m.r. spectroscopists in general, since much of the basic material presented is applicable to other quadrupolar nuclei.

B. D. Flockhart

M. R. F. Ashworth, *The Determination of Sulphur-containing Compounds, Volume 2. Analytical methods for Thiol Groups*, Academic Press, London, 1976, x + 288 pp, price £9.80 ($21.50).

This is the second volume of a monograph dealing with the analysis of sulphur-containing compounds; the first volume was concerned with the analysis of sulphones, sulphoxides, sulphonyl halides, thiocyanates and isothiocyanates. In the main, the present volume gives analytical methods for compounds containing thiol groups attached to a carbon atom joined either to hydrogen or to another carbon atom.

Whilst this covers alkane- and arene-thiols it also includes compounds containing such other functional groups as mercapto-carboxylic acids, mercapto-amines, mercapto-alcohols and some thio-amino acids. In view of the large amount of work associated with mercaptobenzothiazole, and the large interest in its uses, the author has wisely decided to include this compound in his discussions.

In the preface the author indicates the dilemma which faced him when deciding whether to give either detailed descriptions of a limited number of experimental methods, or to give a brief description (in some cases just a reference) to a large number of methods and compounds. He chose the latter method and although this occasionally results in very brief sections and short chapters, it was in the opinion of this reviewer the correct decision. The book is not aimed at beginners in chemistry but at those who have a reasonably broad and basic understanding of the techniques and principles of modern analytical chemistry. It is designed for those who, from the work of others, can deduce a likely solution to their own immediate analytical problems. For such a book to be useful it must perforce be arranged for easy and rapid reference; and as well as having a good coverage of the relevant literature, it must have a comprehensive index. This book fulfils these requirements; it should become a source book for methods for the determination of sulphur containing groups.

L. S. Bark

Z. Holzbecher, L. Divis, M. Kral, L. Sucha and F. Vlacil, *Handbook of Organic Reagents in Inorganic Chemistry*, Ellis Horwood, Chichester, (J. Wiley, Halsted Press), 734 pp., price £19.00 ($41.80).

In recent years, there have been few significant texts dealing exclusively with the use of organic reagents in inorganic analysis. Since Frank Welcher's classic compendium of organic reagents in 1948, there has been, with little exception, no determined attempt to produce a worthwhile discussion of the very many developments which have occurred in the intervening years, apart perhaps from D. D. Perrin's two valuable contributions dealing with organic complexing reagents (1964) and masking and demasking (1968), in which organic reagents play a dominant role. This new volume, designated as a handbook of organic reagents, would appear to fill an important gap in the modern literature and should be expected to stimulate considerable interest in this indispensible area of analytical chemistry. Alas, a perusal of the contents fails to convince this reader that these objectives have been realised.

It is undoubtedly easier to damn than to praise, but is it really necessary to devote the first 180 pages of this book to the theoretical aspects of co-ordination chemistry and solution equilibria, matters which form the basis of many other excellent texts?

Even the general discussion, which follows, of the use of organic reagents in established analytical processes, such as gravimetry, titrimetry, photometry, chromatography, solvent extraction, etc. seems far too long (200 pages) for a book of this nature.

The practising chemist will use this book essentially for reference purposes and most of this preliminary material, however laudable its inclusion may be, is superfluous to his immediate needs. He will be more concerned with the hard core of the book in which the analytical applications of organic reagents are discussed element by element. This section occupies about 200 pages, i.e. a little over one quarter of the total length of the book. The information is presented in tabular form, selected reagents for each element being summarised under headings such as method, conditions, range and remarks.

A final chapter of some 100 pages is really an appendix. It contains a selection of common organic reagents presented in alphabetical order, with structures, properties and principal analytical applications.

In many ways this book is just restating facts which are better discussed elsewhere. The important section on the organic reagents themselves lacks the authority which one might have expected from the experiences of the Czechoslovak authors. There is no attempt at critical selection, and indeed, the actual selections are often curious and certainly not always representative of the literature. As one of many examples, the use of EDTA for the alkali metals is listed. The sequence of events following the precipitation of the alkali metal perchlorates is astounding, but the EDTA is eventually used to titrate nickel ions. Still with the alkali metals, the Reeve reagent, α-methoxyphenylacetic acid, has been discredited as a precipitant for sodium, and yet no mention is made of dihydroxytartaric acid or the excellent Selleri and Caldini reagent, orotic acid, for this purpose. There are many other equally curious omissions and inclusions. One hesitates to raise the Calcion—Calcichrome disputation, but Calcion is at least worth a mention as a photometric reagent for calcium. Again, several reagents for the precipitation of the sulphate ion which are superior to the time-honoured (but carcinogenic) benzidine have been recommended over the last twenty-five years, but none is mentioned.

To conclude, this book fails to provide the necessary stimulus and interest which its subject demands. It is prosaic, mundane and uninspiring. Even as a shelf reference book, it will not find too many users, for its referencing is not always complete or even accurate. It presents too little new information to be of any real value. Just for the record, Blau (1888) made no analytical use of 2,2′-bipyridine or 1,10-phenanthroline, and J. F. Flagg's book was published in 1948.

W. I. Stephen

N. Catsimpoolas (Ed.), *Isoelectric Focusing*, Academic Press Ltd., New York and London, 1976, xii + 265 pp., price £16.00.

Isoelectric focusing is one of the very specialised electrical methods of separation, introduced just over 20 years ago: it is specialised because its application is restricted to amphoteric molecules and bioparticles. Nevertheless, it is a very important technique indeed for those molecules, e.g. proteins, to which it is applicable. This book contains nine chapters contributed by international authorities from Australia, Germany, Great Britain, Sweden and the U.S.A. The coverage is comprehensive and up-to-date; the production is excellent in all respects. There is no doubt that this book will be of great interest to immunologists, geneticists, microbiologists and biochemists and to those analytical chemists concerned with biological macromolecules.

Panos Grammaticakis, *Spectres d' absorption Ultraviolets de Composes Organiques Azotes et Correlations Spectrochemiques, Premier Fascicule*, Technique et Documentation, Paris, 1977, 107 pp., price FF 120.

This is yet another collection of ultraviolet and visible spectra, reproduced directly from a typed manuscript (in French). The author is a well-known spectroscopist and this production is clearly to be regarded as a personal *tour de force* for its author: this first volume contains about 1250 spectra and it is his intention to go on to publish in this form the 5000 spectra that he has accumulated during his researches over the past 40 years. The spectra themselves are presented as reproductions of the actual spectrograms, on to which details of the chemical compound concerned, its formula and concentration etc. have been "pasted up". The result is frequently an entanglement of lines and small print; some of the reproductions are unsatisfactory in terms of clarity. A selling-point claimed for this book is that the spectra were obtained from compounds of high purity prepared by the author himself, that samples of these compounds are available from the author, and that all spectra were obtained by the same operator on the same spectrometer. Formidable!

L. S. Dent Glasser, *Crystallography and its Applications*, Van Nostrand Reinhold, London, 1977, viii + 224 pp., price £12.00 (cloth), £5.95 (paper).

This is a splendid book, written by an expert crystallographer for advanced undergraduates and those industrial and academic research workers who "might wish to use some of the crystallographic techniques to help them along". The result is a most attractive production — possibly rather wordy — but very easily read and understood, with lots of useful, clear diagrams. This is just the sort of book that students need, and a book that many other

crystallographers will wish they had written. There are useful references at the end of each chapter and a further list of 4 pages of suggestions for further reading at the end of the book, a helpful index, and two of the chapters invite the reader to work out answers to problems based on some of the figures. The main chapters deal with Pattern and Symmetry; Elementary Optical Crystallography; Diffraction of X-rays; Single Crystal Diffraction Photographs; Simple Single Crystal Studies; The Uses and Abuses of the Powder Method; Structure Determination; Other Diffraction Methods; Assessing Crystal Structure Analyses; A Crystallographic Cost-benefit Analysis. The teaching of crystallography will be much simpler from now onwards!

D. M. W. Anderson

Announcements

International Symposium on Advances in Chromatography "Chromatography '77"

The Twelfth International Symposium on Advances in Chromatography will be held during November 7—10, 1977 at the International Congress Centre RAI, in Amsterdam, The Netherlands.

The meeting will include papers by outstanding researchers from throughout the world in all fields of chromatography. In particular, new developments in gas, liquid and high-performance thin-layer chromatography will be included.

A total of 83 papers will be presented at the Symposium, representing contributions from 19 countries. A special feature of the meeting will be an exhibition of the latest instrumentation and books. Informal discussion groups will also meet during the Symposium.

Registration should be made in advance. The programs, registration forms and hotel reservation cards can be obtained from:
Organisatie Bureau Amsterdam b.v., International Congress Centre RAI, P.O.Box 7205, Europaplein 14, Amsterdam, The Netherlands
or Prof. A. Zlatkis, Chemistry Department, University of Houston, Houston, Texas 77004, U.S.A.

Sixth International CODATA Conference

The Sixth International CODATA Conference will be held in Taormina, Italy, on May 22—25, 1978. CODATA covers all disciplines within the member unions of ICSU. The following aspects will be dealt with in the Conference: data evaluation methodology; compilation procedures; mathematical modelling data requirements; correlation, extrapolation and estimation procedures; data systems analysis; machine techniques for storage, retrieval,

and dissemination of numerical data. Users of data, and those involved in data compilation, evaluation and handling are invited to submit papers before October 1, 1977. Further information is available from the CODATA Secretariat, 51 Boulevard de Montmorency, 75016 Paris, France.

7th International Geochemical Exploration Symposium

The Association of Exploration Geochemists is sponsoring the 7th International Geochemical Exploration Symposium, to be held in Golden, Colorado, April 16—20, 1978. In addition to technical sessions, a number of geochemically-oriented field trips are planned to various mining districts in the western United States. Spouse/guest activities are also planned. Synopses in English up to 750 words in length are being requested in order to select papers to be presented at the Symposium. Deadline for synopses is October 1, 1977. Further information concerning the Symposium and details on submission of synopses will be sent to those making a request (by Airmail if overseas) to: M. A. Chaffee, Secretary, Organizing Committee, 7th International Geochemical Exploration Symposium, U.S. Geological Survey, 5946 McIntyre Street, Golden, Colorado 80401, U.S.A.

National Bureau of Standards — Conference Briefs

October 3—6 *Alternatives for Cadmium Electroplating in Metal Finishing*, NBS, Gaithersburg, MD; sponsored by NBS, Consumer Product Safety Commission, Department of Defense, Department of the Interior, Occupational Safety and Health Administration, Environmental Protection Agency, Food and Drug Administration, and General Services Administration. Contact, Fielding Ogburn, B166, Polymers Building, National Bureau of Standards, Washington, D.C. 20234; 301/921-2957.

October 11—13 *Materials for Coal Conversion and Utilization*, NBS, Gaithersburg, MD; sponsored by NBS, Energy Research and Development Administration, Electric Power Research Institute. Contact S. J. Schneider, B308 Materials Building, National Bureau of Standards, Washington, D.C. 20234, 301/921-2893.

October 11—14 *13th Meeting of the Computer Performance Evaluation Users Group*, New Orleans, LA; sponsored by NBS. Contact, Dennis M. Conti, A265 Technology Building, National Bureau of Standards, Washington, D.C. 20234, 301/921-3485.

October 17—19 *Time and Frequency Calibration: Methods and Resources*, NBS, Boulder, Colo.; sponsored by NBS. Contact, Roger Beehler, National Bureau of Standards, Boulder, Colo., 80302, 303/499-1000, ext. 3281.

October 19—20 *Reliability Technology for Cardiac Pacemakers*, NBS, Gaithersburg, MD; sponsored by NBS. Contact Harry A.

Schafft, A327 Technology Building, National Bureau of Standards, Washington, D.C. 20234, 301/921-3625.

November 13—17 *Workshop on Rapid Solidification Technology*, Sheraton-Reston, Reston, VA; sponsored by NBS and the Advance Research Projects Agency. Contact, Arthur W. Ruff, Jr., B264 Materials Building, National Bureau of Standards, Washington, D.C. 20234, 301/921-2811.

December 5—7 *Winter Simulation Conference*, NBS, Gaithersburg, MD; sponsored by NBS, the Association for Computing Machinery, the Institute of Electrical and Electronic Engineers, Operations Research Association of America, the Institute for Management Sciences, American Institute for Industrial Engineers, and the Society for Computer Simulation. Contact, Paul F. Roth, B250 Technology Building, National Bureau of Standards, Washington, D.C. 20234, 301/921-3545.

1978

April 10—13 *Trace Organic Analysis: A New Frontier in Analytical Chemistry*, NBS, Gaithersburg, MD; sponsored by NBS. Contact, Harry S. Hertz, A105 Chemistry Building, National Bureau of Standards, Washington, D.C. 20234, 301/921-2153.

April 17—20 *Acoustic Emission Working Group Meeting*, NBS, Gaitherburg, MD; sponsored by NBS. Contact, John A. Simmons, B118 Materials Building, National Bureau of Standards, Washington, D.C. 20234, 301/921-3355.

April 23—26 *American Nuclear Society Topical Conference on Computers in Activation Analysis and Gamma Ray Spectroscopy:* Mayaguez, Puerto Rico; sponsored by NBS, American Chemical Society, American Nuclear Society, Energy Research and Development Administration, U. of Puerto Rico, Puerto Rico Nuclear Center. Contact, B. S. Carpenter, Bldg. 235, NBS, Washington D.C., 20234, 301/921-2167.

May 8—10 *Symposium on Real-Time Radiographic Imaging*, NBS, Gaithersburg, MD; sponsored by NBS and the American Society for Testing and Materials. Contact, Donald A. Garrett, A106 Reactor Building, National Bureau of Standards, Washington, D.C. 20234, 301/921-3634.

June 26—29 *Conference on Precision Electromagnetic Measurements*, Ottawa, Ontario, Canada; sponsored by Institute of Electrical and Electronics Engineers, U.S. National Committee-International Union of Radio Science, and NBS. Contact, Dee Belsher, National Bureau of Standards, Boulder, Colo., 80302, 303/499-1000, ext. 3981. (477-4)

Analytica Chimica Acta, 93 (1977) 372—373
©Elsevier Scientific Publishing Company, Amsterdam — Printed in The Netherlands

ERRATA

R. Reisfeld, H. Harnik, S. Levi and W. J. Levene, The Microdetermination of Nickel, Cobalt and Zinc by Reflectance Spectrometry, *Anal. Chim. Acta*, 91 (1977) 379—383.

Page 381, Table 1, footnote[b] should read:

[b] 1—250 ppm corresponds to $7 \cdot 10^{-9}$—$1.75 \cdot 10^{-6}$ g in a drop.

J. F. Alder, C. A. Pankhurst, A. J. Samuel and T. S. West, The use of Silk and Animal Hairs as Standards for Analysis, *Anal. Chim. Acta*, 91 (1977) 407—410.

Page 410 was inadvertently omitted during the printing process. The complete page is as follows:

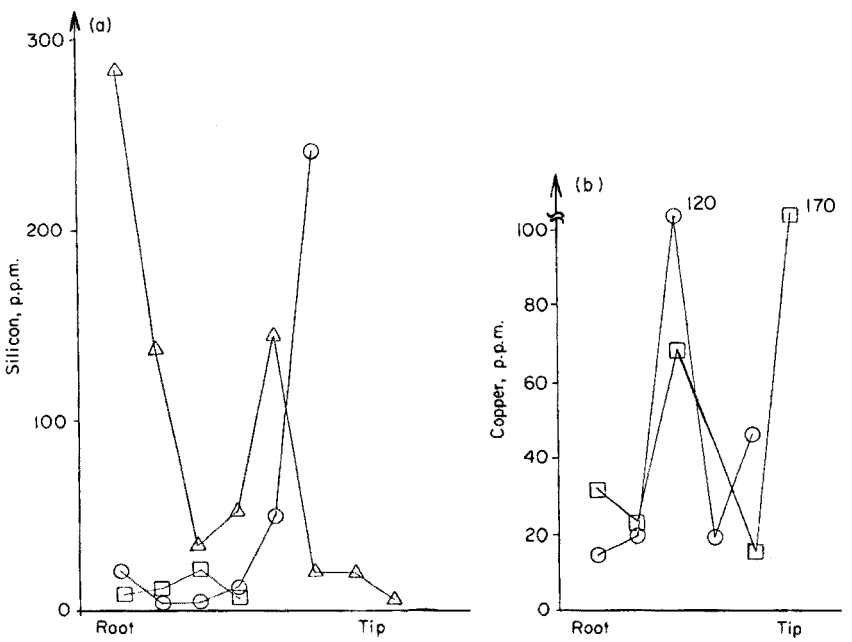

Fig. 1. Analysis of animal hairs. (a) For silicon (○ dog, △□ cat). (b) For copper (cat only).

The data obtained for the cat and dog hairs indicate that the metals are distributed randomly as in human hairs; animal hairs therefore offer, without doping, no advantage over human hair as a standard material.

Conclusion

Except for Cu and Fe, the results obtained for silk were not satisfactory; together with the difficulty in handling the material, this suggests that silk

will not make a suitable reference material for hair analysis. The results for cat and dog hairs suggest that they are also of little use as standards.

The authors are indebted to the Home Office for the loan of the equipment used and for financial support (to J. F. A. and A. J. S.), and to the S.R.C. for financial support (to C.A.P.).

REFERENCES

1 G. D. Renshaw, C. A. Pounds and E. F. Pearson, J. Forensic Sci., 18 (1973) 143.
2 J. F. Alder, D. Alger, A. J. Samuel and T. S. West, Anal. Chim. Acta, 87 (1976) 301.
3 J. F. Alder, A. J. Samuel and T. S. West, Anal. Chim. Acta, 87 (1976) 313.
4 I. Obrusnik, J. Gislason, D. Maes, D. K. McMillan, J. D'Auria and B. D. Pate, J. Radioanal. Chem., 15 (1973) 115.
5 L. C. Bate, J. Forensic Sci., 10 (1965) 60.
6 A. J. Van der Berg, M. de Bruin and J. P. N. Houtman, Proc. Symp. Amsterdam, May (1967) p. 661.
7 E. R. Theis and T. F. Jacoby, J. Am. Leather Chemists Assoc., 36 (1941) 545.

ANALYTICA CHIMICA ACTA, VOL. 93 (1977)

AUTHOR INDEX

ANALYTICA CHIMICA ACTA, VOL. 93 (1977)

SUBJECT INDEX

ANALYTICA CHIMICA ACTA
(including COMPUTER TECHNIQUES AND OPTIMIZATION)

INFORMATION FOR AUTHORS

Analytica Chimica Acta publishes original papers, short communications, and reviews dealing with every aspect of modern chemical analysis, both fundamental and applied. The section on *Computer Techniques and Optimization* is devoted to new developments in chemical analysis by the application of computer techniques and by interdisciplinary approaches, including statistics, systems theory and operation research.

Reviews are written by invitation of the editors, who welcome suggestions for subjects. Short communications are usually complete descriptions of limited investigations, and should generally not exceed four printed pages. Preliminary communications of important urgent work can be printed in this category within 4 months of submission, if the authors are prepared to forego proofs.

Submission of papers

Authors should submit three copies of the manuscript in double-spaced typing on one side of the paper only, with a margin of 4 cm, on pages of uniform size. If any variety of machine copying is used (e.g. xerox), authors should ensure that all copies are easily legible and that the paper used can be written on with both ink and pencil. Authors are advised to retain at least one copy of the manuscript. Manuscripts should be preceded by a sheet of paper carrying (a) the title of the paper, (b) the name and full postal address of the person to whom proofs are to be sent, (c) the number of pages, tables and figures.

Manuscripts should be sent to the editorial addresses given on the covers of current issues; submission to the publisher leads to delays. Submission of a manuscript implies that the work described has not been, and will not be, published elsewhere (except as an abstract, or as part of a lecture, review or academic thesis). On acceptance of the manuscript, the copyright passes to the publishers, if it has not been previously reserved by a government institution or company.

The preferred language of the journal is English, but French and German manuscripts are also acceptable. For authors whose first language is not English, French or German, linguistic improvement is provided as part of the normal editorial processing.

Notes on the preparation of manuscripts

Authors are given every latitude, consistent with clarity and brevity, in the style and form of their papers. Very useful advice is provided in the Handbook for Authors issued by the Chemical Society and American Chemical Society.

Title and initial layout. All manuscripts should be headed by a concise but informative title. This is followed by the names of the authors, and the address of the laboratory where the work was carried out. The author to whom correspondence should be addressed must be indicated by an asterisk (without a footnote). If the present address of an author is different from that mentioned, it should be given in a footnote. Acknowledgements of financial support should not be made in footnotes.

Summary. Research papers and reviews begin with a Summary (50—250 words) which should comprise a brief factual account of the contents of the paper, with emphasis on new information. Uncommon abbreviations, jargon and reference numbers must not be used. The Summary should be suitable for use by abstracting services without rewriting. Papers in French or German require a Résumé or Zusammenfassung followed by a Title and Summary in English; authors are encouraged to provide translations where necessary. Short communications do not require summaries.

Introduction. The first paragraphs of the paper should contain accounts of the reasons for the work, any essential historical background (as briefly as possible and with key references only) and preliminary experimental work.

Experimental. The experimental methods may be described after the introductory material, or after the discussion of results, depending on the nature of the paper. Detailed experimental descriptions should, however, be restricted to one section of the paper, and not scattered throughout the text. Working procedures should be given in the imperative mood; sufficient detail should be given to allow any reasonably experienced worker to carry out the procedure. Detailed descriptions of well-known techniques and equipment are unnecessary, as are simple preparations of reagents or solutions, and lists of common chemicals. Manufacturers need be named only if the product differs essentially from that of other manufacturers. Local suppliers for multi-national concerns need not be named. In writing, complete sentences should be used, and procedural steps should not be numbered.

Results and discussion. These may be treated together or separately. In discussing results, unnecessary repetition of experimental detail, unsupported elaboration of hypotheses, and verbose exposition of ideas should be avoided. Chemical formulae should not be used in the text unless confusion is likely to arise from the use of names. Formulae should, however, be used for brevity in Tables and Figures. Calculations well known to specialists are unnecessary. Conclusions should be added only if needed for interpretation; they should not be used as extended summaries.

Acknowledgements. These should be kept as short as possible, and placed, without a heading, at the conclusion of the text.

References

The references should be collected at the end of the paper, numbered in the order of their appearance in the text (*not* arranged alphabetically), and typed on a separate sheet. If the paper forms part of a series, the reference to the previous part should appear as the first reference, the number being cited at the title of the paper. References given in Tables should be numbered according to the position of the Table in the text. Every reference listed must be cited in the text. Reference numbers in the text are set in square brackets on the line. Numerals referring to equations are placed in parentheses.

In the list of references, the following forms should be adopted.

Journals

1 W. Lund and M. Salberg, Anal. Chim. Acta, 76 (1975) 131.
2 M. McDaniel, A. D. Shendrikar, K. D. Reizneir and P. W. West, Anal. Chem., 48 (1976) 2240.

The title of the journal must be abbreviated as in the Bibliographic Guide for Editors and Authors.

Books

1 D. D. Perrin, Masking and Demasking of Chemical Reactions, Interscience-Wiley, New York, 1970, p. 188.
2 G. G. Guilbault, in G. Svehla (Ed.), Wilson and Wilson's Comprehensive Analytical Chemistry, Vol. 8, Elsevier, Amsterdam, 1977, p. 49.

Titles of papers are unnecessary. Citations of reports which are not widely available (e.g. reports from government research centres) should be avoided if possible. Authors' initials should not be used in the text, unless real confusion could be caused by their omission. If the reference cited contains three or more names, only the first author's name followed by et al. (e.g. McDaniel et al.) should be used in the text; but the reference list must contain the initials and names of *all* authors.

Tables, Computer Programs and Figures

Tables and Figures must be essential for the clear and concise presentation of the material. The same information should not be given in Tables and Figures, and material from the published literature should not be reproduced.

Tables. All Tables should be numbered with Arabic numerals, and have brief descriptive headings; they should be typed on separate pages. The layout should be given serious thought, so that the significance of the results can be grasped quickly. Column headings should be brief.

Tables with only two or three headings are printed best horizontally, e.g.

Hg^{2+} added (μg)	1.0	2.0	3.0	5.0
Extraction (%)	95.0	99.8	99.5	89.0

Experimental information which is relevant to all the results in the Table is best given in parentheses immediately after the heading. No column should contain the same number or unit throughout its length. Footnotes to Tables are denoted by superscript a, b, c .... The units used should be clearly stated. Confusion can arise from the use of powers in column headings. The following usage is recommended: e.g. if molar absorptivities are listed, the heading should be $\epsilon(\times 10^4\ l\ mol^{-1}\ cm^{-1})$ so that a number 2.32 in the column signifies 23 200.

Alphanumeric computer output is usually unsuitable for reproduction and should therefore be retyped and presented as Tables; capitals can be used to simulate computer output if such simulation is essential for illustration.

Computer programs. Computer algorithms should be described clearly; a standard high-level programming language or a suitable algorithmic notation should be used as necessary. Complete program listings, however, are not normally admissible. Extensive flow charts should be avoided if the material can equally well be given in descriptive or tabular form. Statements on the portability of the software described to other computer systems, as well as on its availability to interested readers, should be given.

Figures. Figures should be prepared in black waterproof drawing ink on drawing or tracing paper of the same size as that on which the manuscript is typed. One original (or sharp glossy print) and two photostat (or other) copies are required. Attention should be given to line thickness, lettering (which should be kept to a minimum) and spacing on axes of graphs, to ensure suitability for reduction during printing. Axes of a graph should be clearly labelled, along the axes, and outside the graph itself.

The following standard symbols should be used in graphs:

▼ ▽ ■ □ + × ● ○ ▲ △

Simple straight-line graphs are not acceptable, because they can readily be described in the text, by means of an equation or a sentence. Explanatory information should be placed not in the figure, but in the legend, which should be typed on a separate sheet of paper. All Figures should be numbered with Arabic numerals, and require descriptive legends.

Photographs should be glossy prints and be as rich in contrast as possible; colour photographs cannot be accepted. In general, line diagrams are more informative than photographs of equipment.

Computer outputs for reproduction as Figures must be of good quality on blank paper, and should preferably be submitted as glossy prints.

Nomenclature, abbreviations and symbols

In general, the recommendations of the International Union of Pure and Applied Chemistry (IUPAC) should be followed, and attention should be given to the recommendations of the Analytical Chemistry Division in the journal *Pure and Applied Chemistry*.

Symbols, formulae and equations should be written with great care, capitals and lower case letters being distinguished where necessary. Particular care should be taken in typing mathematical expressions containing superscripts and subscripts, and in proof-reading such equations. Greek letters and unusual symbols employed for the first time should be defined by name in the left-hand margin.

Basic SI and other accepted metric nomenclature are given in the Appendix. In accordance with IUPAC rules, the mass number, atomic number, number of atoms and ionic charge should be designated by a left upper index, a left lower index, a right lower index and a right upper index, respectively, placed round the atomic symbol. For example, the phosphate ion should be designated as PO_4^{3-} (*not* PO_4^{-3} or PO_4^{---}), and phosphorus-32 as ^{32}P (*not* P^{32} or P-32).

The Stock notation for the indication of stoichiometric valency states (and indirectly the proportion of the constituents) is recommended. Examples are iron(III) chloride in preference to ferric chloride, and potassium hexacyanoferrate(II) in preference to potassium ferrocyanide. These rules are valid for French and German as well as English usage.

The use of nanometre (nm) and micrometre (μm), for the expression of analytical wavelengths has now superseded mμ or Å or μ, all of which should be avoided, although Å is sensibly retained in crystallographic work.

Natural or Naperian logarithms should be denoted by ln and decadic logarithms by log.

In analytical chemistry, the term normality (N) serves many useful purposes and will be retained. It should not however, be used, if no ambiguity is introduced by the use of molarity (M). The term formality (F) should be avoided.

Unusual abbreviations require definition when first used. Abbreviations for long chemical names (e.g. EDTA, HEDTA, TBAH, en, pn, Tris) are useful, especially in equations, Tables or Figures. For ease of distinction, well-known techniques should be abbreviated by using lower-case letters and full stops, such as, g.c.-m.s., u.v., i.r., a.a.s., n.m.r., a.s.v., d.p.p., etc.

Ambiguity in expressing dilution can be avoided by the use of e.g. (1 + 2) rather than 1:2 which could mean either one part diluted with 2 parts or one part diluted to twice its volume.

The solidus / may be used in equations to economize vertical space, but its use should be consistent. For example:

$$A/b = x^2/(u + v)^{5/6}$$

Decimal points should be indicated by full stops in papers written in English and by commas in French and German papers.

Appendix

Basic SI units.

metre	m	candela	cd
kilogram	kg	mole	mol
second	s	(an Avogadro number of any	
ampere	A	particle: atoms, molecules,	
degree Kelvin	K	ions, electrons, etc.)	

Derived SI units.

joule	J	$kg\ m^2\ s^{-2}$	farad	F	$A\ s\ V^{-1}$
newton	N	$J\ m^{-1}$	weber	Wb	V s
watt	W	$J\ s^{-1}$	henry	H	$V\ s\ A^{-1}$
coulomb	C	A s	tesla	T	$V\ s\ m^{-2}$
volt	V	$J\ A^{-1}\ s^{-1}$	hertz	Hz	s^{-1}
ohm	Ω	$V\ A^{-1}$	degree Celsius	°C	K − 273.15

Other units.

litre	l	$10^{-3}\ m^3$	hour	h	3.6×10^3 s
gram	g	10^{-3} kg	dyne	dyn	10^{-5} N
poise	P	$10^{-3}\ m^{-1}\ s^{-1}$	atmosphere	atm	101.325 kN m^{-2}
electron volt	eV	1.6021×10^{-19} J	molar	M	mol l^{-1}
calorie	cal	4.184 J	molal	*m*	mol kg^{-1}
minute	min	60 s	curie	Ci	$37 \times 10^9\ s^{-1}$

Prefixes to Abbreviations for the names of units indicating

Multiples		Sub-multiples			
tera ($\times 10^{12}$)	T	milli ($\times 10^{-3}$)	m	pico ($\times 10^{-12}$)	p
giga ($\times 10^9$)	G	micro ($\times 10^{-6}$)	μ	femto ($\times 10^{-15}$)	f
mega ($\times 10^6$)	M	nano ($\times 10^{-9}$)	n	atto ($\times 10^{-18}$)	a
kilo ($\times 10^3$)	k				

Wilson and Wilson's Comprehensive Analytical Chemistry

edited by G. SVEHLA, *Reader in Analytical Chemistry, the Queen's University of Belfast.*

VOLUME VIII: Enzyme Electrodes in Analytical Chemistry, Molecular Fluorescence Spectroscopy, Photometric Titrations, Analytical Applications of Interferometry.

by G. G. GUILBAULT, *Chemistry Department, Louisiana State University in New Orleans,* M. A. LEONARD, *Chemistry Department, Queen's University, Belfast, and* W. NEBE, *Jena, D.D.R.*

The aim of *Comprehensive Analytical Chemistry* is to provide a self-sufficient reference work, as well as a starting point for analytical investigation. This volume contains four chapters by internationally known experts. The first chapter, on the application of enzyme electrodes, covers a growing subject which will be of particular interest to the biochemist. The two optical methods, fluorescence spectroscopy and photometric titrations, described in Chapters 2 and 3 respectively, are now well-established in chemical laboratories. Chapter 4 gives an extensive survey of the analytical applications of interferometry.

CONTENTS: **Chapters 1. Enzyme Electrodes in Analytical Chemistry.** Introduction. Preparation and properties of enzyme electrodes. Analytical applications of enzyme electrodes. The future of enzyme electrodes. **2. Molecular Fluorescence Spectroscopy.** Introduction to luminescence. Instrumentation. Practical considerations. Structural and environmental effects. Phosphorescence. Determination of inorganic ions. Determination of organic compounds. Assay of enzymes. **3. Photometric Titrations.** Introduction. Theory. Instrumentation. Acid-base photometric titrations. Photometric complexometric titrations. Precipitation titrations. Redox titrations. Spectrofluorimetric titrations. Organic functional group photometric titrations. Miscellaneous photometric titration methods. **4. Analytical Applications of Interferometry.** Historical background of analytical interferometry. Symbols. Theoretical background of interference measurements. Apparatus and accessories. Methods for interferometric analysis of homogeneous substances. Interferometric analysis of inhomogeneous substances. References. Index.

Jan. 1977 xvi + 590 pages US$ 77.75/Dfl. 190.00 Subscription price: US$ 65.75/Dfl. 161.00 ISBN 0-444-41163-1

Information on other volumes in the series may be obtained from: Elsevier Promotion Department, P.O. Box 330, Amsterdam, The Netherlands.

The Dutch guilder price is definitive. US$ prices are subject to exchange rate fluctuations.

ELSEVIER

P.O. Box 211, Amsterdam
The Netherlands
52 Vanderbilt Ave
New York, N.Y. 10017

7031

Aspects of Degradation and Stabilization of Polymers

edited by H. H. G. JELLINEK, *Department of Chemistry, Clarkson College of Technology, Potsdam, New York.*

Polymer degradation has wide ramifications. The present volume deals with properties of polymers which are important for their stability and with the various modes of breakdown of macromolecules. The practical implications of polymer degradation are highlighted. A large number of topics related to the environment are included. Quantitative aspects are emphasized throughout the text.

Reflecting the broad scope of the subject, this book covers a wide range of topics such as: mechanical degradation; effect of degradation on mechanical properties of polymers; reactions of polymers with pollutant gases; ignition of polymers and flame propagation; polymer degradation processes in ablation; and biodegradation. Thermal degradation is treated in detail as far as the relevant fundamental kinetics is concerned but is not discussed for specific polymers. This has been done adequately in previous publications. However, some limited topics are dealt with in detail, e.g., ceiling temperatures, TGA and DTA, and thermal and mass chromatography.

The extensive coverage of the practical aspects of polymer degradation makes this book of particular value to research workers. It will also be suitable as a text for graduate students in universities and polytechnics, especially for those following courses in polymer chemistry, kinetics, and environmental science.

Nov. 1977 x + 670 pages US $124.50/Dfl. 305.00 ISBN 0-444-41563-7

ELSEVIER

P.O. Box 211, Amsterdam
The Netherlands
52 Vanderbilt Ave
New York, N.Y. 10017

7059

The Dutch guilder price is definitive. US $ prices are subject to exchange rate fluctuations.

(continued from inside page of the cover)

(continued from page 4 of cover)

Short Communications

CONTENTS

(continued on inside page of the cover)